

# **Chemical Kinetics**

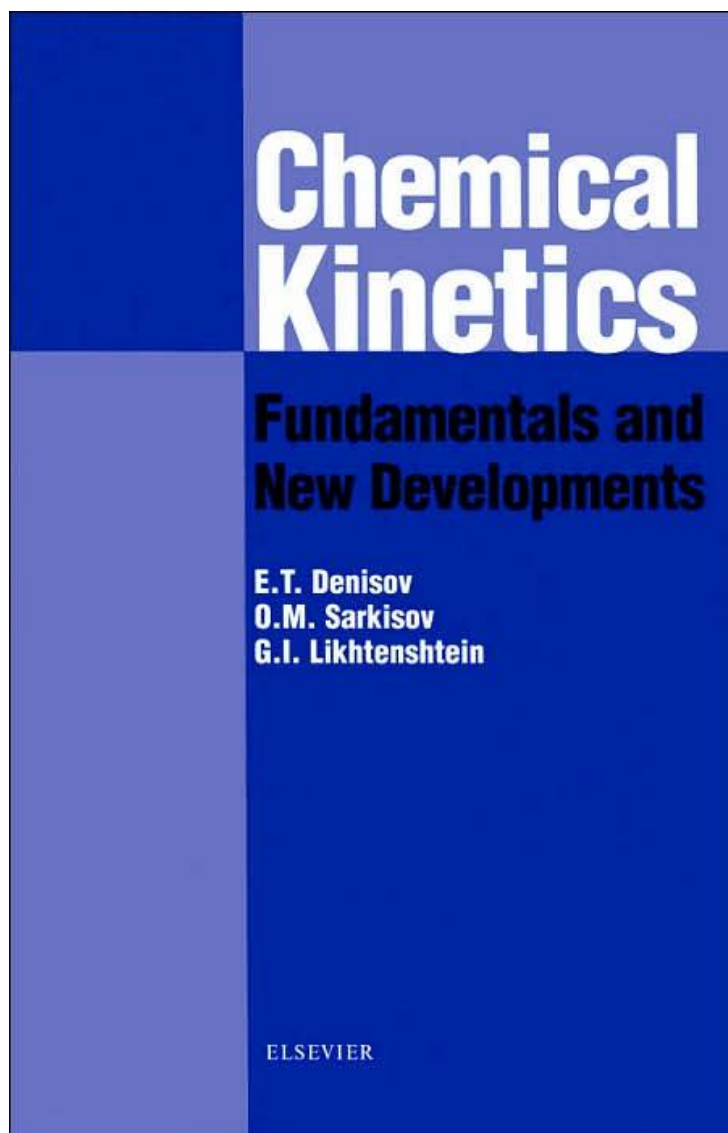
## **Fundamentals and New Developments**

**E.T. Denisov  
O.M. Sarkisov  
G.I. Likhtenshtein**

ELSEVIER

# Chemical Kinetics: Fundamentals and New Developments

by [Evgeny T. Denisov](#), [Gertz I. Likhtenshtein](#), [Oleg Sarkisov](#)



- ISBN: 0444509380
- Pub. Date: May 2003
- Publisher: Elsevier Science & Technology Books

## PREFACE

The object of this book is to present the basis of chemical kinetics in combination with its modern applications in chemistry, technology, and biochemistry. A brief historical note is given below. The material is traditionally divided into formal kinetics and kinetics in the gaseous phase.

The main concepts of chemical kinetics were formulated during the end of the 19<sup>th</sup> century when C. Guldberg and P. Waage formulated the law of action mass (1867) and Arrhenius his famous equation (1889) of the temperature dependence of the rate constant. The book "Etudes de dynamique chimique" (1884) written by Vant-Hoff was the first monograph on chemical kinetics. In this monograph, chemical kinetics was presented as simple chemical reactions. It was in the beginning of the 20<sup>th</sup> century that researchers faced complicated mechanisms of chemical reactions and during the period 1910-1935, chain reactions were discovered (M. Bodenstein, N. Semenov, S. Hinshelwood). In this period, chemical kinetics was transformed into the science of complex chemical reactions in gaseous and liquid phases. Simultaneously, the theory of the elementary act of monomolecular and bimolecular reactions was advanced. The absolute rate theory was developed in the 1930s by S. Glasstone, K. Laidler and H. Eyring. New advancements in the theory of chemical reactions began with the appearance and development of quantum chemistry. The advanced theory of electron and proton transfer as "simple" models of chemical reactions opened the way for a profound understanding of the quantum-mechanical factors affecting elementary chemical processes and stimulated a cascade of experimental studies in chemistry and biology (R. Marcus, V.G. Levich and J. Jortner).

The study of chain reactions initiated interest in reactions involving active intermediates as free atoms and radicals. An array of new experimental methods for the study of these very fast reactions was invented in the middle of the 20<sup>th</sup> century. The most important was EPR, viz., a method of study of free radical reactions. A large number of experimental measurements of the rate constants of various reactions were performed during the last half of the century.

A new field of chemistry was opened, namely the chemistry of labile particles: atoms, free radicals, radical ions, carbenes, etc. The fast development of experimental techniques suitable for monitoring fast and ultrafast processes led to the study of mechanisms of energy exchange in collisions of particles and initiated the formation of nonstationary kinetics.

The objects of study in modern kinetics are a variety of different reactions of molecules, complexes, ions, free radicals, excited states of molecules, etc. A great variety of methods for the experimental study of fast reactions and the behavior of reacting particles close to the top of the potential barrier were invented. Appropriate quantum-chemical methods are progressing rapidly. Computers are widely used in experimental research and theoretical calculations. Databases accumulate a vast amount of kinetic information.

One of the greatest creations of nature, biological catalysis, appears as a challenging problem to chemists of the 21<sup>st</sup> century. The unique catalytic properties of enzymes are their precise specificity, selectivity, high rate, and capacity to be regulated. Classical and modern physical chemistry, chemical kinetics, organic, inorganic and

quantum-chemistry provide a variety of physical methods and establish a basis for investigation of structure and action mechanisms of enzymes. The general properties of enzymes, the "ideal" chemical catalysts, are the formation of intermediates, smooth thermodynamic relief along the reaction coordinate, fulfilment of all selection rules, the ability to proceed and to stop temporarily and spatially, and compatibility with the ambient media. These properties are attributable to multifunctional active centers, to the unique structure of protein globules, possessing both rigidity and flexibility, and the formation of catalytic ensembles.

Biochemistry gives chemistry a plethora of knowledge about nearly "ideal" catalysts, the enzymes as catalysts close to the enzymes and opens the way for chemical modeling of the enzyme reactions.

A major advantage of this work is that it is a comprehensive manual embracing practically all the classical and modern areas of chemical kinetics. Special sections deal with important subjects, which are not covered sufficiently in other manuals: 1) Methods of calculation and determination of rate constants of reactions in gas and liquid phases; 2) Modern areas such as laser chemistry (including pico- and femtochemistry), magnetochemistry, etc.; 3) Modern theories of electron transfer, including long-distance electron transfer; 4) Analysis of kinetics and mechanisms and voluminous illustrations of "classical" processes, such as chain reactions, gas phase and homogeneous reactions (including homogeneous catalysis), etc.; 5) Discussion of enzymatic reactions from the viewpoint of chemical kinetics with emphasis on the special gains biocatalysis offers chemistry; 6) Analysis of the situations where enzymes cope with "tough" chemical problems under mild conditions: hydrolysis peptides, substrate oxidation, nitrogen fixation, long-distance electron transfer conversion of light energy to chemical energy, etc.; and 7) Chemical modeling of enzymes: achievements and problems.

This monograph is intended for scientists working in various areas of chemistry and chemical and biotechnology, as well as for instructors, graduate and undergraduate students in departments of chemistry and biochemistry.

The authors appreciate to the fullest extent the enormous contribution to the foundation and development of modern chemical kinetics by a number of the most prominent scientists, the patriarchs, whose photos appear at the beginning of this book.

The authors are deeply indebted to Profs. R. Lumry, J. Jortner and S Efrima for the encouragement and interest in this book. They are grateful to Drs. Elena Batova, Vassili Soshnikov, Mr. Pavel Parkhomyuk-Ben Arye and Mrs. Nataly Medvedeva for their invaluable help in preparation of the manuscript.



Henry Eyring  
(1901-1981)



Linus Pauling  
(1901-1994)



Viktor N. Kondrat'ev  
(1902-1976)



Nikolay N. Semenov  
(1896-1986)



Rufus Lumry



Rudolf Marcus



Evgeny T. Denisov was entitled by the Ph.D. degree in 1957 and by the Doctor of Science degree in 1967. Since 1956 he has been working at the N.N. Semenov Institute of Chemical Physics and since 1967 up to 2000 as the Head of the Laboratory of Kinetics of Free Radical Liquid-Phase Reactions. Now he is a Principal Researcher of this Institute. He was elected as Active Member of Academy of Creative Endeavors in 1991 and International Academy of Sciences in 1994. From 1979 to 1989 he was a member of IUPAC Commission on physicochemical symbols, terminology, and units and in 1989-1991 the Chairman of Commission on Chemical Kinetics. Prof. Denisov was the Chairman of the Kinetic Section of the Scientific Council on Structure and Chemical Kinetics of the Academy of Sciences of Russia (1972-1997), and he is Chairman of Scientific Council on Qualification in Physical Chemistry and Chemical Kinetics of the

Institute of Problems of Chemical Physics (from 1974 up now). His scientific interests lie in the following fields of chemical kinetics: elementary reactions of free radicals in solutions and polymeric matrix and the kinetics of oxidation and inhibiting action of antioxidants. Prof. Denisov is author of 17 monographs and 390 papers on chemistry of oxidation and free radical kinetics.



Oleg M. Sarkisov received his Ph.D. degree in 1971 at the N.N. Semenov Institute of Chemical Physics, Russian Academy of Science. The title of the thesis was "Excited species in the mechanism of  $F_2 + H_2(D_2)$  reaction". In 1967 he started to work in the Institute of Chemical Physics as a scientific researcher and obtained in 1981 the degree of Doctor of Physical and Mathematical Sciences. Oleg M. Sarkisov currently is the Professor of Chemistry and vice director at N.N. Semenov Institute of Chemical Physics of the Russian Academy of Sciences and the Professor at the Faculty of Molecular and Biological Physics of Moscow Institute of Physics and Technology. He is the author of more than 200 publications. His scientific interests: kinetics and dynamics of elementary reactions, laser spectroscopy, and photochemistry.



Gertz I. Likhtenshtein received his Ph.D. degree in 1963 at the N.N. Semenov Institute of Chemical Physics, Russian Academy of Sciences. The topic of his thesis was "Oxidative Destruction and Inhibition of Polymers". Then his research interest moved to enzyme catalysis and he began his carrier at the Institute of Molecular Biology, Academy of Sciences. In 1965 Likhtenshtein returned to the Institute of Chemical Physics and was appointed on the position of the Head of Laboratory of Chemical Physics of Enzyme Catalysis. This Institute granted him the degree of Doctor of Science (1972) and the Professor title (1976). In 1977 he was awarded with the USSR State Prize for his pioneering research on spin labeling in molecular biology. In 1992 Likhtenshtein moved to the Department of Chemistry, Ben-Gurion University of the Negev, Beer-Sheva on the full professor position and was in charge of the Laboratory of Chemical Biophysics. At present his main scientific interests focuses on the long-distance electron transfer in proteins and model systems, multielectron and

synchronous processes in chemistry and biology, distribution of electrostatic potential around molecules of biological importance, and developments of novel fluorescence-photochrome biosensing of fluidity of biomembranes, express immunoassay, analysis of nitric oxide in solution, and antioxidant status of bioobjects. Likhtenshtein authored 6 books and about 350 scientific papers.

## Part 1

**General problems of chemical kinetics***Chapter 1***General ideas of chemical kinetics***1.1. Subject of chemical kinetics*

The chemical process of transformation of reactants into products is the subject of studying of chemical kinetics. One can say against it that the chemical reaction is also the subject of studying of several other chemical disciplines, such as synthetic and analytical chemistry, chemical thermodynamics and technology. Note that each of these disciplines studies the chemical reaction in its certain aspect. In synthetic chemistry, the reaction is considered as a method for preparation of various chemical compounds. Analytical chemistry uses reactions for the identification of chemical compounds. The chemical thermodynamics studies the chemical equilibrium as a source of work and heat, *etc.* The kinetics also has its specific approach to the chemical reaction. It studies the chemical transformation as a *process that occurs in time according to a certain mechanism* with regularities characteristic of this process. This definition needs to be decoded. What precisely does the kinetics study in the chemical process?

First, the reaction as a process that occurs in time, its rate, a change in the rate with the development of the process, the interrelation of the reaction rate and concentration of reactants - all this is characterized by kinetic parameters.

Second, the influence of the reaction conditions, such as the temperature, phase state of reactants, pressure, medium (solvent), presence of neutral ions, *etc.*, on the rate and other kinetic parameters of the reaction. The final result of these studies is the quantitative empirical correlations between the kinetic characteristics and reaction conditions.

Third, the kinetics studies the methods for controlling the chemical process using catalysts, initiators, promoters, and inhibitors.

Fourth, the kinetics tends to open the *mechanism of the chemical process*, to reveal from which elementary steps it consists, what intermediate compounds are formed in it, *via* what routes reactants are transformed into products, and what factors are responsible for the composition of products. In the result of the kinetic study, authors compose the scheme of the mechanism of the process, analyze it and compare with experimental data, state new testing experiments, and if necessary supplement the scheme and repeat checking. Various elementary reactions of formation and transformation of active species, radicals, ions, radical ions, molecular complexes, *etc.*, participate in many complex chemical processes.

Therefore, fifth, an important task of the kinetics became the study and description of elementary reactions involving chemically active species. *Elementary acts* of the chemical transformation are diverse, they can be theoretically described by the methods of quantum mechanics and mathematical statistics.

Sixth, the chemical kinetics studies a relation between the structure of particle-reactants and their *reactivity*. In most cases, the chemical transformation is preceded by physical processes of the activation of particle-reactants. These processes often accompany chemical processes and manifest themselves, under certain conditions, resulting in the perturbation of the equilibrium particle distribution of the energy. These processes are the subject of the *nonequilibrium kinetics*.

Seventh, the chemical transformation, under laboratory and technological conditions, is often accompanied by mass and heat transfer. *Macrokinetics* studies these complex processes using mathematical methods for analysis and description. Thus, the subject of the chemical kinetics is the comprehensive study of the chemical reaction: regularities of its occurrence in time, the dependence on the conditions, the mechanism, a relation between the kinetic characteristics with the structure of reactants, energy of the process, and physics of particle activation.

Since the kinetics studies the reaction as a process, it has the specific methodology: the body of theoretical concepts and experimental methods, which allow the study and analysis of the chemical reaction as an evolution process that develops in time. The experimental kinetics possesses various methods to perform the reaction and control it in time. The kinetic methods for studying fast reactions (stop-flow, pulse, *etc.*) have been developed during recent 40 years along with procedures and methods for the generation and study of active intermediate compounds: free atoms and radicals, labile ions and complexes. The methods for "perturbation" of the chemical reaction during its course were invented. Mathematical simulation and modern computer technique are widely used for the theoretical description of the reaction as a process.

What scientific disciplines are boundary for the chemical kinetics? First of all, synthetic chemistry, which possesses a large experimental material on chemical reactions, namely, knowing what reactants under which conditions are transformed into

these or other products. The structure of matter provides necessary data on the structure of particles, interatomic distances, dipole moments, and others. These data are required for the development of assumed mechanisms of transformations. The chemical thermodynamics makes it possible to calculate the thermodynamic characteristics of the chemical process. The kinetics borrows from mathematics the mathematical apparatus necessary for the description of the process, analysis of the mechanism, and development of correlations. The kinetics uses molecular physics data when the process is analyzed at different phase states of the system where the reaction occurs. Spectroscopy and chromatography provides the kinetics with methods of process monitoring. Laser spectroscopy serves as a basis for the development of unique methods for studying excited states of molecules and radicals.

In turn, results of the chemical kinetics compose the scientific foundation for the synthetic chemistry and chemical technology. The methods for affecting the reaction developed in the kinetics are used for controlling the chemical process and creation of kinetic methods for the selective preparation of chemical compounds. The methods for retardation (inhibition) of chemical processes are used to stabilize substances and materials. Kinetic simulation is used for the prognostication of terms of the operation of items. The kinetic parameters of reactions of substances contained in the atmosphere are used for prognosis of processes that occur in it, in particular, ozone formation and decomposition (problem of the ozone layer). The kinetics is an important part of photochemistry, electrochemistry, biochemistry, radiation chemistry, and heterogeneous catalysis.

### *1.2. History of the appearance of chemical kinetics*

Chemical kinetics is a rather young science among other chemical disciplines. The first book on the kinetics "Études de dynamique chimique" by J. Van't Hoff appeared in 1884. If counting off the chronology of kinetic studies from this date, the kinetics is about 100 years old. However, the first kinetic studies in which the rate of chemical reactions was studied appeared much earlier. In 1850 German physicist L. F. Wilhelmy published the work "The Law of Acid Action on Cane-Sugar" in which he established for the first time the empirical relation between the rate of the chemical reaction of cane-sugar hydrolysis to glucose and fructose and the amount of reactants involved in the transformation. This relationship was expressed as the equation  $-dZ/dT = MZS$ , where  $T$  is time,  $Z$  is the amount of the reactant (sugar) and  $M$  is that of the acid, and  $S$  is constant). The law of mass action, which was substantiated later, was expressed in this equation for the first time. Twelve years after French chemists M. Berthelot and L. Pean de Saint Gilles published the results of studying the esterification reaction between acetic acid and ethanol. They showed that the reaction does not go to the end and deduced the empirical equation for this reaction as for a reversible process. It had the form

$$dx/dt = k(1 - x)/l \quad (1.1)$$

where  $dx/dt$  is the esterification rate,  $k$  is constant,  $x$  is the amount of the reacted starting substance, and  $l$  is the limiting value of the amount of the transformed substances.

They studied in detail the influence of conditions (temperature, solvent) on the reaction occurrence. One of the main kinetic laws, the law of mass action, was formulated by Sweden scientists, mathematician C. M. Guldberg and chemist P. Waage in the series of works in 1864÷67. Based on the results of M. Berthelot and L. Pean de Saint Gilles and their own great work, they formulated the law of mass action for both the reaction occurring in one direction and the reversible reaction in the equilibrium state. The law was derived in the general form for the reaction with any number of reactants, and the derivation was based on the concept of molecular collisions as an event preceding the reaction of collided particles. For the reaction of the type



$$\text{Reaction rate } v = k [A]^a [B]^b [C]^g \quad (1.2)$$

where  $a$ ,  $b$ , and  $g$  are stoichiometric coefficients of reactants entered into the reaction.

The law was formulated in this form in 1879. The idea of the "rate of chemical transformation" was introduced somewhat earlier by V. Harcourt and W. Esson (1865÷67). They studied the oxidation of oxalic acid with potassium permanganate and pioneered in deriving formulas for the description of the kinetics of reactions of the first and second orders.

Our compatriot N. A. Menshutkin made a great contribution to the development of the kinetics. In 1877 he studied in detail the reaction of formation and hydrolysis of esters from various acids and alcohols and was the first to formulate the problem of the dependence of the reactivity of reactants on their chemical structure. Five years later when he studied the hydrolysis of *tert*-amyl acetate, he discovered and described the autocatalysis phenomenon (acetic acid formed in ester hydrolysis accelerates the hydrolysis). In 1887÷90, studying the formation of quaternary ammonium salts from amines and alkyl halides, he found a strong influence of the solvent on the rate of this reaction (Menschutkin reaction) and stated the problem of studying the medium effect on the reaction rate in a solution. In 1888 N. A. Menschutkin introduced the term "chemical kinetics" in his monograph "Outlines of Development of Chemical Views."

The book by J. Van't Hoff "Etudes de dynamique chimique" published in 1884 was an important scientific event in chemistry. In this book, the author generalized data on kinetic studies and considered the kinetic laws of monomolecular and bimolecular transformations, the influence of the medium on the occurrence of reactions in solutions, and phenomena named by him "perturbing factors." The large section of the outlines is devoted to the temperature influence. Van't Hoff had come right up against the law, which was several years later justified by S. Arrhenius. Using the

correlation for the chemical equilibrium and temperature

$$d\ln k/dT = q/2T^2 \quad (1.3)$$

(where  $K$  is constant, and  $q$  is the heat of equilibrium), he deduced for the rate constant the dependence in the form  $d\ln K/dT = A/T^2 + B$ . In 1889 Arrhenius theoretically substantiated and interpreted this dependence in the form  $k = A\exp(-E/RT)$  (where  $E$  is the activation energy of reacting molecules, and  $\exp(-E/RT)$  is the fraction of active collisions).

At the end of XIX - beginning of XX centuries researchers concentrated their attention on studying multistage reactions. In 1887 W. Ostwald and D.P. Kononov derived the formula that described the kinetics of autocatalytic reactions in the form of the equation

$$dx/dt = (k_1 + k_2x)(A - x) \quad (1.4)$$

where  $k_1$  and  $k_2$  are the rate constants of the spontaneous and catalytic reactions,  $A$  is the concentration of the starting substance, and  $x$  is the concentration of the reaction products.

Reversible, consecutive, and parallel reactions were described and examined by V.A. Kistiakovski in 1894. Three years later, A. N. Bach and G. Engler proposed the peroxide theory of oxidation and introduced the notion about a labile intermediate product, "moxide," in oxidation processes. N.A. Shilov studied the kinetics of various conjugated oxidation reactions and developed the theory of self-conjugated reactions.

As a whole, the grounds of the kinetics as a section of chemistry studying rates of chemical reactions under different conditions and at different natures of reactants were founded in the latter half of the 19th - beginning of the 20th century. In this period two main laws of chemical kinetics were formulated, formulas describing the kinetics of simple reactions were obtained, complex reactions were found, and such important ideas as a reaction rate constant, an activation energy, an intermediate product, and conjugated reactions were introduced. In the first part of the 20th century the kinetics developed *via* several directions. First, simple gas phase reactions were studied and their theory was worked out (encounter theory, theory of absolute reaction rates). Second, various chain reactions (at first in the gas phase and then in solutions) were discovered and studied. Third, various organic reactions in solutions were intensely studied. Fourth, correlations became very popular for the comparison of kinetic data. Fifth, quantum-chemical calculations are widely used for theoretical simulation of chemical reactions.

### 1.3. Rate of chemical reaction

One should distinguish the rate of changing the concentration of the substance,

which enters into or is formed during the chemical transformation, the rate of transformation (conversion), and the rate of chemical reaction. When reactant A enters into the chemical reaction, the rate of its transformation  $v_A = -d[A]/dt$ . For the final reaction product Z, the rate of its formation is  $v_Z = d[Z]/dt$ . Evidently, the change in the concentration is expressed in units [concentration] : [time] and, depending on the concentration units, can be presented in the form  $1 \text{ mol/(s)} = 10^3 \text{ mol/(m}^3 \text{ s)} = 10^{-3} \text{ mol/(cm}^3 \text{ s)} = 6.022 \cdot 10^{23} \text{ cm}^{-3} \text{ s}^{-1} = 12.19 T^{-1} \text{ kilogram-force/(cm}^3 \text{ s)} = 1.6 \cdot 10^{-2} T^{-1} \text{ Hg mm/s} = 1.22 \cdot 10^{-4} T^{-1} \text{ Pa/s}$ . Degree of transformation (conversion) of the reactant x is equal to the ratio of the amount of the transformed substance to its initial amount. The conversion rate is

$$x = v_A^{-1} (dn_A/dt), \quad (1.5)$$

where  $n_A$  is the stoichiometric coefficient of reactant A, and  $n_A$  is the amount (number of moles) of the reactant.

Stoichiometric coefficients should be taken into account for the estimation of reaction rates.

*Reaction rate* is the rate of conversion in the volume unit V

$$v = V^{-1} (dx/dt) = x/V \quad (1.6)$$

The reaction rate is related to the rate of transformation of substances involved in the chemical reaction through stoichiometric coefficients. The reaction rate



equals

$$v = -\frac{1}{v_A} \frac{d[A]}{dt} = -\frac{1}{v_B} \frac{d[B]}{dt} = \frac{1}{v_Y} \frac{d[Y]}{dt} = \frac{1}{v_Z} \frac{d[Z]}{dt} \quad (1.7)$$

The rate of the simple homogeneous reaction is equal to the number of elementary chemical acts that occur in the volume unit per time unit. The reaction rate coincides with the rate of reactant consumption if its stoichiometric coefficient is equal to unity. In the complex multistage reaction, the rate of the overall process can differ substantially from the rates of individual stages. The rate of the overall process cannot be judged, as a rule, by a change in the concentration of intermediates.

When reactants are uniformly distributed over the whole volume, the reaction occurs with the same rate in each microvolume of the reactor. For the nonuniform distribution of reactants over the volume, the reaction rate is the integral value

$$\bar{v} = v_i^{-1} V^{-1} \int_0^V \frac{dc_i(x, y, z)}{dt} dV \quad (1.8)$$

where  $c_i(x, y, z)$  is the concentration of the  $i$ -th reactant in the microvolume with the coordinates  $x, y, z$ .

If the volume of the system changes during the reaction (the reaction is carried out at a constant pressure), the concentration of reactants and products changes due to both the chemical transformation and change in the volume.

This should be taken into account in the calculation in the reaction rate. In this case, we have

$$v = -\frac{d[A]}{v_A dt} - \frac{[A]_0}{V_0} \frac{dV}{dt} \quad (1.9)$$

When the reaction is performed in an open system, the concentration of the substance changes due to both the chemical reaction and the income of reactants into the reactor and removal of products. In a well-stirred reactor in the steady-state regime of the work, the reaction rate is the following:

$$v = (\mu/Vn_A)([A]_0 - [A]) \quad (1.10)$$

where  $\mu$  is the volume feed rate of the reactant to the reactor with the volume  $V$ , and  $[A]_0$  and  $[A]$  are the concentrations of the reactant at the inlet and outlet of the reactor, respectively.

In the heterophase system where the reaction occurs at the interface, the rate of chemical transformation is referred not to the volume unit but to the surface unit where the transformation occurs. In these systems the reaction rate can be determined as the number of chemical transformations occurred on the surface unit per time unit and can be expressed in  $\text{mol}/(\text{m}^2 \text{ s})$ . The average volume rate of transformation  $\bar{v}$  is related to the process rate  $v_S$  that occurs on the surface by the correlation

$$v_S (\text{mol m}^{-2} \text{ s}^{-1}) = \bar{v} (V/S) (\text{mol l}^{-1} \text{ s}^{-1}). \quad (1.11)$$

Usually the information on the kinetics of the process is obtained in the form of a kinetic curve from which the reaction rate is calculated. The average reaction rate within the time interval  $Dt$  is obtained as the ratio  $\bar{v} = D[A]/n_A Dt$ , where  $D[A]$  is the change in the concentration of reactant A for this time period. The reaction rate at the moment  $t$  is obtained graphically as the slope of the tangent drawn to the kinetic curve in the point corresponding to time  $t$ . Since various errors in the determination of the reactant or product concentration result in the scatter of points, the following procedure can be applied to obtain the most exact results. The kinetic curve is expressed in the analytical form as  $c(t)$ , optimizing the numerical parameters that characterize it. The rate of the chemical reaction is obtained by differentiating

$$v = -v_i^{-1} dc/dt \quad (1.12)$$

For example, if  $c = c_0 - at + bt^2$ , then

$$v = -v_i^{-1} (a - bt) \quad (1.13)$$

and the initial rate  $v_0 = av_i^{-1}$ . There are methods for the direct measurement of the chemical process rate when the measured value is proportional to  $v$  or  $f(v)$  as, e.g.,

the intensity of chemiluminescence appeared upon the reaction or the intensity of heat release measured on a differential calorimeter.

#### 1.4. Law of mass action

In the initial form the law of mass action was substantiated for simple reactions; afterwards it was also applied empirically for multistage reactions. The law is based on the simple concept. Several, e.g., two particles of the reactant must collide to enter into the reaction, and the probability of the collision is proportional to the product of their concentrations. Therefore, the reaction rate must be proportional to the product of concentration of reacting substances. In the general case, the rate of the reaction



depends on the concentrations of the reactants as follows:

$$v = k[A]^{n_A} [B]^{n_B} = k \prod_i c_i^{n_i} \quad (1.14)$$

where  $n_i$  is the number of particles of the reactant  $i$  participating in the reaction.

The exponent  $n_A$  is named the *reaction order with respect to reactant A*, and  $n_B$  is the reaction order with respect to reactant B. For simple reactions  $n_A$  and  $n_B$  are integers (1 or 2). In complex reactions the reaction order can be fractional and even negative. The order with respect to each reactant is a particular order. The overall reaction order  $n$  is equal to the sum of exponents with respect to all reactants:  $n = \sum n_i$ . Usually  $n = 1$  or  $2$ , rarely  $3$ . The idea of "order" for the complex reaction has somewhat different sense. The particular order with respect to a certain reactant characterizes the influence of the concentration of this reactant on the overall reaction rate. This influence can change depending on the concentration of this or other reactants.

#### 1.5. Order and rate constant of the reaction

The order of the reaction with respect to each reactant and its *rate constant* are important kinetic characteristics of the chemical reaction. When several reactants are involved in the reaction, two following methods are used.

1. One of the reactants, e.g., A, is taken in deficient in order to neglect the consumption of other reactants during the time of experiment. In this case, a change in the reaction rate both in time and from experiment to experiment is determined only by the concentration of this reactant:  $v = \text{const}[A]^{n_A}$ . Then the reaction order can be found by one of the methods described below in this Section.

2. All reactants are taken in the stoichiometric ratio  $[A]_o : [B]_o = n_A : n_B$ . In this case, the reactant concentrations are consumed in a constant ratio, and the reaction rate is determined by the concentration of any product and the overall reaction order  $n = n_A + n_B$ . In fact, according to the law of mass action, at the ratio  $[A]_o : [B]_o = n_A : n_B$  the rate is

$$v = k v_B^{n_B} v_A^{-(n_B+1)} [A]^n \quad (1.15)$$

Below we describe the methods for determination of the order and rate constants of the reaction, which obeys the law of mass action.

*Dependence of the initial reaction rate on the reactant concentration*

The initial reaction rate is determined by this or another method from the initial region of the kinetic curve. A series of experiments with different initial concentrations of reactants is carried out.

A. The reaction order is determined from the dependence

$$\log n_A = \text{const} + n \log [A]_o \quad (1.16)$$

When other reactants (B) are taken in excess, then  $n = n_A$  and

$$\text{const} = \log k + \log \left( v_A^{-1} [B]_o^{n_B} \right) \quad (1.17)$$

When the reactants are taken in a stoichiometric ratio, then  $n = n_A + n_B$  and

$$\text{const} = \log k + \log \left( v_B^{n_B} v_A^{-(n_B+1)} \right) \quad (1.18)$$

Thus, knowing const, we can determine the reaction rate constant. A combination of these two methods (a series of experiments with an excess of reactant B and a series of experiments with a stoichiometric ratio of the reactants) allows the determination of  $k$ ,  $n_A$ , and  $n$ . For the reliable determination of the reaction order, the concentration of the reactant should be varied in a sufficiently wide interval because the error in determination of  $n$  is inversely proportional to  $\log([A]_{01} - [A]_{02})$ . For example, at  $D \log [A]_o = 0.6$  when  $[A]_o$  fourfold changes, the error in estimation of  $n$  using the results of two experiments is equal to 3.5% at an error in measurement of the rate of 5%. In the case of complex reactions, the reaction order can change with a change in the reactant concentration.

*Dependence of the reaction rate changing in time on the current concentration of the reactant (Van't Hoff method)*

Since the reactant is consumed during the reaction and this influences on the

process rate, the order and rate constant can be estimated in the same experiment comparing the current reaction rate  $v_t$  with the current concentration of the reactants  $c_i(t)$  or one reactant  $[A]_t$ . The reaction order is determined as in the previous case from the dependence

$$\log v_t = \text{const} + n \log [A]_t \quad (1.19)$$

The value of const is used to determine the reaction rate constant from formulas (1.17) or (1.18), depending on the ratio of concentrations of the reactants. The reaction order determined through  $v_t$  coincides with  $n$  determined through  $v_0$  if the reaction is simple and a change in the medium due to the accumulation of products does not affect the rate constant of the reaction.

*Time of conversion by 1/p part*  
(Noyes—Ostwald method)

The time of conversion of the reactant by the  $1/p$  part is unambiguously related to the order and rate constant of the reaction. At  $n = 0$  the time  $t_{1/2} = [A]_0 / 2k_0$ . Thus, the conversion period is always proportional to  $[A]_0$ . At  $n = 1$

$$t_{1/2} = k_1^{-1} \ln 2 \text{ and } t_{1/p} = \ln[p/(p-1)] \quad (1.20)$$

that is, it is independent of the reactant concentration. At  $n = 2$

$$t_{1/2} = k_2^{-1} [A]_0^{-1} \text{ and } t_{1/p} = [1/(p-1)]([A]_0 k_2)^{-1} \quad (1.21)$$

that is,  $t_{1/2}$  is inversely proportional to the reaction rate constant. The interrelation between  $t_{1/p}$  and  $[A]_0$  depends on the reaction order: at  $n > 1$  the higher  $[A]_0$ , the longer  $t_{1/p}$ ; at  $n < 1$  the lower  $[A]_0$ , the shorter  $t_{1/p}$ ; and at  $n = 1$  it is independent of  $[A]_0$ . The reaction order with respect to reactant A or the overall order of the reaction is found from a series of experiments with different  $[A]_0$  using the Noyes-Ostwald formulae

$$\log \frac{t'_{1/p}}{t_{1/p}} = (n-1) \log([A]'_0/[A]_0) \quad (1.22)$$

where  $t_{1/p}$  and  $t'_{1/p}$  are referred to experiments with  $[A]_0$  and  $[A]'_0$ .

One experiment can also be used when measuring, e.g.,  $t_{1/4}$  and  $t_{1/2}$ . The ratio  $t_{1/2}/t_{1/4} = 2.4$  ( $n = 1$ ), 3 ( $n = 2$ ), 3.86 ( $n = 3$ ), and at  $n \neq 1$

$$t_{1/2}/t_{1/4} = (2^{n-1} - 1)[(4/3)^{n-1} - 1]^{-1} \quad (1.23)$$

In the general case, at  $n \neq 1$  the ratio

$$\frac{t_{1/p}}{t_{1/q}} = \frac{[p(p-1)]^{n-1} - 1}{[q(q-1)]^{n-1} - 1} \quad (1.24)$$

at  $n = 1$

$$\frac{t_{1/p}}{t_{1/q}} = \frac{\lg[p(p-1)]}{\lg[q(q-1)]}. \quad (1.25)$$

All these formulas give adequate values of  $n$  and  $k$  if both the order and rate constant of the reaction remain unchanged during the experiment.

*Kinetics of consumption of the starting substance*  
(Powell method)

In the general case, the kinetics of reactant consumption is described by the differential equation of the type  $-d[A]/dt = k'[A]^n$ , where  $k'$  depends on the rate constant  $k$ , stoichiometric coefficient  $n_A$ , and other parameters (see above). At  $n = 1$  the ratio of concentrations is  $x = [A]/[A]_0 = \exp(-t)$ , where  $t = k't$ . In the general case, at  $n \neq 1$

$$x = [1 + (n - 1)t]^{-1/(n - 1)}, \quad (1.26)$$

where

$$t = k' [A]_0^{n-1} t$$

Since

$$\log(k' [A]_0^{n-1}) + \log t = \log t$$

superposing the plot of the experimentally found  $x$  and  $t$  values with the theoretically calculated plot of  $x$  and  $t$  in the coordinates  $x - \log t$ , we can determine  $n$  from the shape of the curve, and  $k'$  can be determined by the superposition of  $\log t$  with  $\log t$ .

Another method is also widely used: experimental data are used to plot the dependence  $f(x) - t$  corresponding to this or another reaction order, e.g.,  $\log(x) - t$  for  $n = 1$  or  $x^{-1} - t$  for  $n = 2$ . The rectification of data by one of these plots is considered as an evidence for the corresponding reaction order. Table 1.1. contains the formulas for kinetic curves of reactant A, which enters into the reaction of the type  $n_A A \rightarrow \text{Products}$  and  $n_A A + n_B B \rightarrow \text{Products}$ . Note that, for the reliable determination of the reaction order from the shape of the kinetic curve, it is necessary that the reaction had occurred to a sufficient depth. For example, the reaction of order I can be distinguished from the reaction of order II if the reaction conversion  $1 - x$  considerably exceeds  $(2dx)^{1/2}$ , where  $dx$  is the error in measurement of the reactant concentration: at  $x = 2\%$  it is needed that  $x < 0.8$ , i.e., the conversion would exceed 20%.

Table 1.1. Integral form of kinetic equations  $x = c_A/c_{A0}$ ,  $k = (c_{B0}n_A/c_{A0}n_B) - 1$ ,  
 $r = n_B/n_A$

$-\frac{dc_A}{k dt}$	k	Equation
		$1 - x = kc_{A0}^{-1}t$
$kc_A^{1/2}$		$1 - x^{1/2} = 0.5kc_{A0}^{-1/2}t$
$kc_A$		$-\ln x = kt$
$kc_A^{3/2}$		$x^{1/2} - 1 = 0.5kc_{A0}^{1/2}t$
$kc_A^2$		$x^{-1} - 1 = kc_{A0}t$
$kc_B^{1/2}$		$(1+k)^{1/2} - (x+k)^{1/2} = 0.5kc_{A0}^{1/2}r^{1/2}t$
$kc_A^{1/2}c_B^{1/2}$		$\ln \left[ \frac{(1+\kappa)^{1/2} + 1}{(x+\kappa)^{1/2} + x^{1/2}} \right] = 0.5kr^{1/2}t$
$kc_Ac_B^{1/2}$	$>0$	$\ln \left[ \frac{(x+\kappa)^{1/2} + \kappa^{1/2}}{x^{1/2} \left\{ (1+\kappa)^{1/2} + \kappa^{1/2} \right\}} \right] = 0.5k(\kappa r)^{1/2}t$
	0	$x^{-1/2} - 1 = 0.5kc_{A0}^{1/2}r^{1/2}t$
	$<0$	$\text{th}^{-1} \left( \frac{1+\kappa}{-\kappa} \right)^{1/2} - \text{th}^{-1} \left( \frac{x+\kappa}{-\kappa} \right)^{1/2} = -0.5k(-\kappa)^{1/2}c_{A0}^{1/2}t$
$kc_A^{3/2}c_B^{1/2}$	$>0$	$\left( \frac{x+\kappa}{\kappa} \right)^{1/2} - (1+\kappa)^{1/2} = 0.5k\kappa c_A r^{1/2}t$
	0	$1/x - 1 = kc_A r^{1/2}t$
$kc_B$		$\ln \left( \frac{1+\kappa}{x+\kappa} \right) = krt$
$kc_A^{1/2}c_B$	$>0$	$\text{th}^{-1} \left( \frac{1}{\kappa} \right)^{1/2} - \text{th}^{-1} \left( \frac{x}{\kappa} \right)^{1/2} = 0.5k\kappa^{1/2}c_{A0}^{1/2}rt$
	0	$x^{1/2} - 1 = 0.5kc_{A0}^{1/2}rt$
	$<0$	$\ln \left[ \frac{(1+\kappa)^{1/2} (x^{1/2} +  \kappa ^{1/2})}{(x+\kappa)^{1/2} (1+ \kappa ^{1/2})} \right] = 0.5k \kappa ^{1/2}c_{A0}^{1/2}rt$
$kc_Ac_B$	$>0$	$\ln \left[ \frac{x+\kappa}{x(1+\kappa)} \right] = k\kappa c_{A0} rt$
	0	$x^{-1} - 1 = kc_{A0}t$

*Dependence of the conversion on time  
(Wilkinson method)*

This method for estimation of  $n$  is a modification of the method described above. The following formula can be used ( $Dx = 1 - x$ ):

$$(1 - Dx)^{1-n} = 1 + (n + 1)t \quad (1.27)$$

where  $t = k[A]_0 t$ .

After the Maclaurin expansion of the power function and transformation, we obtain the following simple formula if restricting our consideration by the terms with  $x$  in I and II powers:

$$\frac{t}{\Delta x} = \frac{1}{k'[A]_0^{n-1}} + \frac{n}{2}t \quad (1.28)$$

The reaction order  $n$  is determined and  $k'$  is estimated from the dependence of  $t/Dx$  on  $t$ . The method of points at any  $Dx$  for  $n = 2$  gives reliable values in the interval  $0 < n < 3$  at  $Dx \leq 0.4$ .

The reaction if being estimated from the dependence of  $n_0$  on  $[A]_0$  can differ from the order determined from the kinetic curve. These orders coincide only for simple reactions under the condition that the formed reaction products have no effect on the mechanism of the reaction and its rate constant. The divergence between the estimations of  $n$  and  $k$  at different methods of performing the experiment and processing experimental data can be used as a method for studying changes that occur in the system during the chemical process.

### *1.6. Arrhenius law*

The law of mass action determines the interrelation between the reaction rate and concentrations of the reactants. The rate constant is a characteristics of the chemical process, it is independent of the reactant concentration but depends, naturally, on the conditions, first of all, temperature. In most cases, before entering into the reaction the reactants are activated, i.e., gain an energy. This is related to the fact that each particle (molecule, radical, ion) is a rather stable structure. Its rearrangement requires a weakening of certain bonds, which needs an energy consumption. This energy, necessary for the chemical transformation of the reactants, is named the *activation energy*. The fraction of particles, more correctly, the fraction of collisions of particle-reactants, whose energy exceeds  $E$ , is equal to  $\exp(-E/RT)$  according to the Boltzmann law. Therefore, the rate constant can be presented in the form

$$k = A \exp(-E/RT), \text{ or } \ln k = \ln A - E/RT \quad (1.29)$$

where  $E$  is the activation energy, and  $A$  is the pre-exponential factor.

The pre-exponential factor characterizes the rate constant with which activated particles react:  $A = k \exp(E/RT)$ ,  $k = A$  at  $E = 0$  and  $k \propto A$  at  $T \propto \infty$ .

The Arrhenius law can theoretically be derived from the equilibrium thermodynamics under the following assumptions (the reaction of a first order is considered for simplicity). 1. In order to enter into the reaction, a molecule must be activated, i.e., must obtain an additional energy not lower than  $E/L$ . 2. Activation of molecules is a reversible process characterized by the equilibrium constant  $K_{\text{act}} = [A]_{\text{act}}/[A]$ . 3. The concentration of active particles is very low, therefore,  $[A]_{\text{act}} = K_{\text{act}}[A]$ . 4. The activated molecules enters into the reaction with the temperature-independent rate, i.e.,  $k = \text{const}[A]_{\text{act}}/[A] = \text{const } K_{\text{act}}$ . According to the thermodynamics,

$$d \ln K_{\text{act}} / dT = E/RT^2 \quad (1.30)$$

from where

$$d \ln k / dT = d \ln K_{\text{act}} / dT = E/RT^2 \quad (1.31)$$

and

$$\ln k = \text{const} - E/RT \text{ or } k = A \exp(-E/RT) \quad (1.32)$$

if we designate  $\text{const} = \ln A$ . It is essential that the activation of particle-reactants occurs only due to the thermal energy and is reversible, and the chemical reaction does not violate the equilibrium energy distribution over degrees of freedom of reacting particles.

The following methods are used for the experimental determination of the activation energy.

1. The initial reaction rate is measured at different temperatures at a constant concentration of reactants. For example, for the bimolecular reaction under the control of reactant A

$$n_0 = v_A^{-1} k [A]_0 [B]_0 = v_A^{-1} A [A]_0 [B]_0 \exp(-E/RT) \quad (1.33)$$

and the activation energy is determined from the dependence

$$\ln n_0 = \ln A + \ln(v_A^{-1} [A]_0 [B]_0) - E/RT \quad (1.34)$$

2. Experiments are carried out at different temperatures; the reaction rate constant is determined for a particular temperature, and the activation energy is found from the dependence of  $\ln k$  on  $T^{-1}$

$$E = -R [D \ln k / D(T^{-1})] \quad (1.35)$$

3. When the kinetics is characterized by the period of conversion of the reactant by the  $1/p$  part, then since always  $t_{1/p} \sim K^{-1}$ , the activation energy is found from the temperature run of  $\ln t_{1/p}$

$$E = RD(\ln t_{1/p})/D(T^{-1}) \quad (1.36)$$

4. Activation energy  $E$  can be determined from a series of kinetic curves of reactant consumption or product formation obtained experimentally at different temperatures. With this purpose, all curves are transformed into one curve, calculating the transformation coefficient  $c: c_{1,2} = t_1/t_2$ , where  $t_1$  and  $t_2$  are the times of achievement of the same conversion in experiments at temperatures  $T_1$  and  $T_2$ , respectively. The activation energy is determined by the correlation

$$E = R[D \ln c / D(T^{-1})] \quad (1.37)$$

The activation energy can be estimated from the results of two experiments at different temperatures. A series of experiments is usually carried out. The lower the error in measurement of the rate constant, the wider the temperature interval, and the greater the number of experiments, the lower the error in determination of the activation energy. For example, if  $k$  is measured with an error of 5%, the results of two experiments give the error in measurement of  $E$   $dE = 5.4$  kJ/mol at  $T_2 - T_1 = 10$  K and  $1.8$  kJ/mol at  $T_2 - T_1 = 30$  K.

The temperature dependence of the reaction rate is expressed sometimes through the temperature coefficient  $a(T)$ , which characterizes the relative acceleration of the reaction with the temperature increase by 10 K:  $a(T) = n(T+10)/n(T)$  is related to the activation energy by the correlation

$$E = 0.1T(T+10)R \ln a(T) \quad (1.38)$$

It is rather conventional to identify experimentally determined  $E_{\text{exp}}$  with the activation energy.  $E_{\text{exp}}$  is approximately equal to the activation energy only for simple gas reactions. Nevertheless, even in this case, one should take into account that  $A$  depends on  $T$ . For example, for bimolecular gas-phase reactions in the framework of the encounter theory,  $A \sim T^{1/2}$  (see below). Reactions in the liquid phase represent a more complex case. The rate constant depends on the medium, its properties that change with temperature. For example, reactions of ions and polar molecules depend on the dielectric constant  $\epsilon$ , and the latter changes with temperature. The degree of solvation of reactants also changes with temperature. The temperature affects the concentration of reactants: with  $T$  increasing the volume of the solution extends and the concentration of the reactants decreases. All this should be taken into account for the correct interpretation of data. There are reactions for which  $E < 0$ . Among complex reactions, it is observed sometimes that the reaction is retarded with an increase in the temperature (reactions with the negative temperature coefficient).

## Part 2

### Elementary Gas Phase Reactions

From the very beginning, the gas phase chemical kinetics developed via two main routes: study of general regularities of the occurrence of complex chemical reactions and investigation of elementary reactions.

The study of complex chemical reactions showed that most of them was a totality of elementary steps that involve very reactive intermediate species - radicals. The general kinetic regularities of radical, chain, and chain branched reactions were established. These general regularities were shown for reactions of oxidation, halogenation, and cracking. The theory of critical phenomena when an insignificant change of some parameter transforms the slow reaction into explosion was given in the framework of this direction. N.N. Semenov and C.N. Hinshelwood made a fundamental contribution to the development of these concepts.

Analysis of the totality of the established regularities showed that the study of complex chemical reactions cannot be restricted by kinetic measurements of concentrations of stable species but must include the detection of the kinetics of atoms and radicals that lead the chain. This induced the development of the second direction of the gas phase chemical kinetics -- investigation of elementary reactions. A considerable contribution to the development of this direction was made by V.N. Kondrat'ev R.G.W. Norrish, and J.C. Polanyi.

Elementary reactions of atoms and radicals were studied first. Then different forms of energy (translational, rotational, and vibrational) were established to be nonequivalent with respect to surmounting the activation barrier. Therefore, simple taking into account reactions of atoms and radicals is insufficient for the kinetic analysis of energetically nonequilibrium processes. Knowing of microscopic steps in which reactants and products in certain quantum states participate is necessary. In this sense, we can say that the gas phase chemical kinetics reached the quantum level where the elementary reactions should already be considered as a complex reaction consisting of various microscopic steps.

A new area of research, femtochemistry, in the framework of which reactions are studied in the femtosecond time scale, has recently appeared along with the term coherent elementary reactions in which phase characteristics of the motion of atoms in the molecular reacting system are taken into account.

The modern approach to revealing the mechanisms of complex chemical reactions is based on the achievements of computer technique. Computer methods make it possible to calculate different variants of chemical mechanisms and reveal key elementary reactions, which are needed to be experimentally studied. Therefore, the experimental chemical kinetics in the gas phase concentrated its attention on studying elementary reactions. Fundamental problems of the chemical kinetics associated with the development of concepts about the physics of the elementary chemical act also lie in this area. Below we present the modern experimental methods and theoretical approaches for studying elementary reactions.

## *Chapter 2*

### **Theory of elementary reactions**

#### *2.1. General statements and definitions*

##### *2.1.1. Types of pairwise collisions*

Molecules in gases for a long time exist at long distances from each other where the interaction is virtually absent. Only when they are brought together at sufficiently short distances, the molecular interaction becomes so substantial that can lead to this or other detected result: charge transfer, excitation energy transfer, chemical reaction, etc. The minimum result of the interaction is the distortion of the trajectory of a moving particle, that is, a change in the motion direction. If some, at least minimum indicated result of the interaction of two particles A and B is observed during their motion, we say that the collision (scattering) occurred. The probability for three molecules to be simultaneously at a short distance from each other is low. Therefore, two colliding particles can be considered as an isolated systems and only pairs of collisions can be taken into account.

Both heavy (atoms, ions, molecules) and light (electrons, photons) particles can be involved in collisions. Polyatomic molecules have internal degrees of freedom (vibrational and rotational motion of atoms) and, in this sense, they have an internal structure.

The modern approach to revealing the mechanisms of complex chemical reactions is based on the achievements of computer technique. Computer methods make it possible to calculate different variants of chemical mechanisms and reveal key elementary reactions, which are needed to be experimentally studied. Therefore, the experimental chemical kinetics in the gas phase concentrated its attention on studying elementary reactions. Fundamental problems of the chemical kinetics associated with the development of concepts about the physics of the elementary chemical act also lie in this area. Below we present the modern experimental methods and theoretical approaches for studying elementary reactions.

## *Chapter 2*

### **Theory of elementary reactions**

#### *2.1. General statements and definitions*

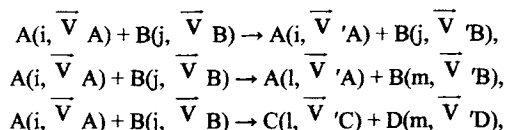
##### *2.1.1. Types of pairwise collisions*

Molecules in gases for a long time exist at long distances from each other where the interaction is virtually absent. Only when they are brought together at sufficiently short distances, the molecular interaction becomes so substantial that can lead to this or other detected result: charge transfer, excitation energy transfer, chemical reaction, etc. The minimum result of the interaction is the distortion of the trajectory of a moving particle, that is, a change in the motion direction. If some, at least minimum indicated result of the interaction of two particles A and B is observed during their motion, we say that the collision (scattering) occurred. The probability for three molecules to be simultaneously at a short distance from each other is low. Therefore, two colliding particles can be considered as an isolated systems and only pairs of collisions can be taken into account.

Both heavy (atoms, ions, molecules) and light (electrons, photons) particles can be involved in collisions. Polyatomic molecules have internal degrees of freedom (vibrational and rotational motion of atoms) and, in this sense, they have an internal structure.

### Collisions of heavy particles

Let particle A exists in the quantum state  $i$  and has the velocity  $\vec{V}_A$  and particle B is in the quantum state  $j$  and has the velocity  $\vec{V}_B$ . The processes of three types can occur at collisions of particles A and B



where  $l, m$  are the quantum states of the particles after the collision; velocities of scattered particles are marked by stroke.

Process 1 corresponds to elastic collisions in which the quantum states of particles A ( $i$ ) and B ( $j$ ) remain unchanged and only the vectors of the velocities of their motion change. Process 2 corresponds to inelastic collisions when the quantum states of particles A and B change along with the velocities. These processes include various forms of exchange of the energy of vibrational, rotational, and electronic motions. Process 3 corresponds to collisions accompanied by the redistribution of atoms to form new particles C and D. In this book, we consider mainly collisions of the last type, which are named chemical collisions or chemical reactions.

#### *2.1.2. Collision cross section*

Such physical magnitudes as the collision cross section and rate constant of the collision are quantitative characteristics of the collision process. Describing processes in experiments on scattering (molecular beams), researchers usually use the notion of "collision cross section," whereas for collision processes in the bulk the notion "rate constant of the process" is used. First, let us introduce the notion "collision cross section".

The scheme of the experiment with molecular beams is presented in Fig. 2.1. Particles A and B with the velocities  $\vec{V}_A$  and  $\vec{V}_B$  can collide in the interaction zone (hatched region in figure). The interaction products fly apart at different angles and are detected by a detector, which can be replaced around the interaction zone.

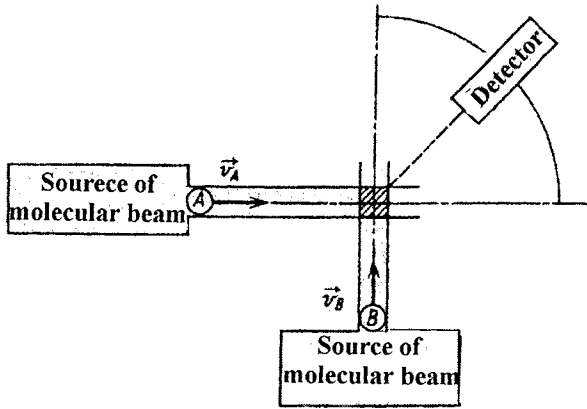


Fig. 2.1. Principal scheme of crossed molecular beams.

Let us consider the collision of particles A and B in the reference system where particles B are at rest (a new laboratory reference system). In this system, particles A have the velocity  $\vec{V} = \vec{V}_A - \vec{V}_B$ , which we call the relative or collision velocity. Accept the direction of vector  $\vec{V}$  as the direction of the x axis. Let us place the zero reference point  $x = 0$  at the boundary of the interception region of the molecular beam with particles B (Fig. 2.2).

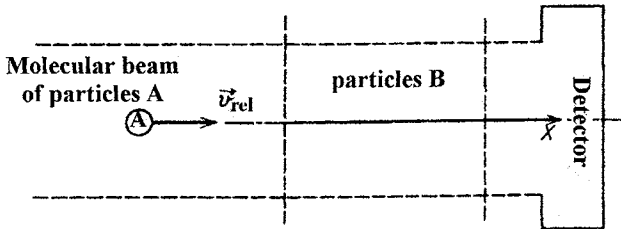


Fig. 2.2. Scheme of experiment to introduce the idea of collision cross section.

Thus, we have the incident beam of particles A moving in the direction of the x axis. Let an imagined detector, which detects particles A that have not collided with particles B, is placed in the x axis. Designate the flux density of particles A as  $I$ . This value is equal to the number of molecules A passed per unit time through the unit surface perpendicular to the x axis, namely,  $I = v[A]$ , where  $[A]$

is the concentration of molecules A in the beam. The concentration  $[A]$  depends on  $x$  because during passing of the beam some fraction of particles A, due to collisions with B, changes the direction of its motion and leaves the beam. As B pass through the target, i.e., with an increase in  $x$ , the flux density  $I$  in the beam decreases. It is clear from physical concepts that the attenuation of the flux density  $dI$  in the way  $dx$  is proportional to the concentration of scattering centers  $[B]$ , flux density  $I$ , and the  $dx$  value

$$dI = -\sigma_0 I(x)[B]dx \quad (2.1.)$$

The sign minus reflects the fact that the flux density of the particles decreases with increasing  $x$ . The proportionality coefficient  $\sigma_0$ , which depends on the collision velocity  $v$ , is named the total collision cross section. Integrating (2.1.), we obtain

$$I = I(0)\exp(-\sigma_0[B]x) \quad (2.2.)$$

where  $I(0)$  is the flux density at the point  $x = 0$ .

Formula (2.2) allows one to determine the dimensionality of  $\sigma_0$ . In fact, since the product  $\sigma_0[B]x$  has to be dimensionless, the quantity  $\sigma_0$  has the dimensionality of the surface area.

In order to reveal the physical sense of  $\sigma_0$ , we consider the structureless spherically symmetrical particles A and B. In this case, only elastic process 1 can occur upon the collision. The theoretical consideration of collision processes is usually performed in the system of coordinates related to the center of mass. In this system of coordinates, the problem of elastic scattering of particles A and B is reduced to the consideration of the motion of a fictitious particle with the mass

$$\mu = m_A m_B / (m_B + m_C) \quad (2.3)$$

and velocity  $\vec{V} = \vec{V}_A - \vec{V}_B$  in the stationary spherically symmetrical force field with the center at the center of mass of the system (Fig. 2.3). The mass  $\mu$  is named the reduced mass of colliding particles

Monitoring the number of particles scattered in some direction at the angle  $\theta$  to the primary direction, we can similarly introduce the notion of the differential cross section  $d\sigma_0$  as the characteristics of the fraction of particle A scattered in the solid angle  $d\Omega = 2\pi \sin\theta d\theta$ . The  $\theta$  angle at which scattering occurs depends on

the distance at which particle A would fly from particle B if they did not interact. This distance is named the impact parameter  $b$ . The scattering angle and impact parameter  $b$  are related to each other: particles that fly with the impact parameters in the range from  $b$  to  $b + db$  are scattered at the  $\theta$  angles in the specified interval  $d\theta$ . It follows from this that

$$d\sigma_0 = 2\pi b db \quad (2.4)$$

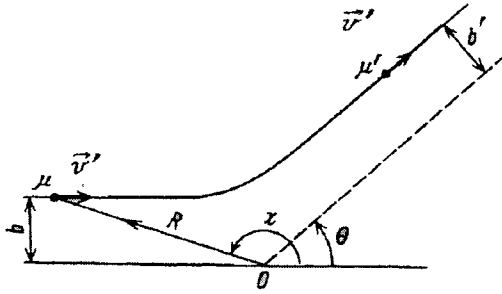


Fig. 2.3. Classical trajectory of elastic scattering in the center-of-mass system.

In order to find the dependence of the differential cross section on the scattering angle, it is sufficient to rewrite expression (2.3) in the form

$$d\sigma_0 = \Sigma b(\theta) |db / \sin \theta d\theta| d\Omega \quad (2.5)$$

where the contributions to the scattering at the specified angle  $\theta$  from different impact parameters are summated.

To determine  $\sigma_0$ , the integration with respect to flight-off angles can be replaced by the integration with respect to the impact parameter. In this case, we can write

$$\sigma_0(v) = \int_0^{b_{\max}} 2\pi b db \quad (2.6)$$

where  $b_{\max}$  is the maximum value of the impact parameter at which scattering takes place yet.

For the model of rigid spheres,  $b_{\max} = R_A + R_B$  (where  $R_A$  and  $R_B$  are the radii of the spheres). Then we have

$$\sigma_0 = \pi(R_A + R_B)^2 \quad (2.7)$$

However, for the real interaction scattering also occurs outside the region of geometric contact. This is especially substantial, for example, for the Coulomb interaction of charged particles. Formulas for the cross section of inelastic processes substantially depend on the fact which form of the energy (electron, vibrational or rotational) changes.

The notion of the partial cross section can be introduced for each of three types of the processes:  $\sigma_1$  (for elastic scattering),  $\sigma_2$  (for inelastic scattering), and  $\sigma_3$  (for the chemical reaction). Each cross section represents the same proportionality coefficient  $\sigma$  in formulas similar to (2.1) obtained under the additional conditions that scattering of particles A is accompanied by one of three processes indicated. In the general case where all three processes are possible, the total collision cross section is summated from the corresponding partial cross sections  $\sigma_0 = \sigma_1 + \sigma_2 + \sigma_3$ .

Let us take that the collision of particles A and B has occurred if any of these three processes takes place. Therefore, we can introduce the probability  $P_\alpha$  of each process

$$P_\alpha = \sigma_\alpha / \sigma_0, \quad \alpha = 1, 2, 3 \quad (2.8)$$

As a rule, the probability of the elastic process  $P_1$  is close to unity, i.e., much higher than  $P_2$  and  $P_3$ .

### 2.1.3. Rate constants of bimolecular reactions

The notion of the rate constant  $\kappa_\alpha^v$  (index  $v$  indicates that the collision velocity of particles  $v$  is unchanged), which is related to the notion of the cross section of the process  $W_3^v$ , is also used for the quantitative characterization of the rate of each of the processes considered.

Let us discuss the most general case of collision 3 in which the internal energy changes and atoms are redistributed. The process rate  $W_3^v$  can be determined from the consumption of the reactant or from the accumulation of the reaction product. These determinations are not equivalent because when the rate is found from the reactant consumption, it includes other possible reaction

channels, e.g., channels of the formation of products C and D in other quantum states. Determine the processes rate as the rate of formation of product C

$$W_3^v = d[C(I)] / dt = k_3^v(i,j \rightarrow l,m)[A(i, v_A)][B(j, v_B)] \quad (2.9)$$

where  $[C(I)]$  is the concentration of product C in the quantum state  $l$ ;  $[A(i, v_A)]$  is the concentration of particles A in the quantum state  $i$  with the velocity  $v_A$ ;  $[B(j, v_B)]$  is the concentration of particles B in the quantum state  $j$  with the velocity  $v_B$ .

With the introduction of the new laboratory reference system (where particles B are at rest), the rate  $W_3^v$  depends only on the relative velocity of particles  $\bar{v} = \bar{v}_A - \bar{v}_B$ . Therefore, for the  $W_3^v$  rate we can write

$$W_3^v = k_3^v(i,j \rightarrow l,m)[A(i,k)][B(j)] \quad (2.10)$$

Let the flux density  $-dI$  of particles A( $i$ ) decreases in collisions with particles B( $j$ ) only due to process 3. Since the  $I$  value is referred to unit surface and time, the decrease in the flux density during passing the  $dx$  distance is equal to the process rate  $W_3^v$  multiplied to the volume of a cylinder with the unit surface area of the base and height  $dx$ , i.e.,

$$-dI = k_3^v(i,j \rightarrow l,m)[A(i, v)][B(j)]dx \quad (2.11)$$

Comparing expressions (2.11) and (2.1), we have

$$k_3^v(i,j \rightarrow l,m)[A(i, v)] = \sigma(i,j \rightarrow l,m) \quad (2.12)$$

and, when taking into account that  $I = v[A(i, v)]$ , then

$$k_3^v(i,j \rightarrow l,m) = v\sigma(i,j \rightarrow l,m) \quad (2.13)$$

For elementary processes in the bulk and in several cases, also for the real experiment in beams, the relative velocity of colliding particles is not the same for each collision act. To obtain the rate constant, in this case, we have to average  $k^v(i,j \rightarrow l,m)$  by the available set of relative velocities  $v$ .

Let the probability that colliding particles have the relative velocity in the interval between  $v$  and  $v + dv$  be  $dP$ . Then

$$dP = f(v)dv \quad (2.14)$$

where  $f(v)$  is the normalized to unity distribution function of the colliding particles over relative velocities.

The rate constant  $k(i,j \rightarrow l,m)$  averaged over relative velocities is expressed through  $k^v(i,j \rightarrow l,m)$  and  $f(v)$  as follows:

$$k(i,j \rightarrow l,m) = \int_0^{\infty} k(i,j \rightarrow l,m) f(v)dv \quad (2.15)$$

Inserting expression (2.13) into (2.15), we obtain

$$k(i,j \rightarrow l,m) = \int_0^{\infty} \sigma(i,j \rightarrow l,m) f(v)dv \quad (2.16)$$

In most real cases, the function  $f(v)$  is the Maxwell distribution function, which is related to the fast establishment of the equilibrium distribution over velocities due to elastic processes. The Maxwell distribution function over relative velocities has the form

$$f(v,T) = 4\pi(\mu / 2 \pi k_B T)^{3/2} v^2 \exp(-\mu v^2 / 2 k_B T) \quad (2.17)$$

where  $k_B$  is the Boltzmann constant.

For this function  $f(v, T)$ , the rate constant averaged over relative velocities is described by the expression

$$k(i,j \rightarrow l,m; T) = 4\pi(\mu / 2 \pi k_B T)^{3/2} \int_0^{\infty} \sigma(i,j \rightarrow l,m) v^3 \exp(-\mu v^2 / 2 k_B T) dv \quad (2.18)$$

The overall rate constant  $Z_0$  of bimolecular collisions we obtain by the replacement of the cross section  $\sigma(i,j \rightarrow l,m)$  in (2.18) by the total collision cross section  $\sigma_0$  and transition to the variable  $E_r = \mu v^2 / 2$  under the integral

$$Z_0 = (8k_B T / \pi \mu)^{1/2} \int_0^{\infty} \sigma_0(E_{tr}) \exp(-E_{tr} / k_B T) E_{tr} dE_{tr} / (k_B T)^2 \quad (2.19)$$

Let us introduce the cross section  $\sigma_0$ , which will be named the kinetic cross section, in such a way that

$$Z_0 = \sigma_0 (8 k_B T / \pi \mu)^{1/2} = \langle v \rangle \sigma_0 \quad (2.20)$$

The rate constant at the temperature  $T$   $k(i,j \rightarrow l,m; T)$  can be presented in the form

$$k(i,j \rightarrow l,m; T) = Z_0 P(i,j \rightarrow l,m; T) \quad (2.21)$$

where  $P(i,j \rightarrow l,m; T)$  is the probability that process 3 occurs during collision.

Expressions (2.18) and (2.21) determine the rate constant of processes where the quantum states of reactants and products are specified. These processes are named microscopic, and rate constants of these processes are named microscopic rate constants.

However, attempts to specify quantum states of reactants and products in real experiments often fail. Therefore, a less detailed information is usually used, that is, such rate constants which are partially averaged over the states of reactants and summated over the states of products. Some examples for these approaches are the following.

(a)  $A(i) + B(j) \rightarrow C + D$ . In this example, the quantum states of the reactants are specified, and it is not defined in what states the products are formed. The averaged rate constant of this process  $k(i,j \rightarrow; T)$  can be obtained by the summation of the probability of the process  $P(i,j \rightarrow l,m; T)$  over all quantum states of the products

$$k(i,j \rightarrow; T) = Z_0 \sum_{l,m} P(i,j \rightarrow l,m; T) \quad (2.22)$$

(b)  $A + B \rightarrow C(l) + D(m)$ . In this example, the reaction occurs from any quantum states of the reactants to the certain quantum state of the products. In this case, the microscopic rate constant  $k(i,j \rightarrow l,m; T)$  should be averaged over

the quantum states of the reactants. With this purpose, the population of various quantum states of reactants A and B should be known. Let

$$[A(i)] = f_A(i)[A] \text{ and } [B(j)] = f_B(j)[B]$$

where  $f_A(i)$  and  $f_B(j)$  are the distribution functions of molecules A and B over quantum states  $i$  and  $j$ , respectively;  $[A]$  and  $[B]$  are the overall concentrations of A and B.

Then

$$k(\rightarrow l, m; T) = \sum_{i, j} f_A(i) f_B(j) k(i, j \rightarrow l, m; T) \quad (2.23)$$

(c)  $A(n_1) + B(n_2) \rightarrow C(n_3) + D(n_4)$  (where  $n_1, n_2, n_3$ , and  $n_4$  are the quantum numbers characterizing the vibrational states of molecules of reactants A, B and products C, D). In this example, the vibrational states of molecules A, B, C, and D are not specified. Then the rate constant  $k(n_1, n_2 \rightarrow n_3, n_4)$  can be obtained by the following averaging:

$$k(n_1 n_2 \rightarrow n_3, n_4; T) = \sum_{N_C, N_D} \sum_{N_A, N_B} f_A(N_A) f_B(N_B) k(n_1, N_A, n_2, N_B \rightarrow n_3, N_C, n_4, N_D; T) \quad (2.24)$$

where  $f_A(N_A)$  and  $f_B(N_B)$  are the distribution functions of molecules  $A(n_1)$  and  $B(n_2)$  over the vibrational states  $N_A$  and  $N_B$ , respectively; the summations are performed over vibrational states  $N_C$  and  $N_D$  of molecules of products  $C(n_3)$  and  $D(n_4)$ .

(d)  $A + B \rightarrow C + D$ . In this sample, neither the quantum states of reactants nor the quantum states of products are specified. We will call this process the elementary reactions and its rate constant will be named the rate constant. It depends on both the distribution function over collision velocities and the distributions  $f_A(i)$  and  $f_B(j)$  of molecules A and B over the quantum states

$$k(T) = \sum_{l,m} \sum_{i,j} f_A(i) f_B(j) k(i,j \rightarrow l,m;T) \quad (2.25)$$

If all indicated distributions are equilibrium, i.e., the velocity distribution is the Maxwell-type and the state distribution is the Boltzmann-type, the equilibrium rate constant is obtained. The term "equilibrium" indicates that the different forms of energy (rotational, vibrational, electronic) are characterized by one temperature  $T$  (energy equilibrium).

Studying thermal reactions, that is, when an external effect on the system (by the light, discharge, etc.) is absent, researchers deal, in most cases, with conditions of the energy equilibrium. Therefore, the term "equilibrium" is usually omitted for the rate constant and simply the rate constant of the elementary reaction is discussed. By contrast, when the reaction occurs under energetically nonequilibrium conditions, this is accepted to be specially marked.

The temperature plot of the rate constant  $k(T)$  of equilibrium elementary reactions is usually presented in the so-called Arrhenius exponential form

$$k(T) = A \exp(-E/k_B T) \quad (2.26)$$

The temperature-independent  $A$  and  $E$  values are named the pre-exponential factor and Arrhenius activation energy, respectively. This is precisely the form which is appropriate for the majority of experimentally measured rate constants of bimolecular reactions. At the same time, as will be shown below, the theory predicts that

$$k(T) = A' T^n \exp(-E_{akt}/k_B T), \quad n = -1 \dots +5 \quad (2.27)$$

In recent time, when  $k(T)$  is measured in a wide temperature interval, it is presented just in the form of (2.27).

#### 2.1.4. Rate constants of unimolecular reactions

Collision processes can result in the formation of the active molecule  $A^*(\epsilon)$ , whose energy  $\epsilon$  on the internal degrees of freedom is higher than some threshold  $E_0$  value necessary for the decomposition of the molecule or rearrangement of atoms. Such active molecules can spontaneously undergo chemical transformations. These chemical reactions are named unimolecular reactions.

The active molecules can be formed by collision processes of energy exchange (thermal activation), bimolecular association reactions of the type  $R + R_1 \rightarrow RR^*_1(\epsilon)$  (chemical activation) and absorption of photons (photoactivation).

The spontaneous unimolecular reaction obeys two laws: conservation of energy and conservation of total angular momentum  $J$ . The rate of spontaneous unimolecular reactions is described by the expression

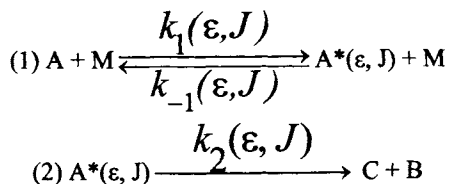
$$dA^*(\epsilon, J)/dt = -k(\epsilon, J)[A^*(\epsilon, J)] \quad (2.28)$$

The coefficient  $k(\epsilon, J)$  is named the microscopic rate constant of unimolecular reaction. Sometimes this rate constant is named microcanonical because all states with equal  $\epsilon$  and  $J$  values are assumed to be equiprobable. If active molecules  $A^*(\epsilon)$  are formed with some distribution  $f(\epsilon, J)$  over the states with the energy  $\epsilon$  and angular momentum  $J$ , the averaged rate constant  $\langle k(\epsilon, J) \rangle$  is described by the equation

$$\langle k(\epsilon, J) \rangle = \int_{E_0}^{\infty} \sum_{j=0}^{\infty} k(\epsilon, J) f(\epsilon, J) d\epsilon \quad (2.29)$$

It should be emphasized that, in principle, the  $E_0$  value (potential barrier) depends on  $J$ .

In the general case, the distribution function  $f(\epsilon, J)$  depends on the rate of obtaining active molecules and experimental conditions. Photoactivation readily provides the conditions for studying the unimolecular reactions involving  $A^*(\epsilon, J)$ . In the case of thermal activation, the chemical unimolecular reaction and processes of energy exchange with the gas  $M$  cannot be distinguished under some experimental conditions. Let us illustrate this point considering the simplified kinetic scheme



Process 1 and the reverse process present energy exchange. It is assumed in the considered kinetic scheme that the active molecule  $A^*(\epsilon, J)$  is formed due to one collision. In addition, it is assumed that the buffer gas M exists in an excess and, hence, energy exchange processes occur only upon collisions with particles M.

In the real experiment, the consumption rate of A due to process 2 is often detected. The macroscopic rate constant of unimolecular reactions  $k_M$  for thermal reactions is determined as

$$k_M(T) = \frac{1}{[M]} \frac{d[A]}{dt}$$

Using quasi-stationarity with respect to  $[A^*(\epsilon, J)]$ , after the summation over J and integration over  $\epsilon$ , we can easily obtain the expression for  $k_M(T)$

$$k_M(T) = \int_{E_0}^{\infty} \sum_{j=0}^{\infty} \frac{k_2(\epsilon, J)[k_1(\epsilon, J) / k_{-1}(\epsilon, J)]}{1 + k_2(\epsilon, J) / k_{-1}(\epsilon, J)[M]} d\epsilon$$

The ratio  $k_1(\epsilon, J) / k_{-1}(\epsilon, J)$  can be found using the principle of detailed balancing. In fact, the following relation is fulfilled at equilibrium:

$$\frac{k_1(\epsilon, J)}{k_{-1}(\epsilon, J)} = \frac{[A^*(\epsilon, J)]}{[A]} = f_B(\epsilon, J) \quad (2.30)$$

where  $f_B(\epsilon, J)$  is the Boltzmann distribution of molecules A over the states with the energy  $\epsilon$  and angular moment J.

Using equation (2.30), we obtain

$$k_M(T) = \int_{E_0}^{\infty} \sum_{j=0}^{\infty} \frac{k_2(\epsilon, J)f_B(\epsilon, J)}{1 + k_2(\epsilon, J) / k_{-1}(\epsilon, J)[M]} d\epsilon \quad (2.31)$$

It is seen from (2.31) that the macroscopic rate constant  $k_M$  depends on the concentration of the buffer gas M. This plot is presented in Fig. 2.4. It is seen that two regions with low and high  $[M]$  values can be distinguished. In the region of low  $[M]$  values, the rate constant  $k_M(T)$  is designated as  $k_0(T)$  to emphasize that  $[M] \rightarrow 0$ . It is seen in Fig. 2.4 that  $k_0(T)$  in this region depends linearly on  $[M]$ . In the region of high  $[M]$  values, we designated the rate constant  $k_M(T)$  as  $k_\infty(T)$  to emphasize that  $[M] \rightarrow \infty$ .

Let us consider the region of low  $[M]$  concentration. The condition of smallness of  $[M]$  is that the condition  $k_2(\epsilon, J) \gg k_{-1}(\epsilon, J)[M]$  is fulfilled in the interval of energies that contribute noticeably to reaction 2.

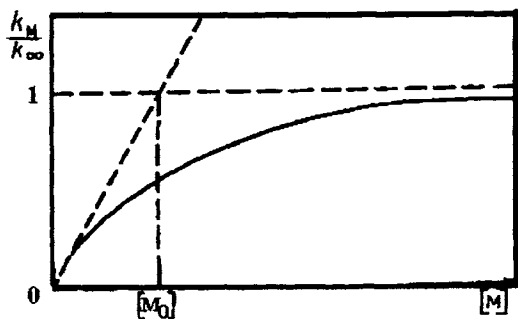


Fig. 2.4. The plot of the rate constant of unimolecular reactions vs. concentration of the buffer gas M.

Taking into account this inequality, we can obtain from (2.31)

$$k_0(T) = [M] \int_{E_0}^{\infty} \sum_{j=0}^{\infty} k_{.1}(\epsilon, J) f_B(\epsilon, J) d\epsilon$$

Usually  $k_{.1}$  is presented in the form (2.21)

$$k_{.1} = Z_0 P \quad (2.32)$$

where  $P$  is the probability of the effective collision.

The  $Z_0P$  can be brought out from under the integral sign. To estimate the integral, let us make several assumptions: molecule  $A^*$  does not rotate, it can be presented as a system of harmonic oscillators, and the density of vibrational states  $\rho(\varepsilon)$  remains to be equal to  $\rho(E_0)$  at  $\varepsilon > E_0$ . In the framework of this approximation,

$$f(\varepsilon) = \frac{\rho(E_0)}{F_{\text{vib}}} \exp\left(-\frac{\varepsilon}{k_B T}\right) \quad (2.33)$$

where  $F_{\text{vib}}$  is the partition function of harmonic oscillators.

Then after integrating, we have the following expression for  $k_0(T)$ :

$$\tilde{k}_{0(T)} = [M] Z_0P \frac{\rho(\varepsilon) k_B T}{F_{\text{vib}}} \exp\left(-\frac{E_0}{k_B T}\right) \quad (2.34)$$

In order to correct the assumptions made, we introduced the correction factors. Then

$$k_0(T) = \tilde{k}_{0(T)} \lambda_\varepsilon \lambda_{\text{anh}} \lambda_{\text{rot}} \lambda_{\text{inrot}} \quad (2.35)$$

where  $\lambda_\varepsilon$  is the factor that takes into account the increase in the density of states  $\rho(\varepsilon)$  at  $\varepsilon > E_0$ ;  $\lambda_{\text{anh}}$  is the factor that takes into account anharmonicity of molecular vibrations;  $\lambda_{\text{rot}}$  takes into account the rotation of molecule  $A$ ; and  $\lambda_{\text{inrot}}$  takes into account the specificity of internal rotations.

The physical essence of the region of low  $[M]$  values is the following. The concentration  $[M]$  is so low that the formation of active molecules occurs more slowly than the decomposition of active molecules. This implies that almost all active molecules  $A^*(\varepsilon, J)$  that are formed decompose before deactivation collision. Therefore,  $k_0 T / [M]$  is the rate constant of the bimolecular reaction of formation of active molecules.

Now let us consider the region of high  $[M]$ . High  $[M]$  concentrations imply those for which the inequality  $k_2(\epsilon, J) \ll k_{-1}(\epsilon, J)[M]$  is fulfilled. Taking into account this inequality, we obtain from (2.31)

$$k_{\infty}(T) = \int_{E_0}^{\infty} \sum_{j=0}^{\infty} k_2(\epsilon, J) f_B(\epsilon, J) d\epsilon \quad (2.36)$$

As can be seen, equation (2.36) coincides with formula (2.29). This implies that the rate constant of decomposition of active molecules  $A^*(\epsilon, J)$  averaged over the Boltzmann distribution  $f_B(\epsilon, J)$  is measured in this region of  $[M]$  values. The fact that the distribution function  $f(\epsilon, J)$  remains Boltzmann implies that at these  $[M]$  values energy exchange processes occur so rapidly that the unimolecular reaction does not virtually violate the Boltzmann distribution. The method for calculation of  $k_2(\epsilon, J)$  and more detailed equation for  $k_{\infty}(T)$  are presented in Sections 2.2.4 and 2.4.6.

The rates of energy exchange processes and reactions of active molecules are comparable in the region of intermediate  $[M]$ . The distribution function  $f(\epsilon, J)$  will not be Boltzmann, and it is very difficult to calculate theoretically the rate constant. Therefore, to express  $k_M(T)$  through  $k_0(T)$  and  $k_{\infty}(T)$ , empirical approaches are used, for example, the following expression:

$$\frac{k_M}{k_{\infty}} = \frac{[M] / [M_0]}{1 + [M] / [M_0]} \gamma(k_0 / k_{\infty}) \quad (2.37)$$

where  $[M_0]$  is the  $[M]$  value at which  $k_0 = k_{\infty}$  (see Fig. 2.4), and  $\gamma(k_0 / k_{\infty})$  is the broadening factor.

The factor  $\gamma(k_0 / k_{\infty})$  can theoretically be calculated using empirical parameters:

### 2.1.5. Principle of microscopic reversibility and equilibrium constants

Above we discussed various types of collisions. A reverse process corresponds to each of these processes. Cross sections and rate constants of forward and reverse elementary processes are mutually related. This relationship is determined by the laws of conservation of energy and total angular momentum.

Process 3 is the most general type of an elementary process for the collision of heavy particles because it is accompanied by the simultaneous redistribution of atoms and energies of internal and translational motions. The principle of microscopic reversibility for this process has the following form:

$$2\mu E_{\text{transl}} g_i g_j \sigma(i, j \rightarrow l, m) = 2\mu' E'_{\text{transl}} g_l g_m \sigma(l, m \rightarrow i, j) \quad (2.38)$$

where  $g_i, g_j, g_l, g_m$  are the multiplicities of states  $i, j, l$ , and  $m$ , respectively;  $\mu$  and  $\mu'$  are the reduced weights of reactants and products;  $E_{\text{transl}}$  and  $E'_{\text{transl}}$  are the translational energies of reactants and products; and  $\sigma(i, j \rightarrow l, m)$  and  $\sigma(l, m \rightarrow i, j)$  are the cross sections of the forward and reverse reactions.

The rate constant and cross section are related between each other through the distribution function  $f(v, T)$  by expression (2.18). Using this expression with the Maxwell distribution function  $f(v, T)$ , we can write expressions for the rate constants of the forward  $k(i, j \rightarrow l, m)$  and reverse  $k(l, m \rightarrow i, j)$  reactions.

The energies  $E_{\text{transl}}$  and  $E'_{\text{transl}}$  are related by the conservation law:

$$E'_{\text{transl}} = E_{\text{transl}} + \Delta U \quad (2.39)$$

where  $\Delta U$  is the difference between the internal energies of products and reactants.

Using expressions (2.38), (2.39), and (2.18), we can easily obtain the expression for the ratio of the rate constants of the forward to reverse reactions

$$\frac{k(i, j \rightarrow l, m; T)}{k(l, m \rightarrow i, j; T)} = \frac{g_l g_m}{g_i g_j} \left( \frac{\mu'}{\mu} \right)^{3/2} \exp \left( -\frac{\Delta U}{k_B T} \right) \quad (2.40)$$

Relationship (2.40) expresses *the principle of detailed balancing* for microscopic processes.

According to this principle, we can speak about an equilibrium between microscopic processes when the rates of the forward and reverse reactions are equal

$$k(i, j \rightarrow l, m; T)[A_i][B_j] = k(l, m \rightarrow i, j; T)[C_l][D_m] \quad (2.41)$$

where  $[A_i]$ ,  $[B_j]$ ,  $[C_l]$ , and  $[D_m]$  are the equilibrium concentrations of reactants and products.

Then the equilibrium constant of the microscopic process is the following:

$$\begin{aligned}
 K(i,j \rightarrow l,m;T) &= \frac{k(i,j \rightarrow l,m;T)}{k(l,m \rightarrow i,j;T)} = \frac{[C_l][D_m]}{[A_i][B_j]} = \\
 &= \frac{g_l g_m}{g_i g_j} \left( \frac{\mu'}{\mu} \right)^{3/2} \exp \left( -\frac{\Delta U}{k_B T} \right) \quad (2.42)
 \end{aligned}$$

The next step is the application of the principle of detailed balancing to partially microscopic or "equilibrium" reactions. In the general case, we have to know distribution functions for various degrees of freedom. This implies that microscopic energy exchange process should be taken into account along with reactions at the microscopic level. Nevertheless, we always can speculatively assume that the addition of some efficient and selective relaxing agents to the system results in the fact that the Boltzmann distribution over these or other degrees of freedom is established much more rapidly than the chemical equilibrium. Then the chemical equilibrium is already established under the condition of the Boltzmann distribution over all or only some internal degrees of freedom. Using the principle of detailed balancing, we can find relationships for the rate constants of forward and reverse processes for macroscopic or partially microscopic reactions.

Table 2.1 contains the expressions for the equilibrium constant for the reaction of the atom A with the diatomic molecule BC. It is accepted that the A and C atoms and the BC and AB molecules are in the nondegenerated electronic states, and the AB and BC molecules can exist in different vibrational and rotational states.

The examples considered in Table 2.1 show that when the quantum states of the reactants and products are not fixed, the statistical sum over the corresponding degrees of freedom appear in the equilibrium constant. The said can be generalized for the case where the A and C particles are not atoms. Then statistical sums will appear for the degrees of freedom of the A and C particles, whose quantum states are not fixed.

Table 2.1. Equilibrium constants of reactions of the atom A with the diatomic molecule BC

$$\begin{aligned}
a) \quad A + BC(n, N_{BC}) &\rightleftharpoons AB(n, N_{AB}) + C - \Delta U_a & K &= \left(\frac{\mu'}{\mu}\right)^{3/2} \frac{(2N_{AB} + 1)}{(2N_{BC} + 1)} \exp\left(-\frac{\Delta U_a}{k_B T}\right) \\
b) \quad A + BC(n, N_{BC}) &\rightleftharpoons AB(n') + C - \Delta U_b & K &= \left(\frac{\mu'}{\mu}\right)^{3/2} \frac{F_{AB}^{\text{rot}}}{2N_{BC} + 1} \exp\left(-\frac{\Delta U_b}{k_B T}\right) \\
c) \quad A + BC(n) &\rightleftharpoons AB(n', N_{AB}) + C - \Delta U_c & K &= \left(\frac{\mu'}{\mu}\right)^{3/2} \frac{(2N_{AB} + 1)}{F_{BC}^{\text{rot}}} \exp\left(-\frac{\Delta U_c}{k_B T}\right) \\
d) \quad A + BC(n) &\rightleftharpoons AB(n') + C - \Delta U_d & K &= \left(\frac{\mu'}{\mu}\right)^{3/2} \frac{F_{AB}^{\text{rot}}}{F_{BC}^{\text{rot}}} \exp\left(-\frac{\Delta U_d}{k_B T}\right) \\
e) \quad A + BC(n) &\rightleftharpoons AB + C - \Delta U_e & K &= \left(\frac{\mu'}{\mu}\right)^{3/2} \frac{F_{AB}^{\text{rot}} F_{AB}^{\text{vib}}}{F_{BC}^{\text{rot}}} \exp\left(-\frac{\Delta U_e}{k_B T}\right) \\
f) \quad A + BC &\rightleftharpoons AB(n') + C - \Delta U_f & K &= \left(\frac{\mu'}{\mu}\right)^{3/2} \frac{F_{AB}^{\text{rot}}}{F_{BC}^{\text{rot}} F_{BC}^{\text{vib}}} \exp\left(-\frac{\Delta U_f}{k_B T}\right) \\
g) \quad A + BC &\rightleftharpoons AB + C - \Delta U_g & K &= \left(\frac{\mu'}{\mu}\right)^{3/2} \frac{F_{AB}^{\text{rot}} F_{AB}^{\text{vib}}}{F_{BC}^{\text{rot}} F_{BC}^{\text{vib}}} \exp\left(-\frac{\Delta U_g}{k_B T}\right)
\end{aligned}$$

*Note.* The difference between the internal energies of products and reactants  $\Delta U$  is determined from formula (2.52),  $F^{\text{rot}}$  and  $F^{\text{vib}}$  are the rotational and vibrational partition functions of the AB and BC molecules,  $N$  is the rotational quantum number, and  $n$  is the vibrational quantum number

The detailed balancing principle for the equilibrium considered appears as follows. When the equilibrium of the macroscopic elementary reaction is observed, any microscopic process, whose totality composes this elementary reaction, are also equilibrium.

We considered adiabatic reactions. If electron-excited species are among reactants or products, the electronic partition function of the reactants or products should also be taken into account.

Case g (Table 2.1) corresponds to the energetically equilibrium elementary reaction. Since the constants of the forward and reverse reactions depend on  $T$  only, the reaction direction is indicated henceforth by an arrow above the rate constant.

The expression for the equilibrium constant  $K$  can also be obtained from the thermodynamics

$$K = \overline{k}(T) / \overline{k}^-(T) = \exp[-\Delta G^\circ(T) / k_B T] \quad (2.43)$$

where  $\Delta G^\circ$  is the change in the Gibbs energy on going from reactants to products.

### 2.1.6. Potential energy surface (PES)

The first task in the calculation of rate constants of elementary reactions is the determination of the potential energy of interaction of colliding particles. In the general case, the potential energy of interaction  $U(r, R)$  depends on the set of coordinates of electrons  $r$  and coordinates of nuclei  $R$  and should contain the contributions from electron-electron, electron-nucleus, and nucleus-nucleus interactions. This task is very labor-consuming and, hence, the *adiabatic approximation* is usually used. It is based on a possibility of separation of motions over different degrees of freedom if the scales of the characteristic times of these motions differ substantially.

Since the mass of any nucleus more than by  $10^3$  times exceeds the mass of an electron, the characteristic times of motions of the electronic and nuclear subsystems differ substantially, that is, the motion of electrons can be studied at any fixed position of nuclei. With a change in the position of nuclei, the electron motion as if without inertia follows the motion of nuclei. This approximation can mathematically be reduced to that the wave function  $\Psi(\overline{r}, \overline{R})$  for each electronic state (which is marked by index  $i$ ) is the product

$$\Psi_i(\overline{r}, \overline{R}) = \varphi_i(\overline{r}, \overline{R}) \chi_i(\overline{R}) \quad (2.44)$$

where  $\varphi_i(\overline{r}, \overline{R})$  and  $\chi_i(\overline{R})$  satisfy the following equations:

$$[T_e + U(\overline{r}, \overline{R})] \varphi_i(\overline{r}, \overline{R}) = U(\overline{R}) \varphi_i(\overline{r}, \overline{R}) \quad (2.45)$$

$$[T_n + U_i(\overline{R})] \chi_i(\overline{R}) = \epsilon_i \chi_i(\overline{R}) \quad (2.46)$$

where  $T_e$  and  $T_n$  are the operators of the kinetic energy of electrons and nuclei, respectively.

Equation (2.45) is the wave equation for the electronic motion when the nuclei are at rest. The  $U_i(\overline{\mathbf{R}})$  values are eigenvalues of the operator  $H_e = T_e + U_i(\overline{\mathbf{R}})$  and named the *adiabatic terms of electronic subsystem*. The functions  $\varphi_i(\overline{\mathbf{r}}, \overline{\mathbf{R}})$  are the electronic wave functions of the system in the  $i$ -th state and named the *adiabatic electronic functions*. The  $\overline{\mathbf{R}}$  coordinates can be considered as parameters on which  $U_i(\overline{\mathbf{R}})$  and  $\varphi_i(\overline{\mathbf{r}}, \overline{\mathbf{R}})$  depend.

Equation (2.46) describes the motion of nuclei. It is seen from this equation that in the indicated approximation  $U_i(\overline{\mathbf{R}})$  is the potential energy of nuclei for the specific  $i$ -th electronic state of the system. The plot of the  $U_i(\overline{\mathbf{R}})$  function in the case where  $\overline{\mathbf{R}}$  is restricted to one variable is named the *potential curve*, and in the case where  $\overline{\mathbf{R}}$  is a set of variables, the *potential energy surface (PES)* is considered.

Elementary processes can be classified as electronically adiabatic and nonadiabatic processes. The sense of the idea "*electronically adiabatic process*" is clear: these are the processes that occur without a change in the electronic state of the system. This is precisely the class of processes for which we can remain in the framework of the adiabatic approximation. However, there are nonadiabatic processes for which the electronic state of the system changes. In the general case it is difficult to predict what processes are electronically adiabatic and what are nonadiabatic. It is clear from qualitative concepts that the higher the difference between the characteristic times of the electron and nuclear motions of the system, the better the description of the system by the adiabatic approximation.

Let

$$\Delta U(\overline{\mathbf{R}}) = U_0(\overline{\mathbf{R}}) - U_1(\overline{\mathbf{R}})$$

where  $U_0$  and  $U_1$  are the PES of the ground and first excited electronic states of the system.

Then the characteristic time of the electron motion can be estimated from the uncertainty relation ( $\tau_e \sim 2\pi\hbar / \Delta U(\overline{\mathbf{R}})$ ). Designating the characteristic length

in which the adiabatic PES  $U_0(\overline{\mathbf{R}})$  of the lowest electronic state changes significantly by  $l$  and the velocity of the nuclear motion by  $v$ , we can evaluate the characteristic time scale of the nuclear motion within which the indicated changes occur as follows:  $\tau_R \sim l/v$ . The ratio of time scales of two motions (fast and slow) is named the *Messi parameter*  $\zeta$  for which, in the considered case, we have

$$\xi \sim (\tau_e / \tau_R)^{-1} = \Delta u l / h v \quad (2.47)$$

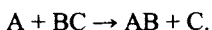
It is clear from qualitative concepts that the better the fulfillment of the condition  $\zeta \gg 1$ , the stronger grounds for using the adiabatic approximation. If the region of  $R$  values for which  $\zeta$  does not much exceed unity (close to unity or even lower) exists for the potential energy surfaces, then transitions to PES of other electronic state can occur in this region. The adiabatic approximation cannot be used in this region of nuclear coordinates and the theory of nonadiabatic transitions should be applied.

In the framework of the adiabatic approximation, the only function of the potential energy  $U_i(\overline{\mathbf{R}})$  which depends only on the coordinates of nuclei  $\mathbf{R} = \{R_1, R_2, \dots, R_{3N-6}\}$ , corresponds to each  $i$ -th electronic state of the system. If the system consists of  $N$  atoms, the  $U_i$  function depends on  $3N - 6$  independent variables. This follows from the fact that six degrees of freedom refer to the motion of the system as a whole (3 translatory and 3 rotational degrees of freedom) and must be subtracted from the number of coordinates of atoms  $3N$ . Therefore, the equation

$$U = U(R_1, R_2, \dots, R_{3N-6}) \quad (2.48)$$

specifies the surface in the space with the  $3N - 6$  dimensionality. Index " $i$ " is omitted because the PES for the ground electronic state is considered below.

The topography of the PES depends on the nature of colliding particles. It has maxima, minima, saddle-points, valleys, *etc.* The PES can depend on many variables  $R_j$ , and this impedes its representation in the clear form. For simplicity, let us consider the collision of the atom A with the diatomic molecule BC. Various elementary processes can occur due to this collision. We will restrict our consideration by the direct exchange reaction



The potential energy of this system depends on three coordinates: the distance between the B and C atoms ( $R_{BC}$ ), the distance from the A atom to the center of mass of the BC molecule ( $R_A$ ), and the angle  $\beta$  between the vectors  $R_A$  and  $R_{BC}$  (Fig. 2.5, a).

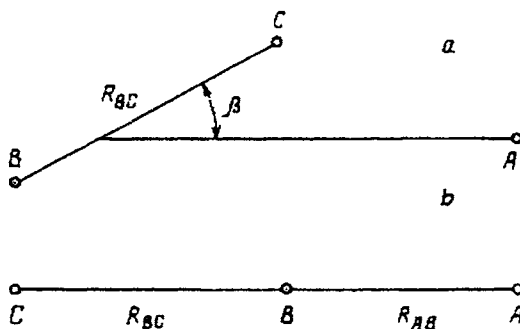


Fig. 2.5. Relative arrangement of three interacting atoms: *a*, noncollinear configuration; and *b*, collinear configuration.

In order to decrease the number of coordinates, we fix the  $\beta$  value,  $\beta = \pi$ , that is, we will consider the collinear collision (Fig. 2.5, b). In this case, the potential energy depends only on two coordinates  $R_{BC}$  and  $R_A$ . Another coordinate can be chosen instead of  $R_A$ , for example, the distance ( $R_{AB}$ ) between the atoms A and B.

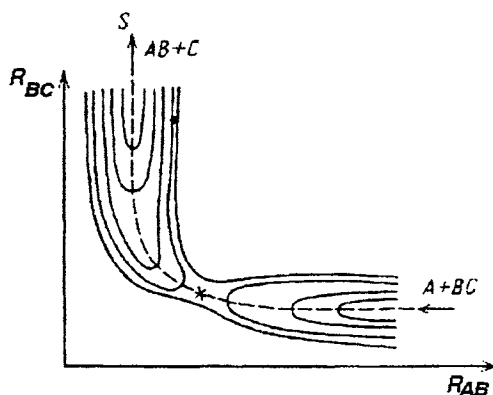


Fig. 2.6. Potential energy surface (PES).

The qualitative form of the PES in these coordinates is presented in Fig. 2.6. Solid lines mark the levels of equal energies. The PES has two valleys corresponding to the reactants and products of the exchange reaction. They are separated by the saddle point (designated by asterisk). At large  $R_{AB}$  values, the potential energy of three atoms should be transformed into the potential energy of the BC molecule in the reactant valley. This implies that if at large  $R_{AB}$  we draw the PES cross section parallel to the  $R_{BC}$  axis, in this cross section we obtain the potential energy curve of the BC molecule.

As the atom A approaches the molecule BC in the cross sections parallel to the  $R_{BC}$  axis, the potential energy curves are more and more transformed simultaneously with an increase in the minimum of the potential energy. When we draw the cross sections parallel to the  $R_{AB}$  axis after passing the saddle-point, the potential energy curve also changes with increasing  $R_{BC}$  in these cross sections, and the value of the potential energy minimum begins to decrease. At large  $R_{BC}$  distances, the potential energy curve of the AB molecule is obtained in the cross section of the outlet valley.

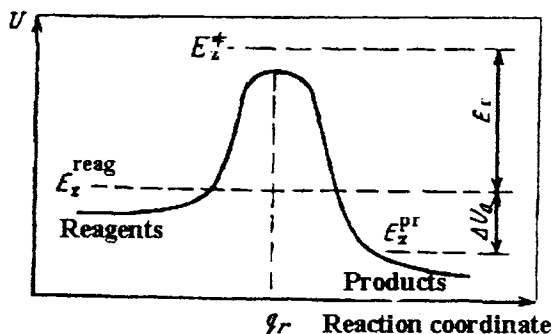


Fig. 2.7. PES cross section along the reaction path.

Two valleys of reactants and products can be connected by the  $S$  line along which the potential energy is minimum, that is, the shift from  $S$  to any side results in an increase in the potential energy. In Fig. 2.6  $S$  is shown by dotted line, being named the *reaction path*. The motion along the reaction path can be described by the *reaction coordinate*  $q_r$ , which measures the distance passed by a representative point along the  $S$  line. The PES cross section along the reaction path gives the dependence of the potential energy on the reaction coordinate:  $U(q_r)$ . The dependence  $U(q_r)$  for the considered PES is presented in Fig. 2.7.

The reaction profile allows one to distinguish two parameters important for the characterization of the elementary process:  $E_0$  and  $\Delta U_0$ . The  $E_0$  parameter

indicates the height of the potential barrier. The  $\Delta U_0$  parameter characterizes the energy of the elementary process, and its sign indicates whether the elementary process occurs with the absorption or liberation of the energy if the reactants and products are in the ground vibrational state.

The  $E_0$  and  $\Delta U_0$  parameters should be determined taking into account the energies of zero-point vibrations for the reactants  $E_Z^r$ , products  $E_Z^p$ , and a quasi-molecule at the saddle-point  $E_Z^\ddagger$ . Then, as can be seen from Fig. 2.7, the  $E_0$  and  $\Delta U_0$  values can be expressed as follows:

$$\Delta U_0 = E_Z^r - E_Z^p, \quad E_0 = E_Z^\ddagger - E_Z^r \quad (2.49)$$

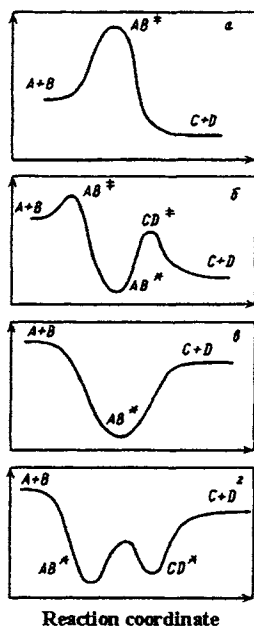


Fig. 2.8. Reaction profiles of the reaction  $A + B \rightarrow C + D$ : a, direct reactions; and b--d, reactions through a long-lived complex.

If  $\Delta U_0 > 0$ , the potential energy increases, that is, the elementary reaction occurs with energy absorption. These reactions are named *endoergic*. Note that the microscopic exoergic process can occur with either the liberation (*exothermic* process) or absorption of the energy (*endothermic* process). In this case, the sign

of the  $\Delta U_0$  value indicates the exothermicity or endothermicity of the process. This value is the difference of the energies of reactants and products in the specified quantum states. For example, for process 3

$$\Delta U = \Delta U_0 - [(E_i + E_j) - (E_l + E_m)] \quad (2.50)$$

where  $E_i$  and  $E_j$  are the internal energies of the A and B reactants; and  $E_m$  and  $E_l$  are the internal energies of the C and D products.

If  $\Delta U_0 > 0$ , the process is exothermic, *i.e.*, occurs with energy liberation; if  $\Delta U_0 < 0$ , the process is endothermic, *i.e.*, occurs with energy absorption. At  $\Delta U_0 = 0$  the process is thermoneutral.

Note that the reaction profiles can differ for different types of elementary reactions (Fig. 2.8). As can be seen in Fig. 2.8, the reaction profiles can have a potential barrier (*a*), can be without a potential barrier (*c*) or with two potential barriers (*b*, *d*). This distinction can be used for the classification of elementary reactions.

#### 2.1.7. Classification of elementary reactions

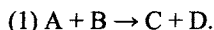
Elementary reactions can be classified by various properties. Some divisions have already been done earlier: adiabatic and nonadiabatic reactions, exoergic and endoergic reactions.

Sometimes reactions are classified by the number of atoms involved in the formation and cleavage of bonds. The reaction  $AB + CD \rightarrow AC + BD$  is the four-center reaction. In this reaction, A, B, C, and D can be either atoms or radicals. Reactions of this type are accompanied by the cleavage of two former bonds and formation of two new bonds. This type of reactions can be exemplified by the reaction  $\cdot CS + O_2 \rightarrow CO + \cdot SO$ .

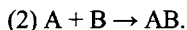
In three-center reactions  $C + AB \rightarrow A + BC$ , one former (simple, double, or triple) chemical bond is cleaved and one new bond is formed. This type of reactions is presented by atom or radical abstraction, for example,  $H + RH \rightarrow H_2 + R$  (*R* is the radical), disproportionation, *e.g.*,  $\cdot CH_3 + \cdot C_2H_5$ , and substitution, for example,  $COS + \cdot O \rightarrow CO_2 + \cdot S$ .

Two types of bimolecular reactions can be distinguished at the macroscopic level of description.

1. Bimolecular exchange reaction when atoms are redistributed upon the collision of two molecules or a molecule and an atom



2. Addition (association) reaction when one particle is formed upon the collision of two particles



However, if reaction 2 is considered in more detail, we see that it consists of several steps. The active molecule  $AB^*(\epsilon)$  is formed due to the addition of A and B ( $A + B \rightarrow AB^*(\epsilon)$ ). This molecule can decompose in the backward direction ( $AB^*(\epsilon) \rightarrow A + B$ ), be deactivated in collisions with other molecules M ( $AB^*(\epsilon) \rightarrow AB$ ) or participate in spontaneous unimolecular reactions to form other products ( $AB^*(\epsilon) \rightarrow C + D$ ). When decomposition in the backward direction and deactivation in collisions with M are the main reactions of  $AB^*(\epsilon)$ , the addition reaction occurs



When the rate of  $AB^*(\epsilon)$  decomposition with the formation of products C and D exceeds the rate of  $AB^*(\epsilon)$  deactivation, the exchange reaction occurs

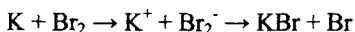


When omitting the formation of the intermediate  $AB^*(\epsilon)$  particle, we have exchange reaction 1. Thus, the same rearrangement of atoms occurs in reactions 1 and 3 but the mechanisms of this rearrangement can differ. Reaction 1 is an elementary reaction, whereas in reaction 3 the formation of products occurs *via* several steps. These distinctions depend on the specificity of the reaction profiles and are most pronounced in studies in crossed molecular beams when the product flight-off is detected under different angles with respect to the direction of the vector of the relative velocities of reactants. In order to emphasize these distinctions, *bimolecular* reactions are divided into two types, which are indicated below.

**Direct reactions.** The characteristic reaction profile of the direct reaction is shown in Fig. 2.8, *a*. The specific feature of this profile is the presence of one extreme (maximum) on the profile of the reaction path. The angular distribution of products in these reactions is strongly asymmetrical relatively to the scattering angle  $\theta = 90^\circ$ . It follows from this that the redistribution of atoms occurs within

the time shorter than one rotation period. The direct reaction is exemplified by  $\cdot\text{H} + \text{RH} \rightarrow \text{H}_2 + \cdot\text{R}$ . A more detailed classification depending on the character of the angular distribution of reaction products can be introduced for direct three-center reactions ( $\text{C} + \text{AB} \rightarrow \text{BC} + \text{A}$ ). If the BC products are mainly scattered in the direction of the motion (in the system of the center of mass) of the C particle (forward scattering), such reactions are named *stripping*. If the products are scattered in the direction of the motion of the AB molecules (backward scattering), such reactions are named *rebounding*. The majority of direct three-center chemical reactions with a noticeable activation energy proceed *via* the mechanism close to rebounding. Cross sections of these reactions are small and strongly depend on the energy.

Unlike rebounding reactions, stripping reactions are usually characterized by large cross sections that are weakly depend on the translational energy. The typical representatives of stripping reactions are the so-called reactions with the electron transfer at the intermediate stage. For example, the reaction  $\text{K} + \text{Br}_2$  proceeds *via* the mechanism



**Reactions occurring *via* the formation of a long-lived intermediate complex.** The long-lived intermediate complex usually corresponds to the strongly vibrationally excited molecule  $\text{AB}^*(\epsilon)$ . This complex does not decompose within the time interval, which exceeds at least several rotation periods. Many vibrations occur in the complex during this time interval, so that the validity of the statistical description of the vibrational energy redistribution can naturally be assumed.

Figure 2.8, *b, c, d* presents various reaction profiles for this class of reactions. Potential wells to which stable AB molecules often correspond are observed everywhere. This class of reactions can be exemplified by the reactions of two radicals. The angular distribution in these reactions is symmetrical relatively to the scattering angle  $\theta = 90^\circ$ .

**Unimolecular reactions** can also be divided into several types, which qualitatively differ by the reaction profiles (Fig. 2.9).

*Reactions of simple bond cleavage.* In this case (Fig. 2.9, *a*), one bond is cleaved and two radicals are formed:  $\text{A} \rightarrow \cdot\text{R} + \cdot\text{R}'$ . *Recombination reactions*, which, as a rule, have no potential barrier, are backward reactions of these unimolecular reactions.

*Concerted decomposition reaction.* In these reactions, several bonds are simultaneously cleaved and formed. An example of this type of reactions can be the reaction  $\text{C}_2\text{H}_5\text{Cl} \rightarrow \text{C}_2\text{H}_4 + \text{HCl}$ . Reactions of this type (Fig. 2.9, *b*) have significant potential barriers ( $\sim 300$  kJ/mol). The reactions  $\cdot\text{R} \rightarrow \text{D} + \cdot\text{R}'$  should also be referred to this type. As a rule, the potential barrier of these reactions is lower.

*Isomerization reactions.* These reactions result in the rearrangement of atoms within one molecule:  $\text{A} \rightarrow \text{A}'$ , for example  $\text{H}_2\text{C}=\text{CHCH}_2\text{NC} \rightarrow \text{H}_2\text{C}=\text{CHCH}_2\text{CN}$ . The reaction profiles of this type of reactions are shown in Fig. 2.9, *c*.

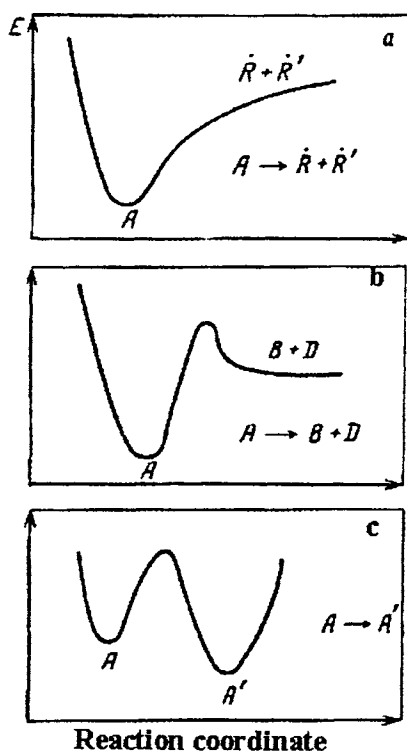


Fig. 2.9. Reaction profiles of unimolecular reactions: *a*, cleavage of one bond; *b*, cleavage of several bonds; and *c*, isomerization.

## 2.2. Methods for calculation of rate constants of elementary reactions

Two approaches, namely, dynamic and statistical, are used for the calculation of cross sections and probabilities of elementary reactions. The *dynamic approach* is the solution of equations of motion for an isolated system of colliding particles with the specified initial state (methods of classical trajectories and semiclassical approximation). The explicit consideration of the rather complicated dynamics of the system can be avoided in the *statistical approach* due to the stochastic character of the nuclear motion during collisions (statistical theories of unimolecular reactions and bimolecular reactions occurred through a long-lived complex) or due to the high degree of averaging of the calculated characteristics of the elementary process (transition state theory). However, an information on the potential energy surface is needed to this or other extent in all methods.

### 2.2.1. Methods for calculation of the potential energy surface (PES)

In the framework of the electronically adiabatic approximation, the calculation of PES is reduced to the solution of the eigenvalue problem for the Schrödinger equation. The exact solution of this problem meets great computational difficulties. Therefore, to obtain an information about the PES, experimental data are used along with theoretical approaches. Depending on sources of the information used, the methods for the determination of the PES are grouped as follows: nonempirical, semiempirical, and empirical. Let us consider each group.

**Nonempirical methods** for the calculation of PES are purely theoretical. The starting information is only data on the composition of the considered system (the number and charges of particles), which allows us to name nonempirical calculations *ab initio* because only first principles are operated in them.

The variation principle in which the minimum of the functional is desired is usually used

$$U = \int H_e \varphi d\tau \quad (2.51)$$

where  $H_e$  is the electronic Hamiltonian,  $d\tau$  is the volume element in the electronic coordinates, and  $\varphi$  is the trial wave function normalized to unity.

It is clear that the minimum of the  $U$  value depends on the form of the probe function  $\varphi$ .

The most popular approximation, which allows to approach the solution of the problem, is the one-electron approach where electrons, according to the Pauli principle, are distributed over the system of levels in some effective potential of nuclei and electrons (in the self-consistent field, SCF). This distribution is named the electronic configuration. There are different variants of the one-electron approximation, and the range of their applicability depends on internuclear distances. The method of molecular orbitals (MO) is the most popular and highly developed method to present time. In this method, molecular orbitals are arranged as a linear combination (LC) of atomic orbitals (AO) from which the method is named MO LCAO.

More accurate nonempirical calculations are performed by the configuration interaction method (MO SCF CI). This method allows most correct taking into account the electron motion.

In order to determine  $U(\overline{\mathbf{R}})$  in **semiempirical calculations**, authors often use experimental data, for example, about the behavior of  $U(\overline{\mathbf{R}})$  in asymptotic regions corresponding to separated fragments of the system. The accuracy loss due to the use of the model function  $\varphi(\overline{\mathbf{r}}, \overline{\mathbf{R}})$  is partially compensated, in this case, by using experiment. Another advantage of these methods is a substantially less labor-consuming character of calculations compared to nonempirical methods. Recently, a possibility of the exact division of the Hamiltonian of the  $N$ -atomic system is used in the method of diatomic fragments in molecules.

$$H = \sum_K^N \sum_{L>K}^N H^{(KL)} - (N-2) \sum_K^N H^{(K)} \quad (2.52)$$

where  $H^{(KL)}$  and  $H^{(K)}$  are the Hamiltonians of isolated diatomic and atomic fragments.

This division makes it possible to choose the basis set of polyatomic functions  $\varphi_m$  in such a way that  $\varphi_m$  are the eigenfunctions the  $H$  operator in the asymptotic regions of the  $\overline{\mathbf{R}}$  values and simultaneously the eigenfunctions of the  $H^{(KL)}$  and  $H^{(K)}$  operators already in the whole region of the  $\overline{\mathbf{R}}$  values. The asymptotic region implies the region of the  $\overline{\mathbf{R}}$  values where the system exists as noninteracting diatomic and atomic fragments. For example, when the system consists of three A, B, and C atoms, in the asymptotic regions the system exists in the forms A and BC, B + AC, C + AB, A + B + C.

**Empirical methods for calculation of PES** are reduced to the specification of the functional form of the PES and determination of the corresponding parameters from spectroscopic, kinetic, and other experiments. Empirical methods are based on a set of model potentials. The elements of this set are potentials of diatomic fragments. Among the most popular potentials are the Lennard-Jones, Buckingham, Morse, and anti-Morse potentials. We present the Buckingham potential as an example

$$U(R) = -\frac{A}{R^6} + B \exp(-CR)$$

where A, B, and C are empirical parameters.

The first term is the attraction energy due to dispersion forces, and the second term is the repulsion energy related to the deformation of electron clouds of colliding particles.

The "flexibility" of the approximation is an important requirement imposed during dynamic calculations to empirical PES.

### *2.2.2. Method of classical trajectories*

The method of classical trajectories has first received wide acceptance for studying the dynamics of electronically adiabatic elementary reactions. In the framework of this method, the dynamics of particles involved in elementary processes is studied by the solution of classical equations of motion (for example, the Hamilton equations). For the generalized coordinates  $R_i$  ( $R_1, R_2, \dots, R_s$ ) and momenta  $P_i$  ( $P_1, P_2, \dots, P_s$ ), the Hamilton equations have the form

$$dR_i/dt = \partial H / \partial P_i; \quad dP_i/dt = -\partial H / \partial R_i \quad (2.53)$$

where  $H$  is the Hamilton function of the system from which the parts corresponding to the motions of the center of mass and rotation of the molecule as a whole are excluded.

This Hamilton function has the following form:

$$H = \sum_{k,i=1}^s \frac{P_i P_k}{2\mu_{ik}} + U(R_1, \dots, R_s) \quad (2.54)$$

Equations (2.53) are solved after the  $R_i$  and  $P_i$  values were specified at the initial moment. The solution gives  $R_i(t)$  and  $P(t)$ , which describe the state of the system at any moment.

The method of classical trajectories provides a very clear picture of elementary processes. The totality of the  $R_i$  coordinates is named the *configuration space of the system* and the totality of the  $R_i$  coordinates and  $P_i$  pulses is named the *phase space*.

At any moment the state of the system is described by a point in the phase space. This point is named the *representative point*. The totality of coordinates of the representative point gives the trajectory in the configuration or phase space, which, under certain initial conditions, parametrically specifies the behavior of the system in time. Knowing the trajectory of the system in the configuration space, we can go to the trajectory of motion over the potential energy surface.

The probability of branching of the elementary process to the  $\alpha$  channel ( $P_\alpha$ ) depends on many initial conditions, including the relative velocity  $v$ , quantum states of reactants  $a$ , quantum states of products  $a'$ , and impact parameter  $b$ . For the random choice of the initial conditions, taking into account the corresponding distribution functions, it is expressed by a rather simple formula

$$P_\alpha = \lim_{N \rightarrow \infty} (N_\alpha / N) \quad (2.55)$$

where  $N$  is the total number of calculated trajectories, and  $N_\alpha$  is the number of trajectories resulting in the reaction products in the channel  $\alpha$ .

However, in real cases, the finite number of trajectories is calculated.

The multiple numerical integration of system (2.55) on a computer for various initial conditions gives the dependence of  $P_\alpha$  on the initial parameters, and the cross section and microscopic rate constants are found from formulae (2.8) and (2.21).

For model PES, the dynamic problem was solved in the framework of both the classical and quantum approaches. A comparison of these calculations shows that the calculated averaged rate constants of chemical reactions usually agree satisfactorily. However, we have to keep in mind that there are classically

forbidden processes, such as tunneling and above-barrier reflection. These processes are most substantial for light particles or at low temperatures. Theoretical analysis in recent years showed that the description of quantum effects can be combined, in several cases, with classical methods.

### 2.2.3. Methods of semiclassical approximation

In these methods, all degrees of freedom of nuclei are divided into two groups, which we designate as  $R$  and  $Q$ . The degrees of freedom  $R$  are referred to the slow motions, and we will consider them as classical. The degrees of freedom  $Q$  correspond to the fast motions and will be considered quantum. The total Hamiltonian of the system is presented in the form

$$H = H_R + H_Q + U[Q, R(t)] \quad (2.56)$$

where  $H_R$  is the Hamilton function of classical degrees of freedom,  $H_Q$  is the Hamilton function of quantum degrees of freedom, and  $U[Q, R(t)]$  is the potential of interaction between the quantum and classical subsystems.

The classical trajectories  $R(t)$  are determined by equations of motion (2.53) for the effective Hamilton function  $H_{\text{eff}} = H_Q + U_{\text{eff}}$  in which  $U_{\text{eff}}$  is the  $U$  value averaged over  $Q$  for the specified state of the quantum subsystem.

The nonstationary Schrödinger equation should be solved for the description of transition between states of the subsystem  $Q$

$$\frac{i\hbar}{2\pi} \partial_x(Q, t) / \partial t = H \chi(Q, t) \quad (2.57)$$

where

$$H' = H_Q + U[Q, R(t)]$$

The wave function  $\chi(Q, t)$  is searched for as the expansion over the eigenfunctions  $\phi_n$  of the Hamiltonian  $H_Q$ . This expansion has the form

$$\chi(Q, t) = \sum_n a_n(t) \varphi_n \exp(-2\pi i E_n t / \hbar) \quad (2.58)$$

where  $E_n$  are the eigenvalues of the Hamiltonian  $H_Q$ .

Inserting expression (2.58) into the Shrödinger equation (2.57), we obtain the system of coupled differential equations for finding the expansion coefficients  $a_m(t)$

$$(i\hbar / 2\pi) \dot{a}_n = \sum_m a_m u_{nm}(t) \exp[-2\pi i (E_n - E_m) t / \hbar] \quad (2.59)$$

where  $u_{nm}$  is the matrix element of interaction

$$u_{nm}(t) = \int \varphi_n U U[Q, R(t)] \varphi_m dQ \quad (2.60)$$

If the matrix elements  $u_{nm}$  are sufficiently small, the coefficients  $a_n(t)$  can be found in the first order of the perturbation theory. If the system primarily (before the collision) existed in the  $m$ -th state and the initial time moment is referred to  $t \rightarrow -\infty$ , the initial conditions have the form

$$a_n(t \rightarrow -\infty) = \begin{cases} 1, n = m \\ 0, n \neq m \end{cases} \quad (2.61)$$

The solution of system (2.61) under these initial conditions, in the framework of the first-order perturbation theory, gives the following expression for  $a_n(t)$ :

$$a_n(t) = 2\pi \int_{-\infty}^t [u_{nm}(t) / i\hbar] \exp[2\pi i (\hbar) E_n - E_m) t] dt \quad (2.62)$$

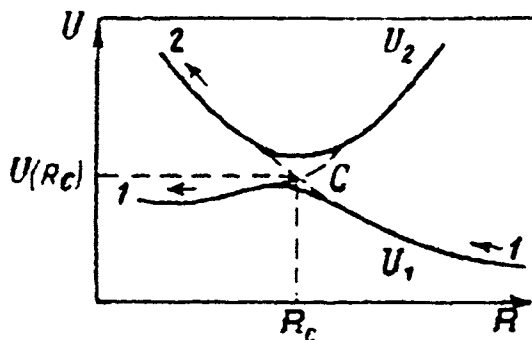


Fig. 2.10. Reaction profiles of the electronically nonadiabatic reaction ( $U_1$  and  $U_2$  are different potential curves):  $1 \rightarrow 1$ , adiabatic path; and  $1 \rightarrow 2$ , nonadiabatic path.

If we believe that the collision covers the time interval from  $-\infty$  to  $+\infty$ , then the probability of the existence of the system in the  $n$ -th state after the collision is the following:

$$P_{nm} = |a_n(t \rightarrow \infty)|^2 = 4\pi^2 \left| \int_{-\infty}^{\infty} \frac{u_{nm}(t)}{h} \exp \left[ -\frac{2\pi i}{h} (E_n - E_m) t \right] dt \right|^2 \quad (2.63)$$

This method can be applied to electronically nonadiabatic processes if in some region of nuclear configuration space the surfaces are strongly brought together. The method of "jumps" between potential energy surfaces is usually used for the description of these processes.

The picture of the dynamics of the nonadiabatic process in the framework of this approach is illustrated in Fig. 2.10. The representative point moves along the trajectory  $R_1(t)$  over the surface  $U_1$  until it reaches the surface  $U_2$ . During the further motion the trajectory is branched. There is the probability  $P_{12}$  that the representative point jumps on the surface  $U_2$  and further moves on this surface along the trajectory  $R_2(t)$ . The representative point remains on the surface  $U_1$  and continues to move on it with the probability  $1 - P_{12}$ . The probabilities of the jump can be calculated in the framework of the semiclassical approximation if we consider that electrons compose the quantum subsystem (the coordinates  $Q$  are replaced by the coordinates of electrons  $r$ ) and nuclei compose the classical

subsystem. Then the  $H$  Hamiltonian implies the electronic Hamiltonian  $H_e$ , and the function  $\chi(Q, t)$  is the electronic wave function  $\varphi(r, t)$ .

Let us consider the following model as an example. Let adiabatic terms 1 and 2 in the region of their approaching have the shapes of hyperbolas (Fig. 2.10). Represent the asymptotes of these hyperbolas in the form  $U_1 = -F_1(R - R_c)$  and  $U_2 = -F_2(R - R_c)$ , where  $F_1$  and  $F_2$  are slopes of hyperbolas in the point of their intersection. Designate the minimum distance between  $U_1$  and  $U_2$  as  $2U_{12}$ . Let us assume that the trajectory  $R(t)$  can be presented in the form

$$R(t) = R_c + v_{\perp} t$$

where  $v_{\perp}$  is the component of the relative velocity of nuclear motion normal to the line of intersection of surfaces.

For this model, Landau and Ziner calculated the probability of the nonadiabatic transition

$$P_{12} = \exp[-2\pi|U_{12}(R_c)|^2 / \hbar v_{\perp} |F_1 - F_2|] \quad (2.64)$$

This formula immediately demonstrates the qualitative result: the lower the velocity  $v_{\perp}$  and the larger the distance between the adiabatic surfaces of the potential energy  $U_1$  and  $U_2$ , the lower the probability of the jump.

#### 2.2.4. Method of activated complex

The method of activated complex (AC) (it is also often called the transition state theory) is applied for the calculation of rate constants of equilibrium adiabatic direct reactions, whose reaction profile has the shape shown in Fig. 2.8, *a*. This method is based on the high degree of averaging of the calculated characteristics of reactions, which makes it possible to calculate the rate constants without the consideration of the collision dynamics. This method was proposed by Eyring, Wigner, Peltzer, Evans, and Polanyi in the thirties and developed in later works.

The theory is based on the fact that the bimolecular or unimolecular reaction occurs through an intermediate state, which is named the *activated complex*. For example,  $A + B \rightarrow AB^{\#} \rightarrow C + D$ , where  $A^{\#}$  is the activated complex. Unlike long-lived intermediate complexes, the activated complex has the short lifetime and decomposes only in the direction of products.

When the reaction is considered by the method of classical trajectories, the system is described by equation (2.55) where the Hamilton function is specified by expression (2.56). Then the reaction can be considered as the motion of the representative point in the phase space  $\Gamma$ .

Let us divide the phase space  $R_i, P_i$  into two subspaces by some critical surface  $S^\#$ . The first subspace corresponds to the reactants, and the second subspace corresponds to the reaction products. Determine the reaction coordination  $R_r = q_r$  in such a way that it is perpendicular to the critical surface  $S^\#$ . The  $q_r$  value on the  $S^\#$  surface that characterizes the configuration of the activated complex will be designated as  $q_r^\#$ . It is assumed that the reaction has occurred if the representative point had crossed the critical surface in the direction of the reaction products. Then the reaction rate is determined as a flow of representative points along  $q_r$  through  $S^\#$  in the direction of the products.

Introduce the dimensionless phase volume

$$d\Gamma = \frac{dR_1 dP_1}{h} \dots \frac{dq_r dP_r}{h} \dots \frac{dR_s dP_s}{h}$$

which characterizes the number of quantum states of the system. Let the distribution of representative points over these states is specified by the  $f(R_i, P_i)$  function. Then the number of representative points (particles) in the phase volume  $d\Gamma$  is determined as

$$dN = f(P_i, R_i) d\Gamma \quad (2.65)$$

and in the whole phase volume as

$$F = \int f(P_i, R_i) d\Gamma \quad (2.66)$$

The  $F$  value is named the statistical integral.

The reaction rate in the elementary volume of the phase space is equal to the rate of changing the number of representative points

$$\frac{dN}{dt} = f(P_i, R_i) \frac{d\Gamma}{dt} = f(P_i, R_i) d\Gamma^\# \frac{dq_r}{dt} dP_r \quad (2.67)$$

where  $d\Gamma' = \prod_{i,r} \frac{dp_i dq_i}{h}$  is the elementary phase volume on the  $S^\#$  surface, *i.e.*, the elementary phase volume of the activated complex.

In order to obtain the full rate  $W$ , we have to integrate equation (2.67) over the whole  $S^\#$  surface and over all rates with which it is intersected. The rate constant of the elementary reaction is determined as the rate of this reaction referred to unit concentrations. Therefore, the  $W$  rate should be divided by the statistical integral  $F$ . As a result, we obtain

$$k_{AK} = \frac{d\Gamma}{dt} \int_0^\infty \int_{\Gamma^\#} f(P_i, R_i) d\Gamma^\# \frac{dq_r}{dt} dP_r \quad (2.68)$$

It is assumed in the activated complex method that  $f(R_i, P_i)$  is equilibrium both in the region of reactants and on the  $S^\#$  surface. Then the distribution function has the form

$$f(P_i, R_i) = \exp[H(P_i, R_i) / k_B T] \quad (2.69)$$

The integral in (2.70) is taken with respect to the phase volume  $d\Gamma^\#$  on the  $S^\#$  surface. Therefore, when inserting  $f(R_i, P_i)$  into (2.68), the Hamilton function in expression (2.69) should also be taken for the  $S^\#$  surface.

The second assumption of the theory is that the Hamilton function of the system on the  $S^\#$  surface can be presented in the form

$$H|_{S^\#} = H^\# + E_{\text{transl}} + E_0 \quad (2.70)$$

where  $H^\#$  is the Hamilton function of the activated complex, which depends on all coordinates of the phase space except for  $q_r$  and  $P_r$ ; and  $E_0$  is the difference of minimal energies on  $S^\#$  and in the space of reactants.

When inserting expressions (2.68) and (2.69) into (2.70) and integrating with respect to  $E_{\text{transl}} (dE_{\text{transl}} = q_r dP_r)$ , we have for the rate constant of the elementary reaction

$$k = \frac{k_B T}{h} \frac{F^\ddagger}{F} \exp[-E_0 / k_B T] \quad (2.71)$$

where

$$F^\ddagger = \int_{\Gamma^\ddagger} \exp[-H^\ddagger / k_B T] d\Gamma^\ddagger \quad (2.72)$$

is the statistical integral for the activated complex.

Expression (2.73) for the rate constant is valid for both uni- and bimolecular reactions. In the case of the bimolecular reaction  $A + B \rightarrow C + D$ , the statistical integral  $F$  is divided into the product of statistical integrals for each molecule, *i.e.*,

$$F = F_A F_B \quad (2.73)$$

Deriving formula (2.73), we assumed that all trajectories crossing  $S^\ddagger$  leads to the reaction products only. In fact, representative points can return into the subspace of the reactants. In order to take into account this possibility, the so-called transmission factor  $\kappa$  is introduced into the formula for the rate constant

$$K_{AK} = \kappa \frac{k_B T}{h} \frac{F^\ddagger}{F} \exp\left(-\frac{E_0}{k_B T}\right) \quad (2.74)$$

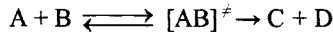
The introduction of the transmission factor also takes into account quantum effects. For example, taking into account the above-barrier reflection leads to  $\kappa < 1$ , and the tunneling effect, by contrast, can result in  $\kappa > 1$ .

Difficulties associated with the choice of the critical surface can appear when the AC theory is used for processes with a low potential barrier. The variational approach was proposed to overcome these difficulties: a search for the minimum of the rate constant varying the position of the critical surface, namely, the  $q_r^\ddagger$  value. This consideration showed that the activated complex was localized at the maximum of the Gibbs energy.

The quantum-mechanical variant of the activated complex theory was also considered. The expression for the rate constant retains the form (2.76) but  $F^\ddagger$

and  $F$  here apply the corresponding quantum partition functions and  $E_0$  is the difference including zero-point vibrational energies and ground state of the activated complex and reactants (see Fig. 2.7).

Let us give the thermodynamic interpretation of the rate constant in the framework of the activated complex theory. The direct bimolecular reaction occurs. If the C and D products are rapidly removed from the system to prevent reverse reaction involving them, then reaction 1 can be presented in the form



The reactants A and B and activated complexes  $[AB]^\ddagger$  are at equilibrium and the C and D products that formed have no effect on the equilibrium concentration of the activated  $[AB]^\ddagger$  complexes. This is the main assumption of the activated complex theory, which was manifested above in the choice of the equilibrium distribution function independent of the reaction products. The equilibrium constant  $K^\ddagger$  between the reactants and activated complexes can be expressed through the corresponding partition functions (see Table 2.1)

$$K^\ddagger = (F^\ddagger / F_A F_B) \exp(-E_0 / k_B T) \quad (2.75)$$

Using (2.77), expression (2.76) can be presented in the form

$$k = \kappa (k_B T / h) K^\ddagger \quad (2.76)$$

Using formula (2.43) for  $K^\ddagger$ , we can write

$$k = \kappa \frac{k_B T}{h} \exp(\Delta G^\ddagger / k_B T) \quad (2.77)$$

where  $\Delta G^\ddagger$  is the difference of the Gibbs energies of the reactants and activated complex under standard conditions.

At a constant temperature the  $\Delta G^\ddagger$  is expressed through the standard changes in the enthalpy  $\Delta H^\ddagger$  and entropy  $\Delta S^\ddagger$

$$\Delta G^\ddagger = \Delta H^\ddagger - T \Delta S^\ddagger \quad (2.78)$$

From (2.80) we obtain the expression for the reaction rate constant through the thermodynamic values

$$k = \kappa \frac{kT}{h} \exp\left(\frac{\Delta S^\ddagger}{k_B}\right) \exp\left(\frac{\Delta H^\ddagger}{k_B T}\right) \quad (2.79)$$

The relationship between the activation energy  $E$  and  $\Delta H^\ddagger$  is given by the expression

$$\Delta H^\ddagger = E_{aKT} - xRT, \quad x = 1 - \Delta n^\ddagger$$

where  $\Delta n^\ddagger$  is the change in the number of moles for the formation of 1 mole of the activated complexes.

Reference books usually give thermodynamic values at the standard state of reactants corresponding to 1 mole of the gas at a pressure of 1 atm (designated as  $\Delta S^\ddagger$ ). Therefore, the rate constant calculated by formula (2.81) has the dimensionality atm/s for bimolecular reactions. The rate constant with the dimensionality  $\text{cm}^3/(\text{mol s})$  for bimolecular reactions and  $\text{s}^{-1}$  for unimolecular reactions has the form

$$k = \kappa \frac{kT}{h} e^{x(RT)^{x-1}} \exp\left(-\frac{\Delta S_p^\ddagger}{R}\right) \exp\left(-\frac{E_{aKT}}{RT}\right) \quad (2.80)$$

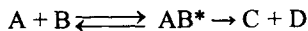
where  $R$  is the gas constant.

For unimolecular reactions  $x = 1$ , and for bimolecular reactions  $x = 2$ .

### 2.2.5. Statistical theory of bimolecular reactions

The statistical theory can be applied to the calculation of rate constants of bimolecular reactions that occur through a long-lived complex. Probable reaction profiles of such reactions are shown in Fig. 2.8.

Let us consider the reaction



where the intermediate excited molecules  $AB^*$  are named the active molecules or the long-lived intermediate complexes.

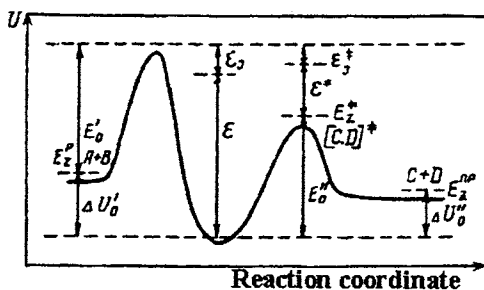


Fig. 2.11. Energy diagram of the bimolecular reaction occurred through the long-lived complex.

The statistical theory of bimolecular reactions is based on two assumptions:

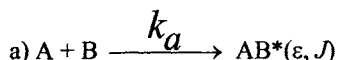
- (1) the formation of active  $AB^*$  molecules and their decomposition are considered independent;
- (2) the rate constants of  $AB^*$  decomposition can be calculated in the framework of the statistical theory of unimolecular reactions.

The latter assumption makes it possible to understand the term "long-lived complex." The lifetime of the  $AB^*$  molecule before its decomposition should have such a value that the energy released at the step of  $AB^*$  formation had time to be statistically redistributed over all internal degrees of freedom of the  $AB^*$  molecule.

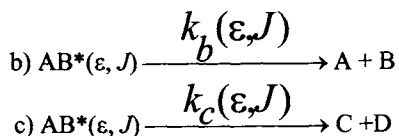
Figure 2.11 exemplifies the energy diagram for reaction 1. At the first step the  $AB^*$  molecule is formed, which, according to the energy conservation law, has the energy  $\Delta U_0 + E_0$ . It consists of two parts: the first part is the rotational energy of the  $AB^*$  molecule, which depends on  $J$  (designate this part of the energy  $\epsilon_J$ ); the second part is the energy on the internal degrees of freedom of the  $AB^*$  molecule. Designate this energy through  $\epsilon$ .

The  $AB^*$  molecules can be characterized as active  $AB^*(\epsilon, J)$  molecules (see 2.1.5) with different values of  $\epsilon$  and  $J$ .

They are formed in the thermal association reaction



The first statement of the statistical theory on the independent character of the steps of  $AB^*(\epsilon, J)$  formation and decomposition allow us to present the further reactions as microscopic reactions



Let us present the rate of formation of the C and D products as  $k_1(T)[A][B]$ . The statistical theory relates  $k_1(T)$  to  $k_a(T)$  and microscopic decomposition rate constants  $k_b(\epsilon, T)$  and  $k_c(\epsilon, T)$ , which can be calculated using the statistical theory.

For polyatomic molecules, in the calculation of decomposition rate constant, their dependence on the quantum number  $J$  can often be neglected. This approximation is possible because polyatomic molecules have very many vibrational degrees of freedom. In the framework of this approximation, the thermal rate constant of reaction 1 can be expressed as follows:

$$k_1(T) = k_a^\infty(T) \int_{\Delta U_0}^{\infty} \frac{k_c(\epsilon)}{k_c(\epsilon) + k_b(\epsilon)} f(\epsilon) d\epsilon, \quad (2.81)$$

where  $f(\epsilon)$  is the normalized distribution function of the  $AB^*(\epsilon)$  molecules over the  $\epsilon$  energy.

In order to obtain the expression for  $f(\epsilon)$ , let us consider the situation where only reactions  $a$  and  $b$  occur at equilibrium. Then the decomposition rate of the  $AB^*(\epsilon)$  molecules within the energy interval from  $\epsilon$  to  $\epsilon + \epsilon$  in the direction  $\sigma$  is the following:

$$W_\sigma = k_a(\epsilon) f_b(\epsilon) d\epsilon[AB] \quad (2.82)$$

It follows from the principle of detailed balancing that this rate is equal to the rate of formation of the  $AB^*(\epsilon)$  molecules in reaction  $a$ , *i.e.*,

$$W_a = k_a(\varepsilon)f_b(\varepsilon) d\varepsilon[AB] \quad (2.83)$$

The overall rate  $W$  of reaction  $a$  is the following:

$$W_a = \int_{E_0}^{\infty} k_a(\varepsilon)f_b(\varepsilon) d\varepsilon \quad (2.84)$$

When accepted that  $f(\varepsilon)$  is equal to the  $W_a(\varepsilon)/W_a$  ratio, then we have

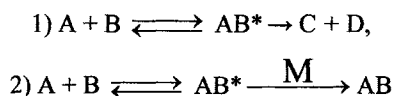
$$f(\varepsilon) = k_a(\varepsilon)f_b(\varepsilon) / \int_{\Delta U'_0}^{\infty} k_b(\varepsilon)f_b(\varepsilon)d\varepsilon. \quad (2.85)$$

If the first step  $a$  occurs with an energy barrier, the  $k_a(T)$  can be calculated by the activated complex theory. If step  $a$  occurs without a barrier (for example, radical recombination), then  $k_a$  has the value close to  $Z_0$ , which can be estimated taking into account dispersion forces of interaction.

A possibility of the deactivation of  $AB^*(\varepsilon)$  was ignored in the considered kinetic scheme. Therefore, in the general scheme, the deactivation process similar to process 1 in Section 2.1.5. should be added to the kinetic scheme consisting of reactions  $a \rightarrow c$



The rate constant of process  $d$  is often accepted according to formula (2.32):  $k_d = Z_0P$ , where  $P$  is the efficiency of the collision. Then reaction 1 can be presented in the form



This scheme contains two channels of the formation of products:  $C + D$  and  $AB$ . If  $k_1(T)$  is the rate constant of the formation of the  $C$  and  $D$  products and  $k_2(T)$  is the rate constant of  $AB$  product formation, then we can write the following expressions for these rate constants:

$$k_1(T) = k_a(T) \int_{E_0}^{\infty} f(\epsilon) \frac{k_c(\epsilon)}{k_c(\epsilon) + k_b(\epsilon) + k_d[M]} d\epsilon \quad (2.86)$$

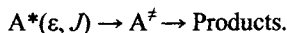
$$k_2(T) = k_a(T) \int_{E_0}^{\infty} \frac{k_c(\epsilon)}{k_c(\epsilon) + k_b(\epsilon) + k_d[M]} d\epsilon \quad (2.87)$$

At high pressures when  $k_d(T) \gg k_b(T)$  and  $k_c(T)$ , it follows from formula (2.88) that  $k_2(T) = k_a(T)$ .

### 2.2.6. Statistical theory of unimolecular reactions

In Section 2.2.4 we obtained expression (2.76) for the rate constant on the basis of the activated complex method. This expression is applicable for the calculation of equilibrium rate constants of unimolecular reactions, in particular,  $k_{\infty}(T)$  under the conditions when the temperature of reactants is constant ( $T = \text{const}$ ).

Then consider the microscopic reaction



The statistical theory makes it possible to calculate the microscopic rate constant  $k(\epsilon, J)$  of this reaction. The main assumption of the statistical theory is that the energy on the internal degrees of freedom in the active molecule and activated complex is statistically redistributed. This assumption is fulfilled rather well for vibrations and internal rotations. As for the rotational energy of the molecule as a whole (active molecule, activated complex), this energy only partially can exchange with the energy of internal degrees of freedom. This is related to the necessity of fulfillment of the law of conservation of the angular momentum  $J$ . Let us return to the rotational energy somewhat later and now we assume that the  $A^*$  and  $A^\ddagger$  molecules do not rotate. Then the dependence of the microscopic rate constant on  $J$  disappears and it can be written as  $k(\epsilon)$ .

For the calculation of  $k(\epsilon)$  we apply the microscopic activated complex theory, which considers probabilities of the existence of a system with the energy between  $\epsilon$  and  $\epsilon + d\epsilon$  in the phase space of the reactants  $\Gamma$  and on the critical surface  $S^\ddagger$ . In this case, we should obtain a formula similar to (2.70). The latter consists of three cofactors:  $1/F$ ,  $\int dE_{\text{trans}}$ , and  $\int f(P_i q_i) d\Gamma^\ddagger$ . For the microcanonical

consideration, the whole phase volume is restricted by the hypersurfaces  $H = \varepsilon$  and  $H + dH = \varepsilon + d\varepsilon$ . Then the following microcanonical analogs should be placed into formula (2.70):

$$\int_{\Gamma} f(P_b, R_i) d\Gamma = \rho(\varepsilon); \quad \int_{\Gamma^\ddagger} f(P_b, R_i) d\Gamma^\ddagger = \rho(\varepsilon^\ddagger)$$

After the insertion of these analogs into (2.70), we have

$$k(\varepsilon) = \int \rho(\varepsilon^\ddagger) dE_{\text{transl}} / h \rho(\varepsilon)$$

If taking into account that  $\varepsilon^\ddagger = \varepsilon - E_0$  and  $\int \rho(\varepsilon^\ddagger) d\varepsilon^\ddagger = W(\varepsilon^\ddagger)$  is the number of quantum states of the activated complex with the energy  $\varepsilon^\ddagger$ , we obtain

$$k(\varepsilon) = W(\varepsilon - E_0) / h \rho(\varepsilon) \quad (2.88)$$

Now let us analyze what contribution to the  $k(\varepsilon)$  is made by rotations of the  $A^*$  molecule and  $A^\ddagger$  as a whole. With this purpose, both the  $A^*$  and  $A^\ddagger$  molecules are simulated by a noninteracting two-dimensional rotator and a one-dimensional rotator with the maximum rotational constant. The one-dimensional rotator corresponds to the rotation about the cleaved bond. In this consideration, the one-dimensional rotator is included into the system of internal free rotations, and the angular momentum  $J$  is ascribed to the two-dimensional rotator. Thus, the rotation of a molecule as a whole increases the number of internal degrees of freedom. Let us understand  $\varepsilon$  as the energy of internal degrees of freedom of the  $AB^*$  molecule taking into account one degree of freedom from the rotation of the molecule as a whole. Designate the energy of the two-dimensional rotator  $\varepsilon_j$  for the active molecule and  $\varepsilon_j^\ddagger$  for the activated complex. The energy diagram is shown in the right part in Fig. 2.11.

The law of conservation of energy requires the equality to obey

$$\varepsilon + \varepsilon_j = \varepsilon^\ddagger + E_0 + \varepsilon_j^\ddagger \quad (2.89)$$

On going from the active molecule to the activated complex, the quantum number  $J$  remains unchanged, and the moments of inertia change. This results in the situation when the difference of the energies  $\Delta\varepsilon_j = \varepsilon_j - \varepsilon_j^\ddagger$  is released on the internal degrees of freedom of the activated complex, and  $\Delta\varepsilon_j$  depends on  $J$ . Taking into account this fact results in  $\varepsilon^\ddagger = \varepsilon + \Delta\varepsilon_j(J) - E_0$  depends on  $J$ . If the

$L$  factor, which takes into account equivalent routes of activated complex decomposition, is added, formula (2.88) can be rewritten in the form

$$k(\epsilon, J) = \frac{W[\epsilon + \Delta\epsilon_j - E_n]}{h\rho(\epsilon)} L \quad (2.90)$$

Thus, the problem is reduced to the calculation of the numbers and densities of quantum states, which can be referred to internal degrees of freedom. These degrees of freedom are sometimes named *active* unlike two degrees of freedom directly related to the conservation of the angular moment, which are named *adiabatic*.

The methods for the calculation of  $k(\epsilon, J)$  are related to the RRKM theory (abbreviation of the first letters of surnames of scientists who developed the theory: Rice, Ramsperger, Kassel, Marcus).

In the framework of this theory, it is assumed for the calculation of  $W(\epsilon + \Delta\epsilon_j (J) - E_n)$  and  $\rho(\epsilon)$  that the active molecule  $A^*$  and activated complex  $A^\ddagger$  is presented as a system of noninteracting between each other  $S(S^\ddagger)$  oscillators and  $r(r^\ddagger)$  free internal rotators.

Due to the quantization of levels, the  $W(\epsilon + \Delta\epsilon_j (J) - E_n)$  and  $\rho(\epsilon)$  functions are discontinuous. Smooth approximations of these functions, which can be found in recommended literature, are used for practical calculations. These formulae are rather cumbersome and, hence, are not presented in this consideration.

The macroscopic rate constant of monomolecular reactions can be calculated if  $k(\epsilon, J)$  and the distribution function  $f(\epsilon, J)$  are known. So, the rate constant of unimolecular reactions  $k_\infty$  in the limit of high concentrations  $[M]$  can be calculated by formula (2.36) if the distribution function  $f_b(\epsilon, J)$  is accepted in the form

$$f_b(\epsilon, J) = \frac{\rho(\epsilon) \exp(-\epsilon/k_B T)}{F_{vib}} \frac{(r_j + 1) \exp(-\epsilon_j/k_B T)}{F_{rot}}$$

and the energy of two-dimensional adiabatic rotators  $\epsilon_j$  and  $\epsilon_j^\ddagger$  is taken into account.

Note that after the calculations the expression for  $k_\infty(T)$  should coincide with

expression (2.71) from the transition state theory.

The considered approach is applicable to unimolecular reactions with a potential barrier (the reaction profiles of these reactions are presented in Fig. 2.9). If the barrier is absent (the reaction profile is shown in Fig. 2.9, a), the potential energy surface does not allow us to determine either the position or the structure of the activated complex.

In this case, the so-called *statistical theory of adiabatic channels* is used. In this theory, the vibration-rotational energy levels  $\epsilon_n^J$  corresponding to the certain  $J$  are calculated at each specified value of the reaction coordinate  $q_r$ . The examples of such potential curves are shown in Fig. 4.12, where  $W(\epsilon + \Delta\epsilon_j(J) - E_\delta)$  is identified with the total number of such potential curves along which with the specified total energy  $E_n = \epsilon + \epsilon_j$  one can get into the region of decomposition products.

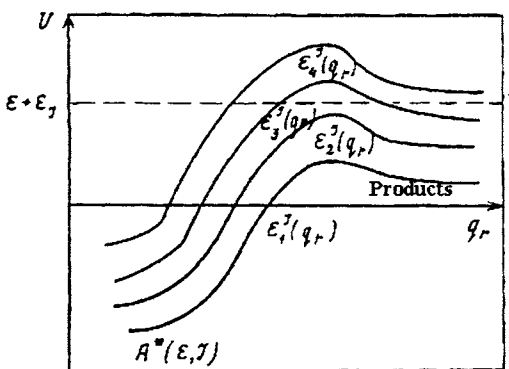


Fig. 2.12. Potential curves of adiabatic channels with different values of the angular momentum  $J$ .

In Fig. 2.12 two potential curves  $\epsilon_1^J(q_r)$  and  $\epsilon_2^J(q_r)$  satisfy this condition. In addition, it is seen in Fig. 2.12 that the potential curves  $\epsilon_n^J(q_r)$  can have maxima corresponding to different activated complexes. In order to introduce the single activated complex, the variational principle is used: at each  $q_r$  value the number of quantum states  $W(\epsilon + \Delta\epsilon_j(J) - E_\delta)$  is calculated.

The value  $q_r = q_r^\#$  at which this value is minimum corresponds to the activated complex.

Thus, the rate constant for this type of unimolecular reactions is also expressed by formula (2.90), and only approaches to calculation change.

*Chapter 3***Methods for Studying Elementary Reactions**

The greatest difficulties appear in studying elementary processes if reactants are atoms, radicals, and rotationally, vibrationally, or electronically excited molecules. Such species very rapidly react with others and, hence, their lifetimes are short. Short-lived reactive species are conventionally named active species.

Any experimental equipment for studying elementary processes involving active species includes methods of their generation and detection. However, the methods for detection and generation of species are determined by conditions under which elementary processes are studied. The choice of these conditions depends on the pressure and temperature region in which the elementary process occurs, the type of the studied elementary process, and the level of microscopicality at which information can be obtained. Depending on these factors, experimental conditions turned out to be so specific that certain approaches based on special techniques had to be developed. So, an elementary process can be studied in shock tubes, crossed molecular beams, under flow conditions, and in static reactor with time-resolved spectroscopy. These approaches were standardized and called methods for studying elementary processes.

*3.1. Instrumental methods for experiments**3.1.1. Supersonic jet and molecular beam*

Supersonic speeds of a moving gas found use for getting very low temperatures ( $<20$  K) with the purpose for studying elementary photophysical and photochemical reactions and spectroscopy of intermediates. Spectroscopists meet experimental difficulties in detection and identification of rotationally resolved spectra in studying both spectra of short-lived species and stable molecules. A great geometrical size of a molecule or a large molecular mass result in relatively small distances between rotational energy levels and, hence, spectral lines in the spectrum. Due to this, a "rich" (with many spectral lines per unit spectral interval) spectrum is observed, and it is difficult to identify it. To obtain a less "rich" spectrum, we can use the fact that at a temperature decrease the population of higher rotational energy levels decreases, which results in a decrease in the intensity of the spectral lines related to transitions from these energy levels. At the same time, the intensity of other lines associated with tran-

sitions from low-lying rotational energy levels increases strongly due to an increase in the population of these levels.

It is much easier to identify such a spectrum, rather "depleted" in lines and obtained by strong cooling. Cooling of molecules or radicals in a supersonic gas jet flowing through a nozzle occurs because the temperature of the gas and the velocity of its motion are related by the energy conservation law. For the adiabatic (without convection and removal of energy) flow of the ideal gas, the total gas energy referred to the unit gas mass  $C_p T + V^2/2 = \text{const}$  is conserved, where  $C_p$  is the specific heat capacity of the gas under a constant pressure,  $T$  is the gas temperature, and  $V$  is the gas velocity.

If at first the gas was at rest in the volume in front of the nozzle, i.e.,  $V_0 = 0$ , and the temperature of the gas was  $T_0$ , then the total energy of the unit gas mass will be related to the parameters of the initial state of the gas by the relation

$$C_p T + V^2/2 = C_p T_0$$

It follows from these relations that the gas is cooled with an increase in the velocity, and vice versa, a decrease in the velocity results in its heating. The mechanism of the transition of the kinetic energy of the chaotic motion of gas molecules to the directed motion of the gas as a whole is related to the fact that molecules upon collision with the nozzle walls "are directed" along the nozzle axis. Thus, the component of motion of molecules along one coordinate increases and the components along other coordinates decrease. The nozzle thus forms the directed gas jet. From the nozzle the beam gets into the first preliminary chamber in which the pressure is  $10^{-3}$  Torr. To form the molecular beam in which collisions between particles are absent, the jet is collimated and then the beam gets into another chamber. Each chamber contains an autonomic pumping out of an excess gas.

### 3.1.2. Crossed molecular beams

The method makes it possible to obtain a less averaged information on elementary processes. The main advantages of the method of crossed molecular beams compared to other methods is that it allows one to study individual collisions of two particles, which have specified quantum states and also determined translational velocities. This method is used for studying the dynamics of an elementary process involving stable molecules in the ground and excited states, atoms and radicals, van der Waals dimers, and ions.

The principal scheme of this method is presented in Fig. 3.1. As can be seen, two molecular beams are needed, which are crossed in a large chamber. To study individual collisions of two particles, the background pressure in the main chamber should be at least  $10^{-6}$  Torr. The elementary process can occur only in the region of crossing molecular beams. Sources of molecular beams should contain a velocity

selector, which provides the variation of velocities in a great enough interval and minimal scatter over velocities in the beam.

In recent time, molecular beams are formed passing the gas through a nozzle with a supersonic speed. From the nozzle the beam gets into the first preliminary chamber in which the pressure is  $10^{-3}$  Torr. After collimating the beam gets into another chamber. Each chamber has an autonomic pumping out of an excess gas.

Modern time-of-flight mass spectrometers, which can be rotated around the region of crossing of molecular beams, are used as detectors. Particles in definite quantum states are detected by laser methods. The method of laser-induced fluorescence is used most frequently.

In some experiments the beam of one particle passes through a collision cell filled with a rarefied gas. This technique is named the "beam-gas" technique. It does not allow one to determine angular and velocity distribution of the scattered particles but gives a pattern of the energy distribution in reaction products with the help of methods of chemiluminescence or laser-induced fluorescence.

### 3.1.3. Static and flow methods

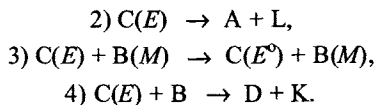
Two types of reactors, static and flow, can be distinguished.

Reactants C (or C and B) and buffer gas M are loaded into a static reactor. The mixture is subjected to flash photolysis to form active species. Active species or reaction products are detected several time intervals after a photopulse. This approach to studying elementary reactions was proposed by Norrish and Porter, and this procedure in 1967 was awarded with the Nobel Prize.

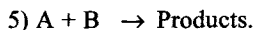
As a result of a short light pulse, the light is absorbed to form an excited species  $C(E)$



The excited species  $C(E)$  either dissociates or participates in the bimolecular process of energy transfer or in the chemical reaction



Thus, processes 2-4, i.e., processes involving excited species, can be studied in a static reactor. However, rather often photodissociation process 2 occurs very rapidly to form the active species A, which can be a radical or other excited species. In the case, the following elementary process is studied:



Therefore, substance C serves for the creation of active species. Concentrations of active species A or C(E) or products of their reactions are detected by absorption or fluorescence spectroscopy. Most often active species are detected by a pulse technique. To study the kinetics of short-lived species, the delay time between the photolyzing and probe pulses is changed.

Presently, studies of elementary processes in a static reactor gained a wide use because of the development of the pulse technique of the creation and detection of active species. With the development of the sensitivity and time resolution of laser spectroscopy methods, possibilities of studies in a static reactor were extended. These possibilities are described schematically in Table 3.1.

Note that sometimes the modification of the method of static reactor is used when the slow flow of the gas is performed through the reactor and photolyzing pulses are repeated. In this modified method, the duration of the gas flow through the reactor is much longer than the duration of studying the reaction and, therefore, the reactor can still be considered static. The role of the slow jet corresponds to the creation of gas mixture without products to the time of the subsequent photolyzing pulse.

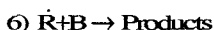
Note one more important feature appeared with the development of the static reactor method. In the classical variant of the method, the whole gas mixture in the reactor was subjected to pulse photolysis, and a high energy of the photolyzing pulse was required. However, laser methods possess a spatial resolution, *i.e.*, they allow the photolysis and detection of species in a local small volume. This provides the use of photopulses with a lower energy, *i.e.*, the generation of active species under milder conditions. When spectroscopy with spatial resolution is used, we have to create conditions under which diffusion processes could be neglected.

Table 3.1. Types of studied elementary processes using time-resolved laser spectroscopy

Time resolution	Types of studied elementary processes
Milli- and microsecond spectroscopy, 10 <sup>-3</sup> —10 <sup>-7</sup> s	Reactions of radicals
Nanosecond spectroscopy, 10 <sup>-8</sup> —10 <sup>-10</sup> s	Inelastic energy transfer processes Instrumental methods for experiments hemical processes at microscopic level: photodissociation, energy distribution in products of elementary reactions, reactions of excited species
Picosecond spectroscopy, 10 <sup>-11</sup> —10 <sup>-13</sup> s	Photodissociation processes, intramolecular processes
Femtosecond spectroscopy,	Dynamics of intramolecular processes

In a flow reactor the reaction is studied in the continuous jet of gases consisting of reactants dilute with an inert gas (helium, argon, nitrogen, etc.). The flow method is used for studying equilibrium reactions of atoms and radicals, although it is recently applied for studying processes involving excited species.

An SHF discharge is usually used as a source of atoms A. Polyatomic radicals are usually generated by fast reactions of atoms with stable molecules C. With this purpose, reactant C is selected in such a way that in its excess all atoms A react very rapidly to form a required radical  $\cdot R$ :  $A + C \rightarrow \cdot R$ . Then we may consider that the flow of radicals  $R\cdot$  moves to which the second reactant B is admixed. To study the reaction



two methods can be used. If the reaction is studied in the zone of reactant mixing, the method is named diffusional. Another limiting case is the study of the reaction under conditions where the complete mixing of reactants took place.

The diffusional method was proposed by M. Polanyi. The simplified method is the following. Active species from a narrow nozzle in a diffusional regime get into a reactor with reactant B and buffer gas M. If collisions with the reactor walls can be ignored, reaction 6 occurs in the spherical zone, and the distribution of the concentrations of  $R\cdot$  over the sphere radius obeys the equation

$$D \left\{ \frac{d^2 [\dot{R}]}{dr^2} + \frac{2}{r} \frac{d[\dot{R}]}{dr} \right\} = k_{\text{eff}} [\dot{R}], \quad (3.1)$$

where  $D$  is the coefficient of diffusion of active species  $R$  in a mixture of gases B and M;  $k_{\text{eff}} = k_6[B]$ .

Taking into account the boundary condition  $[\dot{R}] = 0$  at  $r \rightarrow \infty$ , the solution of (3.1) has the form

$$[\dot{R}(r)] = \frac{k_{\text{eff}} \int_0^\infty [\dot{R}(r)] r^2 dr}{Dr} \exp \left( -r \sqrt{\frac{k_{\text{eff}}}{D}} \right). \quad (3.2)$$

When measured somehow the concentration  $[\dot{R}]$  in different points of the diffusional cloud, we can find  $k_{\text{eff}}$  and, hence, the rate constant  $k_6$ .

Further several researchers developed this method as applied to the conditions of the fast gas flow. V.L. Talroze and A.M. Dodonov created the method of mass spectrometric probing of the diffusion cloud in the flow along the axis of a cylindrical reactor where the flow velocity is maximum. In this case, the diffusion cloud is extended along the reactor axis.

Another modification of the diffusion method is the integral diffusion method developed by Yu.M. Gershenzon and B.F. Monin. In this method the cut of the nozzle is located at the inlet to the cavity of an ESR spectrometer. The reaction is studied directly in the zone of diffusional mixing of reactants. The ratio of the ESR signals in the presence and absence of reactant B is measured. Since the ESR signal is proportional to the total number of active species in the diffusion cloud, the method is integral.

In the jet method, for mixed reactants the concentration of active species  $R\cdot$  due to reaction 6 decreases along the jet. This decrease, which is experimentally detected by spectrometric methods, allows  $k_6$  to be determined. Difficulties appeared in this method are associated with the decay of active species in collisions with the reactor surface, necessity to take into account longitudinal and transversal diffusion, and nonuniformity of the distribution of the flow velocity over the tube cross section. Experiments are usually performed under conditions where the distribution of the concentration of active species and the nonuniformity related to Poiseuille's flow can be neglected.

Then the change in the concentration of active species is described by the equation

$$D \frac{d^2 [\dot{R}]}{dx^2} - \bar{U} \frac{d[\dot{R}]}{dx} + (k_{\text{eff}} + k_r) [\dot{R}] = 0 \quad (3.3)$$

where  $\bar{U}$  is the average flow velocity;  $x$  is the axis directed along the flow;  $k_r$  is the rate constant of heterogeneous decay of radicals in the kinetic region referred to volume unit ( $k_{\text{eff}} = evd$ , where  $d$  is the diameter of the reactor,  $v$  is the thermal velocity of molecules, and  $e$  is the probability of decay of an active species within one collision with the reactor surface).

Equation (3.3) has the following solution:

$$[\dot{R}] = [\dot{R}]_0 \exp(-\beta x) \quad (3.4)$$

where

$$\beta = \frac{\bar{U}}{2D} \left[ \sqrt{1 + \frac{(4k_{\text{eff}} + k_r)D}{\bar{U}^2}} - 1 \right] \quad (3.5)$$

The desired rate constant  $k_6$  can be calculated from the expression

$$k_6 [B] = \bar{U} \beta + D \beta^2 - k_r \quad (3.6)$$

The  $b$  value is experimentally determined, and the  $k_r$  value is found in special experiments ( $[B] = 0$ ).

In several cases, in studying elementary processes we can create conditions where longitudinal diffusion can be neglected. This is possible when the inequality

is fulfilled

$$4(k_{\text{eff}} + K_{\text{B}}^{\text{e}})D/\bar{U}^2 \ll 1 \quad (3.7)$$

Then in expression (3.6) the diffusional term is neglected.

### 3.1.4. Method of shock tubes

Modern kinetic shock tubes are "wall-less" high-temperature reactors in which after passage of the shock wave within the time  $< 10^{-6}$  s the gas jumpwise increases the pressure and temperature and remains at unchanged values of pressure and temperature for  $10^{-2} \div 10^{-1}$  s. An elementary reaction is studied in the shock wave. The walls of the shock tube have room temperature. The shock tube consists of low- and high-pressure sections separated by a ruptured diaphragm. Light gases He and H<sub>2</sub>, which generate most intense shock waves, are usually used as collision gases that fill the high-pressure section.

The low-pressure section is filled with gases, which can serve as either reactants or for the generation of active species (photolysis, dissociation). These gases are usually strongly diluted to fulfill isothermic conditions by non-reactive diluents (Ar, N<sub>2</sub>, etc.). After the diaphragm is ruptured, the compression wave is propagated with the supersonic speed over the gas mixture in the low-pressure section. To determine the density  $\rho^2$ , temperature  $T^2$ , and pressure  $p^2$  behind the incident shock wave, the system of equations of mass, momentum, and energy conservation from both sides of the shock wave front are used. Taking into account these conservation laws along with equations of state of the gas in front and behind the shock wave results in the following expressions:

$$\begin{aligned} p_2 &= \frac{\gamma M_1^2 - (\gamma - 1)}{\gamma + 1} p_1 \\ T_2 &= \frac{(2\gamma M_1^2 - \gamma + 1)(\gamma - 1)M_1^2 + 2}{M_1^2 (\gamma + 1)^2} T_1 \\ \rho_2 &= \frac{(\gamma + 1) M_1^2}{(\gamma - 1) M_1^2 + 2} \rho_1 \end{aligned}$$

where  $M_1 = v_1/a_1$ ,  $a_1 = \sqrt{\gamma RT_1/\mu}$  is the sound speed in the undisturbed gas;  $\gamma = C_p/C_v$  is the ratio of heat capacities of the mixture under study at constant pressure and volume;  $p_1$ ,  $T_1$ , and  $\rho_1$  are the pressure, temperature, and density in front of the incident wave;  $v_1$  is the velocity of the front of the shock wave.

Dissociation of any molecules usually serves as a source of active species. Recently, an shock tube is used in combination with flash photolysis. Active species

are detected in time by absorption or emission spectroscopy.

For a long time the method of shock waves is the main method for studying elementary processes at high temperatures (higher than 1000 K). However, this method is presently applied for studying reactions at low temperatures. In this case, pulse photolysis and spectroscopic detection of active species are carried out in the rarefaction wave.

### *3.1.5. Method of laser-induced heating of gas mixture*

The most part of high-temperature studies of elementary processes was performed by the method of shock tubes. However, the method of heating of the gas mixture by laser radiation has recently appeared.

The method is based on fast and energetically equilibrium heating of the gas mixture at cool walls of the reactor using laser radiation. Powerful lasers radiating in the IR region ( $\text{CO}_2$  lasers) are usually used. Pulse  $\text{CO}_2$  lasers in combination with a static reactor are used more frequently with these purposes, although works are known where continuous  $\text{CO}_2$  lasers are used in combination with a flow-type reactor.

The gas mixture in the reactor consists of the buffer gas M, reactants A (or A and B), and molecules C, which efficiently absorb laser radiation. The absorbed energy should be enough for equilibrium heating of the gas to a required temperature. The conditions should be provided under which vibrational-translational relaxation of excited species occurred more rapidly than the reaction of species A and B. When designating the characteristic time of the  $V$ - $T$  relaxation of molecules C in collisions with M, A, and B through  $t_1$  and the characteristic time of heat relaxation of the gas due to the collision with the reactor surface through  $t_2$ , the condition  $t_1 \ll t_2$  must be fulfilled. Then in time  $t_1$  the gas takes the equilibrium temperature  $T$ , which depends on the distance  $r$  from the reactor axis. Molecules A and B undergo chemical transformations in the reactor. When designating the characteristic time of the chemical transformation of molecules A through  $t_3$ , the condition  $t_3 \ll t_2$  should be fulfilled to perform the reactions under conditions close to isothermic.

The kinetics of chemical transformation is usually detected by spectroscopic methods.

Thus, essence of the method is that to study the reaction kinetics in time when processes of  $V$ - $T$  relaxation are over and thermal relaxation has not yet taken place. The main difficulty is that the temperature of the gas in the reactor depends on time and also on the coordinate  $r$ . This implies that for kinetic studies one has to measure the profile  $T(t, r)$ , and this is rather difficult. To prevent this difficulty, researchers try to use chemical (or physical) references when  $T(t, r)$  can be determined from some measurements (for example, by the rate of the reactant in the reaction with the well-known rate constant).

### 3.2. *Methods of detection of active species*

Spectroscopic methods are most reliable. They are based on the interaction of light particles (photons and electrons) with molecular systems. Molecular spectroscopy is divided into spectral regions depending on the energy of light species used. Chemistry mainly operates with vibrations of atoms and motion of valence electrons. Infrared, visible, and ultraviolet regions of electromagnetic radiation corresponds to this type of motions in molecular systems. This range of the electromagnetic field is named optical or simply the light. This is optical spectroscopy where the most considerable success was achieved related to the use of lasers for studying processes in gases. Therefore, here we present mainly methods of optical laser spectroscopy.

In spectroscopic methods, the result of the interaction of the light with molecular systems is detected as a response function. It reflects either a change in any parameter of the acting light wave (amplitude, frequency, and direction of the wave, phase characteristics, polarization, propagation rate, etc.) or the appearance of a new property (for example, generation of radiation by molecules). The dependence of the response function on the light wave intensity determines the division into linear (a linear dependence) and nonlinear (a nonlinear dependence) spectroscopies. Here we present the methods of both linear laser spectroscopy (absorption and fluorescence spectroscopy; Raman spectroscopy) and some methods of nonlinear optical spectroscopy (two-photon absorption, nonlinear scattering). The methods of femtosecond spectroscopy will be described elsewhere.

#### 3.2.1. *Elementary processes involving a photon and a heavy particle*

Linear methods of laser spectroscopy are based on elementary processes of interaction of one photon with the molecular system. Let the photon has the energy  $h\nu$  ( $\nu$  is the photon frequency), and  $B(j)$  is the heavy particle in the quantum state  $j$ . Instead of indicating the frequency and velocity of the photon, we introduce the designation  $h\nu(\vec{k})$ , where  $\vec{k}$  is the wave vector related to the photon momentum  $\vec{p}$  by the relation  $\vec{p} = h\vec{k}$ . During the interaction with the photon, processes similar to processes 1-3 for heavy particles occur. So, the Raleigh scattering is an analog of process 1

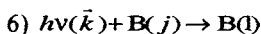
$$4) h\nu(\vec{k}) + B(j) \rightarrow h\nu(\vec{k}') + B(j)$$

which occurs without changing the photon energy; Raman scattering with changing the photon energy is an analog of inelastic collision

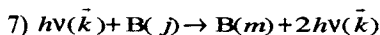
$$5) h\nu(\vec{k}) + B(j) \rightarrow h\nu(\vec{k}') + B(l)$$

When the photon is formed or disappears, these processes can be considered as analogs of 3. In this case, when the particle  $B(j)$  collides with the photon, both

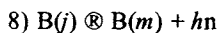
induced (stimulated by the presence of identical photons) absorption



and induced radiation



can occur. In process 4, the internal energy of particle B increases ( $E_i > E_j$ ), and in induced radiation 5 the internal energy of particle B decreases ( $E_i < E_j$ ). In addition to these processes, a process of spontaneous radiation is possible



For induced radiation, the photon that formed has the same wave vector as the incident photon had. For spontaneous radiation, the wave vector of the photon formed can have any direction.

### 3.2.2. Laser absorption spectroscopy (LAS)

This method based on process 4 is most frequently used for kinetic measurements. In the simplest case, the dependence of the radiation intensity passed through the gas on the wavelength  $\lambda$  of the incident light is measured. Quantitative measurements are based, as a rule, on the Lambert-Beer law

$$I(\lambda) = I_0 \exp(-s_l[n_j]x) \quad (3.8)$$

where  $I_0$  is the initial light intensity,  $I(\lambda)$  is the light intensity after passage through the gas of detected molecules,  $[n_j]$  is the concentration of analyzed molecules in the quantum state  $j$ , and  $s_l$  is the spectral absorption cross section at the light wavelength  $\lambda$ .

The value of the spectral absorption of the light  $a_\lambda$  is related to the spectral absorption cross section by the relation

$$a_\lambda = a_l([n_j] - g_l/g_j[n_i])$$

where  $[n_i]$  is the concentration of excited molecules in the quantum state  $i$ ; and  $g_i$  and  $g_j$  are the degeneracy coefficients of the corresponding levels.

However, if  $[n_j] \gg g_l/g_j[n_i]$ , this relation has the form

$$a_\lambda = s_l[n_j]$$

In practice the  $[n_i]$  value is often replaced by the overall concentration of molecules  $[n]$ . This implies that researchers are not interested in the quantum state of molecules B because they are populated according to the Boltzmann distribution.

In this method, the ratio of intensities of the incident ( $I_0$ ) and passed waves  $I(\lambda)$  is measured, and experimental data are presented through the following values: transmission  $[T = I(\lambda)/I_0]$ ; absorption  $(A = 1 - T)$ , and absorbance  $D [D = \ln(I_0/I(\lambda))]$ .

Spectral absorption (transmission) lines are not monochromatic, due to which physical values characterizing transitions of the molecular system from one quantum state to another are also energetically diffused. Therefore, any spectral quantity  $F$  (absorption cross section, absorption coefficient, Einstein coefficients, and others) can be of three types:  $F_l$  is the spectral value,  $F_o$  is the maximum value corresponding to the frequency  $n_o$ , and  $F = \delta F_n dn$  is the integral value for the spectral line. The integral and spectral values are related by the following relationship:

$$Fn = G(n - n_o)F$$

The function  $G(n - n_o)$  characterizes the profile of the spectral line. This function was normalized in such a way that  $\delta G(n - n_o)dn = 1$ .

There are different mechanisms of broadening of spectral lines. They can be distinguished to uniform and nonuniform mechanisms. For uniform broadening, all particles participating in absorption or radiation make the same contribution to the profile of the spectral line. These are broadenings associated with the finite lifetime of molecular systems. For nonuniform broadening, different regions of the spectral line are determined by different groups of particles. For example, the broadening due to the Doppler effect is nonuniform. In this case, the profile is the superposition of uniform profiles of particles with different velocities.

It is most reasonable to use continuous lasers in absorption spectroscopy. However, pulse lasers are also used because their use makes it possible to expand the spectral region of the light source. Lasers on dye solutions are used for studying in the near-UV and visible regions. Semiconductor diode lasers are widely applied for the IR spectral region. There are nonlinear optical methods, which allow one to obtain the radiation with the difference ( $n_3 = n_1 - n_2$ ) and summary frequencies. If one of the lasers are tunable, the radiation frequency  $n_3$  can be tuned in both UV and IR spectral regions.

In order to increase the sensitivity of the absorption method, the frequency modulation of the incident wave, an increase in the optical path by multiway cells, and accumulation procedures are used.

### 3.2.3. Laser magnetic resonance (LMR)

In the absorption method described above, the frequency of laser radiation was tuned in such a way to coincide with the center of the absorption line of the detected particle. If the frequency of laser radiation is unchanged and close to the frequency of the absorption line, to obtain resonance, one can tune the absorption line by the action of the electric or magnetic field on detected particles. The variant of absorption spectroscopy with the electric field is named *laser Stark spectroscopy*, and the variant using the magnetic field is called *laser magnetic resonance*. Laser Stark spectroscopy can be applied for the detection of stable molecules. Such paramagnetic par-

ticles as atoms and radicals can conveniently be detected using laser magnetic resonance.

The essence of the method is the following. The molecular level  $E_0$  with the total angular momentum  $J$  is split in the external magnetic field  $B$  into  $2J + 1$  Zeeman components. The sublevel with the magnetic quantum number  $m$  (the projection of the total angular momentum to the direction of the magnetic field) is shifted from the energy level  $E_0$  at the zero magnetic field according to the equation

$$E = E_0 g m_0 B m$$

where  $m_0$  is the Bohr magneton,  $B$  is the magnetic field intensity, and  $g$  is the Lande factor, which depends on the scheme of coupling of different angular momenta (electronic orbital angular momentum, electron spin, molecular rotation momentum, and nuclear spin).

An increase or a decrease in the energy of the level depends on the sign of  $m$ . Due to splitting, the frequency  $\omega$  of the transition is tuned by the magnetic field from  $n_0$  ( $B = 0$ ) to  $n$ , which is determined by the expression

$$n = n_0 + m_0(g'm' + g''m'')B/h$$

where stroke and two strokes indicate the lowest and highest quantum states of the transition.

According to technical realization, IR LMR in the IR spectral region of 5-10 mm and FIR LMR in the far IR spectral region at wavelengths shorter than 20 mm are distinguished. In the first case, absorption is caused by rotational-vibrational transitions. In FIR LMR absorption is due to rotational transitions. In this case, lasers on  $\text{CH}_3\text{OH}$ ,  $\text{HCOOH}$ ,  $\text{N}_2\text{H}_4$ ,  $\text{CF}_4$ , and other molecules, whose optical pumping is performed by  $\text{CO}_2$  lasers, are usually used.

In order to increase the sensitivity, frequency modulation is used: the high-frequency magnetic field is applied on the sample simultaneously with the slowly changing magnetic field. If the constant magnetic field is 2000-3000 Oe, then the high-frequency magnetic field does not exceed 100 Oe. Modulation is performed at a frequency of 100 kHz. The second point increasing the sensitivity is the arrangement of the reactor inside the laser cavity. The sensitivity will increase due to an increase in the light intensity in the cavity (see 3.2.5).

LMR is the development of the ESR method in gases. It turned out that the modulation frequency of a series-produced ESR spectrometer is close to the optimal modulation frequency of an LMR spectrometer, which allowed Gershenzon to create a new class of combined ESR/LMR spectrometers. The scheme of such a spectrometer is shown in Fig. 3.1. A gas sample is placed simultaneously in the cavity of an ESR spectrometer and in the cavity of an IR laser.

A disadvantage of the method is that the wavelength is not tuned smoothly. To increase the number of lines of laser generation at different wavelengths, gas mix-and oxygen atoms ( $^{16}\text{O}_2$ ,  $^{17}\text{O}_2$ , and  $^{18}\text{O}_2$ ), are used as an active medium.

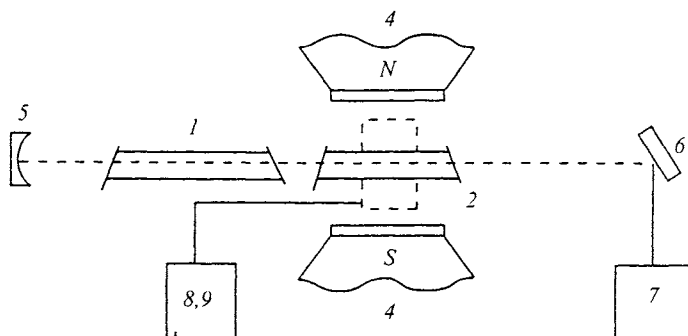


Fig. 3.1. Scheme of the combined ESR/LMR spectrometer technique: 1, active laser medium (for example, CO<sub>2</sub>); 2, cavity of ESR spectrometer; 4, electromagnet; 5, mirror; 6, diffraction lattice; 7, detector of laser radiation; and 8, 9, klystron and SHF detector.

First only continuous lasers were used in the LMR method but presently LMT spectrometers in the pulse variant with the microsecond time resolution are created. The high sensitivity of this variant of the method is achieved due to signal accumulation. The parameters of the LMR method are presented in Table 3.2.

#### 3.2.4. Intracavity laser spectroscopy (ICLS)

The method is based on the influence of the studied substance on the parameters of laser radiation. The method is based on that the reactor with the gas is placed into the laser cavity with a broad amplification contour as it is shown in Fig. 3.2. The main thing is to select parameters of the active medium of the laser so that the amplification of the light intensity in it would compensate losses on mirrors and would not compensate losses related to the studied absorption. These losses differ in frequency dependence. (The losses on mirrors are broad-band compared to narrow absorption lines of detected gas molecules.)

For easier understanding of the main principles of the ICLS, let us use the model of a multimode laser described by the system of balance equations for the number of photons in each mode of the cavity  $M_q$  and population inversion  $N$ . Let us assume for simplicity that the contour of the amplification line in the laser is uniformly broadened and the interaction of the modes and quantum noises are absent.

$$\begin{aligned} dM_q/dt &= -bM_q + B_qNM_q - a_qcM_q \\ dN/dt &= P - N/t - NSB_qM_q \end{aligned}$$

Here  $q$  is the number of the mode;  $b$  are broad-band losses in the cavity, which are the same for all modes;  $a_q$  is the absorption coefficient of the intracavity absorption;  $P$  is the pumping power;  $t$  is the lifetime of the upper laser level;  $B_q$  is the Einstein coefficient;  $c$  is the speed of light; and  $N$  is the total number of generating modes.

First let us consider the case where the absorption coefficient is the same for all modes,  $B_q = B$ , the narrow-band absorption is absent, i.e.,  $a_q = 0$ , the approximation  $t \ll 1/b$  is valid. In this case, stationary solutions of the equations written above have the following form:

$$N_0 = b/B$$

$$(M_q)^0 = (h - 1)P_{th}B_n$$

Here  $P_{th} = b/Bt$  is the threshold pumping power, and  $h = P/P_{th}$  is the increase of the pumping over the threshold.

Now let us consider the case where the pumping power  $a_q$  differs from zero only for one mode of the resonator  $q_0$ . In this case, the values of the threshold and population inversion are determined by modes with the lowest modes and, hence, have the same value as in the previous case. After switching-on pumping, if the  $a_q$  value is not very high, generation appear on all modes. After stationary values of the inversion  $N_0$  and intensity of the generation  $M_0$  are achieved, the intensity in the mode  $q_0$  decreases by the exponential law according to Eq. (1) in which the first two terms in the right part are mutually compensated

$$M_q = (M_q)^0 \exp[-a(w_0)ct]$$

It is assumed in the derivation of this formula that a decrease in the photon density at the frequency  $w_0$  has almost no effect on the concentration of active particles  $N$  and on the amplification coefficient at the same frequency. It can be shown that a change in the amplification coefficient at this frequency is proportional to  $\exp(-2pg/Dw_p)$ , where  $g$  is the width of the uniform amplification line, and  $Dw_p$  is the absorption linewidth of the analyzed substance. Therefore, we may conclude that the necessary condition for the case where the derived formula for the time evolution of the number of photons with the frequency  $w_0$  is fulfilled can be formulated as follows:

$$Dw_p \ll 2pg$$

For gases  $Dw_p$  is usually lower than  $1 \text{ cm}^{-1}$ , whereas  $2pg$  for condensed active media lies in the interval from  $10$  to  $10^3 \text{ cm}^{-1}$ . Thus, the ICLS method can successfully be used for many active media, liquid organic dyes (380—1000 nm), crystalline active media (1—3 mm).

The number of photons in each mode of the cavity is proportional to the spectral

intensity  $I(w_0)$ . Therefore, we can write

$$I(w_0) = I_0(w_0)\exp[-a_0(w_0)ct]$$

This formula is valid if the whole cavity is filled with an absorbing substance. In many cases, only a part of the cavity is filled with the substance. When the cavity length is designated through  $L$  and  $l$  is the length of the absorbing layer, then the coefficient of cavity filling should be introduced into formula. Then we obtain the final formula

$$I(w_0) = I_0(w_0)\exp[-a_0(w_0)(l/L)ct]$$

The absorption coefficient  $a_0(w_0)$  ( $w_0$  is the frequency at which the substance under study absorbs) at which the generation intensity in the chosen mode decreases by  $e$  times is determined by the duration of the generation  $t_g$

$$a_0 = 1/ct_g = 1/L_{ef}$$

Thus, the intracavity spectrometer corresponds to the traditional absorption spectrometer with a cell having the equivalent length

$$l_{ef} = ct_g l/L \quad (3.9)$$

It is seen from this formula that the sensitivity depends on the generation time of the laser. The ICLS spectrum is shown in Fig. 3.7. These spectra are processed in the same manner as in absorption laser spectroscopy, due to which the value  $y = a(w_0)(l/L)ct$  is determined.

When organic dyes are used as active media, it has experimentally been shown that the effective length is proportional to the generation time up to  $t_g$  is equal to 0.1 s. At long generation times of the laser, deviations from this law begin. When the rate of absorption by the sample is comparable with the rate of spontaneous radiation, an increase in the generation duration already gives no gain. From this condition we can estimate that the minimum value of the absorption coefficient, which can be measured by this method, is  $3 \cdot 10^{-11} \text{ cm}^{-1}$ .

The theory shows that expressions (3.8) and (3.9) are fulfilled to times of 1 s. If we accept that the detected gas fills the whole laser resonator, at a time of laser generation of 1 s the optical path length is 300 000 km.

Note that the great length of the optical path can be realized at small geometrical sizes of the reaction vessel. At the same time, the brightness of the light source remains great, and spectrographs with a high spectral resolution can be applied. The sensitivity of the ICLS method to selective absorption is restricted by the presence of spontaneous noises. The theory and experiment show that the absorption coefficient  $s[n]$  can reach  $10^{-11} \text{ sm}^{-1}$ .

Laser with the following active media satisfy the necessary conditions of ICLS:

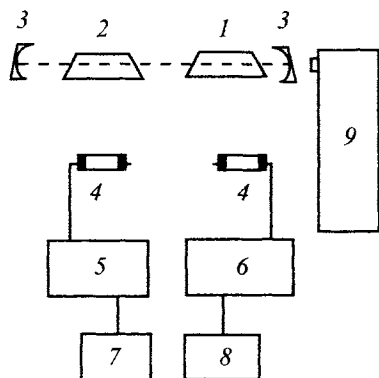


Fig. 3.2. Scheme of the kinetic intracavity laser spectroscopy technique: 1, active medium of the laser; 2, reactor; 3, mirrors; 4, pulse lamps for photolysis of a mixture and pumping of the laser; 5, feeding source for photolysis; 6, feeding source for the laser; 7, controlling unit; 8, unit for time delay between photolyzing and laser pulses; and 9, detector of the spectrum.

glass activated by neodymium; solutions of organic dyes; alkali-halide crystals with coloring centers; crystals of the Ti type; sapphire, etc. Lasers operating in both pulse and continuous modes are used. Lamp pumping, which provides a long generation time, is often used for the work in the pulse mode. Continuous generation of dye lasers is performed using ionic argon and krypton lasers for pumping. The typical scheme of the technique is presented in Fig. 3.2. Most frequently the ICLS method is applied for studies in a static reactor in combination with pulse photolysis. The characteristics of ICLS are given in Table 3.2.

### 3.2.5. Ring-Down spectroscopy

We considered the effect of placing the reactor inside the cavity of multimode lasers (ICLS). Evidently, the sensitivity will increase also when the gas mixture under study is placed into the cavity of a laser. Let us consider the case of intracavity spectroscopy for external passive cavities, which contain no active medium. Such passive cavities are, in fact, reactors with the corresponding edge mirrors. The use of an external cavity, which represents an improved modification of multiway cells, was developed when the technology of creation of mirrors with a high reflection coefficient was improved. This new type of spectroscopy was named Ring-Down spectroscopy.

The method is the following. Let a light pulse is "injected" into a cavity. Let the reflection coefficients of two mirrors of the cavity are  $R_1 = 1$  and  $R_2 = 1 - T_2$  (the absorption in the mirrors is neglected). If the radiation power after the outlet from the passive cavity is designated as  $P_{out}$ , then the power inside the cavity is  $P_{in} = qP_{out}$ , where  $q = 1/T_2^2$ . At  $al \ll 1$  ( $l$  is the length of the absorbing cell), the power absorbed at the frequency  $w_0$  ( $DP(w_0)$ ) in the absorbing cell is the following:

$$DP(w_0) = qa(w_0)lP_{out}$$

If the absorbed energy can directly be measured by some method (for example, from fluorescence), the signal is by  $q$  times higher than that through the cell inside the cavity. At  $T_2 = 0.01$ , the amplification factor is 100 times. This position is valid until saturation effects are absent. The aforesaid can be understood in the following way. The photon in the cavity passes, on the average,  $q$  times between the cavity mirrors before it exits from the cavity. Therefore, the photon has a  $q$ -fold higher probability to be absorbed in the analyzed substance. This increase in the sensitivity can be realized also in external passive cavities. The amplification factor can be higher if mirrors of the cavity have a very low transmission. Recent success in the preparation of mirrors allows one to have mirrors with  $T = 10^{-5}$  and better.

Evidently, the intensity outside the cavity decreases according to the law

$$I(t) = I_0 \exp(-t/t)$$

where  $t$  is the lifetime of the photon in the cavity. The absorption signal in this method is determined by measuring the decay rate constant of the photon or the time of its decay according to the expression

$$k = 1/t = (T + L + s(l)nl)/t_0$$

$t_0 = L/c$  is the time of light propagation in the cavity with the length  $L$ ,  $T$  are losses associated with the transmission coefficient through the outlet mirror,  $L$  are losses associated with the absorption and scattering on the mirrors;  $s(l)$  is the absorption cross section at the wavelength  $l$  by the studied sample with the concentration  $n$  and length  $l$ , which is placed inside the passive cavity. Absorption per passage can be obtained from the measurement of the lifetime of the photon in the absence of the sample ( $t_0$ ) and in the presence of the studied sample ( $t$ )

$$k_0 = 1/t_0 = (T + L)/t_0$$

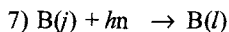
$$s(l)nl = (k - k_0)t_0 = (1/t - 1/t_0)t_0$$

Thus, measuring  $I(t)$  (Fig. 3.8), one can find the  $t$  value and, hence,  $s(l)$ . In this method, the signal/noise ratio is very low and, hence, lower changes in the radiation intensity can be measured. This method allows one to measure the absorption coefficients to  $10^{-7} \text{ cm}^{-1}$ . It can successfully be applied to kinetic studies.

### 3.2.6. Laser-induced fluorescence spectroscopy (LIF)

In this method, the absorbed light energy is measured from fluorescence of detected species, which absorbed the light. The physics of the LIF method includes two types of processes of excitation of the detected species and processes involving the excited species. The first type of the process is realized for the irradiation of the gas mixture with the monochromatic light, most frequently in the visible or UV spectral regions. The light frequency  $\nu$  is selected in such a way that the detected particle

$B(j)$  undergoes transition to the electronically excited state  $B(l)$  due to the process

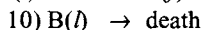
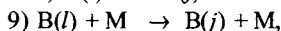
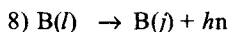


Let the duration of the pump light pulse is short and any processes involving  $B(j)$  and  $B(l)$  have no time to occur within the pulse action. Then some fraction  $b$  of the initial concentration of particles  $B(j)$  transits to the electronically excited state

$$[B(l)] = b[B(j)] \quad (3.10)$$

where  $b$  is proportional to the photon cross section  $s$  and light intensity  $I_0$ .

Excited particles  $B(j)$  can participate in other processes



Process 9 is the deactivation of  $B(l)$  due to collisions with other molecules  $M$  of the gas. Process 10 includes different nonradiative processes in which  $B(l)$  is transformed into either other species or  $B(j)$ . The fluorescence intensity  $I_f$  is detected, which is determined by the expression

$$I_f(t) = Ck_8b[B(j)]\exp\{-(k_8 + k_9[M] + k_{10})t\}$$

where  $C$  is the coefficient characterizing the fraction of fluorescence detected by the equipment.

This coefficient depends on the instrument. In practice it is often convenient to measure the fluorescence quantity integral in time  $I_n^\circ$

$$I_n^\circ = \int_0^\infty I_f(t) dt = CI_0 \sigma \phi[B(j)] \quad (3.11)$$

where  $j = k_8(k_8 + k_9 + k_{10})$  is the quantum yield of fluorescence.

As can be seen from (3.11), the fluorescence signal is proportional to both the concentration of radiating particles and the intensity of the irradiating light. However, with an increase in  $I_0$  the dependence of  $I_n^\circ$  on  $I_0$  becomes smoother. This is related to the fact that with an increase in the intensity of the irradiating light the real absorption decreases due to an increase in the rate of the process of induced irradiation  $B(l) + h\nu \rightarrow B(j) + 2h\nu$ .

It follows from formula (3.11) that the higher the quantum yield  $B(j)$  and the larger the cross section of photon absorption  $j$ , the more efficient the detection of the particle  $B(j)$ . The rate constants  $k_7$  and  $k_8$  characterize the interactions of particle  $B$  with the light and, hence, are related to the Einstein coefficients:  $k_7 \sim B_{ll}$ ,  $k_8 \sim A_{il}$ . They are given by the known expressions

$$A_{il} = (8\pi h\nu^3/c^3)B_{il} \quad (3.12)$$

$$B_{il} = (24\pi^4 n^3 / 3hc^3) |m_{il}|^2 \quad (3.13)$$

where  $m_{il}$  is the transition moment.

When deriving these formulas, averaging over all directions and two orthogonal polarizations was performed.

There are two variants of LIF: using continuous and pulse lasers. The use of LIF with pulse lasers seems more promising because, first, in several problems a high time resolution is necessary, which can easier be achieved using pulse lasers; second; the spectral region covered by continuous lasers is much narrower than that of pulse lasers. This strongly restricts a set of particles, which can be detected.

LIF is used most frequently in combination with the method of crossed molecular beams or with flash photolysis in a static reactor. The latter combination is applied more frequently, which is related to the relative simplicity of such installations. The principal scheme of a variant of the combination of laser photolysis with the LIF method is shown in Fig. 3.3. Omitting details, the technique consists of the following main parts: a laser for photolysis 1, a system of lasers exciting fluorescence 2, a measuring cell 3, and a detection system 4.

Lasers for LIF should correspond to the following main requirements: to have a possibility of tuning of the radiation line, to possess a narrow spectral width of the generation line, a short pulse duration, and a high spectral brightness. The repetition frequency of pulses should be rather high to perform the procedure of accumulation of fluorescence signals.

Tuned dye lasers are used most frequently in the LIF method. Nd:YAG lasers, excimer and nitrogen lasers are applied as pumping lasers. The spectral range of generation of dye lasers is presently 300-1200 nm. To extend this range over the UV region, different methods of nonlinear optics are used: generation of harmonics and summation of frequencies in nonlinear crystals. The char-

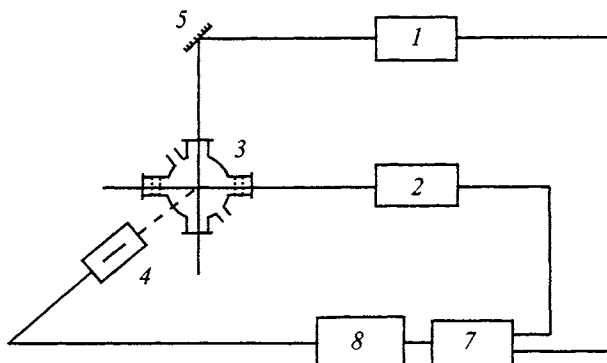


Fig. 3.3. Scheme of the combined technique: laser photolysis/laser-induced fluorescence: 1, laser for photolysis; 2, laser for excitation of fluorescence; 3, measuring cell; 4, detection system of fluorescence; 5, mirror; 6, controlling unit; 7, unit for time delay between pulses of lasers 1 and 2.

acteristics of this method are presented in Table 3.2.

### 3.2.7. Raman light scattering (RLS)

This method is based on elementary process 4). Two schemes illustrating Raman scattering are shown in Fig. 3.4. The states with the energy  $E$  and  $E'$  can be referred to vibrational, rotational, and electronic states. As is seen, the radiation appears at the frequency  $\nu_K = [h\nu - (E' - E)]/h$ . If  $E' > E$ , the radiation occurs at the frequency  $\nu_{st} < \nu_1$  and named Stokes. If  $E' < E$ , the radiation occurs at the frequency  $\nu_a > \nu_1$  and named anti-Stokes.

In the presented scheme, the intermediate state  $E + h\nu$  in the scattering process is considered as a virtual level. The real level can be higher or lower than the virtual level. In the case if the virtual level coincides with the real level, they speak about resonance Raman scattering. In the latter case, the radiation intensity increases sharply.

The use of tuned lasers increases possibilities of the RLS method, however, the radiation intensity still remains much lower than the intensity of the exciting light. This linear spectroscopic method possesses a very low sensitivity and, therefore, it is rarely used for studies in the gas phase. The sensitivity of nonlinear scattering methods is much higher.

### 3.2.8. Methods of nonlinear spectroscopy

We considered the methods which are applicable when the intensity of the incident light is low. However, with an increase in the light intensity processes of absorption, fluorescence, and scattering can occur, when immediately several photons from

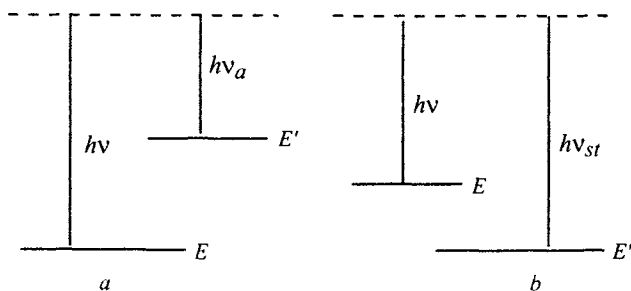


Fig. 3.4. Energy scheme illustrating Raman scattering:  $a$ , radiation at the anti-Stokes frequency  $\nu_a$ ;  $b$ , radiation at the Stokes frequency  $\nu_{st}$ .

the incident electromagnetic waves participate simultaneously in these processes. These photons can be from either one light beam and several beams from one or several lasers. If incident photons are in resonance with the energy levels of the molecular system,

this process can be considered as a sequence of one-photon processes. Such processes are named step-ladder or cascade. The nonlinear multiphoton process implies the process in which the primary act is virtual, i.e., the resonance between the photon energy and levels of the molecular system is absent. The methods based on these processes are named methods of nonlinear spectroscopy. These methods allowed the development of new principles of species detection. Multiphoton absorption and nonlinear light scattering are of greatest interest for the gas kinetics.

Multiphoton absorption can be presented as the elementary process



The summation is performed over all photons  $n_i$ , which are absorbed by the molecule. If photons with the same frequency are present ( $n_1 = n_2 = \dots = n_k = n$ ), this process can be written as



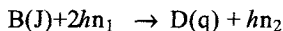
The simplest example of multiphoton absorption is two-photon absorption. Two-photon transitions have selection rules, which differ from the selection rules for one-photon absorption. It is required for one-photon transitions that the levels  $j$  and  $l$  have the opposite parity, and for two-photon transitions the levels  $j$  and  $l$  should have the same parity.

The probability of the two-photon transition is proportional to the product of the intensities  $I_1$  and  $I_2$ . In the case of one laser beam, this product should be replaced by  $I_2$ . High peak powers are required to make the probability of the transition noticeable. Therefore, pulse lasers in which high peak powers are achieved are usually used for two-photon processes.

Thus, multiphoton absorption spectroscopy supplements one-photon spectroscopy and allows one to observe transitions between states with the same parity, which are forbidden for one-photon transitions, to form highly excited states of molecules using the visible frequency range, to perform spectrally more resolved intra-Doppler spectroscopy, and to perform multiphoton ionization, which is used in mass spectroscopic and other ionization methods of detection of active species.

Nonlinear scattering is exemplified by hyper-Raman scattering, induced Raman scattering, coherent anti-Stokes Raman scattering (CARS).

*Hyper-Raman light scattering* is that, unlike linear scattering (see Section 3.2.5), two photons with the frequency  $n_1$  participate in the inelastic collision with the particle  $B(J)$ . As a result, a molecule in the different energy state and one photon with the energy  $\hbar n_2$  are formed



The laws of energy and momentum conservation should be fulfilled for these

processes. Since the momentum of molecules during collision with photons remains virtually unchanged, the momentum conservation law should be fulfilled for photons. The photon momentum is proportional to the wave vector. Therefore, the momentum conservation law is presented as the equality to zero of the vector sum of the wave vectors of photons involving in the nonlinear process. This law in optics is called the condition of *phase synchronism*.

Techniques combining induced and spontaneous Raman scattering is under vigorous development in recent time. We speak about *coherent anti-Stokes Raman spectroscopy* (CARS). The schemes of levels illustrating CARS is shown in Fig.3.5. The method is based on the fact that in the field of rather intense light beams with the frequencies  $\nu_1$  and  $\nu_2$  satisfying the condition  $W = \nu_1 - \nu_2$  ( $W$  is the frequency of molecular vibrations) molecular vibrations with the frequency  $W$  are "swinging." As a result, the light beam with the frequency  $\nu_1$  begins to scatter on the excited states with the appearance of radiation with the anti-Stokes frequency  $\nu_a = 2\nu_1 - \nu_2$ . The detected molecules are irradiated with two lasers at the frequencies  $\nu_1$  and  $\nu_2$ . Fluorescence is detected at the frequency  $\nu_a$ , whose intensity is given by the expression

$$I_a = [n]^2 I_1^2 I_2 \quad (3.16)$$

where  $[n]$  is the concentration of detected particles,  $I_1$  is the intensity of the laser radiation at the frequency  $\nu_1$ , and  $I_2$  is intensity of the laser radiation at the frequency  $\nu_2$ .

To obtain a rather intense radiation at the frequency  $\nu_a$ , it is necessary that the wave vectors of light beams with the frequencies  $\nu_1$  and  $\nu_2$  correspond to the condition of phase synchronism. This condition is fulfilled for gases if the wave vectors are collinear. However, this configuration decreases the spatial resolution of the method. There are approaches which allow one to obtain a high sensitivity in this method along with the good spatial resolution. The second harmonic of the Nd:YAG laser (frequency  $\nu_1$ ) and the tuned laser on dye solutions (frequency  $\nu_2$ ) are used most frequently in the CARS method. In the CARS method, the signal level exceeds the level of spontaneous Raman scattering by  $10^4$ – $10^5$  times. The characteristics of the method are indicated in Table 3.2.

### 3.2.9. Kinetic mass spectrometry (KM)

Along with optical methods, mass spectrometric methods are successfully used for analysis of stable and short-lived products in studying elementary reactions. These methods are combined with a jet reactor for studying reactions involving radicals. The diffusional variant of a jet reactor developed by A.M. Dodonov and V.A. Talroze is most successful. This method allows the detection of both radicals and excited species. The simplified scheme of the method is shown in Fig. 3.6. A sample is taken from a definite point along the axis of the diffusion cloud; the removal of a capillary filled with the second reactant allows one to change the reaction time. To

avoid the decay of active species before getting into the ionization chamber, the sample is conveyed into a mass spectrometer by a molecular beam.

One of the permanent difficulties in mass spectrometric detection is that the mass spectrum of an active species (for example, a radical) can be superimposed on the mass spectrum of a stable molecule, which contains this active species as a fragment. The appearance of the radical-fragment requires energy expenses for the dissociation of the stable molecule. Therefore, the energy of electrons necessary for the creation of ions from the primary radical and stable molecule differs by the dissociation energy of the stable molecule. The use of ion sources with a low energy of electrons and a high degree of monochromaticity with respect to energy allows one to avoid these difficulties. The best selectivity with respect to active species and stable molecules can be achieved if the multiphoton ionization of the detected particles is carried out with the use of lasers. In this case, absorption of several photons results in the formation of a species at the excited level from which it is ionized. This process can be written as follows:



The energy conservation law for this process can be written in the form

$$nh\nu = E_n - E_e$$

where  $E_n$  is the ionization potential, and  $E_e$  is the kinetic energy of an electron.

As can be seen, selecting the wavelength of the light, we can change the kinetic energy of an electron. The mass spectrum consisting of a smaller number of ions can thus be obtained. The characteristics of mass spectrometric detection are presented in Table 3.2.

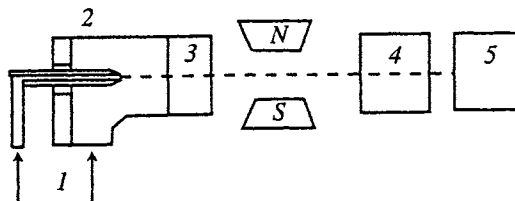


Fig. 3.6. Scheme of a kinetic mass spectrometer: 1, convey of reactants; 2, reactor; 3, system of molecular beam formation; 4, ion source; and 5, mass analyzer.

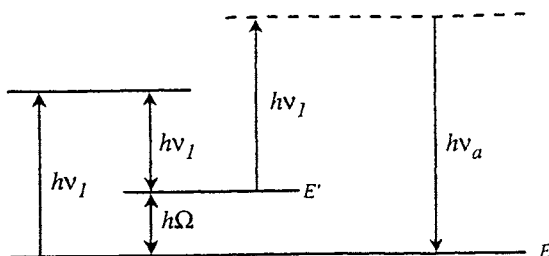


Fig. 3.5. Energy scheme illustrating CARS

### 3.2.10. Comparison of methods for detection of active particles

The methods described above supplement each other. Nevertheless, there are conditions and areas of investigation where this or another method has advantages. Possibilities to use detection methods for studying elementary processes of different types depend on many factors and are determined, first, by the following parameters: sensitivity, time resolution (characterizes the high-speed of the method), spectral resolution (allows one to detect particles in definite quantum states), spatial resolution (shows possibilities of local analysis), and spectral range of action (characterizes the versatility of the method, i.e., a possibility to detect a great variety of active species). These are the characteristics, which allow one to judge what type of elementary processes in combination with what method of investigation is preferential to be used. Table 3.2 contains the characteristics of the methods described above. Emphasize that the figures presented there are not best but typical values. The sensitivity depends on the method and also on the photo or ionization cross section (during collision with an electron) of the detected particle. Since for different molecules these values differ, the sensitivity of the method is presented by average values, which correspond to the an absorption cross section of  $10^{-18} \text{ cm}^2$ .

Table 3.2. Characteristics of different methods for detection of active particles

Method	Sensitivity, $\text{cm}^3$	Time resolution, s	Spectral resolution, $\text{cm}^{-1}$	Spatial resolution	Spectral reso- lution of action, $\mu\text{m}$
LAS	$10^{11}$	$10^{-5}$	$10^{-3}$	1 mm	0.2-10
LMR	$10^9$	$10^{-3}(10^{-6})$	$10^{-3}$	1 mm	IR region
ICLS	$10^9$	$10^{-6}$	$10^{-3}$	1 mm	0.4-0.3
LIF	$10^7$	$10^{-14}$	$10^{-3}$	$10^{-6} \text{ cm}^3$	0.2-1.0
CARS	$10^{12}$	$10^{-13}$	$10^{-3}$	$10^{-6} \text{ cm}^3$	Visible an UV regions
KM	$10^9$	$10^{-3}$	—	—	—

\*Parameters of the LMR method with high time resolution are given in parentheses.

The method of kinetic mass spectrometry is universal for such active particles as radicals and makes it possible to detect radicals with different sets of atoms. The low time resolution is related to the fact that kinetic mass spectroscopy is usually combined with a jet reactor. It is difficult to detect particles in definite quantum states by this method. It is reasonable to use another method with these purposes.

The absorption method is most universal because it operates in a wide spectral

range. However, it is exceeded in sensitivity by other methods. The LAS method is combined with method of shock waves or a jet reactor. The concentration of active species in shock waves are usually rather high and the universal character of LAS makes it possible to observe simultaneously several particles. A combination with a jet reactor restricts the time resolution. In LAS both continuous and pulse lasers are used.

The LMR method is less universal because it acts so far only in the IR range. In addition, lasers with stepwise, not smooth rearrangement of the generation frequency are used in this method. The LMR method can detect only paramagnetic species, whereas the absorption method detects any particles. However, the sensitivity of the LMR method is much higher. The combination of the LMR method with ESR in the same instrument allows one to determine absolute concentrations of radicals by ESR for which the procedure of measurement of absolute concentration already exists. The LMR method and absorption method using continuous lasers are usually combined with a jet reactor, due to which a low time resolution is obtained. This time resolution is sufficient for reactions of radicals, however, can be not enough for studying elementary processes at the microscopic level. There is the modification of the LMR method, which makes it possible to obtain a time resolution of  $10^{-6}$  s but in this case the sensitivity of the method is much lower.

The methods of laser spectroscopy in the IR spectral region are preferential for studying reactions involving radicals. However, in this case, the Doppler absorption linewidth is rather narrow, due to which an increase in the general pressure results in an increase in the absorption linewidth and a sharp decrease in the sensitivity. In the IR region we can study elementary processes at pressures lower than 50 Torr.

The ICLS method allows one to work with a high sensitivity at higher pressure. It also has a rather high time resolution. The ICLS method makes it possible to detect with a high sensitivity not only absorption but also the amplification of light when the population inversion of different energy levels is present in the gas under study. A disadvantage of ICLS is the restriction of the spectral range from the side of the UV spectral region (to 400 nm).

The absorption method, as well as ICLS, LMR, and KM, do not allow local analysis. Nevertheless, in the cases where the reaction medium is symmetrical over some axis, these methods can be applied to analysis of the spatial distribution of active species. In this sense, Table 3.2 indicates a spatial resolution of 1 mm. This value practically corresponds to the spatial width of the laser beam.

Local analysis can be carried out only by the LIF and CARS methods. They have the highest time resolution. The CARS method or any other method of Raman spectroscopy are universal but have low sensitivity. Therefore, it is reasonable to use resonance Raman spectroscopy because its sensitivity is higher. Due to a low sensitivity, Raman spectroscopy is combined with a pulse source of generation of active

species. Then concentrations sufficient for CARS detection can be created in a small volume. The method is usually used for studying microscopic elementary processes.

Unlike CARS, the LIF method possesses the highest sensitivity in the areas where it is applicable. The method is not universal because the radiational relaxation of excitation relaxation in many cases is weak. However, in the cases where the quantum yield of fluorescence of the detected molecule is high, this method becomes indispensable for studying microscopic processes if it is necessary to detect the quantum state of a species, its velocity, and orientation. LIF is used in combination with supersonic jets, molecular beams, jet or static reactors.

### 3.2.11. *Methods of femtosecond spectroscopy*

In previous sections we described the experimental methods which make it possible to detect the time evolution of reactants and products. In recent years, a new instrument appeared in laser technique: light pulses with a duration of 10—100 femtoseconds. The peculiarities of light pulses with such a short duration opened new experimental possibilities, the main of which are the following.

a) The short time duration of pulses makes it possible to study the time evolution of processes with the time resolution even better than the duration of the light pulse ( $10^{-14}$  s). If we accept the velocity of an atom  $10^5$  cm/s and  $t = 10^{-14}$  s, changes in the internuclear distances of 0.1 Å can be detected. This implies that not only product formation but also the time evolution of the nuclear configuration in the time scale of vibrational motion can be detected with a good accuracy in the real time scale.

b) The spectral width of pulses is determined by the uncertainty relation

$$\Delta\nu \Delta t = \text{const.}$$

The const value depends on the shape of the pulse envelope. For the Gauss pulse  $\text{const} = 0.44$ . The pulse with a duration of  $10^{-14}$  s has a spectral width of  $1100 \text{ cm}^{-1}$ . This implies that the femtosecond light pulse can simultaneously excite several vibrational states.

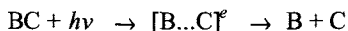
c) Coherent character of the light pulse. This point along with the previous point implies a possibility of the coherent excitation of several vibrational or rotational states. This new type of excited states is named *nonstationary quantum state* or *coherent nuclear wave packet*. The sense of these states is that in the molecule immediately several stationary energy states with correlated relative phases are excited.

d) High intensity (peak power) of femtosecond pulses at an insignificant pulse energy. This point implies that multiphoton absorption processes can easily be performed, that is, the formation of highly excited molecular systems by visible light and the use of numerous nonlinear spectroscopic methods without heating the sample. The action of such light pulses on the target (solid, liquid) can generate light

pulses in a wide spectral range (supercontinuum), electron and X-ray pulses. Also note that it is relatively easy to obtain light field intensities ( $10^{10}$  W/cm<sup>2</sup>) even exceeding intramolecular fields. This can be used for the directed distortion of the potential energy surface (PES) at definite time moments.

Thus, femtosecond light pulses allow one to provide the high time resolution, create nonstationary quantum states, form highly excited molecules, influence on PES, and generate ultrashort light, electron, and X-ray pulses.

The specific features of a new instrument presented above defined a new area of studies, which was named "*femtochemistry*". The problems of femtochemistry are the study of the dynamics of intramolecular processes and transition state during chemical transformation, the study of the kinetics of superhigh processes, and controlling the chemical transformation by femtosecond pulses. We especially emphasize a possibility of studying the dynamics of the transition state in the real time. Note that the transition state implies the whole totality of configurations through which the reacting molecular system passes *via* the route from reactants to products. To distinguish the transition state from the activated complex  $BC^\ddagger$ , we will designate the transition state as  $[B...C]$ . In the case where the transition state exists on the electronically excited PES, we will designate it as  $[B...C]^e$ . Then the dissociation process can be presented in the form



The main experimental methods in femtochemistry are based on the "pump—probe" methods. The pump pulse at the frequency  $\nu_1$  creates a wave packet in the electronically excited state and determines the zero time moment at which the internuclear distance in the transition state is  $R_0 = R_0(t=0)$ . The dynamics of the wave packet, which can be considered as its motion over the PES, represents the dynamics of transition state, that is, the time evolution of the internuclear distance in  $[B...C]^e$ . After some delay time  $t$ , the second femtosecond pulse is produced at the frequency  $\nu_2$ . This pulse is called the probe pulse because it determines the existence of the wave packet on the PES, *i.e.*, the internuclear distances  $R(t)$  in the time moment  $t = t$ .

The transition state will absorb photons from the second pulse if the configuration of the transition state corresponds to such an  $R$  value at which light with the frequency  $\nu_2$  transforms  $[B...C]^e$  into the higher electronically excited state  $U_2$  according to the equality

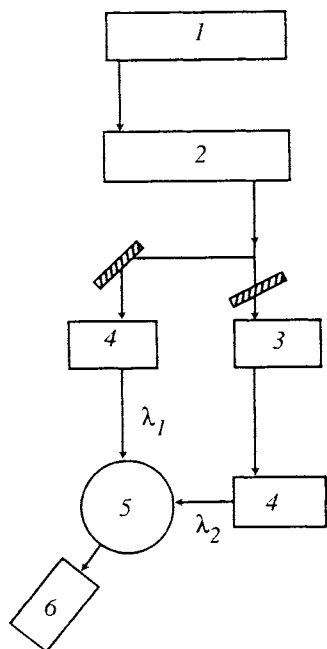
$$h\nu_2 = U_2(R) - U_1(R)$$

The population in the electronic state  $U_2$  depends substantially on the time delay between the pump and probe pulses. From the highest electronic state the molecule can fluoresce (then the fluorescence intensity changes), decompose (the decomposition product is detected by the methods described in this chapter), or be ionized (the

current or ions are detected by mass spectroscopic methods). In all cases, the dependence of the measured quantity (fluorescence intensity, concentration of the product or ion fragment) on the time delay between the pump and probe pulses is detected. In some methods, the probe pulse performs the transition to the lowest electronic state due to the induced radiation on Raman transitions. Note that the high intensity of femtosecond pulses allows one to efficiently use all methods of nonlinear spectroscopy developed to date.

The general scheme of the technique for femtosecond experiments is presented in Fig. 3.7. The generator of femtosecond pulses produces light pulses with a duration of  $10^{-13}$ - $10^{-14}$  s. If the pulse energy is insufficient for the experiment to be performed, the pulse is amplified. Then a portion of amplified pulses goes to the formation of pump pulses, and another portion is consumed to the formation of probe pulses. The time delay between the pump and probe pulses can be varied changing the optical path length. Varying the optical path of the probe pulse, one can change the time delay between the pulses. The converters of wavelengths serve for choosing wavelengths of the pump and probe pulses.

The pump and probe pulses with the specified delay time are directed to the studied object. This is usually a molecular beam or gas placed into a cell. Supersonic jets are used for measurements at very low temperatures.



Note that methods, in which the probe pulse is focused on the target to obtain electron or X-ray pulses, begin to develop now. In these methods, the dependence of electron or X-ray diffraction on the time delay between the pulses is detected. These methods provide an information on the time evolution of the nuclear arrangement in the course of the chemical reaction.

Fig. 3.7.

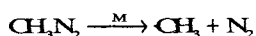
General scheme of the technique for studying the dynamics of the transition state: 1, generator of femtosecond pulses; 2, optical light amplifier; 3, optical line of the time delay between the pump and probe pulses; 4, devices for changing the wavelength of light pulses; 5, reactor; and 6, system of detection of fluorescence or ion current induced by probe pulses.

### 3.3. Methods for obtaining active species

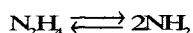
There are two main methods for obtaining active species: using chemical reactions and photophysical methods. Both these methods are used in the chemical kinetics.

#### 3.3.1. Chemical methods

In these methods, radicals are products of chemical reactions. For example, the reaction

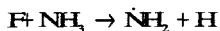


can be a source of the radical  $\cdot\text{CH}_3$  in shock waves because at high temperatures decomposition occurs so rapidly that reactions of the radical  $\cdot\text{CH}_3$  do not virtually occur within these times. If the activation energy is low, high equilibrium concentrations can be at high temperatures, and they are conveyed into a jet reactor.  $\text{N}_2\text{F}_4$  is an example of substances of this type. At comparatively low temperatures, one can achieve the conditions where the equilibrium



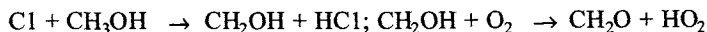
is shifted towards the radicals  $\text{NF}_2$ . This is due to the low energy of the N—N bond, which is equal to -80 kJ/mol.

Jet methods are more frequently used for studying bimolecular reactions of atoms with stable molecules. For example, the reaction



can be a source of the radical  $\cdot\text{NH}_2$ .

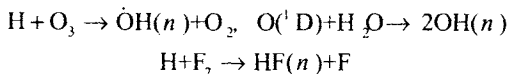
In jet methods, atoms are usually obtained using the SHF discharge. In some cases, a more complex set of elementary reactions is used. For example, the radicals  $\text{HO}_2\cdot$  are obtained in the following reactions:



Such sources are applied in some cases in a static reactor as well, where the atom is formed due to flash photolysis. The main thing in chemical methods is that the characteristic time of generation of the a needed radical would be much shorter than the time of the reaction of this radical with a particular reactant.

In some cases, the chemical methods can be used for the formation of not only

radicals but also excited species. For example, vibrationally excited species can be obtained in the reaction



### 3.3.2. Photophysical methods

Light irradiation of molecules is the most popular method for the formation of active species. Light absorption can result in either the excitation of particles or photodissociation of molecules to form atoms and radicals. Both continuous and pulse light sources are used. Various types of lasers or lamps are used as light sources. The main disadvantages of nonlaser techniques are a comparatively long time of the formation of particles (usually it exceeds  $10^{-5}$  s) and a wide spectral composition of the pulse of lamps: nonmonochromaticity results in noncontrolled dissociation channels, and a low time resolution does not allow primary and secondary elementary processes to be separated. Laser light sources are free of these disadvantages.

One-photon, two-photon, and multiphoton absorption is used to create active species using light. One-photon absorption is technically the simplest. When photodissociation is used for the generation of active species, the irradiation is usually carried out by excimeric lasers, especially KrF ( $\lambda = 248$  nm) and ArF ( $\lambda = 193$  nm) lasers. The fourth harmonic of an Nd: IAG laser ( $\lambda = 265$  nm) is also often used. The advantages of these lasers for photolysis are the short pulse duration ( $<10^{-8}$  s), a convenient spectral range for photodissociation, and high spectral brightness and repetition frequency (allows one to accumulate the signal).

When the energy corresponding to the vacuum ultraviolet region is required for photodissociation, multiphoton absorption using lasers in the visible and UV region is used.

Laser methods made it possible to obtain vibrationally highly excited species when the polyatomic molecule exists near the dissociation threshold. There are several methods for the formation of vibrationally highly excited species.

1. Due to photon absorption, a particle in the electronically excited state is formed, from which it undergoes nonradiative transition to the ground electronic state with a high vibrational excitation. This method is poorly versatile. It allows one to excite molecules in a very narrow energy interval, *i.e.*, with a sufficiently monoenergetic vibrational distribution. In several cases, the transition from the electronically excited state to the ground electronic state can be performed due to the stimulated emission of the molecule under the action of another photon.

2. Particles are excited to high vibrational levels of the ground electronic state due

to the absorption of a photon. In this case, since the cross section of this absorption is very small, one should use a rather intense laser radiation. A possibility to apply this method appeared due to the development of sensitive methods of the detection of the fluorescence spectrum of the reaction products.

3. The formation of vibrationally highly excited polyatomic particles occurs due to the multiphoton absorption of the intense IR radiation. In this case, the wavelength of an IR laser should coincide with the fundamental absorption band. The disadvantage of this method for radical generation is the formation of molecular ensembles with different vibrational excitations, which can participate in side elementary processes. Therefore, this method should be applied only in the cases where radical cannot be formed by one-photon absorption.

Laser methods make it possible to obtain particles with both a definite value and direction of the velocity vector and a definite orientation in the space. If a laser producing the radiation with the spectral width much shorter than the width of the absorption line is used for the excitation of a molecule, whose contour of the absorption line is due to the Doppler broadening, only molecules moving with a definite velocity in the direction of the laser beam will undergo excitation. For example, if the generation frequency of the laser corresponds to the frequency of the center of the absorption line of molecule, then only molecules "at rest" will be excited.

Another method for the formation of particles with a specified velocity vector is based on photodissociation processes. So, it is known that hot hydrogen atoms can be obtained by laser photolysis of HI and HBr molecules using excimer lasers. In this process, the energy of the translational motion of the H atom depends on the wavelength of the irradiating laser radiation.

## Experimental studies of gas-phase reactions

In this Chapter, we discuss results of experimental and theoretical studies of various elementary reactions. The examples represent the values of rate constants of different classes of elementary reactions and approaches to the solution of these or other kinetic problems. Several examples were taken from scientific articles, reviews, and monographs, which are presented in the recommended literature.

### 4.1. Unimolecular reactions

There are three methods for the formation of active molecules  $A$  ( $\epsilon > E_0$ ), which could participate in the unimolecular reaction: thermal activation, chemical activation, and photoactivation. Let us consider unimolecular reaction taking into account the method of activation.

#### 4.1.1. Unimolecular reactions for activation by collisions

In Section 2.1.4, we presented the simplified kinetic scheme for the description of unimolecular reactions for thermal activation. The macroscopic rate constant of the unimolecular reaction  $k_{uni}$  depends on the total concentration of the buffer gas  $[M]$ . In the limit of low  $[M]$  concentration, the rate constant  $k_0$  characterizes the activation process, and in the limit of high  $[M]$  concentrations the rate constant  $k_\infty$  characterizes the unimolecular reaction. Under the conditions of medium  $[M]$  concentrations, the activation rate is comparable with that of unimolecular reactions. Thus, only  $k_\infty$  bears an information on the chemical unimolecular act in the pure form.

The total concentration of the buffer gas  $[M]$  corresponding to the rate constant  $k_\infty$  depends substantially on the number of atoms in the studied molecule, vibrational frequencies, and temperature: the smaller the number of atoms and the higher the temperature, the higher the  $[M]$  concentrations at which  $k_\infty$  is achieved. For molecules with a small number of atoms at high temperatures, the  $[M]$  concentrations can be so high that they can barely be achieved in experiment. In this case,  $k_{uni}$  is determined in the fall-off region of concentrations  $[M]$ . The methods for extrapolation of experimental  $k_{uni}$  values for finding  $k_\infty$  are available.

When the dependence of  $k_{uni}$  on  $[M]$  is experimentally determined up to the val-

ues close to  $k_{\infty}$ , correction can be performed as follows. In the first approximation, it is accepted that at high  $[M]$  values the found experimental  $k_{\text{uni}}$  values are  $k_{\infty}$ . In the framework of this approximation, the  $E_0'$  value and frequencies of vibrations of the transition complex are determined. Taking into account these parameters, one calculates the theoretical plot of  $k_{\text{uni}}$  vs.  $[M]$ , then compares it with the experimental plot, and corrects the  $k_{\infty}$  and  $E_0$  values and frequencies of vibrations of the transition complex.

The following types of unimolecular reactions can be distinguished: cleavage of the ordinary bond and formation of two radicals; elimination to form stable molecules; isomerization reactions. Table 4.1 contains the examples and Arrhenius parameters of the rate constant for these types of reactions. The experimental studies presented in Table 4.1 were carried out in shock tubes except for the decomposition of  $\text{CCl}_2\text{HCH}_2\text{Cl}$  when laser heating of the gas mixture was used. It is seen from these data that the highest pre-exponential factors belong to the rate constants of decomposition at the ordinary bond. Recombination reactions, which, as a rule, occur without a barrier, are inverse for these reactions. Unlike recombination reactions, inverse reactions of elimination and isomerization have substantial potential barriers.

*In chemical activation*, the formation of the active molecule  $\text{A}^*(\epsilon)$  also occurs due to collisions. However, in this case, not the process of energy transfer but the chemical reaction is the result of collision. Association reactions are most often used for chemical activation: radical recombination, addition at the unsaturated bond. The kinetic scheme for chemical activation coincides with that for bimolecular reactions occurring through a long-lived complex. In the microscopic variant, this scheme has the form

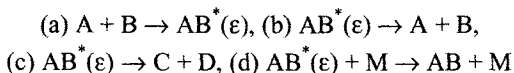


Table 4.1. Arrhenius parameters for decomposition, elimination, and isomerization reactions

Reaction	$A_{\infty}, \text{s}^{-1}$	$E_{\text{act}}, \text{kJ/mol}$
$\text{CH}_4 \rightarrow \dot{\text{C}}\text{H}_3 + \dot{\text{H}}$	$1.0 \cdot 10^{15}$	420
$\text{C}_2\text{H}_5\text{Cl} \rightarrow \text{C}_2\text{H}_4 + \text{HCl}$	$2.0 \cdot 10^{13}$	236.6
Cycloheptatriene $\rightarrow$ Toluene	$1.3 \cdot 10^{14}$	220.5

To consider the energy behavior during chemical activation, we can use Fig. 4.11. The average energy of chemically activated molecules is determined by the expression

$$\langle \epsilon \rangle = E_0' + \Delta U_0' + Q$$

where  $\Delta U_0'$  is the difference of zero-point energies of reactants and molecule AB;  $E_0'$  is the

height of the potential barrier for dissociation reaction  $c$ ; and  $Q$  is the average thermal energy of reactants A and B, which is not indicated in Fig. 4.11 and can often be neglected.

For simplification, let us consider the case when the second maximum in Fig. 4.11 lies much lower than the first one. This corresponds to the case when  $\langle \epsilon \rangle > E_0$ . Then decomposition in the direction of reactants can be neglected, *i.e.*,  $k_b$  is equalized to zero. The rate of formation of decomposition products D and the rate of formation of molecules AB are measured in experiment. We designate them as  $V_D$  and  $V_{AB}$ . The averaged over  $\epsilon$  decomposition rate constant  $\langle k_c \rangle$  is determined from the relation

$$\langle k_c \rangle = k_g[M] V_D / V_{AB} \quad (4.1)$$

Represent the reaction as that occurring via two channels: (1)  $A + B \rightarrow C + D$ , (2)  $A + B \rightarrow AB$ . Then the ratio  $V_D / V_{AB}$  can be defined as

$$\frac{V_D}{V_{AB}} = \frac{k_1(T)[A][B]}{k_2(T)[A][B]} = \frac{k_1(T)}{k_2(T)}$$

The rate constants  $k_1(T)$  and  $k_2(T)$  are determined by formulas (4.88) and (4.89). Inserting the expressions for  $k_1(T)$  and  $k_2(T)$  into expression (6.1), we obtain

$$\langle k_c \rangle = k_g[M] \frac{\int_{E_0}^{\infty} f(\epsilon) k_c(\epsilon) / \{k_c(\epsilon) + k_g[M]\} d\epsilon}{\int_{E_0}^{\infty} f(\epsilon) k_g(\epsilon) / \{k_c(\epsilon) + k_g[M]\} d\epsilon} \quad (4.2)$$

In chemical activation, as well as in thermal activation, one can introduce rate constants in the limit of low concentration  $[M]$  (the condition  $k_g[M] \ll k_c(\epsilon)$  is fulfilled) and high concentration  $[M]$  (the condition  $k_g[M] \gg k_c(\epsilon)$  is valid). The expressions for these rate constants have the form

$$\langle k_c \rangle_0 = k_g[M] \int_{E_0}^{\infty} f(\epsilon) d\epsilon \quad \Bigg/ \quad \int_{E_0}^{\infty} f(\epsilon) \frac{k_g[M]}{k_c(\epsilon)} d\epsilon = \langle k_c^{-1}(\epsilon) \rangle \quad (4.3)$$

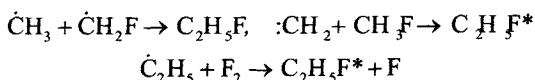
$$\langle k_c \rangle_{\infty} = k_g[M] \int_{E_0}^{\infty} f(\epsilon) \frac{k_c(\epsilon)}{k_g(\epsilon)} d\epsilon \quad \Bigg/ \quad \int_{E_0}^{\infty} f(\epsilon) d\epsilon = \langle k_c(\epsilon) \rangle \quad (4.4)$$

It can easily be seen that the following equality is fulfilled:

$$\langle k_c \rangle_{\infty} / \langle k_c \rangle_0 = \langle k_c(\epsilon) \rangle / \langle k_c^{-1}(\epsilon) \rangle \quad (4.5)$$

Chemical activation has the significant distinction from thermal activation: the distribution functions substantially differ. For chemical activation, the  $f(\epsilon)$  function is determined by formula (4.89). The calculations by this formula using the RRKM theory showed that for chemical activation this function is very narrow and often 70-90% molecules  $A$  ( $\epsilon > E_0$ ) have energies differed from the average energy by not more than 10%. This implies that, in many cases, one can believe to a good approximation that chemically activated molecules have quite certain energy. The validity of this approximation can be checked experimentally by measuring  $\langle k_c \rangle_{\infty}$  and  $\langle k_c \rangle_0$ . If their ratio is close to unity, this approximation is valid. The deviation of  $\langle k_c \rangle_{\infty} / \langle k_c \rangle_0$  from unit can serve as a measure of energy scatter.

Chemical activation has two substantial advantages over thermal activation. Selecting different reactants, one can obtain the same molecule  $A$  ( $\epsilon > E_0$ ) with different storages of the internal energy. For example, chemically activated ethyl fluoride was obtained by three reactions



The average excitation energies of the  $\text{C}_2\text{H}_5\text{F}$  molecules formed in these reactions are close to 370, 450, and 290 kJ/mol, respectively.

Calculations using the RRKM theory rather well describe the experimentally determined plots of the decomposition rate constants vs. excitation energy. To illustrate this, some results of studying the elimination of hydrogen halide from chemically activated alkyl halides, which were obtained by radical recombination, are presented in Table 4.2. The experimental and theoretical values of the decomposition rate constants of these reactions are presented in the last column in the table.

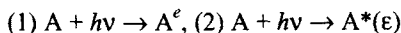
Table 4.2. Calculated and measured rate constants of elimination of hydrogen halides from chemically activated alkyl halides at 700 K

Chemically activated molecule	Eliminated molecule	$E_0$ , kJ/mol	$\langle \epsilon \rangle$ , kJ/mol	$\langle k \rangle \cdot 10^{-9}$ , s <sup>-1</sup> exp.	calcd.
$\text{C}_2\text{H}_5\text{Cl}$	HCl	230	379	2.6	2.5
$\text{C}_2\text{H}_5\text{Br}$	HBr	217	380	6.1	5.8
$\text{C}_2\text{H}_5\text{F}$	HF	212	450	0.9	1.1

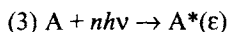
### 4.1.2. Reactions during photoactivation

#### *Types of photodissociation*

Photon absorption can result in the formation of either electronically excited molecule  $A^e$ , or vibrationally excited molecule  $A^*(\epsilon)$  in the ground electronic state

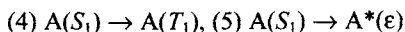


Multiphoton absorption is also used, which usually takes place for the irradiation of molecule  $A$  by powerful infrared radiation. Multiphoton absorption is most often used for the formation of vibrationally excited molecules  $A^*(\epsilon)$



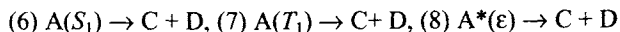
where  $n$  is the number of absorbed photons.

Excited molecules  $A^e$  and  $A^*(\epsilon)$  can participate in various deactivation processes upon collisions with other molecules. Usually unimolecular reactions involving excited molecules  $A^e$  and  $A^*(\epsilon)$  are carried out under such experimental conditions where no collision with other molecules occurs within the time of the unimolecular reaction. However, electronically excited molecule  $A^e$  can participate in non-radiative intramolecular transitions from one potential energy surface to another. Let us assume for determinacy that in process 1 molecule  $A^e$  is formed in the first singlet electronic state (designate  $A^e$  as  $A(S_1)$ ). Molecule  $A(S_1)$  can participate in non-adiabatic non-radiative processes and transform into the triplet electronic state  $T_1$  and ground electronic state  $S_0$



where  $A(T_1)$  designates molecule  $A$  in the first triplet electronically excited state.

Molecules  $A(S_1)$ ,  $A(T_1)$ , and  $A^*(\epsilon)$  can participate in unimolecular reactions



If in process 1 molecule  $A^e$  is formed in higher electronic states, then the molecules in these states participate in either unimolecular reactions, or intramolecular processes of transition to lower electronic states.

Three types of photodissociation processes are distinguished. If molecule  $A^e$  undergoes decomposition on the same PES on which it was formed in process 1, this process is named direct dissociation (reaction 6). If molecule  $A^e$  first transits to another electronically excited state (process 4) and dissociation occurs from this state (reaction 7), we may speak about electronic pre-dissociation. If  $A^e$  transits to the ground electronic state (process 5) to form  $A^*(\epsilon)$ , vibrational pre-dissociation (reaction 8) is discussed.

Experimental studies of unimolecular reactions during photoactivation can be

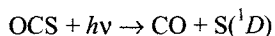
reduced to the following tasks: identification of reaction products, determination of the lifetime  $\tau$  of the excited species (the rate constant of the unimolecular reaction is equal to  $1/\tau$ ), measurements of the energy distribution over electronic, vibrational, rotational, and translational degrees of freedom, and establishment of a correlation between the velocity of species separation and rotational angular momenta of products. Such experimental studies are necessary for analysis of the mechanism and development of theoretical models of unimolecular reactions during photoactivation.

In these studies, not only rotational and vibrational states of products should be detected, but also the distribution of the velocity of the separation of products. Either time-of-flight mass spectroscopy, or the LIF method with a high spectral resolution is used for this purpose. When LIF is used, the Doppler contour of the line in the excitation spectrum is measured. Since atoms with different velocity vectors, according to the Doppler effect, absorb (emit) the light in different manners, this reflects the shape of the line in the excitation spectrum. Therefore, using the experimentally determined contour of the line in the excitation spectrum, one can obtain information about the values and direction of the velocity of the separation of products.

#### *Photodissociation of electronically excited molecules*

Any elementary process is determined by two laws: conservation of energy and conservation of angular momentum. The law of energy conservation characterizes the scalar properties of the elementary process, and the law of angular momentum conservation characterizes the geometric properties of the elementary process. It is difficult to use the latter if activation occurs during collisions of molecules. This is related to the fact that the angular momenta of colliding particles, as a rule, are unknown. The problem is substantially simplified for photoactivation. The angular momentum of a photon is known, and the angular momentum of the reactant can be determined with a high accuracy in the experiment in a supersonic molecular beam using the polarized light.

To illustrate the correlation between the vector of scatter velocity and the angular momentum of the product, let us consider the results of studies by M.R. Doker on the photodissociation of carbon sulfoxides under irradiation with  $\lambda = 222$  nm



The law of angular momentum conservation requires that

$$\bar{J}_{\text{OCS}} + \bar{J}_{\text{F}} = \bar{J}_{\text{S}} + \bar{J}_{\text{CO}} + \bar{l} \quad (4.6)$$

where  $\bar{J}_{\text{OCS}}$  and  $\bar{J}_{\text{CO}}$  are the rotational angular momenta of the corresponding molecules,  $\bar{J}_{\text{S}}$  is the electronic angular momentum of the sulfur atom,  $\bar{J}_{\text{F}}$  is the angular momentum of a photon, and  $\bar{l}$  is the orbital angular momentum of the relative motion of the separating atom and molecule.

The absolute value of the angular momentum of a photon equals unity. The S

atom has only the electronic angular momentum. Since the mass of electrons is very small, the absolute value of the electronic angular momentum is usually much lower than the absolute values of the angular momenta of the molecules. Therefore, in formula (4.6), the angular momentum of a photon and electronic angular momentum of the S atom can be neglected. The use of cooling of the reactant in the supersonic jet makes it possible to obtain the OCS molecule in the lowly excited rotational states when  $|\vec{J}_{\text{OCS}}|$  is close to zero. At the same time, the experiment shows that rotation-excited CO molecules with  $N_{\text{CO}} \approx 60$  ( $N_{\text{CO}}$  is the rotational quantum number of the CO molecule) are predominantly formed in the reaction. This implies that in absolute value  $|\vec{J}_{\text{CO}}| \gg 1$ . Thus,  $|\vec{J}_{\text{CO}}| \gg |\vec{J}_{\text{OCS}}|, |\vec{J}_{\text{S}}|, |\vec{J}_{\text{F}}|$ . Therefore, the equality is fulfilled

$$\vec{J}_{\text{CO}} \rightarrow -\vec{l}$$

This means that the orbital angular momentum and internal angular momentum of the product are antiparallel. The orbital momentum is related to the separation velocity  $\vec{v}$  through the impact parameter  $b$  by the relation

$$\vec{l} \rightarrow \mu [\vec{v} \vec{b}]$$

where  $[\vec{v} \vec{b}]$  is the vector product.

It follows from this that the vector of separation velocity of products  $\vec{v}$  is perpendicular to the rotational angular momentum of the CO molecule. This correlation between the vectors  $\vec{v}$  and  $\vec{J}_{\text{CO}}$  was experimentally confirmed from analysis of the Doppler contours of the excitation spectra of the CO molecule. The use of the law of energy conservation showed that the sulfur atom in the electronic state  $^1D$  is formed in this reaction.

To study the scalar properties of photodissociation, the energy distribution over the vibrational, rotational, and translational degrees of freedom is experimentally detected. If the photodissociation products are formed in the ground electronic state, the law of energy conservation has the form

$$E = \epsilon_{\text{vibr}} + \epsilon_{\text{rot}} + \epsilon_{\text{tr}}$$

where  $E$  is the total energy released in the photodissociation process;  $\epsilon_{\text{vibr}} + \epsilon_{\text{rot}} + \epsilon_{\text{tr}}$  are the energies of the vibrational, rotational, and translational motions of the products.

The experimental data on the average fractions of the energy released to different degrees of freedom during the direct photodissociation of electronically excited molecules are presented in Table 4.3. The wavelengths of the irradiating light are indicated in the first column. It is seen from the table that for the presented examples of photodissociation, a great fraction of the energy is released to the translational degrees of freedom of the products. In addition, the decomposition of all these molecules occurs within times of  $\sim 10^{-13}$  s. Let us discuss in more detail the photodisso-

ciation of HONO, which was studied at different wavelengths of the irradiating light ( $\lambda = 193, 342, 355$ , and  $369$  nm). In all cases, the decomposition products were formed in the ground electronic state. Decomposition occurred so rapidly that the molecule had no time to significantly change its orientation within the time between photon absorption and decomposition. The reaction products were detected by the LIF method. No formation of vibrationally excited products was observed. Analysis of the Doppler contours of the excitation spectrum of the  $\cdot\text{OH}$  radical showed that a considerable portion of the released energy goes to the translational energy of scattering products. Thus, the experimental data indicate that at different wavelengths of the irradiating light direct dissociation occurs, probably, from the repulsive electronic term.

Table 4.3. Energy distribution in dissociation products at different degrees of freedom

Reaction	$\lambda$ , nm	$P_{\text{tr}}$	$P_{\text{vibr}}$	$P_{\text{rot}}$
$\text{CH}_3\text{I} + h\nu \rightarrow \dot{\text{C}}\text{H}_3 + \text{I}^*$	266	0.87	0.13	—
	248	0.89	0.11	—
	193	0.92	0.08	—
$\text{CH}_3\text{Br} + h\nu \rightarrow \dot{\text{C}}\text{H}_3 + \text{Br}^*$	222	0.94	0.06	—
$\text{HONO} + h\nu \rightarrow \dot{\text{O}}\text{H} + \dot{\text{N}}\text{O}$	193	0.94	—	0.03

Electronic spectra of HONO are similar to those of aliphatic nitrates of the RONO type. Therefore, for molecules of this class we can expect the general mechanism of dissociation under irradiation with  $\lambda = 300 \div 400$  nm. Indeed, it was experimentally shown that the mechanism of photodissociation of the  $\text{CH}_3\text{ONO}$  and  $(\text{CH}_3)_3\text{VONO}$  molecules is similar to the mechanism of HONO photodissociation. H. Reisler, M. Noble, and S. Wittig in their reviews gave the detailed description of the photodissociation of nitrogen-containing molecules.

For these fast decompositions, the statistical energy redistribution over the vibrational degrees of freedom of the molecule has no time to occur. Therefore, the statistical theory is not applicable to these unimolecular reactions. The theoretical description of such a fast dissociation of electronically excited molecules requires dynamic calculations, which are very complicated and need the knowledge of the specific features of the potential energy surface of excited electronic states.

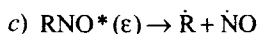
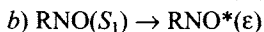
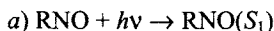
#### *Photodissociation of vibrationally excited molecules*

Three methods for obtaining high-vibrational excited molecules in the ground electronic state are available. Each method has its advantages and disadvantages and, hence, it seems reasonable to discuss unimolecular reactions of vibrationally excited molecules taking into account the method of their generation.

The first method includes processes 1 and 5. In process 1 electronically excited

molecule  $A^e$  is formed, which undergoes non-adiabatic non-radiative transition 5. As a result, vibrationally excited molecule  $A^*(\epsilon)$  in the ground electronically excited state is formed. Photodissociation of nitroso compounds of the RNO type is an example of this method for the formation of high-vibrationally excited molecules in the ground electronic state.

Nitroso compounds have general specific features of the electronic structure. Figure 4.1 presents the shape (typical of nitroso compounds) of three lowest potential curves along the reaction coordinate, resulting in the elimination of NO. As can be seen, the formation of products from state  $S_1$  can occur through surmounting of a high potential barrier. Therefore, the molecules in state  $S_1$  formed in process 1 can transit to the ground electronic state  $S_0$  (process 5). Then the photodissociation of nitroso compounds occurs as follows:



The kinetics of formation of the products R and NO is determined by either process *b*, or reaction *c*. If the rate constant of process *b* is higher than that of reaction *c*, the rate constant  $k_c$  is determined from the kinetic data. By contrast, if  $k_c \gg k_b$ , then the  $k_b$  value is determined from the kinetic data. To reveal which process is slower, the rate constant of decomposition of the vibrationally excited molecule  $\text{RNO}^*(\epsilon)$  is calculated using the statistical theory and the results of the calculation are compared with the experimentally determined rate constant. If the calculated  $k_c$  value is much higher than that determined experimentally, the photodissociation process is limited by the non-adiabatic non-radiative transition, *i.e.*, process *b*. Let us illustrate aforesaid by several examples.

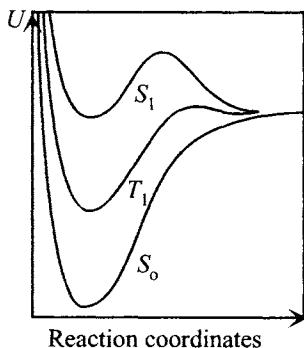
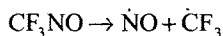


Fig. 4.1. Potential energy curves of nitroso compounds.

Consider the decomposition of *tert*-butylnitrosomethane (*tert*-BuNO). *tert*-BuNO molecules cooled in a supersonic jet to a temperature of several Kelvin were excited by the radiation of a dye laser. Fluorescence of the initial *tert*-BuNO molecules was observed. The reaction product, *viz.*, NO molecules, was detected by the LIF method. It was found that also fluorescence of *tert*-BuNO disappeared 40 ns after excitation (which corresponds to the lifetime of the electronically excited state of *tert*-BuNO), the NO molecules appeared much more later, with the characteristic time longer than 1  $\mu\text{s}$ . The presence of the induction period for product formation indicates that the decomposition of the *tert*-BuNO proceeds in two stages: fast non-

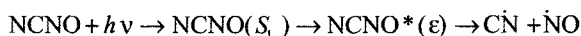
radiative conversion and the relatively slow decomposition of the high-vibrationally excited molecule of *tert*-butylnitrosomethane.

The next example is decomposition



The mechanism of decomposition of this molecule is also determined by stages *a-c*. This example is of interest because the time of appearance of the product (NO molecule) coincides with the radiative lifetime of  $\text{CF}_3\text{NO}$ . The indicated lifetime of the reactant is much longer than that calculated by the RRKM theory for decomposition from the ground electronic state  $S_0$ . This indicates that dissociation occurs more rapidly than non-radiative transitions, and the decomposition rate is limited by the slow non-radiative transition. As for the distribution of the formed NO molecules over internal degrees of freedom, it coincides with the statistical distribution at the excitation energy near the dissociation threshold. If the excitation energy is increased, insignificant deviations from statistics appear. They are likely related to the contribution of the triplet state to the decomposition process.

One more example: HCNO decomposition. The reaction was studied in a supersonic jet. The wavelength of the light exciting the HCNO molecule in process *a* was changed in such a way that the energy interval is  $\Delta\epsilon = h\nu - E_0$  above the dissociation threshold was  $\Delta\epsilon = 0.65$  kJ/mol. The vibrational and rotational distributions of both reaction products, viz., CN and NO, were detected. The experimental data indicate that unimolecular decomposition proceeds via the following mechanism:



This mechanism is substantiated by the fact that the vibrational distribution of the products agrees well with the calculations using the statistical theory at various exceedings of the excitation energy  $\Delta\epsilon$  over the dissociation threshold. Below we present the relative populations of the vibrationally excited products  $P_{\text{CN}} = [\text{CN}(v=1)] / \sum_v [\text{CN}(v)]$  and  $P_{\text{NO}} = [\text{NO}(n=1)] / \sum_n [\text{NO}(n)]$  obtained in experiment and calculated using the statistical theory

$\Delta\epsilon$ , kJ/mol	77.5	116	141
$P_{\text{CN}}^{\text{exp}}$	0.07	0.2	0.27
$P_{\text{CN}}^{\text{theor}}$	0.08	0.22	0.26
$P_{\text{CN}}^{\text{exp}}$	0.12	—	—
$P_{\text{CN}}^{\text{theor}}$	0.14	—	—

The second method for the preparation of vibrationally excited molecules in the

ground electronic state is process 2:  $A + h\nu \rightarrow A^*(\epsilon)$ .

Designating the frequency of the normal vibrational mode as  $\nu_o$ , we can obtain in process 2 the excited molecules with the energy close to  $2h\nu_o$ ,  $3h\nu_o$ , ...,  $nh\nu_o$ . Absorption lines at these frequencies are named *overtones* (first, second, and higher). The probability of formation in process 2 of the excited molecule with the energy corresponding to the higher overtone decreases rapidly. Therefore, the normal

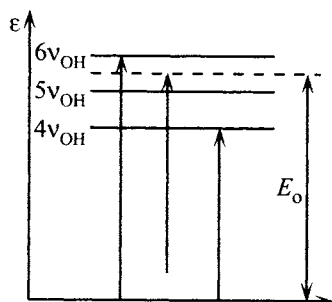
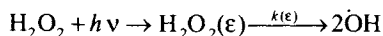


Fig. 4.2. Energy diagram of hydrogen peroxide dissociation

vibrational mode corresponding to the high vibrational frequency (compared to other normal vibrational modes) is separated. In this case, the excitation of a lower overtone is sufficient for the energy to be enough for unimolecular decomposition.

As a rule, at the starting momentum after irradiation, the energy of vibrational excitation is localized. The statistical energy redistribution over all vibrational degrees of freedom occurs with time. The time of statistical energy redistribution depends on the number of atoms and frequencies of normal vibrations in the molecule and is approximately equal to 10-12 s. Therefore, rate constants of decomposition of molecules can be calculated using the statistical theory.

As an example, let us consider the results obtained by F. Krim on studying the unimolecular decomposition of hydrogen peroxide ( $H_2O_2$ )



Hydrogen peroxide decomposition requires surmounting of the potential barrier  $E_o$  equal to 210 kJ/mol. The  $H_2O_2$  molecule has the high-frequency normal vibration ( $\sim 3600\text{ cm}^{-1}$ ), which corresponds to vibrations of the O and H atoms along the O—H bonds in the  $H_2O_2$  molecule. Let us designate the frequency of this normal vibrational mode as  $\nu_{OH}$ . Figure 6.2 presents the energy of vibrational overtones  $4\nu_{OH}$ ,  $5\nu_{OH}$ , and  $6\nu_{OH}$ . Retuning the wavelength of the exciting laser, one can excite vibrations with different overtones. As can be seen in this figure, only the vibrational energy of the sixth overtone exceeds that energy of the O—O bond cleavage. However, decomposition can also occur during the excitation of vibrations of the fifth overtone if photons are absorbed by the thermally excited  $H_2O_2$  molecules. To remove this light absorption, the  $H_2O_2$  molecules are cooled during supersonic expansion. Then the decomposed  $H_2O_2(\epsilon)$  molecules will have certain energy, which is equal to the energy of the absorbed photon ( $\sim 230\text{ kJ/mol}$ ).

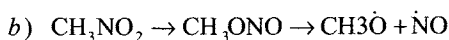
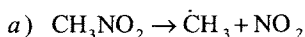
The excitation spectra of different overtones and the OH radicals in different rota-

tional states were experimentally detected. When the sixth overtone is excited, the molecule has an energy excess over the dissociation threshold equal to  $\sim 20$  kJ/mol. The detection of the rotational states of the hydroxyl radicals shows that the rotationally excited  $\cdot\text{OH}$  radicals are mainly formed in the reaction. The distribution function has a rather smooth shape and extends to  $\cdot\text{OH}$  ( $N = 10$ ) ( $N$  is the rotational quantum number). The levels with  $N = 4$  and  $5$  are most populated.

To determine the rate constant  $k(\epsilon)$ , the spectral width  $\Delta\nu$  of particular lines of the overtone excitation spectrum of the  $\text{H}_2\text{O}_2$  was measured. The lifetime of the excited molecule  $\tau$  was determined by the uncertainty:  $\tau = 1/\Delta\nu$ . The microscopic rate constant was determined from the relation  $\tau = 1/k(\epsilon)$ . In principle, this method for determination of  $k(\epsilon)$  should be used with care because not only dissociation but also non-uniform broadening can contribute to the measured spectral width  $\Delta\nu$ . However, in this example, the measured lifetime is  $\tau = 3.5$  ps and, hence,  $k(\epsilon) = 2.9 \cdot 10^{11} \text{ s}^{-1}$  agrees with the calculation using the statistical theory.

The third method of formation of  $\text{A}^*(\epsilon)$  is process 3:  $\text{A} + nh\nu \rightarrow \text{A}^*(\epsilon)$ . V.A. Bagratashvili presents in detail this method of photoexcitation in his monograph. After irradiation with a pulse of an infrared laser, the excited molecules  $\text{A}^*(\epsilon)$  have some distribution over the vibrational energy. This distribution depends on the laser radiation intensity. If the laser intensity is low, the excited molecules have an insignificant excess over the dissociation energy. Molecules are excited to high energies with an increase in the intensity of laser irradiation. Thus, changing the radiation intensity, one can obtain molecules with different excesses of the vibrational energy over the dissociation threshold.

This excitation method is rather efficient for studying reactions with two channels of decomposition. For example, it was shown that the  $\text{CH}_3\text{NO}_2$  molecules could decompose *via* two channels



The cleavage of the weakest bond occurs in channel a. These reactions have no potential barrier, and their decomposition required that the excitation energy would be higher than the C—N bond energy. The profiles of the reaction routes of this type are shown in Fig. 4.9a. Isomerization first occurs in channel b and then decomposition takes place. These reactions have potential barriers. The profiles of the reaction paths of this type are shown in Fig. 4.9c.

The ratio of rate constants of channels *a* and *b* and energy distribution in the reaction products are determined by mass spectrometry and laser spectroscopy. Using these data and calculations by the RRKM theory, information about the excitation energy of the  $\text{CH}_3\text{NO}_2$  molecule and the potential barrier  $E_0$  for channel *b* is obtained. Below thus determined potential barriers for some reactions are presented

	kJ/mol
$\text{CH}_3\text{NO} \rightarrow \text{CH}_3\text{ONO}$	231
$\text{C}_2\text{H}_5\text{NO}_2 \rightarrow \text{C}_2\text{H}_4 + \text{HONO}$	192
$\text{CH}_3\text{CO}_2\text{C}_2\text{H}_5 \rightarrow \text{C}_2\text{H}_4 + \text{CH}_3\text{CO}_2\text{H}$	208

#### 4.2. Bimolecular reactions

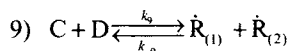
*Thermal electronically adiabatic reactions* (Section 4.2.1), which occur under the conditions of the Maxwell—Boltzmann distribution, compose the largest class of bimolecular reactions. Diverse experimental studies of this class of reactions are resulted first by requests of practice. Information on elementary reactions is necessary for understanding complicated chemical reactions, which are important in the chemistry of atmosphere, combustion, for technologies, *etc.*

In some cases, the kinetics of bimolecular reactions cannot be described in the framework of one PES, and the experimental data to be explained needs the use of two PES. These reactions are named electronically non-adiabatic (Section 4.2.2).

Kinetic analysis of energetically non-equilibrium processes (gas lasers, plasmachemistry, photochemistry, *etc.*) needs the knowledge of microscopic rate constants. Rate constants and cross sections of microscopic reactions (Section 4.2.3) give less averaged information than rate constants of thermal reactions and, therefore, favor the development of concepts about the physics of elementary act.

##### 4.2.1. Thermal electronically adiabatic reactions

Reactions between stable molecules, as a rule, have high activation energies ( $E_0 \approx 160$  kJ/mol). Therefore, rate constants of these reactions have much lower values than rate constants of reactions of stable molecules with radicals. Radicals are usually the products of thermal reactions of stable molecules. Let us consider the reaction of stable molecules with the formation of two radicals



The kinetics of such reactions is experimentally studied at high temperatures when their rates can be detected. The main method of studying is the method of shock waves. Indirect methods are often used because it is difficult to measure low reaction rates.

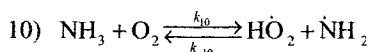
Reactions inverse to 9 are usually exothermic and have much higher values of rate constants. This makes it possible to study inverse reactions at lower temperatures using direct spectroscopic methods. After the rate constant  $k_{-9}$  was experimentally

determined, one can calculate the  $k_9$  value from the expression

$$k_9 = k_{-9}K$$

where  $K$  is the equilibrium constant.

Thus, reactions of radicals can be used for the determination of rate constants of slow reactions between stable molecules. Let us consider the following reaction as an example:



The reaction inverse to 10 was studied by direct methods and it was found that  $k_{10} = 2 \cdot 10^{13} \text{ cm}^3/(\text{mol s})$ . The equilibrium rate constant  $K$ , as it is known, is expressed through the change in entropy  $\Delta S$  and enthalpy  $\Delta H(T)$  in the reaction for the reactants and products in the standard state

$$K = \exp[-(\Delta H^\circ/RT) + (\Delta S^\circ/RT)] \quad (4.7)$$

If it is accepted that  $\Delta H^\circ(298 \text{ K}) = 237 \text{ kJ/mol}$  and  $\Delta S^\circ(298 \text{ K}) = 26.2 \text{ kJ/(mol K)}$ , we can find the  $K$  value at 298 K. Then  $k_{10}(298 \text{ K}) = 1.1 \cdot 10^{-27} \text{ cm}^3(\text{mol s})$ .

As can be seen, this procedure makes it possible to determine such low values of rate constants that cannot be measured experimentally. Since the reaction of the  $\text{HO}_2\cdot$  radicals with  $\text{NH}_2$  takes place at each collisions, it can be assumed that  $k_{-10}$  is temperature-independent and the Arrhenius parameters of the rate constant  $k_{10}$  can be estimated:  $E_{\text{act}} = 237 \text{ kJ/mol}$ ,  $A = 8.5 \cdot 10^{14} \text{ cm}^3/(\text{mol s})$ .

As already mentioned in Section 4.1.7, bimolecular reactions can be classified as *direct reactions and reactions occurring through long-lived complex*. These two types of reactions differ by profiles of reaction paths (see Fig. 4.8).

For direct reactions, the reaction path profile has one potential barrier. In the framework of the theory of activated complex, the deviations of the temperature dependence of the rate constant from the Arrhenius equation for direct reactions can be explained by the temperature dependence of statistical sums of the reactants and activated complex. After inserting rotation, vibration, and translational statistical sums into expression (4.76), the temperature dependence of the rate constant is presented by the expression

$$k = \text{const } T^n \exp(-E_o/RT) \quad (4.8)$$

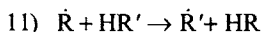
where  $E_o$  is the difference of the ground state energy levels of the activated complex and reactants.

Depending on the structure of reactants, the parameter  $n$  and, hence, the temperature dependence of the pre-exponential factor changes and can reach a value of 3-3.5. However, if the reaction is studied in a narrow temperature interval, the

Arrhenius law (4.26) well describes experimental data.

The calculation of the rate constant by the method of activated complex using formula (4.76) needs the knowledge of  $E_0$ ,  $F$ , and  $F^\ddagger$ . The partition functions of the reactants  $F$  can be calculated through the molecular parameters (vibrational frequencies, rotational constants), which are available from the corresponding reference books. As for  $E_0$  and the statistical sum  $F^\ddagger$ , the calculations of PES are necessary. However, note that the calculation of  $F^\ddagger$  is not very sensitive to the specific features of PES. Therefore, to choose the structure of the activated complex, as a rule, approximate approaches are sufficient.

The reactions of the elimination of the atom by the radicals  $\dot{R}$



are typical direct reactions. The calculated values of pre-exponential factors for several reactions of hydrogen atom elimination at the approximate choice of the activated complex structure are presented in Table 4.4. The height of the potential barrier for hydrogen atom elimination can be estimated most simply by the empirical method "bond energy - bond order." In addition, computer facilities make it possible to calculate PES by semiempirical and non-empirical methods.

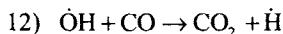
Table 4.4. Experimental and theoretically calculated pre-exponential factors for some reactions

Reaction	$\ln A_{\text{exp}}$	$\ln A_{\text{theor}}$	Temperature interval, K
$\dot{H} + CH_4 \rightarrow \dot{C}H_3 + H_2$	13.7	13.9	500-100
$\dot{C}H_3 + C_3H_8 \rightarrow CH_4 + \dot{C}_3H_7$	11.52	21.4	500-700
$\dot{Cl} + CH_4 \rightarrow HCl + \dot{C}H_3$	13.35	13.66	200-500

Note. The  $A_{\text{theor}}$  values were calculated at  $T = 500$  K,  $A_{\text{exp}}$  were determined in the temperature interval indicated in the table.

Note that it is sometimes rather difficult to determine without quantum-mechanical calculations whether the reaction is direct or proceeds through a long-lived complex. When the reaction proceeds through the long-lived complex, this is usually indicated by the dependence of the rate constant on the pressure of buffer gas  $M$ .

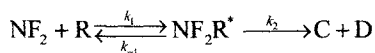
The reaction



is of interest by the fact that the temperature dependence of the rate constant of this reaction differs substantially from the Arrhenius law. At low temperatures ( $< 500$  K), the rate constant is temperature-independent and begins to increase at higher tem-

peratures. This dependence cannot be understood in the framework of the direct reaction. The reaction  $\cdot\text{H} + \text{CO}_2 \rightarrow \cdot\text{OH} + \text{CO}$ , which is inverse to 12, was studied using laser spectroscopy with picosecond time resolution. It was found that the reaction proceeds through the long-lived intermediate complex  $[\text{OHCO}]^*$ . The temperature dependence can be explained from these positions if we accept that the barrier for the decomposition of the intermediate complex toward reactants and products are close. The structure of the activated complex with three collinear heavy atoms corresponds to the barrier toward the products.

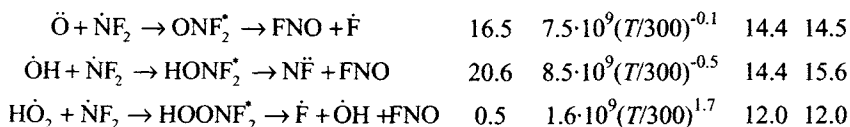
The largest class of reactions occurring through the formation of a long-lived complex includes the reactions of radicals with atoms or radicals. As an example, let us consider the studies of Yu.M. Gershenzon of the reactions of the  $\cdot\text{NF}_2$  radical with atoms and radicals. The method combining LMR and ESR was used in these studies. Atoms were detected by ESR, and LMR was used to detect radicals. Experiments were carried out at pressures of 3–10 Torr in a temperature interval of 300–800 K. Under these conditions, the long-lived complex is not deactivated, *i.e.*, only the decomposition channels can be considered



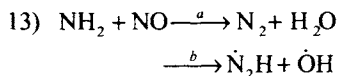
The found temperature dependences of the rate constants are presented in Table 4.5. It is seen that there are both positive and negative temperature dependences of the rate constants. In addition to the experiment, the rate constants were calculated at different temperatures. At the specified structures of the activated complex, the temperature run of the rate constants can be adjusted with the experimental one of varying the potential barriers of  $\text{NF}_2\text{R}^*$  decomposition toward reactants ( $E_0''$ ) and products ( $E_0'$ ). The values of parameters at which the correspondence of the theoretical and experimental data for the studied reactions is observed are indicated in Table 4.5. This example shows that the study of the temperature dependence of the rate constant sometimes allows one to determine the parameters of the potential energy surface. Note that it was assumed in the described case that the reaction proceeds through one long-lived complex.

Table 4.5. Experimental and theoretical results of studying the kinetics of reactions of  $\dot{\text{N}}\text{F}_2$  with atoms and radicals  $\dot{\text{R}}$  ( $\dot{\text{R}} = \dot{\text{H}}, \dot{\text{O}}, \dot{\text{H}}\text{O}, \dot{\text{H}}\text{O}_2$ ).

Reaction	$\Delta U_0$ , kJ/mol	$k(T)$ , $\text{cm}^3/(\text{mol s})$	$E_0''$	$E_0'$
$\dot{\text{H}} + \dot{\text{N}}\text{F}_2 \rightarrow \text{HNF}_2^* \rightarrow \dot{\text{N}}\text{F}(\text{}^1\Delta) + \text{HF}$	8.4	$2.3 \cdot 10^{10} (T/300)^{-0.5}$	18.5	18.0
$\dot{\text{N}} + \dot{\text{N}}\text{F}_2 \rightarrow \text{NNF}_2^* \rightarrow \dot{\text{N}}_2\text{F} + \text{F}$				9.0
$6 \cdot 10^9 (T/300)^{0.25}$	7.2			
7.32				



A more detailed analysis of the kinetics of the reaction proceeding through several long-lived intermediate complexes can be exemplified by the reaction of  $\cdot\text{NH}_2$  with  $\cdot\text{NO}$ . Interest in this reaction is caused by the fact that in it the chemically active nitrogen atom is transformed into the inert  $\text{N}_2$  molecule. This determined the significance of this reaction for the atmospheric chemistry and purification of industrial gases from nitrogen oxides.  $\text{N}_2$ ,  $\text{H}_2\text{O}$ , and  $\cdot\text{OH}$  were observed in the reaction products. The presence of these products assumes two reaction channels



It follows from the thermodynamic calculations that the bond energy of  $\text{NH}$  in the  $\cdot\text{N}_2\text{H}$  species does not exceed 40 kJ/mol and, therefore, it will decompose rather rapidly to the channel  $\text{N}_2 + \text{H}$ .

The published data on the temperature dependence of the total rate constant  $k_{13} = k_a + k_b$  of this reaction are presented in Table 4.6. The reaction was studied in both static and flow-type reactors using different methods for detecting the  $\cdot\text{NH}_2$  and  $\cdot\text{OH}$  radicals. The divergence, although insignificant, between the results of independent authors is observed.

Table 4.6. Temperature plots of the rate constant of the reaction of  $\cdot\text{NH}_2$  with  $\text{NO}$  obtained by different methods

$k$ , l/(mol s)	$T$ (K)	Reactor	Method for radical formation	Method for radical detection
$1.08 \cdot 10^{10} (T/298)^{-1.25}$	300-500	Static	Flow-type	Flash photolysis
$1.2 \cdot 10^{10} (T/298)^{-1.63}$	216-480	Static	The same	LIF
$0.7 \cdot 10^{10} (T/298)^{-1.85}$	210-480	Flash	Chemical	LIF
$1.2 \cdot 10^{10} (T/298)^{-2.2}$	298-620	Static	Absorption spectroscopy	HRLS

The most difficulties appear for the determination of the rate constants of each channel of this reaction. Channel *a* is the main at room temperature:  $k_a = 0.87k_{13}$ ,  $k_b = 0.13k_{13}$ . The role of channel *b* increases with temperature: at  $T = 1000$  K  $k_b = 0.5k_{13}$ .

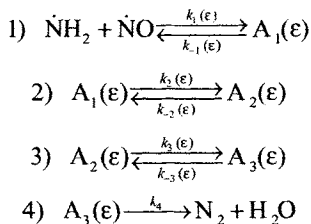
The negative temperature dependence of the overall rate constant immediately indicates that reaction 13 proceeds through a long-lived intermediate complex. To explain the available experimental material on this reaction, theoretical calculations

were performed.

The quantum-chemical calculations performed by John A. Harrison and others show that along the reaction path the system passes through several long-lived complexes. The simplified energy diagram along the reaction path is shown in Fig. 4.3. The reaction proceeds through the long-lived complexes  $A_1$ ,  $A_2$ , and  $A_3$  and activated complexes  $A_{1,2}^*$ ,  $A_{2,3}^*$ , and  $A_{3,4}^*$ . The structures of these complexes are also shown in Fig. 4.3. The index  $i = 1, 2, \dots$  in the presented structures indicates the number of the N and H atoms.

It is seen from the energy diagram that the highest potential barrier is attributed to the transformation of the long-lived complex  $A_2$  into the long-lived complex  $A_3$ . Nevertheless, this barrier also lies below the minimum energy of the reactants. In the activated complex  $A_{3,4}^*$  the  $N_{(1)}-H_{(2)}$  and  $N_{(2)}-O$  bonds are cleaved to form  $H_2O$  and  $N_2$ . It is clear that the reaction should proceed through channel *b* when the  $H_{(2)}-O$  and  $N_{(2)}-O$  bonds are cleaved.

In the framework of the energy diagram in Fig. 4.3, reaction 13 can be presented by the following kinetic scheme:



If we use quasi-stationarity with respect to  $A_1(\epsilon)$ ,  $A_2(\epsilon)$ , and  $A_3(\epsilon)$ , the rate constant  $k_{13}(\epsilon)$  can be presented in the form

$$k_{13}(\epsilon) = k_1(\epsilon)P(\epsilon)$$

where

$$P(\epsilon) = \frac{k_1(\epsilon)k_2(\epsilon)k_3(\epsilon)k_4(\epsilon)}{k_{-1}(\epsilon)k_{-2}(\epsilon)k_{-3}(\epsilon) + k_{-1}(\epsilon)k_2(\epsilon)k_4(\epsilon) + k_2(\epsilon)k_3(\epsilon)k_4(\epsilon) + k_{-1}(\epsilon)k_3(\epsilon)k_4(\epsilon)} \quad (4.9)$$

Let us compare formula (4.9) with the probability  $P(\epsilon) = k_c(\epsilon)/[k_c(\epsilon) + k_b(\epsilon)]$ , which was used in Section 2.2.5 under the assumption of one long-lived complex. The probability  $P(\epsilon)$  of this type can be obtained from expression (4.9) if we neglect the first two terms in the denominator. However, the real calculations of  $k_i(\epsilon)$  by the formulas of the RRKM theory showed that only the first term in the denominator of formula (4.9) can be neglected, and then the probability  $P(\epsilon)$  is the following:

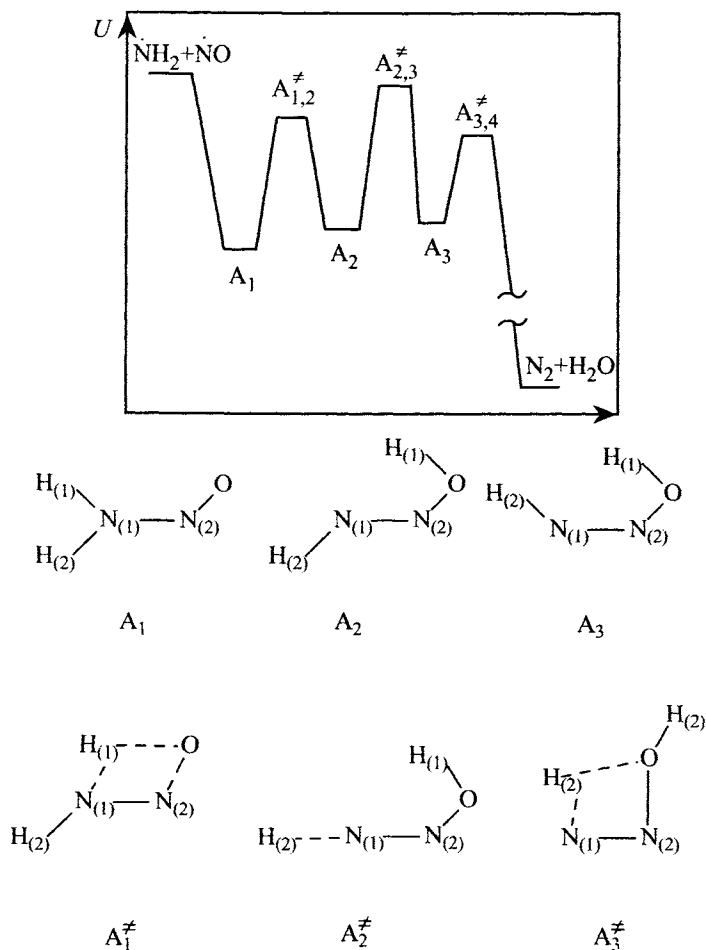


Fig. 4.3. Qualitative profile of the path of the reaction  $\text{NH}_2 + \text{NO} \rightarrow \text{N}_2 + \text{H}_2\text{O}$  and structures of the long-lived and activated complexes.

$$P(\epsilon) = \frac{k_1(\epsilon) k_2(\epsilon) k_3(\epsilon) k_4(\epsilon)}{k_{-1}(\epsilon) k_{-2}(\epsilon) k_4(\epsilon) + k_2(\epsilon) k_3(\epsilon) k_4(\epsilon) + k_4(\epsilon) k_3(\epsilon) k_4(\epsilon)}$$

It is seen from this comparison that information on the reaction path is necessary for the calculation of the rate constant to know how many long-lived complexes should be taken into account for the calculation of  $k$ .

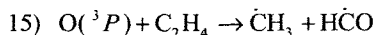
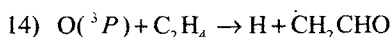
To obtain the thermal rate constant  $k_{13}(T)$ , we have to average  $k_{13}(\epsilon)$  over the dis-

tribution  $f_B(\epsilon)$  for the reactants  $\cdot\text{NH}_2$  and  $\cdot\text{NO}$ . All rate constants  $k_f(\epsilon)$  can be calculated using the formulas presented in Chapter 4. The calculations showed that the calculated  $k_{13}(T)$  satisfactorily describes the observed experimental negative temperature dependence of the rate constant of this reaction.

#### 4.2.2. Electronically non-adiabatic reactions

In the recent time, data appeared that the reactions of  $\text{O}(^3P)$  with unsaturated hydrocarbons can proceed *via* the electronically non-adiabatic mechanism. The reaction of the oxygen atom with ethylene is studied in most detail. Let us consider this reaction to demonstrate the reasons for which it cannot be described in the framework of one potential energy surface.

The reaction of  $\text{O}(^3P)$  with ethylene was studied in both molecular beams and standard reactors. Primary intermediate products were detected by mass spectroscopy and various spectroscopic methods:  $\text{H}$ ,  $\text{CH}_2\text{CHO}$ , and  $\text{HCO}$ . This allowed one to propose two main channels of this reaction



It was revealed that the overall rate constant of this reaction  $k_{\text{overall}} = k_{14} + k_{15}$  is independent of the buffer gas pressure in an interval of 0.5–760 Torr, and the channel ratio  $k_{14}/k_{15}$  decreases with the pressure increase. The question arises what should be the mechanism of this reaction to explain the experimental facts.

The quantum-chemical calculations for the system  $\text{O}(^3P) + \text{C}_2\text{H}_4$  make it possi-

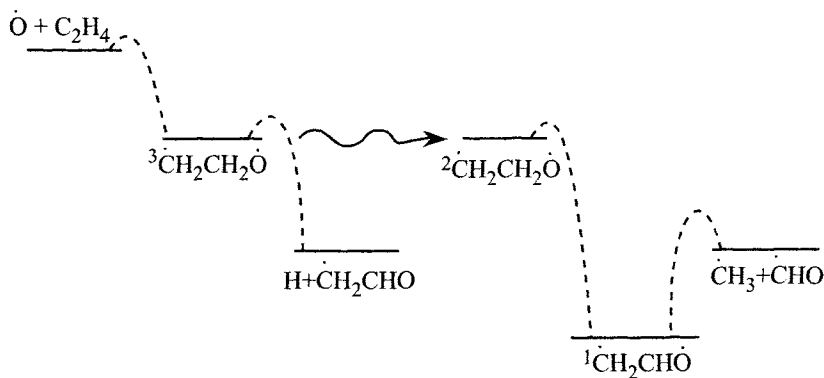
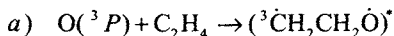


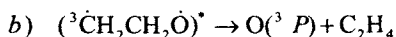
Fig. 4.4. Energy diagram for the reaction of  $\text{O}(^3P)$  with ethylene.

ble to plot the energy diagram, which is presented in the simplified variant in Fig. 4.4.

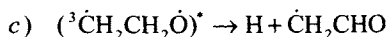
In the first act, the  $O(^3P)$  atom adds to ethylene to form the long-lived complex, viz., the vibrationally excited triplet non-symmetrical biradical  $^3\dot{C}H_2CH_2\dot{O}$



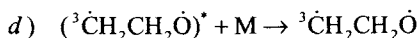
It can decompose back to the reactants



or to the hydrogen atom and  $\dot{C}H_2CHO$

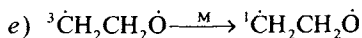


In addition, the vibrationally excited molecule can be stabilized during collisions with molecules

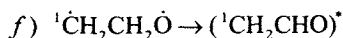


Other channels, for example, isomerization  $^3\dot{C}H_2CH_2\dot{O} \rightarrow ^3\dot{C}H_2CH_2\dot{O}$ , is possible in the framework of one triplet potential energy surface. However, these channels are not indicated in Fig. 4.4 because, according to the quantum-mechanical calculations, to occur they need surmounting of considerable potential barriers. Therefore, taking into account only one potential surface, only reaction 14 can occur. This reaction can be considered as that proceeding through a long-lived complex; its rate constant  $k_{14}$  can be calculated using formula (4.88).

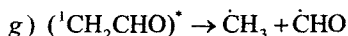
To explain the occurrence of reaction 15 and the experimentally observed dependence of the  $k_{14}/k_{15}$  ratio on the pressure of the buffer gas, the singlet PES has to be taken into account. It is assumed that the triplet-singlet transition can occur, perhaps, due to collision with molecules of the buffer gas M



This transition is shown in Fig. 4.4 by wavy line. Further transformations will occur on the singlet potential energy surface. The formed  $^1\dot{C}H_2CH_2\dot{O}$  biradical can be isomerized with surmounting of a insignificant potential barrier to form the vibrationally excited molecule  $^1\dot{C}H_3CHO^*$



The excited acetaldehyde molecule decomposes to form HCO and  $CH_3$



Thus, reaction 14 proceeds through the triplet state, and reaction 15 proceeds through the singlet state. The contribution of each reaction to the overall reaction rate depends on the singlet-triplet transition  $e$  and, hence, on the overall pressure. The mechanism of the reaction proposed by V.I. Vedeneev explains the experimental data.

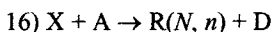
#### 4.2.3. Microscopic reactions

The studies of microscopic reactions are directed first to the development of concepts on the chemical physics of the elementary act. The results of these studies can also be used for the description of non-equilibrium physicochemical processes in the solution of specific applied problems.

It is difficult to experimentally detect simultaneously reactants and products in definite quantum states. Either the quantum state of products or the quantum state of reactants is usually detected. In the first case, we have to speak about the energy distribution in the reaction products, and in the second case, about the reaction of excited molecules. These approaches are equivalent because the corresponding rate constants are related by the principle of microscopic reversibility.

The energy distribution in products is usually studied for strongly exothermic elementary reactions. The mean total energy of products for such reactions can be considered to be equal to  $\Delta U_0 + E_0$  (see Fig. 4.11). This energy is much higher than the thermal energy  $Q$ ; therefore, we can believe that the energy  $E$  released in the reaction products is constant and equal to  $\Delta U_0 + E_0$ .

Let us study the reaction



The product  $\text{R}(N, n)$  is detected in different quantum states (where  $N$  and  $n$  is the set of quantum numbers characterizing the rotational and vibrational states of the particle  $\text{R}$ ). The microscopic rate constant, which will be designated as  $k_{16}(\rightarrow N, n)$ , represents the rate constant of reaction 16, due to which the molecules  $\text{R}(N, n)$  and  $\text{D}$  are formed in any quantum state. The reactants in reaction 16 exist in certain electronic states but under the condition of the Maxwell-Boltzmann distribution over other degrees of freedom. The following functions can be the characteristics of the energy distribution in the product  $\text{R}(N, n)$  over the rotational and vibrational degrees of freedom:

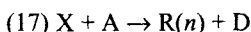
$$P_n(N) = k_{16}(\rightarrow N, n) / \sum_N k_{16}(\rightarrow N, n) \text{ at } n = \text{const} \quad (4.10)$$

$$P(n) = k(\rightarrow n) / \sum_n k(\rightarrow n) \quad (4.11)$$

To determine  $P_n(N)$ , experiments are performed in such a way that the species  $R(N, n)$  formed in reaction 16 can be detected before they collide with other molecules. Under these conditions, the spectrally allowed absorption, emission, or fluorescence excitation spectrum bears information about the rotational distribution for each vibrational state of the product. The main difficulties are the dependence of the sensitivity of the equipment on the wavelength, unequal saturations of absorption lines for different  $n$ , and a possibility of pre-dissociation at some  $N$  values.

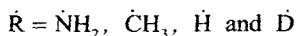
The procedure similar to that applied to rotational distributions is used sometimes for the determination of the distribution function  $P_n(N)$  over vibrational states. To determine  $P(n)$ , the obtained rotational distributions  $P(n)$  for different vibrational levels are integrated. However, transitions with different  $N$  are separated spectrally to a much great extent than those with different  $n$ , which can result in a substantial change in the parameters of the experimental setup on going from one vibrational number to another. This increases the inaccuracy of  $P(n)$  determination and makes the obtained by this method vibrational distribution much less reliable than the rotational distribution.

In some works, the authors develop another approach to the determination of vibrational distributions. It makes it possible to exclude absolute measurements of concentrations and to restrict measurements by relative ones, whose accuracy is higher. This approach, which can be named "kinetic", looks as follows. Let we are interested in the distribution function  $P(n)$ . The experimental conditions are such that the reaction and subsequent rotational relaxation of  $R(N, n)$  occur much more rapidly than the vibrational relaxation of  $R(n)$ . In this case, the reaction



should be written instead of reaction 16.

Then the distribution function  $P(n)$  determines the initial conditions for the concentrations  $[R(n)]$  in different vibrational states, beginning from which deactivation process  $R(n) + M \rightarrow R(n-1)$  occur. The concentrations of radicals  $[R(n)]$  in certain vibrational states measured in relative units depend on the distribution function  $P(n)$ . This allows one to obtain information on  $P(n)$  by the solution of the inverse problem. This "kinetic" approach was used to study the distribution of the vibrational energy in the reaction



The results obtained by measuring the kinetics of formation and decay of  $\cdot\text{OH}(n)$  by the LIF are presented in Table 4.7.

As can be seen, there is the inversion of the population OH(1) and OH(2). The  $P(n)$  values marked by asterisk were obtained by the extrapolation of the experimental data on the basis of the information theory approach.

Table 4.7. Vibrational distribution functions for the  $\cdot\text{OH}$  radical in the reaction

$P(n)$	RH=NH <sub>3</sub>	CH <sub>4</sub>	H <sub>2</sub>	D <sub>2</sub>
$P(n=0)$	0.2	0.18	0.28	0.16
$P(n=1)$	0.32	0.29	0.3	0.29
$P(n=2)$	0.34	0.37	0.24	0.26
$P(n=3)$	0.14	0.15	0.14	0.11
$P(n=4)$	0	0.01*	0.04*	0.11*
$P(n=5)$	0	0	0	0.07*

Let us briefly discuss this approach. Its idea is the comparison of the experimentally obtained distribution with the so-called the *prior distribution*, which would be obtained under the condition of the equiprobable energy distribution over all degrees of freedom of the products. Prior distributions, which we designate as  $P_n^o(N)$  and  $P^o(n)$ , have a maximum entropy and, hence, give the minimum of information about the dynamics of the reaction. The real distribution obtained in experiment has lower entropy than that of the a priori one. As model trajectory calculations and analysis of data of numerous experiments show, the distribution functions over rotational  $P_n(N)$  and vibrational  $P(n)$  states can be expressed through the corresponding a priori distributions as follows:

$$P_n(N) = P_n^o(N) \exp(-\lambda_N f_N) \quad (6.12)$$

$$P(n) = P^o(n) \exp(-\lambda_n f_n) \quad (6.13)$$

$$f_N = \epsilon_{\text{rot}}/(E - \epsilon_{\text{vibr}}), \quad f_n = \epsilon_{\text{vibr}}/E$$

where  $\epsilon_{\text{vibr}}$  is the vibrational energy,  $\epsilon_{\text{rot}}$  is the rotational energy at a fixed value of the vibrational quantum number  $n$ , and  $\lambda_N$  and  $\lambda_n$  are some constants named *surprisals parameters*.

It follows from (4.12) and (4.13) that the quantities

$$I(n) = \ln P(n)/P^o(n) \text{ and } I_n(N) = \ln P_n(N)/P_n^o(N)$$

depend linearly on  $f_n$  and  $f_N$ . The quantities  $I(n)$  and  $I_n(N)$  are named vibrational and rotational surprisals. Helpfulness of representation of experimental data in the framework of the information theory approach follows already from the fact that the linear dependence of the vibrational surprisals on  $f_n$  allows the extrapolation of experimental data to the  $P(n)$  values, which cannot be experimentally measured. This procedure of extrapolation allowed one to obtain the  $P(n)$  values marked in Table 4.7 by asterisk. Non-linearity of the plot of the surprisal suggests that the reaction occurs *via*

several microscopic channels resulting in the same products but with the different energy distributions (bimodal distribution).

According to the considered approach, three types of distributions are possible. When  $\lambda_n = 0$ , the observed distribution coincides with the a priori one. At the negative  $\lambda_n$  value, the observed distribution is "hotter" than the a priori one, and at  $\lambda_n > 0$ , it is "cooler." The  $|\lambda_n|$  value indicates the measure of deviation of the real distribution from the prior one.

Tab. 4.8. Surprisal parameters for the reaction  $O(^1D) + RH \rightarrow \dot{O}H(n) + \dot{R}'$

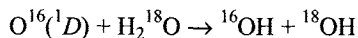
RH	$\lambda_N$	$\lambda_n$
H <sub>2</sub>	-3.5	-1.4
NH <sub>3</sub>	0	-11.0
CH <sub>4</sub>	-6.5*	14.0
C <sub>2</sub> H <sub>6</sub>	-12.0*	-9.0
C <sub>3</sub> H <sub>8</sub>	-15.0*	-11.4
C(CH <sub>3</sub> ) <sub>4</sub>	-25.0*	—

\* The presence of the bimodal distribution.

For all reactions presented in Table 4.8, the experimental data on the vibrational distribution  $P(n)$  are well described by the linear dependence of the vibrational surprisal on  $f_n$ . As for the rotational surprisal  $P(N)$ , for the reactions of  $O(^1D)$  with H<sub>2</sub> and NH<sub>3</sub>, the plot of the rotational surprisal is linear, and for the reaction of  $O(^1D)$  with various alkanes, the plot of the surprisal for  $n = 1$  is described by two linear functions. One of them corresponds to the linear plot of surprisal with the negative values of surprisal parameters (these values are presented in Table 4.8). The second linear function of the plot corresponds to the positive surprisal parameters (are not indicated in the table). This bimodal distribution  $P_n(N)$  suggests that in these reactions two microscopic reaction mechanisms take place. In the first mechanism, the reaction occurs through the direct collinear elimination of the hydrogen atom ("cool" rotational distribution) and in the second mechanism, through the insertion of the  $O(^1D)$  atom into the C—H bond ("hot" rotational distribution). The quantitative processing of the experimental data for the reaction of  $O(^1D)$  with methane in the framework of two microscopic mechanisms results in the situation that the branching ratio of the channel of hydrogen atom elimination with respect to the channel of insertion is equal to 0.05. As alkane becomes more complicated, the reaction rate in the channel of hydrogen atom elimination increases and reaches 0.9 for the reaction of  $O(^1D)$  with C(CH<sub>3</sub>)<sub>4</sub>.

As can be seen, the surprisal parameter for the vibrational distribution function of all reactions in Table 4.8 is negative. This implies that hydroxyl radicals formed in these reactions are much more vibrationally excited than it is expected from the statistical distribution. This fact indicates the predominant vibrational excitation of the

newly formed bond. In this respect, an interesting example is the reaction of  $O(^1D)$  with  $H_2O$  where two  $\cdot OH$  radicals are formed: one is formed from the newly formed bond, and another is formed from water. Studying the reaction

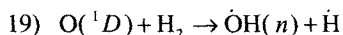


the authors succeeded to show that almost all energy of the vibrational excitation is concentrated on the newly formed bond, whereas the excitation of the "old" bond is insignificant.

Table 4.9. Experimental and theoretically calculated  $P(n)$  for the reaction  $O(^1D) + H_2 \rightarrow \dot{O}H(n) + H$

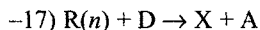
$P(n)$	Experiment	Calculation
$P(0)$	0.28	0.32
$P(1)$	0.32	0.3
$P(2)$	0.24	0.2
$P(3)$	0.14	0.12
$P(4)$	0.04	0.04

Trajectory calculations are needed to obtain more detailed information about the dynamics of the elementary reaction. However, the potential energy surfaces of the reacting species, which are necessary for these calculations, are known only for simplest three-atomic systems. Table 4.9 contains the vibrational distribution functions for the reaction



which were obtained experimentally from the trajectory calculations performed using the non-empirical PES. It is seen that the experimental and theoretical  $P(n)$  values agree quite satisfactorily. This fact can be considered as the experimental confirmation of the mechanism, which follows from the trajectory calculations. According to this mechanism, the  $O(^1D)$  atom comes perpendicularly to the axis of the  $H_2$  molecule. As a result, a complex of the highly excited water molecule is formed in which bending, symmetrical, and non-symmetrical stretching vibrations are excited. After several bending vibrations, the  $H_2O$  molecule decomposes, and energy of bending vibrations is transformed into the translational and vibrational energies of the products, and the energy of symmetrical and asymmetrical stretching vibrations of water is transformed into the vibrational energy of the  $\cdot OH$  radical.

Reactions of vibrationally excited molecules can be considered as reactions reverse to reaction 17



The rate constant of this reaction, which will be designated as  $k_{17}(n \rightarrow)$ , can be calculated using the principle of microscopic reversibility if the rate constant of the reverse reaction  $k_{17}(n \rightarrow)$  is known. According to the formulas for the equilibrium constants presented in Table 2.1, the  $k_{17}(n \rightarrow)/k_{17}(n \rightarrow)$  ratio is determined by the expression

$$\frac{k_{17}(n \rightarrow)}{k_{17}(n \rightarrow)} = \frac{q'}{q} \left( \frac{\mu'}{\mu} \right)^{3/2} \frac{F_A F_X}{F_D F_R^{\text{rot}}} \exp \left[ \frac{E - \epsilon_{\text{vibr}}}{k_B(T)} \right] \quad (4.14)$$

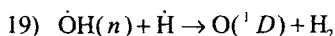
where  $F_R^{\text{rot}}$  is the rotational partition function of the R particle;  $q$  and  $q'$  are the degeneracy factors of the reactants and products.

Let us consider reaction 19 as an example for the calculation of the rate constant of reverse reactions. The rate constant  $k_{19}$  can be expressed, according to (4.11), in the form

$$k_{19}(\rightarrow n) = k_{19}(T)P(n) \quad (4.15)$$

where  $k_{19}(T) = \sum_n k_{19}(\rightarrow n)$  is the thermal rate constant of the reaction  $\text{O}(^1D) + \text{H}_2 \rightarrow \dot{\text{O}}\text{H} + \dot{\text{H}}$  (at  $T = 300$  K the  $k_{19}$  value is close to the number of double collisions  $Z_0$ ).

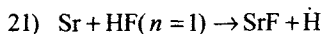
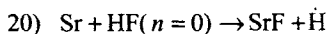
The values of the  $P(n)$  function are presented in Table 4.7. Knowing  $P(n)$  and  $k_{19}(\rightarrow n)$ , using formula (4.14), we can easily calculate the rate constants  $k_{19}(n \rightarrow)$  of the reverse reactions



The calculation gives the following values of the rate constants:  $k_{19}(1 \rightarrow) = 4 \cdot 10^{-11}$ ,  $k_{19}(2 \rightarrow) = 3 \cdot 10^{-4}$ ,  $k_{19}(3 \rightarrow) = 9 \cdot 10^2$ , and  $k_{19}(4 \rightarrow) = 6 \cdot 10^8$  cm<sup>3</sup>/(mol s). It is seen from these data that the reaction rate constant increases substantially with increasing the vibrational energy of the  $\dot{\text{O}}\text{H}$  radical.

Another way of consideration of microscopic reactions is the direct study of the reaction involving the excited species. This approach is more often used for endoergic reactions. In this case, the excited species is obtained by laser excitation. R.N. Zare studied by this method, for example, the reaction of  $\text{HCl}(n=1)$  with the Cl, Br, and F atoms. The measured rate constants are given in Table 4.10.

The efficiency of the vibrational excitation is compared with the efficiency of the translational energy of the reactants in studies in crossed molecular beams. As an example, we present the results of studying the reactions



Exoenergeticity of reaction 20 is 27 kJ/mol. The experiments showed that the cross

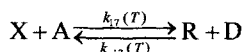
section of reaction 21 at a relative translational energy of 7 kJ/mol is approximately 15 times higher than the cross section of reaction 20 at a relative energy of 54 kJ/mol.

Table 4.10. Ratios of rate constants  $k(n \rightarrow)$  of reactions of excited molecules to rate constant  $k(T)$  of thermal reactions

Reaction	$\Delta U_0$ , kJ/mol	$k(n \rightarrow)/k(T)$	$T$ , K
$\text{HCl}(n=1) + \text{O} \rightarrow \text{OH} + \text{Cl}$	0	102	300
$\text{HCl}(n=2) + \text{Br} \rightarrow \text{HBr} + \text{Cl}$	-65	$7 \cdot 10^3$	712
$\text{HCl}(n=1) + \text{F} \rightarrow \text{HF} + \text{Cl}$	120	3.7	300

The reactions in Table 6.10 can be considered as those reverse to 17 if we accept that  $\text{X} = \text{Cl}$ ,  $\text{A} = \text{HZ}$ ,  $\text{R}(n) = \text{HCl}$  ( $n = 1$ ) or  $\text{HCl}(n = 2)$ , and  $\text{D} = \text{Z}$  ( $\text{O}$ ,  $\text{Br}$ ,  $\text{Cl}$ ).

In the study of the reaction under the conditions of the Maxwell-Boltzmann distribution over the translational and rotational energies, the efficiency of the vibrational form of the energy is judged from the comparison of  $k_{17}(n \rightarrow)$  with the rate constant  $k(T)$  of the thermal reaction. This comparison can be performed if in correlation (4.14)  $k_{17}(n \rightarrow)$  is expressed through the equilibrium constant  $K(T)$  of the thermal reaction



The rate constant of reaction 17 can be presented in the form

$$k_{17}(n \rightarrow) = k_{17}(T)P(n) = K^{-1}k_{17}(T)P(n) \quad (4.16)$$

Inserting this expression into formula (4.14), we obtain

$$\frac{k_{17}(n \rightarrow)}{k_{17}(T)} = K^{-1} \frac{q'}{q} \left( \frac{\mu'}{\mu} \right)^{3/2} \frac{F_A F_X}{F_D F_R^{\text{rot}}} \exp \left[ - \frac{E - \varepsilon_{\text{vibr}}}{k_B(T)} \right] \quad (4.17)$$

Since the cofactor  $\exp(-\Delta U_0/k_B T)$  enters the equilibrium constant, and  $E = \Delta U_0$  under the condition of the zero activation energy in reaction 17, we can approximately accept that the dependence of  $k(n \rightarrow)/k(T)$  on the vibrational energy is determined by the cofactor  $P(n)\exp(\varepsilon_{\text{vibr}}/k_B T)$ . The qualitative criteria of the efficiency of the vibrational form of the energy in surmounting of the activation barrier immediately follow from this. The vibrational energy is completely inefficient if the distribution function in the reverse reaction  $P(n)$  decreases proportionally to  $\exp(-\varepsilon_{\text{vibr}}/k_B T)$ . The vibrational energy is efficient in surmounting the barrier if the function  $P(n)$  in the reverse reaction gives the inverse population of vibrational degrees of freedom.

The  $k(n \rightarrow)/k(T)$  values for some reactions are presented in Table 4.10. As can be seen, the vibrational excitation slightly increases the rate constant in exoergic reac-

tions and does very strongly in endoergic reactions.

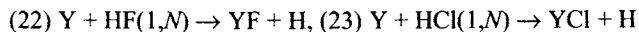
The concepts on the efficiency of the vibrational energy in surmounting of the activation barrier are based on the theoretical consideration of the dependence of the dynamics of the elementary act on the specific features of PES.

The qualitative consideration of the simplified two-dimensional problems corresponding to the reaction of an atom with a diatomic molecule in which all three particles move along one line showed that two points along the reaction path are substantial for understanding of the role of the vibrational form of the energy in the reaction. The first point corresponds to the maximum curvature of the reaction path. The second point is the saddle point. The position of the saddle point relative to the point of maximum curvature, which can also be named the *turning point of reaction path*, determines the efficiency of the vibrational energy. The transition of the vibrational form of the energy of the reactants to the translational energy can be efficient in the turning point of the reaction path due to the centrifugal effect. Therefore, it is necessary for the saddle point to be after the point of maximum curvature, and the longer the distance between these points, the more efficient the vibrational form of the energy. It is known from the general rule of plotting PES that the saddle point for endoergic reactions is shifted toward the products, and for exoergic reaction, it is shifted toward the reactants.

Thus, we can immediately conclude that the vibrational energy is very efficient for endoergic reactions, less efficient for thermoneutral reactions, and inefficient for exoergic reactions. The above examples qualitatively agree with these concepts.

Similar approaches can be used for studying the efficiency of the rotational excitation in reactions. Using the data on the distribution  $P_n(N)$  in reaction 16, where  $\text{RH} = \text{NH}_3$ , we can calculate the rate constants of reactions of the rotationally excited OH radicals at fixed values of the vibrational quantum number. The calculations show that the rotational energy is efficient in the reaction  $\cdot\text{OH}(0,N) + \text{NH}_2 \rightarrow \text{O}({}^1D) + \text{NH}_3$ .

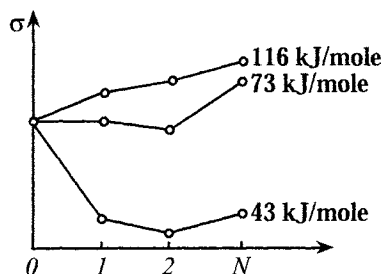
Another approach (it is presented in the review by V. Grot et al.) when rotationally excited particles are obtained by laser excitation is exemplified by the reactions



where Y is the alkali atom.

These reactions were studied in crossed molecular beams or on setups combining the beam with the rarefied gas of another reactant. IR radiation from HF or HCl lasers was used to obtain  $\text{HF}(1,N)$  and  $\text{HCl}(1,N)$ . The reaction products were detected by LIF. The results of studying the reaction  $\text{K} + \text{HF}(1,N) \rightarrow \text{KF} + \text{H}$  are presented as an example (Fig. 4.5). The studies showed that the shape of the cross section  $\sigma(N)$  as a function of the quantum number substantially depends on the translational collision energy. At low translational collision energies (43 kJ/mol), the cross section decreases

Fig. 4.5. Dependence of the total cross section  $\sigma$  of the reaction  $K + HF$  ( $n = 1, N$ )  $\rightarrow KF + H$  on the rotational quantum number at different translational collision energies.



es monotonically with  $N$  increasing. At the same time, at high translational collision energies (116 kJ/mol), the cross section increases monotonically with an increase in the rotational number  $N$ .

Experiments showed that the cross section of the reaction  $\sigma(N)$  substantially depends on the light polarization and, hence, on the orientation of the molecule  $HF(1, 2)$ . These specific features of the behavior of the dependence of  $\sigma(N)$  on the translational energy of the reactants and polarization of the exciting light are related to anisotropy of the interaction of the reactants, which results in the dependence of the potential barrier on the collision angle of the reactants. Therefore, the reaction cross section is determined by the geometry of collision.

Studies in crossed molecular beams make it possible to obtain a specific diagram of products scattering at different angles with respect to the direction of the vector of the relative velocity of the reactants. Angular distributions of the products can be of different shapes. Their most important characteristic is the presence or absence of symmetry relative to the scattering angle by  $90^\circ$ . This characteristic allows one to judge whether the direct reaction occurs or through a long-lived complex. In the case of direct reactions, the effective direction of the attack of the reactants corresponds to the asymmetric scattering of the products. The extreme case of this asymmetry is represented by angular distributions when the product scattering takes place predominantly forward ( $\sim 0^\circ$ ) or in the backward direction ( $\sim 180^\circ$ ). For example, for the reaction  $K + CH_3I \rightarrow KI + CH_3$  the product  $KI$  is mainly scattered in the backward direction ( $\sim 180^\circ$ ). This angular distribution can be interpreted in such a way that the  $K$  atom predominantly attacks the  $CH_3I$  molecule from the side of the iodine atom coming along the axis  $I-C$ . Steric effects were checked by passing of the molecular beam through the electrostatic fields, which create the predominant orientation of the molecule (when the electric field direction changes, the orientation of molecules changes). Experiments showed that the reaction cross section is really greater when the potassium atom attacks the molecule from the side of the iodine atom.

If the reaction proceeds through a long-lived complex, then, since many rotations occur within the lifetime of the complex, the memory about the direction of the attack is partially lost, and the complex decomposes isotropically to a certain extent. However, in this case, the structure of the complex reflects the angular distribution of the products.

When the translational collision energy changes, the mechanism of the elementary act can change. The cases are known when at low energies of the translational motion the reaction proceeds through the long-lived complex, and the direct reaction occurs when the translational collision energy increases.

### 4.3. Femtochemistry

A new area of research named femtochemistry has being vigorously developed in the recent years.

Experimental methods of femtochemistry are based on the achievements of femtosecond spectroscopy (see Section 3.2.11). Three main directions of this new area can be distinguished: dynamics of intramolecular process and transition state during chemical transformation; kinetics of superfast chemical reactions; and control of the intramolecular dynamics and elementary chemical act. These three directions are briefly described in the next sections. The examples are taken from the review by A. Zewail.

#### 4.3.1. Dynamics of transition state during chemical transformation

According to definition given by J. Polanyi and A. Zewail, the "transition state" is implied as the whole totality of configurations of the molecular system on going from reactants to products.

As already mentioned, the coherent light femtosecond pulse, due to the great spectral width, excites the non-stationary quantum state, viz., the coherent nuclear wave package (rotational, vibrational, electronic). Figure 4.6 shows the formation of a diatomic molecule in the stationary and non-stationary quantum states upon light absorption. The bottom line designates the quantum state of the molecule, which absorbs the light. The potential curve of a higher electronic term is presented above. The horizontal lines inside the parabola are vibrational quantum energy levels. After light absorption, the molecule transits to the excited state. Solid lines indicate vibrational energy levels. The molecule in the non-stationary quantum state is formed upon its irradiation with the femtosecond light pulse, whose duration is shorter than the period of excited vibrations (Fig. 4.6, *a*), and the molecule in the stationary quantum state is formed upon irradiation with the monochromatic light (Fig. 4.6, *b*). It is seen from Fig. 4.6 that the nuclear wave package is a superposition of stationary vibrational states. The number of excited vibrational states is determined by the spectral width of the femtosecond light pulse  $\Delta\nu$ .

The wave function of the wave package can be found from the solution of the

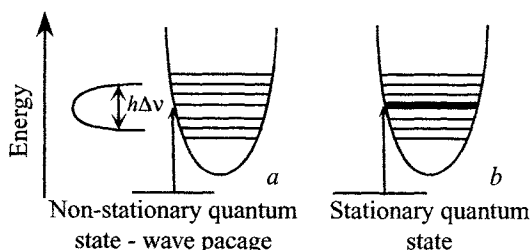


Fig. 4.6. Stationary (a) and non-stationary (b) quantum states of the molecule after light absorption.

non-stationary Shroedinger equation and can be presented in the form

$$\psi(t, r) = \sum a_k \phi_k(r) \exp(-i\omega_k t) \quad (4.18)$$

where  $\phi_k(r)$  are the wave functions of  $\kappa$ -x stationary states,  $\omega_k$  is the circular frequency of the  $\kappa$ -th quantum state,  $r$  is the set of nuclear coordinates, and  $a$  is the amplitude of probability for finding the molecule in the  $\kappa$ -th quantum state.

Summation is performed over all stationary states (Fourier components) from which the wave package consists. The substantial peculiarity of the wave package is the fact that the square of the wave function, which characterizes the probability of finding the nuclei at certain distances, depends on time, unlike the stationary states. This implies that the dynamics of the nuclear motion is manifested in the time evolution of the wave package, which can formally be considered as the “motion” of the wave package over the PES. The high time resolution makes it possible to detect the dynamics of the nuclear motion in the real time.

The concept of the wave package was introduced in 1926 by Shroedinger; however, it was not virtually used in chemistry. The vibrational wave package has a special significance for chemistry, when immediately several vibrational states are coherently excited in the molecular system. In this case, the intramolecular dynamics of nuclei is described by the time evolution of vibration-rotational wave packages. Account for phase characteristics of the nuclear motion is a substantial specific feature of this description.

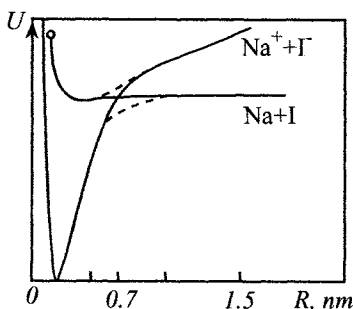
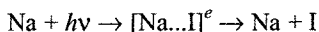


Fig. 4.7. Potential energy curves of the NaI molecule.

Let us consider the dynamics of the transition state for the photodissociation of the diatomic molecule NaI



This reaction is a non-adiabatic process. The potential curves for the NaI molecule are shown in Fig. 4.7. It is seen that there is a pseudo-crossing between the curves of the excited covalent state and ionic ground electronic state. The femtosecond light pulse forms the coherent nuclear wave package in the excited electronic state. We mentioned above that the intramolecular dynamics could be interpreted

as the “motion” of the wave package over the PES. At first the wave package “moves” along the potential curve of the excited state, and the distance between the Na and I atoms increases. When the distance becomes close to the point of pseudo-crossing (0.7 nm), two possibilities appear: to continue the motion along the same potential curve or “jump” to another curve.

Both the dynamics of the transition state  $[\text{Na}\dots\text{I}]^\ddagger$  and the kinetics of formation of the reaction product (Na atom) were detected by the LIF method. Figure 4.8 demonstrates the time plots of the fluorescence intensity  $I(t)$  for the transition state and for the free Na atom. It is seen that the nuclear motion in the transition state has an oscillatory character with considerable decay (Fig. 4.8, b). This decay is due to the fact that some molecules “jump” on another potential energy curve to form the products, viz., the Na and I atoms. The energy of the transition state is not enough to form ions of the sodium and iodine atoms.

The time dependence of the fluorescence intensity of the free Na atom has the stepped character (Fig. 4.8, a). Each step corresponds to the single pass through the pseudo-crossing. The region with the constant value of the fluorescence signal corresponds to the situation when the distances between the nuclei in the transition state differ substantially from 0.7 nm. The ascending region of formation of the Na atoms corresponds to finding of the transition state near the region of pseudo-crossing. Note that the kinetics of formation of the Na atoms is not exponential, which is explained by coherency (the phase characteristics of the stationary states in the wave package

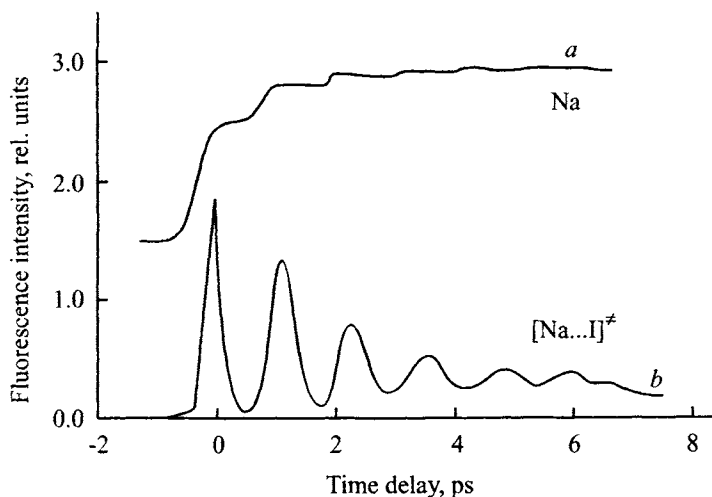


Fig. 4.8. Dependence of the fluorescence signal  $I(t)$  on the delay time between the excited and probe pulses: *a*,  $\lambda = 590$  nm, the free Na atom is detected; and *b*,  $\lambda = 615$  nm, the transition state is detected.

are correlated) of the motions. Therefore, this kinetics is named coherent. When the kinetics is averaged over all phases of the wave packages, we obtain the exponential kinetics.

The most important magnitude, which can be determined from such experiments, is the probability of "jump" from one adiabatic potential curve to another. It can be determined from experimental data using the decay of oscillations. This probability is named the *Landau—Zener probability* and can be calculated from formula (4.66), from which we can see that the probability of "jump" must increase with an increase in the relative velocity of atoms in the region of quasi-crossing. The relative velocity of atoms should increase with a decrease in the wavelength of the exciting light pulse. Indeed, the increase in the decay of oscillations with a decrease in the wavelength of the exciting pulse is observed in experiment. It was experimentally found that the Landau—Zener probability is equal to 0.1 for the exciting pulse with a wavelength of 311 nm.

#### 4.3.2. Kinetics of superfast chemical reactions

In studying the kinetics of any process, we are interested in the time evolution of the concentration of the reactant or product. This implies that populations of the quantum states should be detected rather than the dynamics of wave packages (we are not interested in the phase characteristics of the nuclear motion). Here the high time resolution and high intensity become the main specific features of femtosecond pulses. Different classes of reactions were studied (Table 4.11). The time scale of the presented reactions is given in the last column of the table.

The first example concerns the superfast dissociation of the electronically excited molecule  $\text{CH}_3\text{OOH}$  (the class of such reactions was discussed in Section 4.1). It should be emphasized here that the methods of femtosecond spectroscopy allowed the study of the kinetics of formation of the photodissociation products, viz., the  $\cdot\text{CH}_3\text{O}$  and  $\cdot\text{OH}$  radicals, in the femtosecond time scale.

The second example is reactions of decomposition of highly vibrationally excited molecules in the ground electronic state (decomposition of  $\text{RCO}$ , where  $\text{R} = \text{CH}_3$ ,  $\text{CH}_5$ ). Interest in these reactions is due to the following circumstances. Many efforts were made to create under light irradiation vibrationally excited molecules with a needed intramolecular vibrational distribution. The purpose of these studies is to control the direction of decomposition to desired products by the creation of different intramolecular distributions. However, it turned out that the majority of unimolecular reactions during photoactivation proceed according to statistical laws. This is related to the fact that the intramolecular energy redistribution occurs within 0.1-1 ps, which is usually faster than the decomposition of highly vibrationally excited molecules. It is needed for control of the yield of decomposition products that decompo-

Table 4.11. Examples of studying the kinetics of chemical reactions in the femtosecond time scale

Classes of reactions	Examples of reactions	$\tau$ , fs
Direct reactions of decomposition of electronically excited species	$\text{CH}_3\text{OOH} \rightarrow \text{CH}_3\dot{\text{O}} + \dot{\text{O}}\text{H}$	$\sim 100$
Reactions of highly vibrationally excited molecules in the ground electronic state	$\text{CH}_3\text{COCH}_3 \xrightarrow{h\nu} \text{CH}_3\dot{\text{O}}^* + \dot{\text{C}}\text{H}$ $\text{CH}_3\text{CO}^* \rightarrow \dot{\text{C}}\text{H}_3 + \text{CO}$	$\sim 50$
Reactions of highly electronically excited molecules	$\text{CH}_2\text{I}_2 \xrightarrow{nh\nu} \text{:CH}_2 + \text{I}_2^*$	$\sim 50$
Bimolecular reactions in the Van der Waals complex (VDWC)	$\text{IHCO}_2$ , - VDWC $\dot{\text{H}} + \text{CO}_2 \rightarrow \dot{\text{O}}\text{H} + \text{CO}$	1000

sition occurs more rapidly than the intramolecular redistribution of the vibrational energy. This requires, in turn, very fast excitation of the molecule to high energies, which can be achieved by femtosecond pulses. When the parent acetone molecule decomposes (excitation energy 775 kJ/mol), the highly vibrationally excited radical  $\text{CH}_3\text{CO}^*$  is formed mainly in the ground electronic state. The distribution of the vibrational energy at different degrees of freedom of the radical is non-equilibrium. Its decomposition is tenfold slower than that according to the statistical RRKM theory when the vibrational energy at all degrees of freedom is uniformly distributed. This divergence with the statistical theory is associated, most likely, with the fact that less vibrational energy is released on the reaction coordinate than it was assumed in the calculation. This implies that the most part of the released vibrational energy is at other degrees of freedom, namely, which are not involved in decomposition. However, even the portion of the vibrational energy, which released on the reaction coordinate, is sufficient for the radical to decompose more rapidly than the transfer of the vibrational energy to the reaction coordinate along the C—C bond. This example shows that the use of femtosecond pulses makes it possible to obtain such highly vibrationally excited molecule, whose decomposition does not obey statistical laws, *i.e.*, the possibility to control the intramolecular vibrational distribution appears and new reaction channels can thus be performed with the formation of products, which cannot be obtained when the reaction is carried out under traditional conditions.

The third example in Table 4.11 is the decomposition of the highly electronically excited molecule  $\text{CH}_2\text{I}_2$  during multiphoton light absorption in the visible spectral range. The following peculiarities are observed: due to the multiphoton absorption of the visible light, the molecule is excited to 1150 kJ/mol; not iodine atoms but molecular iodine is formed in the products; the reaction product (iodine molecule) exists in the non-stationary quantum state; the reaction occurs within 50 fs. This example

demonstrates the possibility of femtochemistry to study reactions involving highly electronically excited molecules.

The fourth example represents bimolecular reactions in Van der Waals complexes. It is difficult to determine the momentum of encounter (the start of the reaction) for bimolecular reactions. Therefore, the question arose: can femtochemistry study bimolecular reactions? The following approach was developed. The Van der Waals complex (for example,  $\text{IHCO}_2$ ) including one of the reactant molecules (for example,  $\text{CO}_2$ ) and  $\text{HI}$  molecule is created in the supersonic molecular beam. Under the action of the exciting femtosecond light pulse, the  $\text{H—I}$  bond is cleaved ( $\text{HI} + h\nu \rightarrow \text{I} + \text{H}$ ) and the hydrogen atom is formed, which reacts with the  $\text{CO}_2$  molecule. In this case, the moment of launching of the exciting pulse can be accepted as the zero time moment. The probing pulse detects the  $\cdot\text{OH}$  radical in different moments after the action of the exciting pulse. Thus, the kinetics of  $\cdot\text{OH}$  radical formation is detected, that is, the kinetics of formation of one of the products of the bimolecular reaction  $\text{H} + \text{CO}_2 \rightarrow \text{OH}$ . The study of this reaction by the indicated method found that the reaction proceeds through the long-lived complex. If the structure of the complex is known (the methods of femtochemistry allow one to study the structure of molecules), the possibility appears to study the bimolecular reaction with the specified rate and impact parameter.

#### *4.3.3. Control of the intramolecular dynamics and elementary chemical act*

The specificity of controlling the intramolecular dynamics in femtochemistry is that femtosecond pulses act upon not the initial state of the reactant but the transition state, whose time evolution is monitored. The first method for controlling is the performance of non-adiabatic electronic transitions of the transition state under the action of femtosecond pulses. The high time resolution allows one to "follow" the change in the transition state in order to act on the system by other femtosecond light pulse in the needed moment and transit the reacting system to other electronic state. Another method for controlling is to create at the zero moment different nuclear wave packages to which different nuclear dynamics correspond. This can be performed changing the phase characteristics of the femtosecond light pulse. Below we present the example of this controlling the reaction.

Before speaking about experimental results on controlling the reaction, we explain what is implied for phase characteristics of the light pulse. The electromagnetic field strength can be written in the form

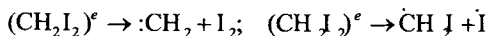
$$E = A \cos(\omega_0 t + \beta t^2/2)$$

where  $A$  is the envelope of the pulse,  $\omega$  is the carrier frequency, and  $\beta$  is the phase modulation (chirp).

The  $\beta$  value is responsible for the phase characteristics of the femtosecond pulse. It can be positive, negative, or equal to zero. If the absolute values of the phase modulation (chirps) of two pulses are equal and the signs are different, only the time dependence of the instant frequency  $\omega$  ( $\omega = \omega_0 + \beta t$ ) changes within the spectral width of the pulse. This implies that the sign of the chirp indicates which frequencies act on the molecular system at first and which frequencies act later. The pulse spectrum remains unchanged. If  $\beta = 0$ , all frequencies irradiate the molecule simultaneously. If  $\beta > 0$ , the molecule is first irradiated by low and then by high frequencies. And on the contrary, if  $\beta < 0$ , the molecule is first irradiated by high and then by low frequencies. Thus, even if all parameters of the pulse remain unchanged and only the sign of the chirp changes, the phase characteristics of the wave package formed by this pulse change. This can result in a change in the nuclear motion and, in turn, the yield of the products.

The first experiments in this direction were performed in studying the dependence of the intramolecular dynamics of diatomic molecules in the absence of the chemical reaction. It was shown for the  $I_2$  molecule that the change in the sign of the chirp of the exciting femtosecond pulse substantially changes the intramolecular dynamics of the vibrational motion of atoms. Similar results were obtained by the study of the dynamics of rotational wave packages.

The work of M. Dantus, where the photodissociation of  $CH_2I_2$  was studied, confirmed that the chirp of the exciting pulse affects the direction of the reaction yield. It is known that at high energies of electronic excitation dissociation proceeds via two channels



The excited molecule  $(CH_2I_2)^e$  was formed during the multiphoton absorption of the light with  $\lambda = 312$  nm and 624 nm. The dependence of the yield of molecular iodine on the phase characteristics and intensity of the femtosecond light pulse was studied. The dependence of the yield of the products on the chirp of the exciting pulse is of greatest interest. The experimental data when the exciting pulse is centered to a wavelength of 624 nm are presented in Fig. 4.9. All data are normed to unity at the zero value of the chirp. It follows from the thermodynamic estimations that the reaction can occur upon the absorption of six photons. This means that the excitation energy is approximately 1150 kJ/mol. It is seen in Fig. 4.9 that the maximum yield of the product is observed at the chirp equal to  $-500$   $fs^{-1}$ , and the minimum yield is observed for a chirp of  $+2400$   $fs^{-2}$ . The yield of the product changes by several times depending on the chirp. Experiments with the multiphoton excitation of the studied molecules by pulses centered at a wavelength of 312 nm were also performed. In this case, the substantially different dependence of the yield of molecular iodine on the value and sign of the chirp is observed. Effects caused by the chirp reflect the characteristics of the potential energy surface, and the obtained results unambiguously show that the phase characteristics of the femtosecond light pulse

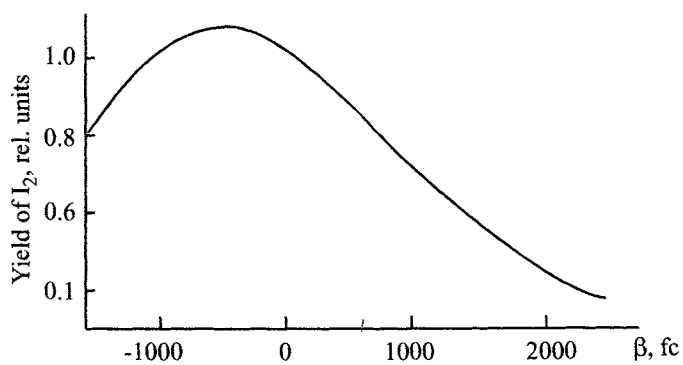


Fig. 4.9. Dependence of the yield of  $I_2$  on the phase modulation.

can be a tool for controlling the yield of products and reaction rate.

### Part 3

## Chemical reactions in liquid phase

### Chapter 5

## Diffusion-controlled reactions in solution

### 5.1. Brief characterization of the liquid state of matter

The liquid state of matter is intermediate in its physical properties between the solid and gaseous states. Chemists who study reactions in solution deal with the so-called normal liquids, very rarely they deal with liquid crystals, and do not virtually work with quantum liquids. In the absence of external actions, normal liquids are macroscopically uniform and isotropic. A liquid is close to a solid in many properties, especially near the melting point. As a solid, a liquid has the interface and withstands strong tensile forces without rupture. The liquid and solid have close values of density, specific thermal capacity, specific thermal conductivity, and electric conductivity. All this is a result of tight contact between molecules in the liquid and solid.

The strong intermolecular interaction of particles in liquid results in the fact that the liquid retains its volume, has the interface and surface tension. In gas at a low pressure ( $p < 1$  MPa) the distance between molecules is much longer than the size of the molecules, whereas in liquid, by contrast, almost the whole volume is occupied by molecules of the substance. Increasing the pressure in the gas, one can create the density of the gaseous substance close to that of the liquid. However, the distinction between the gas and liquid is that the gas always occupies the volume of the vessel, and the liquid always has its intrinsic volume. This distinction is based on the circumstance that in the gas the kinetic energy of a molecule is higher than the energy of intermolecular interaction, while in the liquid, by contrast, molecules interact (are attracted) more strongly than they are repulsed on collision.

The main distinction between the liquid and solid is that the liquid possesses fluidity, and the solid retains its shape. This follows from a great difference in molecular mobility. For example, gold atoms in liquid mercury diffuse with the coefficient  $D = 8 \cdot 10^{-10} \text{ m}^2 \cdot \text{s}^{-1}$ , while for gold atoms in metallic silver  $D = 2 \cdot 10^{-32} \text{ m}^2 \cdot \text{s}^{-1}$  (285 K).

In turn, such a great difference is a consequence of the different structures of the solid and liquid. In the solid crystalline body molecules, metal atoms, or ions are in the nodes of the crystalline lattice where they execute a vibrational motion. Particle diffusion occurs due to migrations of vacancies of the crystalline lattice. In the liquid, as shown by X-ray diffraction analysis, only the short-range order exists between molecules, which is rather rapidly violated, so that each molecule migrates at a distance of the molecular diameter within the time of an order of  $10^{-10}$ - $10^{-8}$  s, which creates a high (as compared to solids) molecular mobility.

Liquid, as an aggregate state, exists in a specific temperature interval  $T_m - T_{cr}$ . Near  $T_m$  the liquid is close in physical properties and structure to the solid. Molecular mobility and intermolecular distances increase with heating. The higher and closer to critical the temperature, the closer the properties and behavior of the liquid to those of the gas. However, far from the critical temperature ( $T < T_{cr}$ ) the liquid is closer to the solid than to the gas. In particular, it follows from a comparison of enthalpies of melting and evaporation:  $\Delta H_m < \Delta H_{vap}$ . For example, for benzene  $\Delta H_m = 11$  kJ/mol and  $\Delta H_{vap} = 48$  kJ/mol, *i.e.*, the transition of the substance from the solid to liquid state requires a much lower energy consumption than that from the liquid to vapor-like state.

The kinetic theory of liquids developed by Ya.I. Frenkel considers a liquid as a dynamic system of particles resembling in part the crystalline state. At temperatures close to the melting point, the thermal motion in liquids is mainly reduced to harmonic vibrations of particles near some average equilibrium positions. Unlike the crystalline state, these equilibrium positions of molecules in liquid have a temporal character for each molecule. After vibrating near one equilibrium position for some time  $t$ , a molecule jumps to a new neighboring position. This jump occurs with the energy consumption  $U$ , then the time of "settled" life  $t$  depends on temperature as follows:

$$\tau = \tau_0 \exp(U/RT) \quad (5.1)$$

where  $\tau_0$  is the period of one vibration near the equilibrium position.

For water at room temperature  $\tau = 10^{-10}$  s,  $\tau_0 = 1.4 \cdot 10^{-12}$  s, *i.e.*, one molecule, executing about 100 vibrations, jumps to the new position where continues to vibrate.

In the crystalline solid particles (atoms, molecules, ions) exist in nodes of the crystalline lattice for a very long time, here particles are arranged in both the short- and long-range orders. The data of X-ray and neutron scattering allow the calculation of the function of density distribution of particles depending on the distance  $r$  from one particle chosen as a center. For the long-range order, the function  $\rho(r)$  has several distinct maxima and minima. In liquid, due to a high mobility of particles, only the short-range order is retained. This follows clearly from X-ray diffraction patterns of liquids: function  $\rho(r)$  for the liquid has the distinct first maximum, diffuse second

maximum, and then  $\rho(r) \approx \text{const}$  (Fig. 5.1). This implies that only the short-range order exists in liquid, and at distances far from a particle the arrangement of particles is chaotic as in gas. The kinetic theory of liquids describes melting as follows. Vacancies (holes) always exist in a minor amount in the crystalline lattice of solids. They migrate slowly over the crystal. With the temperature increase, the amplitude of thermal vibrations of particles in the lattice nodes and the number of defects in the crystalline lattice increase. The closer the temperature to  $T_m$ , the higher the concentration of holes and the faster their migration over the sample. At the melting point, the hole formation process gains a cumulative character, particles become mobile, the long-range order disappears, and fluidity appears. The decisive role in melting belongs to the formation of a free volume in liquid, which makes the system fluid. The free volume in liquid is, to some extent, a sphere somewhat higher than that in crystal, where a particle vibrates and, to some extent, it has the shape of volume fluctuations commensurable with the particle volume, that is, holes, whose migrations over liquid makes it fluid. At temperatures close to the melting point the liquid microstructure is similar to that for the crystal. With the temperature increase the intensity of jumps of molecules from one position to another increases because the concentration of holes in liquid and rate of their migration increase. The number of molecules in the first coordination sphere decreases. The liquid, as a system of particles, becomes still more mobile, the particles move more rapidly, and their mutual arrangement becomes more chaotic. Near the boiling point the chaotic motion of particles in liquids now resembles particle motion in the dense (compressed) gas.

It is clear from the aforesaid that the most important distinction between the liquid and solid crystalline body is that the liquid contains a free volume a considerable part of which looks like holes, whose migration over the liquid imparts fluidity to it. The number of these holes, their volume and mobility, depend on the temperature. At a low temperature the liquid, if it has not been transformed into a crystalline body, becomes an amorphous solid with a very low fluidity due to a decrease in the volume and mobility of the

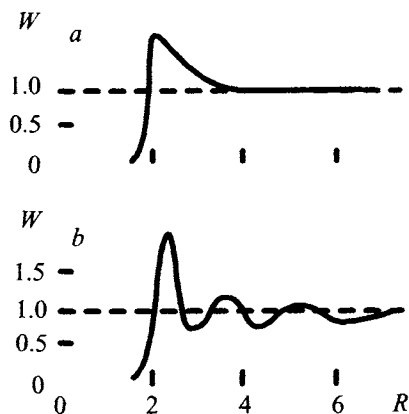


Fig. 5.1. Density function  $W$  of particle distribution at different distances  $R = r/r_0$  ( $r_0$  is the particle radius): *a*, in gas; *b*, in liquid.

holes.

The statistical theory of liquids based on calculations using high-performance computers is successfully being developed in the recent decade along with the kinetic theory.

### 5.2. Reactions controlled by molecular diffusion

Various bimolecular reactions with a very wide range of rate constants from  $10^{-10}$  to  $10^{10}$  l/(mol·s) occur in solution. Activationless reactions, in particular, the recombination of atoms, ions, and many radicals, occur very promptly. In liquid the rate of such processes is determined by the frequency of bimolecular encounters and depends on diffusion.

When particle-reactants after encounter in solution react with each other more rapidly than come apart, the reaction of this type is diffusion-controlled. The role of diffusion in fast chemical reactions and physicochemical processes in liquid was considered by M. Smoluchowski (1917). Later S. Chandrasekhar (1943), F. Collins and G. Kimbrell (1949), T. Waite (1957), and R. Noyes (1961) dealt with this problem. A substantial difficulty in the solution of the problem is that each elementary act of the fast reaction is a microscopic process; however, laws of macroscopic diffusion are used for its description. Nevertheless, this problem can be solved with several assumptions and careful consideration of boundary conditions.

The problem was solved under the following assumptions. Particle-reactants A and B are in the state of thermal equilibrium with the medium, which is considered as a continuous isotropic continuum. These particles diffuse according to the laws of macroscopic diffusions, *i.e.*, in agreement with Fick's law, which is valid in the absence of high gradients. This, however, is violated for the convergence and interaction of particles A and B, which react rapidly. The boundary conditions are determined by the chemical reaction occurred in the system. Particle B is considered as fixed, and particles A migrate with the diffusion coefficient  $D = D_A + D_B$ . The concentration  $c$  of particles A in the vicinity of particle B, which is considered as a sphere of the radius  $R = r_A + r_B$ , depends on the distance  $r$  and time  $t$  and is described by the following equation ( $c_r$  is the concentration of molecules B at the distance  $r$  from A, and  $J$  is the diffusion flow):

$$c_r = c_\infty - J/4\pi rD \quad (5.2.)$$

If the reaction does not violate the concentration of molecules B in the vicinity of molecule A, it would occur with the rate  $v = k c_\infty c_A$ . Since the chemical reaction violates the concentration distribution,  $J = k c_{AB}$ , and the concentration of A.B pairs is the following:

$$c_{AB} = c_{\infty} (1 + k/4\pi r_{AB} D_{AB})^{-1} \quad (5.3)$$

and the experimentally measured rate constant

$$k_{\text{exp}} = 4\pi r D / (1 + 4\pi r D k^{-1}) \quad (5.4)$$

In the limiting case where each collision of the reactants results in the reaction,  $k_{\text{exp}} = 4\pi r D$ , and if  $r$  is expressed in meters,  $D$  in  $\text{m}^2/\text{s}$ , and  $k$  in  $\text{l}/(\text{mol}\cdot\text{s})$ , then

$$k_{\text{exp}} = 4 \cdot 10^3 \pi r D L \quad (5.5)$$

This expression is valid for  $k \gg 4\pi r D$ , which is not always fulfilled. An accurate choice of boundary conditions is necessary for a more rigid solution. The solution of this problem for nonstationary conditions, where at  $t = 0$  in the whole space around A at the distance exceeding  $r$  the concentration of B is equal to  $c_B$ , has the form

$$J = \frac{4\pi r D c_B}{1 + 4\pi r D k^{-1}} \left[ 1 - \frac{k \exp(x^2) \text{erfc}(x)}{4\pi r D} \right] \quad (5.6)$$

where  $x = (Dt)^{1/2} (1 + k/4\pi r D)/r$  and  $\text{erfc}(x)$  is the function of errors.

At not very short times when  $(Dt)^{1/2} (1 + k/4\pi r D)/r \gg 1$ , for the rate constant calculated from experimental data we obtain

$$k_{\text{exp}} = \frac{4\pi r D}{1 + 4\pi r D k^{-1}} \left[ 1 + \frac{r}{(\pi r D)^{1/2} (1 + 4\pi r D k^{-1})} \right] \quad (5.7)$$

This formula is valid in the normal liquid for  $t \gg 10^{-11}$  s and is transformed into Eq. (5.4) at  $t > 10^{-7}$  s; however, in glasses and solid polymers it can be applied at rather long times ( $t \approx 10^2 \div 10^5$  s).

Although the expressions presented above describe satisfactorily experimental data, their approximate character is worthy of notion. Noyes marks the following five distinctions of real systems from systems with ideal diffusion described by Fick's laws. 1. The solvent is not an isotropic continuum, and this is significant when reactants are drawn together at a distance of several molecular diameters. 2. The increment of diffusion displacement is often close to the size of a molecule, however, along with this, it can be much more smaller, and facts indicating this are available. 3. The motion of molecules A includes inevitably correlated motions of neighboring molecules B, which is ignored by the theory. 4. The presence of other molecules A perturbs the concentration gradient of molecules B around isolated molecule A. Therefore, the spherical symmetry of the concentration gradient is valid, rigidly speaking, only at infinite dilution. 5. The average concentration of molecules B in the solution is close to their concentration at the infinite removal from A for infinite dilu-

tion of molecules A in the solution.

Diffusion controls such processes as the recombination of atoms: below we present rate constants of recombination of several atoms at 300 K

Atom (solvent).....	H(H <sub>2</sub> O)	Br(CCl <sub>4</sub> )	I(CCl <sub>4</sub> )
$2k_t \cdot 10^{-9}$ , l/(mol·s).....	20	20	19

Reactions of recombination and disproportionation of alkyl radicals are diffusion-controlled

Radical.....	CH <sub>3</sub>	C <sub>2</sub> H <sub>5</sub>	CH <sub>3</sub> CH <sub>2</sub> $\dot{\text{C}}\text{H}_2$	CH <sub>3</sub> CH <sub>2</sub> $\dot{\text{C}}\text{H}_2$
Solvent (300 K).....	Cyclohexane	Cyclohexane	Cyclohexane	Benzene
$2k_t \cdot 10^{-9}$ , l/(mol·s).....	10	6.4	3.4	0.4

The greater the radical volume, the slower its diffusion, which agrees with the hole theory of diffusion. In benzene the alkyl radical diffuses more slowly than in cyclohexane due to the formation of complexes of the radical with solvent, which decreases, naturally, the rates of diffusion and, correspondingly, recombination.

Many alkoxyl radicals recombine with the diffusion rate constant

Radical	HO	(CH <sub>3</sub> ) <sub>3</sub> C $\dot{\text{O}}$	Ph $\dot{\text{O}}$	Ph $\dot{\text{N}}\text{H}$	(CH <sub>3</sub> ) <sub>3</sub> $\dot{\text{S}}\text{i}$
Solvent (300 K)	H <sub>2</sub> O	CCl <sub>4</sub>	H <sub>2</sub> O	H <sub>2</sub> O	[(CH <sub>3</sub> ) <sub>3</sub> CO] <sub>2</sub>
$2k_t \cdot 10^9$ , l/(mol·s)	10	0.2	5.6	1.5	5.5

Considering radical and atom recombination, one should keep in mind that, when having got into one cage, a radical pair reacts in the case where their spins are antiparallel, and the probability of formation of these pairs is equal to 1/4. Therefore, for radical recombination the rate constant ( $-d[R\cdot]/dt = 2k_t [R\cdot]^2$ ) is the following:

$$2k_t = k_D = 4\pi rD \cdot 1/4 = \pi rD = 2RT/3000 \eta \quad (5.8)$$

The temperature run of  $k_D$  is determined by the activation energy  $E_D$ , which is close to the  $B$  value in the dependence of  $\eta$  on  $T$ :  $\eta = \eta_0 \exp(B/RT)$ . The  $B$  values in kJ/mol for several solvents are presented below.

CCl <sub>4</sub>	C <sub>2</sub> H <sub>5</sub> OH	CH <sub>3</sub> COOH	(CH <sub>3</sub> ) <sub>2</sub> CO	<i>n</i> -C <sub>6</sub> H <sub>14</sub>	H <sub>2</sub> O
9.9	13.5	11.1	6.7	6.9	16.8

It is seen that in low-viscosity solvents the activation energy of diffusion changes within limits of 5÷15 kJ/mol. The same figures are obtained when  $E_D$  is estimated through  $\Delta H_{\text{vap}}$  ( $E_D = 1/3\Delta H_{\text{vap}}$ ).

The formulae presented above describe the diffusion and collision of two neutral particles. The situation changes when reactants are charged particles, *i.e.*, ions or radical ions. Long-range forces of attraction or repulsion appear between such particles, which is, reflected, of course, on the frequency of their diffusion collisions.

In this case, the diffusional flow of molecules B to molecule A depends on the potential of interaction  $U$  of particles A and B rather than the gradient of concentrations of particles B and is described by the differential equation (P. Debye, 1942)

$$\frac{dc}{dr} + \frac{c}{kt} \frac{dU}{dr} = \frac{J}{4\pi rD} \quad (5.9)$$

whose solution results in the expression similar to (5.7) with the distinction that  $r_{\text{eff}}$  should be written instead of  $r$ . The  $r_{\text{eff}}$  value is determined by the expression

$$r_{\text{eff}}^{-1} = \int_{r_{00}}^{\infty} \exp(U/kT) dr/r^2 \quad (5.10)$$

Atoms or unlikely charged metal ions meet in the cage and immediately enter into the reaction, whose rate is limited by translatory diffusion. Many radicals, in particular, hydroxyl, alkoxy, alkyl, and phenoxy radicals, react in the same way. For such reactions  $k_{\text{exp}} \sim \eta^{-1}$  and

$$k_{\text{exp}} \approx k_D = 4 \cdot 10^3 \pi D r L \quad (5.11)$$

However, among reactions of radical recombination, there are such reactions for which  $k_{\text{exp}} \ll k_D$  but  $k_{\text{exp}} \sim \eta^{-1}$ , i.e., they are not limited by the translatory diffusion of reactants but depend, nevertheless, on the molecular mobility of the environment. They were named "pseudo-diffusion" reactions. They are the recombination of 2,6-disubstituted phenoxyls, whose substituents are phenyl, methoxy, and *tert*-butyl groups. They are characterized by proportionality  $k_{\text{exp}} \sim \eta^{-1}$  but  $k_{\text{exp}}$  is by 1, 2 or 3 orders of magnitude lower than the calculated  $k_D$  value. This phenomenon can qualitatively be explained as follows.

These reactants possess anisotropic reactivity: the reaction occurs at a certain mutual orientation, which does not take place at each collision. In the first approximation, these reactants can be considered as spheres each of which has a small reaction spot. The reaction occurs when the spheres collide by their spots. The reaction occurs without an activation energy. The size of the spot in the form of a circumference on the sphere-reactant can be characterized by the angle  $q$ , the relative surface area of the spot on the sphere is equal to  $\sin^2(\theta/2)$ , and the probability of collision with the favorable mutual orientation of two identical particles is  $\sin^4(\theta/2)$ . This is the *geometric steric factor*  $P_r = \sin^4(\theta/2)$  or  $P_r = \sin^2(\theta_A/2)\sin^2(\theta_B/2)$  if the sizes of the spots differ for A and B. After collision the particle-reactants exist near each other for some time and turn relatively to each other. The rate of turn of the particles depends, naturally, on viscosity because the coefficient of rotational diffusion depends on viscosity

$$D_r = kT/8\pi\eta r^3 \quad (5.12)$$

This results in an increase in the steric factor because the probability of collision

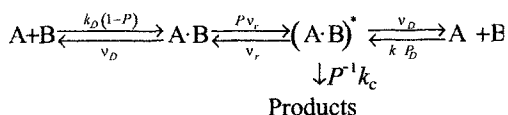
of the reactants by their reaction spots increases due to the cage effect. Several mathematical models describing this interaction are considered in literature. All of them give rather close  $P_{\text{eff}}$  values calculated from  $P_r$ . The reaction of this type (without an activation energy with  $P_r \ll 1$ ) occurs with the rate constant

$$k_{\text{exp}} = 4 \cdot 10^{-3} \pi D L r_{\text{eff}} \quad (5.13)$$

where  $r_{\text{eff}} = (3/16) r \pi \sin^2(\theta/2)$ .

When  $\theta$  is a sufficiently small angle and  $r_{\text{eff}} \ll r$ , we deal with the reaction, whose rate is limited by the rotational diffusion of particle-reactants, and the term "pseudo-diffusional" is unsuccessful.

Taking into account the mutual orientation of particles in the cage, the bimolecular reaction of A with B can be presented by the following simple kinetic scheme, which takes into account in the simple form both the translatory and rotational motion of the particles ( $P$  is the steric factor, and  $\nu_r$  is the rotation frequency of particles):



This scheme allows us to distinguish 3 limiting cases.

1. The reaction occurs very slowly ( $k_c P^{-1} \ll \nu_D$ ,  $k P^{-1} \ll \nu_r$ ), so that this is the chemical interaction which limits the process. In this case,  $k_{\text{exp}} = k_c K_{\text{AB}} \ll k_D$  and  $k_{\text{exp}}$  is independent of the viscosity of the solution.

2. The reaction in the cage occurs rapidly, and the particles are rapidly oriented in the cage ( $k_c P^{-1} \gg \nu_D$ ,  $P\nu_r \gg \nu_D$ ). In this case, the reaction is limited by translatory diffusion,  $k_{\text{exp}} = k_D$ .

3. The oriented particles react rapidly ( $k_c \gg P\nu_r$ ,  $k_c \gg P\nu_D$ ) but the steric factor is low, so that the rate of mutual orientation of particles limits the process. In this case,  $k_{\text{exp}} = \nu_r P K_{\text{AB}}$ . The reaction rate constant depends on viscosity ( $\nu_r \sim \eta^{-1}$ ) but is much lower than  $k_D$ . The last two cases where  $P^{-1}$  is very high can be combined by one expression

$$\frac{1}{k_{\text{exp}}} = \frac{1}{k_D} + \frac{1}{K_{\text{AB}} \nu_r P} \quad (5.14)$$

At a sufficiently high  $P$  where  $K_{\text{AB}} \nu_r P \gg k_D$ ,  $k_{\text{exp}} \approx k_D$ , the reaction is limited by translatory diffusion. By contrast, at low values of the steric factor the process is limited by the rate of particle-reactant orientation and  $k_{\text{exp}} \approx K_{\text{AB}} \nu_r P$ . In both cases, we have diffusion-controlled reactions: in the first case, translatory diffusion is lim-

iting, and in the second case, rotational diffusion limits the process.

### 5.3. Cage effect in liquid

#### 5.3.1. Experimental evidence

When molecules dissociate in the gas phase, the formed radicals immediately fly apart. In liquid these radicals are surrounded by molecules creating a cage, and a pair of radicals is present for some time in this cage until they react or one of the radicals diffuses from the cage.

The time of existence of a pair of particles in the cage for low-viscosity liquids at 300-400 K is  $10^{-10}$ - $10^{-8}$  s. This concept of the cage was formulated by J. Franck and E. Rabinovich in 1934 and naturally followed from the kinetic theory of liquid by Ya.I. Frenkel.

During the decomposition of molecules to radicals, the cage effect is manifested as follows.

1. In the gas phase, the quantum yield of dissociation of a molecule to radicals (atoms) is equal to unity. In the liquid phase it is much lower than unity because the radicals that formed partially recombine in the cage. For example, for iodine dissociation in  $\text{CCl}_4$  at 298 K the quantum yield  $\phi = 0.14$ , and for bromine under the same conditions  $\phi = 0.22$ . For the photodissociation of azo compounds in a solution  $\phi = 0.25 \pm 0.10$ .

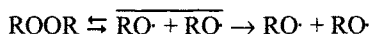
2. For the same reason, at the thermal decomposition of an initiator in the liquid the rate constant of radical generation  $k_i = 2ek$ , where  $k$  is the decomposition rate constant,  $e < 1$ , and  $e$  is the probability of radical escape to the volume.

3. The cage effect affects the product composition: products of the intracage recombination of radicals are formed. For example, the decomposition of azomethane in isooctane gives 65% ethane calculated per decomposed azomethane, whereas in the gas phase only about 3% ethane are formed among its decomposition products. Such a great difference is the result of an intense intracage recombination of methyl radicals. However, when the yield of ethane in azomethane photolysis in a solution is extrapolated to  $\eta \rightarrow 0$ , it is close to unity.

4. Experiments on cross radical recombination provide the distinct evidence of the intracage recombination of primarily formed radical pairs in the solution. According to the probability of recombination of the  $\cdot\text{CH}_3$  and  $\cdot\text{CD}_3$  radicals, the photolysis of an equimolar mixture of azomethane and perdeuterioazomethane in the gas phase affords ethane molecules in the ratio  $\text{C}_2\text{H}_6:\text{C}_2\text{H}_3\text{D}_3:\text{C}_2\text{D}_6 = 1:2:1$ , whereas in a solution of isooctane  $\text{C}_2\text{H}_6 + \text{C}_2\text{D}_6$  is 75%, that is, the predominant recombination

nation of the  $\cdot\text{CH}_3 + \cdot\text{CH}_3$  and  $\cdot\text{CD}_3 + \cdot\text{CD}_3$  pairs occurs in the cage. The thermal decomposition of a mixture of  $\text{CH}_3\text{COOOCOCH}_3$  and  $\text{CD}_3\text{COOOCOD}_3$  in a solution also results in the predominant formation of  $\text{C}_2\text{H}_6$ ,  $\text{C}_2\text{D}_6$ ,  $\text{CH}_3\text{COOCH}_3$ , and  $\text{CD}_3\text{COOCD}_3$ . Some amount of nonsymmetric dimers is formed by the photolysis of a mixture of normal and perdeuterated diacylperoxide in pentane. However, the yield of these dimers decreases sharply in a medium of more viscous decalin.

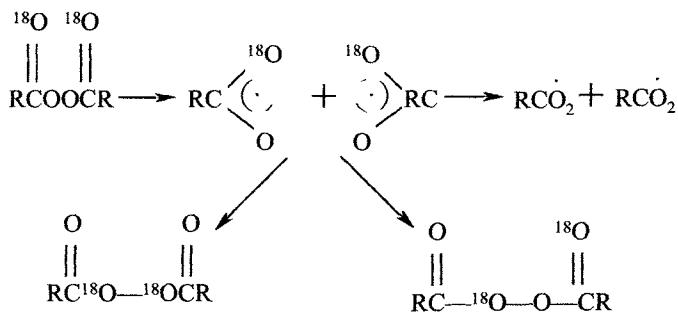
5. The influence of viscosity on molecule decomposition and efficiency of initiation are tightly related to the cage effect. When the initiator decomposes to radicals with the cleavage of only one bond, the radicals that formed can recombine again with some probability to form the initial molecule



The higher the viscosity of the solvent, the lower the rate of radical escape from the cage and the higher the probability of the inverse reaction. Therefore, in these cases, the higher the solvent viscosity, the lower the experimentally observed rate constant of the reaction. On the other hand, with an increase in viscosity  $k_i$  decreases and  $k_i = 2ek$ .

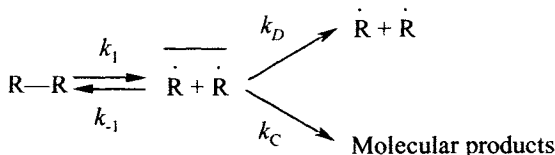
6. The decomposition of an optically active substance, if it occurs with the cleavage of one bond, is accompanied by the racemization of a portion of the nondecomposed substance. Racemization is a result of radical recombination in the cage. For example, the photolytic decomposition of optically active 2-phenyl-2-azobutane in hexadecane is accompanied by its racemization, and after decomposition to 40% the remaining substance is racemized by 26%.

7. When acyl peroxides and some peresters labeled by  $^{18}\text{O}$  at the carbonyl group decompose, isomerization is observed, namely, the transition of  $^{18}\text{O}$  from the carbonyl to peroxide group. Isomerization occurs due to the recombination of the radical pair in the cage

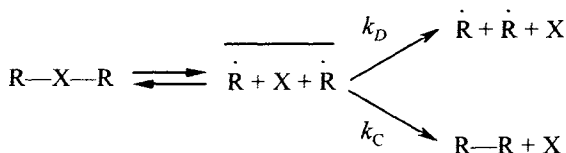


### 5.3.2. Kinetic schemes of cage effect

When the decomposition of a molecule occurs with the cleavage of several bonds, the products of intracage recombination differ from the initial substance



in this case  $e = k_D/k_I = k_D/(k_D + k_C)$  or  $1/e = 1 + k_C/k_D$ . If the molecule decomposes with the cleavage of one bond and the radicals that formed escape to the volume or recombine to form the initial molecule or other products according to the scheme



then

$$e = \frac{k_D/x}{1 - k_I/x}; \quad x = k_{-1} + k_D + k_C$$

and this coincides with the equation of the preceding scheme  $e^{-1} = 1 + k_C/k_D$ ,

$$\frac{1}{k_{\text{exp}}} = \frac{1}{k_I} \left( 1 + \frac{k_{-1}}{k_C + k_D} \right) \quad (5.15)$$

The consideration of the cage effect in the framework of the simple kinetic scheme ignores the following circumstance. When escaping from the cage, two radicals can meet again due to diffusion. The probability of this collision when radicals are close to each other is higher than that of collision with a radical from another cage. Therefore, in several works the cage effect is considered in the framework of the diffusion model.

### 5.3.3. One-dimensional translatory diffusion in isotropic medium

The decomposition of a molecule in liquid results in a pair of radicals at the distance  $l$  from each other. The liquid contains a radical acceptor in the concentration  $c_A$  reacting with radicals with the rate constant  $k_A$ . Due to the Brownian motion, the distance between the radical centers changes continuously. The radical pair disappears when one of the radicals reacts with the acceptor or two radicals come together at a distance equal to the sum of radii of two particles  $2r$  and react with the rate constant

$k_c$ . The medium is considered as a continuum with viscosity  $\eta$ .

The distribution function of radical pairs in this system is described by the diffusion equation

$$(D/x)d^2(nx)/dx^2 - 2k_Anc_A = 0 \quad (5.16)$$

where  $x$  is the distance between radical centers, and  $n$  is the concentration of radical pairs.

The solution of this equation for the boundary conditions ( $n = n_S$  at  $x = 2r$  and  $n = 0$  at  $x \rightarrow \infty$ ) gives the following expression for the probability of radical escape from the cage:

$$e = 1 - \frac{2r}{\ell} \frac{\exp[-a(\ell - 2r)]}{1 + 8\pi r D(\ell + 2ar)/k_c} \quad (5.17)$$

where  $a = 2k_Ac_A/D$ .

Let us estimate the  $2ar$  value, i.e., the contribution of the acceptor to the disappearance of radical pairs. Accepting  $k_A = 10^9$  l/(mol·s) (maximum value),  $c_A = 10^{-2}$  M,  $D = 10^{-5}$  cm<sup>2</sup>/s, and  $r = 2 \cdot 10^{-8}$  cm, we obtain  $2ar = 10^{-2}$ , i.e.,  $2ar \ll 1$ . Thus, even very active radical acceptors cannot affect the cage effect.

Equation (5.17) can be simplified

$$\frac{1}{1-e} = \frac{\ell}{2r} + \frac{\ell}{2r} \frac{8kT}{3k_c} \quad (5.18)$$

or

$$e = 1 - \frac{2r}{\ell} (1 + 8\pi r D / k_c)^{-1} \quad (5.19)$$

Experimental data on azomethane photodecomposition in various solvents agree with equations (5.18) and (5.19) and for the  $1/2r$  ratio give a value of 1.1.

Noyes developed the theory of cage effect applied to halogen photodissociation in a solution considering the solvent as an isotropic viscous medium. When a biatomic molecule with the bond energy  $E$  absorbs a photon with the energy  $h\nu$ , it dissociates to atoms. The energy excess  $h\nu - E$  is transformed into the kinetic energy of atoms  $h\nu - E = 1/2\mu u_0^2$ , which move in the viscous medium and lose an excess of the kinetic energy. Considering a ball with the weight  $m$  and radius  $r$ , for the change in the rate of its motion  $u$  in the viscous medium we have

$$-du/dt = 6\pi r \eta u / m \text{ and } u = u_0 \exp(-6\pi r \eta t / m) \quad (5.20)$$

During the time  $t$  the atom passes the way  $s$

$$s = \int_0^t u dt = (\mu u_0 / 6\pi r \eta) [1 - \exp(-6\pi r \eta t / m)] \quad (5.21)$$

The full distance at which the atoms come apart to the moment when  $u = 0$  is the following:

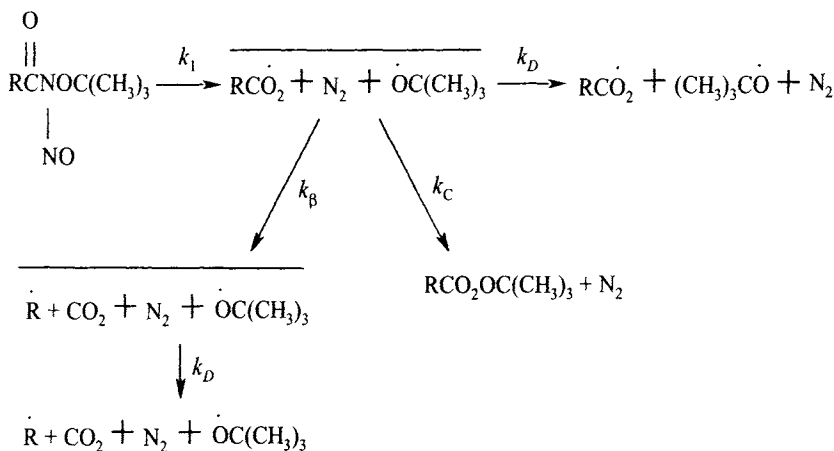
$$s_p = 2r + (2mu_o / 6\pi\eta r) = 2r + (\sqrt{m} / 3\pi\eta)(h\nu - E)^{1/2} \quad (5.22)$$

According to this model, when thermal dissociation occurs, atoms go apart with the rate  $u_o = (3kT/2)^{1/2}$ , and the distance at which they diverge is the following:

$$s_t = 2r + (mkT/6)^{1/2} / \pi\eta r \quad (5.23)$$

The quantum yield of atom dissociation, taking into account the possibility of their repeated collision and recombination, is  $\phi = 1 - 4r^2/s_p d$ . The  $\phi$  values calculated using this formula agree satisfactorily with experimental values for such energies  $h\nu$  when  $s_p$  is much shorter or much longer than the diameter  $d$  of the solvent molecule. A bad correspondence is observed for  $s_p \approx r$ , that is, the approximation of a discrete medium consisting of molecules by a continuous viscous continuum is unsatisfactory.

Somewhat different dependence of  $e$  on  $\eta$  was obtained experimentally and derived theoretically by T Koenig for the decomposition of initiators including the concerted and unconcerted decomposition:



The yield  $y$  of the decomposition product  $\text{RC(O)OOC(CH}_3)_3$  is related to the rate constants of the reactions of radical pair transformation by the following correlation

$$\frac{1}{y} - 1 = \frac{k_D}{k_C} + \frac{k_B}{k_C} \quad (5.24)$$

The rate constant of diffusional separation of the radical pair in the time-depend-

ent form can be expressed through the ratio

$$k_D = r/(\rho - r_0)t \quad (5.25)$$

where  $r$  is the root-mean-square displacement of radical centers for time  $t$ ;  $\rho$  is the collision diameter of particles;  $r_0$  is the distance between the centers of particles at the initial moment.

According to the theory of Brownian motion,  $r = (2Dt)^{1/2}$ , where  $D$  is the diffusion coefficient of the radical pair. From this

$$k_D = \left(\frac{2D}{t}\right)^{1/2} \frac{1}{k_c(\rho - r_0)} + \frac{k_\beta}{k_c} \quad ; \quad \frac{1}{y} - 1 = \left(\frac{2D}{t}\right)^{1/2} \frac{1}{k_c(\rho - r_0)} + \frac{k_\beta}{k_c} \quad (5.26)$$

The characteristic time within which the radical pair can escape from the cage is restricted by the lifetimes of the pair in competing processes, namely,  $\tau_\beta$  and  $\tau_c$ ,

$$\frac{1}{y} - 1 = \frac{\text{const}}{\sqrt{\eta}} + \frac{\tau_c}{\tau_\beta} \quad (5.27)$$

If there is no route  $\beta$  ( $\tau_\beta = \infty$ ), then  $1/y - 1$  depends linearly on  $1/\eta^{1/2}$ . For the decomposition of  $\text{RCO}_2\cdot$  to  $\text{R}\cdot$  and  $\text{CO}_2$ , an interception is observed in the  $(1/y - 1) - 1/\eta^{1/2}$  plot.

Assuming the following dependence between  $k_D$  and  $\eta$ :

$$\eta = A_V \exp(E_V/RT); \quad k_D = E_D \exp(-E_D/RT)$$

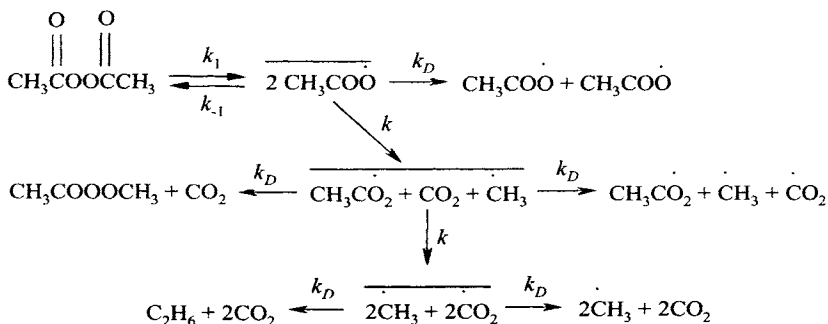
then for  $k_{\text{exp}}$  we obtain the function ( $E_D = 0.5E_V$ )

$$k_{\text{exp}}^{-1} \approx k_1^{-1} + \frac{k_{-1} \sqrt{\eta}}{k_1 A_D \sqrt{A_V}} \quad (5.28)$$

The extrapolation of  $k_{\text{exp}}^{-1}$  to  $\eta = 0$  allows the determination of  $k^1$ , and the dependence of  $k_{\text{exp}}$  on  $\eta$  helps to make choice between the concerted and unconcerted mechanisms of decomposition.

### 5.3.4. Quantitative data on cage effect

The higher the solvent viscosity, the higher the fraction of cage pairs recombining to form the initial molecule. Therefore, an increase in the solvent viscosity decreases the experimental rate constant of decomposition. For acyl peroxides, due to the instability of the oxyacyl radical, several transformations occur in the cage resulting in both the initial peroxide and other products of cage recombination. The scheme of transformations for acetyl peroxide has the following form:



An increase in viscosity, on the one hand, decreases the decomposition rate constant and, on the other hand, increases the fraction of products of intracage recombination, methyl acetate and ethane. Intracage recombination with the formation of the initial peroxide molecule is clearly proved by experiments on isotope isomerism: the decomposition of peroxide labeled by  $^{18}\text{O}$  at the carbonyl group is accompanied by the transition of  $^{18}\text{O}$  into the peroxide group.

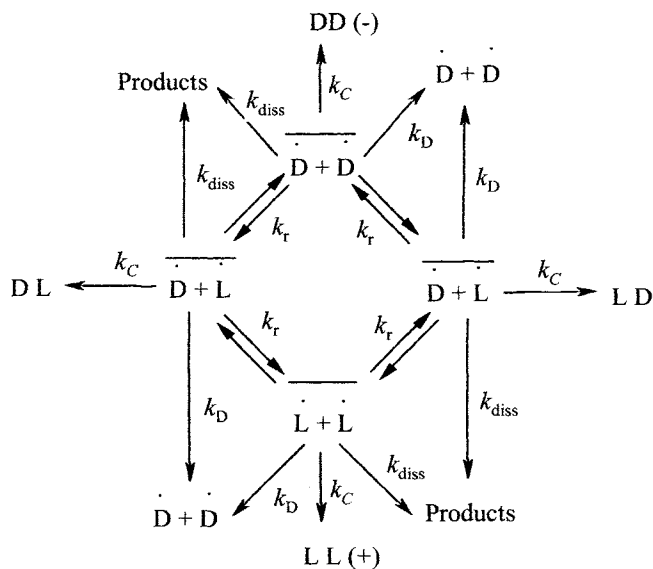
The calculations according to the Noyes theory were compared to the results on the quantum yield of iodine atoms during photolysis of iodine in various solvents. The calculation agrees well with experiments for solvents with a low viscosity. In the case of chlorine-containing solvents, the theory predicts higher  $F$  values than those obtained in experiment. An increase in the viscosity does not decrease  $F$  to such an extent as it follows from the theory. In very viscous solvents at  $\eta \rightarrow \infty$   $F \rightarrow F' \neq 0$ . All these deviations indicate that the model of cage as a uniform viscous medium surrounding a pair of particles describes the phenomenon approximately and in a limited interval of changing viscosity.

Noyes draws a similar conclusion in another work comparing the calculation and experiment on the influence of the wavelength of the irradiating light on the quantum yield of iodine atoms. When the absorbed light energy exceeds slightly the dissociation energy of  $I_2$ , the calculation and experiment virtually coincide. An increase in the energy of irradiating quanta results in a considerable divergence between the calculation and experiment. The authors believe that the divergence is reasoned by the fact that the solution is not a continuum but a discrete medium.

Nevertheless, the Noyes theory is often valid for changing viscosity of the solvent in a sufficiently wide interval: for azomethane photodecomposition,  $(1 - e)^{-1} = 1.1 + 6.5 \cdot 10^{-5} T^{1/2}/\eta$ ; for perfluoroazomethane,  $(1 - e)^{-1} = 1.1 + 4.0 \cdot 10^{-4} T^{1/2}/\eta$ ; and for *tert*-butyl peroxy- $\alpha$ -phenyl isobutyrate,  $(1 - e)^{-1} = 1.24 + 5.75 \cdot 10^{-4} T^{1/2}/\eta$ . However, in solvents with a low viscosity (at high  $\sqrt{T}/\eta$ ), a deviation of  $(1 - e)^{-1}$  from the straight line is observed, i.e., in this case, the model of liquid as an isotropic medium is invalid.

Both theoretical models (Noyes and K oenig) can be combined in the framework of one kinetic scheme. Assuming in the general case  $k_D = \text{const}/\eta^\alpha$  and considering  $\alpha$  as an empirical parameter ( $1 \geq \alpha \geq 0$ ), we obtain  $k_D \approx \eta^{-\alpha}$ , where  $\alpha$  differs from unity. This approach agrees with the comparison of  $E_D - E_c$  from the data on cage effect with  $E_V$  for the temperature run of viscosity:  $\eta = A_V \exp(E_V/RT)$ . As a rule,  $E_D - E_c \neq E_V$ , and from this it follows more often  $\alpha \neq 1$  (at  $E_c \approx 0$ ). It is quite understandable that  $E_D$  and  $E_V$  do not coincide:  $E_D$  refers to the diffusion of the radical (easiest) from the cage, and  $E_V$  is attributed to the diffusion of solvent molecules. When  $k_D$  of the radical and solvent molecule are close, the model of cage as a pair of radicals surrounded by a structureless viscous medium is well described by the Noyes model. The stronger the difference between mobilities of the radical and solvent molecule, the greater the divergence between the theory and experiment. For a mixed solvent, the macroscopic viscosity cannot be considered at all as a magnitude reflecting the microdiffusion of particles.

Valuable data on intracage processes are provided by the study of the decomposition of optically active compounds. Radicals with the free valence at the asymmetric C atoms can recombine in different ways. The recombination product can retain the mutual arrangement of fragments and give an optically active molecule (dimer). If one of the radicals in the cage turns by  $180^\circ$ , the recombination of this pair gives a mesoform. If both radicals turn by  $180^\circ$ , an optically active dimer with an inverse sign of rotation is formed by recombination. The scheme of cage processes during the decomposition of optically active azo compounds have the following form:



Unlike the schemes considered previously, in this scheme we introduced the states of pairs differed by mutual orientation and  $k_r$  is the rate constant of mutual turn of the radicals. For the dimer obtained by the recombination of two  $\alpha$ -phenylethyl radicals formed in the decomposition of optically active azo- $\alpha$ -phenylethane (benzene with the acceptor of alkyl radicals), the following composition is observed: 31% DD(-) (configurations of both radicals remained unchanged), 48% meso (one of the radicals had time to turn), and 21% LL(+) (both radicals turned). The ratio  $k_r/k_c = 15$ , *i.e.*, the rotation of radicals in the cage occurs very promptly. The close results were obtained for the recombination of the  $\alpha$ -phenylethyl—benzyl radical pair:  $k_r/k_c = 16$  (benzene, 383 K). The decomposition of optically active peroxides in the cage affords predominantly recombination products of radicals, which did not retain the initial mutual orientation.

Singlet or triplet radical pairs can appear during the photodecomposition of molecules. The triplet radical pair does not recombine, recombination requires its transformation into the singlet pair, *i.e.*, for triplet pairs the probability of intracage recombination is lower than that for singlet pairs. The latter exist during direct photolysis of molecules. The triplet radical pair is formed when a photosensitizer is used.

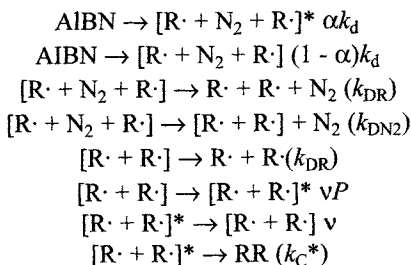
### *5.4 Cage effect in solid polymers*

Polyolefins are semicrystalline polymers, so that low-molecular-weight substances penetrate and diffuse virtually in the amorphous phase only. Each particle or a pair of particles is surrounded by segments of the macromolecule. Since the segments in the amorphous phase are not packed so tight as in the crystalline phase, there are holes moving through the polymer. Due to the high molecular weight of macromolecules, the "concentration" of holes and the rate of their motion in polymers are lower than in liquids. This is because the diffusion rate of molecules in polymers is much lower than in liquids. Slow molecular diffusion in polymers leads to a high probability of free radical pair recombination in a polymer cage. In polymers the probability of a free radical pair to escape recombination in the cage is a value of 0.1–0.01 and lower in comparison with 0.3–0.8 in liquids. An attempt to estimate the cage effect in polymers was made reckoning from the cage effect in liquids and taking into account slower translational diffusion in polymers and gave the results that are in disagreement with experimental measurements.

#### *5.4.1. Schemes of cage effect with translational and rotational motion of particles*

Free radicals in the cage execute translational and rotational motions. The latter can be important for free radicals to react, because such a reaction requires a pair of

free radicals to be oriented in an appropriate manner for overlapping of odd electron orbitals and singlet spin orientation. One can expect that discrepancies between the above schemes and experimental data are the result of an important role of rotation in the cage effect. The following scheme of AIBN decomposition in polymer was considered.



Four types of cages are supposed for reactions in the polymer matrix: primary cage  $[\text{R}\cdot + \text{N}_2 + \text{R}\cdot]$ , cage  $[\text{R}\cdot + \text{R}\cdot]$  with random orientation of radicals,  $[\text{R}\cdot + \text{N}_2 + \text{R}\cdot]^*$ , and  $[\text{R}\cdot + \text{R}\cdot]^*$  where free radicals are oriented conveniently for the reaction. Radical recombination occurs with the steric factor  $P$ . The cage  $[\text{R}\cdot + \text{R}\cdot]^*$  is transformed into  $[\text{R}\cdot + \text{R}\cdot]$  with the frequency  $\nu$  and back transformation occurs with the frequency  $\nu P$ . The probability of  $[\text{R}\cdot + \text{R}\cdot]^*$  cage formation after AIBN decomposition is  $\alpha$  and that of  $[\text{R}\cdot + \text{R}\cdot]$  cage formation is  $(1 - \alpha)$ . The rate constant of radical recombination in the  $[\text{R}\cdot + \text{R}\cdot]^*$  cage is equal to  $k_{\text{C}}^*$ . The ratio  $k_{\text{DN}_2}/k_{\text{DR}} = \beta$  and the ratio  $\nu/k_{\text{DR}} = \gamma$ . This scheme leads to the following dependence of  $e$  on the parameters of molecular mobility:

$$(\beta + 1)e - \frac{1}{(\beta + 1)(1 - e)} = \frac{\nu}{k_{\text{C}}^* (\gamma P + \alpha)} + \frac{1 - \alpha}{\gamma P + \alpha} \quad (5.29)$$

The experimental data on AIBN decomposition in polypropylene were found to accord with this scheme and equation 7.29. The following values were calculated for the parameters of this equation, and the  $k_{\text{C}}^*$  values were calculated at  $P = 0.1$ .

$T$ .....	333 K	343 K	353 K
$k_{\text{C}}^* (\gamma P + \alpha)/s^{-1}$ .....	$5.8 \times 10^{10}$	$10.0 \times 10^{10}$	$29 \times 10^{10}$
$(1 - \alpha)(\gamma P + \alpha)^{-1}$ .....	0.165	0.125	0.065
$k_{\text{C}}^*/s^{-1}$ .....	$4.0 \times 10^{10}$	$7.0 \times 10^{10}$	$2.0 \times 10^{11}$

The data on lauroyl peroxide decomposition in polymers were treated in the scope of the analogous scheme, which takes into account the possibility of the reverse recombination of radicals  $\text{C}_{11}\text{H}_{23}\text{CO}_2\cdot$ , their decarboxylation with the rate constant  $k_{\text{D}}$ , and rotation of radicals in the cage. According to the scheme, the probability of free radical diffusion out of the cage was found to be

$$v(1 - e) = k_C^* (1 + 2.4P)e - k_C^*(1 - \alpha) \quad (5.30)$$

The experimental data on lauroyl peroxide decomposition are in agreement with the dependence of  $e$  on the molecular mobility  $n$  (polypropylene, 353 K). Assuming  $P = 0.1$ , we find  $k_C^* = 2.7 \times 10^{10} \text{ s}^{-1}$ ,  $\alpha = 0.96$ . Thus, the experimental data on the cage effect at the decomposition of AIBN and lauroyl peroxide in comparison with the molecular mobility in the polymer matrix evidence that the fate of a radical pair in a polymer cage depends on the rate constant of radical recombination (disproportionation) and their translational and rotational diffusion. The lower the rate of rotation, the more important the influence of the rotation of particles on the cage effect. So, the important role of rotational diffusion in the cage effect (which is not important in liquids) is specific for a polymer matrix.

#### 5.4.2. Concept of a hard cage of polymer matrix

Another phenomenon specific for polymers is the cage effect in slow bimolecular reactions. It is well known that the viscosity of liquids does not influence on the rate of slow bimolecular reaction, which occurs with an activation energy and is not controlled by the rate of diffusion of reactants. However, slow reactions in the polymer matrix occur more slowly than in the liquid under the same conditions. It was proved by comparison of the experimental rate constants of the reaction of 2,4,6-*tert*-butylphenoxyl radical with hydroperoxide groups of polypropylene (PP) and polyethylene (PE).

Media	$v \times 10^{-7}$ ( $\text{s}^{-1}$ )	$k$ ( $\text{l mol}^{-1} \text{ s}^{-1}$ ) ( $T = 295 \text{ K}$ )	$E$ ( $\text{kJ mol}^{-1}$ )	$\log A$ ( $\text{l mol}^{-1} \text{ s}^{-1}$ )
PP.....	6.7	$3.5 \times 10^{-3}$	67	9.4
PP + 8% C <sub>6</sub> H <sub>5</sub> Cl.....	240	0.38	52	7.8
PE.....	44	0.014	69	10.4
C <sub>6</sub> H <sub>6</sub> .....	850	0.115	45	7.1

Rate constants of these reactions were found to correlate with the molecular mobility, which was calculated from the ESR spectra of the nitroxyl radical. The higher the molecular mobility, the higher the rate constant of the reaction.

These experimental data initiated us to put forward the model of the hard cage of polymer matrix. The medium of the polymer matrix affects the bimolecular reaction differently than in the liquid phase. The interaction of two reactants in the liquid phase occurs in the cage formed by labile molecules. All geometric shapes of such a cage are energetically equivalent due to the high flexibility of molecules surrounding the pair of reacting particles, and this cage may be regarded as "soft." The formation of a transition state in the soft cage of the nonpolar liquid does not need an addition-

al energy for the reorganization of the molecules surrounding the pair of reactants.

In the polymer matrix each particle or a pair of particles is surrounded by segments of the macromolecule. These segments connected by C—C bonds form a rigid cage. In such a rigid cage, there are geometrically and energetically unequal orientations of particles. This is why, a pair of reactants reacting in the polymer matrix needs an additional energy to gain the necessary orientation to react in a rigid cage. Therefore, the rate constant of bimolecular reaction in the polymer matrix includes an additional coefficient  $F_s$ , which describes the influence of the cage walls on the mutual orientation of reactants:  $k_s = A \times F_s \exp(-E/RT)$ . This coefficient must depend on the temperature because it includes the Boltzmann factor equal to  $\exp(-U_{or}/RT)$ , where  $U_{or}$  is the difference between the energy of the energetically most convenient orientation of particles and that necessary for the reaction to occur. A particle in the polymer cage is regarded as being in the field of forces of intermolecular interaction, which is approximated by a cosine function (the reaction is regarded in one plane).

$$U(\theta) = 0.5 U_o(1 - \cos n_\theta \theta) \quad (5.31)$$

where  $U_o$  is the energy barrier dividing two energetically convenient positions of the particle in the cage, and  $2n_\theta$  is the number of such positions. For the reaction to occur, particles A must be oriented in the cage at an angle of  $\theta_A \pm \Delta\theta_A$ .

The pre-exponential factor of the bimolecular reaction in the polymer in the scope of such a model is the following:

$$A_s = \frac{A \exp(-U_{or}/RT)}{4\pi^2 I_o(U_o/2RT) \exp(-U_o/2RT)} \quad (5.32)$$

where  $I_o(x)$  is the modified Bessel function with respect to imaginary argument. In liquids all orientations of reactants are energetically equivalent. Therefore, the ratio of rate constants in the polymer and liquid is

$$\frac{k_s}{k_l} = \frac{\exp(-U_{or}/RT)}{\exp(-U_o/2RT) I_o(U_o/2RT)} \quad (5.33)$$

This cage model gives a simple equation for the frequency of rotation of the particle in the polymer  $v_s$  and liquid  $v_l$ :

$$v_s = v_l \exp(-U_o/RT) \quad (5.34)$$

Such a model explains the above mentioned peculiarities of free radical reactions in polymers. First, the reaction occurs more slowly in polymer than in liquid on the account of the reorganization of surrounding polymer segments to achieve the transition state (potential  $U_{or}$ ). Second, the correlation between  $k_s$  and molecular mobility  $v_s$  finds its natural explanation because  $k_s$  and  $v_s$  depend on the same potential  $U_o$ .

$$\ln \frac{k_l}{k_s (v_s/v_l)^{1/2}} = m \ln \frac{v_l}{v_s} \quad (5.35)$$

where  $m = U_{or}/U_o$ . Experimental data are in good agreement with this formula (see Table 5.1).

**Table 5.1 Comparison of rate constants and molecular mobility in the polymer matrix and liquids, values of  $U_0$  and  $U_{or}$ .**

Polymer	$v_s/v_l$	$k_s/k_l$	$U_0$ (kJ mol <sup>-1</sup> )	$m$	$U_{or}$ (kJ mol <sup>-1</sup> )
Reaction of 2,4,6-1,1-dimethylethylphenoxyl with hydroperoxide groups, $T = 295$ K					
PE.....	$5.62 \cdot 10^{-3}$	$8.40 \cdot 10^{-2}$	12.7	0.74	9.3
PP.....	$1.22 \cdot 10^{-3}$	$3.12 \cdot 10^{-3}$	36.8	0.74	12.2
PP + 2%C <sub>6</sub> H <sub>5</sub> Cl...	$1.43 \cdot 10^{-2}$	0.125	10.4	0.78	8.1
PP + 8%C <sub>6</sub> H <sub>5</sub> Cl...	$5.00 \cdot 10^{-2}$	0.332	7.3	0.72	5.2
Reaction of 4-benzoyloxy-2,2,6,6-tetramethylpiperidine-N-oxyl with 2,6-bis-1,1- dimethylethylphenol, $T = 313$ K					
PE.....	$8.93 \cdot 10^{-3}$	$7.25 \cdot 10^{-2}$	13.1	0.81	10.7
PE + 5.5%C <sub>6</sub> H <sub>5</sub> Cl.	$1.07 \cdot 10^{-2}$	0.123	11.7	0.74	8.6
PE + 36%C <sub>6</sub> H <sub>5</sub> Cl..	$6.67 \cdot 10^{-2}$	0.502	10.7	0.69	7.4
PP.....	$4.25 \cdot 10^{-3}$	$7.25 \cdot 10^{-2}$	14.1	0.73	10.3
PP + 2%C <sub>6</sub> H <sub>5</sub> Cl...	$1.11 \cdot 10^{-3}$	$7.22 \cdot 10^{-2}$	11.7	0.61	7.1
$T = 323$ K					
PE.....	$8.93 \cdot 10^{-3}$	0.267	12.6	0.55	6.9
PE + 4%C <sub>6</sub> H <sub>5</sub> Cl...	$1.56 \cdot 10^{-2}$	0.370	11.1	0.52	5.8
PP.....	$4.31 \cdot 10^{-3}$	0.125	14.6	0.63	9.2
PP + 1%C <sub>6</sub> H <sub>5</sub> Cl....	$6.45 \cdot 10^{-3}$	0.208	13.5	0.57	7.6
$T = 333$ K					
PE.....	$1.11 \cdot 10^{-2}$	0.345	12.4	0.51	6.5
PP.....	$6.67 \cdot 10^{-3}$	0.251	13.8	0.53	7.4
PP + 1%C <sub>6</sub> H <sub>5</sub> Cl....	$9.61 \cdot 10^{-3}$	0.345	13.0	0.51	6.6
PP + 2%C <sub>6</sub> H <sub>5</sub> Cl....	$1.39 \cdot 10^{-2}$	0.417	11.8	0.49	5.7
PS + 9%C <sub>6</sub> H <sub>5</sub> Cl....	$2.08 \cdot 10^{-3}$	0.133	17.0	0.56	9.5
PS + 38%C <sub>6</sub> H <sub>5</sub> Cl..	$4.17 \cdot 10^{-3}$	0.526	8.8	0.52	4.6
Reaction of 4-benzoyloxy-2,2,6,6-tetramethylpiperidine-N-oxyl with 1-naphthol, $T = 333$ K					
PE + 6%C <sub>6</sub> H <sub>5</sub> Cl	$1.39 \cdot 10^{-3}$	$7.04 \cdot 10^{-2}$	18.1	0.63	11.4
PS + 18%C <sub>6</sub> H <sub>5</sub> Cl	$4.59 \cdot 10^{-3}$	0.252	14.9	0.52	7.9
PS + 50%C <sub>6</sub> H <sub>5</sub> Cl	$6.67 \cdot 10^{-2}$	0.588	7.4	0.55	4.1

As seen from this table, the parameter  $m$  is constant in all experiments and lies in the limits of  $0.5 \div 0.75$ . The energetic barrier for orientation varies from 7 to 12

$\text{kJ}\cdot\text{mol}^{-1}$ . This model explains also the compensating effect, *i.e.*, the increase in the pre-exponential factor with an increase in the activation energy. An empirical linear correlation between the rate constant of bimolecular reaction in the polymer matrix and the transition state volume was found.

$$RT \ln(k_t/k_s)/\text{kJ mol}^{-1} = a (V^\ddagger - b) \quad (5.36)$$

$T/\text{K}$ .....	303	333	363
$A \cdot 10^2 \text{ kJ cm}^{-3}$ .....	2.50	2.23	1.98
$B/\text{cm}^3 \text{ mol}^{-1}$ .....	127	110	17

### 5.5. Pulse methods for studying the kinetics of fast reactions

The recombination of atoms and radicals in a solution occurs so promptly that special methods are necessary to study its kinetics. Several methods are based on the participation of free radicals in chain processes: these methods are considered in Chapter 16. Pulse methods (pulse photolysis and pulse radiolysis) have received wide recognition for studying fast radical reactions beginning from sixties. The method of pulse laser photolysis appeared later. The first pulse photolysis technique was developed by J. Porter in 1950; at first this method was used for studying gas phase radical reactions, later for reactions in solutions. Pulse radiolysis was developed in 1959-60 by four research groups: M. Matheson and L. Dorfman (USA), A. MacLachlan and R. McCarthy (USA), J. Keene (England), and J. Boag (England).

The principle of the pulse method is the following. The initial substance, a source of radicals, is irradiated for a short time with a powerful flash of light or particles, which results in the formation of a sufficiently high nonequilibrium radical concentration. Their consumption is monitored by the method of high-performance spectrophotometry, and the consumption kinetics allows one to understand in which reaction and with which rate constant radicals are consumed.

#### 5.5.1. Pulse photolysis

An experimental pulse photolysis technique consists of a pulse lamp with an energy source and equipment for charging and discharging, a reaction vessel with a reflector, and a device for the spectroscopic detection of short-lived intermediates. The light source must provide for a very short time a high intensity of light and give flashes reproducible by both intensity and spectral parameters. A gas-discharge tube for discharging capacitors is used: capacity of capacitors from 4 to 10  $\mu\text{F}$ , voltage from 4 to 20 kV, energy consumption from 10 to 3000 J. An empirical dependence is observed between the flash duration and energy of gas-discharge tubes: the higher

the flash energy, the longer its duration. For example, at an energy of 1 J the flash duration  $t \cong 0.3 \cdot 10^{-6}$  s; at 100 J  $t \cong 4 \cdot 10^{-6}$  s. Each system is characterized by its optimum time and energy of the flash. To increase the number of photons absorbed by the solution, a pulse lamp and a reaction vessel are arranged nearby and surrounded by a reflector.

The reaction course is monitored by the absorption of light with the wavelength usually corresponding to the absorption maximum of the radical under study. With this purpose, the light, which was preliminarily passed through a spectrograph, is passed through the solution, and at a chosen wavelength its intensity is detected by a photoamplifier. The photocurrent comes to an oscillograph, on the display of which the kinetics of changing the absorbance is detected. The data are processed, as a rule, using a personal computer to obtain the kinetic characteristics of the process. If a particle is consumed according to the first order, the reaction rate constant is calculated; if the order is second, the product  $\epsilon_R k$  is calculated, where  $\epsilon_R$  is the molar absorption coefficient of the analyzed particle R, which is determined by special experiments, often being a complicated problem. Several methods for its solution are available. 1. The final products of radical transformation after a series of successive flashes are analyzed, and their sum is used for the determination of the initial concentration of radicals in each experiment. To determine reliably  $\epsilon_R$ , all products should be analyzed and the mechanism of their formation should be known. 2. Radicals are generated in the presence of an appropriate radical acceptor, which is transformed into an easily analyzed stable product. For example, radicals  $\text{RO}\cdot$  and  $\text{RO}_2\cdot$  react promptly with phenols. 2,4,6-Tri-*tert*-butylphenol is introduced into the system where these radicals are generated. It rapidly "intercepts" all radicals appeared during the flash and is transformed into the stable phenoxyl radical. This radical has a high molar absorption coefficient, and it can easily be determined spectrophotometrically. If the presence of phenol does not reflect on photoinitiation, it is not difficult to calculate the molar absorption coefficient of the initial  $\text{RO}\cdot$  and  $\text{RO}_2\cdot$  radicals.

The kinetics of radical consumption with  $t_{1/2} \cong 10^{-5} \text{ s}^{-1}$  can be studied at a flash duration of  $\sim 1 \text{ } \mu\text{s}$ . This allows the study of the kinetics of the bimolecular reaction with  $\cong 10^6 \text{ s}^{-1}$  or  $k \cong$ ; at a length of the reactor of 10 cm  $l \cong 0.1$ . Usually  $\cong 1/(\text{mol}\cdot\text{s})$ , and constants up to  $10^{11} \text{ l}/(\text{mol}\cdot\text{s})$  are accessible for measurement. The method is widely used for measuring rate constants of atom and radical recombination in solution, reactions of molecules in the excited triplet state, electron transfer between radicals, and fast reactions of radicals with molecules (see Chapter 7).

Pulse lamps do not allow one to obtain short ( $< 10^{-6} \text{ s}$ ) flashes with a high radiation intensity. This difficulty can be overcome using laser light sources. Lasers have three important advantages: their peak power can be very high, the irradiated light is coherent and monochromatic, and the light pulse is symmetric in time. Lasers make it possible to record the kinetics in the nanosecond range. Using laser photolysis, researchers study reactions of singlet-excited aromatic molecules, kinetics of disap-

pearance of radical pairs formed during photolysis of molecules, transformations of charge transfer complexes, and processes with electron transfer, and changes in the physical state of molecules (for example, polarization) can also be detected.

### 5.5.2. *Pulse radiolysis*

This method is a radiation-chemical analog of pulse photolysis. High-performance spectrophotometry is used for the identification of particle detection. The kinetic information is processed by a computer. Active particles are generated by the electron impact with a short pulse of high-energy electrons, which induce the ionization and electron excitation of molecules, and excited molecules dissociate to form radicals and atoms.

To create an electron pulse, the following instruments are used: a microwave linear accelerator (electron energy  $2\div 12$  MeV, pulse duration  $100\div 1000$  ns), a Van der Graaf accelerator (electrons with an energy of  $2\div 4$  MeV, duration  $1\div 100$  ns), and a febetron (electrons with an energy of  $0.6\div 2$  MeV, duration  $10\div 50$  ns). A reaction cell is prepared from quartz, which is rather resistant toward radiation coloring. Since electrons are rapidly retarded in liquid and lose their capability of ionizing molecules, the cell thickness should not exceed  $1\div 2$  cm. The electron energy in the beam usually ranges from 1 to 30 MeV. The higher this energy, the more uniform over the vessel the initiation.

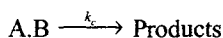
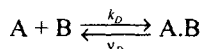
The method of pulse radiolysis was used to study in detail reactions of particles appeared in water during its electron irradiation: hydrogen atoms, hydroxyl radicals, and  $\text{HO}_2\cdot$ . Very valuable data were obtained for reactions of a hydrated electron with various ions, radicals, and molecules. A radical anion is formed when an electron is captured by an aromatic molecule, and reactions involving radical anions are also studied by pulse radiolysis.

## Bimolecular reactions in solutions Influence of medium

### 6.1. Theory of encounters in liquid

In gases an elementary act of the bimolecular reaction occurs by the collision of two particle-reactants if an excessive energy of colliding particles exceeds the activation barrier and the configuration of the formed pair is convenient for the reaction. In liquid (solution) the bimolecular act occurs in somewhat different way. At first particle-reactants diffuse in solution and get into the same cage, neighboring for some time, they collide in it and undergo transformation in one of the collisions if the same conditions are fulfilled as those for the bimolecular reaction in the gas phase. The situation is somewhat more difficult when molecular complexes or electrostatic interactions appear between molecules in solution, which will be considered in the next chapter. The time of existence of a particle in the cage in low-viscosity liquids at room temperature is  $10^{-10} \div 10^{-8}$  s, and one collision between adjacent particles occurs for  $10^{-13} \div 10^{-12}$  s.

Due to the described above process of encounter and collision of two particles in liquid (and, in general, in the condensed phase), the following general scheme is valid for the bimolecular reaction in solution:



where  $A.B$  is the pair of particles in the solvent cage;  $k_D$  is the rate constant of diffusional encounter of particles  $A$  and  $B$ ,  $l/(\text{mol}\cdot\text{s})$ ;  $v_D$  is the rate constant of diffusional escape of one particle from the cage,  $\text{s}^{-1}$ ; and  $k_c$  is the rate constant of transformation of the pair of particles into products,  $\text{s}^{-1}$ .

The full solution of the system of equations describing the process has the following form ( $v = k_c[A.B] = k_{\text{exp}}[A][B]$ ):

$$k_{\text{exp}} = \frac{k_D k_c}{v_D + k_c} \{1 - \exp[-(v_D + k_c)t]\} \quad (6.1.)$$

At  $t \gg (v_D + k_c)^{-1}$

$$k_{\text{exp}} = k_D k_c (v_D + k_c)^{-1}$$

In low-viscosity liquids, the time of establishment of the kinetically equilibrium concentration of A.B is very low ( $10^{-9} \div 10^{-8}$  s) but in glasses and polymers where diffusion occurs slowly the diffusion time is  $10^2 \div 10^4$  s. When the reaction occurs with an activation energy, in liquid usually  $k_c \ll v_D$  and the equilibrium concentration of A.B pairs is established

$$[A.B] = K_{AB}[A][B], K_{AB} = k_D v_D^{-1}$$

Assuming that molecules of reactants and solvent are close in size, shape, and character of intermolecular interaction and the medium that surrounds the A.B pair is a continuum, then the concentration of the pairs is the following:

$$[A.B] = 4\pi \cdot 10^{-3} L r_{AB}^2 \delta r [A][B] = K_{AB}[A][B] \quad (6.2)$$

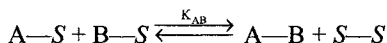
where  $r_{AB}$  is the average distance between the centers of particles in the cage ( $r_{AB} \approx r_A + r_B$ ), and the cell thickness is  $\delta r = r_B + r_S$ , where  $r_S$  is the radius of the solvent molecule.

At  $r_A + r_B = r_S = 5 \cdot 10^{-10}$  m,  $K_{AB} = 0.94 \approx 1$  l/mol  $\approx 1.5 \cdot 10^{-21}$  cm<sup>3</sup>/molecule.

When particles of the same type react, then

$$K_{AB} = 2 \cdot 10^3 L r_{AA}^2 \delta r \text{ l/mol.} \quad (6.3)$$

This expression was obtained in the framework of the concept of solid spheres and describes the behavior of reactant pairs, which do not interact with each other and with the solvent. In a more general case, this interaction takes place, so that the formation of the A.B pair in a solution can be presented as the equilibrium of the type



where  $S$  is the solvent molecule, and dash designates the intermolecular interaction.

According to the thermodynamic theory of solutions (E. Guggenheim, 1952), the equilibrium constant of this type

$$K_{AB} = (n/[S]) \exp(2U_{ABS}/RT) \quad (6.4)$$

where  $U_{ABS}$  is the difference between potential energies of the interaction of pairs A—S, B—S, and A—B, S—S.

These energies can be estimated, first, by the partition coefficient of the substance between two liquid phases and, second, by the critical temperature of mutual dissolution of two phases. The ratio of the number of neighbors in the cage  $n$  to the number of moles of the solvent  $S$  (in mol/l) is usually close to unity. According to the encounter theory, the rate constant of bimolecular reaction  $k \sim z_0$ , where  $z_0$  is the frequency factor of bimolecular collisions. In liquid a molecule is surrounded by  $n$  molecule-neighbors, vibrates in this cage with the frequency  $n$ , and collisions with each neighbor  $6v$  times and with one molecule  $6v/n$  times. The vibration of a particle sur-

rounded by molecules can be considered as harmonic when the particle with the weight  $m$  vibrates with the amplitude  $a$  and frequency  $\nu$

$$\nu = (3/2)(kT/\pi m)^{1/2} \quad (6.5)$$

Amplitude  $a$  can be related to the temperature coefficient of linear expansion of liquid  $\alpha_1$ :  $a = 2\alpha_1 T$ . At the same time, the amplitude can be related to the free volume of liquid  $V_f$

$$a = 2(3V_f/4\pi L)^{1/3}$$

In turn, the free volume of liquid can be estimated, e.g., by the heat of evaporation

$$V_f = (2RT/\Delta H_{\text{vap}})^3 V \quad (6.6)$$

The vibration frequency of molecules can be estimated by the velocity of sound in liquid  $u_l$

$$\nu = u_l(3L/4\pi V)^{1/3} \quad (6.7)$$

(where  $V$  is the volume of one mole of liquid) and by the viscosity of liquid  $\eta$  ( $\rho$  is the liquid density)

$$\nu = 3 \cdot 10^4 \eta / \rho r_{AB}^2 \quad (6.8)$$

For most liquids and standard molecules ( $M \approx 100$ )  $\nu$  changes in an interval of  $10^{12} \div 10^{13} \text{ s}^{-1}$ . The chemical reaction can be induced by such vibrations due to which molecules get in tight contact and experience repulsion. This is observed when the vibration energy exceeds some energy  $E'_v$  and the vibration amplitude exceeds the  $a'$  value. The frequency of these encounters

$$\nu' = \nu \exp(-E'_v/RT)$$

The factor  $\exp(-E'_v/RT)$  takes into account, in essence, the situation that the chemical interaction is a result of encounters with such an amplitude which perturbs the harmonic character of vibrations. For harmonic vibrations the repulsion energy is proportional to  $\Delta r^{-2}$ , and a more tight approaching changes this dependence ( $r^{-n}$ ,  $n \approx 6 \div 12$ ) according to the Lenard—Jones potential of intermolecular interaction. Thus, the frequency of efficient encounters of the A.B pair in solution

$$\nu' = (3/2\alpha_1)(k/\pi m T)^{1/2} \exp(E'_v/RT) \quad (6.9)$$

where  $m$  is the reduced weight of particles A and B.

In the framework of the encounter theory in gas (see Chapter 2), the rate constant of bimolecular reaction

$$k = z_0 P \exp(-E/RT)$$

The exponential factor expresses the fraction of encounters, whose energy is equal to or higher than  $E$ . This expression follows from the fact that the contribution to the activation energy is made only by the translatory motion of particles A and B. In liquid the character of motion of particles A and B changes: it becomes vibrational, whose full energy (kinetic and potential) is described by two quadratic terms. Due to this, the fraction of encounters of two particles A and B with an energy exceeding  $E$  is equal to  $(E/RT)\exp(-E/RT)$ . The rate constant of transformation of a pair of particles in solution

$$k_c = \nu' P(E/RT) \exp(-E/RT) \text{ s}^{-1}$$

and the experimentally observed bimolecular rate constant

$$k_{\text{exp}} = K_{\text{AB}} k_c = (n/[S]) P(E/RT) \exp[-(E + E'_\nu - 2U)/RT] \quad (6.10)$$

As already mentioned,  $n/[S] \approx 1$ ,  $\nu' \approx 10^{12} \div 10^{13} \text{ s}^{-1}$ , the energy  $E'_\nu$  depends on forces of intermolecular interaction, free volume, and temperature. Near the freezing temperature  $E'_\nu \approx 0$  and increases with temperature, reaching 8-15 kJ/mol near the boiling point. The algebraic sum of potentials of intermolecular interactions can be either positive or negative:  $-10 \leq U_{\text{AB}} \leq 10 \text{ kJ/mol}$  ( $P$  and  $E$  are determined by the structure and reactivity of reactants).

The rate constant is calculated from experimental data in the Arrhenius form

$$k_{\text{exp}} = A \exp(-E/RT) \text{ l/(mol}\cdot\text{s)}.$$

Since the theoretical expression for  $k_{\text{exp}}$  includes both the exponential term and the temperature-dependent pre-exponential factor  $B(T)$ , which is seen from (6.10) and (6.9), then

$$E_a = E + E'_\nu + 2U_{\text{AB}} + RT d \ln B(T) / d \ln(T)$$

and

$$E = E_a - E'_\nu + 2U_{\text{AB}} + 3/2RT - RT d \ln V / d \ln T @. \quad (6.11)$$

The last term reflects the contribution of the thermal expansion of liquid to the temperature dependence of  $k_{\text{exp}}$ . If the collision frequency in liquid is expressed by viscosity (formula 8.8)  $\eta = \eta_0 \exp(E_\eta/RT) @$ , then

$$E = E_a - E'_\nu + 2U_{\text{AB}} + E_\eta \quad (6.12)$$

According to (6.10), the pre-exponential factor  $A$  is the following:

$$A = B(T) \exp[d \ln B(T) / d \ln T] = 0.19 \alpha^{-1} (k/mT)^{1/2} (n/[S]) (E/RT) P \exp(d \ln V / d \ln T)$$

### 6.2. Theory of activated complex

The specificity of a bimolecular act in liquid, as already mentioned, is that particle-reactants at first meet in the same cage and then, at a sufficient activation, react in the environment of solvent molecules. The formation of the A.B pair is accompanied, in the general case, by a change in entropy  $\Delta S_{AB}$  and enthalpy  $\Delta H_{AB}$  of the system; equilibrium rate constant  $K_{AB}$  is related to them by the known correlation

$$-RT \ln K_{AB} = \Delta H_{AB} - T \Delta S_{AB} \quad (6.13)$$

The experimentally measured rate constant of the slow ( $k_{\text{exp}} \ll k_D$ ) adiabatic reaction is

$$k_{\text{exp}} = K_{AB} k_c = (kT/h) \exp[(\Delta S^\ddagger + \Delta S_{AB})/R] \exp[-(\Delta H^\ddagger + \Delta H_{AB})/RT] \quad (6.14)$$

Therefore, the  $\Delta S_{\text{exp}}$  and  $\Delta H_{\text{exp}}$  values calculated from experimental data are the following:

$$\Delta S_{\text{exp}} = \Delta S^\ddagger + \Delta S_{AB}, \quad \Delta H_{\text{exp}} = \Delta H^\ddagger + \Delta H_{AB}$$

Compare the expressions for bimolecular rate constants according to the encounter theory and activated complex theory. Since  $K_{AB}$  enters the expression for  $k_{\text{exp}}$  in both considerations, only  $k_c$  should be compared

$$\frac{6V}{n} P \frac{E}{RT} \exp[-(E + E'_v)/RT] = \frac{kT}{h} \exp(\Delta S^\ddagger/R) \exp(-\Delta H^\ddagger/RT) \quad (6.15)$$

It follows from this equality that  $\Delta H^\ddagger = E + E'_v$  and

$$\Delta S^\ddagger = R[\ln(6VhEPL/n) - 2\ln(RT)] @. \quad (6.16)$$

Activation entropy  $\Delta S^\ddagger$  is related to the pre-exponential factor  $A$  by the correlation

$$A = (RT/Lh)(n/[S]) \exp(\Delta S^\ddagger/R) \exp(d \ln V / d \ln T) @, \quad (6.17)$$

and the Arrhenius activation energy

$$E_a = \Delta H^\ddagger + 2U_{AB} + RT(d \ln V / d \ln T) \quad (6.18)$$

The formation of an activated complex from two particle-reactants is accompanied by a change in the volume. Therefore, the external pressure influences the rate constant of bimolecular reaction. Since the internal pressure about  $10^8$ - $10^9$  Pa exists in liquid due to the intermolecular interaction (in  $\text{CCl}_4$  at 293 K it is  $3.48 \cdot 10^8$  Pa), the external pressure of an order of  $10^8$ - $10^{10}$  Pa should be created for a noticeable effect on the liquid. The study of the pressure effect on the reaction provides data on a change in the system volume during the formation of an activated complex.

Measuring the reaction rate constant  $k_{\text{exp}}$  at different pressures  $p$ , one can find  $\Delta V_{\text{exp}}$  from the dependence

$$(\delta \ln k / \delta p) T = -(\Delta V_{\text{exp}} / RT) + \Delta n^* \gamma \quad (6.19)$$

where  $\Delta n^*$  is the change in the number of particles during activated state formation (for the bimolecular reaction  $\Delta n^* = 1$ );  $\gamma = V_S^{-1}(dV/dp)T$  is the correction for the solvent compressibility.

The  $\gamma$  correction is not high ( $RT\gamma \approx 1 \div 4 \text{ cm}^3/\text{mol}$ ) and often neglected. Usually the dependence of  $\ln k$  on  $p$  is nonlinear because with the pressure increase the energy of intermolecular repulsion increases and the effect of further compression of the system becomes difficult. The following empirical equation is used for the description of this dependence:

$$\ln k = \ln k_0 - (V_0/RT)[p/(1 + bp)] \quad (6.20)$$

Here  $b = 9.2 \cdot 10^{-9} \text{ Pa}^{-1}$  is the empirical parameter that allows the determination of  $\Delta V_{\text{exp}}^*$  at  $p = 0$  by the formula

$$\Delta V_{\text{exp}}^* = V_{\text{exp}}^* (1 + bp)^2 \quad (6.21)$$

Since in liquid the bimolecular reaction occurs in two steps:  $A + B \rightleftharpoons A.B \rightarrow (A.B)^* \rightarrow \text{Products}$ , this should be taken into account in the interpretation of  $V_{\text{exp}}^*$  calculated from experiment

$$V_{\text{exp}}^* = \Delta V_{AB} + \Delta V^* \quad (6.22)$$

The change in the volume during the formation of the equilibrium A.B pair can be either positive or negative, depending on the density of the solvate shell around A and B, on the one hand, and from the A.B pair, from the other hand. If reactants react more vigorously with each other than with solvent molecules, then  $\Delta V_{AB} < 0$ , and this value is added to the negative  $\Delta V^*$  value. The  $\Delta V^*$  values for several bimolecular reactions are presented below as an example.

Reaction	Solvent	T	$V_{\text{exp}}^*$ , cm <sup>3</sup> /mol
PhN(CH <sub>3</sub> ) <sub>2</sub> + C <sub>2</sub> H <sub>5</sub> I.....	(CH <sub>3</sub> ) <sub>2</sub> CO	303	-16.4
(CH <sub>3</sub> CO) <sub>2</sub> O + C <sub>2</sub> H <sub>5</sub> OH.....	PhCH <sub>3</sub>	333	-19.6
	C <sub>2</sub> H <sub>5</sub> OH	303	-15.9
Dimerization of <i>cyclopentadiene</i> ....	C <sub>6</sub> H <sub>6</sub>	303	-23.1
<i>o</i> -(CH <sub>3</sub> )C <sub>6</sub> H <sub>4</sub> N(CH <sub>3</sub> ) <sub>2</sub> + CH <sub>3</sub> I.....	CH <sub>3</sub> OH	313	-26.6

It is seen that  $V_{\text{exp}}^*$  changes from -15 to -25 cm<sup>3</sup>/mol, with the temperature increase  $V_{\text{exp}}^*$  increases, which is related to the thermal expansion of liquid.

Since the rate constant depends on both the temperature and pressure, the reaction can be described in two forms

$$k_p = A_p \exp(-E_p/RT), \quad k_v = A_v \exp(-E_v/RT), \\ E_p = RT^2(d\ln k_{\text{exp}}/dT)_p, \quad E_v = RT^2(d\ln k_{\text{exp}}/dT)_v$$

Since the following equality is valid:

$$(\delta \ln k / \delta T)_v = (\delta \ln k / \delta T)_p - (\delta V / \delta T)_p (\delta p / \delta V)_T (d \ln k / dp) T \quad (6.23)$$

and the coefficients of isothermic and isobaric expansion are

$$\alpha_1 = (d \ln V / dp) T \quad \text{and} \quad \alpha_2 = (d \ln V / dT) T$$

then  $E_p$  and  $E_v$  are related by the correlation

$$E_v = E_p + (RT^2 \alpha_2 / \alpha_1) (\delta \ln k / \delta p)_T \quad (6.24)$$

For the dimerization of liquid *cyclopentadiene* at  $p = 10^5 \div 3 \cdot 10^8$  Pa

$$k_p = 2.7 \cdot 10^7 \exp(-74/RT), \quad k_v = 5.0 \cdot 10^8 \exp(-82/RT) \text{ l/(mol} \cdot \text{s)}$$

If polar particles participate in the reaction, the rate constant depends on the dielectric constant of the medium  $\epsilon$  (see below), which, in turn, changes with the pressure increase. The change in  $\epsilon$  with the pressure increase is described by the formula ( $\epsilon = \epsilon_0$  at  $p = p_0 = 10^5$  Pa)

$$\epsilon_0 / \epsilon = 1 - a \ln[(b + p)/(b + p_0)] \quad (6.25)$$

$$E_v = E_p + (RT^2 \alpha_2 / \alpha_1) (\partial \ln k / \partial p) T$$

### 6.3. Comparison of bimolecular reactions in gas and liquid phases

Fast activationless reactions, such as recombination of atoms and radicals, of course, occur more slowly in liquid than in gas because they are limited by the rate of particle self-diffusion, and diffusion in liquid occurs more slowly than in gas. Therefore, it is of interest to compare slow reactions, which are not limited by diffusion in liquid, to those with rate constants  $k < 10^7$  l/(mol·s) in the gas phase. As we will see further, the solvation effects and formation of molecular complexes influence strongly on the chemical reaction in liquid. Since solvation is absent from the gas phase, for the correct comparison we have to consider reactions in which at least one reactant is a nonpolar particle, for example, hydrocarbon. Reactions of radicals with nonpolar C—H bonds are most suitable for this comparison. The data on such

reactions, whose rate constants are measured in the gas and liquid phases, are presented in Table 6.1. It is seen that, in all cases, the rate constants of bimolecular reactions of radical abstraction in the liquid phase are higher than those in the gas phase.

Table 6.1. Rate constants of bimolecular radical reactions in liquid (H<sub>2</sub>O) and gas phases [ $T = 298$  K,  $V_f/V = 2.1 \cdot 10^{-3}$ ,  $k_{\text{gas}}$  and  $k_{\text{liq}}$  in l/(mol·s)]

Reactions	$k_{\text{gas}}$	$E_{\text{gas}}$ , kJ/mol	$k_{\text{liq}}$	$k_{\text{liq}}/k_{\text{gas}}$	$\frac{E}{RT} \left( \frac{V}{V_f} \right)^{1/3}$	
H + CH <sub>3</sub> OH	$1.2 \cdot 10^4$	36	$1.6 \cdot 10^6$	133	143	0
H + C <sub>2</sub> H <sub>5</sub> OH	$1.4 \cdot 10^5$	29	$1.6 \cdot 10^7$	114	90	0
H + CH <sub>3</sub> COCH <sub>3</sub>	$3.0 \cdot 10^4$	35	$3 \cdot 10^5$	10	109	6
H + H <sub>2</sub> O <sub>2</sub>	$2.5 \cdot 10^6$	16	$4 \cdot 10^7$	16	50	3
$\dot{\text{C}}\text{H}_3$ + CH <sub>3</sub> OH	7	42	220	31	131	5
$\dot{\text{C}}\text{H}_3$ + C <sub>2</sub> H <sub>5</sub> OH	23	40	590	26	125	4
$\dot{\text{C}}\text{H}_3$ + (CH <sub>3</sub> ) <sub>2</sub> CHOH	340	25	$3.4 \cdot 10^3$	10	78	5
$\dot{\text{C}}\text{H}_3$ + CH <sub>3</sub> CH <sub>2</sub> COCH <sub>3</sub>	240	34	$2.9 \cdot 10^3$	12	106	5
$\dot{\text{C}}\text{H}_3$ + CH <sub>3</sub> COOH	4	43	200	50	134	$E_v$
2						vy/mol
$\dot{\text{H}}\text{O} + \text{H}_2$	$3 \cdot 10^6$	22	$1.5 \cdot 10^8$	50	69	kJ/mol
0						
$\dot{\text{H}}\text{O} + \text{CH}_4$	$6 \cdot 10^6$	16	$1.5 \cdot 10^8$	25	50	2

In the framework of the encounter theory, this is a result of the following two distinctions between the gas and liquid phases. First, if the pressure in the gas is not very high, particles move over the whole volume  $V$  and the frequency of bimolecular encounters  $z_0$  gas depends only on the temperature  $T$ , weights of particles  $m_A$  and  $m_B$ , and encounter cross sections ( $r_A$  and  $r_B$ )

$$z_{0 \text{ gas}} = 10^{-3} L(r_A + r_B)^2 [8RT(m_A^{-1} + m_B^{-1})/\pi]^{1/2} \quad (6.26)$$

In liquid reactants at first get in one cage where they multiply collide. The main part of the volume is occupied by solvent molecules. Encounters of particles occur due to their motion in the free volume  $V_f$ , and  $V_f \ll V$ , where  $V$  is the volume of a mole of solvent. In liquid with  $z_0$  gas we have to compare  $K_{AB} z_{0 \text{ liq}} = K_{AB} 6v/n$ , where  $n$  is the number of solvent molecules surrounding one particle. In the framework of the concept of solid spheres,  $K_{AB}$  is expressed by equation (6.2) through  $r_A$ ,  $r_B$ , and  $\delta r$

$$K_{AB} = 4 \cdot 10^{-3} L(r_A + r_B)^2 \delta r \text{ l/(mol·s)}$$

where  $r_A$ ,  $r_B$ , and  $\delta r$  are expressed in cm.

The vibrational frequency of a particle in the cage is expressed by equation (6.5),

for a pair of particles  $m$  should be replaced by the reduced weight:  $(Lm)^{-1} = M_A^{-1} + M_B^{-1}$ . After insertion we obtain

$$z_{o \text{ liq}} K_{AB} = 4 \cdot 10^{-3} L(r_A + r_B)^2 \delta r \left( \frac{4L}{3V_f} \right)^{1/3} [RT(M_A^{-1} + M_B^{-1})/\pi]^{1/2} \quad (6.27)$$

The cage thickness  $\delta r$  can be accepted equal to the diameter of the solvent molecule:  $\delta r = (V/L)^{1/3}$ . For the frequency of collision frequencies in the gas and liquid phases we obtain

$$z_{o \text{ gas}}/K_{AB} z_{o \text{ liq}} = 0.097 n (V_f/V)^{1/3} \quad (6.28)$$

The number of neighbors  $n \approx 8 \div 12$ . Accepting  $n = 10$ , we have  $z_{o \text{ gas}}/K_{AB} z_{o \text{ liq}} \approx (V_f/V)^{1/3}$ . Since  $V_f \ll V$  (usually  $V_f \approx 0.2 \div 2\%$  of  $V$ ), in liquid particles collide more frequently.

Second, in liquid the character of particle motion changes, and this reflects the proportion between the total number of collisions and collisions leading to excitation. In the gas phase where excitation occurs due to the translatory motion of collided particles, the fraction of collisions, whose energy exceeds  $E$ , is equal to  $\exp(-E/RT)$ . This is a result of the fact that the energy depends on the kinetic energy of two particles  $0.5m_A v_A^2$  and  $0.5m_B v_B^2$ , i.e., is described by two quadratic terms. In liquid the character of particle motion changes from translatory to vibrational: each particle in solution executes vibrational motions in the field of molecular forces of solvent molecules. In this case, the fraction of encounters of two particles, whose energy exceeds  $E$ , is equal to  $(E/RT)\exp(-E/RT)$ . In addition, as already mentioned, in liquid only vibrations with the encounter energy higher than some threshold value  $E'_v$  participate in the activation of all vibrations [see (6.9)]. Therefore, the ratio of rate constants for the same reaction occurred with the same  $P$  and  $E$  in the gas and liquid phases is the following:

$$\begin{aligned} \frac{k_{\text{liq}}}{k_{\text{gas}}} &= \frac{z_{o \text{ liq}} K_{AB} (E/RT) \exp(-E_v/RT)}{z_{o \text{ gas}}} \approx \\ &\approx \left( \frac{V}{V_f} \right)^{1/3} \frac{E}{RT} \exp(-E'_v/RT) \end{aligned} \quad (6.29)$$

Since  $V/V_f$  ranges from 200 to 30, and  $E/RT$  changes from 8 to 40, at  $E'_v = 0$   $k_{\text{liq}}/k_{\text{gas}} \approx 20 \div 200$ , and  $\exp(-E'_v/RT)$  usually changes in an interval of  $1 \div 0.02$ . The data presented in Table 6.1 agree with the following estimations: in all cases,  $k_{\text{liq}} > k_{\text{gas}}$ , the average energy value is  $E'_v \approx 3$  kJ/mol.

Similar conclusions are drawn when this problem is considered in the framework of the transition state theory. The rate constant of the bimolecular reaction in the gas phase

$$k_{\text{gas}} = e^2(RT/Lh)\exp(\Delta S^\ddagger/R)\exp(E_{\text{gas}}/RT) \quad (6.30)$$

In the liquid phase

$$k_{\text{liq}} = e^2(RT/Lh)\exp(\Delta S^\ddagger/R)\exp(E_{\text{liq}}/RT) \quad (6.31)$$

Assume that  $E_{\text{gas}} = E_{\text{liq}}$  and the activation entropy differs only because of the free volume  $V_f$ . Let us consider the reaction that occurs in equal volumes  $V_{\text{gas}} = V_{\text{liq}} = V$ . Almost the whole volume  $V$  is accessible for motion in gas. In liquid almost the whole volume is occupied by solvent molecules, and only the free volume  $V_f$  is accessible for motion. Therefore, when a particle goes from the gas to liquid, the entropy related to the translatory motion of particles changes by the value

$$\Delta S = S_{\text{gas}} - S_{\text{liq}} = R\ln(V/V_f) \quad (6.32)$$

Since

$$\Delta S^\ddagger = S^\ddagger - S_A - S_B, \text{ then } \Delta S_{\text{liq}}^\ddagger = \Delta S_{\text{gas}}^\ddagger + R\ln(V/V_f)$$

and

$$k_{\text{liq}}/k_{\text{gas}} = V/eV_f \approx 10 \div 70$$

Evidently, such factors as the delayed rotation of particles in liquid, solvation of reactants and transition state reflect this ratio. Situations are possible where the liquid medium impedes the bimolecular act, and the reaction in gas occurs more promptly than in liquid. However, in all cases, the effect of free volume is retained, which as if accelerates the bimolecular act. This effect should also take place in strongly compressed gases where the substance density approaches that of liquid.

#### 6.4. Reactions of polar particles

Many molecules have polar groups (O—H, C—Cl, C=O, and others). In this group the electron density of bond-forming electron pairs is shifted toward the atom with the highest electron affinity. Polar molecules possess the dipole moment  $m$  because the centers of gravity of positive and negative charges do not coincide. The exception are molecules in which polar groups form a symmetric structure, so that group-dipoles compensate each other and the resulting dipole moment is equal to zero (for example,  $\text{CCl}_4$ ,  $\text{CO}_2$ , etc.). Below we present dipole moments of several molecules in the gas phase expressed in  $\text{C}\cdot\text{m}\cdot 10^{30}$ .

HCl	HBr	HI	NH <sub>3</sub>	H <sub>2</sub> O	CH <sub>3</sub> Cl	CH <sub>3</sub> OH	CH <sub>3</sub> COCH <sub>3</sub>
3.48	2.67	1.28	4.93	6.09	6.56	5.68	9.49

This particle-dipole is solvated in the solvent. When the solvent is considered as a medium with the dielectric constant  $\epsilon$ , the solvation Gibbs energy calculated per mole, according to Kirkwood (1943), is the following ( $m$  is the dipole moment,  $r$  is the particle radius):

$$\Delta G_{\text{solv}} = -\frac{L\mu^2}{r^3} \frac{\epsilon - 1}{2\epsilon + 1} \quad (6.33)$$

When two particle-dipoles A and B get into the same cage in liquid, they form the associate A.B due to the dipole-dipole interaction. If each particle is considered as a sphere with the radius  $r_A$  or  $r_B$  with the point dipole moment  $\mu_A$  or  $\mu_B$ , and the associate is considered as a bisphere executing rotation around two axes perpendicular to the line connecting the centers of spheres A and B, then the constant of equilibrium associate formation calculated through the sums of states

$$K_{AB} = 10^3 L (V_{r_{AB}} / V_{CB}) (8\pi h^2 / m_{AB} kT)^{1/2} \exp(-\Delta G_{\text{el}} / RT) \quad (6.34)$$

where  $r_{AB} = r_A + r_B$  is the radius of the dimer,  $m_{AB} = m_A m_B (m_A + m_B)^{-1}$  is the reduced weight of the associate,  $V$  and  $V_f$  are the full and free volumes of solvent, and  $\Delta G_{\text{el}}$  is the change in the electrostatic energy due to associate formation.

This energy is summated from the change in the energy of interaction of dipoles A, B, and A.B with the medium and the change in the polarization energy of particles by the medium ( $\alpha_A$  and  $\alpha_B$  are the polarizabilities of particles A and B)

$$\Delta G_{\Sigma} / L = -\frac{2\mu_A^2 \mu_B^2}{3kT r_{AB}^6} - \frac{\mu_A^2 \alpha_B}{r_{AB}^6} - \frac{\mu_B^2 \alpha_A}{r_{AB}^6} \quad (6.35)$$

As a result, we have the following expression:

$$kT \ln K_{AB} = \ln \left( \frac{10^3 L V r_{AB}^2}{V_f} \right) + \frac{1}{2} \ln \left( \frac{8\pi h^2}{m_{AB} kT} \right) - \frac{\epsilon - 1}{2\epsilon + 1} \left( \frac{\mu_A^2}{r_A^3} + \frac{\mu_B^2}{r_B^3} - \frac{\mu_{AB}^2}{r_{AB}^3} \right) + \frac{2\mu_A^2 \mu_B^2}{3kT r_{AB}^6} + \frac{\mu_A^2 \alpha_B}{r_{AB}^6} + \frac{\mu_B^2 \alpha_A}{r_{AB}^6} \quad (6.36)$$

The energy  $\Delta G_{\text{el}}$  can reach a value of  $-20$  kJ/mol. The experimentally observed rate constant is  $k_{\text{exp}} = K_{AB} k_c$ , where  $k_c$  is the rate constant of transformation of the pair A.B into the reaction products. During transformation the pair A.B with  $\mu_{AB}$  is transited to the transition state (A.B) $^\ddagger$  with  $\mu_{AB}^\ddagger$ . In the general case, the transition state has the different configuration than the equilibrium pair A.B, and  $\mu_{AB} \neq \mu_{AB}^\ddagger$ . The contribution of electrostatic repulsions to the formation of the transition state taking into account the equilibrium formation of the A.B pair is

$$\Delta G = G_{AB}^\ddagger - G_{A.B} = \frac{\epsilon - 1}{2\epsilon + 1} \left( \frac{\mu_{AB}}{r_{AB}^3} - \frac{\mu_{AB}^\ddagger}{r_{AB}^\ddagger{}^3} \right) \quad (6.37)$$

Correspondingly, the  $G_{AB}^*$  value determined from  $k_{\text{exp}}$  is

$$\Delta G_{\text{exp}}^* = \Delta G_o^* + \varphi \frac{\varepsilon - 1}{2\varepsilon + 1}; \quad \varphi = \frac{\mu_{AB}^2}{r_{AB}^3} - \frac{\mu_A^2}{r_A^3} - \frac{\mu_B^2}{r_B^3}. \quad (6.38)$$

According to this expression, a linear dependence of  $\log k$  on  $(1 - \varepsilon)/(2\varepsilon + 1)$  is observed very often. The measurements of  $k_{\text{exp}}$  at different temperatures makes it possible to divide (conventionally) the contribution of the electrostatic interaction to the activation entropy and enthalpy. Since  $\Delta S = (-dG/dT)$ , neglecting the contribution of the  $\varepsilon$  change with temperature to the temperature run of  $k_{\text{exp}}$ , we obtain

$$\Delta S_{\text{el}}^* = \frac{d\varphi}{dT} \frac{\varepsilon - 1}{2\varepsilon + 1} = \sigma \frac{\varepsilon - 1}{2\varepsilon + 1}, \quad (6.39)$$

because the potential  $j$ , as shown in experiment, changes linearly with the change in  $T$ :  $\varphi = \lambda + T\sigma$ . Then for  $\Delta H_{\text{el}}^*$  we have the expression

$$\Delta H_{\text{el}}^* = \lambda(\varepsilon - 1)/(2\varepsilon + 1) \quad (6.40)$$

The same expression is obtained for the activation energy. For hydrolysis of phthalyl chloride in aqueous-dioxane media,  $\lambda = 62.3$  kJ/mol,  $\sigma = 219.5$  J/(mol·K).

The transition state appeared from two polar particles can be considered in a different way, namely, as two interacting dipoles. The energy of interaction  $j$  of two dipoles with dipole moments  $\mu_A$  and  $\mu_B$  depends on the distance  $r$  between them, dielectric constant of the medium  $\varepsilon$ , and mutual orientation of dipoles

$$\varphi = -\frac{\mu_A \mu_B}{\varepsilon r_{AB}^3} F(\theta_A, \theta_B, \psi_{AB}) \quad (6.41)$$

where  $\theta_A$  and  $\theta_B$  are the slope angles of two polar axes of dipoles to the line connecting their centers, and  $\psi_{AB}$  is the angle between two planes each of which passes through the axis of the corresponding dipole and axis connecting their centers.

Depending on the  $F$  value, the potential  $\varphi$  changes from  $-2\mu_A\mu_B r_{AB}^{-3}$  to  $+2\mu_A\mu_B r_{AB}^{-3}$ . If  $\mu_A = \mu_B = 6 \cdot 10^{-48}$  C·m,  $r_{AB} = 4 \cdot 10^{-10}$  m, and  $\varepsilon = 80$ , then  $2\mu_A\mu_B r_{AB}^{-3} = 8.5$  kJ/mol.

Considering the transition state as the sum of interacting dipoles, we should expect that the following correlations are valid:

$$E = E_o + (\alpha\mu_A\mu_B/\varepsilon r_{AB}^3) \ln k = \ln k_o - \alpha\mu_A\mu_B/RT\varepsilon r_{AB}^3 \quad (6.42)$$

These correlations are often confirmed by experiment. For example, for the reaction of alkyl halides with amines (quaternary ammonium salts are formed), a linear increase in  $E$  is observed with increasing both the product  $\mu_A\mu_B$  and  $\varepsilon^{-1}$ . The plots of the type  $\Delta E \sim \Delta[(\varepsilon - 1)/(2\varepsilon + 1)]$  and  $\Delta E \sim \Delta(\varepsilon^{-1})$  at sufficiently high  $\varepsilon$  ( $\varepsilon > 3$ ) virtually coincide. Therefore, when based on experimental data only, we cannot distinguish these two models of transition state. Note that the transition state can be considered as a sum of two dipoles if the distance between polar groups exceeds their sizes. And vice versa, if polar groups in the transition state are very close, they can

be considered as one resulting dipole.

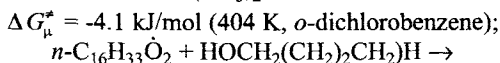
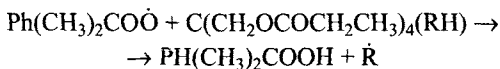
The transition state as an array of interacting dipoles manifests itself in reactions of polar polyfunctional compounds. A molecule of the polyfunctional compound with  $n$  polar groups represents, from the point of view of the electrostatic interaction, a semirigid carcass of atoms on which group-dipoles having a restricted freedom of rotation are mounted in certain sites. The distance between centers of the dipoles usually exceeds the length of the group-dipole. The dipoles interact with each other, and the interaction energy of each pair of dipoles  $i$  and  $j$  is described by expression (6.46). The total energy of interaction of all  $n$  dipoles  $U_n = 0.5 \sum U_{ij}$ . The dipoles are oriented in such a way that the energy of their interaction is minimum. The energy of dipole interaction is rather high. For example, in the bifunctional molecule with an interdipole distance of 0.3 nm and  $\mu_1 = \mu_2 = 6.7 \cdot 10^{-30}$  C·m  $U_{\min} = -18$  kJ/mol. When this molecule is attacked by a particle-dipole, the transition state is a multidipole consisting of  $n + 1$  dipoles. Naturally, the energy of dipole-dipole interaction in it, in the general case, differs from the energy of this interaction in the molecule. Therefore, the multidipole interaction contributes to the Gibbs activation energy

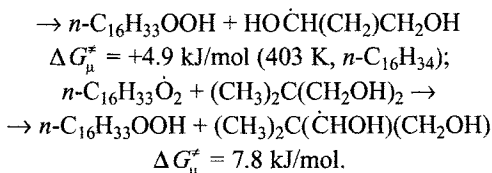
$$\Delta G_u^* = L (U_{n+1}^* - U_n) = \frac{L}{2\epsilon} \left( \sum_{ij}^{n+1} \frac{\mu_i \mu_j}{r_{ij}^3} F - \sum_{ij}^n \frac{\mu_i \mu_j}{r_{ij}^3} \right) \quad (6.43)$$

The contribution of the interaction of several dipoles to  $\Delta G^*$  can be estimated from experimental data by comparison of the rate constants of the same type reactions with structurally similar monofunctional ( $k_1$ ) and polyfunctional compounds if  $kn$  is attributed to one group ( $k_n/n$ )

$$\Delta G_\mu^* = RT \ln(nk_1/k_n) \quad (6.44)$$

Multidipole effect manifests itself in reactions of H abstraction from esters by peroxy radicals, reaction of  $RO_2\cdot$  addition at the double bond of unsaturated esters, reactions of  $O_2$  with the C—H bond and double bond of the corresponding esters, reactions of  $RO_2\cdot$  with polyatomic alcohols, and reactions of polyfunctional  $RO_2\cdot$  with phenols. The multidipole effect appears only when a polar particle attacks a polyfunctional molecule. For example, nonpolar  $\cdot CCl_3$  radicals attack with the almost equal rate constants the  $—CH_2OCOCH_2CH_3$  group in esters  $R_{4-n}C(CH_2OCOCH_2CH_3)_n$ ,  $n = 2, 3, 4$  [ $1/nk_n = 46$  l/(mol·s) at 373 K in  $CCl_4$ ]. The same result was obtained for the attack of the  $n$ -undecyl radical of *mono*-, *bi*-, and *tetra*-functional esters (373 K, PhCl). For the attack with polar  $RO_2\cdot$  ( $\mu \approx 8 \cdot 10^{-30}$  C·m) of esters and polyatomic alcohols, the multidipole effect is manifested, which is seen from the following examples:





Since the activation energy of the reaction of  $\text{RO}_2\cdot$  with the C—H bond is equal to 25–50 kJ/mol, the contribution of the multidipole interaction to the activation barrier is considerable and can either increase or decrease this barrier. Below we present the results of studying the addition reactions of  $\text{RO}_2\cdot$ ,  $\text{ROOH}$ , and  $\text{O}_2$  at the double bond of mono- and polyfunctional unsaturated (acrylate) esters.

Reactant	$\text{RO}_2$ (styrene)	$\text{RO}_2$ (acrylate)	$\text{Ph}(\text{CH}_3)_2\text{COOH}$	$\text{O}_2$
$T, \text{K}$ .....	323	323	343	343
$k, \text{l}/(\text{mol}\cdot\text{s})$ .....	101	0.8	$2.4\cdot 10^{-6}$	$4\cdot 10^{-10}$
$\Delta H^{\circ}, \text{kJ/mol}$ .....	-46	-	30	130
$\Delta G_{\mu}^{\circ}, \text{kJ/mol}$ .....	0.5	1.5	5.6	13.8

As can be seen, the higher  $\Delta H^{\circ}$ , i.e., the more endothermic the process, the higher the contribution of the dipole-dipole interaction to  $\Delta G^{\ddagger}$ . It is most likely that this is related to the fact that the more endothermic the reaction, the closer the structure of the transition state to that of the final product, which is polar in nature, and the higher the energy of interaction of the dipole of the attacking particle with other dipoles.

Note that the description of the interaction of the polar particle with the medium (also polar molecules) as a continuum with the dielectric constant  $\epsilon$  is a great simplification. Each polar particle is surrounded by solvent molecules and interact with them as with dipoles due to orientation forces to induce their polarization, interact due to dispersion forces and often form molecular complexes due to hydrogen bonds or donor-acceptor interaction. As a whole, the solvation of one particle or a pair of reacting particles appears. This solvation makes the corresponding contribution to  $\Delta G^{\ddagger}$ , positive or negative. Since the configuration of the transition state differs, as a rule, from the mutual orientation of particles in the equilibrium state, the transition  $\text{A.B} \rightarrow (\text{A.B})^{\ddagger}$  should be accompanied by the reorganization of solvent molecules forming the walls of the cage, i.e., the first coordination sphere of the A.B pair. This reorganization includes a change in the average radius of the solvate shell, coordination number, symmetry of arrangement of molecules creating the solvate shell, orientation of molecule-dipoles, values of the induction-induced dipoles, and energy of the dispersion interaction between A.B and nearest molecule-neighbors. Each of the listed types of reorganization is characterized by its relaxation time.

How rapidly does the rearrangement of the solvate shell occur compared to the elementary act time? The latter, according to the transition state theory, occurs for the

time  $kT/h \approx 10^{-13}$  s. 1. The average radius of the solvate shell changes, most likely, for the time comparable with that of vibrations of a molecule ( $10^{-13}$  s) for nonviscous liquids at room temperature (see Chapter 5). 2. The change in the coordination number of solvent molecules around the A.B pair is comparable, most likely, with the time of existence of a particle in the cage, i.e., it is  $10^{-10} \div 10^{-11}$  s. 3. The period of retaining symmetry of molecules that form the cage lies, most likely, between  $\tau_{(1)}$  and  $\tau_{(2)}$ , i.e., of an order of  $10^{-12}$  s. 4. The time of the rotational relaxation of a dipole in liquid is  $10^{-10} \div 10^{-11}$  s. 5. The induction polarization of solvent molecules occurs due to the displacement of the electron density very rapidly, within  $10^{-16} \div 10^{-15}$  s. 6. Dispersion interaction occurs also so rapidly. Thus, different interactions of molecules in solution occur with different rates covering the range from  $10^{-10}$  to  $10^{-15}$  s. Electron polarization occurs very promptly, a change in the position of molecules surrounding a pair of particles is comparable with the elementary act, all spheres are rearranged very slowly, and molecular complexes decompose slowly, for example, the complex formed by the hydrogen bond lives for  $10^{-8} \div 10^{-10}$  s. Each type of the interaction contributes to the solvation energy of the transition state, so that we can write

$$\Delta G^\ddagger = \Delta G_{\text{or}}^\ddagger + \Delta G_{\text{ind}}^\ddagger + \Delta G_{\text{disp}}^\ddagger \quad (6.45)$$

where the first, second, and third terms characterize the contributions of the orientation, induction, and dispersion interactions, respectively.

In nonpolar solvents  $\Delta G_{\text{or}}^\ddagger = 0$ , and in polar solvent  $\Delta G_{\text{or}}^\ddagger$  makes the main contribution to the solvation of the polar transition state. The dependence of  $\ln k$  on  $(\epsilon - 1)(2\epsilon + 1)^{-1}$  is related to  $\Delta G_{\text{or}}^\ddagger$ , whereas the dependence of  $\ln k$  on  $(n^2 - 1)(2n^2 + 1)$ , where  $n$  is the refractive index, is related to  $\Delta G_{\text{ind}}^\ddagger + \Delta G_{\text{disp}}^\ddagger$ . In the entire form the dependence of  $\Delta G_{\text{solv}}^\ddagger$  is expressed by the formula

$$\Delta G_{\text{solv}}^\ddagger = a \frac{\epsilon - 1}{2\epsilon + 1} + b \frac{n^2 - 1}{2n^2 + 1} \quad (6.46)$$

where  $a$  and  $b$  are related to  $\mu_A$ ,  $\mu_B$ ,  $\mu^\ddagger$ , and  $r_A$ ,  $r_B$ ,  $r^\ddagger$ .

Activation preceding the reaction influences both the reacting A and B particles and solvate shell, and the elementary act in liquid is a cooperative process to a great extent.

Such parameters of the solvent as  $\epsilon$  and refractive index  $n$  do not always allow the explanation and description of the empirical influence of the solvent on the chemical reaction rate. Therefore, several functions were proposed for such a purely empirical description (correlation).

E. Grunwald and S. Winstein proposed (1948) to characterize the solvent by its ionizing strength  $Y = \log(k/k_0)$ , where  $k$  and  $k_0$  are the rate constants of solvolysis of  $(\text{CH}_3)_3\text{CCl}$  in a given solvent and in 80%  $\text{C}_2\text{H}_5\text{OH}$  at 298 K. The dependence of  $k$  of any reaction on  $Y$  has the form

$$\log k = \log k_0 + mY \quad (6.47)$$

where  $m$  characterizes the effect of solvents on the given reaction as compared to the effect of *tert*-butyl chloride on solvolysis. In essence, this is the interrelation between  $\log k$  of the reaction under study and solvolysis of  $(\text{CH}_3)_3\text{CCl}$  in the chosen series of solvents. The ionizing strength of the solvent changes nonlinearly with its polarity expressed through  $(\epsilon - 1)(2\epsilon + 1)^{-1}$ .

The  $Y$  function is convenient for the description of the solvent effect on solvolytic reactions.

### 6.5. Reactions of ions

Compounds with the ionic bond (salts) that form in the solid state the ion crystalline lattice dissociate to ions. Being dissolved, acids and bases undergo complete or partial dissociation where a noticeable chemical interaction of ions with solvents occurs. Each ion in the solvent, e.g., in water, is surrounded by the dense solvate shell of polar molecules. This shell appears due to the ion-dipole interaction. Solvation is manifested, first, in that the dissolution of a salt in  $\text{H}_2\text{O}$  is accompanied by a decrease in the volume and, second, liberation of a great amount of heat. This is seen from the  $\Delta H$  values where the ion from the gas phase is transferred to an aqueous solution ( $\Delta H_{\text{Li}^+} = \Delta H_{\text{F}^-}$ ,  $\Delta H$  in kJ/mol)

	$\text{H}^+$	$\text{Li}^+$	$\text{Na}^+$	$\text{Mg}^{2+}$	$\text{Zn}^{2+}$	$\text{Cl}^-$	$\text{Br}^-$	$\text{OH}^-$
$\Delta H, \dots$	1070	512	399	1952	2057	374	341	399

The strong interaction of the ion with the solvent is reflected all physicochemical properties of solutions of electrolytes. The classical electrostatic theory considers the  $i$ -th ion as a sphere with the radius  $r_i$  with the charge  $z_i e$  and the solvent as a medium with the dielectric constant  $\epsilon = \epsilon_0 \exp(-L_e T)$ .

In this simplified approach, the electrostatic components of the  $G$ ,  $H$ , and  $S$  functions are the following ( $e$  is the charge of an electron):

$$G_e = Le^2 z_i^2 / 2\epsilon r_i, \quad H_e = \frac{Le^2 z_i^2}{2\epsilon r_i} (1 - L_e T), \quad S_e = \frac{Le^2 z_i^2 L_e}{2\epsilon r_i} \quad (6.48)$$

Since many ions are present in a solution and they interact, this reflects both the ion distribution in the solution and their thermodynamic characteristics.

The reaction between two ions A and B is preceded by their encounter in a solution. If the reaction is not limited by encounter acts, then the experimentally observed rate constant  $k_{\text{exp}} = K_{\text{AB}} k_c$ , where  $K_{\text{AB}}$  is the equilibrium constant of ion pair formation. It depends on the properties of both ions (charge, sizes) and medium ( $\epsilon$ , ion

strength  $I$ ). Comparing  $K_{AB}$  in two solvents with  $\epsilon_0(K_{AB}^0)$  and  $\epsilon(K_{AB})$  and taking into account the effect of the ion strength of the solution according to the Debye-Hückel theory, for  $k_{exp}$  we obtain the expression

$$\ln k_{exp} = \ln k_c + \ln K_{AB}^0 + \frac{z_A z_B e^2}{kTr_{AB}} (\epsilon_0^{-1} - \epsilon^{-1}) + \frac{z_A z_B e^2 I^{1/2} (kT)^{-1}}{1 + r_{AB} I^{1/2}} \quad (6.49)$$

For  $K_{AB}^0$  Bjerrum obtained the following expression:

$$K_{AB}^0 = 4 \cdot 10^{-3} \pi L \left( \frac{|z_A z_B| e^2}{\epsilon_0 kT} \right) \int_2^b \frac{e^x}{x^4} dx, \quad (6.50)$$

where  $b = |z_A z_B| e^2 / \epsilon_0 kTr_{AB}$ , and  $r_{AB}$  is the distance between atoms at their tight contact.

Two important sequences follow from (6.55). First, the rate constant of the ion reaction depends on the ionic strength of the solution and in dilute solution where  $I^{1/2} r_{AB} \ll 1$ ,  $\Delta \ln k_{exp} \sim I^{1/2}$ , which is confirmed by a large experimental material. In the case of the reaction of likely charged ions, the slope of  $\Delta \ln k / \Delta(I^{1/2})$  is positive (the ion atmosphere facilitates the reaction); in the case of the reaction between unlike ions, this slope is negative, and the higher the product of charges  $z_A z_B$ , the higher the absolute value of the tangent slope. Deviations due to specific features of reaction mechanisms are often observed. Second,  $k_{exp}$  depends on  $\epsilon$  in such a way that  $\Delta \ln k_{exp} \sim \Delta(\epsilon^{-1})$ . In this case, the higher the product  $|z_A z_B|$ , the greater the slope; for like charges the slope is negative, and for the unlike ions, the slope is positive.

It is reasonable to consider the problem about the equilibrium concentration of ion pairs in a solution from the point of view of changing the thermodynamic functions  $\Delta G$ ,  $\Delta S$ , and  $\Delta H$ . Since dispersion and electrostatic forces act between ions, and the latter depend on the polarity of the medium and concentrations of other ions expressed through the ion strength, the equilibrium constant of ion association can be presented in the form

$$K_{AB} = K_{AB}^0 \exp(-\Delta G_e / RT) \exp(-\Delta G_l / RT)$$

where

$$\Delta G_e = \frac{2L z_A z_B e^2}{r_{AB}} \left( \frac{1}{\epsilon} - \frac{1}{\epsilon_0} \right), \quad \Delta G_l = -\frac{2L z_A z_B e^2}{\epsilon} \left( \frac{2\pi L I}{10\epsilon} \right) \quad (6.51)$$

Correspondingly, for the components of enthalpy we obtain

$$\begin{aligned} \Delta H_e &= \frac{d(\Delta G_e / T)}{d(1/T)} = \frac{L z_A z_B e^2}{r_{AB}} \left( \frac{1}{\epsilon} - \frac{1}{\epsilon_0} \right) \times \\ &\quad \times \left[ 1 + \frac{1}{3} \frac{d \ln V}{d \ln T} - \frac{d \ln(\epsilon^{-1} - \epsilon_0^{-1})}{d \ln T} \right], \\ \Delta H_l &= -\frac{L z_A z_B e^2}{\epsilon} \left( \frac{8\pi L I}{10^3 \epsilon} \right)^{1/2} \left[ 1 + \frac{3}{2} \frac{d \ln V}{d \ln T} - \frac{1}{2} \frac{d \ln I}{d \ln T} \right] \end{aligned} \quad (6.52)$$

For the activation energy, which is determined from experimental data  $E_a = RT(d \ln k / d \ln T)$ , we have the expression [see equation (6.18)]

$$E_a = E + E_V' - 3/2RT + \Delta H_{AB}^0 + \Delta H_\epsilon + \Delta H_I - RT \frac{d \ln n}{d \ln T} \quad (6.53)$$

For the entropy contributions to ion association we obtain ( $S = -dG/dT$  at  $p = \text{const}$ )

$$\Delta S_\epsilon = \frac{Lz_A z_B e^3}{r_{AB} \epsilon} \frac{d \ln \epsilon}{dT} + \frac{1}{3} \frac{d \ln V}{dT} \left( 1 - \frac{\epsilon}{\epsilon_0} \right) \quad (6.54)$$

$$\Delta S_I = \frac{Lz_A z_B e^3}{\epsilon} \left( \frac{8\pi L I}{10^3 \epsilon} \right)^{1/2} \left( \frac{3}{2} \frac{d \ln \epsilon}{dT} - \frac{1}{2} \frac{d \ln V}{dT} \right) \quad (6.55)$$

According to this, the pre-exponential factor

$$A_{\text{exp}} = A_{AB}^0 \frac{kT}{h} \exp(\Delta S/R) \exp[(\Delta S_\epsilon + \Delta S_I)/R] \quad (6.56)$$

When the A ion reacts with the B molecule, the equilibrium association constant has the form

$$\ln K_{AB} = \ell n K_{AB}^0 + \frac{Lz_A^2 e^2}{2 \cdot 10^3 kT} \left( \frac{1}{\epsilon} - \frac{1}{\epsilon_0} \right) \left( \frac{1}{r_A} - \frac{1}{r_{AB}} \right) - \frac{L \cdot 10^{-3} \mu_B^2}{kT} \frac{\epsilon - 1}{r_B^3 2\epsilon - 1} \quad (6.57)$$

The considered above electrostatic models of ion interaction are, undoubtedly, simplified. Each ion is surrounded by the solvate shell, whose character and sizes are determined by the ion, its charge and radius, and sizes of solvent molecules and such their parameters as the dipole moment of their polar groups, structure and sizes of the molecule. The solvent, its solvating ability, and the influence on the ion interaction are not reduced to the medium with the dielectric constant  $\epsilon$  only. Similarly, the interaction of ions is not restricted by the formation of only the ion atmosphere: ion pairs, triples, and associates of several ions appear in the solution. Ion pairs, which can be separated by the solvate shell or be in contact to form contact pairs, also differ in structure. As a whole, the situation is more complex and diverse than its description by the classical theory of interaction of spherical charges in the liquid medium of dielectrics. The solvating ability of the solvent is determined only in part by its dielectric constant. For aprotic solvents, the ability of their heteroatoms to be donors of a free pair of electrons for cations is very significant. The donating ability of the solvent is characterized by its donor number DN, which for the solvent is equal to the enthalpy of its interaction with  $\text{SbCl}_5$  in a solution of 1,2-dichloroethane

	$\text{CH}_3\text{NO}_2$	$\text{C}_6\text{H}_5\text{NO}_2$	$\text{CH}_3\text{CN}$	$\text{CH}_3\text{COCH}_3$	$(\text{CH}_3)_2\text{SO}$	$\text{C}_5\text{H}_5\text{N}$
DN.....	2.7	4.4	14	17	30	33

In protic solvents, the ability of the solvent to form hydrogen bonds is important in ion solvation. In mixed solvents an ion forms a set of solvates with various compositions.

### 6.6. Correlation equations in chemical kinetics

The question about the relation between the reactivity of reactants and their structure is one of the fundamental problems of chemistry. This problem as one of the main directions of chemical kinetics was formulated in the general form about 100 years ago by N.A. Menshutkin in his works on hydrolysis of esters. One of the most important directions in this area is correlation equations relating the reaction rate constant to thermodynamic and structural parameters of reactants. The first correlation was proposed by Ch. Taylor (1914) who noticed a proportionality between the ionization rate constant of the catalyst and rate constant of the catalyzed reaction. The systematic work on correlations in chemical kinetics started from the works of J. Brönsted and K. Pedersen who, using the results of their study of the reactions catalyzed by acids ( $k_{\text{HA}}$ ) and bases ( $k_{\text{A}}$ ), proposed the equations relating the rate constants of catalytic reactions to the dissociation constants of acids  $k_{\text{HA}}$  (1924)

$$k_{\text{HA}}/p = G(K_{\text{HA}}q/p)^{\alpha}, \quad k_{\text{A}}/q = G(K_{\text{HA}}q/p)^{\beta} \quad (6.58)$$

where  $p$  and  $q$  are the number of equivalent protons in acid HA and the number of equivalent charges in conjugated base  $\text{A}^-$ ;  $\alpha$ ,  $\beta$ , and  $G$  are empirical constants.

Based on a large experimental material, L. Hammett in 1937 proposed the known  $\rho\sigma$ -equation relating the rate constant of the reaction of an aromatic compound to the dissociation constant of the corresponding benzoic acid. A year later, M. Evans and M. Polanyi derived the empirical correlation  $\Delta E = \alpha\Delta H$  for the reaction of sodium atoms with alkyl halides. In 1954 N. N. Semenov considered and showed the applicability of this correlation to many reaction of radical abstraction. Simultaneously (1952-1953) R. Taft advanced a postulate about the additive influence of structural factors. A diverse experimental material on various reactions of aromatic and aliphatic compounds and application of the Hammett, Taft, and Polanyi-Semenov equations to them was obtained in fifties-seventies.

A relation between the activation energy  $E$  and  $\Delta H$  of the reaction is rather evident when the reaction is endothermic ( $\Delta H > 0$ ). In this case, always  $E \geq \Delta H$  and the stronger the cleaved bond in the reactant, the higher  $E$  and the lower the reactivity of compounds estimated either through  $k$  or through  $\Delta G^\ddagger$ . The Polanyi-Semenov correlation is very often fulfilled for exothermic reactions:  $E = A - \alpha q$ . A diverse experimental material on activation energies of radical reactions showed that for different

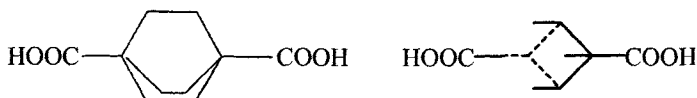
types of reactions the coefficients  $A$  and  $\alpha$  are different. These data are considered in more detail in Chapter 9.

The role of polar effects, among which the inductive, field, and conjugation effects are distinguished, is very important in reactions of ions and polar molecules. Polar groups appear because atoms of elements differ in electronegativity and upon the formation of the A—B bond the electron density of the bond-forming electron pair is shifted toward a more electronegative atom. Inductive effect is that the polar group acts on the nearest  $s$ -bonds to shift the electron density at the adjacent groups. The polar character of the bond can be concluded by its dipole moment, which also depends on the bond length.

Bond	C—O	C=O	C—F	C—Cl	C—Br	C—I
$\mu \cdot 10^{30}$ , C.m.....	3.6	8.2	6.0	6.8	6.7	5.9

The inductive effect  $I$  is transmitted along the system of  $s$ -bonds of molecules and decays according to the approximately exponential law:  $I^1 \sim z^n$ , where  $z$  is the conductivity coefficient, and  $n$  is the number of groups separating the polar group and the bond under consideration. For example, for the  $\text{CH}_2$  group  $z = 0.36$  and the inductive effect, which propagates over the C—C bonds, in the  $\gamma$ -position is proportional to  $0.36^3 = 0.046$ , i.e., lower than 5%. The fast decay of the inductive effect is associated with the weak polarizability of orbitals of  $\sigma$ -bonds.

The influence of the polar or electric charge-bearing group is transmitted to another group or reaction center of the transition state and directly through the space. This is the so-called *field effect*. When the acting group is a dipole, the action energy is determined by the dipole moment, distance, and orientation of the dipole ( $I$ -effect  $\sim \cos\theta/r^2$ ). The polar effect in aliphatic compounds is transmitted by two ways: along the system of  $\sigma$ -bonds and directly through the space. Two these methods were compared by the comparison of calculation and experiment using as an example the dissociation of dibasic acids with the structure



The comparison showed that the field effect prevailed. It is most likely that this takes place when the groups are separated by more than one C—C bond.

Another effect, which affects strongly the reactivity, is *conjugation effect*. The interaction between the bonds and groups occurs due to overlapping of  $n$ - and  $p$ -orbitals in a molecule containing  $\pi$ -bonds of heteroatoms with unshared pairs of  $p$ -electrons. The conjugation is especially pronounced in the influence of  $p$ -bonds on the strength of  $s$ -bonds in the  $\alpha$ -position. For example, in the methyl group of propane  $D_{\text{C-H}} = 422$  kJ/mol, in the  $\text{CH}_3$  group of propylene  $D_{\text{C-H}} = 368$ , and in toluene  $D_{\text{C-H}} = 375$  kJ/mol. This great difference is a result of the conjugation of an

unpaired electron of the  $\text{CH}_2$  group of the allyl and benzyl radical with  $\pi$ -electrons of the double bond and benzene ring, respectively. The conjugation effect also affects the values of dipole moments due to a high polarizability of  $p$ -orbitals. For example, for  $\text{CH}_3\text{NO}_2$   $m = 12 \cdot 10^{-30}$ , and for  $\text{PhNO}_2$   $\mu = 14 \cdot 10^{-30} \text{ C} \cdot \text{m}$  (gas phase). The higher dipole moment for nitrobenzene is resulted by the conjugation of  $p$ -electrons of the aromatic ring with the nitro group.

The accessibility of the molecular fragment, which is attacked and transformed, is very significant for bimolecular reactions. The degree of accessibility often depends on the fact whether bulky substituents are present near the reaction center or not. The presence of these substituents creates steric hindrances for the reaction. For example, phenols form associates due to the hydrogen bond of the  $\text{O} \cdots \text{H} \cdots \text{O}$  type but when the phenol molecule contains two *tert*-alkyl groups in the ortho-position, this prevents the formation of a molecular complex through the hydrogen bond.

Various linear correlations are widely used for the quantitative comparison of the kinetic characteristics with the structure of molecules and their thermodynamic parameters. Linear correlations are based on the linear correlation of free energies. This principle is the following. When one fragment is systematically replaced in the reactant structure by this or other substituent, the proportionality of the type  $\Delta G_2^* \sim \Delta G_1^*$  and  $\Delta G_2^* \sim \Delta G_1^*$  is observed, where 1 and 2 are indices of the corresponding reaction series. Formally the principle looks as follows. Let molecules  $\text{R}-\text{Y}-\text{X}$  and  $\text{H}-\text{Y}-\text{X}$ , where X is the reaction center, enter into the same reaction, which is designated by index 1. The reaction of each reactant is characterized by its change in the Gibbs energy; the difference in these energies  $\Delta G_1(\text{R}) - \Delta G_1(\text{H}) = \delta_{\text{R}}\Delta G_1$ . The same correlation is valid for another reaction with index 2. If this reaction is irreversible, then  $\delta_{\text{R}}\Delta G_2 = \Delta G_2(\text{R}) - \Delta G_2(\text{H})$ . The principle of linear correlation of free energies is fulfilled if the following correlation is valid:

$$\delta_{\text{R}}\Delta G_2 = \alpha \delta_{\text{R}}\Delta G_1 \quad (6.59)$$

Going from DG to the equilibrium constant and from DG# to the reaction rate constant, we obtain

$$\log(k_{\text{R}}/k_{\text{H}})_2 = \alpha \log(K_{\text{R}}/K_{\text{H}})_1 \quad (6.60)$$

Linear correlations of this type are very popular, and their use allowed a large experimental material on various reactions in solutions to be systematized. The Hammett equation is widely used for reactions of aromatic compounds

$$\log(k/k_0) = \rho\sigma \quad (6.61)$$

where  $k$  and  $k_0$  are the rate constants of the reactions of substituted and unsubstituted aromatic compounds;  $\sigma = \log(K/K_0)$ ;  $K$  and  $K_0$  are the dissociation constants of substituted and unsubstituted benzoic acids in water at 298 K.

The equation is valid for benzene derivatives with substituents in the *para*- and

*meta*-positions to the reaction center. The coefficient  $r$  characterizes the influence of the substituent on a certain reaction series. The polar substituent has the inductive effect plus conjugation effect on the reaction center if the substituent contains  $\pi$ -bonds or an atom with a lone pair of  $p$ -electrons (N, O, etc.). If the reaction is the attack of an ion with the charge  $z_A$  at a molecule with the substituent X with the dipole moment  $\mu_X$ , then in the framework of the electrostatic model

$$2.3\sigma = \frac{\mu_X e \cos\theta_i}{298 k \epsilon_{H_2O} r_i^2} \text{ and } 2.3\rho\sigma = -\frac{z_A e \mu_X \cos\theta}{k T r_\#^2 \epsilon} \quad (6.62)$$

where  $r_i$  and  $r_\#$  are the radii of the ion of substituted benzoic acid and transition state, respectively.

It is seen from this that  $\rho$  depends on both the temperature ( $\rho \sim 298/T$ ) and solvent ( $\epsilon$ ).

The following functions are also used for reactions of aromatic compounds.

1.  $\sigma^H$  is the standard Hammett constant,  $\sigma^H = \sigma$  for substituents *m*-CH<sub>3</sub>, *m*-Cl, *m*-I, *m*-COCH<sub>3</sub>, *m*-NO<sub>2</sub>, *p*-COCH<sub>3</sub>, and *p*-NO<sub>2</sub>, and for other substituents  $s$  is determined from reaction series. The constants  $\sigma^H$  reflect the inductive effect only, they do not take into account the conjugation effect.

2.  $\sigma^+$  is the Brown constants,  $\sigma^+ = \rho_o^{-1} \log(k_X/k_o)$ , where  $\rho_o^{-1} = -4.54$ , and  $k_o$  and  $k_X$  are the rate constants of solvolysis of nonsubstituted and substituted cumyl chloride in a mixture of 90% acetone + 10% water at 298 K.

3.  $\sigma^- = \log(K_o/K_X)$ , where  $K_o$  and  $K_X$  are the constants of acid dissociation of non-substituted and substituted phenol in water at 298 K.

4.  $\sigma^o = \rho_o^{-1} \log(K_o/K_X)$ , where  $\rho_o = 0.46$ , and  $K_o$  and  $K_X$  are the dissociation constants of nonsubstituted and substituted phenylacetic acids in water at 298 K.

The Taft constant  $\sigma^*$  is used for reactions of aliphatic compounds

$$\sigma^* = \frac{1}{2.48} \left[ \log \left( \frac{k_B}{k_{AH}} \right) - \log \left( \frac{k_{0B}}{k_{0AH}} \right) \right] \quad (6.63)$$

where  $k_{HA}$  and  $k_B$  are the rate constants of acid and base hydrolysis of esters of substituted acetic acids  $XCH_2COOR$ ; constants with index "zero" correspond to  $X = H$ .

The dependence has the form  $\log(k_X/k_o) = \rho^* \sigma^*$ . Later this equation was modified. Taft introduced the principle of additivity of the influence of different factors on the reactivity of a compound: each factor, being it inductive, conjugation or steric, affects  $\Delta G^\ddagger$  independently, so that for each reaction series  $\log(k/k_o)$  or  $\log(K/K_o)$  can be presented as the sum  $\sum \rho_i \sigma_i$ , where  $\sigma_i$  reflects the contribution to a change in  $\Delta G^\ddagger$  of the corresponding factor related to the substituent. For aliphatic compounds the Taft equation has the form

$$\log(k/k_o) = \rho_I \sigma_I + \rho_s E_s \quad (6.64)$$

Here  $\sigma_I$  characterizes the inductive effect of the substituent:  $\sigma_I = 0.276 \log(K/K_o)$  ( $K$  and  $K_o$  are the dissociation constants of  $XCH_2COOH$  and  $CH_3COOH$  in  $H_2O$  at 298 K),  $\sigma_I = 0.45 \sigma^*$ . The constant  $E_s$  characterizes the steric factor,  $E_s = \log(k_{AH}/k_{oAH})$ , as in the case of  $\sigma^*$ ;  $k_{AH}$  and  $k_{oAH}$  are the rate constants of acid

hydrolysis of  $\text{XCH}_2\text{COOR}$  and  $\text{CH}_3\text{COOH}$ , respectively.

A series of multiparametric equations was proposed to characterize the reactivity of aromatic compounds, one of them has the form

$$\log(k/k_0) = \rho_I \sigma_I + \rho_R \sigma_R^\circ + \rho_s E_s \quad (6.65)$$

where  $\sigma_I$  is the inductive constant;  $E_s$  reflects the steric influence (see above);  $\rho_R$  is the resonance constant, which is determined as follows:  $\sigma_R^\circ = 2.17 \log(K/K_0)$ , where  $K$  and  $K_0$  are the dissociation constants of substituted  $\text{XC}_6\text{H}_4\text{COOH}$  and nonsubstituted phenylacetic acids ( $\text{H}_2\text{O}$ , 298 K).

The constant  $\sigma_R^\circ$  reflects the resonance effect of a substituent, it is calculated from the following equations: for *para*-substituents  $\sigma_R^\circ = 1.14\sigma_I - \sigma$  and  $\sigma_R^\circ = 2.63(\sigma - \sigma_I)$  for *meta*-substituents,  $\sigma$  is the Hammett function.

The principle of linear correlation of free energies is fulfilled rather often but not always. It must be fulfilled when the following conditions satisfy. 1. When one-stage equilibrium reactions ( $\text{XCH}_2\text{COOH} \rightleftharpoons \text{XCH}_2\text{CO}_2^- + \text{ROH}$ ) or irreversible reactions ( $\text{XCH}_2\text{COOR} + \text{OH}^- \rightarrow \text{XCH}_2\text{COO}^- + \text{ROH}$ ) are compared. Complex multistage processes including various equilibria may also obey the correlations but such correlations are often random: breaks in the  $\log k - \sigma$  plot are observed *etc.* 2. When the reactions centers of the reaction under study and those of the correlation used are close. For example, the correlation of  $\log k$  with  $\sigma$  (for aromatic) and  $\sigma_I$  (for aliphatic compounds) is suitable for acid hydrolysis. 3. When substituents in the reaction series are selected in such a way that they affect the reaction center by the same mechanism, for example, inductive, or create only steric hindrances, *etc.* 4. When reaction conditions (solvent, temperature) in two compared reaction series are identical or close. Coefficients  $\rho$  are often used to substantiate the reaction mechanism. Since  $\rho$  depends on the conditions and in the multistage reaction it also depends on the mechanism and similarity factors may be between reaction centers different in structure, arguments of this kind are always doubtful.

The linear correlation of free energies results in the linear correlation of activation energies if one of two conditions is fulfilled: in the considered reaction series all pre-exponential factors are equal ( $A_i = A = \text{const}$ ) and then  $\log(k/k_0) = (E_0 - E)/2.3RT$ , or  $\Delta \log A_i \sim \Delta E_i$ .

In the framework of the transition state theory, the following proportionality corresponds to the linear dependence  $\Delta \log k_i \sim \Delta E_i^\ddagger$ :

$$\delta_R \Delta G^\ddagger = (\beta - T) \delta_R \Delta S^\ddagger \quad (6.66)$$

It should be kept in mind that this effect appears as a result of errors in the measurement of  $E$ . If the true activation energy is  $E_0$  and it was determined as  $E$ , then since  $\log A$  is calculated as  $\log A = \log k + E/2.3RT$ , the overestimation of  $\log A$  by a value of  $\Delta E/2.3RT$  corresponds to the increase in  $E$  by  $\Delta E = E - E_0$ . For  $\Delta E = 6$  kJ/mol  $\Delta \log A = 1.05$  at 300 K. Therefore, the variation of  $A$  within one—two orders

in one reaction series can result in errors in the measurement of  $E$ . However, there are many examples that  $\log A$  changes in wider limits: for the solvolysis of substituted benzoyl chlorides, e.g.,  $A$  changes in an interval of 15 orders of magnitude.

The compensation effect is absent from gas-phase reactions of atoms and radicals with molecules, it is not either observed for radical reactions in solutions when one of two reactants is a nonpolar particle. One of the sources of this effect is the influence of the medium on the elementary act of polar particles. The rate constant of bimolecular reaction in a solution depends on the association constant of particles  $K_{AB}$ , amplitude of vibrations of particles  $a \sim V_f^{1/3}$ , and dielectric constant  $\epsilon$ . All these values are temperature-dependent, which contributes to the experimentally determined activation energy and create the compensation effect (see Sections 8.2 and 8.4). Another source of the effect is a complex mechanism of the reaction and the dependence of its observed rate constant of various equilibria into which reactant-molecules enter.

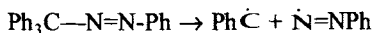
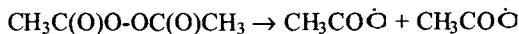
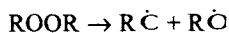
## Radical reactions

### 7.1. Decomposition of molecules to radicals

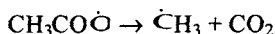
Many organic molecules are stable in the liquid state and decompose to radicals only in the gas phase. Their decomposition occurs often as chain reactions (see Chapter 10). A restricted scope of compounds decompose with a noticeable rate in the liquid phase. They are compounds with rather weak O—O, C—N, and S—S bonds. The decomposition of such compounds as peroxides and azo compounds, which are widely used in technology and research practice as initiators of chain liquid-phase reactions, was studied in detail. Using these compounds, the following three mechanisms of molecule decomposition were found and studied: decomposition with the cleavage of one bond, concerted decomposition with the cleavage of several bonds, and decomposition with chimerical interaction.

#### 7.1.1. Decomposition of molecules with cleavage of one bond

In this case, an excess of vibrational energy in a molecule is concentrated at one of the weakest bonds, and the latter is decomposed to two radicals. Hydrocarbons, dialkyl peroxides, many diacyl peroxides, peresters, and some oxo compounds decompose in such a way



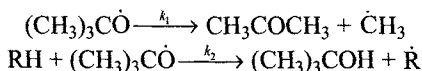
The radicals that formed can undergo further fragmentation, for example,



In this case, the successive (stepped) fragmentation of a molecule to radicals occurs or the so-called nonconcerted decomposition at several bonds.

The nonconcerted decomposition of molecules to several fragments is characterized by the following features.

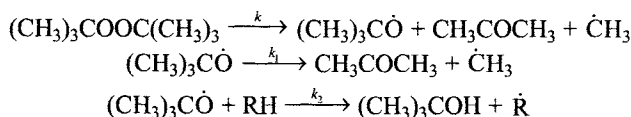
1. A certain dependence of the composition of products on the concentration of a free radical acceptor. For example, the decomposition of *tert*-butyl peroxide afford as primary product two *tert*-butoxy radicals, each of which enters into one of two possible reactions (RH is considered as an acceptor of RO $\cdot$  radicals)



The following linear kinetic correlation is fulfilled for this mechanism of alcohol and acetone formation:

$$\frac{[\text{CH}_3\text{COCH}_3]}{[(\text{CH}_3)_3\text{COH}]} = \frac{k_1}{k_2} [\text{RH}]^{-1} \quad (7.1)$$

If this peroxide decomposes according to the mechanism of concerted decomposition, we would deal with the following mechanism of the formation of alcohol and acetone:



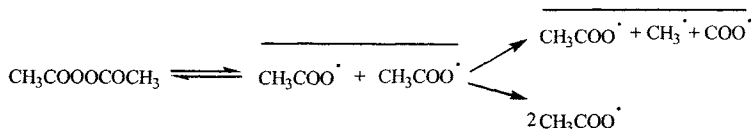
and

$$\frac{[\text{CH}_3\text{COCH}_3]}{[(\text{CH}_3)_3\text{COH}]} = 1 + 2 \frac{k_1}{k_2} [\text{RH}]^{-1} \quad (7.2)$$

*i.e.*, this dependence would be nonlinear.

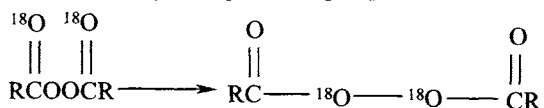
2. For the cleavage of one bond, the volume of the activated complex is larger than that of the initial molecule and, hence, an increase in pressure retards this decomposition (see below). The opposite situation is observed for the concerted decomposition of two bonds.

3. If the molecule is decomposed with the cleavage of only one bond, a portion of free radicals formed in the cage recombines to form the initial molecule, for example,



In these cases, first, the decomposition rate constant depends on the solvent vis-

cosity (the higher the viscosity, the lower the observed decomposition rate constant). Second, an optically active compound is partially racemized at its incomplete decomposition. When diacyl peroxides labeled by  $^{18}\text{O}$  at the carbonyl group,  $^{18}\text{O}$  is partially transferred from the carbonyl into peroxide group

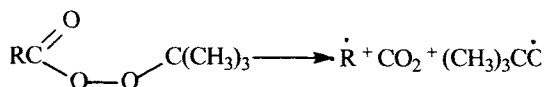


4. The activation energy of decomposition with the cleavage of one bond is equal to the energy of this bond cleavage, and the pre-exponential factor is not lower than  $10^{13} \text{ s}^{-1}$ . In the case where one O—O bond is cleaved,  $\Delta H^\ddagger \approx \Delta H^\circ$ . The different picture is observed when perester decomposition proceeds as the concerted cleavage of two bonds.

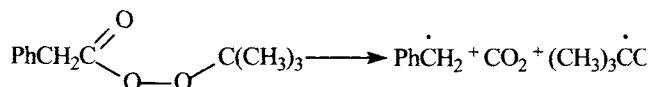
### 7.1.2. Decomposition with concerted cleavage of two bonds

Sometimes a molecule decomposes to give not two but three or more fragments. This concerted cleavage of two bonds in the molecule with the formation of a new molecule and two radicals occurs when it is energetically more favorable than the simple decomposition of one bond. The decomposition of perester with the cleavage of only one O—O bond requires the energy expense equal to the energy of this bond, i.e., 140–160 kJ/mol.

Decomposition of the type



becomes energetically favorable only when the R—C bond is weakened, and this takes place in the case where the R· radical is stabilized. This decomposition with the simultaneous cleavage of the C—C and O—O bonds occurs, e.g., during the decomposition of phenyl peracetate



In this case, the concerted mechanism is favored by the comparatively weak  $\text{PhCH}_2\text{—C}$  bond; the enthalpy of concerted decomposition is only 34 kJ/mol.

Decomposition with concerted bond cleavage is characterized by the following properties.

1. The activation energy of molecule decomposition for the concerted cleavage of bonds is much lower than that for the decomposition of one bond for this class of

compounds. For example, the activation energy of the decomposition of peresters at the O—O bond lies in the interval from 140 to 160 kJ/mol, and for the concerted cleavage of the O—O and C—C bonds the  $E$  value varies from 90 to 125 kJ/mol. The comparison of  $\Delta H^\ddagger$  with  $\Delta H^0$  for concerted decomposition shows that always  $\Delta H^\ddagger < \Delta H^0$ , i.e., the energy state of the activated complex differs noticeably from that for the reaction products.

2. The cleavage of one bond in the molecule is always accompanied by an increase in its sizes. Therefore,  $\Delta V^\ddagger$  always higher than zero, and an increase in pressure retards decomposition. For the decomposition of peroxide compounds with one bond cleavage  $\Delta V^\ddagger = 10 \pm 3 \text{ cm}^3/\text{mol}$ . Concerted decomposition occurs with the formation of a more compact transition state. Therefore, its  $\Delta V^\ddagger$  is lower than that for the decomposition of one bond, in some cases  $\Delta V^\ddagger < 0$ . The pressure accelerates or weakly affects concerted decomposition.

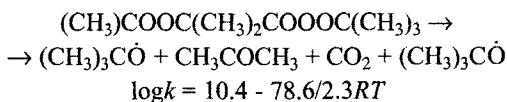
3. For the same reason, the activation entropy for the concerted decomposition of peresters is low ( $-20 \div +20$ ), whereas for the decomposition with the cleavage of one O—O bond  $\Delta S^\ddagger$  lies in the  $40 \div 80 \text{ J}(\text{mol}\cdot\text{K})^{-1}$  interval. The  $\Delta H^\ddagger$  and  $\Delta S^\ddagger$  values can be used to choose between two mechanisms (concerted and nonconcerted). However, one should be very careful in using  $\Delta H^\ddagger$  and  $\Delta S^\ddagger$ , first, because they are very sensitive to the medium (solvent) even for nonconcerted decomposition; second, because of an inaccuracy in measurement of both  $E$  ( $\Delta H^\ddagger$ ) and  $A$  ( $\Delta S^\ddagger$ ). The decomposition rate constant at a constant temperature is more reliable.

4. The transition state at the concerted decomposition of peresters and diacyl peroxides has the polar structure of the  $\text{R}^+ \dots \text{CO}_2 \dots \bar{\text{O}}\text{R}$  type. Therefore, the concerted decomposition of peroxide compounds depends on the solvent polarity: the higher the polarity, the faster the decomposition.

5. Decomposition to a molecule and two radicals makes it impossible to recover the initial molecule in the cage from primary reaction products. Therefore, the solvent viscosity has almost no effect on the concerted decomposition of molecules.

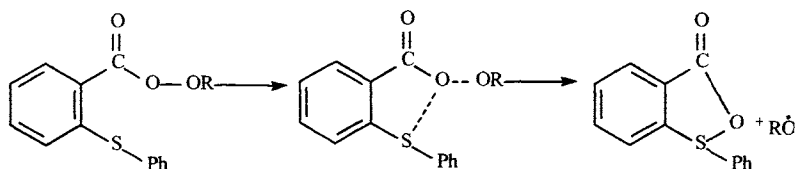
6. In the decomposition of azo compounds, the concerted decomposition is manifested in the fact that  $k$  and  $E$  of the decomposition of symmetric and nonsymmetric azo compounds differ strongly, whereas the difference is low for the decomposition of only one bond.

The following reaction is a very interesting example of decomposition with the concerted cleavage of three bonds:

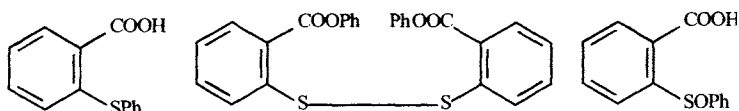


### 7.1.3. Decomposition with chimerical interaction

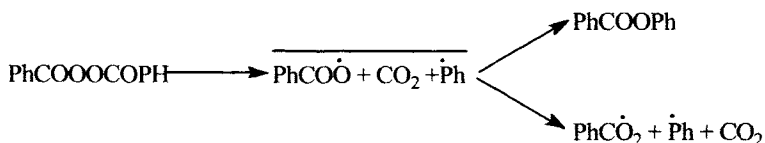
Chimerical decomposition with the cleavage of one bond and formation of another bond is close to concerted decomposition. *ortho*-Substituted esters of perbenzoic acid decompose very rapidly if the substituent X is the iodine atom, RS radical or a substituent with the double bond. The accelerating effect of these *ortho*-substituents is explained by the fact that the cleavage of the O—O bonds in the transition state is compensated in part by O...X bond formation, for example,



Radical I appears as an intermediate product and gives the products



Generally speaking, the substance can decompose in parallel via two and more routes through different transition states. For example, benzoyl peroxide decomposes mainly with the cleavage of one O—O bond. However, as shown by the method of chemical nuclei polarization, its concerted decomposition also occurs in part



The ratio between the directions of decomposition changes depending on the conditions: temperature, polarity of the solvent, its viscosity, and pressure. The existence of parallel routes of decomposition is, most likely, the main source of contradictory conclusions of independent authors concerning the mechanism of decomposition of this or other initiator.

### 7.1.4. Influence of pressure

When a molecule decomposes to radicals, one of the bonds is stretched, and the molecule in the transition state occupies somewhat larger volume:  $\Delta V^\ddagger = V^\ddagger - V > 0$ , usually  $V$  being expressed in  $\text{cm}^3/\text{mol}$ . The  $\Delta V^\ddagger$  value is calculated from results of experiments on substance decomposition at different pressures (the pressure is usually varied from  $10^8$  to  $10^9$  Pa). According to the transition state theory,

$$\frac{d \ln k}{dp} = -\frac{1}{RT} \left( \frac{\partial \Delta G^\ddagger}{\partial p} \right)_T = -\frac{\Delta V^\ddagger}{RT} \quad (7.3)$$

$$\Delta V^\ddagger = -RT d \ln k / dp \quad (7.4)$$

Since decomposition occurs in the liquid phase, the cage effect should be kept in mind



The decomposition rate constant measured in experiment is  $k_1(1 + k^{-1}/k_c)^{-1}$ . Therefore,  $\Delta V_{\text{exp}}^\ddagger$  calculated from experimental data, in this case, is equal to

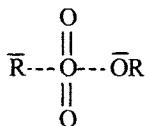
$$\Delta V_{\text{exp}}^\ddagger = \Delta V^\ddagger + RT \partial [\ln(1 + k^{-1}/k_c)] / \partial p \quad (7.5)$$

In turn,

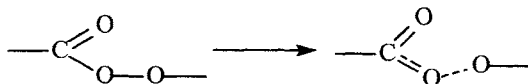
$$\Delta V^\ddagger = \Delta V_d^\ddagger + \Delta V_s^\ddagger$$

where  $\Delta V_d^\ddagger$  is the change in volume due to bond extension, and  $\Delta V_s^\ddagger$  is the change in volume related to the change in the solvation shell in the transition state.

The term  $\Delta V_s^\ddagger$  contributes to  $\Delta V^\ddagger$  during the decomposition of peroxide compounds with the cleavage of two bonds when the polar transition state is formed



This results in "thickening" of the solvate shell, makes  $\Delta V_s^\ddagger < 0$ , and decreases substantially  $\Delta V^\ddagger$ , so that sometimes  $\Delta V^\ddagger < 0$ . At the same time, the decomposition of peroxide compounds with the cleavage of two bonds proceeds through the compact transition state because the extension of two C—O and O—O bonds is partially compensated by the shortening of another C—O bond due to the formation of the double bond



An interesting method to determine  $\Delta V^\ddagger$  without using pressure was proposed for the measurement of  $k$  of the decomposition of *tert*-butyl perbenzoate in several solvents with different internal pressures. Starting from  $\Delta V^\ddagger = 12 \text{ cm}^3/\text{mol}$ , the values of this pressure in each solvent were calculated and used for the estimation of  $\Delta V^\ddagger$ .

The dependence of  $\log k$  on  $p$  is often nonlinear. In the general form, the dependence of  $k$  on  $p$  is the following:

$$\ln k = \ln k_1 - \frac{1}{RT} \int_1^p \Delta V^\ddagger \quad (7.6)$$

The dependence of  $\Delta V^\ddagger$  on pressure is theoretically unknown and, hence, it was determined empirically from the plot of the dissociation rate constant of electrolytes versus pressure. Under the assumption of the linear change in free energy, we have

$$\log(K/K_1)_i = \beta \log(k/k_1)_j$$

where index  $i$  is referred to equilibrium, and index  $j$  is referred to the  $j$ -th reaction.

The plot of  $k$  versus  $p$  has the following form:

$$\log k = \log k_0 - \frac{V}{2.3 RT} \frac{p}{1 + bp} \quad (7.7)$$

where index 0 is referred to the state at  $p = 0$ ;  $b = 9.20 \cdot 10^{-10} \text{ Pa}^{-1}$ .

The  $\Delta V^\ddagger$  value is related to the pressure by the dependence

$$\Delta V^\ddagger = \Delta V_0^\ddagger (1 + bp)^{-2} \quad (7.8)$$

The factor  $(1 + bp)^{-2}$  takes into account the fraction of the volume effect at  $p = 0$  that takes place at pressure  $p$ .

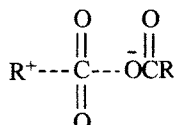
### 7.1.5. Influence of medium

In the liquid phase, both the initial molecule and activated complex exist in the field of molecular forces of surrounding molecules, and these forces exert a pressure of  $(1.5) \cdot 10^8 \text{ Pa}$  on each particle. This internal pressure in liquid has an effect on molecule decomposition. For the homolytic decomposition of one bond, the volume of the activated complex is somewhat greater than that of the initial molecule:  $\Delta V^\ddagger - V = \Delta V^\ddagger$ ,  $\Delta V^\ddagger = 10 \text{ cm}^3/\text{mol}$  for the decomposition of benzoyl peroxide. On going from the gas to liquid with an internal pressure of  $2 \cdot 10^8 \text{ Pa}$ ,  $\Delta \log k = -0.30$ , i.e.,  $k_{\text{gas}}/k_{\text{liq}} = 2$  at  $\Delta V^\ddagger = 0.01 \text{ l/mol}$  and  $T = 400 \text{ K}$ . Therefore, the internal pressure in liquid should somewhat retard homolytic decomposition with the cleavage of one bond.

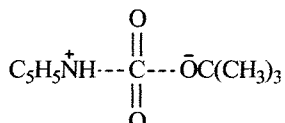
In addition, due to the cage effect some radical pairs recombine in the cage to form the starting molecules. For example, when acetyl peroxide decomposes, as shown by the study with  $^{18}\text{O}$ , approximately one third of radical pairs in acetic acid recombine to form peroxide. Thus, it can be expected that in the liquid phase decomposition rate constants of substances with the cleavage of one bond are two- to three-fold lower than those in the gas phase. The comparison of experimental data shows that the rate constants and activation energies of decomposition of these molecules are close in fact. Usually kinetic measurements in the gas phase are carried out at a higher temperature than in solution; extrapolation by temperature serves as an additional source of data divergence. If two bonds are consistently cleaved, then  $\Delta V^\ddagger < 0$ , and the internal pressure of the liquid, in this case, should have a weak effect on

decomposition. Experimental data on the decomposition of such substances in the gas phase are lacking.

The solvent has a strong effect on concerted decomposition, which was proved for the decomposition of isobutyryl peroxide, whose decomposition rate constant varies from  $3 \cdot 10^{-5}$  in isooctane to  $58 \cdot 10^{-5} \text{ s}^{-1}$  in nitrobenzene (313 K). A linear dependence between  $\log k$  and  $(\epsilon-1)/(2\epsilon+1)$  is fulfilled for polar solvents, and nonpolar solvents are characterized by a linear dependence of  $\log k$  and solvent polarizability. The solvent effect on the decomposition rate is related to the polar structure of the transition state



The authors believe that this is confirmed by a linear correlation between the change in logarithms of decomposition rate constants  $k$  and those of the reaction of pyridine with *tert*-butyl perester of formic acid  $k'$ :  $\Delta \log k \sim \Delta \log k'$ .

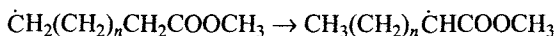


## 7.2. Isomerization of free radicals

The first case of radical isomerization was established by Urri and Kharash in 1944 for the neopentyl radical. Many other examples of radical isomerization were discovered during next 40 years. In most cases, it was proved by the composition of formed molecular products of multistage radical transformation. Quantitative data on this class of reactions are yet insufficient. Various isomerization reactions of radicals can be grouped as follows: isomerization of hydrogen atom abstraction, with group migration, with closure and breakage of the cycle, and *cis-trans*- isomerization of allyl radicals.

### 7.2.1 Isomerization with hydrogen atom abstraction

Free radicals are prone to the abstraction of the hydrogen atom from C—H bonds. In several cases, reactions of this type occur intramolecularly and then the position of the free valence in the radical changes. These reactions occur with a noticeable rates in structures where the five-, six- or seven-membered transition state can be formed, for example,

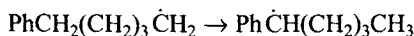


The starting radical was photochemically generated from a molecule of the corresponding bromide; the radical obtained was fixed by the nitroso compound (radical trap). The position of the alkyl radical added to the molecule-trap was established from the EPR spectrum of the formed stable nitroxyl radical. The rate constant is determined by the radical structure and, depending on the number of methylene groups  $n$ , it equals (benzene, 313 K)

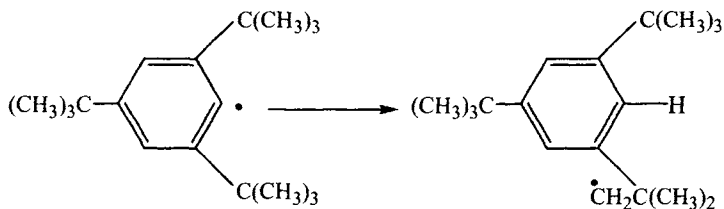
$n$ .....	2	3	4
$k, \text{s}^{-1}$ .....	$7.8 \cdot 10^5$	$1.3 \cdot 10^5$	$1.8 \cdot 10^4$

Isomerization occurs with the highest rate when the geometrically most favorable six-membered cycle of the transition state is formed. This isomerization from position 1 to position 2 does not occur due, most likely, to great deformations of bond angles in the three-membered cycle of the transition state.

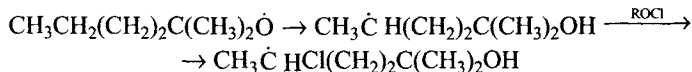
#### Isomerization



occurs with  $k = 2 \cdot 10^4 \text{ s}^{-1}$  (323 K, benzene). The following isomerization occurs slowly:



Similar isomerization was found for alkoxy radicals, for example,

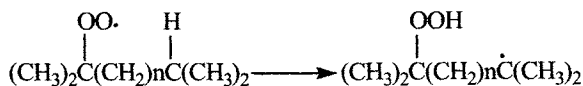


The occurrence of this reaction was judged from the formation of the corresponding chloride upon the decomposition of hypochloride. Since the *tert*-alkoxy radical decomposes to form acetone, the ratio of rate constants of isomerization to decomposition was estimated from the [chloride] : [acetone] ratio. The composition of the ROCl products was studied in which  $\text{R} = \text{CH}_3(\text{CH}_2)_n\text{C}(\text{CH}_3)_2$ ,  $n = 2, 3, 4$ . At  $n = 2$  only the methyl group is attacked, and at  $n = 3$  and 4 only the methylene group is attacked. The rate constants calculated for 273 K at  $k_d = 5.1 \cdot 10^4 \text{ s}^{-1}$  are the following:

n.....	2	3	4
$k, s^{-1}$ .....	$2.4 \cdot 10^4$	$3.2 \cdot 10^5$	$1.5 \cdot 10^4$
$E, kJ/mol$ .....	38	32	39

It is seen that isomerization is most fast at  $n = 3$ , *i.e.*, when the six-membered cycle in the transition state is formed.

The intramolecular attack of the free valance at the C—H bond is also observed for peroxy radicals. The oxidation of branched paraffins is accompanied by isomerization



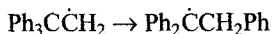
due to which biatomic hydroperoxide is formed. The rate of intramolecular attack depends on the number of methylene groups separating the reaction centers

n.....	0	1	2	3
$k, s^{-1}$ .....	0.2	18	8	1
$E, kJ/mol$ ...	94	73	71	79

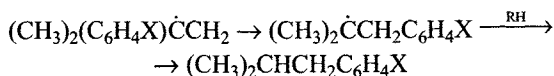
The number  $n=1$  corresponds to six-membered cycle of the transition state at which the maximum isomerization rate is observed. The activation energy of  $\text{RO}_2$  isomerization is much higher than that of  $\text{RO}\cdot$ , which is resulted by the difference in  $\Delta H$ .

### 7.2.2. Isomerization with migration of group

The migration of the phenyl group in alkylaryl radicals is well known, for example,



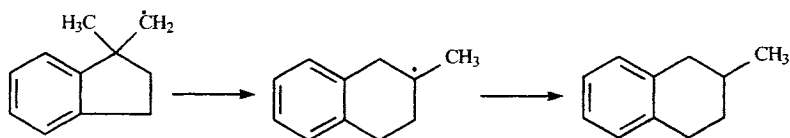
Alkyl radicals rapidly detach H from  $\text{R}_3\text{SnH}$ . For the reaction of  $\text{Ph}_3\text{CCH}_2\text{Cl}$  with  $\text{Ph}_3\text{SnH}$  the products of the reaction of  $\text{R}_3\text{SnH}$  with both radicals were found, namely,  $\text{Ph}_3\text{CCH}_3$  and  $\text{Ph}_2\text{CHCH}_2\text{Ph}$ . The isomerization rate constant was estimated by the method of competitive reactions to be  $5 \cdot 10^7 s^{-1}$  (373 K). Substituents affect isomerization of this type, which is seen from the yield of the isomerization products



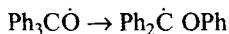
depending on the X substituent (RH is tetramine, 403 K)

X.....	<i>n</i> -OCH <sub>3</sub>	<i>n</i> -CH <sub>3</sub>	H	<i>n</i> -Br	<i>n</i> -NO <sub>2</sub>
% $(\text{CH}_3)_2\text{CHCH}_2\text{C}_6\text{H}_4\text{X}$ ....	19	35	44	60	96

The migration of the phenyl group in radicals of fused aromatic structures is accompanied by an increase in the sizes of the cycle

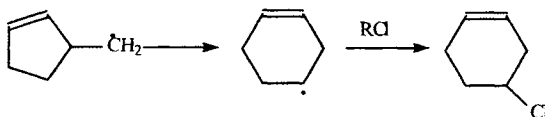


Arylalkoxyl radicals undergo similar isomerization, for example,

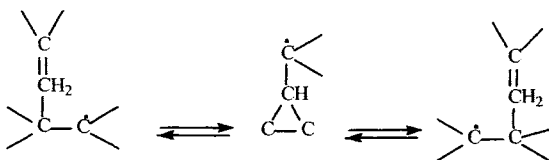


The rate constant of this reaction is higher than  $10^6 \text{ s}^{-1}$  (300 K).

Isomerization with the displacement of the free valance if the radical contains a double bond is also known, for example,

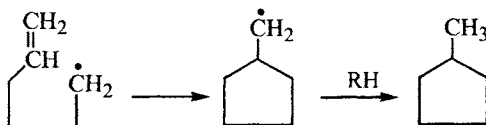


The following mechanism of rearrangement is proposed as the most probable:



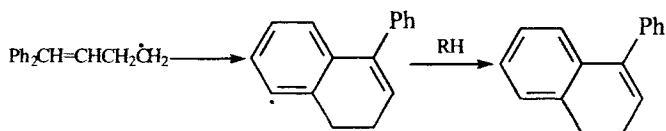
### 7.2.3. Isomerization with cycle closure and opening

Alkyl radicals bearing the double bond are prone to cycle formation if this is allowed by the geometry of the carbon skeleton of the radical, for example,

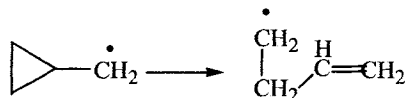


The reaction is rather prompt,  $k \approx 10^5 \text{ s}^{-1}$  (313 K).

The following cyclization occurs rapidly ( $k = 6 \cdot 10^5 \text{ s}^{-1}$ , 398 K):

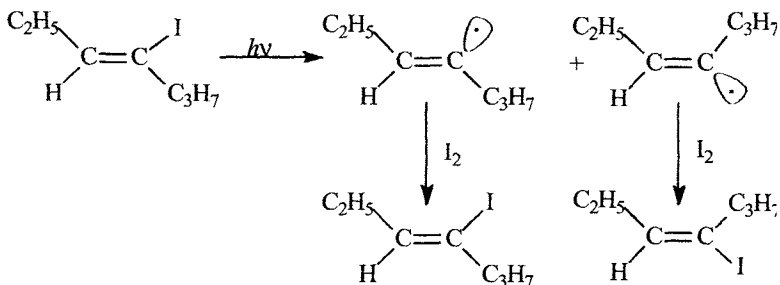


By contrast, radicals with the cyclic structure are isomerized with ring opening, for example,



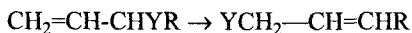
#### 7.2.4. Isomerization of unsaturated compounds

*cis-trans*-Isomerization of vinyl compounds proceeds *via* the intermediate radical state, for example,

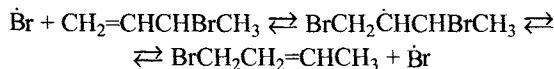


For some time the radical retains the *trans*-configuration of the initial molecule; the transition to the *cis*-configuration is related to overcoming of an activation barrier of approximately 60 kJ/mol.

The allyl rearrangement of the type

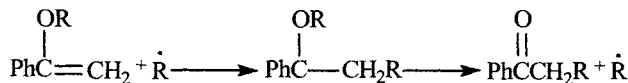


is also initiated by free atoms and radicals as it is seen from the following example:



The theoretical estimation gives  $k = 3 \cdot 10^{13} \exp(-70/RT) \text{ s}^{-1}$  for the isomerization of the allyl radical.

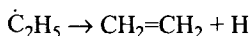
The Claisen rearrangement also proceeds *via* the radical mechanism, which requires either a high temperature ( $T > 700 \text{ K}$ ) or the introduction of an initiator at a moderate temperature



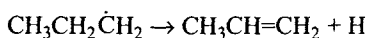
### 7.3. Decomposition of free radicals

Radicals with the structure that allows the energy compensation of the cleavage of one bond by the appearance of another bond are prone to fast decomposition. This is observed for radicals of the  $R-CH_2-\dot{C}H_2$  type, where the cleavage of the  $R-C$  bond is partially compensated by the formation of the  $\pi-C-C$  bond, and radicals of the  $R_1R_2R_3C-Y\cdot$  type, where the cleavage of the  $R_1-C$  bond is compensated by the appearance of the  $C-Y$  bond, and in similar structures.

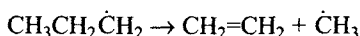
The ethyl radical decomposes with  $C-H$  bond cleavage to ethylene and hydrogen atom



The activation energy is virtually equal to the endothermic effect of the reaction, and the decomposition rate constant in the gas phase is  $k_d = 3 \cdot 10^{13} \exp(-170/RT) \text{ s}^{-1}$ . The propyl radical decomposes via two parallel routes, namely, with the cleavage of the  $C-H$  and  $C-C$  bonds



$$k = 6.3 \cdot 10^{13} \exp(-159/RT) \text{ s}^{-1}$$

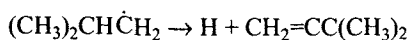


$$k = 4.0 \cdot 10^{13} \exp(-138/RT) \text{ s}^{-1}$$

The isobutyl radical also decomposes via two directions with the cleavage of the same bonds



$$k = 1.6 \cdot 10^{14} \exp(-137/RT) \text{ s}^{-1}$$



$$k = 5 \cdot 10^{13} \exp(-153/RT) \text{ s}^{-1}$$

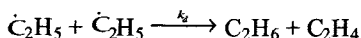
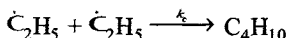
### 7.4. Recombination and disproportionation of radicals

Recombination of atoms differs basically for the gas and condensed phases. In the gas atoms recombine upon the collision of two atoms with the third particle, which receives a portion of the energy liberated in the recombination act. In the liquid the excited molecule formed in the recombination act immediately donates an excessive energy in collisions with surrounding molecules, *i.e.*, the recombination of atoms in the liquid and solid is bimolecular with the rate constant of diffusion collisions (see

Chapter 5).

### 7.4.1. Alkyl radicals

Recombination of alkyl radicals, as that of atoms, occurs practically without an activation energy. In the gas phase at a sufficiently high pressure the recombination of methyl radicals is bimolecular with the rate constant close to  $(1/4)z_0$  (where  $z_0$  is the frequency factor of bimolecular collisions, and the factor  $1/4$  reflects the probability of collisions of particles with the antiparallel orientation of spins). The theoretical estimation of the constant at a collision diameter of  $3.5 \cdot 10^{-10}$  m agrees with the experimental value  $2k = 2 \cdot 10^{10}$  l/(mol·s) (300 K). This  $k$  value agrees with the estimation by the theory of absolute reaction rates under the assumption that the free rotation of methyl groups is retained in the transition state. In the liquid the recombination of methyl radicals is bimolecular with the rate constant of diffusion collisions (see Chapter 5). For example, in water  $2k = 3.2 \cdot 10^9$  l/(mol·s) (298 K). Ethyl radicals react with each other by two methods: recombine and disproportionate



The overall constant  $2(k_c + k_d) = 2.2 \cdot 10^9$  l/(mol·s) in  $\text{H}_2\text{O}$  at 298 K. The ratio  $k_d/k_c = 0.13$  in the gas phase and 0.18 in isooctane. This ratio increases with viscosity: it is equal to 0.27 in ethylene glycol. This is explained by the fact that transition states for recombination and disproportionation are different, and disproportionation occurs through a more contact transition state. The difference  $V_c - V_d = 2.6$  cm<sup>3</sup>/mol (273 K), and the  $k_d/k_c$  ratio depends, therefore, on the internal pressure of the liquid  $p_s$

$$(k_d/k_c) = -1.08 + 1.5 \cdot 10^{-5} p_s^{1/2} \quad (7.9)$$

The  $k_d/k_c$  ratio depends slightly on temperature:  $k_d/k_c = 0.087 \cdot \exp(1.55/RT)$ . The ratio between recombination and disproportionation depends, naturally, on the structure of the alkyl radical, which can be seen from the presented data (decane, 303 K)

Radical....	$\dot{\text{C}}_2\text{H}_5$	$\text{CH}_3\text{CH}_2\dot{\text{C}}\text{H}_2$	$(\text{CH}_3)_2\dot{\text{C}}\text{H}$	$(\text{CH}_3)_3\dot{\text{C}}$	$\text{Ph}(\text{CH}_3)_2\dot{\text{C}}$
$k_d/k_c$ .....	0.12	0.13	1.2	7.2	0.05

A comparison of the *tert*-butyl and cumyl radicals shows that the delocalization of an unpaired electron dramatically decreases the probability of disproportionation. At the same time, the  $k_d/k_c$  ratio increases for alkyl radicals in the sequence primary < secondary < tertiary. A rigid conception that describes quantitatively this competition is lacking.

### 7.4.2. Aminyl radicals

Aliphatic aminyl radicals, as alkyl radicals, enter into disproportionation and recombination reactions. The reaction direction depends on the radical structure. For example, methylaminyl radicals predominantly recombine and diisopropylaminyl radicals disproportionate

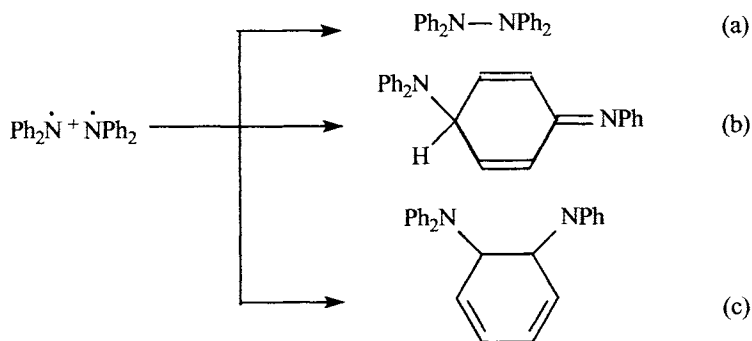


The reaction between two aminyl radicals is not always limited by diffusion, which follows from the following data ( $\text{C}_6\text{H}_6$ , 300 K):

Radical.....	$(\text{C}_2\text{H}_5)_2\dot{\text{N}}$	$(\text{CH}_3)_3\text{CN}\dot{\text{H}}$	$[(\text{CH}_3)_2\text{CH}]_2\dot{\text{N}}$
$2k$ , l/(mol·s).....	$1 \cdot 10^9$	$2 \cdot 10^7$	$4.5 \cdot 10^6$

The bulky *tert*-butyl substituent loses the free rotation of methyl groups during aminyl radical recombination. This results in the loss of entropy during the formation of the transition state and a decrease in the rate constant. Two isopropyl groups in the corresponding aminyl radical sterically hinder recombination and, therefore, disproportionation occurs. The transition state is rather compact in this case, and its formation is also accompanied by the entropy loss, which explains the low value of  $k_d$ .

Diphenylaminyl radicals recombine by three different methods

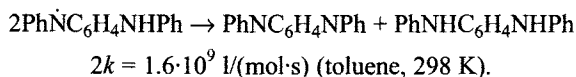


The ratio between them is the following: 1.0 (a) : 0.15 (b) : 0.03 (c), *i.e.*, the formation of the dimer with the N—N bond prevails. The overall constant  $2k_c = 2.7 \cdot 10^7$  l/(mol·s) (toluene, 298 K). Electropositive substituents in the para-position retard recombination, whereas electronegative substituents accelerate it. The following linear correlation is fulfilled between  $\log k_c$  and  $\sigma$  Hammett constant:

$$\log k = 7.24 + 1.50\sigma \quad (7.10)$$

It is seen that the recombination of aromatic aminyl radicals is not limited by dif-

fusion but is determined by their structure. Recombination is accompanied by the entropy loss due to the loss of the free rotation of the phenyl rings and occurs with the activation energy. For example, for the recombination of the *p*-methoxydiphenylaminyl radicals  $E = 12$  kJ/mol,  $\Delta S^\ddagger = -97$  J/(molK). Naphthylaminyl radicals recombine only with the formation of N—C and C—C bonds likely due to steric hindrances created to the formation of N—N dimers by the naphthyl rings and to the instability of hydrazines that formed. Aminyl radicals formed from *p*-diamines disproportionate with diffusion rate constants

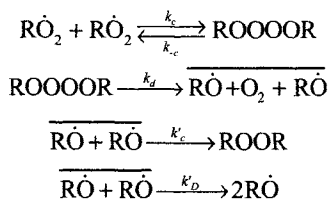


#### 7.4.3. Peroxyl radicals

Disproportionation of peroxyl radicals was studied in detail because in the liquid-phase oxidation of organic compounds chains terminates by this reaction. The experimentally measured rate constants of  $\text{RO}_2\cdot$  decay change in a wide interval depending on the structure of the radical (303 K)

Radical	$\text{RCH}_2\text{O}\dot{\text{O}}$	$\text{RCHOO}\dot{\text{O}}$	$\text{R}_3\text{CO}\dot{\text{O}}$	$\text{RC(O)O}\dot{\text{O}}$
$2k_t$ , l/(mol·s)	$(2 \div 4)10^8$	$(1 \div 10)10^6$	$(1 \div 50)10^3$	$(3 \div 20)10^7$

The mechanism of peroxyl radical disproportionation is rather complicated and includes several stages. Tertiary peroxyl radicals react in a solution as follows:

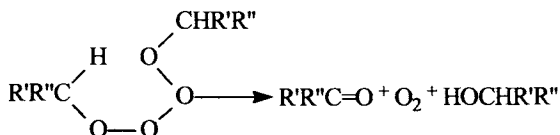


Below we present the  $K_c$  values (303 K),  $\Delta H$ , and  $\Delta S$  for the first stage

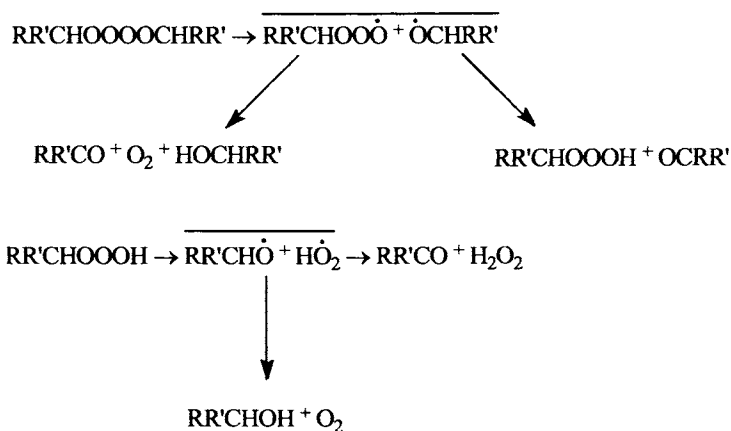
$\text{R}\dot{\text{O}}_2$ .....	$K_c$ , l/mol	$-\Delta H$ , kJ/mol	$\Delta S$ , J/(mol·K)
$(\text{CH}_3)_3\text{CO}\dot{\text{O}}$ .....	12.2	37	142
$\text{C}_2\text{H}_5(\text{CH}_3)_2\text{CO}\dot{\text{O}}$ ....	8.5	31	121
$\text{Ph}(\text{CH}_3)_2\text{CCO}\dot{\text{O}}$ .....	2.2	38	134

The following expressions for the rate constants of individual stages at 303 K were found for the *tert*-butylperoxyl radical:  $k_c = 3 \cdot 10^9 \exp(-8/RT) = 10^7$  l/(mols),  $k'_c = 4 \cdot 10^{15} \exp(-44/RT) = 9 \cdot 10^7 \text{ s}^{-1}$ ,  $k_d = 10^{17} \exp(-67/RT) = 3 \cdot 10^5 \text{ s}^{-1}$ ,  $k'_D = 6 \cdot 10^{10} \text{ s}^{-1}$ . Since  $k_d \ll k_c$ , the experimentally measured value  $2k_t = 2k_d k_c k'_D (k'_c + k'_D)^{-1}$ .

For primary and secondary  $\text{RO}_2\cdot$  Russel proposed the concerted decomposition of tetraoxide



with the formation of ketone and alcohol. However, this decomposition does not explain the following facts. The disproportionation of primary and secondary  $\text{RO}_2\cdot$  results in chemiluminescence, whose source is ketone (or aldehyde) in the triplet state. According to the law of spin conservation, ketone (aldehyde) can be formed during concerted decomposition only in the ground singlet state.  $\text{RO}_2\cdot$  was found among the products of  $\text{CH}_3\text{PhCHO}\cdot$  disproportionation, which does not either confirm the concerted decomposition of tetraoxide. It is highly probable that the successive fragmentation of tetraoxide occurs with the intracage transformations of the radicals

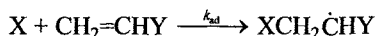


This scheme explains both the formation of triplet ketone from  $\text{RR}'\text{CHOOO}\cdot$  and  $\text{H}_2\text{O}_2$  from labile hydrotrioxide. According to the scheme, ketone and alcohol can be formed during disproportionation in a nonequivalent ratio, which is also observed in experiment. It cannot be ruled out that the concerted and nonconcerted decompositions of tetraoxide occur in parallel.

## 7.5. Free radical addition

### 7.5.1. Enthalpy and entropy of radical addition

The radical addition reactions



involve the rupture of the C=C bond and the formation of a C—X  $\sigma$ -bond. A  $\pi$ -bond is normally stronger than a  $\sigma$ -bond; hence, radical addition is an exothermic reaction. This can be clearly seen when comparing the reaction enthalpies  $\Delta H$  and the strengths of the bonds being formed  $D(\text{EtX})$  given in Table 1; the stronger the EtX bond, the larger the  $-\Delta H$  value. Yet another important factor influencing the reaction enthalpy is the energy of stabilization of the radical  $\text{XCH}_2\dot{\text{C}}\text{HY}$  formed: the higher this energy, the greater the heat of the addition of the  $\text{X}\cdot$  radical to an alkene. Stabilization energy can be characterized as the difference between the strengths of the C—H bonds in  $\text{Pr—H}$  and  $\text{EtYHC—H}$ . Below we present the data characterizing the contribution to the enthalpy of this reaction of the stabilization energy of the  $\text{MeCH}_2\dot{\text{C}}\text{H}\cdot\text{Y}$  radical, resulting from the addition of a methyl radical to the monomer  $\text{CH}_2=\text{CHY}$ .

Y	H	C(O)OMe	Cl	CN	Ph
$D_{\text{Pr-H}} \quad D_{\text{EtYHC-H}}/\text{kJ mol}^{-1}$	0.0	23.2	24.1	33.6	57.9
$-\Delta H/\text{kJ mol}^{-1}$	95.8	102.0	104.3	129.7	143.0

It can be seen that the greater the energy of radical stabilization, the smaller the reaction enthalpy.

All the addition reactions are accompanied by a decrease in entropy (two species are combined to give one species, see Table 7.1). Therefore, for addition reactions,  $\Delta G < \Delta H$  ( $\Delta G$  is the Gibbs energy) and, when the temperature is sufficiently high, exothermic addition is reversible because  $\Delta G = \Delta H - \Delta TS$ .

Free radical addition can be considered to be reversible if the equilibrium concentration of the  $\text{X}\cdot$  radicals is commensurate with the concentration of the  $\text{XCH}_2\dot{\text{C}}\text{HY}$  radicals formed, *i.e.*, if the  $[\text{X}\cdot] : [\text{XCH}_2\dot{\text{C}}\text{HY}]$  ratio in the equilibrium state is not smaller than 0.05. When  $[\text{CH}_2=\text{CHY}] = 10 \text{ mol/l}$  and  $T = 300 \text{ K}$ , this condition results in the inequality  $K \geq 200$  ( $K$  is the equilibrium constant). In turn,  $-RT \ln K = \Delta G$ ; therefore,  $\Delta G \geq RT \ln 200 = 13 \text{ kJ mol}^{-1}$ .

For addition reactions,  $S \approx 100$ ; therefore, the enthalpy of irreversible addition of a free radical to an alkene should be smaller than  $43 \text{ kJ mol}^{-1}$  (at  $T = 300 \text{ K}$ ).

Table 7.1. Bond strength ( $\text{kJ mol}^{-1}$ ), enthalpy ( $\text{kJ mol}^{-1}$ ), entropy ( $\text{J mol}^{-1} \text{K}^{-1}$ ), and Gibbs energy ( $\text{kJ mol}^{-1}$ ) for the addition of atoms and radicals to ethylene ( $T = 298 \text{ K}$ )

X·	$\Delta H$ , $\text{kJ mol}^{-1}$	$\Delta S$ , $\text{kJ mol}^{-1}$	$\Delta G(298 \text{ K})$ $\text{kJ mol}^{-1}$
H·	150	84	125
Cl·	82	88	56
C·H <sub>3</sub>	100	122	64
Me <sub>2</sub> C·H	92	134	52
PhC·H <sub>2</sub>	63	122	27
N·H <sub>2</sub>	81	109	49
HO·	122	100	93
CH <sub>3</sub> O·	82	118	46
HO <sub>2</sub> ·	63	134	23

The  $\Delta H$  values for radical addition reactions listed in Table 7.1 comply with this condition. Naturally, as the temperature rises, the boundary value of  $\Delta H$  increases in absolute magnitude.

### 7.5.2. Empirical correlation equations

Activation energy and heat of reaction. A linear correlation between the change in the activation energy ( $\Delta E$ ) of the monomer addition to a macroradical and the change in the heat of the reaction ( $\Delta q$ ) of the type

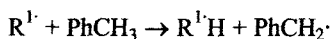
$$\Delta E = -\alpha \Delta q \quad (7.11)$$

where  $\alpha$  is an empirical factor of proportionality, was found by Evans et al. Later, Semenov confirmed this correlation and extended it to a wider range of addition reactions. However, even for a narrow series of reactions, for example, for the addition of methyl radical to  $\text{CH}_2=\text{CHY}$ , this correlation is nothing but a trend. Indeed, the correlation coefficient for the variation of  $\Delta \log k$  as a function of  $\Delta q$  is 0.85 ( $k$  is the reaction rate constant). Evidently, apart from the heat of reaction, other factors also influence the activation energy. *Q-e* Scheme. The Alfrey and Price *Q-e* scheme takes account of two factors affecting activation energy, namely, the energy of stabilization of the radical formed in the reaction and the interaction between polar groups in the radical and the monomer. This scheme was based on the analysis of empirical rate constants for copolymerization. The rate constant for the reaction of a radical with a monomer is postulated to have the following form:

$$k_{AB} = P_A Q_B \exp(-e_A e_B) \quad (7.12)$$

where the factors  $P_1$  and  $Q_2$  reflect the reactivity and  $e_1$  and  $e_2$  are the charges of the radical and the monomer, respectively. The  $Q$  and  $e$  parameters are calculated from the corresponding rate constants for copolymerization. When developing the  $Q$ - $e$  scheme, the researchers assumed that the charges on the molecule and on the radical are equal and constant (polarization in the transition state was not taken into account) and that the copolymerization rate constants do not depend on the dielectric constant of the medium. Subsequently, these assumptions have been criticized. The  $Q$ - $e$  scheme made it possible to systematize the vast experimental information on radical copolymerization of various monomers. It permits rough prediction of the rate constants for copolymerization. The  $Q$  and  $e$  values for monomers in radical polymerization are listed in Table 7.2.

The Bamford and Jenkins  $\alpha$ - $\beta$  scheme. These researchers suggested that the reactivities of a radical and a monomer should be described by three parameters, namely, rate constant for the reaction of the macroradical (for example,  $R^{\cdot}$ ) with toluene ( $k_T$ )

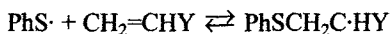


the product of coefficient  $\alpha$  with the Hammett constant  $\sigma$ , which takes into account the polar effect, and the coefficient  $\beta$ , reflecting the difference between the radical reactivities towards the monomer and towards toluene. Thus the equation for the rate constant for the addition of  $R^{\cdot}$  to the monomer  $M^1$  is represented as follows:

$$\ln k_{11} = \ln k_T + \alpha_1 \sigma_1 + \beta_1 \quad (7.13)$$

the coefficients  $\alpha_1$  and  $\sigma_1$  are calculated from the dependence of  $\ln(k_{11}/k_T)$  on  $\sigma$ , and the rate constant  $k_T$  is determined experimentally at  $T = 333$  K. The values of  $\alpha$  and  $\beta$  for a number of monomers are listed in Table 7.2.

The Ito and Matsuda KP scheme. In terms of this scheme, the activation energy of an addition reaction is represented as the sum of two terms,  $E_1$  and  $E_2$ . The first term  $E_1$  is proportional to the change in the Gibbs energy in the reversible addition of the thiyl radical  $\text{XC}_6\text{H}_5\text{S}^{\cdot}$  to the monomer,  $E_1 \sim \log K$ , where  $K$  is the equilibrium constant of the reaction



The second term  $E_2$  reflects the contribution of the polar interaction between the radical and the monomer to the activation energy. The contribution of the Gibbs energy to the activation energy is determined by the coefficient present in the linear dependence on  $\log K$  of the logarithm of the rate constant ( $k_X$ ) for the addition of the  $\text{XC}_6\text{H}_5\text{S}^{\cdot}$  radical to the monomer  $\text{CH}_2=\text{CHY}$

$$\log k = \alpha_Y \Delta \log K \quad (7.14)$$

The  $\alpha_Y$  value depends on the nature of the substituent Y in the monomer, this

dependence being used to estimate the contribution of the polar effect to the activation energy. This contribution is characterized by the increment  $P$

$$P = \alpha_Y + 2(\alpha_Y - \alpha_{\text{styrene}}) \quad (7.15)$$

The parameters  $K$  and  $P$  are listed in Table 9.2.

All the above schemes include, in essence, different variants of empirical linear equations in which the rate constants for chain propagation in the free radical polymerization are brought into correlation with thermodynamic (heat, Hammett constant ( $\sigma$ ), the change in the Gibbs energy in the equilibrium reaction) and kinetic (logarithms of the rate constants of the reference reaction and the reaction under study) characteristics of the addition reaction.

Table 7.2. Correlation parameters for the reactivity of monomers towards radical polymerization in terms of the Alfrey Price ( $Q$ ,  $e$ ), Bamford - Jenkins ( $\alpha$ ,  $\beta$ ), and Ito Matsuda ( $K$ ,  $P$ ) schemes

Monomer	$Q$	$e$	$\alpha$	$\beta$	$K$	$P$
$\text{CH}_2=\text{CHPh}$	1.00	-0.80	0.00	4.85	2.28	1.00
$\text{CH}_2=\text{CHSEt}$	0.27	-1.33	-0.50	4.21	1.30	2.78
$\text{CH}_2=\text{CHSO}_2\text{Et}$	0.07	1.29	-4.0	4.62	-1.40	-0.26
$\text{CH}_2=\text{CHCO}_2\text{Me}$	0.45	0.60	-3.0	5.20	0.00	0.58
$\text{CH}_2=\text{CHOCOMe}$	0.03	-0.88	0.0	3.00	-1.36	0.81
$\text{CH}_2=\text{CHCN}$	0.48	0.12	-3.0	5.30	0.89	-1.00
$\text{CH}_2=\text{CHOEt}$	0.02	-1.17	0.0	2.97	-0.59	1.63
$\text{CH}_2=\text{CMePh}$	0.98	-0.81	-1.0	4.72	1.30	1.69
$\text{CH}_2=\text{CMeCO}_2\text{Me}$	0.78	0.40		4.90	1.89	0.25
$\text{CH}_2=\text{CHCH}=\text{CH}_2$	1.70	-0.50	0.0	5.03	-	1.00
$\text{CH}_2=\text{CMeCH}=\text{CH}_2$	1.99	-0.55	0.0	4.92	-	1.09
$\text{CH}_2=\text{CClCH}=\text{CH}_2$	10.52	1.20	-1.5	5.82	-	0.10
$\text{CH}\equiv\text{CPh}$	0.45	0.5	0.5	4.41	-	1.00

### 7.5.3. Quantum-chemical calculations of the activation energy

Quantum-chemical methods are widely used to study addition reactions. The results obtained, in particular, the activation energies, depend significantly on the program chosen for calculations. For example, Wong et al. calculated the activation energy of the methyl radical addition to ethylene using the QCISD(T) program package. The results of calculations by this program are in good agreement with experimental data.

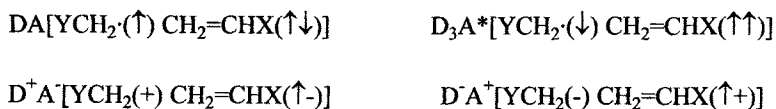
When atoms C of alkyl radical approaches to atom C of double bond and a tran-

sition state is formed, the bond angles at the carbon atom attacked by an atom or radical substantially change. The geometry of the transition state is characterized by the distance  $r(\text{C}-\text{C})$ , the angle of attack  $\varphi_{\text{at}}(\text{C}-\text{C}-\text{C})$  and the pyramidal angle  $\varphi_{\text{pyr}} = \varphi(\text{H}-\text{C}-\text{C})$ . The last-mentioned parameter is the angle of deviation of the two  $\text{C}-\text{H}$  bonds of ethylene from the plane in which they have been located in the initial molecule (the four hydrogens and both carbons of ethylene lie in one plane). Table 7.3 presents the values of the three above parameters and the activation energies for the addition of methyl radicals and the  $\text{C}\cdot\text{H}_2\text{OH}$  and  $\text{C}\cdot\text{H}_2\text{CN}$  radicals to ethylene.

Table 7.3. Interatomic distances and bond angles in the reaction center and the activation energies for the addition of the  $\text{XC}\cdot\text{H}_2$  radicals to ethylene (quantum-chemical calculations)

X	H	OH	CN
$r(\text{C}-\text{C})$ , Angstrom	2.246	2.226	2.173
$\varphi_{\text{att}}^\circ$	109.9°	108.2°	109.3°
$\varphi_{\text{pyr}}^\circ$	25.0°	25.9°	28.0°
E, kJ mol <sup>-1</sup>	39.8	35.0	42.3

The energy profile of the addition reaction is calculated using specific quantum-chemical programs as a superposition of four different electron configurations of the reactants, namely



where D is the radical, A is the molecule, the arrows mark the orientation of the electrons involved in the reorganization, and (+) and (-) are the charges on the radical and on the molecule. The results (the activation energies) thus obtained are considered with allowance for the influence of two values, namely, the reaction enthalpy and the polar effect.

#### 7.5.4. Parabolic model of radical addition

Within the framework of the parabolic model, radical addition



is represented as a result of intersection of two potential curves, each of them describing the potential energy of the stretching vibrations of atoms as a parabolic function of the amplitudes of vibrations of atoms in the outgoing (i) and incoming (f) bonds. In terms of the parabolic model, radical addition can be characterized by the following parameters:

1. Reaction enthalpy  $\Delta H_c$ 

$$\Delta H_c = D_i - D_f + 0.5hL(v_i - v_f) = \Delta H + 0.5hL(v_i - v_f) \quad (7.16)$$

where  $D_i$  and  $D_f$  are dissociation energies,  $h$  is the Planck constant,  $L$  is Avogadro's number, and  $i$  and  $f$  are the stretching vibration frequencies of bonds  $i$  and  $f$ , respectively. The second term is the difference between the zero-point energies of the reacting bonds.

2. Activation energy  $E_e$ , which includes the zero-point energy of the bond being attacked ( $0.5hLv_i$ ) and depends on the experimentally determined activation energy  $E$

$$E_e = E + 0.5(hLv_i - RT) \quad (7.17)$$

3. Distance  $r_e$ , which is equal to the sum of the amplitudes of vibrations of the atoms of the reacting bonds in the transition state.

4. Parameters  $b_i$  and  $b_f$ , which are dynamic characteristics ( $2b^2$  is the force constant) of the outgoing bond ( $b_i = \pi v_i(2\mu_i)^{1/2}$ ) and the incoming bond ( $b_f = \pi v_f(2\mu_f)^{1/2}$ ) where  $i$  and  $f$  are the reduced masses of atoms forming the bonds.

The above parameters are related to one another by the following expression:

$$br_e = \alpha(E_e - \Delta H_c) + E_e \quad (7.18)$$

By using the parameter  $br_e$ , one can calculate other characteristics of a whole group of reactions with  $br_e = \text{const}$ , for example, the activation energy of the thermally neutral reaction  $E_{e0}$  for  $\Delta H_c = 0$

$$E_{e0} = br_e(1 + \alpha)^{-1} \quad (7.19)$$

and the position of the transition state  $r^\#$

$$r^\# = r_e(1 + \alpha)^{-1} \quad (7.20)$$

As a rule, each reaction within one group is characterized by the same pre-exponential factor  $A$  (determined in relation to one reaction center). This allows the activation energy to be expressed in terms of the rate constant  $k$  using the Arrhenius equation

$$E = RT \ln(A/k) \quad (7.21)$$

Since for any elementary reaction,  $E > 0$ , relation (13) holds when  $\Delta H_c > \Delta H_{c,\min}$ , whereas for  $\Delta H_c < \Delta H_{c,\min}$ , the activation energy is very small and amounts to  $0.5RT$ . In accordance with the parabolic model,  $\Delta H_{c,\min}$  is related to  $br_e$  and  $\alpha$  by the expression

$$\alpha^2 \Delta H_{c,\min} = -(br_e)^2 + 2br_e(0.5hLv_i)^{1/2} + 0.5hLv_i(\alpha^2 - 1) \quad (7.22)$$

The physical, thermodynamic and kinetic parameters for 15 classes of reactions involving addition of atoms and radicals to carboncarbon and carbonoxygen multiple bonds are listed in Table 7.4.

Table 7.4. Parameters of various classes of addition of atoms and radicals to multiple bonds used in the parabolic model

Reaction	$\alpha$ (kJ/mol) <sup>1/2</sup> m <sup>-1</sup>	$b \times 10^{-11}$ , kJ mol <sup>-1</sup>	$0.5hLv_i$ , kJ mol <sup>-1</sup>	$0.5hL(v_i - v_f)$ , kJ mol <sup>-1</sup>	$A \times 10^{-10}$ l mol <sup>-1</sup> s <sup>-1</sup>
H· + CH <sub>2</sub> =CHR	1.440	5.389	9.9	-7.5	10
H· + CH≡CR	1.847	6.912	12.7	-4.7	40
H· + O=CR <sup>1</sup> R <sup>2</sup>	1.600	5.991	10.3	-11.4	10
D· + CH <sub>2</sub> =CHR	1.461	5.389	9.9	-2.7	10
Cl· + CH <sub>2</sub> =CHR	1.591	5.389	9.9	4.8	9
Br· + CH <sub>2</sub> =CHR	1.844	5.389	9.9	5.8	5
R· + CH <sub>2</sub> =CHR	1.202	5.389	9.9	1.7	0.1
R· + CHCR	1.542	6.912	12.7	3.8	0.1
R· + O=CR <sup>1</sup> R <sup>2</sup>	1.570	5.991	10.3	3.7	0.05
N·H <sub>2</sub> + CH <sub>2</sub> =CHR	1.410	5.389	9.9	3.1	0.008
	⌋	RO· + CH <sub>2</sub> =CHR	1.413	5.389	9.9 3.3
		0.05			
RO <sub>2</sub> · + CH <sub>2</sub> =CHR	1.737	5.389	9.9	4.6	0.1
R <sub>3</sub> Si· + CH <sub>2</sub> =CHR	2.012	5.389	9.9	4.1	0.1
R <sub>3</sub> Si· + O=CR <sup>1</sup> R <sup>2</sup>	2.518	5.991	10.3	7.0	0.08
PhS· + CH <sub>2</sub> =CHR	2.282	5.389	9.9	6.3	0.07

The parabolic model makes it possible to develop an empirical hierarchy of addition reactions. All the known addition reactions are divided *a priori* into classes in accordance with the atomic structure of the reaction center in the transition state. Each class is characterized by a pair of force constants of the outgoing and incoming bonds or by the parameters  $b = b_i$  and  $\alpha = b_i/b_f$  (see above). Subclasses are distinguished in each class. Each subclass is characterized by  $r_e = \text{const}$  or  $br_e = \text{const}$ , which is confirmed by analysis of a large array of experimental results. Each subclass of reactions can be described additionally by the energy of the thermally neutral reaction  $E_{eo}$  (see Eq. (7.19) and by the threshold value  $\Delta H_{e,\text{min}}$ , for which  $E = 0.5RT$  provided that  $\Delta H_e < \Delta H_{e,\text{min}}$  (see Eq. (7.22). The kinetic parameters for various subclasses of addition reactions are listed in Table 7.5. It can be seen that each subclass is characterized by individual values of these parameters. For instance,  $E_{eo}$  varies from 31.4 kJ mol<sup>-1</sup> for the addition of PhS to 105.3 kJ mol<sup>-1</sup> for the addition of the phenyl radical to an alkene double bond.

Table 7.5 Kinetic parameters  $E_{e0}$ ,  $b(1 + a)^{-1}$ ,  $r_e$ ,  $(r^\#/r_e)_0$ , and  $\Delta H_e$  min calculated from Eqs. (7.20) and (7.22) for addition reactions of various subclasses

Y·	$E_{e0}$ kJ mol <sup>-1</sup>	$b(1+\alpha)^{-1} \cdot 10^{11}$ kJ <sup>1/2</sup> mol <sup>-1/2</sup> m <sup>-1</sup>	$r_e \cdot 10^{11}$ , m	$(r^\#/r_e)_0$	$\Delta H_{e,min}$ kJ mol <sup>-1</sup>
Y· + CH <sub>2</sub> =CHX → YCH <sub>2</sub> C·HX					
H·	101.6	2.21	4.56	0.41	211.9
D·	99.6	2.19	4.56	0.41	204.9
Cl·	50.5	1.86	3.82	0.39	82.9
Br·	31.2	1.69	3.30	0.35	37.9
C·H <sub>3</sub>	82.6	2.45	3.71	0.45	194.4
C <sub>6</sub> H <sub>5</sub> ·	105.3	2.45	4.19	0.45	252.0
N·H <sub>2</sub>	61.0	2.24	3.49	0.41	226.0
RO·	65.2	2.23	3.62	0.41	119.0
RO <sub>2</sub> ·	90.5	1.97	4.83	0.36	150.4
R <sub>3</sub> Si·	76.6	1.78	4.92	0.33	117.5
PhS·	31.4	1.64	3.42	0.30	34.7
Y· + HC≡CX → YCH=C·X					
H·	125.1	2.43	4.60	0.35	229.3
C·H <sub>3</sub>	97.7	2.72	3.63	0.39	184.7
Y· + O=CR <sup>1</sup> R <sup>2</sup> → YOC·R <sup>1</sup> R <sup>2</sup>					
H·	102.9	2.30	4.41	0.38	149.7
C·H <sub>3</sub>	72.9	2.33	3.66	0.39	112.2
R <sub>3</sub> Si·	114.5	1.70	6.29	0.28	176.8

#### 7.5.5. Contribution of enthalpy of an addition to its activation energy

The parabolic model postulates a non-linear relationship between the activation energy and the enthalpy of a reaction (see Eq. 7.18). The contribution of enthalpy to the activation energy  $\Delta E_H$  can be estimated as the difference  $\Delta E_{e0} = E_e - E_{e0}$ .

Transformation of Eq. (7.18) gives the following equation for  $\Delta E_H$  as a function of  $\Delta H_e$ , and  $br_e$ :

$$(\alpha^2 - 1)\Delta E_H = 2a(br_e)^2 \{ [a^2 - 1]^2 (br_e)^{-2} \Delta H_e - 1 \}^{1/2} - 1 \} + a^2 \Delta H_e \quad (7.23)$$

When the range of variation of  $\Delta H_e$  is narrow, this dependence is close to linear.

$$\Delta E_{\text{H}} = \frac{\alpha}{1+\alpha} \Delta H_{\text{e}} + \frac{\alpha}{(2br_{\text{e}})^2} \Delta H_{\text{e}}^2 \quad (7.24)$$

The  $E_{\text{e0}}$  values calculated from experimental bre parameters made it possible to evaluate correctly the contribution of the enthalpy of addition to its activation energy. As an example, Table 7.6 presents the results of this comparison for two groups of addition reactions.

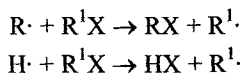
Table 7.6. Contribution  $\Delta E_{\text{H}}$  of the reaction enthalpy  $\Delta H$  to the activation energy  $E$ .

R	Y	$-\Delta H$ kJ mol <sup>-1</sup>	$E_{\text{e}}$ kJ mol <sup>-1</sup>	$-\Delta E_{\text{H}}$ kJ mol <sup>-1</sup>
Reaction: $\text{H}\cdot + \text{CH}_2=\text{CRY} \rightarrow \text{CH}_3\text{C}\cdot\text{RY}$				
H	H	162.1	22.5	79.1
H	Me	165.3	21.0	80.6
Me	Me	173.3	18.0	83.6
H	Cl	179.5	19.8	81.8
H	Ph	204.1	19.2	93.0
Ph	Ph	213.3	19.0	98.7
Reaction: $\text{C}\cdot\text{H}_3 + \text{CH}_2=\text{CRY} \rightarrow \text{CH}_3\text{CH}_2\text{C}\cdot\text{RY}$				
H	H	98.5	39.0	43.6
H	Me	96.1	36.9	45.7
Me	Me	98.3	35.7	46.9
H	Cl	104.3	33.6	49.0
H	Ph	143.3	26.6	63.4
Ph	Ph	154.0	24.5	69.3

It can be seen that these reactions are highly exothermic and the contribution of enthalpy to the activation energy is fairly high; it varies from 44 to 99 kJ mol<sup>-1</sup>, *i.e.*, amounts to 40%-50% of  $\Delta H$ .

### 7.5.6. Force constants of reacting bonds

The activation energy of a thermally neutral reaction is determined by two parameters: the distance  $r_{\text{e}}$  and the force constants of the reacting bonds  $\alpha$  and  $b$ . In some classes of radical abstraction reactions, namely in those presented below,



only the force constants change on passing from one class to another; thus, only the

parameters  $a$  and  $b$  determine the activation energy of a thermally neutral reaction. There are no such examples among addition reactions; therefore, it is expedient to compare different classes of reactions assuming (conditionally) that  $r_e = \text{const}$ . The parameter  $r_e$  for each reaction was taken to be  $3.713 \cdot 10^{-11} \text{ m}$ , as for the addition of the methyl radical to  $\text{CH}_2=\text{CRY}$ , while the parameters  $a$  and  $b$  were varied in conformity with the structure of the reaction center. The calculations were carried out using Eq. (7.9).

Reaction	$E_{\text{co}}$ (calculated), $\text{kJ mol}^{-1}$	$E_{\text{co}}$ (experimental), $\text{kJ mol}^{-1}$
$\text{H}\cdot + \text{C}=\text{C}$	67.3	101.6
$\text{H}\cdot + \text{O}=\text{C}$	73.2	102.9
$\text{H}\cdot + \text{C} \quad 81.3$	125.2	
$\text{C}\cdot\text{H}_3 + \text{C}=\text{C}$	82.6	82.6
$\text{C}\cdot\text{H}_3 + \text{O}=\text{C}$	74.9	68.1
$\text{C}\cdot\text{H}_3 + \text{C}=\text{C}$	64.0	97.7

Comparison of the calculated and experimental  $E_{\text{co}}$  values shows a substantial influence of, on the one hand, the force constants (the range of variation of  $E_{\text{co}}$  is  $64$ – $83 \text{ kJ mol}^{-1}$ ) and, on the other hand, the parameter  $r_e$ .

### 7.5.7. Triplet repulsion in addition reactions

The activation energy of radical abstraction is influenced by the so-called triplet repulsion in the transition state. This influence is manifested in the fact that the stronger the  $\text{X}-\text{R}$  bond towards which the hydrogen atom moves in the thermally neutral reaction  $\text{X}\cdot + \text{RH}$ , the higher the activation energy of this reaction. The triplet repulsion is due to the fact that three electrons cannot be accommodated in the bonding orbital of  $\text{X}-\text{C}$ ; therefore, one electron occupies the non-bonding  $\text{X}-\text{C}$  orbital. Meanwhile, the stronger the  $\text{X}-\text{C}$  bond, the higher the energy of the non-bonding orbital and the higher the activation energy of abstraction. How do matters stand with radical addition? Comparison of  $E_{\text{co}}$  and  $r_e$  with the energy of dissociation of the resulting bond  $D_e$  has shown that this influence certainly does exist. The parameters  $E_{\text{co}}$  and  $r_e$  are juxtaposed with the dissociation energy of the bond formed  $D_e(\text{X}-\text{C})$  in Table 7.7. For reactions of one class, namely,  $\text{X}\cdot + \text{CH}_2=\text{CHY}$ , the linear correlation  $E_{\text{co}} = \text{const} [D_e(\text{X}-\text{C})]^2$  holds;  $\text{const} = 5.95 \cdot 10^4 \text{ mol kJ}^{-1}$ . The following correlation was found to be fulfilled for reactions of all the thirteen classes considered:

$$r_e = (0.98 \cdot 10^{13} / \text{m mol kJ}^{-1}) \times D_e(\text{X}-\text{C}) \quad (7.25)$$

This correlation should be regarded as an empirical proof of the fact that the non-bonding orbital of the bond being formed actually does participate in the generation of the activation energy of addition. The stronger this bond, the higher the energy of the non-bonding orbital and the higher the activation energy. Empirical correlation

(7.7) can be used to estimate roughly the activation energies of diverse addition reactions.

Table 7.7. Parameters of various classes of radical addition ( $E_{co}$ ,  $r_e$ ) and strengths of the bonds formed

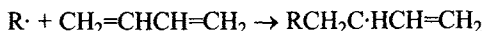
Reaction	$E_{co}$ kJ mol <sup>-1</sup>	$r_e \times 10^{11}$ , m	$D_e(X-C)$ , kJ mol <sup>-1</sup>	$\frac{r_e}{D_e(X-C)} \times 10^{13}$ m · kJ mol <sup>-1</sup>
H· + CH <sub>2</sub> =CHR	101.6	4.563	439	1.04
D· + CH <sub>2</sub> =CHR	99.6	4.557	439	1.04
Cl· + CH <sub>2</sub> =CHR	50.5	3.427	357	0.96
Br· + CH <sub>2</sub> =CHR	31.2	2.949	299	0.99
N.H· + HC≡CR	125.2	4.608	462	1.00
H· + O=CR <sup>1</sup> R <sup>2</sup>	102.9	4.402	459	0.96
C·H <sub>3</sub> + CH <sub>2</sub> =CHR	82.6	3.713	378	0.98
Me <sub>2</sub> C·H + CH <sub>2</sub> =CHR	78.3	3.617	372	0.97
Me <sub>3</sub> C· + CH <sub>2</sub> =CHR	68.3	3.377	360	0.94
C <sub>6</sub> H <sub>5</sub> · + CH <sub>2</sub> =CHR	105.3	4.194	436	0.96
N·H <sub>2</sub> + CH <sub>2</sub> =CHR	62.1	3.53	360	0.98
RO· + CH <sub>2</sub> =CHR	65.2	3.617	359	1.01
R· + O=CR <sup>1</sup> R <sup>2</sup>	68.1	3.540	365	0.97

#### 7.5.8. Influence of neighboring bonds on the activation energy of radical addition

Radical abstraction reactions that involve molecules with  $\pi$ -bonds in the vicinity of the reaction center are characterized by higher  $E_{co}$  values than the corresponding reactions involving similar hydrocarbons without these bonds. This is due to triplet repulsion. In these reactions, the three electrons of the reaction center interact with the neighboring  $\pi$ -electrons; as a consequence, the energy of the non-bonding orbital in the transition state increases and, hence, the activation energy also increases. Do neighboring  $\pi$  bonds influence the  $E_{co}$  values of radical addition? In order to answer this question, let us compare the  $b_{re}$  and  $E_{co}$  parameters for the addition of hydrogen atom to the monomers CH<sub>2</sub>=CHY and monomers with double bonds in the  $\alpha$ -position relative to the double bond being attacked. If the monomer contains an aromatic ring or a double bond in the  $\alpha$ -position, the activation energy of a thermally neutral reaction increases; if there are two aromatic rings in the  $\alpha$ -position,  $E_{co}$  increases to even a greater extent (Table 7.8). The difference between  $E_{co}(\pi)$  and  $E_{co}(\text{CH}_2=\text{CHY})$  can be used to evaluate the contribution of this factor to the activation barrier

$$\Delta E(\pi) = E_{co}(\pi) - E_{co}(\text{CH}_2=\text{CHY}) \quad (7.26)$$

Triplet repulsion also manifests itself in the reactions in question; for example, in the reaction



a multicenter multielectron  $R\cdots C\cdots C\cdots C$  bond arises in the transition state; this increases the strength of the bond, and, hence, enhances the triplet repulsion and its contribution to the activation energy. It can be seen from the data of Table 7.8 that this contribution can reach  $20 \text{ kJ mol}^{-1}$ . The increase in the dissociation energy  $D_e(X-C)$  caused by this electron delocalization can be estimated using relation 7.16.

Table 7.8. Influence of a  $\pi$ -bond adjacent to the reaction center on the activation energy of the radical addition to alkenes

Reaction ( $\text{kJ mol}^{-1}$ ) <sup>1/2</sup>	$br_e$ $\text{kJ mol}^{-1}$	$E_{co}$ $\text{kJ mol}^{-1}$	$\Delta E_\pi$ $\text{kJ mol}^{-1}$	$\Delta D_e(\pi)$ $\text{kJ mol}^{-1}$
$H\cdot + CH_2=CHR$	24.59	101.6	0	0
$H\cdot + CH_2=CHPh$	25.85	112.2	10.6	24.1
$H\cdot + CH_2=CPh_2$	26.47	117.7	16.1	36.0
$H\cdot + 1,3\text{-cyclo-C}_6\text{H}_8$	26.47	117.7	16.1	36.0
$H\cdot + CH_2=CHCN$	25.45	108.8	7.2	16.4
$C\cdot H_3 + CH_2=CHR$	20.01	82.6	0	0
$C\cdot H_3 + CH_2=CHPh$	20.82	89.4	6.8	15.5
$C\cdot H_3 + CH_2=CMePh$	20.67	88.7	6.1	12.6
$C\cdot H_3 + CH_2=CPh_2$	21.33	94.4	11.8	25.2
$C\cdot H_3 + CH_2=CHCH=CH_2$	20.88	89.9	7.3	16.6
$C\cdot H_3 + MeCH=CHCH=CHMe$	21.15	92.2	9.6	21.8
$C\cdot H_3 + CH_2=CMeCMe=CH_2$	21.03	91.2	8.6	19.5
$C\cdot H_3 + 1,3\text{-cyclo-C}_6\text{H}_8$	22.27	102.3	19.7	43.2
$C\cdot H_3 + 1,4\text{-cyclo-C}_6\text{H}_8$	22.23	101.9	19.3	42.5
$N\cdot H_2 + CH_2=CHR$	18.82	61.0	0	0
$N\cdot H_2 + (E)\text{---}CH_2=CHCH=CH_2$	20.52	72.5	10.4	23.7
$RO\cdot + CH_2=CHR$	19.49	61.8	0	0
$RO\cdot + CH_2=CHPh$	21.09	76.4	14.6	30.6
$RO_2\cdot + CH_2=CHR$	26.04	90.5	0	0
$RO_2\cdot + CH_2=CHPh$	27.23	99.0	8.5	22.8
$RO_2\cdot + CH_2=CPh_2$	28.04	105.0	14.5	38.3

$R_3Si\cdot + CH_2=CHR$	26.46	76.6	0	0
$R_3Si\cdot + CH_2=CHPh$	28.52	89.0	12.4	27.9
$R_3Si\cdot + O=CR^1R^2$	37.62	114.5	0	0
$R_3Si\cdot + O=CMePh$	39.74	127.6	13.1	22.5
$R_3Si\cdot + O=CPh_2$	40.02	129.3	14.8	25.5

The same trend is observed for the addition of the benzyl radical to the monomers  $CH_2=CRY$ .

R	Y	$br_e/(kJ/mol)^{1/2}$	$E_{eo}/kJ\ mol^{-1}$
Me	OMe	24.98	128.7
H	OEt	24.85	127.8
H	Ph	24.88	127.7
Me	Ph	24.93	128.2

The average  $E_{eo}$  value for these reactions is  $128.0\ kJ\ mol^{-1}$ , respectively; the value for the addition of methyl radical is  $82.6\ kJ\ mol^{-1}$ . The greater  $E_{eo}$  value found in the case of the addition of benzyl radicals points to stronger triplet repulsion caused by electron delocalization.

The substantial influence of the  $\pi$ -bonds located near the reaction center on the activation energy can also be followed for the addition of methyl radicals to the  $C=O$  group in *p*-benzoquinone. This can be clearly seen when comparing the corresponding parameters for the addition of a methyl radical to acetone and to *p*-benzoquinone.

$R^1C(O)R^2$	$br_e/(kJ/mol)^{1/2}$	$E_{eo}/kJ\ mol^{-1}$	$10^{11}r_e/m$
MeC(O)Me	21.95	68.1	3.54
OC <sub>6</sub> H <sub>4</sub> O	23.15	81.1	3.86

The observed difference in the parameters is due most likely to the electron delocalization in the aromatic ring and, hence, to the increase in the triplet repulsion. The difference between the  $E_{eo}$  values for the reactions considered amounts to  $13\ kJ\ mol^{-1}$ . For the addition of polystyrene radical to *p*-benzoquinone,  $br_e = 25.03\ (kJ/mol)^{1/2}$  and  $E_{eo} = 94.8\ kJ\ mol^{-1}$ . In this case, the  $E_{eo}$  value is  $26.7\ kJ\ mol^{-1}$  greater than that for the reaction of the methyl radical with acetone. The very large  $\Delta E(\pi)$  value can be accounted for by the interaction of the electrons of the two neighboring benzene rings with the reaction center. With allowance for the examples considered above, correlation (7.15) can be extended and written in the following form:

$$r_e = (0.98 \times 10^{13} / m\ mol\ kJ^{-1}) \times [D_e(X-C) + \Delta E(\pi)] \quad (7.27)$$

### 7.5.9. Role of the radius of the atom bearing the free valence

The greater the radius of the atom carrying the free valence, the higher the  $E_{\text{eo}}$  for radical abstraction. Does the radius of the atom which attacks the double bond influence the activation energy of addition reactions? This question was answered as a result of analysis of experimental data on the addition of triethylsilyl and phenylthiyl radicals to alkenes.

Since the strength of the C—X ( $D_e$ ) bond being formed influences the parameter  $r_e$  (see Eq. (7.25), the characteristic to be compared for the addition of various radicals to alkenes is the  $r_e/D_e$  ratio (Table 7.9). The lengths  $r(\text{C—X})$  of the bonds formed upon the addition of radicals such as  $\text{CH}_3\cdot$  and  $\text{RO}\cdot$  to the C=C bond and upon the addition of  $\text{CH}_3\cdot$  to the C=O bond are close; therefore, the ratio  $r_e/D_e = \text{const}$ . However, in the case of addition of  $\text{PhS}\cdot$  and  $\text{R}_3\text{Si}\cdot$  to the C=C bond, the  $r_e/D_e$  ratio is much greater and a linear correlation is observed between  $r_e/D_e$  and  $r(\text{C—X})$ . The correlation has the following form:

$$r_e = (8.81 \times 10^4 / \text{mol kJ}^{-1}) - [r(\text{X—C}) - 0.42 \cdot 10^{10} \text{m}](D_e / \text{kJ mol}^{-1}) \quad (7.28)$$

Thus, the radius of the atom carrying the free valence has a substantial influence on the activation barrier to the addition reaction: the greater the radius of this atom, the higher the activation energy. Apparently, this effect is due to repulsion in the transition state, the repulsion being due to the interaction between the electron shells of the double bond being attacked and the atom which attacks this bond.

Table 7.9. Strengths ( $D_e/\text{kJ mol}^{-1}$ ) and lengths ( $r(\text{C—X})$  or  $r(\text{O—X})/\text{m}$ ) of the bonds formed upon the addition of  $\text{X}\cdot$  radicals to C=C or C=O double bonds

X	$D_e/\text{kJ mol}^{-1}$	$10^{10} r(\text{C—X}), \text{ or } 10^{10} r(\text{O—X})/\text{m}$	$10^{11} r_e/\text{m}$	$10^{11} r_e/D_e / \text{m mol kJ}^{-1}$
Reaction: $\text{X}\cdot + \text{CH}_2=\text{CHY} \rightarrow \text{XCH}_2\text{CHY}$				
$\text{C}^{\text{H}}\text{H}_3$	378	1.52	3.71	0.98
$\text{N}^{\text{H}}\text{H}_2$	360	1.47	3.53	0.98
$\text{RO}^{\text{H}}$	359	1.43	3.62	1.01
$\text{RS}^{\text{H}}$	284	1.79	3.41	1.20
$\text{R}_3\text{Si}^{\text{H}}$	378	1.89	4.91	1.30
Reaction: $\text{X}\cdot + \text{O}=\text{CR}^1\text{R}^2 \rightarrow \text{XOC}\cdot\text{R}^1\text{R}^2$				
$\text{C}^{\text{H}}\text{H}_3$	365	1.43	3.54	0.97
$\text{R}_3\text{Si}^{\text{H}}$	487	1.64	6.28	1.20

### 7.5.10. Interaction of two polar groups

The polar effect involved in radical addition has been repeatedly discussed in the scientific literature. The parabolic model opens up new prospects for the correct estimation of the polar effect. It permits one to determine the contribution of this effect to the activation energy using experimental data. This contribution ( $\Delta E_\mu$ ) is estimated by choosing a reference reaction which involves the same reaction center but in which one or both reactants are nonpolar. The reference reaction is characterized by the parameter  $br_e$  and the reaction with two polar reactants is characterized by the parameter  $(br_e)_\mu$ . The component of the activation energy caused by polar interaction ( $\Delta E_\mu$ ) is calculated from the equation

$$\Delta E_\mu = [(br_e)^2 - (br_e)_\mu^2](1 + \alpha)^{-2} \quad (7.29)$$

Table 7.10 presents the results of calculation of  $\Delta E_\mu$  for the reactions of six polar radicals with a number of polar monomers. It can be seen that the polar interaction in the transition states for the addition can either decrease ( $\Delta E_\mu < 0$ ) or, in other cases, increase ( $\Delta E_\mu > 0$ ) the activation energy. The  $\Delta E_\mu$  values vary from +19.5 to -23 kJ mol<sup>-1</sup>, *i.e.*, they can be rather large.

Table 7.10. Contribution of the polar effect ( $\Delta E_\mu$ /kJ mol<sup>-1</sup>) to the activation energy of the addition of polar radicals to polar monomers CH<sub>2</sub>=CRY (calculated from the data of several studies)

X, Y	Radical					
	Me <sub>2</sub> (HO)C·	Me <sub>2</sub> (CN)C·	Me <sub>3</sub> COC(O)C·H <sub>2</sub>	<i>sec</i> -RO <sub>2</sub> ·	<i>tert</i> -RO <sub>2</sub> ·	HO <sub>2</sub> ·
H, EtO	-1.9	-4.9	13.2	-	-	-
Me, MeO	-6.5	-9.4	10.1	-	-	-
H, AcO	-15.1	-11.2	17.5	9.5	7.3	11.5
Me, AcO	-16.4	-4.3	19.5	-	-	-
Me, Cl	-8.2	-4.4	10.8	-	-	-
Cl, Cl	-10.2	-3.8	13.4	-	-	-
H, C(O)OMe	-20.1	-1.4	13.1	-0.3	-2.0	-
Me, C(O)OMe	-	-3.4	-	-5.2	-6.4	-4.7
H, CN	-23.2	-0.9	13.8	-9.0	-10.8	-7.9

### 7.5.11. Multidipole interaction in addition reactions

The multidipole interaction in a bimolecular reaction arises if one or both reactants contain several polar groups. The multidipole effect shows itself as a deviation of the rate constant for the addition of a polar radical to a polyfunctional compound (calculated in relation to one reaction center) from the rate constant for the addition to a monofunctional compound. The multidipole effect was discovered for radical

abstraction of a hydrogen atom from polyfunctional esters induced by peroxy radicals. Later, this effect has also been found in the addition of peroxy radicals to the double bonds of polyatomic unsaturated esters. Table 7.11 summarizes the results of calculations of the contribution of the multidipole effect to the activation energy performed using relation (7.19). A monofunctional ester of the corresponding structure served as the reference compound. It can be seen that the role of the multidipole interaction in these reactions is fairly low: the contribution of the interaction of several polar groups  $\Delta\Delta E_\mu$  varies from 0.8 to 2.3 kJ mol<sup>-1</sup>.

Table 7.11. Multidipole effect in the addition of cumylperoxy radicals to unsaturated polyatomic esters ( $n$  is the number of reacting double bonds in the ester molecule)

Ester	$k$ (323 K), l mol <sup>-1</sup> s <sup>-1</sup>	$k/n$ , l mol <sup>-1</sup> s <sup>-1</sup>	$\Delta\Delta E_\mu$ , kJ mol <sup>-1</sup>
CH <sub>2</sub> =CHCOOMe	0.50	0.50	0
(CH <sub>2</sub> =CHCOOCH <sub>2</sub> ) <sub>2</sub> CMe <sub>2</sub>	0.76	0.38	0.8
(CH <sub>2</sub> =CHCOOCH <sub>2</sub> ) <sub>2</sub> CHOCOCH=CH <sub>2</sub>	1.05	0.35	1.0
(CH <sub>2</sub> =CHCOOCH <sub>2</sub> ) <sub>4</sub> C	1.28	0.32	1.2
CH <sub>2</sub> =CMeCOOMe	1.79	1.79	0
(CH <sub>2</sub> =CMeCOOCH <sub>2</sub> ) <sub>2</sub> CHOCOMeC=CH <sub>2</sub>	3.93	1.31	0.9
(CH <sub>2</sub> =CMeCOOCH <sub>2</sub> ) <sub>4</sub> C	3.08	0.77	2.3

The multidipole effect is also manifested in the addition of chlorine atoms to chloroalkenes. The scope of influence of this factor on the activation energy of these reactions can be judged from the data given in Table 7.12. The interaction of a polar reaction center with one polar C—Cl group increases the activation energy by 17 kJ mol<sup>-1</sup>, whereas the interaction with several polar C—Cl groups, conversely, results in a lower activation energy.

Table 7.12. Parameters  $br_c$ ,  $\Delta E_\mu$ , and  $\Delta\Delta E_\mu$  for the addition of chloride atom to chloroalkenes

Alkene	$br_c$ (kJ mol <sup>-1</sup> ) <sup>1/2</sup>	$\Delta E_\mu$ kJ mol <sup>-1</sup>	$-\Delta\Delta E_\mu$ kJ mol <sup>-1</sup>
CH <sub>2</sub> =CHCl	21.23	17.0	0.0
<i>cis</i> -CHCl=CHCl	20.43	11.4	5.6
CH <sub>2</sub> =CCl <sub>2</sub>	19.64	6.6	10.4
CCl <sub>2</sub> =CHCl	20.50	11.8	5.2
CCl <sub>2</sub> =CCl <sub>2</sub>	19.46	5.6	11.4

### 7.5.12. Steric hindrance

The addition of trialkylsilyl radicals to 1,2-disubstituted ethylene derivatives is subject to a steric effect. This shows itself in the  $E_{\infty}$  value for the  $\text{Et}_3\text{Si}\cdot$  addition to  $\text{RCH}=\text{CHR}$  being greater than that for the addition of the same radical to  $\text{CH}_2=\text{CHR}$ . The contribution of steric repulsion to the activation energy can be characterized by the increment  $\Delta E_{\text{S}}$

Alkene	$br_{\text{f}}/(\text{kJ/mol})^{1/2}$	$E_{\infty}/\text{kJ mol}^{-1}$	$\Delta E_{\text{S}}/\text{kJ mol}^{-1}$
$\text{CH}_2=\text{CHR}$	26.46	76.6	0.0
$\text{RCH}=\text{CHR}$	27.54	83.0	6.4

No effect of this type is manifested for the addition of alkyl radicals to the same alkenes. Evidently, the steric effect involved in the addition of trialkylsilyl radicals to 1,2-disubstituted ethylene derivatives is due to the repulsion between the carbon and silicon atoms, caused by the large size of the silicon atom, in the reaction center of the transition state.

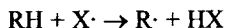
The addition of tris(*tert*-butyl)phenoxy radical to styrene can serve as an example of reaction subject to the steric effect. This reaction is characterized by  $br_{\text{f}}/(\text{kJ/mol})^{1/2} = 23.89$ , whereas the addition of the *tert*-butoxy radical to styrene (a reaction with a similar structure of the reaction center) has the parameter  $br_{\text{f}}/(\text{kJ/mol})^{1/2} = 21.09$ . The difference between these values is matched by the difference between the activation energies of the corresponding thermally neutral reactions,  $E_{\infty} = 21.6 \text{ kJ mol}^{-1}$ ; this can be regarded as a rough estimate of the energy of additional repulsion in the transition state of the reacting system. This repulsion in the transition state is brought about by two *tert*-butyl groups of the phenoxy radical.

### 7.6. Radical abstraction reactions

A simplified model of an elementary bimolecular reaction, the intersecting parabolas model (the parabolic model), was used in the analysis of the activation energies for a wide variety of radical abstraction reactions. This model can be regarded as a further development of the empirical approach initiated in the studies of Polanyi and Semenov. As a result, it became possible to separate diverse radical abstraction reactions into classes and to differentiate in each class groups of isotypical reactions. Each reaction is described by two parameters referring to the entire given class of reactions: one parameter, characteristic of the group of reactions, and one individual parameter, namely the enthalpy of reaction, characteristic of the given reaction. The creation of a hierarchical system of reactions made it possible to identify at an empirical level the physical characteristics of the reactants determining the height of the activation barrier.

### 7.6.1. Intersecting parabolas model

In the parabolic model, the radical abstraction reaction



in which a hydrogen atom is transferred from the initial (RH) to the final (XH) molecule, is regarded as the result of the intersection of two potential curves, one of which describes the potential energy  $U_i(r)$  of the vibration of the H atom along the bond being dissociated in the initial molecule and the other describes the potential energy  $U_f(r)$  of the vibration of the same atom along the bond being formed in the reaction product ( $U$  is the potential energy and  $r$  the amplitude of the atomic vibrations along the valence bond). The stretching vibrations of the H atom in RH and XH are regarded as harmonic and are described by the parabolic law

$$U(r)^{1/2} = br \quad (7.30)$$

The following parameters are used to characterize the elementary step in the parabolic model.

1. The enthalpy of reaction  $H_e$  which includes the difference between the zero-point energies of the broken and generated bonds:

$$\Delta H_e = D_i - D_f + 0.5hL(v_i - v_f) \quad (7.31)$$

where  $D_i$  and  $D_f$  are the dissociation energies of the cleaved (i) and generated (f) bonds,  $v_i$  and  $v_f$  are the stretching vibration frequencies of these bonds,  $h$  is the Planck constant, and  $L$  is Avogadro's number. The activation energy  $E_e$ , which is linked to the experimentally determined Arrhenius energy  $E$  by the relation

$$E_e = E + 0.5(hLv_i - RT) \quad (7.32)$$

2. The coefficients  $b_i$  and  $b_f$ , which describe the dependence of the potential energy on the atomic vibration amplitude along the initial (i) and final (f) valence bonds. There is a parabolic relation between the potential energy and the vibration amplitude.

3.

$$U_i = b_i^2 r^2 \quad \text{and} \quad U_f = b_f^2 (r_e - r) \quad (7.33)$$

The quantity  $2b^2$  is the force constant of the corresponding bond with  $b = \pi v(2\mu)^{1/2}$ , where  $\mu$  is the reduced mass of the atoms forming the bond.

4. The distance  $r_e$ , which characterizes the displacement of the abstracted atom in the elementary step.

In the parabolic model, these parameters are linked by the relation

$$br_e = \alpha(E_e - \Delta H_e)^{1/2} + E_e^{1/2} \quad (7.34)$$

where  $b = b_i$ , *i.e.*, refers to the attacked bonds in the molecule, while the coefficient  $\alpha = b_i/b_f$  represents the ratio of the force constants of the ruptured and generated bonds raised to the power 1/2. In the case of structurally isotypical reactions ( $br_e = \text{const}$ ), a thermally neutral reaction ( $\Delta H_e = 0$ ) proceeds with an activation energy  $E_{eo}$ , which is determined by two parameters, namely  $b$  and  $br_e$ :

$$E_{eo} = (br_e)^2 (1 + \alpha)^2 = [b_i b_f r_e / (b_i + b_f)]^2 \quad (7.35)$$

On substituting the parameter  $br_e$  in Eq. (7.35) by its value from Eq. (7.34), we obtain

$$(1 + \alpha) E_{eo}^{1/2} = (E_e - \Delta H_e)^{1/2} + E_e^{1/2} \quad (7.36)$$

Comparison of Eqs. (7.34) and (7.35) makes it possible to understand the kinetic significance of the parameter  $br_e$ : it is directly proportional to the activation energy for a thermally neutral reaction raised to the power 1/2. The transition state in the parabolic model is characterized by the distance  $r^\#$ , which is linked to the other parameters by the relation

$$r^\# / r_e = E_e^{1/2} / br_e = [1 + \alpha(1 - \Delta H_e / E_e)]^{-1} \quad (7.37)$$

In the case of a thermally neutral reaction with  $\alpha = 1$ , *i.e.*, when the force constants of the attacked and generated bonds are equal,  $r^\#$  is equal to half the distance  $r_e$ . In the general case,

$$(r^\# / r_e)_0 = (1 + \alpha)^{-1} \quad (7.38)$$

The parabolic model is in essence empirical, since the parameter  $b$  is calculated from spectroscopic ( $\nu_i$  and  $\nu_f$ ) and atomic ( $\mu_i$  and  $\mu_f$ ) data, while the parameter  $br_e$  (or  $E_{eo}$ ) is found from the experimental activation energies  $E$  (Eqs. (7.34) and (7.35)) or *via* the rate constant  $k$  by the Arrhenius equation

$$E = RT \ln(A/k)^{-1} \quad (7.39)$$

where  $A$  is the pre-exponential factor typical of such reactions. The enthalpy of such reaction is calculated by Eq. (7.31) from the experimental bond dissociation energies. The calculations showed that  $br_e = \text{const}$  for structurally similar reactions.

### 7.6.2. Classification of radical abstraction reactions

The bond dissociation energy is an individual characteristic of the molecule entering into the reaction or formed. The force constants for the stretching vibration of bonds ( $2\pi^2\nu^2\mu$ ) of each type (C—H, O—H, *etc.*) are virtually identical for the entire class of isotypical compounds. This important factor makes it possible to classify radical abstraction reactions in terms of the type of reacting bonds and the coef-

ficients  $b$  characterizing them. A pair of coefficients,  $b_i$  and  $b_f$  or  $b = b_i$  and the coefficient corresponds to each class of such reactions. In the calculation of the activation energy  $E_e$  from  $E$  and conversely, the zero-point vibration energy of the ruptured bond also becomes important (see Eq. (7.32)). The quantities  $\alpha$ ,  $\beta$ , and  $0.5hLv_i$  for the radical abstraction reactions of compounds in different classes are listed in Table 7.13.

Table 7.13. Kinetic parameters of radical abstraction reactions of different classes. Here and henceforth AmH is amine, AmOH is hydroxylamine, Am $\cdot$  is aminyl radical, and AmO $\cdot$  is nitroxyl radical.

Reaction	$\alpha$ (kJ mol <sup>-1</sup> ) <sup>1/2</sup>	$b \cdot 10^{11}$ kJ mol <sup>-1</sup>	$0.5hLv_i$ kJ mol <sup>-1</sup>	$0.5hL(v_i - v_f)$	$(r^\#/r_e)_0$
H $\cdot$ + H <sub>2</sub>	1.00	4.133	26.3	0.0	0.500
H $\cdot$ + HCl	0.953	3.937	17.9	-8.4	0.488
H $\cdot$ + HBr	0.851	3.516	15.2	-11.1	0.460
H $\cdot$ + HI	0.743	3.072	13.8	-12.5	0.426
H $\cdot$ + RH	0.906	3.743	17.4	-8.9	0.475
H $\cdot$ + NH <sub>3</sub>	1.042	4.306	20.0	-6.3	0.510
H $\cdot$ + HOCH <sub>3</sub>	1.137	4.701	21.7	-4.6	0.532
H $\cdot$ + HSiR <sub>3</sub>	0.668	2.756	12.6	-13.6	0.400
H $\cdot$ + H <sub>2</sub> S	0.831	3.434	15.6	-10.7	0.454
HO $\cdot$ + CH <sub>4</sub>	0.790	3.743	17.4	-4.4	0.441
HO $\cdot$ + NH <sub>3</sub>	0.908	4.306	20.0	-1.8	0.472
HO $\cdot$ + HOCH <sub>3</sub>	0.992	4.701	21.7	-0.1	0.498
HO $\cdot$ + SiH <sub>4</sub>	0.591	2.861	13.1	-8.7	0.372
HO $\cdot$ + HS <sub>2</sub>	0.724	3.434	15.6	-6.2	0.420
R $\cdot$ + R'H	1.00	3.743	17.4	0.0	0.500
R $\cdot$ + H <sub>2</sub> NR'	1.207	4.517	20.9	3.5	0.547
R $\cdot$ + HSiR' <sub>3</sub>	0.723	2.756	12.6	-4.8	0.420
R $\cdot$ + HSR'	0.808	3.026	13.8	-3.6	0.447
RO $\cdot$ + RH	0.796	3.743	17.4	-4.3	0.443
RO $\cdot$ + HSiR' <sub>3</sub>	0.581	2.756	12.6	-9.1	0.3668
RO <sub>2</sub> $\cdot$ + RH	0.814	3.743	17.4	-3.8	0.449
RO <sub>2</sub> $\cdot$ + HOOR	1.00	4.600	21.2	0.0	0.500
RO <sub>2</sub> $\cdot$ + HOAr	1.00	4.665	21.5	0.3	0.500
RO <sub>2</sub> $\cdot$ + HOAm	1.00	4.665	21.5	0.3	0.500

Knowing these parameters, it is easy to find the analogous characteristics of the reverse reactions. For a reverse reaction, to which the index  $f$  corresponds, we have  $\alpha_f = \alpha^{-1}$ ,  $b_f = b/\alpha$ , and  $0.5hLv_f = 0.5hLv_i/\alpha$ .

The class of radical abstraction reactions may include a single reaction (for exam-

ple,  $H + HCl$ ), one group of reactions (for example,  $R\cdot + NH_3$ , where  $R\cdot$  is any alkyl radical), or several such groups (for example, the class of reactions  $RO\cdot + R'H$ , where  $R'H$  is a hydrocarbon, consists of three groups of reactions:  $RO\cdot + HR^1$ ,  $RO\cdot + HR^2$ , and  $RO\cdot + HR^3$ , where  $R^1H$ ,  $R^2H$ , and  $R^3H$  are any aliphatic, unsaturated, and aromatic alkyl-substituted hydrocarbons respectively. All the reactions belonging to one group are characterized by a single parameter  $r_e$  or  $br_e$ . The quantities  $br_e$  calculated on the basis of parabolic model for reactions  $RO\cdot + HR^1$  involving aliphatic hydrocarbons having different structures are very close; the average values of  $br_e$  for reaction  $RO\cdot + HR^1$  is equal  $15.30 \pm 0.59$  (kJ/mol)<sup>1/2</sup>. The quantity  $A$  calculated per reacting C—H bond is  $10^9$  l mol<sup>-1</sup> s<sup>-1</sup> for the liquid phase and  $2 \cdot 10^8$  l mol<sup>-1</sup> s<sup>-1</sup> for the gas phase. Knowing the parameter  $br_e$ , it is possible to calculate an important characteristic of the reactivity of each group of reactions such as the activation energy for a thermally neutral reaction  $E_{co}$  (Eq. (7.35)). The energies  $E_{co}$  may differ significantly for reactions of different classes. Thus, the following values were obtained (kJ mol<sup>-1</sup>) for reactions involving aliphatic hydrocarbons  $R^1H$ :

Reaction:	$H\cdot + R^1H$	$R\cdot + R^1H$	$RO_2\cdot + R^1H$	$RO_2\cdot + ArOH$
$E_{co}$ ,	64.8	68.2	58.1	45.3

The classification of radical reactions carried out in this way makes it possible to observe empirically (on the basis of the parameter  $br_e$ ) structural differences between reactants within one class, to compare the classes and groups of reactions in terms of reactivity (in terms of the parameter  $br_e$  or  $E_{co}$ ), and to identify the physical and structural factors determining the reactivities of groups of reactants.

The activation energy for any individual reaction within the limits of the given group of reactions may be calculated correctly from the parameter  $br_e$ . Within the framework of the parabolic model, the quantity  $E_e$  was calculated by the following formula

(1) for  $\alpha = 1$ ,

$$E_e^{1/2} = 0.5br_e + \Delta H_e/2br_e \quad (7.40)$$

(2) for  $\alpha \neq 1$

$$E_e^{1/2} = br_e (1 - \alpha^2)^{-1} \{ 1 - \alpha [1 - (1 - \alpha^2)(br_e)^{-2} \Delta H_e]^{1/2} \} \quad (7.41)$$

(3) for  $\Delta H_e(1 - \alpha^2) \ll (br_e)^{-2}$

$$E_e^{1/2} = br_e(1 + \alpha)^{-1} + \alpha \Delta H_e/2br_e \quad (7.42)$$

### 7.6.3. Dissociation energies and force constants of the attacked and generated bonds

A clear-cut dependence of the activation energy on the heat (enthalpy) of reac-

tion, which is equal in its turn to the difference between the dissociation energies of the ruptured ( $D_i$ ) and formed ( $D_f$ ) bonds, was established for radical abstraction reactions. In parabolic model the values of  $D_{ei}$  and  $D_{ef}$ , incorporating the zero-point energy of the bond vibrations, are examined. The enthalpy of reaction  $\Delta H_e$  therefore also includes the difference between these energies (see Eq.7.31).

As noted above, all radical abstraction reactions can be divided into groups and the activation energy  $E_{eo}$  for a thermally neutral reaction can be calculated in each group. The possibility of calculating the activation energy for any reaction of the given series (group) from the value of  $E_{eo}$  (or  $br_e$ ) and of estimating the contribution of the enthalpy to the activation energy follows from this important factor. This contribution ( $\Delta E_H$ ) represents the difference between the activation energies for the given ( $i$ th) reaction and a thermally neutral reaction characterized by the quantity  $E_{eo}$

$$\Delta E_H = E_{ei} - E_{eo} \quad (7.43)$$

As an example, Table 7.14 presents the values of  $\Delta E_H$  for the reactions of peroxy radicals with antioxidants of different classes. It follows from the table that the ratio  $\Delta E_H/\Delta H$  for these groups of reactions is close to 1/2.

Table 7.14. Contributions of the enthalpy  $\Delta E_H$  to the activation energy  $E$  for the reactions of a secondary peroxy radical with various inhibitors YH ( $\Delta H$ ,  $E$ , and  $\Delta E_H$  in  $\text{kJ mol}^{-1}$ )

YH	$\Delta H$ , $\text{kJ mol}^{-1}$	$E$ , $\text{kJ mol}^{-1}$	$\Delta E_H$ , $\text{kJ mol}^{-1}$
$\text{C}_6\text{H}_5\text{OH}$	1.5	25.9	0.7
$4\text{-CH}_3\text{C}_6\text{H}_4\text{OH}$	-7.7	21.4	-3.8
$4\text{-CH}_3\text{OC}_6\text{H}_4\text{OH}$	-16.5	17.3	-7.9
$4\text{-C}_6\text{H}_5\text{CH}_2\text{C}_6\text{H}_4\text{OH}$	-18.0	16.6	-8.6
$4\text{-CH}_3\text{COC}_6\text{H}_4\text{OH}$	4.0	27.2	2.0
$2,3\text{-(CH}_3)_2\text{C}_6\text{H}_3\text{OH}$	-12.0	19.4	-5.8
$1\text{-HOC}_{10}\text{H}_7$	-24.1	13.9	-11.3
$2,6\text{-}[(\text{CH}_3)_3\text{C}]_2\text{-C}_6\text{H}_3\text{OH}$	-18.8	22.8	-8.9
$2,6\text{-}[(\text{CH}_3)_3\text{C}]_2\text{-4-CH}_3\text{C}_6\text{H}_2\text{OH}$	-26.5	19.3	-12.4
$2,6\text{-}[(\text{CH}_3)_3\text{C}]_2\text{-4-CH}_3\text{OC}_6\text{H}_2\text{OH}$	-34.8	15.8	-15.9
$2,6\text{-}[(\text{CH}_3)_3\text{C}]_2\text{-4-C}_6\text{H}_5\text{CH}_2\text{C}_6\text{H}_2\text{OH}$	-27.8	18.8	-12.9
$2,6\text{-}[(\text{CH}_3)_3\text{C}]_2\text{-4-C}_6\text{H}_5\text{SC}_6\text{H}_2\text{OH}$	-19.1	22.6	-9.1
$\text{Si}[2,6\text{-}[(\text{CH}_3)_2\text{C}]_2\text{-4-CH}_2\text{CH}_2\text{OC}_6\text{H}_2\text{OH}]_4$	-24.6	20.2	-11.5
$(\text{C}_6\text{H}_5)_2\text{NH}$	-0.8	12.0	-1.5
$(4\text{-CH}_3\text{C}_6\text{H}_4)_2\text{NH}$	-14.9	5.7	-7.8
$(4\text{-CH}_3\text{OC}_6\text{H}_4)_2\text{NH}$	-24.3	1.8	-11.7
$4\text{-CH}_3\text{OC}_6\text{H}_4\text{NHC}_6\text{H}_5$	-18.3	4.2	-9.3
$1\text{-C}_{10}\text{H}_7\text{NHC}_6\text{H}_5$	-13.6	6.2	-7.3

4-C <sub>6</sub> H <sub>5</sub> NHC <sub>6</sub> H <sub>4</sub> NHC <sub>6</sub> H <sub>5</sub>	-18.6	4.1	-9.4
[(CH <sub>3</sub> ) <sub>3</sub> C] <sub>2</sub> C=NOH	-27.0	27.1	-12.7
C <sub>6</sub> H <sub>5</sub> CH=CHC(O)N(OH)C(CH <sub>3</sub> ) <sub>3</sub>	-44.1	19.8	-20.0
C(CH <sub>3</sub> ) <sub>2</sub> CH <sub>2</sub> CHOHCH <sub>2</sub> C(CH <sub>3</sub> ) <sub>2</sub> N(OH)	-63.3	12.4	-27.4
C <sub>6</sub> H <sub>5</sub> SH	-37.1	11.9	-15.0
4-CH <sub>3</sub> C <sub>6</sub> H <sub>4</sub> SH	-30.7	13.7	-13.2

In terms of the parabolic model, it is possible to obtain simple and physically clear equations for the estimation of  $\Delta E_H$  as a function of  $\alpha$ ,  $br_e$ , and  $\Delta H_e$ . The following simple expressions follow from the combination of Eqs. (7.40-7.43):

(1) for  $\alpha = 1$

$$\Delta E_H = 0.5\Delta H_e + 0.25(br_e)^{-2} \Delta H_e^2 \quad (7.44)$$

for  $\alpha \neq 1$

$$(1 - \alpha^2)\Delta E_H = 2(br_e)^2 - \alpha^2\Delta H_e - 2\alpha(br_e)^2[1(1 - \alpha^2)(br_e)^2\Delta H_e]^{1/2} \quad (7.45)$$

for  $\Delta H_e(1 - \alpha^2) \ll (br_e)^2$

$$\Delta E_H = (1 + \alpha)^{-1}\Delta H_e + 0.25\alpha(br_e)^2\Delta H_e^2 \quad (7.46)$$

It is seen from Eqs. (7.44) and (7.46) that, for low values of the enthalpy of reaction,  $\Delta E_H$  is directly proportional to  $\Delta H_e$  which agrees with the Polanyi-Semenov equation. The slope of the linear plot of  $\Delta E_H$  as a function of  $\Delta H_e$  depends on, i.e., on the force constants of the bonds. The ratio  $\Delta E_H/\Delta H_e = \alpha(1 + \alpha)^{-1}$  at low  $\Delta H_e$  and may serve as a parameter of the sensitivity of activation energy to  $\Delta H_e$  for low values of the latter. For reactions of different classes, the coefficient varies in the range from 0.6 to 1.7 and the coefficient  $(1 + \alpha)^{-1}$  therefore varies from 0.38 to 0.63.

The activation energy increases with increase in  $\Delta H_e$  and diminishes with increase in  $|\Delta H_e|$  for  $\Delta H_e < 0$ . On the other hand, according to the law of conservation of energy,  $E > 0$  for exothermic reactions and  $E > \Delta H_e$  for endothermic reactions. It follows from the law of conservation of energy and Eqs. (7.40) (7.42) that the parameter  $br_e$  for one group of reactions is constant, while  $\Delta H_e$  varies in the range  $\Delta H_{e \min} < \Delta H_e < \Delta H_{e \max}$ . For highly endothermic reactions with  $\Delta H_e > \Delta H_{e \max}$  the activation energy is  $E = \Delta H + 0.5RT$ , whilst for exothermic reactions with  $\Delta H_e < \Delta H_{e \min}$  it is  $0.5RT$ . The limiting values of enthalpies of reaction  $\Delta H_{e \max}$  and  $\Delta H_{e \min}$  are related to the parameters  $br_e$  and in the following way:

$$\Delta H_{e \max} = (br_e)^2 - 2\alpha br_e(0.5hLv_f)^{1/2} + 0.5(\alpha^2 - 1)hLv_f \quad (7.47)$$

$$\Delta H_{e \min} = (br_e/\alpha)^2 + 2\alpha^{-2}br_e(0.5hLv_i)^{1/2} + 0.5(1 - \alpha^2)hLv_i \quad (7.48)$$

As can be seen from Eqs. (7.47) and (7.48), the range of variation of  $\Delta H_e$  in which

$br_e = \text{const}$  is wider the greater the parameter  $br_e$ . For the reactions of alkyl radicals with aliphatic hydrocarbons ( $\alpha = 1$ ,  $br_e = 17.23 \text{ (kJ/mol)}^{1/2}$ ), we have  $\Delta H_{e \text{ max}} = \Delta H_{e \text{ min}} = 153.1 \text{ kJ mol}^{-1}$ , i.e., the range of enthalpies  $\Delta H_e$  where  $br_e = \text{const}$  is  $306 \text{ kJ mol}^{-1}$ .

Yet another important characteristic of radical abstraction reactions is the force constants of the ruptured and generated bonds. The dependence of the activation energy for reactions of the type  $R\cdot + R^1X \rightarrow RX + R^1$ , where  $X = \text{H, Cl, Br, or I}$ , on the coefficients  $b_i$  and  $b_f$  was demonstrated experimentally. It was found that parameter  $r_e = \text{const}$  in these reactions, whilst the square root of activation energy for a thermally neutral reaction is directly proportional to the force constant of the ruptured bond. The smaller is the force constant of the  $\text{C—X}$  bond, the lower  $E_{eo}$  and that the relation  $E_{eo}^{1/2}$  to  $b(1 + \alpha)^{-1}$  is linear. The same result was obtained also for reactions of the hydrogen atoms with  $\text{RCl}$ ,  $\text{RBr}$ , and  $\text{RI}$ . This results confirm the important role of the force constant of the reacting bonds in the formation of the activation barrier. The activation energies for the  $R\cdot + \text{RX}$  reactions can be easily estimated from the empirical formula

$$(E_{eo}/\text{kJ mol}^{-1})^{1/2} = 4.80 \cdot 10^{11} b(1 + \alpha)^{-1} \quad (7.49)$$

#### 7.6.4. The triplet repulsion in the transition state

The hydrogen atom migrates from  $\text{Y}$  to  $\text{X}$  in the  $\text{X}\cdot + \text{HY}$  reaction. The transition state of this reaction can be regarded conventionally as a labile formation containing the  $\text{X}\dots\text{H}\dots\text{Y}$  pseudobond. The characteristics of this bond may influence the activation energy. This influence can be observed with the aid of the parabolic model, since it makes possible to convert the activation energy for an individual reaction into the activation energy for a thermally neutral reaction (see Eq. (7.45) and also to take into account the influence of the force constants of the  $\text{X—H}$  and  $\text{Y—H}$  bonds on  $E_{eo}$ . When the hydrogen abstraction reactions are compared in relation to different classes of compounds, it is useful to employ the parameter  $r_e$ , in which the influence of  $\Delta H_e$ ,  $b_i$ , and  $b_f$  on the activation energy for the reaction has already been taken into account.

In the  $\text{X}\dots\text{H}\dots\text{Y}$  transition state, the  $\text{X}\dots\text{Y}$  pseudobond is formed by three electrons. According to the Pauli principle, one molecular orbital may be occupied by only two electrons with opposite spins. Two molecular orbitals therefore participate in the transition state: the bonding orbital of the  $\text{X—Y}$  bond, in which two electrons are accommodated, and its nonbonding orbital containing the third electron. The energy of the nonbonding orbital  $D_T$  is higher the stronger the  $\text{X—Y}$  bond; its value is described by the Sato formula

$$D_T = D_e \{ \exp(-br_e^{1/2}) + 0.5 \exp(2br_e^{1/2}) \} \quad (7.50)$$

where  $D_e$  and  $D_T$  are the energies of the bonding and nonbonding X—Y orbitals respectively,  $2b^2$  is the force constant, and  $r$  is the amplitude of the vibration of this bond. In the given case,  $r = r_{XH} + r_{YH} - r_{XY} + r_e$ . The involvement of the nonbonding orbital of the X—Y bond in the formation of the activation barrier has come to be referred to as triplet repulsion. This effect constitutes the basis of three semiempirical methods for the calculation of the activation energies for radical substitution reactions: the “bond energy bond order” (BEBO) method, the “bond energy bond length” (BEBL) method, and the Zavitsas method. In all these methods, the activation energy corresponds to the maxima on the “potential energy bond order” (BEBO) curves or the “potential energy bond length” (BEBL, Zavitsas method) curves while the potential energy curve represents a superposition of two Morse curves corresponding to the Y—H and X—H reacting bonds and the curve for the non bonding orbital of the X—Y bond (Eq. (7.50).

The role of triplet repulsion in radical abstraction can be clearly traced on comparing reactions in which the energies of the X—Y bonds differ significantly. The values of  $E_{eo}$  and  $r_e$  for a series of radical abstraction reactions found by the parabolic method as well as the energies  $D_e$  of the X—Y bond are presented below.

X...H...Y	$E_{eo}$ , kJ mol <sup>-1</sup>	$r_e \times 10^{11}$ , m	$D_e$ , kJ mol <sup>-1</sup>
R...H...R	68.2	4.414	382
R...H...N<	60.2	3.862	361
ArO...H...OAm	41.8	2.772	~0
RO <sub>2</sub> ...H...O <sub>2</sub> R	43.1	2.854	88
RO <sub>2</sub> ...H...OAr	45.3	2.885	~0
RO <sub>2</sub> ...H...OAm	45.6	2.895	~0

The difference between the reactions with a high energy of the X—Y (C—C and C—N) bond, for which  $E_{eo} \sim 60 \div 70$  kJ mol<sup>-1</sup>, and the reactions with a very low energy of this bond (O—O), for which  $E_{eo} \sim 40 \div 45$  kJ mol<sup>-1</sup> can be clearly traced. Within the limits of the error of the measurement, the parameter  $r_e$  for the last four reactions is constant:  $r_e = (2.85 \div 0.05) \cdot 10^{-11}$  m. This value is characteristic of reactions with zero triplet repulsion in the transition state. On substituting this quantity in Eq. (7.35), we obtain the following equation for the estimation of the contribution of triplet repulsion  $\Delta E_T$  to the activation energy  $E_{eo}$ :

$$\Delta E_T = (b_i b_f)^2 (b_i + b_f)^{-2} (r_e^{-2} - 2.852 \cdot 10^{22}) \quad (7.51)$$

For reactions of the R· + RH class, this contribution is 40.0 kJ mol<sup>-1</sup>, i.e., a considerable proportion of the activation energy  $E_{eo} = 68$  kJ mol<sup>-1</sup> is due precisely to the triplet repulsion in the transition state.

### 7.6.5. The electron affinity of atoms of reaction center.

Another important characteristic of the X—Y bond is its polarity induced by the different electron affinities of the atoms or radicals X and Y. The greater the difference, the greater the polarity of the bond, its strength and its dipole moment. According to Pauling, the polarity of the X—Y bond may be characterized by the extent to which its strength differs from half the sum of the bond dissociation energies of the XX and YY molecules by virtue of the different electronegativities of the atoms X and Y

$$\Delta EA(XY) = D_{XY} - 0.5(D_{XX} + D_{YY}) \quad (7.52)$$

The question arises whether the polarity of the X—Y bond affects the  $X\cdot + YH$  abstraction reactions. We shall compare two reactions:  $H\cdot + H_2$  and  $Cl\cdot + H_2$ .

Reaction	$E_{co}$ , kJ mol <sup>-1</sup>	$r_e \cdot 10^{11}$ , m	$D_{XY}$ , kJ mol <sup>-1</sup>
$H\cdot + H_2$	58.2	3.69	436.0
$Cl\cdot + H_2$	36.7	3.04	431.6

Evidently the dissociation energies of the H—H and Cl—H bonds are very close and the triplet repulsion in the transition states of these reactions is therefore almost identical. Nevertheless, the quantities  $E_{co}$  and  $r_e$  in these two reactions differ very considerably. The reason for this is that the H—H bond is nonpolar, while the Cl—H bond is polarized and  $\Delta E_A = 92.3$  kJ mol<sup>-1</sup> (Eq. (7.52) for the latter. As in the HCl molecule, in the transition state there is evidently a strong attraction between Cl and H, which in fact induces a decrease in  $r_e$  and  $E_{co}$ . If the  $Cl\cdot + H_2$  reaction was characterized by the same parameter  $r_e = 3.69 \cdot 10^{11}$  m as the  $H\cdot + H_2$  reaction, the activation energy  $E_{co} = 56.5$  kJ mol<sup>-1</sup> would have been obtained for it. The difference between the observed and expected activation energies ( $\Delta E_{EA} = 36.7 - 56.5 = 19.8$  kJ mol<sup>-1</sup>) must be attributed to the influence of the unequal electronegativities of the hydrogen and chlorine atoms on  $E_{co}$  in the  $Cl\cdot + H_2$  reaction.

The  $R\cdot + RH$  and  $RO\cdot + RH$  reactions may serve as another example.

Reaction	$E_{co}$ , kJ mol <sup>-1</sup>	$r_e \cdot 10^{11}$ , m	$D_{XY}$ , kJ mol <sup>-1</sup>
$R\cdot + RH$	68.2	4.414	376
$RO\cdot + RH$	54.8	3.553	361

In this case, the similarity of the R—R and RO—R bond dissociation energies also leads to the similarity of the triplet repulsion energies in the  $R\cdots H\cdots R$  and  $RO\cdots H\cdots R$  transition states. However, in these reactions too the quantities  $E_{co}$  and  $r_e$  differ appreciably. The polarity of the O—C bond in the  $RO\cdot + HR$  reaction is manifested here. On substituting the dissociation energies  $D(CH_3-CH_3)$ ,  $D(CH_3-OOCH_3)$ , and  $D(CH_3-OCH_3)$  in Eq. (7.52), we obtain  $\Delta E_A = 80$  kJ mol<sup>-1</sup>. Calculation of the contribution of the electronegativities of the O and C atoms to the activation

energy for the  $\text{RO}\cdot + \text{RH}$  reaction yields  $\Delta E_{\text{EA}} = 26.1 \text{ kJ mol}^{-1}$ , which should be regarded as very considerable bearing in mind that  $E_{\text{eo}} = 54.8 \text{ kJ mol}^{-1}$ .

### 7.6.6. The radii of atoms of reaction center

When the fragments X and Y approach one another in the  $\text{X}\cdots\text{H}\cdots\text{Y}$  transition state, their outer electron shells begin to repel one another. It is to be expected that the repulsion will be stronger, the larger the radii of the atoms X and Y. The examples presented below confirm this conclusion. We shall compare the  $\text{R}\cdot + \text{RH}$ ,  $\text{R}\cdot + \text{HSiR}_3$ , and  $\text{R}_3\text{Si}\cdot + \text{HSiR}_3$  reactions.

Reaction	$r_e \cdot 10^{11}, \text{ m}$	$r_{\text{X}-\text{Y}} \cdot 10^{11}, \text{ m}$	$D_{\text{XY}}, \text{ kJ mol}^{-1}$	$\Delta E_{\text{A}}, \text{ kJ mol}^{-1}$
$\text{R}\cdot + \text{RH}$	4.414	15.13	376	0.0
$\text{R}\cdot + \text{HSiR}_3$	4.782	18.70	376	11.0
$\text{R}_3\text{Si}\cdot + \text{HSiR}_3$	4.967	23.59	354	0.0

An evident parallel variation of the increment in  $r_e$  and in the bond length  $r_{\text{XY}}$  is observed. On the other hand, the strengths of the  $\text{X}-\text{Y}$  bonds in this series are similar, so that the increase in  $r_e$  is not caused by a change in the triplet repulsion. The electronegativities of the C and Si atoms are also similar and in the first and third reactions  $\Delta EA \approx 0$ .

The empirical dependence of the parameter  $r_e$  (in m) on  $D_{\text{XY}}$ ,  $\Delta EA$ , and  $r_{\text{XY}}$  in the interaction of radicals carrying a free valence on the C and O atoms with the  $\text{C}-\text{H}$ ,  $\text{O}-\text{H}$ ,  $\text{Si}-\text{H}$ , and  $\text{S}-\text{H}$  bonds has the following form:

$$r_e^2 \cdot 10^{22}, \text{ m} = 13.7(D_{\text{XY}}/D_{\text{HH}}) - 22.4(\Delta EA/D_{\text{HH}}) + 9.4(r_{\text{XY}}/r_{\text{HH}}) - 12.4 \quad (7.53)$$

These formulas make it possible to estimate the contribution of each factor, namely, triplet repulsion  $\Delta E_{\text{T}}$ , electronegativity,  $\Delta E_{\text{EA}}$ , and repulsion of the electron shells of the X and Y atoms  $\Delta E_{\text{R}}$  in the transition state, to the activation barrier  $E_{\text{eo}}$  for each class of radical abstraction reactions. Since  $E_{\text{eo}} = br_e(1 + \alpha)^{-1}$ , it follows that, by employing the corresponding increments from Eqs. (7.51) and (7.53), it is possible to calculate the contribution of a particular factor. Table 7.15 presents the results of such calculation for 21 classes of radical abstraction reactions.

It is seen from the data presented in Table 7.15 that the triplet repulsion  $\Delta E_{\text{T}}$  makes an additional contribution to the activation energy  $E_{\text{eo}}$ . The difference between the electronegativities of the fragments X and Y lowers the activation energy.

When the discrepancy between the electron affinities is large, this decrease may be very considerable. For example,  $\Delta E_{\text{EA}} = 45 \text{ kJ mol}^{-1}$  for the  $\text{HO} + \text{SiH}_4$  reaction and  $\Delta E_{\text{EA}} = 43 \text{ kJ mol}^{-1}$  in the reaction of hydrogen atom with water.

Table 7.15. The contributions of triplet repulsion ( $\Delta E_T$ ), the electron affinity of the fragments X and Y ( $\Delta E_{EA}$ ), and the repulsion of the atoms forming the X—Y bond ( $\Delta E_R$ ) to the activation energy  $E_{co}$  for the  $X\cdot + HY$  reaction.

Reaction	$b(1 + \alpha)^{-1} \cdot 10^{-11}$ (kJ/mol) <sup>1/2</sup>	$r_e \cdot 10^{11}$ , m	$\Delta E_T$ , kJ mol <sup>-1</sup>	$\Delta E_{EA}$ , kJ mol <sup>-1</sup>	$\Delta E_R$ , kJ mol <sup>-1</sup>
R· + HR	1.87	4.41	41	0	25
R· + H <sub>2</sub> NR	2.05	3.84	45	-8	32
R· + HOOR	2.06	3.80	37	-7	29
R· + HOAr	2.08	3.80	35	-19	26
R· + HSiR' <sub>3</sub>	1.60	4.78	30	-3	27
R· + HSR	2.13	4.09	44	0	46
HO· + HR	2.09	3.67	53	-22	30
HO· + SiH <sub>4</sub>	1.79	3.30	55	-45	28
RO· + HR	2.08	3.55	49	-20	30
RO· + HSiR' <sub>3</sub>	1.74	3.68	45	-34	26
RO <sub>2</sub> · + HR	2.06	3.80	37	-7	29
RO <sub>2</sub> · + HOOR	2.30	2.85	15	-0	28
RO <sub>2</sub> · + HOAr	2.33	2.88	0	0	45
AmO· + HR	2.08	3.66	28	-23	26
AmO· + HOAr	2.33	2.77	0	0	42
R <sub>3</sub> Si· + HSiR' <sub>3</sub>	1.38	4.97	18	0	27
H· + HR	1.96	3.76	53	-8	10
H· + NH <sub>3</sub>	2.11	3.45	63	-21	9
H· + H <sub>2</sub> O	2.20	3.91	76	-43	8
H· + SiH <sub>4</sub>	1.69	4.09	34	-2	15
H· + H <sub>2</sub> S	1.88	3.60	42	-5	16

The repulsion of the electron orbitals of the atoms forming the reaction center  $\Delta E_R$  plays an important role in all the radical abstraction reactions. In the interaction of radicals with molecules, the contribution of this repulsion ranges from 25 to 46 kJ mol<sup>-1</sup>. In reactions of molecules with hydrogen atoms, the contribution is naturally smaller, varying from 8 to 16 kJ mol<sup>-1</sup>.

#### 7.6.7. Influence of the $\pi$ -bond and steric effect

An aromatic ring and a double or triple bond in the  $\alpha$ -position relative to a C—H bond weaken the latter by virtue of the delocalization of the unpaired electron in its interaction with the  $\pi$ -bond. The weakening of the C—H bond is very considerable: for example,  $D(C-H)$  is 418 kJ mol<sup>-1</sup> in ethane, 368 kJ mol<sup>-1</sup> in the methyl group of propene ( $\Delta D = 50$  kJ mol<sup>-1</sup>), and 375 kJ mol<sup>-1</sup> in the methyl group of toluene ( $\Delta D =$

43 kJ mol<sup>-1</sup>). Such decrease in the strength of the C—H bond diminishes the enthalpy of the radical abstraction reaction and hence its activation energy. This effect is illustrated below in relation to the reactions of the methyl radical with hydrocarbons.

Hydrocarbon	C <sub>2</sub> H <sub>6</sub>	CH <sub>3</sub> CH=CH <sub>2</sub>	C <sub>6</sub> H <sub>5</sub> CH <sub>3</sub>
$\Delta H$ , kJ mol <sup>-1</sup>	-22.0	-72.0	-65.0
$E$ , kJ mol <sup>-1</sup>	52.4	37.4	39.3
$\Delta E$ , kJ mol <sup>-1</sup>	0.0	-15.0	-13.1

Comparative analysis of the kinetics of the reactions of atoms and radicals with paraffinic (R<sup>1</sup>H), olefinic (R<sup>2</sup>H), and aromatic alkyl-substituted (R<sup>3</sup>H) hydrocarbons within the framework of the parabolic model permitted a new important conclusion. It was found that the  $\pi$ -C—C bond occupying the  $\alpha$ -position relative to the attacked C—H bond increases the activation energy for thermally neutral reaction. The corresponding results are presented in Table 7.16.

Table 7.16. Influence of adjacent  $\pi$  bond on activation energy of hydrogen atom abstraction reaction.

R·	RH	$br_e$ , (kJ/mol) <sup>1/2</sup>	$E_{co}$ , kJ mol <sup>-1</sup>	$\Delta E_\pi$ , kJ mol <sup>-1</sup>
H·	R <sup>1</sup> H	14.49	57.9	
H·	R <sup>2</sup> H	15.58	66.9	9.0
H·	R <sup>3</sup> H	15.34	64.9	7.0
R·	R <sup>1</sup> H	17.23	74.2	
R·	R <sup>2</sup> H	18.86	88.9	14.7
R·	R <sup>3</sup> H	18.11	82.0	7.8
RO·	R <sup>1</sup> H	13.37	55.2	
RO·	R <sup>2</sup> H	14.41	64.1	8.9
RO·	R <sup>3</sup> H	14.16	61.9	6.7
RO <sub>2</sub> ·	R <sup>1</sup> H	14.23	61.5	
RO <sub>2</sub> ·	R <sup>2</sup> H	15.68	74.7	13.2
RO <sub>2</sub> ·	R <sup>3</sup> H	14.74	66.0	4.5
AmO·	R <sup>1</sup> H	13.72	58.0	
AmO·	R <sup>2</sup> H	15.66	75.5	17.5
AmO·	R <sup>3</sup> H	14.42	64.0	6.0

Evidently the activation energy for a thermally neutral reaction with participation of a hydrogen atom or a radical (alkyl, alkoxy, *etc.*) is higher in those cases where there is an  $\alpha$ -bond or an aromatic ring next to the attacked C—H bond. Evidently this effect is a property of the structures themselves and the  $\pi$ -bond exerts a dual effect on the reaction center. On the one hand, by weakening the C—H bond the  $\pi$ -bond in the  $\alpha$ -position lowers the enthalpy and hence the activation energy for the reaction.

On the other hand, by interacting with the electrons of the reacting bonds, the  $\pi$ -orbital increases the strength of the C—Y bond in the  $Y\cdot + HR$  reaction, which increases the energy of the non bonding C—Y orbital and intensifies triplet repulsion.

The influence of bulky substituents, for example *tertiary* alkyl groups, on the kinetics of diverse chemical reactions is well known. A steric effect occurs also in radical reactions. Such substituents usually influence both the enthalpy of the reaction and its activation energy. The parabolic model examined in the present review make it possible to separate these effects and to estimate separately the contribution of steric hindrance to the activation energy. We shall examine the thoroughly investigated radical reactions in which a radical attacks the O—H bond of a sterically hindered phenol ( $Ar^2OH$ ) containing two *tert*-butyl groups in the ortho-position relative to the phenolic group. Comparison of the energies  $E_{eo}$  for isotypical reactions involving both sterically unhindered ( $Ar^1OH$ ) and sterically hindered ( $Ar^2OH$ ) phenols makes it possible to estimate the contribution of steric hindrance  $\Delta E_S$  to the activation energy

$$\Delta E_S = E_{eo}(Ar^2OH) - E_{eo}(Ar^1OH) \quad (7.54)$$

The results of the comparison are presented in Table 7.17. The steric hindrance increases the activation energy for a thermally neutral reaction by 8.2, 8.2, and 24 kJ mol<sup>-1</sup> when oxygen-centered, nitrogen-centered, and alkyl radicals are involved respectively. The data obtained with the aid of the parabolic model. The steric effect is manifested similarly also in the reactions of sterically hindered ( $Ar^2O$ ) phenoxyl radicals with various substrates. The reactions of the sterically hindered diphenylpicryl radical (DPPH $\cdot$ ) and the unhindered diphenylaminyl radical may serve as another example. In the reactions of DPPH $\cdot$  with phenols, the contribution of the steric effect to  $E_{eo}$  ranges from 23 to 30 kJ mol<sup>-1</sup>, *i.e.*, is very considerable.

Table 7.17. The contributions of the steric effect ( $\Delta E_S$ ) to the activation energies for thermally neutral reactions of sterically hindered phenols, phenoxyl radicals, and diphenylpicryl hydrazyl.

Reaction	$br_e$ (kJ/mol) <sup>1/2</sup>	$E_{eo}$ , kJ mol <sup>-1</sup>	$\Delta E_S$ , kJ mol <sup>-1</sup>
$RO_2\cdot + Ar^1OH$	13.76	45.3	
$RO_2\cdot + Ar^2OH$	14.40	51.8	6.5
$CH_3\cdot + Ar^1OH$	17.38	59.8	
$CH_3\cdot + Ar^2OH$	18.92	84.2	24.4
$Ar^1O\cdot + Ar^1OH$	12.61	39.7	
$Ar^1O\cdot + Ar^2OH$	13.31	44.3	4.6
$Am\cdot + Ar^1OH$	10.93	27.6	
$Am\cdot + Ar^2OH$	12.15	34.2	6.6

$\text{AmO}\cdot + \text{Ar}^1\text{OH}$	12.93	41.8	
$\text{AmO}\cdot + \text{Ar}^2\text{OH}$	14.54	52.9	11.1
$\text{Ar}^1\text{O}\cdot + \text{HOOR}$	13.46	45.3	
$\text{Ar}^2\text{O}\cdot + \text{HOOR}$	14.40	51.8	6.5
$\text{Ar}^2\text{O}\cdot + \text{Ar}^2\text{OH}$	14.37	51.6	7.3
$\text{Ar}^1\text{O}\cdot + \text{AmH}$	10.13	27.6	
$\text{Ar}^2\text{O}\cdot + \text{AmH}$	11.59	36.2	8.6
$\text{Am}\cdot + \text{RH}$	16.87	81.7	
$\text{DPPH}\cdot + \text{RH}$	18.59	99.3	17.6
$\text{Am}\cdot + \text{Ar}^1\text{OH}$	10.93	27.6	
$\text{DPPH}\cdot + \text{Ar}^1\text{OH}$	14.85	51.0	23.4
$\text{Ar}_2\text{O}\cdot + \text{Ar}^2\text{OH}$	12.15	34.2	
$\text{DPPH}\cdot + \text{Ar}^2\text{OH}$	16.74	64.8	30.6

### 7.6.8. Polar effect in radical reactions

An extensive literature was devoted to polar effects in chemical reactions. The parabola model permits a fresh approach to this important problem. The introduction of a functional group into a hydrocarbon molecule alters the dissociation energy of the neighboring C—H bonds, which is indicated by the examples presented below.

Compound	$\text{C}_2\text{H}_5\text{—H}$	$\text{CH}_3\text{CH—H(OH)}$	$\text{CH}_3\text{C—H(O)}$	$\text{C}_2\text{H}_5\text{OCH—HCH}_3$
$D, \text{ kJ mol}^{-1}$	422	400	338	399

The change in the C—H bond strength affects the enthalpies and through them the activation energies for radical abstraction reactions. If a molecule is attacked by a nonpolar group (hydrogen atom, alkyl radical), then the influence of the polar group on the activation energy is confined to a change in  $\Delta H$ . This was confirmed by data on the reactions of the methyl radical with the C—H bonds of hydrocarbons and their derivatives (alcohols, ethers, *etc.*), which are characterized by a virtually identical parameter  $br_e = 17.23 \text{ (kJ/mol)}^{1/2}$ . Thus a polar group (OH, OR, *etc.*) influences only the enthalpy of reaction and not the energy of a transition state of the type  $\text{C}\cdots\text{H}\cdots\text{C}$  and  $\text{H}\cdots\text{H}\cdots\text{C}$ .

A different picture is observed when a polar radical reacts with a C—H bond of a polar molecule. For example, the reaction of an oxygen atom with a methane C—H bond is characterized by the parameter  $br_e = 13.11 \text{ (kJ/mol)}^{1/2}$  while the reaction with a methanol C—H bond is characterized by the corresponding parameter of  $12.55 \text{ (kJ/mol)}^{1/2}$ . For these values of  $br_e$ , the difference between the activation energies is  $4.6 \text{ kJ mol}^{-1}$ . The decrease in activation energy can be explained by the fact that the polar O—H group in the  $\text{O}\cdots\text{H}\cdots\text{C—OH}$  transition state interacts with the  $\text{O}\cdots\text{H}\cdots\text{C}$  polar reaction center.

The parabolic model make it possible to isolate from the overall effect of the sub-

stituent its contribution to  $E$ . In the calculation, use is made of the values of  $\Delta H$  and the activation energy for a thermally neutral reaction of the given group (reaction series), because the activation energy can be represented by the sum  $E_e = E_{eo} + \Delta E_H$  (see above), where the second term takes into account only the influence of enthalpy. The polar interaction in the transition state may be inferred by comparing the values of  $E_{eo}$  in various reactions of the same radical involving a hydrocarbon and the corresponding polar molecule. The contribution of the polar interaction to the activation energy ( $\Delta E_\mu$ ) can be estimated from the formula

$$\Delta E_\mu = [(br_e)^2 - (br_{eRH})^2](1 + \alpha)^{-2} \quad (7.55)$$

where the parameters  $(br_e)$  and  $(br_{eRH})$  refer to reactions involving a polar compound YH and a reference hydrocarbon RH respectively. The results of the calculation of the energy  $\Delta E_\mu$  (in  $\text{kJ mol}^{-1}$ ) for the  $X + HY$  gas-phase reactions are presented below

X·/HY	CH <sub>3</sub> OH	CH <sub>2</sub> (O)	RCH(O)	CH <sub>3</sub> C(O)CH <sub>3</sub>	(CH <sub>3</sub> ) <sub>2</sub> O
O	4.6	-4.6	-7.9	-9.4	-5.1
HO·	2.4	1.8	1.5	-11.4	2.8
CH <sub>3</sub> O·	-6.0	0	-12.2	-	-
(CH <sub>3</sub> ) <sub>3</sub> CO·	-	-4.2	-3.1	-17.8	-

polar groups on the activation energies for abstraction reactions were obtained by analyzing experimental data on reactions with participation of alkoxy and peroxy radicals in the liquid phase. These data are presented in Table 7.18. As can be seen from the table, the interaction of a polar group with a O...H...C or O—O...H...C polar reaction center can both diminish and increase the activation energy. A very marked decrease in activation energy (from -11 to 19  $\text{kJ mol}^{-1}$ ) was observed in the reactions of RO· and RO<sub>2</sub>· with aldehydes and ketones. The alcoholic group diminishes slightly the height of the activation barrier (by 1-3  $\text{kJ mol}^{-1}$ ), the reaction of RO· with benzyl alcohol being an exception. In the reactions with ethers, an increase in activation energy is observed.

Table 7.18. Kinetic parameters of the reactions of alkoxy and peroxy radicals with the C—H bonds of oxygen-containing compounds YH.

YH	RO·	RO <sub>2</sub> ·	YO <sub>2</sub> ·	YO <sub>2</sub> ·/RO <sub>2</sub> ·
	$\Delta E_\mu$ , $\text{kJ mol}^{-1}$	$\Delta E_\mu$ , $\text{kJ mol}^{-1}$	$\Delta E_\mu$ , $\text{kJ mol}^{-1}$	$\Delta \Delta E_\mu$ , $\text{kJ mol}^{-1}$
AlkOH	-1.5	-2.2	-5.8	-3.6
Cyclo-C <sub>6</sub> H <sub>11</sub> OH	-1.1	-2.2	-5.6	-3.4
C <sub>6</sub> H <sub>5</sub> CH <sub>2</sub> OH	-8.8	-2.8	-12.7	-9.9
C <sub>6</sub> H <sub>5</sub> CH(O)	-19.0	-8.2	-15.8	-7.6
RCH(O)	-12.2	-8.8	-15.8	-7.0
RC(O)CH <sub>2</sub> R	-10.6	-15.4	-13.0	-2.4
RC(O)CHR <sub>2</sub>		-15.7	-21.2	-5.5

$C_6H_5CH_2C(O)R$	-5.2	-11.2	-12.9	-1.7
$(R_3CH_2)_2O$	-1.7	3.4	5.7	2.3
$(R_2CH)_2O$	2.3	6.3	3.5	-2.8
$(C_6H_5CH_2)_2O$		-1.4		
$(C_6H_5RCH)_2O$		6.1	3.7	-2.4
$(RO)_2CH_2$	-3.9	1.8	1.4	-0.4
$(RO)_2CHCH_3$	-0.4	6.2	3.8	-2.4
<i>cyclo</i> - $C_6H_{11}OCH_3$		8.4		
<i>cyclo</i> - $CH_2OCH_2$		-3.8	-3.8	0.0
<i>cyclo</i> - $RCHOCH_2$		-3.4	-5.3	-1.9
<i>cyclo</i> - $OCH_2OR$		-2.4	-0.2	2.2
$CH_3OC(O)R$	6.3	8.7		
$RCH_2OC(O)R$	8.0	8.9	-11.2	-20.1
<i>cyclo</i> - $C_6H_{11}OC(O)CH_3$	6.1	8.8		

### 7.6.9. Effect of multidipole interaction

Yet another effect, namely multidipole interaction, is manifested in the reactions of polar radicals with polyfunctional compounds. This effect consists in the unequal reactivities of the same group, for example,  $R_2CH(OH)$ , in compounds with one and several functional groups. The corresponding kinetic data were analyzed within the framework of the parabolic model. The multidipole interaction is manifested, in particular, in the reactions of peroxy radicals  $RO_2\cdot$ , containing functional groups, with oxygen-containing compounds YH (Table 7.18). The magnitude of this effect in the transition state may be inferred from the change in the activation energy for a thermally neutral reaction on passing from a monofunctional compound YH to a polyfunctional compound ZH

$$\Delta\Delta E_{\mu} = [(br_e)^2_{ZH} - (br_e)^2_{YH}] (1 + \alpha)^{-2} \quad (7.56)$$

As can be seen from Table 7.19, the highest values of  $\Delta\Delta E_{\mu}$  correspond to the transition from  $RO_2\cdot$  to  $YO_2\cdot$  containing a carbonyl or ester group. Apparently this effect is induced by the dipole-dipole interaction in the transition state. Table 7.19 presents data concerning the influence of ester groups on the reactivity of  $CH_2$  groups in reactions with peroxy radicals. The multidipole effect always reduces the activation energy for reactions of this group and in certain cases the decrease is extremely significant (down to  $-10 \text{ kJmol}^{-1}$  and even further).

Table 7.19. Kinetic parameters of the reactions of cumylperoxyl radicals with compounds containing ester groups.

Ester	$\Delta H_e$ , kJ mol <sup>-1</sup>	$E_e$ , kJ mol <sup>-1</sup>	$br_e$ , (kJ/mol) <sup>1/2</sup>	$\Delta E\mu$ , kJ mol <sup>-1</sup>	$\Delta\Delta E\mu$ , kJ mol <sup>-1</sup>
[CH <sub>3</sub> OC(O)] <sub>2</sub>	31.7	72.5	13.70	-3.6	-12.3
[CH <sub>3</sub> (CH <sub>2</sub> ) <sub>4</sub> C(O)OCH <sub>2</sub> ] <sub>2</sub>	23.7	71.0	14.02	0.3	-8.6
[CH <sub>3</sub> (CH <sub>2</sub> ) <sub>4</sub> C(O)OCH <sub>2</sub> CH <sub>2</sub> ] <sub>2</sub>	23.7	68.8	13.73	-0.4	-9.3
CH <sub>3</sub> O(O)C(CH <sub>2</sub> ) <sub>3</sub> C(O)OCH <sub>2</sub> CH <sub>3</sub>	23.7	74.8	14.46	2.2	-6.7
CH <sub>2</sub> [CH <sub>2</sub> C(O)O(CH <sub>2</sub> ) <sub>2</sub> CH <sub>3</sub> ] <sub>3</sub>	23.7	76.6	14.67	6.0	-2.9
CH <sub>2</sub> [CH <sub>2</sub> C(O)O(CH <sub>2</sub> ) <sub>3</sub> CH <sub>3</sub> ] <sub>3</sub>	23.7	76.1	14.61	5.5	-3.4
[CH <sub>3</sub> CH <sub>2</sub> C(O)OCH <sub>2</sub> ] <sub>2</sub> C(CH <sub>3</sub> ) <sub>2</sub>	23.7	78.6	14.89	8.0	-0.9
[CH <sub>3</sub> (CH <sub>2</sub> ) <sub>3</sub> C(O)OCH <sub>2</sub> ] <sub>4</sub> C	23.7	76.8	14.69	6.2	-2.7
[CH <sub>3</sub> (CH <sub>2</sub> ) <sub>6</sub> C(O)OCH <sub>2</sub> CH <sub>2</sub> ] <sub>2</sub> O	23.7	77.3	14.72	6.5	-2.4
[CH <sub>3</sub> C(O)OCH <sub>2</sub> ] <sub>4</sub> C	23.7	77.6	14.78	7.0	-1.9
[CH <sub>3</sub> CH <sub>2</sub> C(O)OCH <sub>2</sub> ] <sub>4</sub> C	23.7	75.8	14.55	5.1	-3.8
[CH <sub>3</sub> (CH <sub>2</sub> ) <sub>8</sub> C(O)OCH <sub>2</sub> ] <sub>4</sub> C	23.7	69.6	13.85	-1.1	-10
[CH <sub>3</sub> CH <sub>2</sub> C(O)OCH <sub>2</sub> ] <sub>3</sub> CCH <sub>2</sub> CH <sub>3</sub>	23.7	77.4	14.76	6.8	-2.1

#### 7.6.10. Solvation of reactants in radical abstraction reactions

Yet another important effect, observed when reactions take place in the liquid phase, is associated with the solvation of the reactants. Theoretical comparison showed that the collision frequencies of the species in a gas and in a liquid are different, the difference being due to the difference between the free volumes. In a gas, the free volume is virtually equal to the volume occupied by the gas species ( $V_f \approx V$ ), while in a liquid it is much smaller than the volume of the liquid species ( $V_f \ll V$ ). Since the motion and collision of the species occur in the free volume, the collision frequency in a liquid is higher than in a gas by an amount  $(V/V_f)^{1/3}$ . The activation energies for the reactions of radicals and atoms with hydrocarbon C—H bonds in a gas and in a liquid are virtually identical, that in a liquid being independent of the solvent polarity. This also applies to the parameter  $br_e$  which can be seen from the following examples referring to the interaction of the hydroxyl radical with hydrocarbons:

RH	C <sub>2</sub> H <sub>6</sub>	C <sub>3</sub> H <sub>8</sub>
$br_e$ , (kJ/mol) <sup>1/2</sup> (gas)	13.74	13.52
$br_e$ , (kJ/mol) <sup>1/2</sup> (H <sub>2</sub> O)	13.48	13.40

A different picture is observed when a polar molecule is attacked by a polar radical (HO·, RO·, RO<sub>2</sub>·). The reaction in a polar solvent is slower than in a nonpolar hydrocarbon solution or in the gas phase. From the change in the parameter  $br_e$ , it is

possible to estimate the extent to which the activation energy increases as a result of the solvation of the polar reactants

$$\Delta E_{\text{sol}} = [(br_e)_l^2 - (br_e)_g^2] \times (1 + \alpha)^{-2} \quad (7.57)$$

The subscripts l and g in Eq. (7.57) refer to the liquid and gas phases, respectively. The results of the comparison are presented in Table 7.20. If the  $\text{HO}\cdot + \text{YH}$  reaction takes place in aqueous solution and not in the gas phase, the parameter  $br_e$  and hence the activation energy increase. This is associated with the solvation of the reactants and the need to overcome the solvation shell by the reacting component in order to effect the elementary step. The contribution of  $\Delta E_{\text{sol}}$  is particularly large in the reaction of the hydroxyl radical with aldehydes.

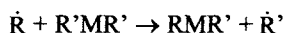
Table 7.20. Contributions of the solvation effect to the activation energies for radical reactions.

RH	$(br_e)_{\text{gas}},$ $(\text{kJ/mol})^{1/2}$	$(br_e)_{\text{liquid}},$ $(\text{kJ/mol})^{1/2}$	$\Delta E_{\text{sol}},$ $\text{kJ mol}^{-1}$
Radical: $\text{HO}\cdot, \text{H}_2\text{O}$			
$\text{CH}_3\text{OH}$	13.91	14.26	3.1
$\text{CH}_3\text{CH}_2\text{OH}$	13.48	14.01	4.6
$(\text{CH}_3)_2\text{CHOH}$	13.31	14.12	7.1
$(\text{CH}_3)_3\text{COH}$	13.39	14.13	6.5
$\text{CH}_3\text{OCH}_3$	13.95	14.70	6.8
$(\text{C}_2\text{H}_5)_2\text{O}$	13.47	14.33	7.6
$\text{CH}_2\text{O}$	13.84	14.98	10.4
$\text{CH}_3\text{CHO}$	13.81	14.99	10.8
$\text{CH}_3\text{COCH}_3$	13.81	14.50	6.3
$\text{CH}_3\text{COOCH}_3$	14.38	14.97	5.5
Radical: $(\text{CH}_3)_3\text{CO}\cdot, \text{CH}_3\text{COCH}_3$			
$\text{CH}_3\text{COCH}_3$	12.67	13.17	7.2

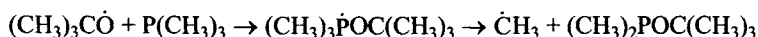
When a radical or atom attacks a polar O—H or N—H bond, the reactant Y forms a hydrogen bond of the type O—H...Y or N—H...Y in polar solvents. The hydrogen bond shields the reactant and slows down the reaction regardless of what kind of radical, polar or nonpolar, attacks it. A universal kinetic scale was proposed for the estimation of the effectiveness of such shielding.

### 7.7. Radical substitution reactions

Substitution (or replacement) reactions of the type

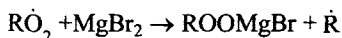


are characteristic of organometallic compounds and compounds bearing O—O, S—S, Sn—Sn, *etc.* bonds. These reactions can be divided into two groups: synchronous substitution reactions that occur in one act and stepwise substitution reactions that occur in two steps, for example,

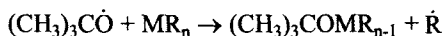


Let us consider briefly the material on synchronous substitution reactions. When an intermediate radical in the stepwise substitution decomposes very rapidly, it is rather difficult to establish the mechanism.

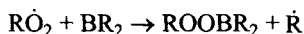
Substitution reactions involving  $\text{RO}_2\cdot$  occur during the oxidation of organomagnesium compounds



The attack of the alkoxy radical at the organometallic compound



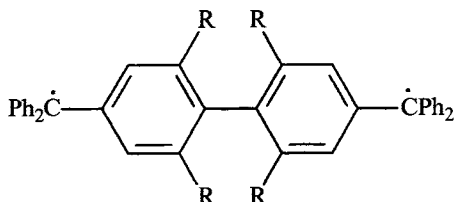
occurs as a stage of the chain process of interaction of peroxides with such compounds as  $(\text{C}_2\text{H}_5)_2\text{Zn}$ ,  $(\text{CH}_3)_2\text{Cd}$ ,  $\text{R}_3\text{B}$ ,  $(\text{CH}_3)_3\text{Al}$ ,  $(\text{C}_2\text{H}_5)_3\text{Ga}$ ,  $(\text{C}_2\text{H}_5)_3\text{Bi}$ , and others. The formation of alkyl radicals in these systems was proved by the ESR method. These reactions occur much more rapidly than H atom abstraction from hydrocarbons, as it can be seen from the following data (303 K) ( $k$  in  $l/(\text{mol s})$ ) (K. Ingold with coworkers, 1970-72):



It is seen that trialkylboron is more reactive than compounds bearing the B—O bond. Secondary alkyl borides are less reactive than primary compounds, perhaps, due to additional steric hindrances. Alkoxyl radicals react with  $\text{R}_3\text{B}$  still more rapidly ( $k \approx 10^7 l/(\text{mol s})$  for the reaction of  $(\text{CH}_3)_3\text{CO}\cdot$  with  $(\text{C}_4\text{H}_9)_3\text{B}$  at 303 K).

### 7.8. Reactions of biradicals

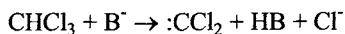
Biradicals can be grouped as follows: species bearing a free valence on two different atoms and species with a deficient of two electrons at the external electron

CN1(C)CC(C)(C)C1=NN=C2C(C)(C)C(C)(C)N2

Among radicals of the second type, carbenes (methylenes) are well studied. The simplest carbene is methylene :CH<sub>2</sub>, which exists in two forms: singlet and triplet. In singlet :CH<sub>2</sub> the HCH angle is equal to 103°,  $r_{\text{C-H}} = 0.112$  nm,  $\Delta H = 393$  kJ/mol. In triplet :CH<sub>2</sub> all three atoms lie on one line,  $r_{\text{C-H}} = 0.103$  nm.

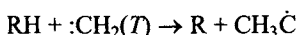
$$\begin{array}{l} \text{R}_2\text{C}=\text{N}_2 \xrightarrow{h\nu} \text{R}_2\text{C:} + \text{N}_2 \\ \text{CH}_2=\text{C}=\text{O} \xrightarrow{h\nu} \text{CH}_2=\text{C}=\text{O}(S) \begin{array}{l} \longrightarrow \text{:CH}_2(S) + \text{CO} \\ \longrightarrow \text{:CH}_2(T) + \text{CO} \end{array} \end{array}$$

upon the action of a strong base on trihalomethane


$$\text{CH}_2\text{N}_2 \rightarrow \text{N}_2 + :\text{CH}_2, \text{CCl}_3\text{SiCl}_3 \rightarrow :\text{CCl}_2 + \text{SiCl}_4$$
$$\text{CCl}_4 + \text{Mg} \rightarrow \text{MgCl}_2 + :\text{CCl}_2$$
$$\text{RH} + \text{:CH}_2 \rightarrow \text{RCH}_3$$

and the insertion rate is independent of the strength of the C—H bond:  $\text{:CH}_2$  is inserted with approximately the same partial rate constant at the primary and secondary C—H bonds. This is seen from the composition of hexanes, which are obtained by the reaction of *n*-pentane with  $\text{CH}_2\text{N}_2$  (methylene source): *n*-hexane (48%), 2-methylpentane (35%), and 3-methylpentane (17%). The fraction of the corresponding hexane in the reaction products corresponds to the number of the attacked C—H bonds. The insertion of methylene at different bonds of isopentane (liquid) occurs with the following relative rates: 1.0 (prim.) : 1.2 (sec.) : 1.5 (*tert.*). The vinyl and allyl C—H bonds also differ slightly with respect to methylene. For example, in propylene the rate of insertion rates of  $\text{:CH}_2$  at the vinyl and allyl C—H bonds is 1 : 1.4 (gas phase).

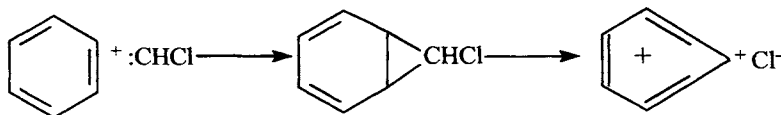
Addition occurs much more rapidly than insertion at the C—H bond. For example, in the case of ethylene, the rates of  $\text{:CH}_2$  addition and insertion are in a ratio of 1 : 0.044 (gas phase). Triplet  $\text{:CH}_2$  detaches H from the C—H bond



This reaction is an efficient method of synthesis of cyclopropanes. Singlet carbenes add at the double bond stereospecifically unlike triplet carbenes. The structure of olefin, naturally, affects the addition rate. Below we present the relative rates of  $\text{:CCl}_2$  addition in dimethoxyethane at 353 K with respect to cyclohexene

$(\text{CH}_3)_2\text{C}=\text{C}(\text{CH}_3)\text{C}_2\text{H}_5$	$\text{CH}_3\text{CH}=\text{C}(\text{C}_2\text{H}_5)_2$	$\text{CH}_2=\text{C}(\text{C}_2\text{H}_5)\text{CH}_2\text{CH}_2\text{CH}_3$
23.2	3.13	2.30
<i>cis</i> - $\text{C}_2\text{H}_5\text{CH}=\text{CHC}_3\text{H}_7$	<i>trans</i> - $\text{C}_2\text{H}_5\text{CH}=\text{CHCHC}_3\text{H}_7$	$\text{CH}_3=\text{CH}(\text{CH}_2)_4\text{CH}_3$
0.84	0.54	0.22

Carbenes are so reactive that add to the benzene ring to form the cyclohepta-trienyl cation



### 7.9. Radical reactions in solid polymer

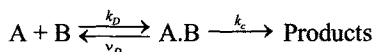
A wide use of polymeric materials in technology and agriculture stimulated studies of chemical reactions in polymeric media. During manufacturing, processing, and exploitation of polymers (polyethylene, polypropylene, rubber, polystyrene, poly(ester acrylates)), free radicals appear in them and various radical reactions occur. Free radical formation occurs under the action of light, penetrating radiation,

during oxidation with oxygen or mechanical actions. The kinetics of radical processes in solid polymers has several specific features, which are worthy of special consideration. These specific features are resulted from the chemical structure and physics of molecular motions in a solid polymer.

In amorphous and amorphous-crystalline polymers chemical processes occur predominantly in the amorphous phase of a polymer in which the solubility of gases and low-molecular substances is higher, diffusion of species and chemical processes occur more rapidly. The amorphous phase consists of segments of macromolecules arranged chaotically due to which the far-range order characteristic of crystals is absent. The amorphous phase of the polymer is micrononuniform: it consists of regions with different packing densities of macromolecular segments. This results in different intensities of molecular motions in these regions, which affects the kinetics of reactions in solid polymers.

### 7.9.1. Rigid cage of polymeric matrix

A collision of two particle-reactants is needed for the bimolecular reaction to occur. In the condensed phase (both in the liquid and solid phase), this reaction occurs in two stages. At first particle-reactants, moving due to the molecular mobility of surrounding solvents particles of polymer segments, approach each other at the reaction distance (get into the same "cage"). Then they react with each other with the rate constant  $k_c$  or diverge with the rate constant  $v_D$  (index  $D$  designates diffusion)



In a liquid the cage is formed by comparatively small molecules (10-100 atoms), which are very mobile. Due to the high mobility and a small volume, these molecules create the energetically equivalent cage of any shape around the reactants. Therefore, the mutual orientation of particles necessary for an elementary act in the liquid does not require an additional energy expense for the rearrangement of surrounding molecules, and the steric factor is independent of the medium viscosity and determined, as in the gas phase, by the structure of the reactants and structure of the reaction center.

The different situation is observed for the reaction in the polymeric matrix. Here two reactants collide in the cage formed by segments of a macromolecule. The macromolecule represents, in the first approximation, a large entangled ball of sequentially linked  $10^2$ - $10^6$  monomeric units ( $10^3$ - $10^7$  atoms). Since these units are linked by sequential chemical bonds, conditions for the predominant appearance of cavities with a certain shape, e.g., cylindrical, are created in the polymer. Therefore, cages in which two particle-reactants collide have energetically nonequivalent shapes in the polymer. The transition from one, energetically favorable shape of the cage to another, less favorable, requires energy expenses. For the bimolecular reac-

tion, reactants should mutually be oriented in such a way that this corresponds to a minimum in the curve of the potential barrier. In the solid polymer, an additional energy is required for the transition from the energetically favorable shape of the cage to that needed for the formation of the orientation, which is necessary for the reaction to occur. Thus, in the polymer the pre-exponential factor  $A_p$  depends on the configuration of the transition state, forces of the molecular interaction of macromolecular segments, and temperatures. This picture provides the following qualitative peculiarities of the bimolecular reaction in the polymer compared to the reaction in the liquid:

Liquid phase	Polymeric matrix
$k_{liq}$	$k_p < k_{liq}$ due to the noncorrespondence of the cage shape most favorable energetically
$k_{lig}$ is independent of viscosity	$k_p$ increases with an increase in molecular mobility
Activation energy $E_{liq}$ is independent of viscosity for $k_{liq} < k_D$	The lower the molecular mobility in polymer, the higher the activation energy $E_p > E_{liq}$ and $E_p$

Table 7.22 presents the comparison of experimental data for three bimolecular reactions along with rotational frequencies of nitroxyl radicals ( $\nu_r$ ) and orientational frequencies of reactants  $\nu_{or} = P\nu_p$ , where  $P$  is the steric factor of the reaction for the liquid phase. It is distinctly seen that in all studied cases  $k_p < k_{liq}$ ; all reactions studied occur in the kinetic regime ( $k_p < k_D$ ), and the rate constant in the polymer is much lower than the orientational frequency of the reactants. The dependence of the rate constant of the reaction of the molecular mobility (rotational frequencies of the reactant, nitroxyl radical) is described by the quantitative model of a particle-gyroscope, which rotates in the cosinoid potential field created by the rigid cage.

A particle is considered as a classical gyroscope with the rotation moment  $J$ , which rotates in the plane around the fixed axis (planar model of a particle in the cage). Segments of the macromolecule forming the cage create around the particle the field potential of intermolecular interaction forces. This field is simulated by the periodical  $n$ -fold continuous cosinoid potential

$$V(\Theta) = 0.5V_0(1 - \cos n_0\Theta) \quad (7.58)$$

where  $V_0$  is the potential barrier separating two energetically favorable positions of the particle, and  $n_0$  is the number of these positions upon the turn of the particle at the angle from 0 to  $\pi$ .

The rotation of a particle in the cage is considered as the rotational Brownian motion of the classical gyroscope around the fixed axis in the potential field  $V(\Theta)$ .

The rotational frequency of the particle  $\nu$  (in  $\text{s}^{-1}$ ) as a series of sequential jumps  $2n_0$  in one direction is the following:

$$\nu = (2 \times n_0 V_0 / 2J\xi) \exp(-V_0/RT) \quad (7.59)$$

where  $\xi$  is the coefficient of rotational friction  $x = 2n_0$ .

Table 7.21. Rate constants of bimolecular reactions with translatory and rotational diffusion of reactants

Medium	$k$ , l/(mol s)	$k_D$ , l/(mol s)	$P$	$\nu_r$ , $\text{s}^{-1}$	$\nu_{or}$ , $\text{s}^{-1}$
ROOH + C <sub>10</sub> H <sub>7</sub> NHC <sub>6</sub> H <sub>4</sub> NHC <sub>10</sub> H <sub>7</sub> , 300 K					
C <sub>6</sub> H <sub>5</sub> Cl	$6.7 \cdot 10^{-4}$	$3 \cdot 10^9$	$6 \cdot 10^{-6}$	$7 \cdot 10^9$	$4 \cdot 10^4$
Polypropylene (PP)	$6.2 \cdot 10^{-5}$	$3 \cdot 10^6$	$6 \cdot 10^{-6}$	$1.5 \cdot 10^7$	90
PhO• + HOOR, 295 K					
C <sub>6</sub> H <sub>6</sub>	0.12	$3 \cdot 10^9$	$6 \cdot 10^{-6}$	$6 \cdot 10^9$	$4 \cdot 10^4$
PP + 8% C <sub>6</sub> H <sub>5</sub> Cl	$3.8 \cdot 10^{-2}$	$8 \cdot 10^7$	$6 \cdot 10^{-6}$	$3 \cdot 10^8$	$2 \cdot 10^3$
PP + 2% C <sub>6</sub> H <sub>5</sub> Cl	$1.4 \cdot 10^{-2}$	$2 \cdot 10^7$	$6 \cdot 10^{-6}$	$8 \cdot 10^7$	500
Polypropylene	$3.5 \cdot 10^{-3}$	$2 \cdot 10^6$	$6 \cdot 10^{-6}$	$8 \cdot 10^6$	500
Polyethylene (PE)	$5.6 \cdot 10^{-3}$	$9 \cdot 10^6$	$6 \cdot 10^{-6}$	$4 \cdot 10^7$	240
>NÖ• + PhOH, 303 K					
C <sub>6</sub> H <sub>5</sub> Cl	$7.2 \cdot 10^{-4}$	$3 \cdot 10^9$	$1.3 \cdot 10^{-6}$	$7 \cdot 10^9$	9
Polypropylene	$6.3 \cdot 10^{-5}$	$3 \cdot 10^6$	$1.3 \cdot 10^{-9}$	$1.4 \cdot 10^7$	0.02

To consider a pair of particles and their mutual orientation, the equilibrium distribution of orientations of the gyroscope (one of the particles) is usually calculated. It has the form

$$W(\theta)d\theta = \frac{\exp[-V(\theta)/RT]}{2\exp(-V_0/2RT)I_0(V_0/RT)} \quad (7.60)$$

where  $I_0(V_0/2RT)$  is the modified Bessel function of the zero order of an imaginary argument.

The orientation of particle A with respect to particle B at the sighting angle  $\Theta$ . is necessary for the reaction to occur. The probability of this orientation  $W(\Theta_A)$  is the following:

$$W_p(\theta_A) = \frac{\Delta\theta_A \exp[-V_{or}(\theta_A)/RT]}{2\pi I_0(V_0/2RT) \exp(-V_0/RT)} \quad (7.61)$$

where  $V_{or} = 0.5V_0(1 - \cos n_0\Theta_A)$  is the potential energy of the orientation (favorable for the reaction to occur) of reactant A in the cage.

Considering the reaction in the framework of the encounter theory, according to

which for the bimolecular reaction

$$k = z_0 K_{AB} P \exp(-E/RT) \text{ l/(mol s)}$$

where  $z_0$  is the factor of collision frequency, and  $K_{AB}$  is the equilibrium constant between reactants A and B in the volume and in the cage,

we obtain

$$k_p = k_{liq} C \exp(-V_{or}/RT)$$

if  $z_0 K_{AB}$  is considered to be the same in the liquid and polymer. The potential of mutual orientation of particles  $V_{or} \leq V_o$ , and for the particular reaction (the  $\Theta_A$  angle is fixed)

$$V_{or} = m V_o$$

where  $m = 0.5(1 - \cos n_o \Theta_A)$ .

The potential barrier  $V_o$  can be expressed in the framework of the accepted model through the rotational frequency of particle A. Since in the liquid  $V_o = 0$ , we can accept the rotational frequency of the particle in the polymer as

$$v_p = v_{liq} \exp(-V_o/RT)$$

and determine

$$V_o = RT \ln(v_{liq}/v_p)$$

Combining the expressions

$$k_p = k_{liq} C \exp(-V_{or}/RT), \\ v_{or} = m V_o, \text{ and } V_o = RT \ln(v_{liq}/v_p)$$

we obtain the universal formula relating the reaction rate constant in the polymer to the molecular mobility of the reactant in the polymer

$$\log\{k_{liq}/k_p(v_p/v_{liq})^{1/2} I_o[0.5 \ln(v_{liq}/v_p)]\} = m \lg(v_{liq}/v_p) \quad (7.62)$$

This formula agrees well with experimental data for the reaction of the nitroxyl radical with phenols and of the phenoxyl radical with ROOH studied in polypropylene, polyethylene, and polystyrene at different temperatures.

### 7.9.2. Alignment of reactivity of reactants in polymers

Yet another important specific feature of bimolecular reactions in the polymer is the narrowing of the range of changing the reactivity of particles (radicals of molecules). This alignment of reactivity is observed not only for diffusion-controlled reactions (in this case, the explanation is trivial) but also for slow reactions that occur with the activation energy. This phenomenon was observed for the first time for the

reaction of peroxide radicals with several phenols. Peroxide radicals were generated due to the decomposition of azoisobutyronitrile in the presence of oxygen; the ratio of rate constants of the reactions  $\text{RO}_2\cdot + \text{InH}$  (InH is phenol) and  $\text{RO}_2\cdot + >\text{NO}\cdot$  ( $>\text{NO}\cdot$  is *p*-methoxydiphenylnitroxyl) was measured by the method of competitive reactions.

In solid polystyrene at 343 K, this ratio for the phenols studied changes 17-fold, whereas in the liquid phase the rate constant of the reaction  $\text{RO}_2\cdot + \text{InH}$  in ethylbenzene for the same compounds changes from  $0.3$  to  $48 \cdot 10^4$  l/(mol s), *i.e.*, 160-fold. The rate constants of the reaction of  $\text{RO}_2\cdot$  with several phenols (measured by the kinetics of the initiated oxidation of isotactic polypropylene (PPI)) change twofold (388 K), whereas in cumene at 333 K for the same phenols they change 20-fold.

A similar regularity is observed for the reaction of  $\text{RO}_2\cdot$  with 2,6-di-*tert*-butylphenols with different substituents in the para-position of PPI (at 353 K in the polymer  $k$  of this reaction changes from  $0.6$  to  $8 \cdot 10^3$  l/(mol s), whereas in ethylbenzene it changes from  $2.8$  to  $200 \cdot 10^3$  l/(mol s)) and for the reactions of several para-substituted 2,6-di-*tert*-butylphenoxy radicals with hydroperoxide groups of polypropylene.

Alignment of the reactivity can easily be explained from the model of rigid case when additionally taking into account the specificity of the propagation of thermal fluctuations in the condensed phase. According to the said above, the activation of not only reacting particles (as in the liquid phase) but also that of the surrounding segments is required in the polymer for the bimolecular elementary act to occur. Therefore, in the polymer the Gibbs activation energy is

$$\Delta G_p^\ddagger = \Delta G_{\text{liq}}^\ddagger + \Delta G_{\text{rc}}^\ddagger$$

where  $\Delta G_{\text{liq}}^\ddagger$  is the Gibbs activation energy for the reaction in the liquid similar to the polymer in the character of intermolecular interactions, and  $\Delta G_{\text{rc}}^\ddagger$  is the reorganization energy of the rigid cage necessary for transition state formation.

In the polymer the activation of a molecule is accompanied by the activation of the segments surrounding it because the thermal fluctuation in the polymers covers an array (group) of adjacent segments. The size of such fluctuations can be judged from the density fluctuations in the polymers, which cover 10 to 100 segments near the vitrification point. Therefore, when the energy  $\Delta G_{\text{liq}}^\ddagger$  is concentrated on the reaction center, the segments surrounding the pair are inevitably activated. Therefore, the activation energy of the cage  $\Delta G_{\text{rc}}^\ddagger$  can be divided into two terms

$$\Delta G_{\text{rc}}^\ddagger = \Delta G_{\text{rc}}^{\ddagger/} + \Delta G_{\text{rc}}^{\ddagger//}$$

one of which ( $\Delta G_{\text{rc}}^{\ddagger/}$ ) is determined by  $\Delta G_{\text{liq}}^\ddagger$ , and the second term ( $\Delta G_{\text{rc}}^{\ddagger//}$ ) is the energy that is additionally necessary for cage activation to form the transition state configuration. It is reasonable to assume that the higher  $\Delta G_{\text{liq}}^\ddagger$ , the higher  $\Delta G_{\text{rc}}^{\ddagger/}$ . When

accepting the simplest, namely, linear relationship

$$\Delta G_{\text{rc}}^{\#} = \beta \Delta G_{\text{liq}}^{\#}$$

then the Gibbs activation energy in the polymer

$$\Delta G_{\text{p}}^{\#} = \Delta G_{\text{liq}}^{\#} (1 - \beta) + \Delta G_{\text{p}}^{\#}$$

Then the correlation reflecting the following alignment should be fulfilled for the reaction rate constants in the polymer  $k_{\text{p}}$  and liquid  $k_{\text{liq}}$ ''

$$\log(k_{\text{liq}}/k_{\text{p}}) = B + \log k_{\text{liq}} B = \Delta G_{\text{rc}}^{\#} / (2.3RT) - \beta \log(RT/NA) \quad (7.63)$$

Evidently, at a sufficiently high  $\Delta G_{\text{liq}}^{\#} \geq \Delta G_{\text{liq}}^{\#} = \Delta G_{\text{rc}}^{\#} / \beta$ ,  $\Delta G_{\text{rc}}^{\#} = 0$ ,  $\Delta G_{\text{p}}^{\#} = \Delta G_{\text{liq}}^{\#}$ , and  $k_{\text{p}} = k_{\text{liq}}$ .

Table 9.23 presents the results of experimental data processing for the reactions  $\text{RO}_2\cdot + \text{ArOH}$ ,  $\text{ArO}\cdot + \text{ROOH}$ , and  $\cdot\text{NO} + \text{ArOH}$  by formula (8.80). As can be seen  $\Delta G_{\text{rc}}^{\#}$  changes from 30 to 60 kJ/mol. Thus, the conception of rigid cage explains the phenomenon of alignment of reactivity.

Table 7.22 Parameters B and  $\beta$  and Gibbs energies  $\Delta G_{\text{rc}}^{\#}$  and  $\Delta G_{\text{liq}}^{\#}$  (kJ/mol) for several radical reactions in the liquid phase and solid polymer

Reaction	T, K	$\beta$	B	$\Delta G_{\text{rc}}^{\#}$	$\Delta G_{\text{liq}}^{\#}$
$\text{RO}_2\cdot + \text{ArOH}$	388	0.53	-3.2	27±2	51
$\text{RO}_2\cdot + \text{ArOH}$	353	0.48	-1.1	34±3	71
$\text{ArO}\cdot + \text{ROOH}$	353	0.57	2.0	61±12	107
$\cdot\text{NO} + \text{ArOH}$	333	0.48	21	53±4	110

### 7.9.3. Transhybridization delay in reactions involving macro-molecules and macroradicals

Trans-hybridization of the orbitals occurs simultaneously in the elementary act of H atom abstraction from the C—H bond:  $sp^3$  hybridization of the orbitals of the C atoms is transformed into  $sp^2$  hybridization. This transition is accompanied by a change in the bond angles of the C—C bonds from 109 to 120°. In reactions of low-molecular compounds and in reactions of polymers in a solution, this rearrangement occurs already in the transition state simultaneously with hydrogen atom abstraction. In the solid polymer when the H atom is detached from the C—H bond of the polymeric chain, trans-hybridization delay is possible. This is related to a change in the bond angle of the C—C bond, which is delayed in the polymeric chain due to the strong van der Waals interaction between the adjacent segments of the macromole-

cules and a low segmental mobility resulting from this. The role of orbital trans-hybridization in abstraction reactions are pronounced for polymers under loading: the C—H bonds of macromolecules, which are in the stretched state, have angles between the C—C bonds exceeding  $109^\circ$  and react more rapidly with ozone.

The contribution of trans-hybridization of orbitals in abstraction reactions in non-strained polymers is less clear. The matter is that the reactivity of molecules and radicals in polymers is lowered, as we saw, because the rigidity of cages in which bimolecular reactions occur. Therefore, the decrease in the rate constant of the abstraction reaction on going from the liquid to solid polymer cannot be ascribed to only one of these two factors. It seems evident that, under conditions of restricted mobility of segments in the crystalline phase and in the glassy state in the amorphous phase (at  $T < T_g$ , where  $T_g$  is the vitrification temperature), trans-hybridization delay can substantially retard the abstraction of the H atom from the polymer by the radical. In the amorphous phase at  $T > T_g$  the segments are rather mobile and, most likely, the effect of trans-hybridization delay is slightly pronounced. In resins where the mobility of macromolecular fragments is high, virtually no trans-hybridization delay is observed.

A similar situation appears in the addition of a macroradical to a molecule with the double bond or to oxygen. In this reaction  $sp^2$  hybridization is transformed into  $sp^3$  with a change in the bond angle of the C—C bonds from  $120$  to  $109^\circ$ . Of course, for the polymeric radical this rearrangement in the solid phase is hindered by the interaction with adjacent segments. Therefore, in the solid polymer the addition of oxygen to the alkyl macroradical is slower than in the liquid phase and occurs with the activation energy.

#### 7.9.4. Polychronous kinetics

As already mentioned, the solid polymer is structurally nonuniform and represents an array of regions differed in packing of segments of macromolecules, density, and molecular mobility. If some physical (diffusion of the gas or dilute) or chemical processes (decomposition, recombination of particles, bimolecular reaction) occurs in the polymer, the polymer is as if a set of microreactors in each of which the process occurs with its intrinsic rate characteristics. Since in the polymer the reaction occurs in the rigid cage, all bimolecular processes controlled by both diffusion and kinetics occur in different microvolumes of the polymer in different ways.

This structural "mosaic" of the polymer results in the so-called polychronous kinetics of physical and chemical processes in the polymer. The polychronous kinetics is manifested as the stepwise process in heating the polymer. When free radicals are generated in the concentration  $[R]_0$  in the polymer, for example, polystyrene, at the low temperature  $T_0$  and then the sample is heated to the temperature  $T_1$ , some radicals decay due to diffusion and recombination, and the new concentration  $[R]_1$  is established rather rapidly (for  $10^2$ – $10^3$  s) and then at  $T_1 = \text{const}$  remains virtually

unchanged in time. This is the specific feature of the polychronous kinetics of the process in the solid polymer and its distinction from the kinetics in the liquid phase.

On subsequent heating of the sample to  $T_2$  the radical concentration decreases to  $[R\cdot]_2$  etc. to the complete disappearance of the radicals at a sufficiently high temperature. When the standard conditions are fulfilled, the value of the step  $[R\cdot]_0 - [R\cdot]_1$  depends on the temperatures  $T_0$  and  $T_1$  only.

The formal kinetics of such polychronous processes was developed. It is based on the fact that the particles are distributed over microreactors (ensembles) in each of which the reaction occurs with the intrinsic activation energy. Formally this looks like the particle distribution over activation energies

for the reaction of the first order

$$n_i = n_0 f(E) \exp(-k_1 t)$$

for the second order

$$n_i = n_0 f(E) \exp(1 + k_2 n_0 t)$$

The rectangular distribution  $f(E)$  in the form

$$f(E) = B(E_{\max} - E_{\min})^{-1}$$

is the simplest and considered in detail.

For this distribution the following (logarithmic) law of particle consumption  $n$  is fulfilled:

$$\frac{n}{n_0} = \frac{E_{\max}}{E_{\max} - E_{\min}} - \frac{RT \ln k_2 n_0 t}{E_{\max} - E_{\min}} \quad (7.64)$$

The polychronous kinetics reflect the deep interrelation between the reaction kinetics in the polymer and molecular mobility of the polymer segments and the nonuniformity of the polymer as a medium for the slow relaxation of physical processes in the polymer.

### 7.9.5. Influence of mechanical strain on chemical reactions in polymer

The mechanical loading on a polymeric item not only changes its shape and sizes but also affect substantially its supramolecular structure. The mechanical loading on the amorphous-crystalline polymer (polyolefins) substantially influences first of all on the amorphous phase of the polymer. The stretching strain results in the conformational transitions: the number of gauche conformations decreases and the number of trans conformations increases (polyethylene, poly(ethylene terephthalate)). Under strain chains of macromolecules are additionally oriented and the rotation of the rad-

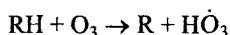
ical-probe in these samples is retarded, diffusion is retarded and the cage effect is enhanced.

The stretching strain results in polymer destruction due to the cleavage of the C—C bonds to form free radicals. Their formation in polypropylene under loading was detected by the consumption kinetics of radicals of 2,2,6,6-tetramethyl-4-oxopiperidine-N-oxyl. It has been established that the higher the strain  $\sigma$ , the higher the rate of radical formation due to the cleavage of the C—C bonds of the macromolecules. The following dependence is observed between the rate of radical generation  $v_i$  and  $\sigma$  (polypropylene, 294 K,  $\sigma = 195\div 430$  MPa):

$$\log v_i \text{ (mol/l s)} = 12 - (125 - 53 \cdot 10^{-6} \sigma) / 2.3RT \quad (7.65)$$

(where  $E = 125 - 53 \cdot 10^{-6} \sigma$  is expressed in kJ/mol,  $\sigma$  is expressed in MPa, and the factor  $53 \cdot 10^{-6}$  is expressed in m<sup>3</sup>/mol). The most strained fragments of macromolecules in the amorphous phase are prone to rupture.

The mechanical loading on the polymeric sample also changes the reactivity of the C—H bonds. This was distinctly shown by A.A. Popov in studies of the reaction of ozone with C—H bonds of polypropylene under loading. Ozone attacks the tertiary C—H bonds of the macromolecule according to the reaction



In the solid phase the reaction occurs with the rate constant  $k = 6 \cdot 10^6 \exp(-48.5 \text{ kJ/mol}/RT) \text{ kg/(mol s)}$ . Under the loading effect, the reactivity of the C—H bonds increases, and the following correlation between  $k_\sigma$  (rate constant of the reaction in the sample under loading  $\sigma$ ) becomes true:

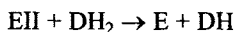
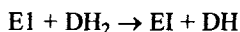
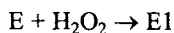
$$\ln k_\sigma = \ln k + \gamma \sigma / RT$$

where  $\gamma = 2 \cdot 10^{-6} \text{ m}^3/\text{mol}$ .

The acceleration of the reaction of the C—H bond with ozone under loading is explained by the following circumstances. In a polymeric molecule each C atom has  $sp^3$  hybridization of the orbitals, due to which the CCC angle is equal to  $109^\circ$ . The reaction of ozone with the C—H bond is accompanied by the formation of a radical in which the C atom is already characterized by the  $sp^2$  hybridization of the orbitals with a CCC angle of  $120^\circ$ . Under loading the CCC angles in the macromolecular segments in the transition chains are deformed. This decreases the transhybridization energy at the carbon atom of the attacked C—H bond and, correspondingly, the activation energy. Loading increases the energy of these macromolecular regions and, hence, decreases the activation barrier. A distinct sybante character was established for the influence of the mechanical loading in the polymer and deformation of angles of the C—C bonds in cyclic hydrocarbon on the reactivity of the C—H bonds in their reaction with ozone. The loading also accelerates the reaction of ozone with double bonds and hydrolysis of polyamides with water vapor.

### 7. 10 Radical reactions in biology

In 1949 Chance in his classical work has constructed the following radical mechanism of substrate (DH<sub>2</sub>) oxidation catalyzed by peroxidase (E)



According to the Chance mechanism, the interaction of H<sub>2</sub>O<sub>2</sub> with the enzyme gives "compound I" (E1). The oxidation of the donor molecules leads to "compound II" (E11) which oxidizes the second donor molecule. The radical intermediates were detected experimentally for such substrates as amines and phenols with relatively high reduction potential (Dunford and Stillman, 1976). The one-electron steps with the formation of free radicals at oxidation of amines and phenols have been proved in the ceruloplasmin, laccase and ascorbic oxidase reactions (Malmstrom et al., 1975).

Recently enzymatic mechanisms that proceed by free radical chemistry initiated by the 5'-deoxyadenosyl radical were discovered. (Frey, 2001). Three radicals were spectroscopically characterized in reaction of the interconversion of L-lysine and L-lysine by lysine 2,3-aminomutase. The enzyme [Fe<sub>4</sub>S<sub>4</sub>]<sup>+</sup> center undergoes the chemical cleavage of S-adenosylmethionine (SAM) with the reversible formation of 5'-deoxyadenosyl radical. In other reactions with SAM, iron-sulfur proteins generate this radical which activate an enzyme to abstract a hydrogen atom from an enzymatic glycyl residue to form a glycyl radical. 5'-deoxyadenosyl radical also arises in adenosylcobalamin reaction as the result of hemolytic cleavage of the cobalt-carbon bonds. In the following reaction this radical initiates abstraction hydrogen atoms from substrates.

The radical rebound mechanism has been proposed and proved in several cases in reaction of hydroxylation catalyzed by cytochrome 450 and methane monooxygenase.

The kinetic methods and analysis of products can provide valuable information about mechanisms of the cytochrome P450 reactions. According to the pioneering works of the Groves group (Groves, 1985) the observed kinetic isotope effect (KIE) is large:  $kH/kD > 11$  for benzylic and aliphatic hydroxylation. This observation was confirmed in kinetics studies of various systems. In one instance a large intramolecular KIE was observed for flour derivative of camphor (Sono et al., 1986). The experimental KIE was attributed to the Groves rebound mechanism in which the iron-oxo species abstracts an H atom from substrate to give an iron-hydroxo species

and an alkyl radical, followed by recombination of the hydroxo-species and the alkyl radical. This mechanism was also supported by experimental results of stereochemistry and regiochemistry in some systems (Ortiz de Montellano, 1995). Thus, stereochemical allylic transformation was demonstrated by using microsomal P450-2B4 as a substrate. The radical mechanism was also supported by the absence of skeleton-rearranged alcohol products, which were expected to be generated from a carbocation intermediate in hydroxylation of substrates as norcaran (Ortiz de Montellano, 1995).

## Reactions of ions and radical ions

### 8.1. Dissociation to ions and ion recombination

#### 8.1.1. Solvation of ions in solution

Ionization of substances in polar solvents is accompanied by the formation around the ion of a solvate jacket consisting of solvent molecules. This solvate jacket is formed due to the ion-dipole interaction of molecule-dipoles with the ion of the dilute. Several methods are used for the estimation of the number of solvent molecules, which create the solvate shell of the ion (solvation number  $SN$ ): NMR, UV and IR spectroscopy, by electroconductivity, viscosity, *etc.*).

Data of different methods diverge. For example, for  $\text{Na}^+$  in water  $SN = 13$  (by the transfer number), 3 (by electroconductivity), 3 (by viscosity), 4 (by compressibility of the solution), 4 (by entropy of dissolution), and from 3 to 4.5 (by NMR). The  $SN$  measured by the NMR method for several cations in  $\text{H}_2\text{O}$  are 3.4 to 5 for  $\text{Li}^+$ , 3-4 for  $\text{Na}^+$ , 1-4.6 for  $\text{K}^+$ , 4 for  $\text{Be}^{2+}$ , 3.8 for  $\text{Mg}^{2+}$ , 4.3 for  $\text{Ca}^{2+}$ , 5.7 for  $\text{Ba}^{2+}$ , and 6 for  $\text{Fe}^{2+}$ ,  $\text{Co}^{2+}$ ,  $\text{Ni}^{2+}$ , and  $\text{Zn}^{2+}$ .

On the other hand, the solvation number depends on the nature of solvent molecules: their polarity and sizes. Below we present the  $SN$  values for  $\text{Na}^+$  in several solvents. They were estimated from viscosity (through the Stokes radius): 9 ( $\text{H}_2\text{O}$ ), 6 ( $\text{CH}_3\text{OH}$ ), 5 ( $\text{C}_2\text{H}_5\text{OH}$ ), 4, ( $n\text{-C}_3\text{H}_7\text{OH}$ ), 4-5 ( $\text{CH}_3\text{COCH}_3$ ), 5-6 ( $\text{CH}_3\text{CN}$ ), 4 (pyridine), 3 ( $\text{C}_2\text{H}_5\text{COCH}_3$ ), 2.6 ( $\text{CH}_3\text{CON}(\text{CH}_3)_2$ ), and 2.0 (Sulpholan). Different methods of solvation are observed in mixed (binary) solvents. 1. Both components participate approximately to the same extent in the formation of the solvate shell. This takes place, e.g., for the solvation of  $\text{Li}^+$  in the  $\text{H}_2\text{O} + \text{D}_2\text{O}$  and  $\text{H}_2\text{O} + (\text{CH}_3)_2\text{SO}_2$  mixtures and of  $\text{Mn}^{2+}$  in the  $\text{H}_2\text{O} + \text{HCON}(\text{CH}_3)_2$  mixture. 2.

The cases where in a binary aqueous solutions water molecules form the solvate shell are more often. This is observed for  $\text{Li}^+$  and  $\text{Na}^+$  in  $\text{H}_2\text{O} + \text{H}_2\text{O}_2$  mixtures, for  $\text{Li}^+$ ,  $\text{Na}^+$ ,  $\text{Cs}^+$ ,  $\text{Tl}^+$ ,  $\text{Ca}^{2+}$ ,  $\text{Mn}^{2+}$ , and  $\text{Co}^{2+}$  in  $\text{H}_2\text{O} + \text{CH}_3\text{OH}$  mixtures, and for  $\text{Na}^+$ ,  $\text{Cs}^+$ ,  $\text{Ca}^{2+}$ ,  $\text{Co}^{2+}$ , and  $\text{La}^{3+}$  in  $\text{H}_2\text{O}$ -dioxane mixtures. 3. Sometimes the solvate shell is formed by the second component (not  $\text{H}_2\text{O}$ ). This is precisely the second component

that forms the solvate shell of the  $\text{Na}^+$  and  $\text{Cs}^+$  ions in the  $\text{H}_2\text{O} + (\text{CH}_3)_2\text{SO}_2$  mixture, and in the  $\text{H}_2\text{O} + \text{CH}_3\text{CN}$  mixture the latter forms the shell around  $\text{Ag}^+$ .

The formation of the solvate shell from solvent molecules is accompanied by a considerable energy release

Ion	$\text{H}^+$	$\text{Li}^+$	$\text{Mg}^+$	$\text{Ba}^+$	$\text{Fe}^{2+}$	$\text{Fe}^{3+}$	$\text{Al}^{3+}$
$\Delta H$ , kJ/mol	1090	514	1920	1590	1920	4370	4660

The higher the charge of the ion and the shorter its radius, the higher the change in the enthalpy during hydration. Hydration is accompanied by a decrease in the entropy of the system  $\Delta S_r < 0$ . The dissolution of ions is accompanied by a change in the solution volume.

On the one hand, the solution volume increases because ions that occupy some volume appear, and on the other hand, solvent molecules forming the solvate shell are arranged more compactly so the volume occupied by the solvent decreases. As a result, the change in the volume upon the dissolution of the ion,  $\Delta V_{\text{sol v}}$  can be either greater or smaller than zero. The higher the charge of the and the shorter its radius, the lower  $\Delta V_{\text{sol v}}$ .

On going from water to other polar solvents, the thermodynamic characteristics of solvation naturally change. In many cases, when the ion is transferred from an aqueous solution into an organic solvent  $\Delta H = \Delta H_{\text{sol v}} - \Delta H_{\text{aq}} > 0$ .

### 8.1.2. Ion pairs

Both isolated ions and ion pairs exist in solutions of electrolytes. The studies of the last two decades showed that ion pairs participate actively in reactions involving ions. The idea "ion pair" was introduced by N. Bjerrum in 1926 for solvated ions at a short distance from each other in a solution. A rich material on ion pairs was accumulated in sixties-seventies.

Contact (tight, nonseparated) and solvate-separated ion pairs are distinguished. In the contact pair the anion replaces one or several solvent molecules in the solvate shell of the cation, so that the cation and anion are nearest neighbors. In the solvate-separated ion pair the anion and cation are separated by solvent molecules, that is, each anion is surrounded by its solvate shell.

If the solvent is considered as a structureless medium with the dielectric constant  $\epsilon$ , the difference in the Gibbs solvation energies for the solvated ion pair with the charges  $z_A$  and  $z_B$  of ions infinitely remote from each other is the following:

$$\Delta G_{\text{sol v ion}} - \Delta G_{\text{sol pair}} = -Lz_A z_B e^2 (1 - \epsilon) / (r_A + r_B) \quad (8.1)$$

and the dissociation constant of the ion pair  $K_{AB}$

$$\ln K_{AB\pm} = -\ln K_{AB}^{\circ} + z_A z_B e^2 / (r_A + r_B) \epsilon R T \quad (8.2)$$

where  $K_{AB}^{\circ}$  is the dissociation constant of the "uncharged" ion pair.

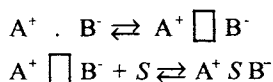
Constant  $K_{AB}^{\circ}$  reflects the influence of dispersion forces, including the polarization of ions and surrounding molecules.

Ion pairs exist as stable forms in a certain interval of temperatures and concentrations. The form, whose bond energy is much higher than  $kT$ , is stable. At a sufficiently high temperature the lifetime of the ion pair becomes comparable with the time of existence of a particle in the case, and the ion pair as a stable form disappears. In the framework of the electrostatic approach, the bond energy in the ion pair, where  $A^+$  and  $B^-$  exist at the distance  $a$ , equals  $z_A z_B e^2 / a \epsilon$ , and the ion pair exists at temperatures lower than  $z_A z_B e^2 / a \epsilon k$ . For example, for singly charged ions at  $a = 1$  nm and  $\epsilon = 80$  the ion pair exists at  $T < 200$  K.

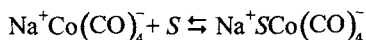
The idea "ion pair" becomes incorrect at a very high ion concentration in the solution where the average distance between them becomes comparable with the distance between ions in the ion pair.

The transition from the solvate-separated to contact ion pair is accompanied by a change in the electrostatic energy. If in the contact pair the distance between ions is equal to  $r_A + r_B$ , and in the solvate-separated pair it is  $r_A + r_B + \Delta r$ , then the transition to the contact pair is accompanied by the release of an energy equal to  $z_A z_B e^2 \Delta r / \epsilon (r_A + r_B + \Delta r)(r_A + r_B)$ . At  $r_A \gg r_B$  and  $r_A + \Delta r$ , this energy becomes insignificant. The structure of the ion pair depends on the solvent: only tight ion pairs are formed in poorly solvating solvents.

The rearrangement of the tight pair into the solvate-separated pair is considered as a two-stage process: at first a hole is formed between ions due to their thermal motion, and then a solvent molecule enters the hole



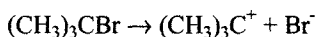
For the solvation of  $\text{NaCo}(\text{CO})_4$  in tetrahydrofuran



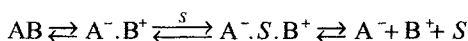
$\Delta H^{\circ} = -30$  kJ/mol,  $\Delta S^{\circ} = -116$  kJ/(mol K) and  $\Delta G^{\circ} = 5$  kJ/mol at  $T = 300$  K and  $\Delta G = -7$  kJ/mol at  $T = 200$  K. Ion pairs along with ions participate in various reactions in solutions.

### 8.1.3. Ionization of molecules in polar solvents

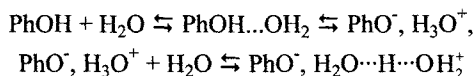
Molecules with polar bonds undergo complete or partial ionization in polar solvents. Ionization occurs due to the heterolytic dissociation of the molecule to form solvated ions, for example,



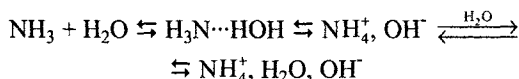
The formation of independently diffusing ions occurs through the stage of contact and solvate-separated ion pairs



Dissociation very often occurs through the chemical interaction of the substance with solvents. Hydroxyl-containing substances dissociate *via* the intermediate formation of an associate with the hydrogen bond, for example,



The solvate-separated pair of  $\text{C}_6\text{H}_5^-$  and  $\text{H}_5\text{O}_2^+$  then dissociates to individual ions. In this polymer ionization represents, in essence, the heterolytic abstraction of a proton from the phenoxyl group with the simultaneous formation of the  $\text{H}_3\text{O}^+$  ion, which is transformed then into the more stable  $\text{H}_5\text{O}_2^+$  ion. Bases (*i.e.*, ammonia), by contrast, abstract the proton from water



The experimentally determined rate constant is evidently the product of the rate constant of the limiting step and equilibrium constants of the preceding steps. Probably, in many cases, the step in which bond ionization occurs limits the process. Rate constants of the dissociation of molecules to ions change in a wide interval depending on their structure. This is illustrated by the examples presented below.

Reaction (in $\text{H}_2\text{O}$ , 298 K)	$k$ , $\text{s}^{-1}$
$\text{H}_2\text{O} \rightarrow \text{H}^+ + \text{OH}^-$	$2.3 \cdot 10^{-5}$
$\text{C}_6\text{H}_5\text{OH} \rightarrow \text{H}^+ + \text{C}_6\text{H}_5\text{O}^-$	6
$\text{H}_2\text{S} \rightarrow \text{H}^+ + \text{SH}^-$	$4.3 \cdot 10^3$
$(\text{CH}_3)_4\text{NOH} \rightarrow (\text{CH}_3)_4\text{N}^+ + \text{OH}^-$	$6 \cdot 10^5$
$\text{PhCOOH} \rightarrow \text{H}^+ + \text{PhCOO}^-$	$2.4 \cdot 10^6$
$\text{HF} \rightarrow \text{H}^+ + \text{F}^-$	$6.7 \cdot 10^7$

This variation in the dissociation constant values is due to the energy of het-

erolytic cleavage of the corresponding bond: the higher this energy, the lower the rate constant of dissociation.

#### 8.1.4. Ion recombination

Ions in a solution recombine with the diffusion rate constant. For ions with the charges  $z_A$  and  $z_B$  the potential of their interaction with a medium with the dielectric constant  $\epsilon$  at the distance  $r$  is equal to  $z_A z_B e^2 / \epsilon r$ . Therefore, in ion recombination the following expression is obtained for the rate constant of diffusional collisions:

$$k_D = 4\pi D r z_A z_B e^2 (\epsilon r k T)^{-1} [\exp(z_A z_B e^2 / \epsilon r k T) - 1]^{-1} \quad (8.3)$$

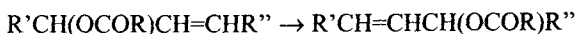
Due to the mutual attraction when  $r_{\text{eff}} > r_{AB}$ , the recombination of unlikely charged ions occurs very promptly, more promptly than radical recombination. This is seen from the data presented below and obtained by the method of temperature jump

Reaction (in H <sub>2</sub> O)	$k$ , l/(mol s)
$\text{H}^+ + \text{SO}_4^{2-} \rightarrow \text{HSO}_4^-$	$10^{11}$
$\text{NH}_4^+ + \text{OH}^- \rightarrow \text{NH}_4\text{OH}$	$4 \cdot 10^{10}$
$\text{H}^+ + \text{OH}^- \rightarrow \text{H}_2\text{O}$	$1.5 \cdot 10^{11}$
$\text{H}^+ + \text{CH}_3\text{COO}^- \rightarrow \text{CH}_3\text{COOH}$	$5 \cdot 10^{10}$

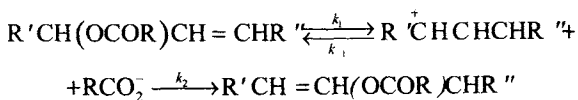
As the calculation shows, the recombination of these ions occurs as soon as they approach at a distance close to three molecular diameters.

#### 8.1.5. Isomerization of molecules through ionization stage

The dissociation of molecules to ions followed by fast ion recombination in the ion pair results in isomerization if the molecule contains the double bond. In particular, the isomerization of allyl esters accompanied by the migration of the double bond occurs in such manner

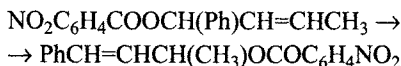


The ester dissociates to the anion of the acid and carbocation, which then recombines rapidly to form both the initial and new forms of the ester

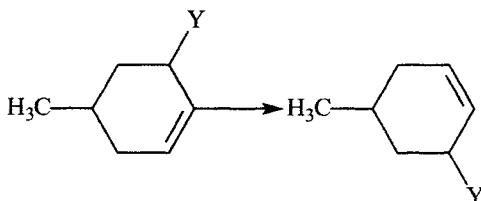


The experimentally observed  $k_{\text{exp}} = k_1 k_2 (k_{-1} + k_2)^{-1}$ . For compounds with the structure  $\text{RCOOCH}(\text{Ph})\text{CH}=\text{CH}_2$  in chlorobenzene at 403 K  $k = 1.3 \cdot 10^{-6} \text{ s}^{-1}$  for R =

$n\text{-NO}_2\text{C}_6\text{H}_4$ ,  $2.3 \cdot 10^{-7} \text{ s}^{-1}$  for Ph, and  $6.3 \cdot 10^{-8}$  for  $\text{CH}_3$ . Isomerization is accelerated by acid, whose accumulation during experiment due to hydrolysis results in autocatalysis. Taking into account acid catalysis,  $k_{\text{exp}} = 1.3 \cdot 10^{-6} + 2.3 \cdot 10^{-4} [n\text{-NO}_2\text{C}_6\text{H}_4\text{COOH}]$ , for the isomerization of  $\text{NO}_2\text{C}_6\text{H}_4\text{COOCH(Ph)CH=CH}_2$ . In more polar solvents where ionization is more mild, isomerization occurs more rapidly. The isomerization of the ester



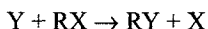
in the solvent containing 70% dioxane and 30% water occurs with  $\Delta H^\circ = 88 \text{ kJ/mol}$  and  $\Delta S^\circ = 5 \text{ J/(mol K)}$ . The isomerization of the ester ( $Y = n\text{-NO}_2\text{C}_6\text{H}_4\text{COO}$ )



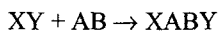
in 60% dioxane occurs with  $\Delta H^\ddagger = 115 \text{ kJ/mol}$  and  $\Delta S^\ddagger = -5 \text{ J/(mol K)}$ , i.e., the activation energy is rather high and the activation entropy is close to zero.

## 8.2. Mechanisms of heterolytic reactions

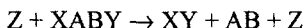
Various organic reactions involving two reactants can be grouped into three large groups: reactions of substitution (*S*), addition (*Ad*), and elimination (*E*). In the substitution reaction the reactant substitutes the atom or group in the molecule of another reactant



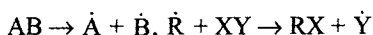
In the addition reaction two reactants are unified to form one molecule



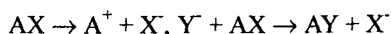
and in the elimination reaction, by contrast, two molecules are formed from one reactant under the action of another reactant Z or on heating



In each reaction one bonds are cleaved and others are formed. This cleavage can occur either homolytically



or heterolytically



so that one fragment removes an electron pair and another reactant has the vacant orbital and the possibility to accept the electron pair on it with filling at the external electron shell. The division of reactants into *agents* and *substrates* remained in synthetic chemistry from the alchemy epoch. It is assumed (conventionally) that the agents acts and the substrate is subjected to the action.

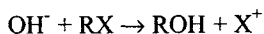
Generalizing the diverse experimental material, Ch. Ingold in 1933-34 introduced the division of reactants (agents) into *nucleophilic* (*N*), which attack the positively charged fragment of the substrate, and *electrophilic* (*E*), which attack the molecular fragment with an excessive electron density.

Thus, three types of reactions were divided into reactions of nucleophilic and electrophilic substitution, addition, and elimination. The kinetic study showed that some reactions involving two reactants occur as bimolecular reactions, whereas others occur as monomolecular reactions with the rate proportional to the substrate concentration and independent of the agent concentration. Thus, all variety of heterolytic reactions involving two reactants is divided into the following 10 groups:

Type of reaction	Reactant	Molecularity of reaction	Designation
Substitution	Nucleophile	1	$S_N1$
		2	$S_N2$
	Electrophile	1	$S_E1$
		2	$S_E2$
Addition	Nucleophile	1	$Ad_N1$
		2	$Ad_N2$
	Electrophile	1	$Ad_E1$
		2	$Ad_E2$
Designation		1	$E1$
		2	$E2$

### 8.2.1. Nucleophilic substitution

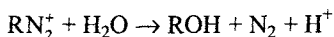
Alkaline hydrolysis of alkyl halides is an example of reactions of this type



along with the alcoholysis of alkyl halides



and deamination



Nucleophilic agents are the anions

$\text{H}^-$ ,  $\text{HO}^-$ ,  $\text{RO}^-$ ,  $\text{HOO}^-$ ,  $\text{RCOO}^-$ ,  $\text{HS}^-$ ,  $\text{S}^{2-}$ ,  $\text{RCOS}^-$ ,  $\text{ArO}^-$ ,  $\text{ArS}^-$ ,  $\text{S}_2\text{O}_3^{2-}$ ,  $\text{NC}=\text{C}(\text{NH}_2)\text{S}^-$ ,  $\text{NH}_2^-$ ,  $\text{RHN}^-$ ,  $\text{R}_2\text{N}^-$ ,  $\text{O}=\text{CNH}^-$ ,  $\text{O}=\text{CNR}^-$ ,  $\text{N}_3^-$ ,  $\text{F}^-$ ,  $\text{Cl}^-$ ,  $\text{Br}^-$ ,  $\text{I}^-$ ;

carbanions

$(\text{RCO})_2\text{C}^-$ ,  $(\text{NC})_2\text{C}^-$ ,  $\text{RC}^-(\text{CN})\text{COOR}$ ,  $\text{RCO}^-$ ,  $(\text{CN})_2\text{C}^-$ ,  $(\text{ROOC})_2\text{C}^-$ ,  $\text{ArC}^-(\text{CN})\text{R}$ ,

$\text{ArC}^-\text{RCOOR}$ ,  $\text{R}_2\text{C}^-\text{NO}_2$ ,  $\text{R}_2\text{C}^-\text{CN}$ ,  $\text{RCO}^-\text{CR}_2$ ,  $\text{R}_2\text{C}^-\text{CCOOR}$ ,  $\text{R}_2\text{C}^-\text{CSOOR}$ ,  $\text{X}_3\text{C}^-$ ,  $\text{R}_3\text{N}^+\text{C}^-$ ,  $\text{RSC}^-\text{R}_2$ ,  $\text{R}_2\text{C}^-=\text{CHCR}_2$ ,  $\text{ArC}^-\text{R}_2$ ,  $\text{RC}\equiv\text{C}^-$ ,  $\text{CN}^-$ ,  $\text{Ar}^-$ ;

and neutral molecules

$\text{H}_2\text{O}$ ,  $\text{H}_2\text{O}_2$ ,  $\text{ROH}$ ,  $\text{ArOH}$ ,  $\text{NH}_3$ ,  $\text{NRH}_2$ ,  $\text{NR}_3$ ,  $\text{RNHNH}_2$ ,  $\text{RCONHNH}_2$ ,  $\text{PH}_3$ ,  $(\text{HO})_2\text{PH}$ ,  $\text{P}(\text{OH})_3$ .

Nucleophilic substitution often occurs as the bimolecular reaction  $\text{S}_{\text{N}}2$  with the rate  $v = k_2[\text{AB}][\text{Y}]$ , where AB is the substrate, Y is the nucleophilic agent, and  $k_2$  is the bimolecular rate constant. Below we present the kinetic parameters for the reactions  $\text{XCH}_3 + \text{Y}^- \rightarrow \text{CH}_3\text{Y} + \text{X}^-$  ( $\text{H}_2\text{O}$ , 298 K)

Reaction	$k$ , l/(mol s)	$E$ , kJ/mol	$\log A$
$\text{CH}_3\text{Cl} + \text{F}^-$	$1.40 \cdot 10^{-8}$	112.4	11.87
$\text{CH}_3\text{Br} + \text{F}^-$	$3.02 \cdot 10^{-7}$	105.3	11.96
$\text{CH}_3\text{I} + \text{F}^-$	$6.92 \cdot 10^{-8}$	105.3	11.32
$\text{CH}_3\text{F} + \text{I}^-$	$2.08 \cdot 10^{-8}$	96.4	9.22
$\text{CH}_3\text{Cl} + \text{I}^-$	$2.00 \cdot 10^{-5}$	83.7	9.98
$\text{CH}_3\text{Br} + \text{I}^-$	$7.02 \cdot 10^{-4}$	76.3	10.22
$\text{CH}_3\text{I} + \text{I}^-$	$4.85 \cdot 10^{-4}$	75.7	9.95
$\text{CH}_3\text{F} + \text{OH}^-$	$5.86 \cdot 10^{-7}$	90.3	9.60
$\text{CH}_3\text{Cl} + \text{OH}^-$	$6.67 \cdot 10^{-6}$	101.5	12.61
$\text{CH}_3\text{Br} + \text{OH}^-$	$1.44 \cdot 10^{-4}$	96.1	13.02
$\text{CH}_3\text{I} + \text{OH}^-$	$6.36 \cdot 10^{-5}$	92.9	12.09

As it is shown by quantum-chemical analysis, the nucleophilic reactant attacks the cleaved bond from the rear, so that the likely charged orbitals of the reactant and substrate overlap. The frontal attack of the nucleophilic reactant (Fig. 8.1, b) is very rare. Moelwyn-Hughes estimated the activation energy of reactions of the  $\text{CH}_3\text{X} + \text{Y}^-$  type as follows.

Both the ion and polar molecule are solvated in a solution. In order to be approached, they must have vacancies in their solvate shells. An energy is needed for

the creation of such a vacancy. The activation energy can be considered as the energy of the creation of such vacancies in nucleophile 1 (ion  $Y^-$ ) and reactant 2 (molecule  $AB$ ).

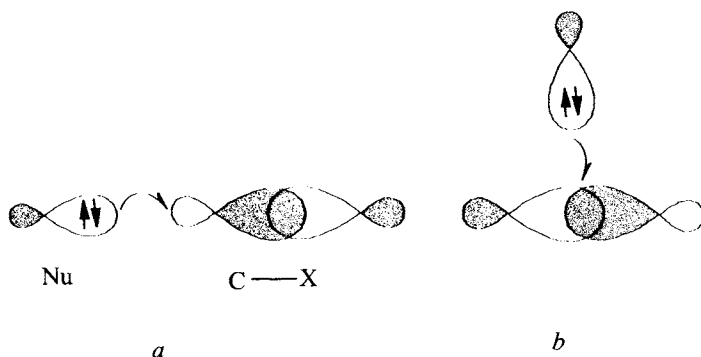


Fig. 8.1. Mechanisms of nucleophilic attack: *a*, attack from the rear with revolution of the configuration; and *b*, frontal attack with retention of the configuration.

Let the solvation number of reactant 1 in the standard state be equal to  $n_1$ , and in the state necessary for the reaction it is  $n_1^*$  ( $n_1 > n_1^*$ ). The energy necessary for the removal of one molecule from the solvate shell of the ion is designated by  $E_{S1}$ . This energy can be estimated through the desolvation energy of the ion  $E'_S$ :  $E_{S1} = E'_S(n_1 - n_1^*)n_1^{-1}$ . For example, for  $Cl^-$  in water  $E'_S = 322$  kJ/mol, and taking  $n_1 = 6$ ,  $n_1^* = 5$ , we obtain the term of the activation energy  $E_{S1} = (1/6)322 = 54$  kJ/mol.

Similarly we accept for the second reactant  $n_2$ ,  $n_2^*$  ( $n_2 > n_2^*$ ) and  $E_{S2}$ . The solvation energy of a polar molecule depends on the dipole moments of the reactant  $\mu_2$  and solvent  $\mu_S$  and the dielectric constant  $\epsilon$ , they were calculated by the formulas

$$E_{S1} = E'_S (n_2 - n_2^*) n_2^{-1}$$

$$E'_S = L[\mu_2 \mu_S (\epsilon + 2)/9\epsilon]^{3/2} a^{-1/2} \quad (8.4)$$

where  $a = 1.0 \cdot 10^{-88} \text{ J cm}^9$ .

The calculation using this simple physical model gave a good correspondence with experiment: for example, for the reaction of  $CH_3I$  with  $Y^-$  in  $H_2O$  the experimental and calculated  $E$  values (kJ/mol) are the following:

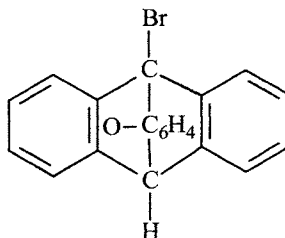
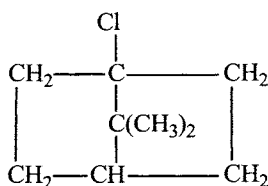
Y.....	$F^-$	$Cl^-$	$Br^-$	$I^-$	$OH^-$
$E_{exp}$ .....	105	92	81	76	93
$E_{calc}$ .....	107	98	87	73	93

It is most likely that in the nonsolvated form these reactions (if they are exother-

mic) can occur without an activation energy. The  $S_N2$  reaction is characterized by the following peculiarities.

1. The reaction rate is proportional to the concentration of each reactant:  $v = k_2[RX][Y]$ . Rigidly speaking, this is valid for dilute solutions, especially in the cases where Y is the anion. Sometimes the reaction order changes from the second to first with an increase in the concentration of one of the components. This is observed, in particular, when Y and RX form a complex, whose concentration at a high concentration of one of the components is determined by the amount of the component taken in deficient.

2. In the reaction of the nucleophilic reactant with the optically active molecule RX according to the  $S_N2$  mechanism, the configuration is inverted (inversion) because the attack of Y at RX is accompanied by the reversion of the tetrahedron of the attacked C atom (see Fig. 8.1). This rule was proved for numerous examples where nucleophilic substitution was bimolecular and accompanied by optical activity inversion. On the other hand, the substitution of the halogen at the carbon atom in a molecule with the bridged structure cannot be accompanied by the reversion of the tetrahedron. Indeed, the mechanism is not realized in the following RX compounds:



3. For nucleophilic substitution in aliphatic compounds, the rate constant decreases in the series  $CH_3X > C_2H_5X > R_1R_2CHX$ . The decrease in the reactivity is due to two effects: the induction influence of the alkyl groups, which decrease the effective positive charge at the attacked carbon atom, and steric hindrances of the alkyl groups. Both the activation energy and entropy change. Below we present the data illustrating the contribution of the induction and steric effects to the activation energy and the change  $\Delta S^\ddagger$  (kJ/mol) for the exchange reaction between  $Br^-$  and alkyl bromides RBr in acetone

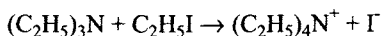
R.....	$CH_3$	$C_2H_5$	$(CH_3)_2CH$	$n-C_3H_7$	$(CH_3)_2CHCH_2$	$(CH_3)_3CCH_2$
$\Delta E_{ind}$ .....	0	4.2	8.4	4.2	4.2	4.2
$\Delta E_{ster}$ .....	0	3.3	6.7	3.3	9.6	30
$\Delta \Delta S^\ddagger$ .....	0	-11.3	-17.1	-19.6	-20.9	-40.1

It is seen that the  $S_N2$  reaction is very sensitive to steric effects.

4. The solvent, *vz.*, its polarity, can affect substantially the rate (rate constant) of the  $S_N2$  reaction. This depends on the charge distribution in the initial reactants and products. The  $S_N2$  reactions can be divided into three groups.

A. Ion + Molecule  $\rightarrow$  Molecule + Ion. For example,  $\text{HO}^- + \text{RCl} \rightarrow \text{ROH} + \text{Cl}^-$ ,  $\text{NH}_3 + \text{R}'\text{SR}'_2 \rightarrow \text{RNH}_3^+ + \text{SR}'_2$ . In these cases, an increase in the solvent polarity results in a slight decrease in the reaction rate constant. The decrease is resulted from some charge distribution and a decrease in the degree of solvation of reactants in the transition state.

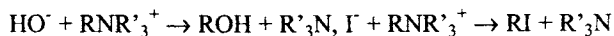
B. Molecule + Molecule  $\rightarrow$  Ion + Ion. For example,  $\text{H}_2\text{O} + \text{RCl} \rightarrow \text{ROH}_2^+ + \text{Cl}^-$ ,  $\text{NH}_3 + \text{RBr} \rightarrow \text{RNH}_3^+ + \text{Br}^-$ . Since ions are solvated to a much greater extent than molecules, in a more polar solvent the reaction is more exothermic, its activation energy is lower, and it occurs more rapidly. In this case, an increase in the solvent polarity results in a greater increase in the reaction rate constant. For example, for the reaction



at 373 K in various solvents  $k$  (l/(mol s)) are the following:

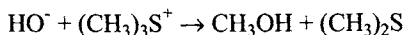
	$\text{C}_6\text{H}_6$	$\text{PhCl}$	$\text{PhCN}$	$\text{PhNO}_2$	$(\text{CH}_3)_2\text{SO}$
$\epsilon$ .....	2.2	5.6	25	35	49
$k \cdot 10^4$ .....	4.1	14.0	112	138	1200

C. Ion + Ion  $\rightarrow$  Molecule + Molecule. For example,



In this case, the products are solvated to a much less extent than the reactants. The transition state is also less polar than the ion-reactants. Therefore, the rate constant of such reactions decreases with an increase in the solvent polarity.

For example, the rate constant of the reaction



changes as follows with an increase in the content of water in a mixture with ethanol (373 K).

% $\text{H}_2\text{O}$ .....	0	20	40	100
$k \cdot 10^4$ , l/(mol s).....	7240	178	15	0.37

Specific solvation is of great importance. Aprotic solvents do not virtually solvate an ion. This strongly facilitates its attack at the positively charged carbon atom of the  $\text{RX}$  substrate. Therefore, in aprotic solvents nucleophilic substitution occurs espe-

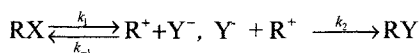
cially rapidly. Below we present the relative  $k_2$  values for the reaction of  $\text{Cl}^-$  with  $\text{CH}_3\text{I}$  at 298 K in several solvents.

	$\text{CH}_3\text{OH}$	$\text{HCONHCH}_3$	$\text{NCON}(\text{CH}_3)_2$	$\text{CH}_3\text{CON}(\text{CH}_3)_2$
$k/k_{\text{CH}_3\text{OH}}$	1	45	$1.2 \cdot 10^6$	$4.4 \cdot 10^6$

In protic solvents the activity of nucleophilic agents depends on the degree of solvation. The smaller the size of the ion, the higher the latter and changes in the series  $\text{F}^- < \text{Cl}^- < \text{Br}^- < \text{I}^-$ . In aprotic solvents where the solvation of an anion is insignificant, the smaller the radius of the halide ion, the more reactive the ion, and the dependence is inverse:  $\text{I}^- < \text{Br}^- < \text{Cl}^- < \text{F}^-$ .

Ions of neutral salts being introduced into a solution have a slight effect on the  $S_N2$  reaction (they slightly accelerate it). Ions formed during the reaction act similarly. The accumulation of these ions in a solution results in some acceleration of the process.

In addition to the  $S_N2$  mechanism, nucleophilic substitution can occur *via* the  $S_N1$  mechanism. This mechanism is multistage and includes the following steps:

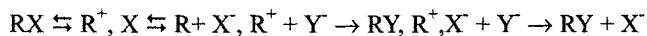


1. Dissociation to ions usually occurs slowly and recombination is very fast. Therefore, at early steps when  $k_{-1}[\text{X}^-] \ll k_2[\text{Y}^-]$ , the reaction rate is limited by the dissociation of  $\text{RX}$  and equals  $v = k_1[\text{RX}]$ . In a more general case,

$$v = k_1 k_2 [\text{RX}] / (k_{-1}[\text{X}^-] + k_2[\text{Y}^-]) \quad (8.5)$$

Thus, the first specific feature of the  $S_N1$  mechanism is that the reaction rate very often is independent of the concentration of the nucleophilic agent, and the reaction has the first order with respect to the substrate  $\text{RX}$ . Its rate is determined by the structure of  $\text{RX}$  and reaction conditions.

2. During the dissociation of  $\text{RX}$ , the tetrahedral structure of  $\text{R}$  is transformed into the planar structure of the  $\text{R}^+$  ion. The nucleophile attacks the central C atom of this ion from any of two sides with equal probabilities. Therefore, nucleophilic substitution *via* the  $S_N1$  mechanism is accompanied by the racemization of the optically active product. The formation of the partially racemized and partially inverted substitution product is often observed experimentally, for example, for the reactions  $\text{C}_6\text{H}_{13}(\text{CH}_3)\text{CHBr} + \text{H}_2\text{O}$  (60%  $\text{C}_2\text{H}_5\text{OH}$ ),  $\text{Ph}(\text{CH}_3)\text{CHCl} + \text{CH}_3\text{OH}$  ( $\text{CH}_3\text{OH}$ ), and  $\text{Ph}(\text{CH}_3)\text{CHCl} + \text{OH}^-$  ( $\text{H}_2\text{O}$ ). This is explained by the fact that ion pairs are formed and participate in the reaction along with free carbocations



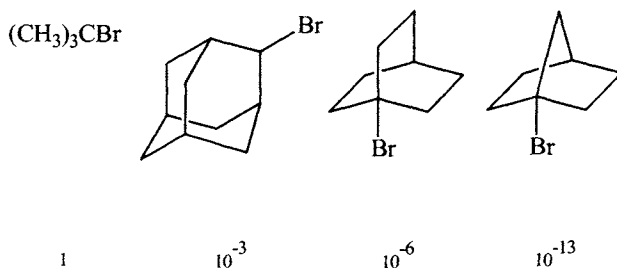
When  $Y^-$  reacts with free  $R^+$ , optically active  $RX$  is transformed into racemized  $RY$ . When  $Y^-$  attacks the ion pair  $R^+, X^-$  in which the agent can approach from one side only, the tetrahedron is inverted and the inverted product is formed as in the  $S_N2$  mechanism.

3. Since the reaction for the  $S_N1$  mechanism is limited by the dissociation of  $RX$  to ions, the lower the dissociation energy, the faster the reaction. Therefore, the reactivity of  $RX$  is determined by the degree of stabilization of the formed  $R^+$  ion. Since alkyl substituents increase the electron density at the carbon atom to which they are bound, the reactivity of  $RX$  increases in the series  $CH_3 < R_{prim} < R_{sec} < R_{tert}$ . For example, the reaction of  $RBr$  with  $H_2O$  in ethanol containing 20% water at 328 K occurs with the rate constant  $k_1 = 2.4 \cdot 10^{-6} s^{-1}$  for  $R = (CH_3)_2CH$  and  $k_1 = 1.0 \cdot 10^{-2} s^{-1}$  for  $R = (CH_3)_3C$ . The vinyl group and aromatic substituent in the  $\alpha$ -position to the attacked C atom facilitate the ionization of  $RX$

$RX$ .....	$(CH_3)_3CCl$	$CH_2=CHCH_2Cl$	$Ph(CH_3)CHCl$	$PhCHCl$
$k_1$ (rel.).....	1	$4 \cdot 10^4$	$8 \cdot 10^4$	$4 \cdot 10^7$

The dissociation of  $RX$  is substantially facilitated when bulky substituents are linked to the attacked C atom. This is resulted by the fact that in  $RX$  the angle between the  $C-C$  bonds is  $109^\circ$  and the bulky substituents experience repulsion. In the  $R^+$  carbocation formed by  $RX$  dissociation, the charge-bearing C atom has  $sp^2$  hybridization, the angles between the  $C-C$  bonds are  $120^\circ$ , and as a result, the arrangement of the substituents is more free.

Therefore, the larger the volume of the substituents at the C atoms linked with X, the faster the ionization of  $RX$ . By contrast, when the formation of the carbocation with  $sp^2$  hybridization is hindered, the rate of the  $S_N1$  reaction is retarded. This situation is observed in cyclic compounds  $RBr$ , and the greater the rigidity of the carbon framework, the slower the reaction (solvolysis of  $RBr$  in 80%  $C_2H_5OH$  at 298 K, relative rates are presented)



4. The ionization of  $RX$  occurs more rapidly in more polar solvents. The ionizing ability of the solvent is unambiguously related to  $\epsilon$  only for aprotic solvents in which dependence of the following type (see Chapter 5) is observed:

$$\log k = \log k_0 + \alpha(\epsilon - 1)/(2\epsilon + 1) \quad (8.6)$$

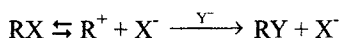
For protic solvents forming hydrogen bonds,  $\epsilon$  is not a characteristics of the ionizing ability of the solvent. Therefore, E. Grunwald and S. Winstein proposed to characterize this ability by the rate constant of solvolysis of  $(\text{CH}_3)_3\text{CCl}$ , choosing a solution of 20%  $\text{H}_2\text{O}$  and 80%  $\text{C}_2\text{H}_5\text{OH}$  as a standard

$$\log(k/k_0) = mY \quad (8.7)$$

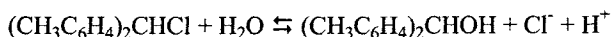
where  $Y$  is the measure of the ionizing ability of the solvent

	$\text{H}_2\text{O}$	$\text{CH}_3\text{OH}$	$\text{C}_2\text{H}_5\text{OH}$	80% $\text{C}_2\text{H}_5\text{OH}$	$\text{CH}_3\text{COOH}$	$\text{CF}_3\text{COOH}$
$Y$ .....	3.49	-1.09	-2.03	0.00	2.05	4.5

5. As already mentioned, the first step of the  $S_N1$  mechanism is reversible



therefore, the reaction is naturally retarded according to equation (8.5) when a salt containing the  $\text{X}^-$  anion is introduced into the solution. Due to the reversibility of the first step of the reaction occurred *via* the  $S_N1$  mechanism is retarded during the reaction, which is experimentally observed from a decrease in the experimentally determined  $k_{\text{exp}}$  ( $v = k_{\text{exp}}[\text{RX}]$ ). For example, the hydrolysis of  $\text{RCl}$



in water (298 K) is accompanied by a decrease in  $k_{\text{exp}}$  during the reaction

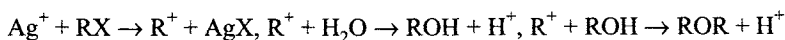
Conversion, %.....	8	16	38	50	70
$k_{\text{exp}} \cdot 10^5, \text{s}^{-1}$ .....	8.7	8.3	7.5	7.3	6.8

In the absence of perturbing factors, the reaction kinetics should be described by the equation ( $x = [\text{RX}]/[\text{RX}]_0$ )

$$v = k_1[\text{RX}]_0(1 - x)(1 + \alpha x)^{-1} \quad (8.8)$$

Neutral salts facilitate  $\text{RX}$  ionization affecting it through the ionic strength of the solution. For example, 0.1 mol/l  $\text{LiCl}$  increases the hydrolysis rate of *tert*-butyl bromide in 90% acetone (10% water) by 40% (323 K), 0.1 mol/l  $\text{LiBr}$  accelerates the hydrolysis of benzhydryl chloride in 80% acetone (20% water) by 17% (298 K), and 0.1 mol/l  $\text{LiCl}$  accelerates the hydrolysis of benzhydryl bromide, under the same conditions, by 27%.

6. The dissociation of alkyl halides to  $\text{R}^+$  and  $\text{X}^-$  is accelerated in the presence of metallic silver. Its surface contains  $\text{Ag}^+$  ions, which react with  $\text{RX}$  to form  $\text{R}^+$

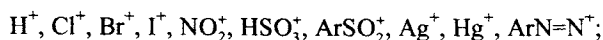


Solvolysis catalyzed by  $\text{Ag}^+$  ions is characterized by the properties of the  $S_N1$  mechanism. First, in reactivity alkyl halides are arranged in the series *tert* > *sec* > *prim*. Second, optically active  $\text{RX}$  are transformed into product-racemates. Third, this reaction results in the formation of products, whose structure indicates the intermediate formation of  $\text{R}^+$  (the rearrangement characteristic of  $\text{R}^+$  is observed).

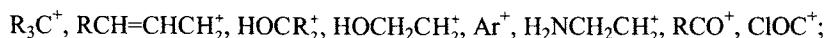
Acid catalysis proceeds via the  $S_N1$  mechanism. For example, the exchange of  $\text{Cl}$  between 1-phenyl-1-chloroethane and radioactive  $\text{Cl}^-$  in nitromethane is accelerated by  $\text{HCl}$ . The reaction rate is  $v = k_1[\text{RCl}] + k_2[\text{RCl}][\text{HCl}]$ . The second term corresponds to the  $\text{HCl}$ -catalyzed reaction. The transition state  $\text{R}\cdots\text{Cl}\cdots\text{H}\cdots\text{Cl}$  is observed in which the formation of the  $\text{H}\cdots\text{Cl}$  bond favors the cleavage of the  $\text{R}\cdots\text{Cl}$  bond.

### 8.2.2. Electrophilic substitution

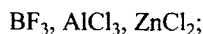
Electrophilic agents have a vacant orbital and, hence, possess a high reactivity with respect to carbanions, unsaturated and aromatic compounds. Electrophilic agents are the cations



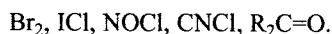
carbocations



Lewis acids



and neutral molecules



Such long ago known in organic chemistry reactions as nitration, sulfonation, and halogenation of aromatic compounds are reactions of electrophilic substitution.

Quantum-chemical analysis of a bimolecular reaction of an electrophilic agent with a substrate shows that the frontier attack of the agent involving the unoccupied orbital at the occupies orbital of the substrate is preferential (Fig. 8.2, a).

Therefore, the geometry of the transition state of electrophilic substitution substantially differs from that of nucleophilic substitution (see Fig. 8.1) where the attack of the agent occurs "from the rear." The electrophilic agent attacks the  $\pi$ -bond of the substrate also in a different manner (Fig. 8.2, b).

Electrophilic substitution reactions are widely abundant among aromatic compounds. The general mechanism of the reaction of the electrophilic agent  $\text{E}^+$  with the aromatic compound  $\text{ArH}$  can be presented by the following scheme:

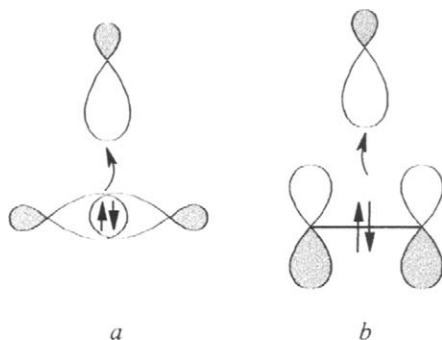
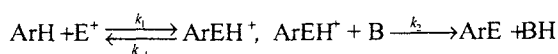


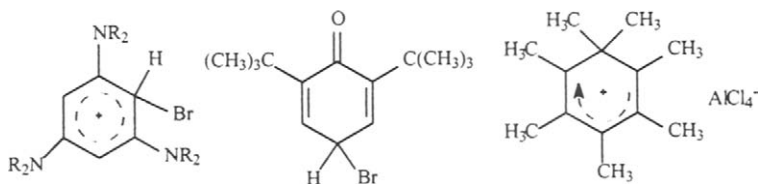
Fig. 8.2. Mechanism of the electrophilic attack: *a*, at the  $\sigma$ -bond; and *b*, at the  $\pi$ -bond.



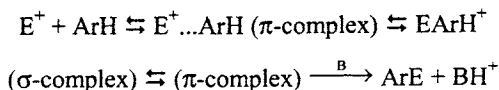
The reaction rate in the general form looks like

$$v = k_1 k_2 [\text{ArH}][\text{E}^+][\text{B}] / (k_1 + k_2 [\text{B}]) \quad (8.9)$$

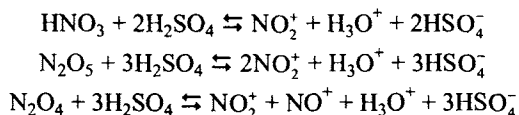
Usually  $k_2[\text{B}] \gg k_1$ , *i.e.*, the second step is very fast. The  $\text{ArEH}^+$  complex is very labile, and evidences for its formation are usually indirect. However, in some cases, this complex was detected and isolated. Below we present the structures of these stable complexes



The formation of the  $\sigma$ -complex is preceded, likely, in many cases, the formation of the  $\pi$ -complex, which occurs almost without an activation energy. Therefore, the sequence of transformations in the  $S_N2$  mechanism can be presented by the multistep scheme



Among electrophilic substitution reactions, the nitration reactions seems to be most completely studied. In this reaction, the nitronium ion, which is formed in a mixture of nitric and sulfonic acids, is the attacking agent in this reaction. The nitronium ion is formed by the equilibrium reactions



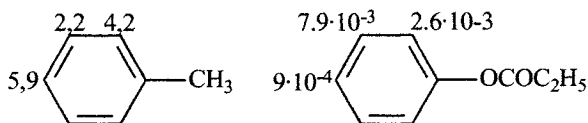
The formation of the nitronium ion in the presence of sulfuric acid was proved by cryoscopic measurements, IR spectroscopy (peaks at 1400 and 1050  $\text{cm}^{-1}$  appear in the spectrum), from analysis of spectra and X-ray patterns of crystalline salts of nitronium, such as  $\text{NO}_2\text{ClO}_4$ ,  $\text{NO}_2\text{FSO}_4$ , and  $\text{NO}_2\text{HS}_2\text{O}_7$ , and by electroconductivity of nitric acid. In a solution of sulfuric acid the nitration rate is  $v = k_2[\text{ArH}][\text{H}_2\text{SO}_4]$ , whereas in nitric acid  $v = k_1[\text{ArH}][\text{HNO}_3]$ . Substituents in the benzene ring affect the rate of  $\text{NO}_2^+$  addition to the aromatic ring: substituents increasing the electron density in the ring accelerate and those decreasing it retard the addition rate

Substituent	H	$\text{CH}_3$	$\text{C}(\text{CH}_3)_3$	Cl	I	$\text{NO}_2$	$\text{N}(\text{CH}_3)_2$
Relative rate	1	24	15	0.033	0.18	$6 \cdot 10^{-8}$	$1.2 \cdot 10^{-8}$

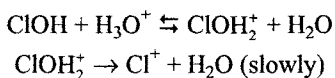
In addition, substituents affect the ratio of ortho-, meta-, and para-isomers formed during nitration. A substituent can have a positive inductive effect on the system of  $\pi$ -electrons, for example,  $\text{CH}_3$  (+I effect), a negative inductive effect, *i.e.*, ester group (-I effect), or a positive conjugation effect, OR group (+K effect). Below we present the classification of these effects according to Ingold

Effect	Substituents	Effect
+I	$\text{CH}_3\text{CH}(\text{CH}_3)_2$	ortho-para, activation
-I	$\text{COOR}$	meta, deactivation
	$\text{S}^+(\text{CH}_3)_2$	meta, deactivation
-I, +K	Cl	ortho-para, deactivation
	OR	ortho-para, activation
+I, +K	$\text{O}^-$	ortho-para, activation

The distribution of partial activities of various positions of the benzene ring in the nitration reaction compared to benzene is presented below for toluene and ethyl benzoate

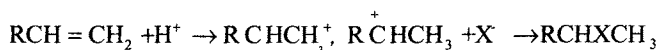


The halogenation of aromatic compounds in acidic media or in the presence of Lewis acids proceeds *via* the  $S_E2$  mechanism. The following species can be electrophilic agents in chlorination (arranged in decreasing their activity):  $\text{Cl}^+$ ,  $\text{ClOH}_2^+$ ,  $\text{Cl}_2$ , and  $\text{ClOH}$ . In nonaqueous solvents,  $\text{Cl}_2$  acts most often as the main agent. In aqueous acidic solutions, it is  $\text{Cl}^+$ , which is formed from  $\text{ClOH}$  by the reactions

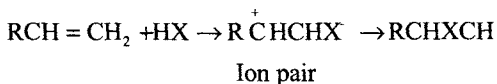


### 8.2.3. Addition reactions

Addition at the double  $\text{C}=\text{C}$  bond occurs *via* various mechanisms: ionic, radical, or molecular. In this Section we consider briefly the mechanisms of heterolytic addition. Electrophilic addition reactions  $\text{Ad}_E$  are widely abundant. Halogens and hydrogen halides often add according to this mechanism. The addition of  $\text{HX}$  to the  $\pi\text{-C}=\text{C}$  bond in a polar medium where  $\text{HX}$  is ionized occurs in two steps



The geometry of interacting electron orbitals for the electrophilic attack of this type is presented in Fig. 8.2, *b*. In aprotic solvents where  $\text{HX}$  exists predominantly in the nondissociated state, this is precisely  $\text{HX}$  which attacks the double bond

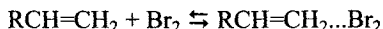


Olefin hydration catalyzed by acids proceeds *via* the mechanism of electrophilic addition. Here carbocations play an important role as intermediates (see Section 8.2.4).

The addition of halogens to olefins in polar media proceeds as a heterolytic process. In acetic acid and other polar solvents at a low content of  $\text{X}_2$ , the rate

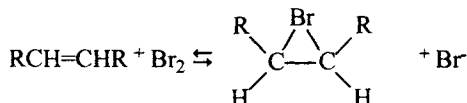
$$v = k[\text{RCH}=\text{CH}_2][\text{X}_2]$$

The following mechanism is assumed:





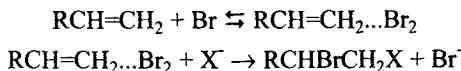
Halogen addition is characterized by stereospecificity. For example, the addition of bromine to acetylenedicarboxylic acid is accompanied by the predominant formation of dibromofumaric acid, that is, occurs in the *trans*-position. Therefore, the formation of labile cations with the bridged structure is assumed



The ion of this type was spectrally proved in the case of the reaction of adamantylideneadamantane with  $\text{Br}_2$ . The intermediate formation of the cation in olefin halogenation is also evidenced by the fact that halide ions accelerate this reaction. In acetic acid olefin bromination in the presence of  $\text{Br}^-$  or  $\text{Cl}^-$  occurs with the rate

$$v = k[\text{RCH}=\text{CH}_2][\text{Br}_2][\text{X}^-]$$

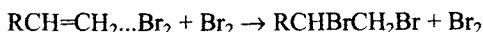
and the following mechanism is proposed:



At a sufficiently high concentration of  $\text{Br}_2$ , olefin bromination in acetic acid occurs as a reaction of the II order with respect to bromine

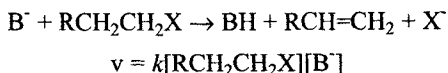
$$v = k[\text{RCH}=\text{CH}_2][\text{Br}_2]^2$$

A similar mechanism is assumed

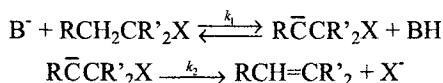


#### 8.2.4. Abstraction (elimination) reactions

Abstraction reactions are reverse to addition reactions. Two types of these reactions are distinguished: monomolecular abstraction *E1* and bimolecular *E2*. Orbitals in the heterolytic abstraction of X are schematically presented in Fig. 8.3. The abstraction of HX from the  $\text{RCH}_2\text{CH}_2\text{X}$  molecule under the action of the B base can occur by different ways. First, as a synchronous process (*E2*)



Second, as a stepped process through the intermediate formation of the carbanion

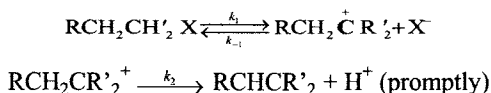


And in this case,  $v \approx [\text{RCH}_2\text{CR}'_2][\text{B}^-]$ , if  $k_2 \gg k_1[\text{BH}]$  or  $k_2 \ll k_1[\text{BH}]$ . In the second case,

$$v = k_1 k_2 [\text{RCH}_2\text{CR}'_2\text{X}][\text{B}^-]/[\text{BH}]$$

Thus, the limiting step can be determined by the influence of the conjugated acid BH on the abstraction process.

Third, elimination can occur through the formation of the carbocation (*E1*) similarly to that as it is observed for  $S_N1$



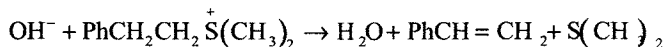
In this case,

$$v = k_1 k_2 [\text{RCH}_2\text{CR}'_2\text{X}](k_{-1}[\text{X}^-] + k_2)^{-1}$$

The following is characteristic of the *E2* mechanism occurred in one step. The reaction rate  $v = k[\text{RCH}_2\text{CR}'_2\text{X}][\text{B}^-]$ . Since the detachment of a proton and the abstraction of the X group occur simultaneously in the elementary act, the reaction is characterized by a sufficiently high isotope effect. For example, for the reaction



the  $k_H/k_D$  ratio is equal to 3.9, and for the reaction



$k_H/k_D = 5.9$  ( $\text{H}_2\text{O}$ , 303 K), and for the reaction



$k_H/k_D = 7.1$  ( $\text{C}_2\text{H}_5\text{OH}$ , 313 K).

The reaction of the *E2* type involving aromatic compounds is very sensitive to substituents in the aromatic ring.

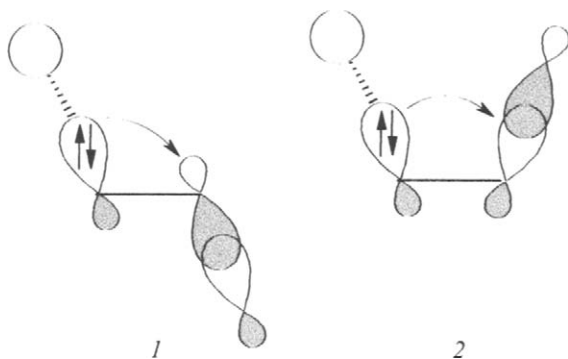
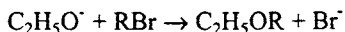


Fig. 8.3. Arrangement of the interacting orbitals for *trans*- (1) and *cis*-elimination (2).

#### 8.2.5. Conventional character of reaction division into nucleophilic and electrophilic

The division of reactions into nucleophilic and electrophilic is conventional, as it was mentioned by Ingold. When the heterolytic interaction of two reactants occurs, one of them is a donor of an electron pair (nucleophile), and another is an acceptor of an electron pair (electrophile). For example, in the reaction



the nucleophilic attack occurs of the  $\text{C}_2\text{H}_5\text{O}^-$  ion at the C atom bound to the bromine (as it is commonly accepted), and at the same time, the electrophilic attack of RBr at the oxygen atom occurs in the ethoxy ion. The division of reactants into agents and substrates descends to the epoch of alchemy when the active male origin was seen in some reactants, and others (substrates) represented the passive female origin.

There are many examples where the same reactant is considered sometimes as an agent and sometimes as a substrate. For example, alkyl halides in reactions of nucleophilic substitution and abstraction are considered as substrates, whereas in alkylation reactions of aromatic compounds they are considered as agents. If both reactants are considered as equivalent, we have to speak about electrophilic-nucleophilic, *i.e.*, heterolytic reactions, in which one reactant is a nucleophile and another is an electrophile.

The situation is similar to that for redox reactions (one reactant is an oxidant and another is a reducing agent) or for reaction involving acids and bases. Another moment, which is important from the viewpoint of the kinetics, is the following. For

the accepted division of reactions, the same group is composed of simple (e.g.,  $S_N2$ ,  $E2$ ) and complex reactions ( $S_N1$ ,  $S_N2$ ,  $E1$ ), reactions involving starting reactants and labile intermediates formed from them, and reactions involving molecules and ions.

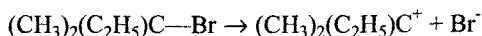
Therefore, reactions of the same group, e.g.,  $Ad_E$  involving olefins and halogens, obey different kinetic regularities, behave differently depending on the polarity of the solvent and the ionic strength, do not always obey the law of acting masses, exhibit anomalies in the temperature dependence, have a complex composition of the final products, etc. The same system, depending on the solvent, temperature, and sometimes the reactant concentration, can be transformed according to this or another mechanism or *via* several directions simultaneously. The competition of different directions is considered in the next Section using reactions involving carbocations as examples.

### 8.3. Reactions of carbocations and carbanions

#### 8.3.1. Carbocations

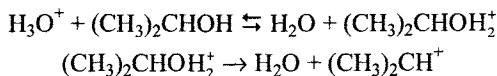
Carbocations are ions with the positively charged carbon atom  $R_3C^+$ , they are formed as intermediates in various heterolytic reactions and participate in reactions of heterolytic substitution, addition, and decomposition. Carbocations are formed in reactions of the following types.

1. Upon heterolysis at the C—X bond, where X is the residue of a strong acid, for example,

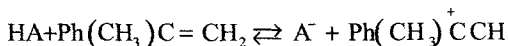


Heterolysis occurs in polar solvents and when the carbocation is rather stable (see below).

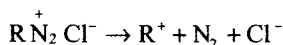
2. Due to the decomposition of protonated alcohol, for example,



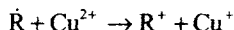
3. Due to the addition of a proton at the multiple  $\pi$ -C—C bond, for example,



4. Upon the decomposition of diazo cations to evolve  $N_2$

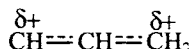


5. By the oxidation of a radical with an ion-oxidant (see below)

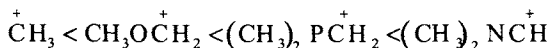


For the detection of stable carbocations, various physicochemical methods are used: spectroscopy (aromatic carbocations possess a high extinction coefficient up to  $10^5 \text{ l}/(\text{mol cm})$ ), NMR spectroscopy, and methods of measuring the electroconductivity and the number of particles in a solution (cryoscopy). Many carbocations are very labile. To prove their formation, "traps" are used, reactants that react very promptly with carbocations:  $N_3^-$ , tetrahydrothiophene.

The positively charged carbon atom in the carbocation exists in the state of  $sp^2$  hybridization. It has a planar structure and angles between the C—C bond of  $120^\circ$  each if this is not prevented by a bulky substituent. The stability of the carbocation depends of its structure. It is higher for ions with substituents with  $\pi$ -C—C bonds (vinyl groups, aromatic rings) in the  $\alpha$ -position to the charge-bearing C atoms. Stability increases in the sequence  $CH_3^+ < CH_3CH=CH_2^+ < CH(CH=CH_2)_2^+$  and  $CH_3^+ < CH_2(Ph)^+ < CHPh_2^+ < Ph_3C^+$ . This is related to the interaction of the positive charge on C with  $\pi$ -electrons of the multiple C—C bond, which results in the delocalization of the charge and  $\pi$ -electrons stabilizing the cation. The following structure is valid for the propylene carbocation:



Due to the same reason, substituents with heteroatoms with a lone electron pair increase the stability of carbocations



The inductive effect is a reason for an increase in the stability of carbocations with an increase in the number of alkyl substituents at the charge-bearing carbon atom:  $CH_3^+ < CH_3CH_2^+ < (CH_3)_2CH^+ < (CH_3)_3C^+$ . The degree of stabilization of  $R^+$  can be judged from a change in the enthalpy in the reaction  $RH \rightarrow R^+ + H^-$ . For the gas phase the enthalpy  $\Delta H$  can be calculated using the strength of the R—H bond  $D_{R-H}$ , the ionization potential  $I_R$  of the radical  $R\cdot$ , and the electron affinity of the hydrogen atom  $EA = 72.4 \text{ kJ/mol}$

$$\Delta H = D_{R-H} + I_R - EA(H)$$

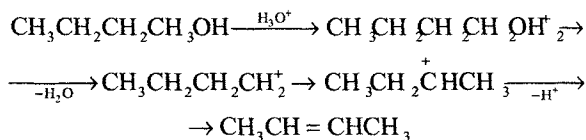
Below we present the values (in kJ/mol) of  $\Delta\Delta H = \Delta H(\text{CH}_3^+) - \Delta H(\text{R}^+)$  characterizing  $\text{R}^+$  relatively to  $\text{CH}_3^+$  in the gas phase ( $\Delta H(\text{CH}_3^+) = 1216$  kJ/mol).

$\text{R}^+ \dots\dots \text{C}_2\text{H}_5^+$	$(\text{CH}_3)_2\text{CH}^+$	$(\text{CH}_3)_3\text{C}^+$	$(\text{C}_2\text{H}=\text{CH}=\text{CH}_2)^+$	$\text{PhCH}_2^+$
$\Delta\Delta H \dots\dots 167$	259	331	237	320

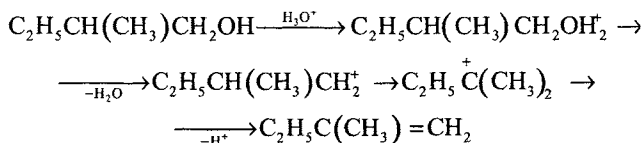
It follows from figures presented above that the influence of the structure on the stabilization of the carbocation is very high. For comparison, we can present, e.g., the difference in strengths of C—H bonds for R—H, which (relatively to methane) is equal to 26 for ethane, 38 for propane (in the  $\text{CH}_2$  group), and 50 kJ/mol for isobutane (in the *tert*-C—H group).

### 8.3.2. Isomerization of carbocations

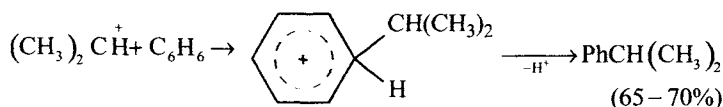
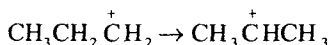
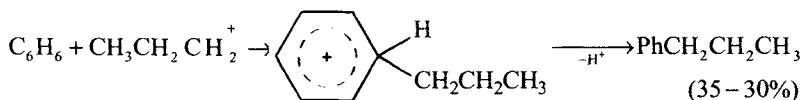
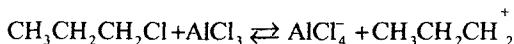
Since carbocations with different carbon skeleton differ strongly in their stability, they are prone to isomerization due to which the most stable of all possible carbocation is formed. The charge on the carbon atom facilitates this isomerization. The isomerization of carbocations results in the appearance of products, whose structure differs from that which is seemingly pre-determined by the structure of the reactant. For example, for *n*-butanol dehydration, one can expect the formation of butene-1 but butene-2 is formed. The reason is the isomerization of an intermediate species, carbocation



A similar situation is observed for the dehydration of 2-methylbutanol-1

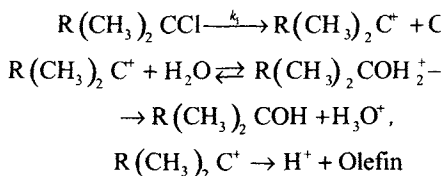


The alkylation of aromatic hydrocarbons with alkyl halides  $\text{RX}$  in the presence of  $\text{AlCl}_3$  (according to Friedel—Crafts) also proceeds through the intermediate  $\text{R}^+$  and, hence, is accompanied by the isomerization of the carbocation, due to which a mixture of alkylated aromatic hydrocarbons is formed. For example, in the alkylation of benzene with *n*-propyl chloride ( $\text{AlCl}_3$ , 255 K) two hydrocarbons are formed



### 8.3.3. Competition of reactions involving carbocations

Carbocations possess a high reactivity and rapidly enter the following reactions: abstract a proton to be transformed into olefin, add to a negative ion ( $\text{R}^+ + \text{X}^- \rightarrow \text{RX}$ ), add to a molecule at the heteroatom with a lone electron pair ( $\text{R}^+ + \text{HQR}' \rightarrow \text{RR}'\text{OH}^+$ ), add to a molecule with the double bond ( $\text{R}^+ + \text{CH}_2=\text{CHX} \rightarrow \text{RCH}_2\text{CHX}$ ), and add to the aromatic ring ( $\text{R}^+ + \text{C}_6\text{H}_6 \rightarrow \text{RC}_6\text{H}_6^+$ ). Some of these reactions very often occur in parallel, due to which the competition of different mechanisms of heterolytic transformation appears. For example, the solvolysis of  $\text{R}(\text{CH}_3)_2\text{CCl}$  in 80%  $\text{C}_2\text{H}_5\text{OH}$  affords the corresponding alcohol ( $\text{S}_{\text{N}}1$  mechanism) and olefin ( $\text{E}1$  mechanism) due to the following reactions:



Below we present the rate constants of the first limiting step and % of ions  $\text{R}(\text{CH}_3)_2\text{C}^+$  transformed into olefin (298 K, 80%  $\text{C}_2\text{H}_5\text{OH}$ , 20%  $\text{H}_2\text{O}$ ).

R.....	$\text{CH}_3$	$\text{C}_2\text{H}_5$	$(\text{CH}_3)_2\text{CH}$	$(\text{CH}_3)_3\text{C}$	$(\text{CH}_3)_3\text{CCH}_2$
$k_1 \cdot 10^6, \text{s}^{-1}$ .....	9.2	15.3	8.1	11.1	206
% (C=C).....	16	34	62	61	65

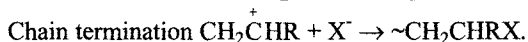
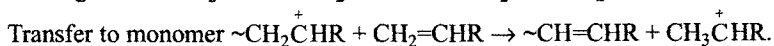
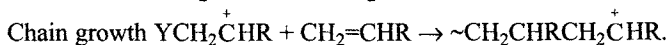
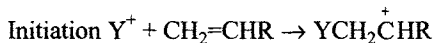
The carbocation reacts both in the stable form and in the composition of the ion pair. This explains the fact that the counterion (anion) influences on the ratio of solvolysis of  $\text{H}^+$  detachment resulting in the formation of olefin. In the solvolysis of  $\text{C}_2\text{H}_5(\text{CH}_3)_2\text{CX}$  in 80%  $\text{C}_2\text{H}_5\text{OH}$  (298 K), the fraction of olefin in the reaction prod-

ucts is 33% for X = Cl, 26% for X = Br, and 26% for X = I.

#### 8.3.4. Cationic polymerization

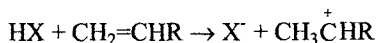
Cationic polymerization is based on the capability of carbocations and other positively charged ions of adding rapidly at double bonds and reacting with heteroatoms of organic molecules. Under certain conditions, a stepwise growth of the carbonium ion appears in the system, and this results in the formation of a monomer. Vinyl monomers and heterocycles containing the heteroatom in the ring are polymerized by the cationic mechanism.

The positively charged ions  $R_3C^+$ ,  $RO^+=CR_2$ ,  $R_3O^+$ ,  $R_3S^+$ , and  $R_2N^+=CR_2$  lead cationic polymerization. In a solution these ions react as either free ions or in the composition of ion pairs, both contact and separated. Cationic polymerization includes the following stages:

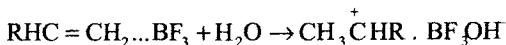
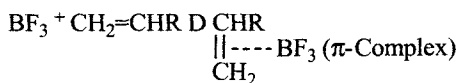


Quite various compounds can initiate cationic polymerization.

1. Protic acids, transferring a proton to a monomer, can lead cationic polymerization

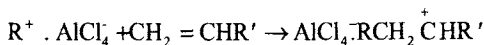
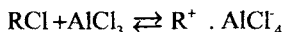


2. Aprotic acids ( $BF_3$ ,  $SnCl_4$ ,  $AlCl_3$ ,  $SbCl_5$ ) are efficient catalysts of cationic polymerization. Usually polymerization needs a cocatalysts, and water is used as the latter. Initiation occurs as several successive stages, for example,

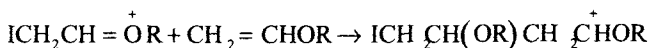
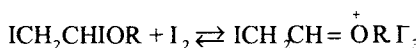


The cocatalyst is introduced in a small amount because a water excess prevents initiation reacting with the ion pair.

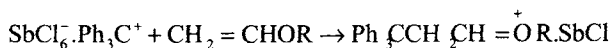
The  $AlCl_3 + RCl$ ,  $Al(C_2H_5)_2Cl + RCl$ , etc. mixtures are widely used for the preparation of polyisobutylene and butyl rubber. The reaction of aluminum chloride with  $RCl$  affords a carbocation, which begins polymerization



3. Alkyl vinyl ethers are rapidly polymerized under iodine. Initiation includes several stages

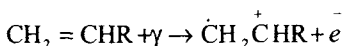


4. Polymerization can be initiated by stable carbocations. The triphenylcarbocation induces the polymerization of alkyl vinyl ethers



Cycloheptatrienyl  $\text{C}_7\text{H}_7^+$  and aminium  $(\text{XC}_6\text{H}_4)_3\text{N}^+$  salts have the same effect.

5. Radical cations are formed under the action of electrons and  $\gamma$ -beams on the monomer



Since in a nonpolar medium the carbocation is very active and reacts with the monomer much more rapidly than the C atom bearing the free valence, cationic polymerization occurs predominantly. This is facilitated by a low temperature at which ion recombination is rather slow.

Chain propagation during the polymerization of olefinic compounds proceeds through the addition of the monomer to the positively charged active site. In a monomer medium under  $\gamma$ -initiation, chain growth on the carbocations that formed occurs very rapidly, as it is seen from the following data ( $k_{\text{gr}}$  is the rate constant of chain propagation (growth) in l/mol s):

Cyclopentadiene.....	Styrene	$\alpha$ -Methylstyrene	Isobutyl vinyl ether
$k_{\text{gr}} = 6 \cdot 10^8$ (195 K).....	$3.5 \cdot 10^6$ (288)	$4 \cdot 10^6$ (273)	$3 \cdot 10^5$ (303)

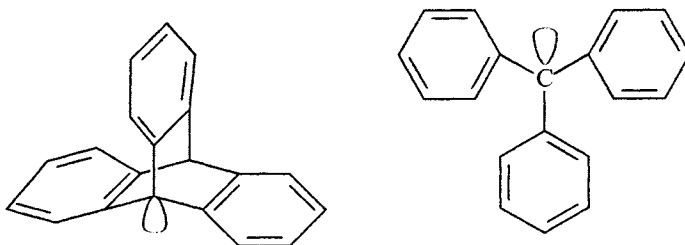
The polarity of the solvent affects chain propagation in cationic polymerization. The higher the polarity, the stronger the equilibrium shift toward separated ion pairs and free ions and the faster the addition of monomers to these ions. For the polymerization of styrene under  $\text{HClO}_4$  in  $\text{CCl}_4$ — $\text{ClCH}_2\text{CH}_2\text{Cl}$  mixtures with different

compositions  $k_{gr}$  at 298 K depends on  $\epsilon$  of the medium as follows:

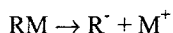
$\epsilon$ .....	2.3	5.2	7.0	9.7
$k_{gr}$ , l/(mol s).....	$1.2 \cdot 10^{-3}$	0.40	3.2	17

### 8.3.5. Reactions of carbanions

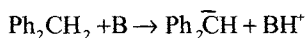
The carbocation contains the carbon atom bearing a positive charge: this atom has a lone electron pair. The carbanionic center has a planar or a pyramidal structure. For example, three C—C bonds in triphenylmethyl carbanion are arranged in one plane, and the trypticyl anion has the structure of a trihedral pyramid



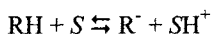
Carbanions are formed in polar solvents during the dissociation of organometallic compounds



and the action of bases on the C—H acid, for example,



Most frequently carbanions in a solution exist as contact or solvate-separated ion pairs. The stability of the  $R^-$  carbanion is characterized by  $pK_a = -\log K_a$ , where  $K_a$  is the constant of acid dissociation of RH:  $K_a = [R^-][H^+]/[RH]$ . At this dissociation the proton adds to the solvent molecule



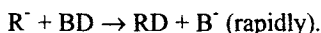
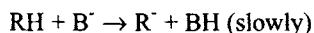
so that  $K_a$  depends on the solvent, as it is seen from the following data ( $pK_a$  are given in three solvents):

Solvent	Benzene	Cyclohexylamine	Dimethyl sulfoxide
9-Phenylfluorene	21	18.5	18.5
Indene	21	20.0	18.2
Fluorene	20.5	23.1	22.1

$(p\text{-PhC}_6\text{H}_4)_2\text{CH}_2$	31	30.2	25.3
$\text{Ph}_3\text{CH}$	33	31.5	27.2
$\text{Ph}_2\text{CH}_2$	35	33.1	28.6

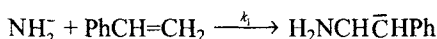
The higher the degree of charge delocalization, the more stable the carbanion. The negative inductive effect also favors its stabilization.

Carbanions rapidly add protons, which is manifested in the deuterioexchange reaction

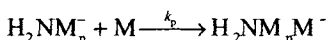


### 8.3.6. Anionic polymerization

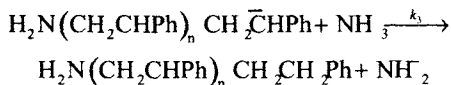
The high reactivity of carbanions with respect to unsaturated compounds results in polymerization. Polymerization occurs under the action of strong bases in aprotic media and begins from the addition of  $\text{R}^-$  or  $\text{NH}_2^-$  to the monomer, for example,



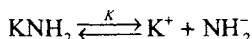
The growth of the macrochain occurs in the reaction of the type



(M is the monomer), and chain termination occurs due to the chain transfer to the solvent, e.g., in a medium of ammonia, *via* the reaction



Under conditions where the  $\text{KNH}_2$  initiator is used, the rates of initiation  $v_i$  and polymerization  $v_p$ , respectively, are equal to  $v_i = k_i K^{1/2} [\text{M}] [\text{KNH}_2]^{1/2}$  and  $v_p = k_i K^{1/2} k_p [\text{M}]^2 [\text{KNH}_2]^{1/2} / k_s [\text{NH}_3]$ , where  $K$  is attributed to the equilibrium



Anionic polymerization often occurs in the absence of reactions of chain termination. Then anionic centers remain unchanged after polymerization, and polymers with such centers at the ends of macromolecules are named *living polymers*. These polymers are formed when solvents incapable of terminating the growing macroanions are used, e.g., tetrahydrofuran, dioxane, and 1,2-dimethoxyethane. Both free carbanion and ion pair participate in chain propagation.

### 8.4. Ion redox reactions

An idea to transfer an electron from one ion to another appeared during studying the isotope exchange: electron exchange between  $\text{Mn}^{2+}$  and  $\text{Mn}^{3+}$  was postulated by M. Polissar in 1936. Experimental evidence for exchange of this type was obtained only in 1950 ( $\text{MnO}_4^- + \text{MnO}_4^{2-}$ , K. Hornig, H. Zimmermann, W. Libby). Several years after an alternative mechanism of electron transfer involving the bridging ligand was proposed (W. Libby, 1952, intermediate complex  $(\text{H}_2\text{O})_5\text{FeXFe}(\text{OH}_2)_5^{4+}$ ), and a year later this mechanism was proved for the reaction of  $\text{Cr}^{2+}$  with  $\text{Co}(\text{NH}_3)_5\text{Cl}^{2+}$  (H. Taube, H. Myers, R. Rich, 1953). Soon afterwards, concepts about the extrasphere, intrasphere, and bridging mechanisms of electron transfer were formed.

#### 8.4.1. Binuclear intermediate complex

As any bimolecular reaction, the redox reaction in a solution includes following three stages, each of which can be reversible:



If the electron transfer in the  $\text{A}^+ \cdot \text{B}$  pair is very fast and irreversible, the reaction is limited by the frequency of diffusional collisions, which depends on the viscosity  $\eta$ , radius  $r$  ( $r_A = r_B$ ), and the Coulomb interaction potential, which is determined by the sign and value of charges  $z_A$  and  $z_B$  (see Chapter 5)

$$k_D = (8RT/3\eta)(z_A z_B s/r) [\exp(z_A z_B s/r) - 1]^{-1} \quad (8.11)$$

where  $s = (1/4\pi)\epsilon^2/\epsilon kT$ .

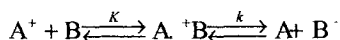
As it can be seen from this formula, the role of the Coulomb interaction between ions is very important. The following (calculated) data illustrate this ( $r = 0.4$  nm,  $\text{H}_2\text{O}$ , 298 K):

$z_A z_B$	+9	+4	+1	0	-1	-4	-9
$\log k_D, \text{l}/(\text{mol s})$	4.3	7.8	9.5	10	10.4	40.9	11.3

Below we present some examples for these reactions ( $\text{H}_2\text{O}$ , 298 K)

$\text{A}^+$	$\text{Co}(\text{H}_2\text{O})_6^{3+}$	$\text{Co}(\text{NH}_3)_5\text{Cl}^{2+}$	$\text{MnO}_4^-$	$\text{Fe}(\text{phen})_3^{3+}$
$\text{B}^+ (\text{B}^-)$	$\text{U}^{3+}$	$\text{Cr}^{2+}$	$\text{Cd}^{2+}$	$\text{MnO}_4^{2-}$
$k_D, \text{l}/(\text{mol s})$	$7 \cdot 10^3$	$6 \cdot 10^5$	$2 \cdot 10^{10}$	$1 \cdot 10^{11}$

Many such electron transfer reactions proceed slowly through a labile intermediate complex

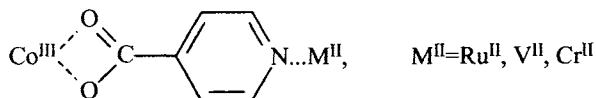


In this case (see Chapter 7),  $k_{\text{exp}} = kK(1 + K[A^+B^+])$ .

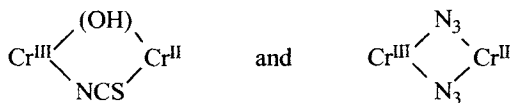
Some reactions of this type are exemplified below.

$A^+(A^-)$	$\text{Fe}(\text{CN})_6^{3-}$	$\text{Ce}^{4+}$	$\text{Ru}(\text{NH}_3)_5\text{Cl}^{2+}$	$\text{Co}(\text{NH}_3)_5\text{H}_2\text{O}^{3+}$
$B^+(B^-)$	$\text{Co}(\text{EDTA})^{2-}$	$\text{IrCl}_6^{3-}$	$\text{Cr}^{2+}$	$\text{Fe}(\text{CN})_6^{4-}$
$K, \text{ l/mol}$	$7 \cdot 10^2$	$2 \cdot 10^2$	70	$1.5 \cdot 10^3$
$k_{\text{exp}}, \text{ s}^{-1}$	$6 \cdot 10^{-3}$	60	$4.6 \cdot 10^2$	0.2

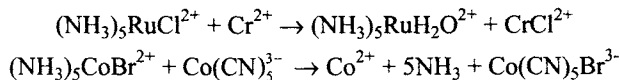
This labile formation can be (1) an ion pair as, e.g., in the reaction of  $\text{Co}(\text{NH}_3)_5\text{H}_2\text{O}^{3+}$  with  $\text{Fe}(\text{CN})_6^{4-}$ ; (2) a chelate complex as in the reaction of  $\text{Co}(\text{NH}_3)_5\text{LH}_2^{2+}$  with  $\text{Fe}^{2+}$  when the  $(\text{NH}_3)_5\text{CoLFe}^{2+}$  complex is formed ( $\text{L}^{3-} = \text{N}(\text{CH}_2\text{COO})_3^{3-}$ ; and (3) a complex with the common bridging ligand, e.g.,  $(\text{CN})_5\text{FeCNCo}(\text{EDTA})^{5-}$ . In these labile formations, the electron transfer can proceed as extrasphere, for example, in the reactions  $\text{Co}^{3+} + \text{Cr}^{2+}$ ,  $\text{Co}^{3+} + \text{V}^{2+}$ ,  $\text{CoCl}^{2+} + \text{V}^{2+}$ , and  $\text{Cr}^{2+} + \text{Co}^{\text{III}}$  (imidazole). Various mechanisms of intrasphere transfer are also known, namely: (1) through the monoatomic bridging ligand in the complexes  $\text{Cr}^{\text{III}}\text{ClIr}^{\text{III}}$ ,  $\text{Cr}^{\text{III}}\text{OHCr}^{\text{II}}$ ,  $\text{Co}^{\text{III}}\text{FV}^{\text{II}}$ , and  $\text{V}^{\text{II}}\text{OHCr}^{\text{III}}$ ; (2) through the ligand consisting of several atoms, e.g., in the complexes  $\text{Co}^{\text{III}}(\text{SCN})\text{V}^{\text{II}}$ ,  $\text{Co}^{\text{III}}(\text{SCN})\text{Cr}^{\text{II}}$ , and  $\text{Co}^{\text{III}}(\text{NC})\text{Fe}^{\text{II}}$ ; and (3) through the polyatomic ligand, for example,



(4) through the double “bridge,” for example,



The electron transfer with the simultaneous transfer of the bridging group is also abundant, for example,



#### 8.4.2. Theoretical models of reaction of electron transfer (ET)

Electron transfer is one of ubiquitous and fundamental phenomena in chemistry, physics and biology. Nonradiative and radiative ET is found to be a key elementary

step of many important processes in isolated molecules and super molecules, ions and excess electrons in solution, condensed phase, surfaces and interfaces, electrochemical systems and biology.

As a light microscopic particle, electron easily tunnels through a potential barrier, therefore, the process is governed by general tunneling law formulated by Gamov. The principle theoretical cornerstone for condensed-phase ET was laid by Franck and Libby (1949-1952) who asserted that the Frank-Condon principle is applicable not only to the vertical radiative processes but also to nonradiative horizontal electron transfer.

Next decisive step in the ET in solution was done by Marcus, Zwolinski, Eyring and Weiss (1954) and then by Marcus (1956-1960). These authors formulated the need for readjustment of the coordination shells of reactants in self-exchange reactions and of the surrounding solvent to the electron transfer. They showed also that the electronic interaction of the reactants give rise to the splitting at the intersection of the potential surfaces, which leads to decrease of activation energy (Fig. 8.4).

Let us now consider the situation involving the transition of a system from one state to another using the concept of energy terms. With a certain value of the coordinate  $S_r$  the energy of the initial (*i*) and final (*f*) states is the same and the law of energy conservation allows to the term-term transition (Fig. 8.4). In the general case, the probability of the transition in the crossing area is described by the Landau-Zener equation 8.12. The theory predicted a key role of the electronic interaction, which is quantitatively characterized by the value of resonance integral  $V$ . If this value is suf-

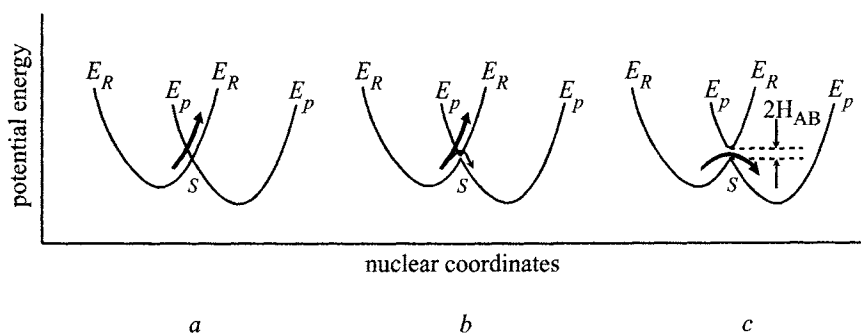


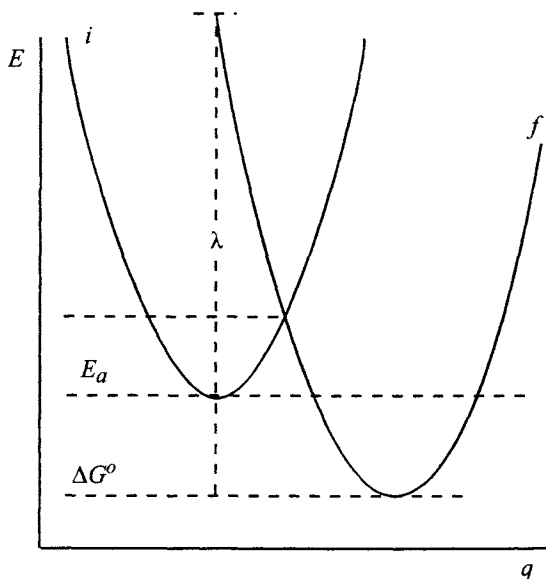
Fig. 8.4 Variation in the energy of the system along the reaction coordinate: (a) diabatic terms of the reactant ( $E_R$ ) and products ( $E_P$ ), the resonance integral  $V = H_{AB} = 0$ ; (b) nonadiabatic terms,  $H_{AB}$  is small; (c) adiabatic terms  $H_{AB}$  is large.

ficiently high, the terms are split with a decreasing activation barrier and the process occurs adiabatically. In another non-adiabatic extreme, where the interaction in the region of the coordinate  $Q_{tr}$  is close to zero, the terms practically do not split, and the probability of transition  $i \rightarrow f$  is very low.

According to the Marcus model, the distortion of the reactants, products and solvent from their equilibrium configuration are described by identical parabolas shifted related to each other according the value of the process driving force, standard Gibbs free energy  $\Delta G_o$  (Fig. 8.5). In the frame of adiabatic regime (strong electron coupling, the resonance integral  $V > 200 \text{ cm}^{-1}$ ), the value of the electron transfer rate constant

$$k_{ET} = (h\nu/kT)\exp[-(1 + \Delta G_o)^2/4\lambda kT] \quad (8.12)$$

where  $\lambda$  is the reorganization energy defined as energy for the vertical electron transfer without replacement of the nuclear frame. The formula 8.12 predicted the  $\log k_{ET} - \Delta G_o$  relationships depending on the relative magnitudes of  $\lambda$  and  $\Delta G_o$  (Fig.X): (1)  $\lambda > \Delta G_o$ , when  $\log k$  increases if  $\Delta G_o$  decreases (normal Marcus region); (2)  $\lambda = \Delta G_o$ , the reaction becomes barrierless; and (3)  $\lambda < \Delta G_o$ , when  $\log k$  decreases with increasing driving force.



The theory of non-adiabatic electron transfer was developed by Levich, Dogonadze and Kuznetsov (1959-1966). These authors, utilizing Landau-Zener theory for the intersection area crossing, proposed a formula for non-adiabatic ET

$$\log k_{ET} = \frac{(2\pi V^2/h)/(4\pi\lambda kT)^{1/2}}{(1 + \Delta G_o)^2/4\lambda kT} \exp[-] \quad (8.13)$$

Involving of intramolecular high-frequency vibrational modes in electron transfer was considered by Jorntner, Bixon and Efrima

Fig. 8.5 The free energy of initial (i) and final (f) terms as a function of generalized classical coordinates.  $G_o$  and  $\lambda$  are the Gibbs and reorganization energy respectively (the Marcus model)

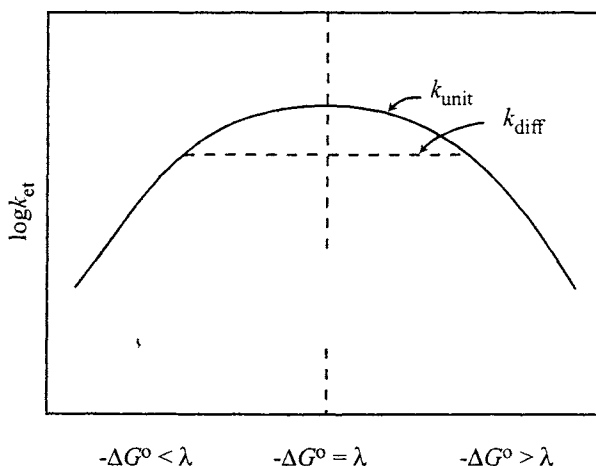


Fig. 8.6 Variation of the logarithm of the rate constant of electron transfer with the driving force for the reaction after Marcus. Three  $\Delta G^\circ$  regions are indicated: normal ( $-\Delta G^\circ < \lambda$ ); activationless ( $-\Delta G^\circ = \lambda$ ); and inverted ( $-\Delta G^\circ > \lambda$ ). The dashed line is for a bimolecular reaction ( $k_{diff}$ ) under diffusion control in the maximum region; the solid line is for a unimolecular reaction ( $k_{uni}$ ).

(1974-1976) and Hopefield and Chernavsky (1974). As an example, when the high-frequency mode ( $h\nu_v$ ) is in the low-temperature limit and solvent dynamic behavior can be treated classically (Jortner, Ulstrup), the rate constant for non-adiabatic ET is given by

$$k_{ET} = \Sigma(2\pi F_j V^2 / h) / (\lambda kT) \exp - [(j h \nu_v + \lambda_s + \Delta G^\circ)^2 / 4 \lambda kT] \quad (8.14)$$

where  $j$  is the number of high-frequency modes,  $F_j = e^{-S}/j!$ ,  $S = \lambda_v / h\nu$ ;  $\lambda_v$  and  $\lambda_s$  are the reorganization energy inside of the molecular and solvent, respectively.

Involvement of the high-frequency modes can cause strong deviation from the Marcus equation (8.12). The inverted Marcus region can not be experimentally observed if the stabilization of the first electron transfer product for account of the high-frequency vibrational mode occurs faster then the equilibrium of the solvent polarization with the momentary charge distribution is established. Another source of the deviation is non-parabolic shape of the activation barrier.

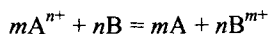
When ET occurs faster then the medium relaxation, the process is governed by the medium dynamics with the medium relaxation time  $\tau_s$ . In such a case the pre-exponential factor in non-adiabatic equation is described by formula

$$k_0 = 1/\tau_s(\pi\lambda 3kT)^{1/2} \quad (8.15)$$

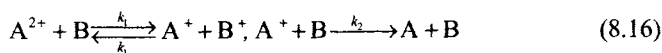
and the ET rate constant becomes independent of the electronic coupling.

#### 8.4.3. Noncomplementary reactions

Above we considered the reactions with one-electron transfer. In the general case, the redox reaction can be written in the following stoichiometric form:



In the framework of this stoichiometric approach, reactions with electron transfer are divided into complementary when  $m = n$  and noncomplementary when  $m \neq n$  (J. Halpern, 1961). Among the latter, the cases where  $m = 1$ ,  $n = 2$  are widely abundant. These reactions occur in two stages. The following mechanism is most frequent:

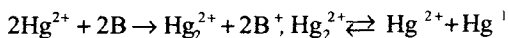


according to which the reaction rate

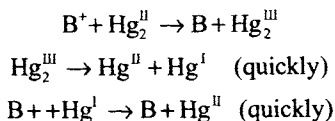
$$v = k_1 k_2 [A^{2+}][B]^2 (k_{-1}[B^+] + k_2[B])^{-1} \quad (8.17)$$

The electron transfer occurs *via* this mechanism in the following schemes (the limiting stage is indicated in parentheses):  $Tl^{III} + V^{III}$  (1),  $Tl^{III} + Fe^{II}$  (1 and 2),  $Tl^{III} + V^{IV}$  (1),  $Tl^{III} + Fe$  (phenanthroline) (1),  $Tl^{III} + Mn^{II}$  (2),  $Tl^{III} + Co^{II}$  (1 or 2),  $Mn^{VII} + V^{IV}$  (1), and  $Sn^{IV} + Fe^{II}$  (2).

Bivalent mercury is reduced to metallic mercury through an intermediate form of the binuclear ion  $(Hg^{2+})_2$  in which mercury is formally monovalent, followed by the reversible decomposition of H to  $Hg^0$  and  $Hg^{II}$



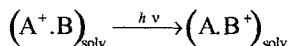
The first stage is limiting, so that the reaction rate  $v = k[Hg^{2+}][B]$ . The reactions of  $Hg^{2+}$  with  $V^{II}$ ,  $Cr^{II}$  and  $Fe^{II}$  occur in such a way. The oxidation of monovalent mercury occurs in several stages of which the first stage limits the whole process



The  $Ce^{IV}$ ,  $Ag^{II}$ ,  $Fe(\text{phenanthroline})^{3+}$ ,  $Ru(\text{bipyridyl})^{3+}$ , and  $IrCl_6^{2-}$  ions oxidize monovalent mercury in such a way.

#### 8.4.4. Photochemical reactions with electron transfer

An electron can be transferred from an ion to an ion photochemically, under the action of a photon



where index "solv" designates the ligand environment of both ions including the bridging ligand and solvate shell.

The jump of an electron occurs so rapidly that the ligand environment and solvate shell remain the same as they were in the initial state (Franck—Condon principle). Therefore, for the new  $A \cdot B^+$  state the environment is designated as  $(A \cdot B^+)_{\text{solv}}^*$  because it must further relax.

Quantum-chemical consideration of the one-electron transition in the binuclear formation  $A^+ \cdot B$  in the framework of the LCAO method gives the following picture. The energies of the main  $E_+$  and excited  $E_-$  states depend on  $\Delta E = E_i - E_f$ , where  $E_i$  refers to the initial  $A^+ \cdot B$  complex, and  $E_f$  refers to  $A \cdot B^+$ , and on the resonance integral

$$\beta = \int \psi_i H \psi_f d\tau \quad (8.18)$$

where  $\psi_i$  and  $\psi_f$  are the wave functions of the  $A^+ \cdot B$  and  $A \cdot B^+$  states,  $H$  is Hamiltonian, and  $d\tau$  is the infinitely small spatial volume.

If  $\beta \ll \Delta E$ , the simple expressions are obtained for  $E_+$  and  $E_-$

$$E_+ = E_i - \beta^2/\Delta E, E_- = E_f + \beta^2/\Delta E \quad (8.19)$$

The transition from the ground to excited states occurs upon light absorption, so that  $h\nu = E_- - E_+$ . If the complex is symmetrical, *i.e.*,  $A$  and  $B$  are identical, then  $h\nu = A'$ , where  $A'$  is the energy of rearrangement of the ligand sphere. If  $A$  differs from  $B$ , then at very low  $\beta$  the energy of transition  $\Delta G_{\text{tr}}$  from the state  $(A^+ \cdot B)_{\text{solv}}$  to  $(A \cdot B^+)_{\text{solv}}$  is  $\Delta G_{\text{tr}} = Lh\nu = \Delta E + A'$ . On the other hand, the thermal electron transition occurs with the activation Gibbs energy  $\Delta G^\ddagger = 1/4A' (1 + \Delta E/A')$ , and  $\Delta G^\ddagger$  and  $\Delta G_{\text{tr}}$  are related by the relationship

$$\Delta G^\ddagger = \Delta G_{\text{tr}}^2/4(\Delta G_{\text{tr}} - \Delta E) \quad (8.20)$$

The energies of transition to the excited state are rather high. Below we present the  $\Delta G_{\text{tr}}$  values obtained from spectral data for several ruthenium complexes

	Cl <sup>-</sup>	Br <sup>-</sup>	I <sup>-</sup>	NCS <sup>-</sup>	S <sub>2</sub> O <sub>3</sub> <sup>-</sup>
$\Delta G_{\text{tr}}$ , kJ/mol.....	407	370	298	369	297

The following expression was obtained for the ratio of the absorption intensity  $I$  and the light frequency (N. Hash, 1957):

$$I/\nu = (I_{\max}/\nu_{\max}) \exp[-(h\nu_{\max} - h\nu)^2/4A'kT] \quad (8.21)$$

from which the relationship between  $\Delta E_{1/2} = h(\nu_{\max} - \nu_{1/2})$  and  $A'$  follows:  $\Delta E_{1/2} = 4(\ln 2)^{1/2}(A'kT)$ , where  $\nu_{1/2}$  is the light frequency at which  $I/\nu_{\max} = 1/2I_{\max}\nu_{1/2}$ .

The absorption intensity is proportional to the square of the dipole moment of the complex  $\mu = \alpha eR_{AB}$ , where  $\alpha$  is the coefficient reflecting the degree of asymmetry of the electron density. Below we present  $\nu_{\max}$ ,  $R_{AB}$ , and  $\alpha^2$  for several binuclear complexes

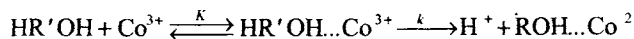
Complex	$\nu$ , $\text{cm}^{-1}$	$R_{AB} \cdot 10^{10}$ , m	$\alpha^2$
$\text{Ti}^{\text{III}} \dots \text{ClTi}^{\text{IV}}$	2.04	5.0	$4.4 \cdot 10^{-4}$
$\text{SbVCl}_6^- \dots \text{SbCl}_6^{3-}$	1.18	7.1	$4.0 \cdot 10^{-4}$
$\text{Fe}^{\text{III}} \dots \text{Fe}^{\text{II}}(\text{CN})_5\text{OS}(\text{CH}_3)_2$	1.61	5.1	$6.0 \cdot 10^{-3}$
$\text{Ti}_3^{\text{I}} \dots \text{Fe}^{\text{III}}(\text{CN})_6$	2.1	-	$1.6 \cdot 10^{-3}$

### 8.5. Redox reactions of ions with molecules

The oxidation of molecules with inorganic oxidants, such as potassium permanganate, chromic acid, and selenium dioxide, has long ago and widely been used in organic synthesis as methods for the selective oxidation of oxygen-containing compounds. Redox reactions of ions with variable valence with various oxygen-containing compounds as intermediate stages of various catalytic oxidation processes were studied in the 1950-60s.

#### 8.5.1. Oxidation of oxygen-containing compounds

The oxidation of alcohols with metal ions in aqueous solutions was studied in detail. Alcohol enters into the inner coordination sphere of the oxidation where the electron transfer from the alcohol to the ion occurs



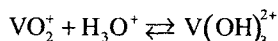
Due to the acid-base equilibrium,



both forms participate in oxidation:  $\text{Me}^{n+}$  and  $\text{MeOH}^{(n-1)+}$ , and the effective rate con-

stant depends on the concentration of hydrogen ions according to the type  $k = a + b/[H^+]$ .

Pentavalent vanadium in an aqueous solution exists in two forms



therefore, the experimentally measured rate constant is referred to either  $VO_2^+$  (1) or  $V(OH)_3^{2+}$  (form 2), depending on the pH, and in the general form it can be written as  $k_{\text{exp}} = K_1 k_1 + K_2 k_2 K_{\text{H}^+} [H_3O^+]$ . Below  $k_{\text{exp}}$  of the oxidation of several alcohols in water at  $[HClO_4] = 1 \text{ M}$  and 323 K are presented (J. Jones, W. Waters, 1962)

n-C <sub>3</sub> H <sub>7</sub> OH	(CH <sub>3</sub> ) <sub>2</sub> CHOH	cyclo-C <sub>6</sub> H <sub>11</sub> OH	CH <sub>2</sub> =CHCH <sub>2</sub> OH	HOCH <sub>2</sub> CH <sub>2</sub> CH <sub>2</sub> OH
$2.3 \cdot 10^{-5}$	$7.6 \cdot 10^{-6}$	$2.4 \cdot 10^{-5}$	$7.0 \cdot 10^{-4}$	$1.0 \cdot 10^{-5}$

Co<sup>III</sup> oxidizes alcohols much more rapidly (H<sub>2</sub>O, 288 K,  $[HClO_4] = 1.57 \text{ M}$ ,  $k$  in l/(mol s); D. Hoare, W. Waters, 1964)

CH <sub>3</sub> OH	C <sub>2</sub> H <sub>5</sub> OH	(CH <sub>3</sub> ) <sub>2</sub> CHOH	C <sub>2</sub> H <sub>5</sub> CH(CH <sub>3</sub> )OH	cyclo-C <sub>6</sub> H <sub>11</sub> OH	(CH <sub>3</sub> ) <sub>3</sub> COH
0.12	0.28	0.37	0.11	0.05	0.03

For isopropanol  $k_{\text{exp}} = 1.0 \cdot 10^{22} \exp(-124/RT) \text{ l/(mol s)}$  (the conditions are the same). Naturally, in nonaqueous solutions oxidation occurs more slowly. For example, cobalt acetylacetonate in a chlorobenzene solution oxidizes alcohols *via* the bimolecular reactions with the following constants (393 K, E. Denisov, V. Solyanikov, V. Martem'yanov, 1966):

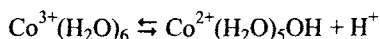
(CH <sub>3</sub> ) <sub>2</sub> CHOH	n-C <sub>4</sub> H <sub>9</sub> OH	cyclo-C <sub>6</sub> H <sub>11</sub> OH	C <sub>6</sub> H <sub>5</sub> OH
$k = 6.8 \cdot 10^{-5}$	$2.7 \cdot 10^{-5}$	$4.8 \cdot 10^{-4}$	$1.5 \cdot 10^{-2}$
$E = 130$	165	130	138

Note that oxidation in aqueous and nonaqueous media occurs with close activation energies (cf. 124 and 130 kJ/mol for isopropanol) but with different activation entropies ( $\Delta S^\ddagger = 168 \text{ J/(mol K)}$  and  $\Delta S^\ddagger = 0$ ). Cerium ions actively oxidize alcohols. The oxidation rate in strongly acidic solutions is  $v = kK(1 + K[ROH])^{-1}[ROH][Ce]^{4+}$ . At a low concentration of  $H_3O^+$ , the  $CeOH^{3+}$  ion also manifests itself as an oxidant. The  $k$  values in l/(mol s) and  $K$  values in l/mol for alcohol oxidation in H<sub>2</sub>O at 293 K and  $HClO_4 = 1 \text{ M}$  (S. Muhammad, K. Rao, 1963) are presented below

CH <sub>3</sub> OH	C <sub>2</sub> H <sub>5</sub> OH	cyclo-C <sub>6</sub> H <sub>11</sub> OH	CH <sub>3</sub> CH(OH)CH(OH)CH <sub>3</sub>
$k = 4.4 \cdot 10^{-4}$	$6.7 \cdot 10^{-3}$	$2.2 \cdot 10^{-3}$	$3.0 \cdot 10^{-3}$
$K = 2.3$	4.3	2.9	24

As it can be seen, the association constant is much higher for the polyatomic alcohol, which can form chelate complexes.

The oxidation of carbonyl compounds resembles in their regularities the oxidation of alcohols. For example, diethyl ketone is oxidized by  $\text{Co}^{3+}$  in a reaction of the second order with the pH-dependent constant:  $k_{\text{exp}} = 3 \cdot 10^{-4} (1 + 13.8[\text{H}_3\text{O}^+])^{-1} \text{ l/(mol s)}$  at 293 K. The dependence of  $k_{\text{exp}}$  on  $[\text{H}_3\text{O}^+]$  is explained by the equilibrium

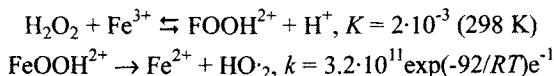


and the high activity of the  $\text{CoOH}^{2+}$  ion as an oxidant. It is assumed that an electron is transferred to  $\text{Co}^{3+}$  from the  $\pi$ -bond of the carbonyl group; the formed radical cation dissociates to the ethyl radical and the  $\text{C}_2\text{H}_5\text{C}=\text{O}$  cation, which is transformed into propionic acid in the reaction with  $\text{H}_2\text{O}$ .

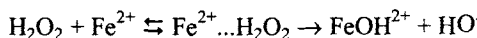
### 8.5.2. Reactions of variable-valence ions with peroxides

Redox reactions of heavy metal ions with peroxides and hydroperoxides in which free radicals are generated are widely used for the initiation of chain polymerization and oxidation reactions. The  $\text{H}_2\text{O}_2 + \text{Fe}^{2+}$  system known as "Fenton's reagent" has long ago been used for the hydroxylation and oxidative dimerization of organic compounds. These reactions occur during the catalytic decomposition of peroxides and in complicated processes of catalytic oxidation.

Hydrogen peroxide can also act as an oxidant accepting an electron:  $\text{H}_2\text{O}_2 + e^- \rightarrow \text{HO}\cdot + \text{HO}\cdot$ , and as a reducing agent donating an electron:  $\text{H}_2\text{O}_2 - e^- \rightarrow \text{HO}_2\cdot + \text{H}^+$ . Therefore,  $\text{H}_2\text{O}_2$  reacts with both ion-oxidants and ion-reducing agents. The redox reaction is preceded by the incorporation of  $\text{H}_2\text{O}_2$  into the inner coordination sphere where an electron overjumps, for example,  $\text{H}_2\text{O}_2$  reacts with  $\text{Fe}^{3+}$  as follows:



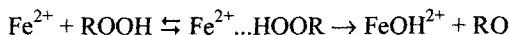
$\text{H}_2\text{O}_2$  is similarly reduced



The constant  $k_{\text{exp}} = kK = 1.5 \cdot 10^7 \exp(-30.5/RT) = 68 \text{ l/(mol s)}$  ( $T = 298 \text{ K}$ ,  $\text{H}_2\text{O}$ ). The rate constants  $k$  ( $\text{l/(mol s)}$ ) for several ion-oxidants and ion-reducing agents ( $\text{H}_2\text{O}$ , 298 K) are presented below.

$\text{Ti}^{3+}$	$\text{Mn}^{3+}$	$\text{Cu}^+$	$\text{Ce}^{4+}$	$\text{Cr}_2\text{O}_7^{2-}$	$\text{MnO}_4^-$
$5.0 \cdot 10^2$	$67.2 \cdot 10^4$	$7.3 \cdot 10^3$	$8.6 \cdot 10^5$	$1.9 \cdot 10^3$	$3.0 \cdot 10^3$

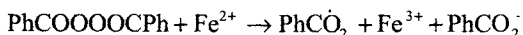
Hydroperoxides are reduced similarly, for example,



In an aqueous solution for  $(\text{CH}_3)_3\text{COOH}$   $k_{\text{exp}} = kK = 2 \cdot 10^8 \exp(-41/RT) = 13$  l/(mol s) (298 K).

The rate constant weakly depends on the structure of the hydrocarbon residue : for example, for cumyl hydroperoxide it is equal to 16.6 l/(mol s) (298 K).

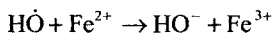
Acyl peroxides are reduced similarly, for example,



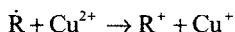
The constant  $k_{\text{exp}} = 2.2 \cdot 10^{11} \exp(-59.4/RT) = 12$  l/(mol s) (303 K,  $\text{C}_2\text{H}_5\text{OH}$ ). The reduction of  $(\text{CH}_3)_3\text{COOH}$  by  $\text{Co}^{2+}$  ions in acetic acid involves both the mononuclear and binuclear cobalt complexes, so that  $k_{\text{exp}} = (7.3 \cdot 10^{-5} + 6.1 \cdot 10^{-3} [\text{Co}^{2+}])$  l/(mol s) at 308 K in  $\text{CH}_3\text{COOH} : \text{H}_2\text{O} = 1 : 1$ . The decomposition of ROOH in the binuclear complex occurs homolytically, as in the mononuclear complex, which is evidenced by the formation of acetone, the decomposition product of the *tert*-butoxyl radical.

### 8.6. Redox reactions of ions with atoms and radicals

These reactions occur in various catalytic and chain processes involving variable-valence ions, such as the catalytic decomposition of peroxides, oxidation of hydrocarbons, and radical polymerization of vinylic compounds (see Chapters 10, 12, 15). A free radical has an unpaired electron and can oxidize an ion-reducing agent, for example,



or reduce an ion-oxidant, for example,

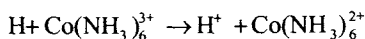


Mechanisms of these reactions are various. In one case, the radical and the ion are brought together, and an electron jumps from the oxidant to the reducing agent. In another case, the radical replaces a ligand in the inner coordination sphere of the complex where the electron transfer occurs. In the third case, the radical reacts with the ligand followed by the rearrangement of the electronic structure of the complex. The rate constants of such reactions change in the  $10^{10} - 1$  l/(mol s), depending on the reactants and conditions.

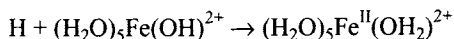
#### 8.6.1. Hydrogen atom

In reactions with ion-oxidants, atomic hydrogen acts as an active reducing agent.

Reduction proceeds through either the electron transfer, as in the case of  $\text{Co}^{\text{III}}$



or through the addition to the ligand followed by the electron transfer to the metal, as in the case of  $\text{Fe}(\text{OH})^{2+}$

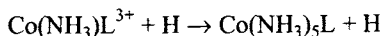


The rate constant of the reaction of hydrogen with  $\text{M}^{\text{n}+1}$  is almost independent of the redox potential of the ion  $E_0$  ( $\text{H}_2\text{O}$ , 298 K)

Ion	$\text{Cu}^{2+}$	$\text{Fe}(\text{CN})_6^{3-}$	$\text{Fe}_{\text{aq}}^{3+}$	$\text{Fe}_{\text{aq}}^{3+}$
$E_0$ , kJ/mol	17	35	74	77
$k$ , l/(mol s)	$5.9 \cdot 10^7$	$4.0 \cdot 10^9$	$2.2 \cdot 10^7$	$1.0 \cdot 10^{10}$

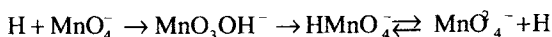
The ligand environment affects the mechanism of electron transfer and noticeably influences on the rate constant of the hydrogen atom with the  $\text{Fe}^{\text{III}}$  and  $\text{Co}^{\text{III}}$  complexes ( $\text{H}_2\text{O}$ , 298 K, method of competing reactions)

Ion	$\text{Fe}_{\text{aq}}^{3+}$	$\text{FeOH}^{2+}$	$\text{FeCl}^{2+}$	$\text{FeCl}_2^+$	$\text{Fe}(\text{CN})_6^{3-}$
$k$ , l/(mol s)	$9.5 \cdot 10^7$	$7.6 \cdot 10^8$	$4.5 \cdot 10^9$	$8.9 \cdot 10^9$	$4.0 \cdot 10^9$



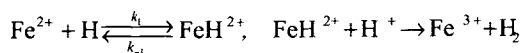
$L$	$\text{NH}_3$	$\text{H}_2\text{O}$	$\text{OH}^-$	$\text{F}^-$	$\text{Cl}^-$	$\text{Br}^-$	$\text{I}^-$
$k$ , l/(mol s)	$1.9 \cdot 10^6$	$4.5 \cdot 10^5$	$3.1 \cdot 10^7$	$1.1 \cdot 10^6$	$7.2 \cdot 10^7$	$4.6 \cdot 10^8$	$3.3 \cdot 10^9$

It is likely that the hydrogen atom first reacts with anion-oxidants in the addition reaction followed by the rearrangement of the electron configuration and the dissociation of the acid that formed, e.g., ( $\text{H}_2\text{O}$ , 298 K, method of competing reactions)

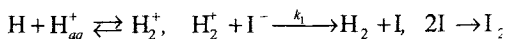


Anion	$\text{NO}_2^-$	$\text{NO}_3^-$	$\text{BrO}_3^-$	$\text{MnO}_4^-$	$\text{Cr}_2\text{O}_7^{2-}$	$\text{IO}_3^-$
$k$ , l/(mol s)	$1.3 \cdot 10^8$	$2.4 \cdot 10^7$	$2 \cdot 10^7$	$2 \cdot 10^{10}$	$2 \cdot 10^{10}$	$6 \cdot 10^7$

In reactions with ion-reducing agents, the hydrogen atom reacts as an oxidant. It oxidizes, for example,  $\text{I}^-$  to  $\text{I}$ ,  $\text{Fe}^{2+}$  to  $\text{Fe}^{3+}$ . The following mechanism was proposed for the last reaction:



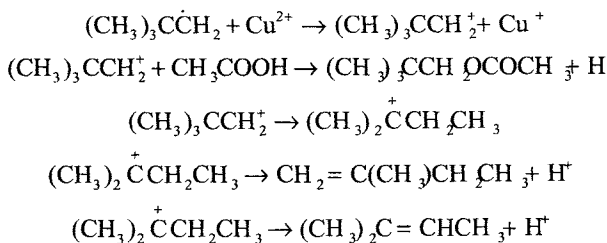
The experimentally observed rate constant is  $k_{\text{exp}} = 2 \cdot 10^7 \text{ l/(mol s)}$  ( $\text{H}_2\text{O}$ , pH 2, 298 K, method of competing reactions). The different mechanism was proposed for the oxidation of the iodide ion, where the  $\text{H}_2^+$  radical ion plays an important role



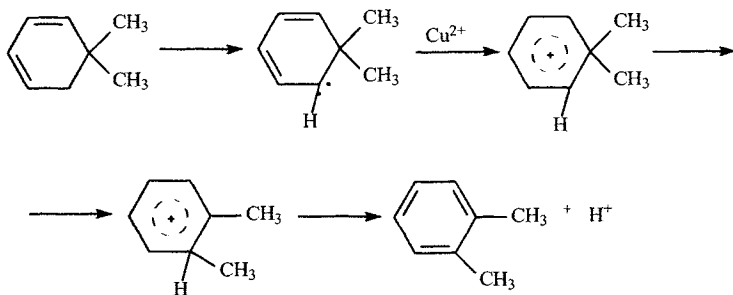
The constant is  $k_1 \approx 10^3 \text{ l/(mol s)}$  ( $\text{H}_2\text{O}$ , 298 K).

### 8.6.2. Oxidation of alkyl radicals

Alkyl radicals are oxidized by ion-oxidants to olefins and alcohols or esters. In many cases, carbocations are formed as intermediates, which proves the composition of the oxidation products. The oxidation of the neopentyl radical with copper acetate in acetic acid results in the formation of isomeric 2-methylbutenes and *tert*-amyl acetate, which agrees with reactions involving intermediate carbocations



The formation of the intermediate carbocation is convincingly proved by the transformation of 1,1-dimethylcyclohexadiene into *o*-xylene in the presence of peroxide (the source of radicals) and copper ions



The  $\beta$ -anisylethyl radical is oxidized with copper acetate in acetic acid predominantly to  $\beta$ -anisylethyl acetate. It is remarkable that radicals labeled with deuterium only in the  $\alpha$ - and only in the  $\beta$ -position give the same mixture of deuterated acetates.

This also indicates the intermediate formation of the carbocation.

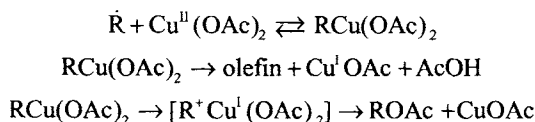
For the oxidation of various alkyl radicals with copper ions in aqueous solutions, the more stable the carbocation that formed, the higher the ratio of the alcohol to olefin

$\dot{R}$ .....	$\dot{C}_2H_5$	$sec-\dot{C}_4H_9$	$tert-\dot{C}_4H_9$	$CH_2=CH\dot{C}H_2$
[Alcohol]/[Olefin]...	0.81	3.4	9.1	Only alcohol

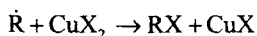
The rate constants of the reactions of alkyl radicals with  $Cr^{II}$  in a mixture of acetonitrile and acetic acid were measured by the method of competing reactions. At 330 K in the mixture  $CH_3CN : CH_3COOH = 1 : 1.5$ , they are the following:

$\dot{R}$ .....	$CH_3CH\dot{C}H_2$	$(CH_3)_2\dot{C}H$	$(CH_3)_3\dot{C}$	$PhCH_2\dot{C}$
$k, l/(mol\ s)$	$3.1 \cdot 10^6$	$5.0 \cdot 10^6$	$4.5 \cdot 10^5$	$1.6 \cdot 10^6$

In many cases, as J. Kochi showed, the ratio between the olefin to alcohol (ester) formed from  $R\cdot$  depends on the ligand environment of copper. Therefore, in these cases, the formation of an intermediate species (complex) is assumed, and this species undergoes further transformations



Alkyl radicals react with copper derivatives predominantly in elimination reactions



The reaction occurs very rapidly. For example, the cyclopropylmethyl radical reacts with  $CuCl_2$  with  $k = 1.1 \cdot 10^9\ l/(mol\ s)$  and with  $CuBr_2$  with  $k = 4.3 \cdot 10^9\ l/(mol\ s)$  (298 K, solvent  $CH_3CN$ ). However, the electron transfer reaction to form the carbocation occurs to a low extent in parallel. This is indicated by the oxidation products of the cyclopropylmethyl radical with  $CuCl_2$

Product.....	$CH_2=CHCH_2CH_2Cl$	$cyclo-C_4H_7Cl$	$cyclo-C_3H_5CH_2Cl$
Yield, %.....	9	2	89

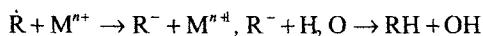
The first two products are formed in the reactions



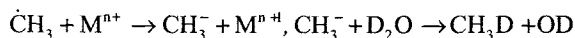
Thus, the oxidation of the alkyl radical with the metal ion proceeds as either the

extrasphere electron transfer to form the free  $R^+$ , or the intrasphere transfer to form  $R\cdot$  in the ligand sphere of copper followed by its subsequent transformation, or as the reaction of  $R\cdot$  with the ligand (detachment or addition). In several cases, these mechanisms compete.

Alkyl radicals are reduced by such ions as  $Fe^{2+}$ ,  $Ti^{3+}$ , and  $Cr^{2+}$  to hydrocarbons in proton-donating solvents



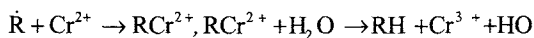
The formation of the carbanion in the free or metal-bound form is proved by experiments on the reduction of methyl radicals with the  $Ti^{3+}$ ,  $V^{2+}$ , and  $Cr^{2+}$  ions. In heavy water ( $D_2O$ ), the methyl radicals are reduced to  $CH_3D$  in the reactions



The stronger the reducing agent, the higher the experimentally measured  $[CH_3D]/[CH_4]$  ratio ( $CH_4$  is formed in the reaction of  $\cdot CH_3$  with  $RH$ ,  $E_0$  is the redox potential)

Ion.....	$Cr^{2+}$	$V^{2+}$	$Ti^{3+}$	$Fe^{2+}$
$E_0$ , kJ/mol	-39.3	-24.6	-	74.3
$[CH_3D]/[CH_4]$	0.22	0.09	0.031	$4.8 \cdot 10^{-4}$

In reduction with chromium, it is assumed that the radical enters into the inner coordination sphere

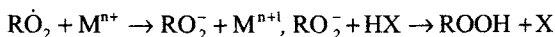


The reaction is very fast. For example, for the  $\omega$ -hexenyl radical  $k = 4 \cdot 10^7$  l/(mol s) (298 K,  $H_2O$ ). Chains of radical polymerization terminate on the ion-reducing agents due to reduction. Below we present  $k$  for chain termination on the ions for the polymerization of acrylamide in aqueous solutions (298 K)

Ion.....	$Ti^{3+}$	$V^{2+}$	$Cr^{2+}$	$Eu^{2+}$	$Ti^{3+}$
$\log k$ , l/(mol s).....	2.76	5.04	5.45	4.92	1.53

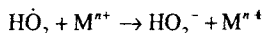
Often radicals are not reduced with ions but form complexes with them, which changes the composition of the transformation products of the radicals. For example, the presence of ions increases the yield of ethane, which is formed during the decomposition of *tert*-butyl hydroperoxide due to the recombination of the methyl radicals.

Peroxy radicals rather rapidly oxidize ion-reducing agents in both polar and hydrocarbon media



The reaction with chelate complexes proceeds, most likely, as the extrasphere electron transfer.

The  $\text{HO}_2^\cdot$  radical can act as an oxidant in reactions with the ion-reducing agent



The rate constants (l/(mol s)) measured by pulse radiolysis for the reactions of both types in aqueous solutions at 298 K are presented below.

Ion.....	$\text{Fe}^{2+}$	$\text{Cu}^+$	$\text{Br}_2^-$	$\text{Br}_3^-$	$\text{CNS}^-$
$k$ .....	$7.2 \cdot 10^5$	$4.3 \cdot 10^9$	$3.8 \cdot 10^8$	$1 \cdot 10^8$	$1.6 \cdot 10^9$
Ion.....	$\text{Fe}^{3+}$	$\text{Cu}^{2+}$	$\text{MnO}_2^-$	$\text{Br}_2$	
$k$ .....	$3.3 \cdot 10^5$	$1.5 \cdot 10^7$	$8 \cdot 10^6$	$1.5 \cdot 10^9$	

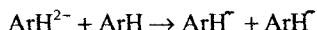
It is seen from these data that the  $\text{HO}_2^\cdot$  radicals are very active as both oxidants and reducing agents. Peroxyl radicals formed in the oxidation of alcohols and aromatic amines possess the same reactivity, which forms a basis for the catalytic mechanism of chain termination in chain reactions of the oxidation of these compounds (see Chapter 11).

### 8.7. Reactions of radical anions

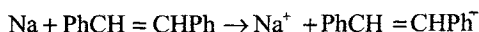
A radical anion is formed due to the addition of an electron to a molecule. It is rather stable if the molecule possesses a positive electron affinity ( $EA$ ). These compounds are aromatic hydrocarbons, ketones, and aldehydes

ArH	Naphthalene	Phenanthrene	Anthracene	Pyrene	Stylbene
$EA$ , kJ/mol	14.7	29.7	53.3	55.9	128
ArH	Acetophenone	Benzaldehyde	1-Naphthaldehyde	2-Naphthaldehyde	
$EA$ , kJ/mol	32.2	40.5	59.8	71.9	

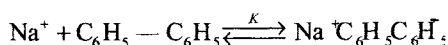
Radical anions are generated by the electrolysis method, in the addition of the solvated electron to the molecule, in the reaction of the anion with the molecule, for example,



and in the reaction of the molecule with the alkaline metal ion, for example,



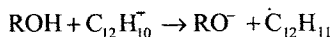
Radical anions of aromatic compounds are rather stable due to charge delocalization over the system of  $\pi$ -bonds. The distribution of the spin density on radical anions was studied by ESR and NMR. The reaction between an alkaline metal and an aromatic hydrocarbon is reversible, and the electron transfer from the metal atom to the molecule is accompanied by the heat release. For example, the reaction



is characterized by the parameters  $\Delta H = -46.8$  kJ/mol,  $\Delta S = -167$  J/(mol K), and  $\Delta G = -2.8$  kJ/mol at 263 K. This equilibrium also depends on the solvent, as it is seen from the data presented below

Solvent	$\text{C}_2\text{H}_5\text{OC}_2\text{H}_4\text{OC}_2\text{H}_5$	$\text{OCH}_2(\text{CH}_2)_4\text{CH}_2$	$\text{CH}_3\text{O}(\text{CH}_2)_3\text{OCH}_3$	$\text{CH}_3\text{OC}_2\text{H}_4\text{OC}_2\text{H}_5$
$K$ (293K)	0.07	0.36	0.49	0.75

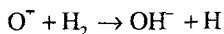
Since radical anions possess both a charge and an unpaired electron, they enter reactions characteristic of both anions and free radicals. In addition, they manifest a high activity as reducing agents and can both donate and accept an electron. The transfer of a proton in the reaction



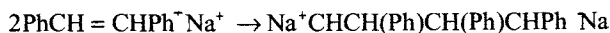
depending on alcohol, occurs with the rate constants (alcohol is medium, 298 K)

ROH.....	$\text{CH}_3\text{OH}$	$\text{C}_2\text{H}_5\text{OH}$	$\text{n-C}_3\text{H}_7\text{OH}$	$(\text{CH}_3)_2\text{CHOH}$
$k$ , l/(mol s)..	$6.9 \cdot 10^4$	$2.6 \cdot 10^4$	$3.2 \cdot 10^4$	$5.5 \cdot 10^3$

As radicals, radical anions can detach a hydrogen atom. For example, the reaction



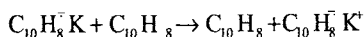
occurs with a rate constant of  $8 \cdot 10^7$  l/(mol s) ( $\text{H}_2\text{O}$ , pH 13, 298 K). Radical anions are prone of adding at the double bond on which anionic polymerization under the action of radical ions is based. As radicals, radical anions recombine to form dimers



However, unlike the recombination of alkyl radicals, which occurs with the diffusional rate constant, radical anions recombine more slowly due to their repulsion upon bringing together. The recombination rate depends on the counterion (tetrahydrofuran, 273 K)

Counterion	Li <sup>+</sup>	Na <sup>+</sup>	K <sup>+</sup>	Cs <sup>+</sup>
<i>k</i> , l/(mol s)	3.3	7.4	13	5.0
<i>E</i> , kJ/mol	63.7	77.3	60.2	59.4

Radical anions are specified by the reaction of electron transfer to a molecule-acceptor (e.g., C<sub>10</sub>H<sub>8</sub> — naphthalene)



The transfer rate constant in tetrahydrofuran at 296 K is equal to  $6 \cdot 10^7$  l/(mol s).

Radical anions are also characterized by the disproportionation reaction of the type



### 8.8. Methods of studying fast ion reactions

Many reactions involving ions, such as ion association, electron and proton transfer, and ligand exchange, occur very promptly, and the equilibrium state is established in the system. Several special methods were developed for the kinetic study of such systems. They can be classified as three types: methods with fast single distortion of the equilibrium state of the system, methods of periodical physical action on a solution in which the equilibrium chemical process occurs, and electrochemical methods for studying ion reactions.

#### 8.8.1. Method of temperature jump

The method is based on the following principle. The temperature of the equilibrium solution is increased very quickly, which removes the system from equilibrium. The kinetics of establishment of the new equilibrium state is monitored by high-speed spectrophotometry. The corresponding kinetic characteristics are calculated from experimental data. For the one-stage reversible reaction, the temperature change  $\Delta T$  results in the corresponding change in the equilibrium concentration of

the  $i$ th component  $\Delta c_i$

$$\Delta c_i = \left( \frac{\partial c_i}{\partial \ln K} \right)_{T,r} \frac{\Delta H}{RT^2} \Delta T \quad (8.22)$$

The first technique for studying equilibria by this method was created by M. Eigen in 1959. The temperature increase is achieved most often by the discharge of a high-voltage capacitor through an aqueous solution. The temperature increases due to the friction of ions moving in the electric field. The rate of the temperature increase depends on the  $RC$  product (where  $R$  is the resistance of the cell, and  $C$  is the capacitance of the capacitor) and is described by the formula

$$\Delta T = \Delta T_{\infty} [1 - \exp(-2t/RC)] \quad (8.23)$$

The temperature jump technique is characterized by the following parameters (Fig. 8.7): the voltage on the capacitor plates is 10–100 kV,  $RC = 1 \div 10$  ms, the cell volume is  $0.2 \div 20$  cm<sup>3</sup>, and  $\Delta T = 6 \div 8$  K. High-speed spectrophotometry is used to monitor a change in the reactant concentration. The method enables one to measure relaxation times from 1 to  $10^{-6}$  s. High requirements are imposed on the reaction cell in the temperature jump technique. The cell must withstand the high-voltage discharge, provide the uniform heating of the liquid, and allow one to use an optical equipment for spectral monitoring.

The reaction cell is usually prepared from Plexiglas, electrodes are brass, and the light is transmitted through quartz rods. Uniform heating is provided by parallel electrodes embracing the reaction cell. Fast heating is achieved by a pulse generator of microwaves. Due to electric relaxation, the liquid absorbs microwaves with a certain frequency and is rapidly heated. Water absorbs the microwave radiation at a frequency of  $10^{10}$  s<sup>-1</sup>, and this allows one to rise the temperature by 1 K for 1 ms. Absorption spectrophotometry is the most popular method of detection.

For a single relaxation process, the kinetics of the  $i$ th component is described by an exponential law

$$c_{i0} - c_i = (c_{i0} - c_{i\infty}) [1 - \exp(-t/\tau)]$$

where  $\tau$  is the relaxation time.

For small changes in the concentration

$$\Delta I = \epsilon_i l \Delta c_i$$

where  $I$  is the change in intensity of the light absorption,  $l$  is the reactor length, and  $i$  is the molar absorption coefficient.

Data are processed on a computer. The method is widely used for studying the kinetics of the acid-base equilibrium, intermolecular transfer, formation of metal complexes, electron transfer reactions, and enzymatic catalysis. The method measures rate constants of up to  $10^{11}$  l/(mol s).

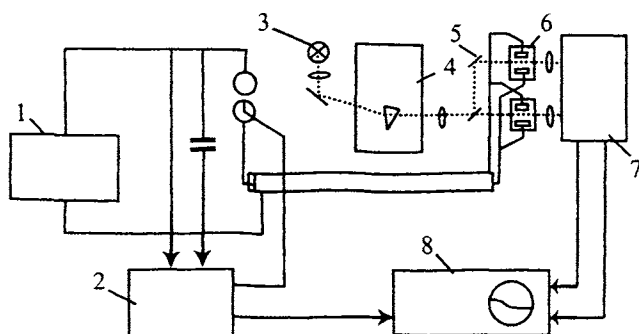


Fig. 8.7. Scheme of the temperature jump technique: 1, high-voltage generator; 2, kilovoltmeter and trigger; 3, monochromator; 7, photoamplifier; and 8, differential amplifier and oscillograph.

### 8.8.2. Method of pressure jump

Chemical reactions with a change in the number of species are accompanied by a change in the volume. The equilibrium constant of such equilibrium reactions depends on the pressure in the system

$$(\partial \ln K / \partial p)_T = -\Delta V / RT \quad (8.24)$$

If in the system with the established chemical equilibrium the pressure is rapidly changed, the equilibrium state changes, and the system relaxes to the new equilibrium state. The method of pressure jump is based on this regularity. The first setups for this method were constructed by S. Ljunggren and O. Lamm in 1958 and by G. Strehlow and M. Becker in 1959.

The setup is an autoclave 4 (Fig. 8.8) in which two conductometric cells 3 are mounted. One cell contains the solution under study, and another is a reference cell.

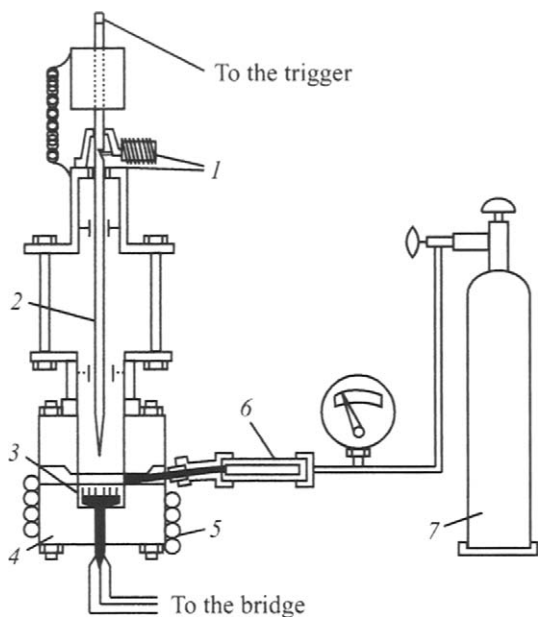


Fig. 8.8. Scheme of a pressure jump instrument: 1, magnetic release; 2, steel needle; 3, cells; 4, autoclave; 5, thermostating coil; 6, capillary; and 7, cylinder with gas.

Kerosene is poured into the bottom part of the autoclave with the cells, the autoclave is closed and thermostatted, and the pressure is applied. After the equilibrium is established in the reaction cell, the steel needle 2 breaks the membrane, and the pressure in the chamber drops within a short ( $\sim 100$  ms) time to atmospheric. The relaxation time of the system  $\tau$  to the new equilibrium state is measured by a change in the electroconductivity of the solution. The pressure change in the solution results in a temperature change

$$\Delta T = (\alpha_1 T / \rho C_p) \Delta p$$

where  $\alpha_1$  is the coefficient of temperature expansion,  $\rho$  is density, and  $C_p$  is temperature.

After the pressure jump, the temperature slowly (within several seconds) returns to the initial value. If the time of chemical relaxation is much shorter, this temperature change can be neglected, considering the process as quasi-adiabatic. If the reaction depth caused by the pressure change is designated through  $\xi$  and to take into

account that it is related to a change in both the pressure and temperature, we have

$$\bar{\zeta} = \bar{\zeta}_p + \bar{\zeta}_T = \left( \frac{d\zeta}{d \ln K} \right) \left( -\frac{\Delta V}{RT} + \frac{\Delta H}{RT^2} \frac{\alpha T}{\rho C_p} \right) \Delta p \quad (8.25)$$

Usually  $\bar{\zeta}_T < \bar{\zeta}_p$ : for example, for water at  $p = 10^7$  Pa,  $\bar{\zeta}_T = 0.2\bar{\zeta}_p$  because  $(\partial T/\partial p)_S = 1.45 \cdot 10^{-6}$  kPa $^{-1}$ . A change in the electroconductivity  $\kappa$  in time is described by an exponential law  $(d\kappa/\kappa) = \text{const} \Delta_p \exp(-t/\tau)$ , where  $\tau$  is related to the kinetic characteristics of the chemical equilibrium. The change in the electroconductivity in time is recorded on an oscillograph. This allows one to measure  $\tau$  from 1 to  $10^{-5}$  s. To study faster reactions, one has to shorten the time during which the pressure changes. With this purpose, impact waves are used in setups with a special construction.

These setups make it possible to shorten the time of pressure jump to 50 ms. The method of pressure jump is used for studying ion equilibria that occur with a change in the number of species, such as ligand exchange, hydration, and the formation of chelate metal complexes.

### 8.8.3. Method of electric pulse

The degree of dissociation of a weak electrolyte  $E$  increases when a strong electric field with the strength  $E$  is applied to a solution of this electrolyte

$$d\alpha/dE \approx 9.6\alpha(1 - \alpha)/(2 - \alpha)\epsilon T^2 \text{ cm/V}. \quad (8.26)$$

For example, when a field of 200 kV/cm is applied,  $\alpha(\text{CH}_3\text{COOH})$  increases by 12%. The change in the degree of dissociation of the electrolyte is monitored by a change in the electric conductivity. In order to exclude the temperature effect, the field is applied for a short time interval, and the relative change  $\alpha$  in two cells is monitored: one cell is filled with a solution of a weak electrolyte, and another contains a solution of a strong electrolyte.

The rectangular electric pulse is fed to the electrodes of the cell within a time interval of  $10^{-8}$  s. This pulse is maintained constant for  $2 \cdot 10^{-4}$  s. During this time a change in the electric conductivity is monitored by an oscillograph. The method makes it possible to measure relaxation times in the  $10^{-6}$  to  $10^{-4}$  s interval.

For solutions with a noticeable electric conductivity, a pulse lasting for  $10^{-7}$  to  $10^{-5}$  s is used. The  $\alpha$  change in time is recorded on an oscillograph. Since there is the relaxation time  $\tau$ , the  $\Delta\alpha(t)$  curve differs from the  $\Delta\alpha_0(t)$  curve at  $\tau = 0$ , namely,  $\Delta\alpha_{\max} < \Delta\alpha_{0, \max}$ :

$$\Delta\alpha_{0, \max}/\Delta\alpha_{\max} = [(1 - b\tau)^2 + \omega^2\tau^2]^{1/2} \quad (8.27)$$

where

$$\Delta\alpha = \Delta\alpha_0 e^{-b\tau} \sin\omega t$$

where  $b$  is the decay constant, and  $\omega/2\pi$  is the vibration frequency of the electric field.

The method makes it possible to measure  $\tau$  in the  $10^{-4}$  to  $10^{-7}$  s interval,  $k_{\max} \approx 4 \cdot 10^{10}$  l/(mol s).

#### 8.8.4. Ultrasonic method

When sound propagates in the liquid, it results in small periodical fluctuations of the temperature and pressure. The reaction, whose equilibrium depends on the temperature or pressure and the relaxation time is comparable with the perturbation period, absorbs sound according to the law  $P = P_0 \exp(-\alpha t)$ , where  $P$  and  $P_0$  are the amplitude at the  $l$  distance and the initial amplitude of the sound vibration, and  $\alpha$  is the absorption coefficient at 1 cm. The absorption coefficient at the wavelength is  $\mu = \alpha\lambda = 2\pi au/\omega$ , where  $\lambda$ ,  $u$ , and  $\omega$  are the wavelength, rate, and angular frequency (rad/s):  $\mu$  depends on  $\omega$  and relaxation time  $\tau$  as follows:

$$\mu = \mu_{\max} \omega \tau (1 + \omega^2 \tau^2)^{-1} \quad (8.28)$$

At  $\omega\tau = 1$

$$\alpha v^{-2} = \text{const}[1 + (2v/\pi\tau)^2] \quad (8.29)$$

Since other process of sound energy absorption occur in the liquid due to viscosity, thermal conductivity, and dipole orientation (background absorption), in the general case we have

$$\alpha v^{-2} = A[1 + (2v/\pi\tau)^2]^{-1} + B \quad (8.30)$$

In experiment  $\alpha$  is measured at different  $v$ , the dependence of  $\alpha v^{-2}$  on  $\log v$  is plotted, and  $\tau = 2\pi v_{\sim}$  is found by the inflection point in this curve, where  $v_{\sim}$  is the frequency corresponding to the inflection point. The ultrasonic method allows one to measure  $\tau$  in the  $10^{-4}$  to  $10^{-9}$  s interval.

In order to measure ultrasound absorption, the following methods are used: pulse (in the frequency region from  $2 \cdot 10^8$  to  $1.5 \cdot 10^6$  s $^{-1}$ ), optical ( $1 \cdot 10^8$  to  $1.5 \cdot 10^6$  s $^{-1}$ ), flow ( $2 \cdot 10^6$  to  $1.5 \cdot 10^5$  s $^{-1}$ ) reverberation ( $1 \cdot 10^6$  to  $5 \cdot 10^4$  s $^{-1}$ ), and resonating sphere ( $1.5 \cdot 10^6$  to  $5 \cdot 10^3$  s $^{-1}$ ).

#### 8.8.5. Method of periodical electric field

A high-frequency alternative field with the frequency  $v = \omega/(2\pi)$  is applied to a solution of a weak electrolyte, which results in the periodical change in the degree of

dissociation of the electrolyte. If  $\tau \ll \omega^{-1}$ , the change in the degree of dissociation virtually coincides with a change in the field intensity  $E$ . If  $\tau \gg \omega^{-1}$ , the degree of dissociation very weakly changes in time. At  $\tau = \omega^{-1}$ , the shift of the phases by frequency between  $E$  and  $\alpha$  is that the maximum absorption of the energy is observed, and  $\tau$  is calculated.

### 8.8.6. Electrochemical methods

The first work on measuring the rate constant of the protolytic reaction by the polarographic method was published in 1947 (R. Brdichka). Later several other electrochemical methods were developed for measuring rates of fast ion reactions. For the electrochemical determination of the reaction rate constant, it is necessary for the chemical equilibrium to exist in the system and for at least one of the reactants to participate in the electrode process. The reaction rate of electron transfer on the electrode increases exponentially with an increase in its potential  $E$  when  $E > E_{eq}$ , where  $E_{eq}$  is the equilibrium oxidation or reduction potential of the reactant on the electrode. The current strength is

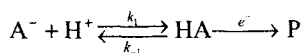
$$i = i_0 \left\{ \exp \frac{\alpha F}{RT} \eta - \exp \left[ -\frac{(1-\alpha)F}{RT} \eta \right] \right\} \quad (8.31)$$

where  $i_0$  is the exchange current, and  $\alpha$  is the transfer coefficient ( $0 < \alpha < 1$ );  $\eta = E - E_{eq}$ .

Increasing  $E$ , we can create such a regime when the reaction on the electrode occurs very rapidly so that the process is limited by the formation of the corresponding reactant on the electrode and depends on its transport characteristics during diffusion from the bulk to the electrode surface.

Analyzing experiments data in the framework of the diffusion equilibrium, taking into account the equilibrium chemical reaction in the bulk, the rate constants of the direct and inverse reactions are determined. Several electrochemical methods were developed.

1. In the *polarographic method* the reaction is studied in a cell with a dropping mercury electrode. Another electrode is calomel. A direct voltage is applied to the electrodes, and the mean current is measured. The rate constant of the corresponding stage is determined from the dependence of the current strength  $i$  on the electrode potential  $E$  under specially selected conditions when the rates of the studied reaction and electrode process and commensurable. For example, when the cell is filled with a weak acid, the following processes occur:



The solution of the diffusion equation ( $i_d$  is the current caused by the diffusion of

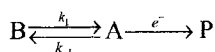
species to the electrode), taking into account the chemical reaction in the bulk, gives the formula, which relates  $i/i_d$  to  $k_{-1}$  ( $t$  is the time of formation of one mercury droplet on the dropping electrode)

$$\frac{i}{i_d} = \frac{0.886(k_{-1}t)^{1/2}[\text{H}^+]}{1 + 0.886(k_{-1}t)^{1/2}[\text{H}^+]} \quad (8.32)$$

The rate constants of dissociation of organic acids and of redox reactions were determined by this method. The method makes it possible to measure times of chemical relaxation to  $10^{-4}$  s.

2. Faster reactions can be studied by the method of *pulse polarography*. In this method, the potential, at which the limiting current appears not immediately but some time after the appearance of the droplet, is applied to the electrode. This makes it possible to shorten the current period  $t$  for the period of droplet formation and to enlarge the interval of measuring rate constants to  $10^{10}$  l/(mol s).

3. The *method of rotating disk* is similar to the polarographic method but a rotating platinum disk is used as an electrode. The current is measured at a constant voltage and different rates of disk rotation. In the case of the reversible reaction of the type



the current density  $i$  and the angular frequency of disk rotation  $\omega$  are related to the  $k_1$  and  $k_{-1}$  constants and diffusion coefficients  $D_A$  and  $D_B$  by the following correlation:

$$\frac{i}{\omega^{1/2}} = \text{const} - \frac{K_1 D_B}{1.6(D^2 \eta / \rho)^{1/6} D_A} \frac{i}{(k_1 / D_B) + (k_{-1} / D_A)} \quad (8.33)$$

where  $D = (k_1 D_A + k_{-1} D_B)(k_1 + k_{-1})^{-1}$ . Using the tangent slope in the  $i\omega^{-1/2} - i$  coordinates, the  $(K_1 D_B / D_A)[(k_1 / D_B) + (k_{-1} / D_A)]^{-1/2}$  value is determined and the  $k_1$  and  $k_{-1}$  constants are calculated at the already known  $K_1$ ,  $D_A$ , and  $D_B$ .

4. The potentiostatic method allows one to estimate the rate constant of the stage preceding the electrode reaction using a change in the current strength in time. For the scheme presented above, the time dependence of the current density  $i$  is described by the equation ( $\lambda^2 = K_1 k_1 t$ )

$$i = nF([A] + [B]) D^{1/2} K_1 k_1^{1/2} e^{\lambda^2} \text{erfc}(\lambda) \quad (8.34)$$

Comparing the experimental curve  $i(t)$  with the calculated one,  $k_1$  is determined ( $K_1$  and  $D = D_A + D_B$  are known). In this method, a hanging dropping mercury electrode is usually used.

5. The galvanostatic method differs from the potentiostatic method by the fact that during experiment the current strength is maintained constant in the electrolytic cell where the chemical reaction occurs, and the voltage increase in time is detected.

The electrochemical methods make it possible to study reactions occurring with a rate constant to  $10^{-8} \text{ s}^{-1}$ . Measurements can be carried out in a cell with a volume to  $1 \text{ cm}^3$  and less. These methods were used to study reactions of proton transfer and complex formation, redox reactions.

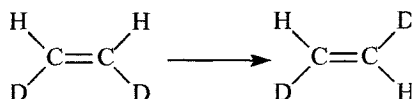
The choice of the systems is restricted by such reactants and products, one of which is reduced on the electrode. The solution must conduct the current and contain a sufficient concentration of a dissolved electrolyte.

## Reactions of molecules

### 9.1. Isomerization and decomposition of molecules

#### 9.1.1. *cis-trans*-Isomerization of olefins

The transition of the *cis*-configuration of olefin to the *trans*-configuration, for example,



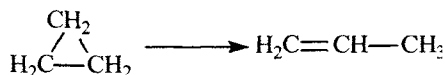
needs the turn of the C atom around the C—C bond. However, this turn by rotation about the  $\pi$ -C—C bond is forbidden by the symmetry rules. Therefore, isomerization occurs through an intermediate biradical state in which the  $\pi$ -C—C bond is cleaved. This state is most probably singlet; since the cleavage requires a large energy consumption, the *cis-trans*-isomerization of olefins occurs with a high activation energy. The pre-exponential factor for a light molecule, for example,  $\text{HDC}=\text{CDH}$ , is equal to  $2(e kT/h) \approx 10^{13} \text{ s}^{-1}$ . In a heavy molecule in the transition state the turn about the C—C bond is comparatively slow, so that  $h\nu/kT \ll 1$  and the sum of the states related to rotation is  $[1 - \exp(-h\nu/kT)]^{-1} \approx kT/h\nu$ . Due to this  $A \approx 2\nu$ ; evidently, in this case,  $\nu < 10^{13} \text{ s}^{-1}$ . These reactions occur with a noticeable rate at 600–800 K and are studied in the gas phase. Below we present  $E$  and  $\log A$  for several olefins ( $A$  is expressed in  $\text{s}^{-1}$ ).

Olefin	$E$ , kJ/mol	$\log A$	Olefin	$E$ , kJ/mol	$\log A$
<i>cis</i> -CDH=CDH	272	13.0	<i>cis</i> -PhCH=CHPh	179	12.8
<i>cis</i> -CH <sub>3</sub> CH=CHCH <sub>3</sub>	263	13.8	<i>cis</i> -CH <sub>3</sub> -cinnamate	174	10.5
<i>cis</i> -CH <sub>3</sub> CH=CHCN	214	11.0	<i>cis</i> -PhCH=CHCN	192	11.6
<i>cis</i> -CH <sub>3</sub> CH=CHCOOCH <sub>3</sub>	242	13.2	<i>cis</i> -CF <sub>3</sub> CF=CFCF <sub>3</sub>	236	3.5

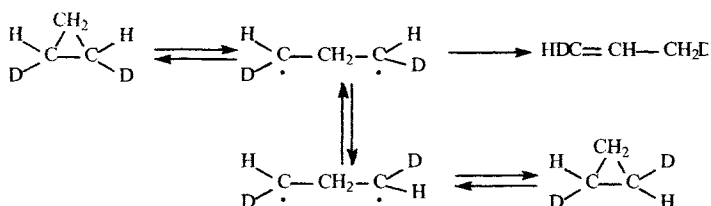
As can be seen from these examples, the activation energy of this reaction is close to that of  $\pi$ -C—C bond cleavage and the  $A$  factor changes from  $10^{10}$  to  $10^{13} \text{ s}^{-1}$ .

### 9.1.2. Reactions of cyclization and decyclization of molecules

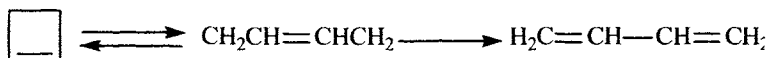
Decyclization of cycloparaffins also proceeds through the biradical transition state, for example,



The study of the transformation of *cis*-1,2-dideuteriocyclopropane showed that the reaction was accompanied by isomerization, which occurs by approximately an order of magnitude more rapidly than decyclization (B.S. Rabinovich et al., 1955). Thus, the reaction mechanism is more complicated and includes the following steps involving the intermediate biradical:



It is most likely that cyclobutene decomposition occurs similarly



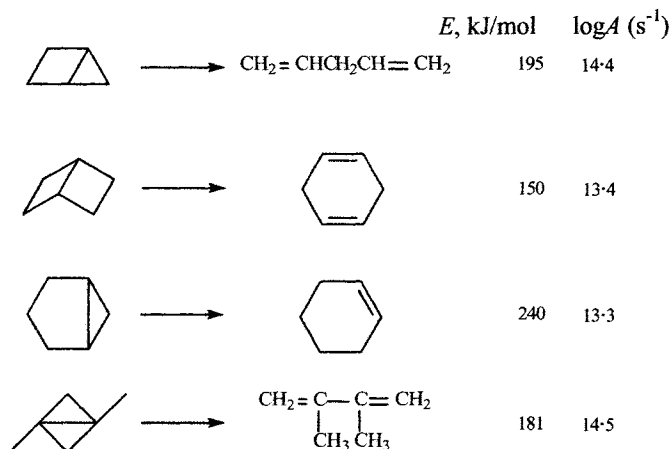
The Arrhenius parameters for several isomerization reactions of cyclic compounds to unsaturated compounds (gas phase) are exemplified below.

Compound	<i>E</i> , kJ/mol	log <i>A</i> (s <sup>-1</sup> )
$\overline{\text{CH}_2\text{CH}_2\text{CH}_2}$	272	15.2
$\text{CH}_3\overline{\text{CHCH}_2\text{CH}_2}$	272	15.4
$\text{CH}_2=\text{CH}\overline{\text{CHCH}_2\text{CH}_2}$	208	13.6
$\overline{\text{CH}=\text{CHCH}_2\text{CH}_2}$	136	13.1
$\overline{\text{CH}_2\text{CH}_2\text{O}}$	238	14.2

It is seen, in particular, that the activation energy of decomposition of vinylcyclopropane is much lower than that of methylcyclopropane. The reason is the stabilization of the biradical formed due to the interaction of its free valence with  $\pi$ -electrons of the vinyl groups. The same reason provides a comparatively low activation

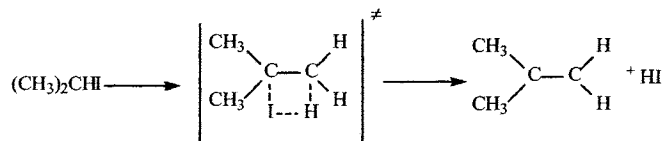
energy for cyclobutene.

The decomposition of bicyclic hydrocarbons proceeds *via* the biradical mechanism. The parameters of such reactions are presented below.



### 9.1.3. Decomposition of molecules

Homolytic decomposition of molecules to radicals was considered in Chapter 7. Let us consider such reactions when one molecule decomposes to two molecules. This decomposition occurs through the cyclic transition state, for example,

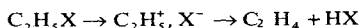


The values of  $\Delta H$ ,  $E$  (kJ/mol), and  $\log A$  for several  $\text{RCl}$  and  $\text{C}_2\text{H}_5\text{X}$  (gas phase,  $A$  in  $\text{s}^{-1}$ ) are presented below.

R.....	$\text{C}_2\text{H}_5$	$n\text{-C}_3\text{H}_7$	$(\text{CH}_3)_2\text{CH}$	$(\text{CH}_3)_3\text{C}$	$\text{PhCHCH}_3$	$\text{CH}_3\text{CHOCH}_3$
$\Delta H$ .....	70	59	66	71	57	69
$E$ .....	236	230	214	188	190	154
$\log A$ ....	13.2	13.45	13.6	13.8	12.9	13.1

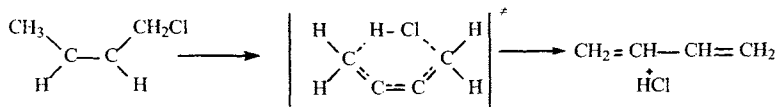
X.....	Cl	Br	I	CN	SH	NO <sub>2</sub>
$\Delta H$ .....	70	83	87	134	125	77
$E$ .....	236	225	209	323	214	188
$\log A$ ....	13.2	13.4	13.4	15.0	13.0	12.4

As can be seen the pre-exponential factor for such reactions are close to  $10^{13}$ - $10^{14}$   $s^{-1}$ , and the activation energy are much higher than the change in enthalpy in the reaction. These reactions are allowed in part by orbital symmetry. The high activation energy can be related to the following circumstances. If the reaction occurs as the synchronous formation of the X—H bond with the simultaneous loosening of the C—H bonds and C—X and the appearance of the  $\pi$ -C—C bond, then the high energy barrier is a result of a considerable change in the bond angles of rearranging bonds and the repulsion of approaching atoms. It was assumed that the reaction proceeds through the preliminary ionization of the C—X bond and formation of the ion pair

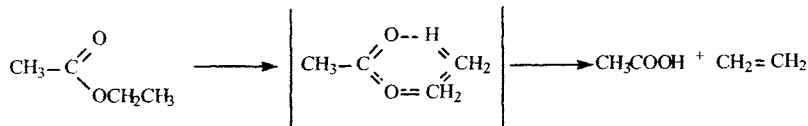


In this case, the high activation energy is associated with energy consumptions to the ionization of the C—X bond in the gas phase. In the liquid phase reactions of this type often involve the solvent and are accompanied by the ions formed. The values of the pre-exponential factor, as S. Benson showed, agree with the elimination of HX *via* the synchronous mechanism. In particular, for  $C_2H_5Cl$  decomposition the theoretical calculation gives  $\log A = 13.1$ , which virtually coincides with the experimental value.

The elimination of HX in positions 1 and 4 occur much more rapidly because in this case the transition state represents a six-membered complex where the strain of angles is minimum



It is most likely that the decomposition of esters in the gas phase proceeds through the six-membered transition state, as follows:

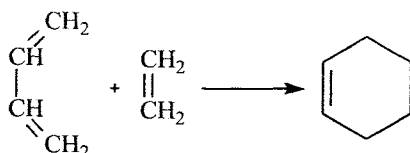


Reactions of this type also occur with a high activation energy and a pre-exponential factor of  $10^{12}$ - $10^{13}$   $s^{-1}$  ( $E$  and  $\Delta H$  in kJ/mol,  $A$  in  $s^{-1}$ )

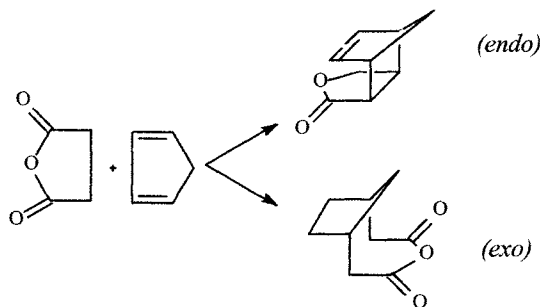
	CH <sub>3</sub> COOC <sub>2</sub> H <sub>5</sub>	<i>n</i> -C <sub>3</sub> H <sub>7</sub> OCOCH <sub>3</sub>	(CH <sub>3</sub> ) <sub>2</sub> CHCH <sub>2</sub> OCOCH <sub>3</sub>	PhCH <sub>2</sub> CH <sub>2</sub> OCOCH <sub>3</sub>
$\Delta H$ .....	51	40	29	38
<i>E</i> .....	201	199	198	190
log <i>A</i> .....	12.6	12.4	11.9	12.4

### 9.2. Bimolecular reactions with concerted rearrangement of bonds

These are Diels-Alder reactions, *viz.*, reactions of addition of unsaturated compounds to dienes. The simplest reaction is the addition of ethylene to butadiene



Three  $\pi$ -bonds are cleaved and two  $\sigma$ -bonds and new  $\pi$ -bond are formed in the transition state. Diene reacts only in the *cis*-form because only in this case  $\pi$ -orbitals of the diene and olefin can overlap. If both compounds are cyclic, the formation of two isomers, *endo*- and *exo*-, are possible, for example,



The dimerization of cyclopentadiene and cyclohexadiene with maleic anhydride affords only *endo*-forms. The dimerization of furan with maleic anhydride in xylene (400 K) gives 28% *endo*-form and 72% *exo*-form.

Diene synthesis is reversible: the product that formed undergoes decomposition to the initial products. The decomposition reaction is named the retro-diene synthesis. The addition of diene to olefin is accompanied by a decrease in both the enthalpy and entropy. A series of examples is given below.

Reaction	Conditions	$-\Delta H$ , kJ/mol	$-\Delta S$ , kJ/mol	$\log K$ (400 K)
$\text{CH}_2=\text{CH}=\text{CH}=\text{CH}_2 +$ $\text{CH}_2=\text{CH}_2$	Gas phase	125	109	10.9
<i>cis</i> - $\text{C}_5\text{H}_6 + \text{cis}$ - $\text{C}_5\text{H}_6$	Gas phase	71	132	2.4
<i>cis</i> - $\text{C}_5\text{H}_6 + \text{cis}$ - $\text{C}_5\text{H}_6$	parafine	68	113	3.0
<i>cis</i> - $\text{C}_5\text{H}_6 + \text{CH}_2=\text{CH}-\text{CHO}$	Gas phase	81	121	4.3
<i>cis</i> - $\text{C}_5\text{H}_6 + \text{OC}_6\text{H}_4\text{O}$	$\text{C}_6\text{H}_6$	73	121	3.2

In all presented examples the equilibrium is shifted toward adducts. In a solution the equilibrium constant is somewhat higher than that in the gas because the internal pressure of the solvent favors the association of species.

In the gas phase and neutral solvents, the diene synthesis occurs as one stage. Below we present the Arrhenius parameters for several reactions in the gas phase ( $A$  in l/mol s), ( $k$  at K).

Reaction	$k$ , l/(mol s)	$E$ , kJ/mol	$\log A$
$\text{CH}_2=\text{CH}-\text{CH}=\text{CH}_2 + \text{CH}_2=\text{CH}_2$	$3.0 \cdot 10^{-8}$	11.5	7.5
$2\text{CH}_2=\text{CH}-\text{CH}=\text{CH}_2$	$1.2 \cdot 10^{-6}$	99	7.0
$2\text{-cis-C}_5\text{H}_6$	$9.2 \cdot 10^{-4}$	70	6.1
<i>cis</i> - $\text{C}_5\text{H}_6 + \text{CH}_2=\text{CH}-\text{CHO}$	$7.0 \cdot 10^{-3}$	64	6.2
$\text{CH}_2=\text{CH}-\text{CH}=\text{CH}_2 + \text{CH}_2=\text{CHCHO}$	$3.1 \cdot 10^{-5}$	82	6.2
$\text{CH}_2=\text{C}(\text{CH}_3)\text{CH}=\text{CH}_2 + \text{CH}_2=\text{CHCHO}$	$6.6 \cdot 10^{-5}$	78	6.0

Although all these reactions are exothermic, they occur with a sufficiently high activation energy. The pre-exponential factor is much lower than the frequency of double encounters, which is resulted by the negative activation entropy. When the transition state is formed, two species are combined in one species and the diene loses the ability of the  $\text{RCH}=\text{CH}$  groups to internal rotation. This results in considerable entropy losses.  $-\Delta S^\ddagger = 120 \text{ J}/(\text{mol K})$  corresponds to the pre-exponent  $A = 10^{7.5}$ . This value is close to the entropy of equilibrium in the reaction of butadiene with ethylene (see above). Therefore, the structure of the transition state is close to that of the final product.

In the absence of catalysts the Diels-Alder reaction occurs as a bimolecular reaction with the concerted rearrangement of  $\pi$ -orbitals. The  $\pi$ -orbitals of diene with the  $\pi$ -orbital of olefin interact in the transition state, which is favored by the geometry of the reactants (a six-membered cycle appears) and the character of (properties of symmetry) of the interacting orbitals. According to the rules of orbital symmetry (Woodward—Hofmann rule), the efficient overlap of the interacting orbitals occurs only when the bonding orbital of one reactant and the antibonding orbital of another reactant have appropriate symmetry. As seen from the scheme presented in Fig. 9.1, the reaction of diene synthesis obeys this condition and, hence, occurs comparative-

ly rapidly. This correspondence is absent in the case of the interaction of two olefins, the reaction is forbidden by the rules of orbital symmetry and to occur it needs one of the reactants to be transformed into the excited state. The general analysis of conditions of concerted addition of polyenes is allowed if the total number of  $\pi$ -electrons is equal to  $4n \pm 2$ . For the addition of olefin to diene this number is equal to 6.

The solvent slightly affects the dimerization of nonpolar reactants.

In a solution the reaction occurs somewhat more rapidly than in the gas phase:  $k_g = 0.85 \cdot 10^{-6}$ ,  $k_l = 1.0 \cdot 10^{-6}$  l/(mol s), which is related, most likely, to a higher frequency of collisions of particles in the liquid (see Chapter 6). This influence is much more pronounced in the case of polar reactants. For example, the dimerization of cyclopentadiene with *p*-benzoquinone, depending on the solvent, occurs with the following rate constant:

Solvent.....	<i>n</i> -C <sub>7</sub> H <sub>16</sub>	CS <sub>2</sub>	CCl <sub>4</sub>	C <sub>6</sub> H <sub>6</sub>	PhCN	PhNO <sub>2</sub>
$k \cdot 10^2$ , l/(mol s) (300 K) ..	0.48	0.64	0.77	1.10	4.67	5.14

The formation of the transition state is accompanied by a decrease in volume because two species are unified to form one associate. The study of cyclopentadiene dimerization under a pressure allowed the estimation of the activation volume  $\Delta V^\ddagger = 33$  cm<sup>3</sup>/mol (298 K, cyclopentadiene). It is equal to the change in the volume upon the formation of the dimer from the initial particles. Therefore, the volume of the transition state is virtually equal to the volume of the dimer.

Acids accelerate the Diels-Alder reaction. The rate of the catalytic reaction is proportional to the acid concentration and the product of the concentrations of the reactants. The activation energy of the catalytic reaction is low. For the reaction of cyclopentadiene with *p*-benzoquinone catalyzed by trichloroacetic acid, it is equal to zero, and the constant  $k = 6.8$  l<sup>2</sup> mol<sup>2</sup>/s at 298 K. The reaction occurs, evidently, through the intermediate formation of the carbocation.

### 9.3. Molecular complexes

In a solution molecules interact with each other. This interaction can be divided in physical and chemical. This division is conventional to a great extent but helpful in many cases. When molecules collide (in both the gas and liquid phases), repulsion forces appear. The repulsion energy depends on the interatomic distance and increases sharply with shortening of the interatomic distance  $r$  according to the law:  $U_{\text{rep}} \approx Ar^{-m}$ ,  $m = 10 \div 12$  or  $U_{\text{rep}} \sim e^{-ar}$ , where  $a \approx 0.3 \div 0.5$  nm<sup>-1</sup>, i.e., repulsion forces are short-range. When molecules are remote from each other, far-range attraction forces appear between them.

If both molecules A and B possess dipole moments, being approached they take

the antiparallel orientation and the dipole-dipole interaction appears between them. The energy of this *orientational interaction* of two particle-dipoles depends on their dipole moments  $\mu_A$  and  $\mu_B$ , the distance between them  $r_{AB}$ , and the dielectric constant of the medium  $\epsilon$ :  $U_{or} = -(2kT)\mu_A^2\mu_B^2/\epsilon r_{AB}^6$ .

If the antiparallel orientation is impossible,  $U_{or}$  depends on angles of mutual orientation. Due to the mobility of the electronic shell in molecule A under the action of the electric field of the adjacent particle-dipole B, a induced dipole appears (is induced). The value of this dipole  $\mu_A$  depends on the polarizability of molecule A  $\alpha_A$ , and the energy of the induced interaction  $U_{ind} = -2\mu_B^2\alpha_A/r_{AB}^6$ . Molecules with  $p$ - and  $\pi$ -electrons possess a high polarizability.

Finally, dispersion forces act between molecules. They appear due to the displacement of nuclei and the electronic shell appeared for a very short time, which results in the formation of an instant dipole. The interaction of such existing for a short time dipoles creates forces of *dispersion interaction* (*London forces*). The energy of dispersion interaction between the same biatomic molecules depends on the polarizability of the molecule  $\alpha$  and the zero-point frequency of vibrations of atoms  $\nu_0$ :  $U_{disp} = -3\alpha^2 h\nu_0/4r^6$ . Depending on the structure and sizes of the molecule, the contributions of the orientation, induced, and dispersion interactions differ. The example is presented below (the energies are expressed in kJ/mol; accepted that  $\epsilon = 1$ ).

Molecule	CH <sub>4</sub>	CO	HCl	NH <sub>3</sub>	H <sub>2</sub> O
$-U_{or}$	0	0.4	2.8	12.6	36.3
$-U_{ind}$	0	0.8	0.8	1.5	1.9
$-U_{disp}$	17.6	8.8	15.8	14.0	8.8
Sum	17.6	10.0	19.4	28.1	47.0

Physical interaction does not change or very weakly affects the structure of interacting particles. In addition to physical interaction, molecules very often form with each other molecular complexes involving definite atoms and molecular orbitals. Molecular complexes are divided into two large classes: complexes with the hydrogen bond and charge transfer complexes (CTC). Molecular complexes occupy an intermediate position between associates of molecules appeared due to the physical interaction, for example, dipole-dipole attraction, and molecules. Physical interaction appears as a result of the electrostatic attraction of molecules with a constant or induced dipole. The number of interacting molecules that form an associate can be rather great and change depending on conditions. The molecular complex has a constant composition (most often 1 : 1 or 1 : 2); if it changes, the complex structure also changes. The hydrogen bond in alcohols appears by the interaction of the O—H group with the electron pair of the oxygen atom of another molecule. Unlike molecules, which are formed from other molecules in reactions that occur with the activation energy, molecular complexes are formed in association processes that occur

without activation energy. Therefore, molecular complexes are at equilibrium with the initial molecules. Molecules in the complex retain their properties, and only groups or bonds, due to the interaction of which the complex is formed, change. The bond energy in molecular complexes changes in a wide range. The complexes are conventionally divided into 3 groups by this property

Weak	Medium	Strong
To 10	From 10 to 15	>35 kJ/mol

Let us consider the properties of CTC. The theory of CTC was developed by R.S. Mulliken in 1952. Two molecules form CTC when the transfer (complete or partial) of an electron from the occupied orbital of the molecule-donor D to the vacant orbital of the molecule-acceptor A is energetically favorable. The wave function of the  $D^+ \cdot A^-$  CTC is described in the first approximation through the wave functions of the initial state D, A and completely ionized state  $D^+ \cdot A^-$

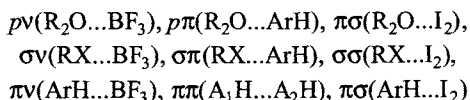
$$\psi(D^{\delta+}A^{\delta-}) = \alpha\psi_0(A...D) + \beta\psi_1(D^+ \cdot A^-) \quad (9.1)$$

If during CTC formation the electron is completely transferred from D to A, the energy of complex formation is the following:

$$U_{CTC} = I_D - E_A - e^2/r_{AD} \quad (9.2)$$

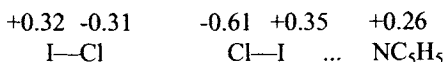
where  $I_D$  is the ionization potential of the donor;  $E_A$  is the electron affinity of the acceptor, and the third term expresses the energy of Coulomb interaction between  $D^+$  and  $A^-$ .

For a polar solvent, we have to supplement the solvation energy of CTC. Electron pairs,  $p$ - and  $\pi$ -electrons, and easily polarized  $\sigma$ -bonds participate in the formation of CTC. Simultaneously  $v$ -,  $\sigma^*$ -, and  $\pi$ -orbitals of the acceptor are involved in CTC formation. According to the type of orbitals involved in the formation of complexes, CTC are divided into 9 groups:



The structure of CTC was studied by visible and UV spectroscopy, NMR, and X-ray diffraction analysis of complexes in the crystalline state. The data show that in some cases the structure of the molecule weakly changes when it is in the composition of CTC. For example, for the formation of the  $Br_2$  complex with two benzene molecules the distance between the bromine atoms remains the same as in the initial molecule, viz., 0.228 nm. In the  $Br_2$  complex with two dioxane molecules, this distance is somewhat greater, namely, 0.231 nm, and the distance between the bromine and oxygen atoms is 0.271 nm, that is, much smaller than the sum of the van der Waals radii. When the molecule contains several fragments, which can participate in CTC formation, depending on the partner, complexes with different structures can

appear. For example, acetophenone forms a complex with  $I_2$  due to the interaction of the  $\pi$ -orbital of the carbonyl group:  $C=O \cdots I_2$ , whereas the complex with tetracyanoethylene is formed due to the interaction of the  $\pi$ -orbitals of the aromatic ring with the  $\pi$ -orbital of olefin. Complex formation is accompanied, naturally, by the redistribution of the electron density between atoms and bond involved in bond formation. The charge distribution in the  $ICl$  molecule and in the pyridine- $ICl$  CTC is exemplified below.



Enthalpy, entropy, and equilibrium constant are important characteristics of CTC. The enthalpy and entropy of CTC formation are negative. The enthalpy of formation changes in a wide range. Below we present the  $\Delta H^\circ$ ,  $\Delta S^\circ$ , and  $K$  for several complexes in  $n$ -paraffins.

Complex	$\Delta H^\circ$	$\Delta S^\circ$	$K$ (300 K)	$K$ (400 K)
$CH_2O \cdot BF_3$	57.2	138.4	380	1.72
$PhH \cdot I_2$	33.4	64.8	268	9.47
$(CH_3)_2S \cdot BF_3$	14.7	58.9	0.26	0.07

Of course, the solvent, first of all its solvating ability, affects the position of equilibrium. For example, for the formation of a CTC between 1,3,5-trinitrobenzene and  $N,N$ -dimethylaniline at 300 K,  $K = 9.5$  l/mol in cyclohexane and 0.15 l/mol in dioxane. The enthalpy of formation of CTC from A and B is determined by two contributions, electrostatic ( $E_A$  and  $E_B$ ) and covalent ( $C_A$  and  $C_B$ ). Drago and Wiland (1971) derived the empirical correlation

$$DH = 4.18(E_A E_B + C_A C_B) \quad (9.3)$$

and estimated the  $E$  and  $C$  parameters in hydrocarbon solvents for several molecules

Acceptor	$C_A$	$E_A$	Donor	$C_B$	$E_B$
$I_2$	1	1	$C_5H_5N$	6.40	1.17
$ClI$	0.83	5.10	$NH(CH_3)_2$	8.73	1.09
$C_6H_5OH$	0.44	4.33	$CH_3CN$	1.34	0.89
$(CH_3)_3COH$	0.30	2.04	$CH_3COCH_3$	2.33	0.99
$BF_3$	3.08	7.96	$(C_2H_5)_2O$	3.25	0.96
$SbCl_5$	3.15	7.38	$HCON(CH_3)_2$	2.58	1.32
$CHCl_3$	0.15	3.31	$C_6H_6$	0.71	0.49

The formation of CTC is influenced by steric factors. If substituents are near the atom involved in bond formation, then this creates interferences and decreases the bond energy of A and D in the complex.

#### 9.4. Molecular halogenation of olefins

The double bond possesses high reactivity; therefore, olefins enter into various reactions with double bond opening. In particular, olefins react with halogens  $X_2$  and with  $HX$  via the ionic and chain-radical mechanisms (see Chapters 7 and 8). Along with these multistage mechanisms, the addition of  $X_2$  and  $HX$  at the double bond under certain conditions occur by the molecular route. The reaction is preceded by the formation of a molecular complex.

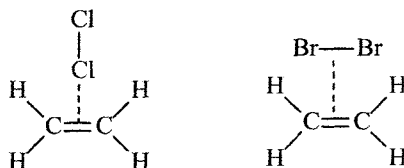
Halogens form with olefins 1 : 1 complexes. For cyclohexene in *n*-hexane, the complexes have the following thermodynamic characteristics:

$X_2$	IBr	$I_2$	$Br_2$	$Cl_2$
$K$ (298 K), l/mol	1.80	0.52	0.36	0.33
$-\Delta H^\circ$ , kJ/mol	31.5	9.6	16.8	11.3
$-\Delta S^\circ$ , J/(mol K)	55	59	46	48

Close values of the parameters are observed for other olefins, for example, for the  $Br_2$  complexes with different olefins the following values were obtained:

Olefin	Hexene-1	Hexene-3	Styrene	4-Methylpentene-1
$K$ (298 K), l/mol	0.23	0.72	0.20	0.33
$-\Delta H^\circ$ , kJ/mol	12.6	16.8	11.7	11.7
$-\Delta S^\circ$ , J/(mol K)	55	59	46	48

As can be seen from the  $K$  and  $\Delta H^\circ$  values, the complexes of halogens with olefins are characterized by the medium bond energy. They are stable at the temperature below 300 K, the equilibrium are shifted toward the formation of these complexes at temperatures below 250 K. The complexes are formed due to the overlapping of the highest occupied orbital of the  $\pi$ -bond of olefin with the antibonding  $\sigma^*$ -orbital of halogen. X-ray diffraction data on these complexes are lacking. The quantum-chemical calculation gave the following probable configurations of the chlorine and bromine complexes with ethylene:



The degree of charge transfer from the  $\pi$ -bond of olefin to halogen estimated from spectroscopic data in the heptene-1 complex is 0.043 for  $I_2$  and  $Br_2$ , 0.029 for  $Cl_2$ , and 0.08 for  $ICl$ , that is, it is insignificant.

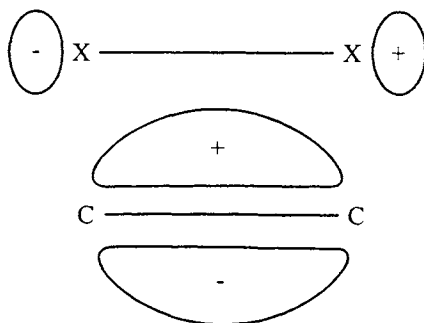


Fig. 9.1. Symmetry of interacting orbitals in the reaction of halogen with olefin.

The formation of halogen complexes with olefins does argue in favor of the molecular mechanism of halogenation because the complexes can participate in ion and radical reactions of transformation. It is difficult experimental problem to prove the molecular mechanism of these reactions because it should be based on the comprehensive kinetic study of the process and strong proofs that ions or radicals do not partici-

pate in the process.

The molecular mechanism was rather reliably proved for several systems. Olefin chlorination in weakly polar solutions (hydrocarbons, halohydrocarbons) in the absence of Brønsted and Lewis acids and in the absence of free radicals at low temperatures ( $<300$  K) proceeds *via* the molecular mechanism. Olefin chlorination is bimolecular with the rate  $v = k[\text{Cl}_2][\text{Olefin}]$  and the negative activation energy  $E = -7.1$  kJ/mol (hexene-1),  $-11.3$  (cyclohexene, heptene-3), and  $-16.8$  (styrene). The negative activation energy is the result of the fact that chlorination is preceded by the formation of a complex and  $\Delta H > E'$ , where  $E'$  is  $E - \Delta H^\circ$ . For example, for heptene-3 chlorination,  $E = -11.3$ ,  $\Delta H^\circ = 16.8$  and  $E' = 16.8 - 11.3 = 5.5$  kJ/mol, i.e., the activation barrier of the transformation of the complex into the products is low. This, at first glance, contradicts the rules of conservation of orbital symmetry under the assumption of a four-membered activated complex. In this complex the  $\sigma^*$ -orbitals of halogen and  $\pi$ -orbitals of olefin should overlap, and the reaction is forbidden due to a change in symmetry of the interacting orbitals (Fig. 9.1). However, in the CTC that formed the electron density is transferred, and this process is enhanced in the transition state. It is quite possible that the polar structure of the transition state removed the forbiddance of the rule of orbital symmetry, and the reaction occurs with a low activation energy.

## Part 4

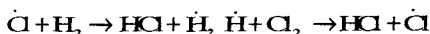
### Chain Reactions

#### Chapter 10

#### Chain non-branched reactions

The discovery of chain reactions was a result of intensive studies of photochemical reactions. In 1912 Einstein formulated the law about the interaction of a photon with a molecule, according to which the quantum yield of the photochemical reaction cannot exceed unity. M. Bodenstein studied a series of reactions that occur under irradiation and discovered that the reaction of chlorine with hydrogen occurs with a huge quantum yield: to million of molecules per absorbed quantum. He proposed that the reaction occurs as a chain of consecutive transformations: the photon knocks out an electron from the molecule. The electron induces the chain of consecutive transformations of  $H_2$  and  $Cl_2$  into  $HCl$ . However, measurements of electroconductivity showed that electrons are not formed in such a system, and Bodenstein proposed in 1916 that the photoexcited chlorine molecule is the active center. This mechanism was not either confirmed by subsequent experiments.

In 1918 Christiansen proposed the mechanism of chain transformation of  $Cl_2$  and  $H_2$  into  $HCl$  involving chlorine and hydrogen atoms and chain propagation in the reactions



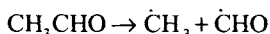
Atomic chlorine is generated under the action of light. This scheme was confirmed experimentally, and its particular steps were thoroughly studied. A new science, viz., kinetics of chain reactions, thus appeared in 1913—1918.

#### *10.1. Steps of chain non-branched reaction and conditions of its accomplishment*

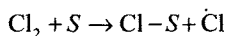
The chain reaction is a complicated process consisting of diverse elementary reactions (stages); these stages are related to one another in a definite way. They are classified as stages of chain initiation, propagation, and termination.

### 10.1.1. Chain generation

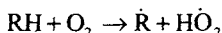
The formation of radicals initiating the chain process occurs *via* various reactions. First, radicals can appear from the starting substances. For example, the chain decomposition of acetaldehyde begins from its monomolecular decomposition at the C—C bond ( $D_{C-C} = 338.6$  kJ/mol)



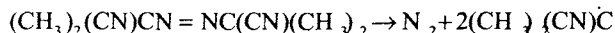
Thermolysis often occurs on the wall  $S$  of the reaction vessel, for example,



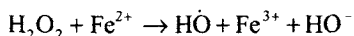
The formation of the chemisorbed chlorine atom facilitates such a process by decreasing the activation energy. Radicals can be regenerated in the bimolecular reaction of the reactants, as, e.g., in hydrocarbon oxidation by the reaction



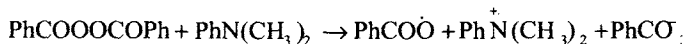
Second, the chain reaction is initiated by the introduction of an initiator or an initiating system. Peroxides and azo compounds are used as initiators of liquid-phase chain reactions. For example, azoisobutyronitrile decomposes to radicals in the reaction



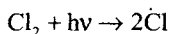
Radicals can appear in redox systems. For example, to initiate emulsion polymerization, the system  $\text{H}_2\text{O}_2 + \text{Fe}^{2+}$  is used, which initiates radicals in the reaction



Dibenzoyl peroxide and dimethylaniline generate radicals by the reaction



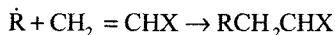
Third, the chain reaction can be initiated by the photochemical generation of radicals, for example,



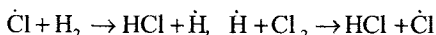
or using the action of penetrating radiation ( $\gamma$  rays, electrons  $\alpha$  particles).

### 10.1.2. Chain propagation

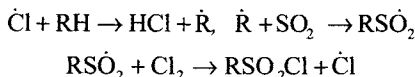
Free atoms and radicals formed in the system react with molecules. If a sequence of radical reactions composing the cycle of transformations with regeneration of the initial radical form appears in the system, then a chain reaction is possible. The cycle of radical transformations with conservation of the free valence and regeneration of the initial species is named the *chain unit*. The chain unit can consist of one or several elementary steps. For the radical polymerization of the vinyl monomer  $\text{CH}_2=\text{CHX}$ , the unit consists of one elementary step ( $\text{R}\cdot$  is macroradical)



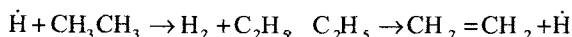
In the chain reaction of chlorine with hydrogen, the chain unit includes two successive reactions



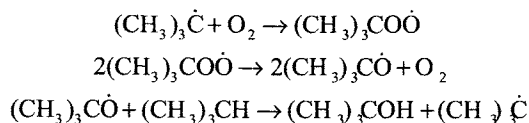
The chain sulfochlorination of hydrocarbon  $\text{RH}$  proceeds as alternation of three elementary acts



Chain propagation can include reactions of radicals with molecules and also decomposition reactions. For example, the chain decomposition of ethane includes the reactions



Sometimes we meet reactions where chain propagation occurs as the reaction of two radicals. For example, isobutane oxidation includes the following steps:

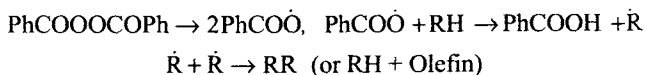


Chain propagation can include not one but two or more parallel cyclic reactions of chain propagation.

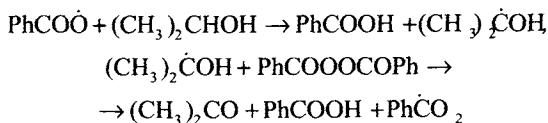
As shown by the analysis of steps of chain propagation in various chain reactions, their occurrence in nature is based on two principles. First, the *principle of non-annihilation of free valence* in reaction involving one free atom or radical. If the radical

is isomerized or decomposes, the reaction products always contains an atom or a radical. If the radical reacts with the molecule, detaches an atom or a group or adds to the multiple bond, in these cases, the free valence is also conserved because the odd number of electrons characteristic of reactants remains unchanged on the external electronic shells of the products. Thus, in reactions of an atom or a radical with a valence-saturated molecule and in monomolecular reactions of free radicals, a species with an odd number of radicals (atom or radical) is necessarily present among the products due to the conservation of the odd number of electrons on the orbitals of the reactants and products.

The appearance of free radicals in the system does not always result in the chain reaction. For example, the decomposition of dibenzoyl peroxide in hydrocarbon RX results in the following reactions:



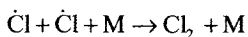
Although in this system radicals are generated and the free valence is conserved in the act of interaction of  $\text{PhCO}\dot{\text{O}}$  with RH, no chain reaction appears because the cyclic sequence of steps with conservation of the free valence is not realized. Therefore, second, the fulfillment of one more condition is very important: *principle of cyclicity* of radical steps with conservation of free valence. The chain reaction to occur requires such a combination of the reactants that the cycle of transformations with conservation of free valence and reproduction of the initial radical (atom) takes place. In the example presented above, it is enough to replace hydrocarbon by secondary alcohol to induce the chain reaction of dibenzoyl peroxide decomposition with the following steps of chain propagation:



### 10.1.3. Chain termination

The principle of conservation of free valence is fulfilled only in reactions of a first order with respect to the free radical. In reactions involving two free radicals or atoms, the free valence, as a rule, is saturated to form molecules as reaction products. Such reactions are exothermic because new bonds are formed in them and they occur with high rate constants. For example, the recombination and disproportionation of alkyl radicals in solution occur with the rate constant of diffusional collisions ( $10^8$ - $10^9$  l/(mol s)). In the gas phase, atoms recombine with the frequency of triple colli-

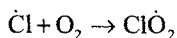
sions ( $\sim 10^{10} \text{ l}^2/(\text{mol}^2 \text{ s})$ ).



transmitting a portion of the evolved energy to the third particle M. If the atom or radical participates in the chain process, the reactions of this type are, in essence, reactions of *chain termination (decay)*. This termination can occur *via* reactions of active sites of either one or different types.

The molecular product formed in the act of chain decay must be stable under the conditions of the chain process. In other case, it decomposes without chain termination in this reaction.

The cyclicity principle necessary for the chain reaction to occur is disturbed if we introduce into the system a substance reacting with one of the chain-leading active sites to form a radical, which does not participate in chain propagation. For example, the presence of  $\text{O}_2$  in the  $\text{H}_2 + \text{Cl}_2$  mixture, where the chain reaction develops, results in chain termination by the reaction



The  $\text{ClO}_2\cdot$  radical that formed does not react with hydrogen and chlorine. Therefore, such a reaction terminates the chain. The reactant terminating the chain is the *inhibitor of chain reaction*. The wall of the reaction vessel can act as a unique inhibitor of the chain reaction if active sites are adsorbed on it followed by their decay.

Processes of propagation and decay of active sites compete with each other. Therefore, the chain reaction is realized only when possibilities for the predominant (priority) occurrence of chain propagation reactions are provided in the system. Only under this condition, the cycle of chain propagation reactions is multiply repeated. The average number of the chain propagation cycles calculated per active site generated in the system is the *chain length*. For the chain non-branched reaction in the quasi-stationary regime, the *chain length*  $\nu$  is equal to the ratio of the chain propagation rate to the chain termination or initiation rate.

Thus, a chain reaction appears due to the principle of indestructibility of free valence in reactions with a first order with respect to the radical. This reaction to occur needs the fulfillment of three conditions. 1. The set and structure of reactants must be such that the cycle of radical transformations with regeneration of the initial radical (atom) could occur in the system. 2. Free radicals must be generated in the system from reactants or by a special initiating action (initiator, light, radiation). 3. The conditions are selected in such a way that propagation occurs much more rapidly than chain termination.

### 10.2. Competition of chain and molecular reactions

The question about the transformations of reactants into products by the molecular reaction (direct way) and chain (complicated, multistage way) was considered in the monograph by N.N. Semenov "On Some Problems of Chemical Kinetics and Reactivity." The new approach appeared because the quantum chemistry formulated the rule of conservation of orbital symmetry in chemical and photochemical reactions (Woodward-Hofmann rule). Let us consider this interesting aspect.

Very often the structure of initial reactants suggests their direct interaction to form the same final products, which are also obtained in the chain reaction, and the thermodynamics does not forbid the reaction with  $\Delta G < 0$ . However, the experiment often shows that many reactions of this type occur in a complicated manner through several intermediate stages. For example, the reaction  $\text{H}_2 + \text{Cl}_2 \rightarrow 2\text{HCl}$  is very exothermic ( $\Delta H = -181 \text{ kJ/mol}$ ) but occurs only *via* the chain route through the intermediate stages involving chlorine and hydrogen atoms. Now, analyzing numerous cases where a molecular transformation is possible but the reaction occurs *via* the chain route, one can distinguish several reasons for which the chain route of transformation has an doubtless advantage over the molecular route.

#### 10.2.1. High chemical reactivity of free radicals and atoms

The high reactivity of radicals and atoms is clearly seen from the comparison of rate constants of reactions of the same type involving close in structure molecules and radicals. For example, the decomposition of propane to the methyl and ethyl radicals occurs very slowly with the rate constant  $k = 4 \cdot 10^{17} \exp(-343/RT) = 2 \cdot 10^{-17} \text{ s}^{-1}$  (500 K), and the n-propyl radical decomposes to the methyl radical and ethylene with  $k = 5 \cdot 10^{11} \exp(-106/RT) = 10 \text{ s}^{-1}$ , that is, by 18 orders of magnitude more rapidly. This distinction is due to the following. The energy expenses for the C—C bond cleavage in the n-propyl radical is partially compensated by the formation of the  $\pi$ -C—C bond of ethylene. In the case of propane decomposition, such a compensation is absent. In turn, ethylene formation during the decomposition of the n-propyl radical is predetermined by the presence of an unpaired electron. In other words, the fast decomposition of the radical compared to the molecule is a result of its high chemical reactivity in the form of a free valence. Similar conclusions are obtained if we compare the decomposition at the C—C bond of alcohol and alkoxy radical, amine and aminyl radical, aldehyde and acyl radical, aliphatic acid and acyloxy radical.

High reactivity is manifested by free atoms and radicals in abstraction reactions. For example, the oxygen atom abstracts the H atom from cyclohexane with the rate constant  $k = 1.3 \cdot 10^{10} \exp(-13.6/RT) = 5.6 \cdot 10^7 \text{ l/(mol s)}$  (300 K), and the oxygen molecule does it with  $k = 7.9 \cdot 10^{12} \exp(-167/RT) = 5.7 \cdot 10^{-17} \text{ l/(mol s)}$  (300 K). Such a great difference is related to the fact that the first reaction is exothermic ( $\Delta H = -22 \text{ kJ/mol}$ ),

and the second reaction is endothermic ( $\Delta H = 167$  kJ/mol). This distinction again follows from the structure of the species and strength of the formed O—H bonds: in the hydroxyl radical  $D_{O-H} = 427$  kJ/mol, and in  $H-O_2$  it is only 202 kJ/mol.

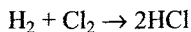
Radicals also exhibit high selectivity in addition reactions. For example, the peroxy radical of oxidizing styrene adds to the double bond of styrene with the rate constant  $k = 68$  l/(mol s), and the oxygen molecule adds with  $k = 5.6 \cdot 10^{-10}$  l/(mol s) (298 K). As in the case of abstraction reactions, the distinction is resulted by the fact that the first reaction is exothermic ( $\Delta H = -100$  kJ/mol), and the second reaction is endothermic ( $\Delta H = 125$  kJ/mol). In this case, the differences are due to the fact that the chemical energy is stored in the free radical. To illustrate this, below we present the  $\Delta H$  values for RH molecules and radicals  $R\cdot$  formed from them. It is seen that this difference ranges from 180 to 280 kJ/mol, that is, very significant

RX.....	H <sub>2</sub>	CH <sub>4</sub>	CH <sub>3</sub> OH	H <sub>2</sub> O	(CH <sub>3</sub> ) <sub>3</sub> COOH
$\Delta H_{RH}$ , kJ/mol.....	0.0	-74.8	-201	-241.8	-267
$\Delta H_R$ , kJ/mol.....	218	146.3	13	39	-81
$\Delta H_R - \Delta H_{RH}$ , kJ/mol.	218	221.1	214	280.8	186

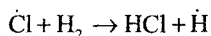
The high chemical reactivity of free atoms and radicals in various chemical reactions is one of the reasons for which radical chain reactions occur much more rapidly than the direct molecular transformation of reactants into products. Although radical formation is the endothermic reaction but, when appeared in the system, radicals rapidly enter into the reaction, and each radical induces the chain of transformations.

### 10.2.2. Rule of conservation of orbital symmetry

One more reason for which chain reactions have an advantage of molecular reactions is the restrictions, which are imposed on the elementary act by the quantum-chemical rule of conservation of symmetry of orbitals of the bonds, which undergo rearrangement in the reaction. If this rule is disturbed, the reaction, even if it is exothermic, requires a very high activation energy to occur. For example, the reaction

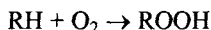


is exothermic ( $\Delta H = -181$  kJ/mol) but its activation energy (according to the calculation) is very high (about 150 kJ/mol). At the same time, the thermoneutral reaction

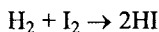


occurs with an activation energy of only 23 kJ/mol and a rate constant of  $8 \cdot 10^6$  l/(mol s) (300 K) because in this act the products conserve the symmetry of orbitals of the reactants. According to the rule of conservation, the reaction is allowed and occurs with a low activation energy (if it is exothermic) if the symmetries of orbitals of the

cleaved and formed bonds coincide. If this symmetry is disturbed, unoccupied high-energy orbitals of reactants should participate in the formation of the transition state, and this results in a very high activation energy of transformation. For example, the reaction



is forbidden by the rule of conservation because the oxygen exists in the triplet state and the formed hydroperoxide is in the singlet state, that is, the spin of the system is not retained. The reaction of this type can involve singlet oxygen. In the reaction



the symmetry of orbitals is also disturbed: the orbitals  $a_1$  and  $b_2$  overlap. In the transition state these orbitals are mixed (Fig. 10.1), which results in the high activation energy of this reaction. A similar situation takes place for the reactions  $\text{H}_2 + \text{Cl}_2$ ,  $\text{H}_2 + \text{Br}_2$ ,  $\text{N}_2 + \text{O}_2$ ,  $\text{ClO} + \text{ClO}$ ,  $\text{N}_2 + \text{H}_2$ ,  $\text{Cl}_2 + \text{CO}$ , and many others. In the case of reactions involving free atoms and radicals, the symmetry of orbitals in reactants and products remains unchanged because a species with an unpaired electron also has one unoccupied bonding orbital, which provides non-overlapping of the orbitals during the formation of the transition state.

### 10.2.3. Configuration of transition state

In abstraction reactions, atoms and some radicals have one more advantage over molecules. When two reacting species form the transition state, the fragments of these species arranged near the reaction center are repulsed. The repulsion energy depends on the configuration of the transition state. In reactions of X atom abstrac-

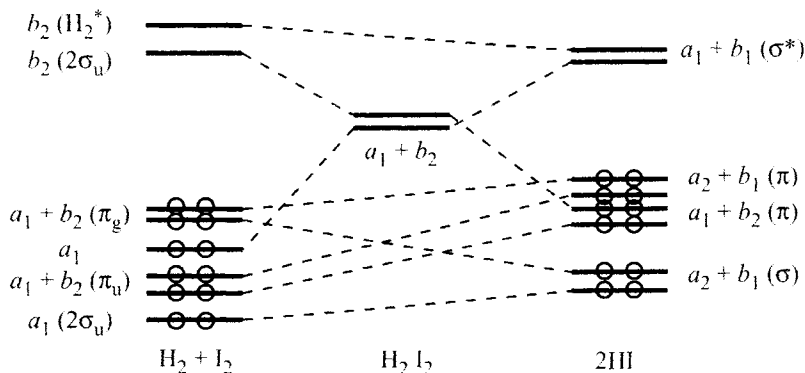
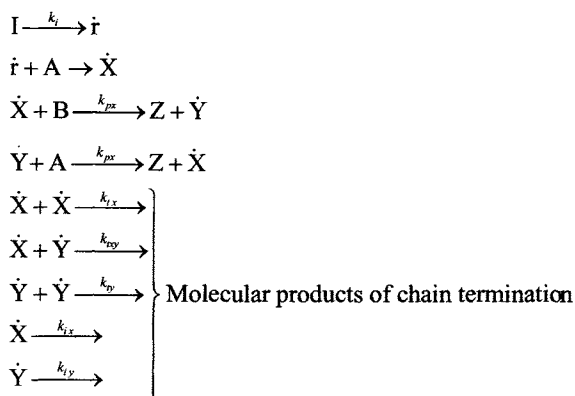


Fig. 10.1. Diagram of molecular orbitals for the reaction  $\text{H}_2 + \text{I}_2$ .

tion from the X—R molecule, the minimum repulsion is provided by the linear configuration of the transition state. This configuration is possible during the attack at the R—X bond of the atom or alkyl radical. As a rule, in reactions between molecules more compact nonlinear configurations appear, which increases the activation energy due to a higher repulsion energy of fragments of molecules in the transition state.

### 10.3. Kinetic regularities of chain reaction

Each particular chain reaction has its specific features. However, all of them have common features and kinetic regularities resulted from the chain mechanism. In this section, we consider the main of them using the following hypothetical scheme as an example (I is initiator, A and B are reactants, X· and Y· are active sites, and Z is product):



The scheme will be analyzed in the quasi-stationary regime with respect to X· and Y· where the initiation and chain termination rates are virtually equal.

#### 10.3.1. Interrelation between reaction rate and character of chain termination

Chain termination can occur through different ways. An active site can decay on the wall of the reaction vessel or in the bulk by the reaction with an inhibitor. For example, in the chain reaction of hydrogen with chlorine in the presence of oxygen, the chains decay in the reaction



because the  $\text{ClO}_2\cdot$  radical does not participate in chain propagation. In these cases, if chains are not terminated on the  $\text{X}\cdot$  sites in the reaction of a first order (in the bulk or on the wall), the inequality  $v_i = k_{tx} [\text{X}\cdot]$  is fulfilled in the quasi-stationary regime, and the chain reaction rate takes the following form:

$$v_Z = 2k_{px} k'_{tx}{}^{-1} [\text{B}] v_i \quad (10.1)$$

If chains are terminated in the bulk on inhibitor molecules, then  $k_{tx} = k_{\text{InH}} [\text{InH}]$ , and if termination occurs on the reactor wall in the kinetic regime when chain termination is not limited by diffusion of active sites centers to the surface  $S$ , then  $k_{tx} = k_S (S/V) \text{ s}^{-1}$ , where  $k_S$  is the specific rate of chain termination on the surface.

A different dependence is obtained when chains are terminated in the reaction of a second order. For chain termination in the reaction  $\text{X}\cdot + \text{X}\cdot$  in the quasi-stationary regime, the initiation rate  $v_i = k_{tx} [\text{X}\cdot]^2$

$$v_Z = 2k_{px} (k_{tx})^{-1/2} [\text{B}] v_i^{1/2} \quad (10.2)$$

that is,  $v_Z \sim v_i^{1/2}$ . In the general case, chains can terminate in parallel by reactions of the first and second orders. In this case,  $v_i = 2k_{tx} [\text{X}\cdot]^2 + k_{tx} [\text{X}\cdot]$ , and the dependence of  $v_Z$  on  $v_i$  is described by the expression

$$\frac{v_i}{v_Z} [\text{B}] = \frac{k_{tx}}{2k_{px}} + \frac{k_{tx}}{k_{px}} \frac{v_Z}{v_i} \quad (10.3)$$

at low  $v_i$  the rate  $v_Z \sim v_p$  and at high  $v_i$  the rate  $v_Z \sim v_i^{1/2}$ . If we introduce the notion of an *order of chain reaction with respect to initiator* ( $v_i \sim [\text{I}]$ ) and determine this order through

$$n_i = d \ln v_Z / d \ln [\text{I}] = d \ln v_Z / d \ln v_i \quad (10.4)$$

then  $n_i = 1$  for chain termination according to the first order and  $n_i = 0.5$  for chain termination by the second order. If chains terminate in parallel in reactions of the first and second orders, the inequality  $1 \geq n_i \geq 0.5$  is fulfilled and  $n_i$  depends on the  $v_i$  value.

### 10.3.2. Chain length

An important characteristic of the chain process is the chain length, viz., the average number of cycles of radical transformations of reactants into products, which are caused by one active center appeared in the system. The chain length is  $\nu = v_B / v_i = v_A / v_i$ . It depends or does not depend on  $v_i$ , which is due to way of chain termination. When chains terminate on the  $\text{X}\cdot$  centers according to the first order (see Eq. (10.1)), the chain length looks as follows:

$$v = 2k_{px}(k'_{ix})^{-1} \quad (10.5)$$

that is, is independent of  $v_i$ . When chains terminate on the  $X\cdot$  centers in the bimolecular reaction (see Eq. (10.2)), the chain length is

$$v = 2k_{px}(2k_{ix})^{-1/2}[B]v_i^{1/2} \quad (10.6)$$

that is, decreases with an increase in  $v_i$ . In the general case, when chain termination occurs in parallel *via* two channels,  $v$  and  $v_i$  are related by the correlation

$$\frac{[B]}{v} = \frac{k_{ix}}{2k_{px}} + \frac{k_{ix}}{4k_{px}^2} \frac{v_i}{[B]} \quad (10.7)$$

and at low  $v_i$  values when  $v_i \ll 2k_{px}k'_{ix}k_{ix}^{-1}[B]$ ,  $v$  is independent of  $v_i$ , and at high  $v_i$  ( $v_i > 2k_{px}k'_{ix}k_{ix}^{-1}[B]$ ) the chain length decreases with an increase in  $v_i$ . For short chains, the contribution of initiation to the overall process becomes noticeable, and the reaction rate should be written in a more complete form, namely,

$$v_A = v_i + k_{px}(2k_{ix})^{-1/2}[B]v_i^{1/2} \quad (10.8)$$

With increasing the initiation rate,  $[X\cdot]$  becomes so high that their recombination occurs more rapidly than chain propagation. Under these conditions, the chain process is transformed into the non-chain radical reaction. This transition takes place when the condition is fulfilled

$$v_i \geq k_{px}^2(2k_{ix})^{-1}[B]^2 \quad (10.9)$$

On the other hand, one can experimentally observe the chain reaction when  $v_A = v_B = 1/2v_Z = v$  is higher than some minimum detected value  $v_{min}$  to which  $v_{i,min}$  corresponds. Therefore, there is a range of  $v_i$  in which the chain reaction can be studied, and this range is determined by the inequality

$$v_{i,min} < v_i < k_{px}^2(2k_{ix})^{-1}[B]^2 \quad (10.10)$$

### 10.3.3. Limiting step of chain propagation

In the quasi-stationary regime at long chains, the rates of the first and second steps of chain propagation are virtually equal:  $k_{px}[B][X\cdot] = k_{px}[A][Y\cdot]$ . If  $k_{px}[B] \ll k_{py}[A]$ , then  $[X\cdot] \gg [Y\cdot]$  and chain termination occurs only in reactions involving  $X\cdot$ . Assume that chain terminate only by reactions of a first order. Then in the quasi-stationary regime  $v_i = k_i[I] = k'_{ix}[X\cdot]$ , and the rate of formation of the product is described by formula (10.1), *i.e.*, is proportional to the concentration of reactant B. If, on the contrary,  $k_{px}[B] \gg k_{py}[A]$ , so that the chains terminate only in the reaction involving  $Y\cdot$ , then  $v_Z \sim [A]$ . Thus, the rate of chain reaction is proportional to the concentration of the reactant with the corresponding active center reacts most slow-

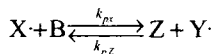
ly. This step of chain propagation is limiting. For the most rigid derivation of the criterion of the limiting step of the chain process, let us consider the general case where both centers participate in chain termination *via* the reaction of a first order. In this case,  $v_i = k'_{tx}[X\cdot] + k'_{ty}[Y\cdot]$  and

$$v_Z = 2k_{px}k_{py}[A][B]v_i/(k_{px}k'_{ty}[B] + k_{py}k'_{tx}[A]) \quad (10.11)$$

If  $k_{py}k'_{tx}[A] \gg k_{px}k'_{ty}[B]$ , then  $v_Z \sim [B]$  and the inequality written in the beginning is the criterion of the fact that the step  $X\cdot + B$  limits chain propagation. For chain termination in reactions of a second order, the criterion of the limiting step gains the character of the inequality  $k_{tx}k_{py}[A] \gg k_{tx}k_{py}[B]$ ; in this case, the inequality  $k_{tx}(k_{py}[A])^2 \gg k_{ty}(k_{px}[B])^2$  is also usually fulfilled. Evidently, changing the ratio of concentrations of reactants, we can transit from one limiting step to another.

#### 10.3.4. Reversible step of chain propagation

One of the steps of chain propagation can be reversible. This substantially reflects the kinetics of the process. Assume that the first step of chain propagation is reversible



Then as Z accumulates, the equilibrium is shifted toward reactant B. The reaction rate measured from the accumulation of Z in this reaction is the following:

$$\begin{aligned} v_Z &= k_{px}[B][X\cdot] - k_{pZ}[Z][Y\cdot] + k_{py}[A][Y\cdot] = \\ &= \left\{ 1 + \frac{k_{py}[A]}{k_{pY}[A] + k_{pZ}[Z]} \right\} k_{px}[B]v_i (k'_{tx})^{-1} \end{aligned} \quad (10.12)$$

Evidently, in this chain reaction the rate of the process decreases with the accumulation of product Z, and its introduction into the initial mixture of A and B also decreases the initial reaction rate.

#### 10.3.5. Variable initiation rate

The initiation rate, which remains unchanged during experiment, can be developed by photochemical or radiochemical radical generation. When initiator I is a source of radicals, which decomposes to radicals with the rate constant  $k_d$ , so that  $k_i = 2ek_d$ , where  $e$  is the probability of escape of radicals into the bulk from the liquid cage, then the initiation rate decreases as the initiator is consumed

$$v_i = 2ek_d[I]_0 \exp(-k_d t) = k_i[I]_0 \exp(-k_d t) \quad (10.13)$$

If chains terminate by the reaction of a first order on centers  $X\cdot$ , the kinetics of formation of product  $Z$  is described by the equation

$$[Z] = [Z]_0 + \Delta[Z]_{\infty}[1 - \exp(-k_d t)] \quad (10.14)$$

where  $\Delta[Z]_{\infty} = 4ek_{px}(k'_{tx})^{-1}[B][I]_0$  is the limiting degree of conversion, which is provided by the introduced initiator seeding.

For the bimolecular chain termination on radicals  $X\cdot$ , we obtain the expression

$$\begin{aligned} [Z] &= [Z]_0 + \Delta[Z]_{\infty}[1 - \exp(-0.5k_d t)], \\ \Delta[Z]_{\infty} &= 4k_{px}(ek_d k'_{tx})^{1/2}[B][I]_0^{1/2} \end{aligned} \quad (10.15)$$

Chain generation sometimes occurs with a sufficient rate due to the dissociation of one of the reactants. This reflects the kinetic regularities of the chain process. Assume that the reactant  $A = X_2$ ,  $v_i = 2k_d[A]$ , and chain termination occurs due to the recombination of  $X\cdot$ . Then the reaction rate

$$v_A = k_{px}[B](2k_d[A]/2k_{tx})^{1/2} \quad (10.16)$$

and the kinetics of  $A$  consumption in the equimolar mixture ( $[A]_0 = [B]_0$ ) has the form

$$[A] = [A]_0 (0.5k_{px} k_d^{1/2} k'_{tx}{}^{-1/2} [A]_0^{1/2} t + 1)^{-2} \quad (10.17)$$

It is characteristic that the rate of chain process depends on both the concentration of  $B$  (the step  $X\cdot + B$  limits chain propagation) and the concentration of  $A$  due to its participation in initiation. For linear chain termination,  $v_i \sim [A]$  and  $v \sim [A][B]$ . If reactant  $B$  generates radicals and participates in the limiting step of chain propagation, then  $v \sim [B]^{3/2}$  or  $v \sim [B]^2$ , depending on the character of chain termination.

### 10.3.6. Establishment of quasi-stationary regime

The chain reaction needs some time to achieve the quasi-stationary regime. This time depends on the character and rate of chain termination. If chain propagation is limited by the step  $X\cdot + B$ , and the chains terminate in the reaction of a first order, then the kinetics of increasing the concentration of active centers  $X\cdot$  is described by the equation

$$[X\cdot] = v_i(k'_{tx})^{-1}[1 - \exp(-k'_{tx}t)] \quad (10.18)$$

and the time of establishment of  $[X\cdot]_{st} = v_i(k'_{tx})^{-1}$  depends only on  $k'_{tx}$ . During the time equal to  $3(k'_{tx})^{-1}$  the concentration of  $X\cdot$  reaches a value of  $0.95[X\cdot]_{st}$ .

For the bimolecular mechanism of chain termination, the quasi-stationary concentration of  $X\cdot$  depends not only on  $k_{tx}$  but also on the initiation rate

$$[X\cdot]_{st} = (v_i/2k_{tx})^{1/2}$$

and the kinetics of achievement  $[X\cdot]_{st}$  is described by the equation

$$[\dot{X}] = [\dot{X}]_{st} \operatorname{th}[2(2v_i k_{tx})^{1/2} t] \quad (12.19)$$

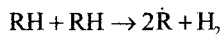
It can be accepted that the quasi-stationary concentration of  $X\cdot$  is achieved during the time  $1.5(2v_i k_{tx})^{-1/2}$ . At  $v_i = 10^{-7} \text{ mol/(l s)}$  and  $k_{tx} = 10^9 \text{ l/(mol s)}$  this time is 0.1 s.

## Oxidation of organic compounds by molecular oxygen

### 11.1. Elementary steps of chain oxidation

#### 11.1.1. Chain generation

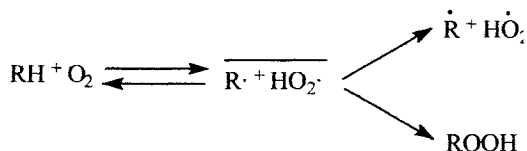
Liquid-phase oxidation of organic compounds is studied in laboratories at 300-500 K. Under these conditions, organic compounds are quite stable, and their decomposition with dissociation at the C—C bond and in the reaction



does not virtually occur.

Chain generation in the absence of initiating additives and those formed by hydroperoxide oxidation occurs *via* the following reactions involving dioxygen.

1. *Via* the bimolecular reaction of the weakest C—H bond with dioxygen



This reaction is endothermic because  $D_{R-H} > D_{H-O_2}$  and occurs slowly with the activation energy close to the enthalpy of the reaction

$$E_2 = D_{R-H} - 221 \text{ kJ/mol}, \quad (11.1)$$

$$\log k_{C-H} (403 \text{ K}) = 7.78 - 0.044 D_{R-H} \quad (11.2)$$

(where  $k_{C-H}$  is referred to one C—H bond), the reaction occurs in a non-polar hydrocarbon medium. Dioxygen reacts with one C—H bond of cyclohexane with  $k_{C-H} = 1.5 \cdot 10^{-10} \text{ l/(mol s)}$  (403 K) and with the C—H bond of cumene with  $k_{C-H} = 2.5 \cdot 10^{-8} \text{ l/(mol s)}$ , with the C—H bond of cyclohexene (in the  $\alpha$ -position to the double bond) with  $k_{C-H} = 1.3 \cdot 10^{-7} \text{ l/(mol s)}$ . Since the transition state of this reaction is polar (its

configuration is close to that of  $R\cdot + HO_2\cdot$ ), in polar media the reaction occurs more rapidly; a linear dependence is observed between  $\log k_2$  and the parameter  $(\epsilon - 1)/(2\epsilon + 1)$ . The reaction of polyatomic esters with dioxygen exhibits the effect of multidipole interaction: the greater the number of ester groups in the molecule, the lower the reactivity of each group in the reaction with dioxygen due to the dipole-dipole interaction of the polar reaction center with polar ester groups.

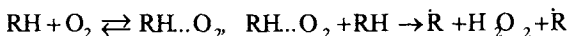
2. In the oxidation of easily oxidized compounds with weak C—H bonds, chain generation proceeds *via* the trimolecular reaction



This reaction is endothermic,  $\Delta H_3 = 2D_{R-H} - 570$  kJ/mol. The rate of radical generation in this reaction is  $v_i = k_3[RH]^2[O_2]$ . A trimolecular reaction is the reaction with concerted bond cleavage. In the transition state two C—H bonds are simultaneously cleaved and two O—H bonds are formed, *i.e.*, the concerted motion of two H atoms, two O atoms, and two C atoms takes place. This concerted motion requires a higher activation energy; therefore,  $E_3 > \Delta H$ . Below we present the  $k_3$  values for a series of compounds.

RH	$\Delta H$ , kJ/mol	$k_3$ , l <sup>2</sup> /(mol <sup>2</sup> s) (400 K)
Tetralin	80	$3.5 \cdot 10^3 \exp(-86.5/RT) = 1.7 \cdot 10^{-8}$
Indene	70	$3.9 \cdot 10^3 \exp(-78.5/RT) = 2.1 \cdot 10^{-7}$
Cyclohexadiene 1,3	70	$7.1 \cdot 10^6 \exp(-74.5/RT) = 1.3 \cdot 10^{-3}$
1,1-Dibutoxyethane	—	$5.2 \cdot 10^3 \exp(-83.6/RT) = 6.1 \cdot 10^{-8}$
Crotonic aldehyde	—	$5.0 \cdot 10^3 \exp(-63/RT) = 2.9 \cdot 10^{-5}$

It is seen that the activation energies somewhat exceed  $\Delta H$ , and the pre-exponential factors are much lower than the frequency factor of triple collisions ( $\sim 10^{10}$  l<sup>2</sup>/(mol<sup>2</sup> s)); both these circumstances are due to the concerted bond cleavage. The trimolecular reaction can occur either through triple collision or in two steps through the preliminary formation of the complex



It is known from spectroscopy of solutions that  $O_2$  forms donor-acceptor complexes with  $\pi$ -orbitals of aromatic hydrocarbons and unsaturated compounds. However, such complexes cannot be precursors of the transition state of the reaction of  $O_2$  with C—H bonds.

As shown by the quantum-chemical analysis of the  $CH_4 \cdots O_2$  pair, dioxygen forms an unstable complex with methane, which is characterized by the right angle H—O—O, an H...O distance of  $2.05 \cdot 10^{-10}$  m,  $\Delta H = 2$  kJ/mol, and charge transfer from O to H by only  $2 \cdot 10^{-3}$  electron charge. Therefore, for reactions in solution it is

hardly possible presently to distinguish the triple collision and the bimolecular reaction of RH with the short-lived encounter complex  $\text{RH}\cdot\text{O}_2$ . Both O—O and C—H bonds are non-polar, and the final reaction product  $\text{H}_2\text{O}_2$  is polar. Reaction (3) is endothermic, and the transition state of this reaction is polar according to the Hammond postulate. Therefore, in the polar medium the reaction should occur more rapidly, which agrees with the experimental data: for benzaldehyde at 303 K  $k_3 = 5.4 \cdot 10^{-5}$  in  $\text{CCl}_4$  and  $1.05 \cdot 10^{-4} \text{ l}^2/(\text{mol}^2 \text{ s})$  in acetic acid.

In an oxidized compound where chain generation occurs in the reaction with  $\text{O}_2$ , reactions (2) and (3) occur simultaneously. The trimolecular reaction will predominate when  $k_3[\text{RH}] > k_2$ . The activation energy is  $E_2 \approx \Delta H_2 = D_{\text{R-H}} - 221 \text{ kJ/mol}$ , and  $E_3 = \Delta H_3 + \Delta E_3 = 2D_{\text{R-H}} - 570 + \Delta E_3$ , where  $\Delta E_3$  is the additional energy barrier caused by the concerted bond cleavage and, according to the oscillatory model, for this reaction

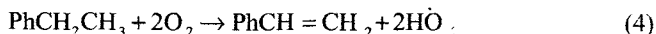
$$\Delta E_3 = 2.3RT \log(\pi E_2/3RT) \quad (11.3)$$

For  $E_2 = 80 \text{ kJ/mol}$  at 400 K  $\Delta E_3 = 12 \text{ kJ/mol}$ . The pre-exponential factor in the hydrocarbon medium for the bimolecular reaction is  $A_2 = 11.2 \pm 2.2$  (for 15 hydrocarbons and esters) and is much lower for the trimolecular reaction:  $A_3 = 4.7 \pm 1.2$  (for 9 hydrocarbons). The condition  $k_3[\text{RH}] > k_2$  is reduced to the following inequality for  $D_{\text{R-H}}$  ( $T = 400 \text{ K}$ ,  $[\text{RH}] = 10 \text{ mol/l}$ ,  $E_2 \approx 100 \text{ kJ/mol}$ ):

$$D_{\text{R-H}} < 344 \pm 10 \text{ kJ/mol} \quad (11.4)$$

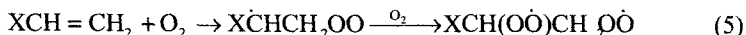
Experimental data agree with this condition. The polar medium accelerates reaction (3) to a greater extent than reaction (2).

For the reaction of ethylbenzene with dioxygen it was established that the rate of chain generation was  $v_{io} = k_4[\text{RH}][\text{O}_2]^2$ , and the following trimolecular reaction was proposed:



which occurred with the rate constant  $k_4 = 6.0 \cdot 10^8 \exp(-10^8/RT) \text{ l}^2/(\text{mol}^2 \text{ s})$ .

2. Vinyl monomers react with dioxygen *via* the bimolecular reaction involving the double bond



For example, styrene reacts with  $k_5 = 3.5 \cdot 10^{11} \exp(-125/RT) \text{ l}/(\text{mol s})$ . The activation energy of this reaction is close to its enthalpy  $\Delta H$ . This reaction also exhibits the effect of multidipole interaction: dioxygen reacts much more slowly with the double bond of polyatomic acrylic ester.

All reactions of chain generation are endothermic and occur with sufficiently high activation energies. On contact with air, the concentration of dissolved dioxy-

gen in organic compounds is low ( $1 \div 2 \cdot 10^{-3}$  mol/l), so that the chain generation rates at moderate temperatures are low ( $10^{-9} \div 10^{-13}$  mol/(l s) at 400 K).

### 11.1.2. Reactions of alkyl radicals with dioxygen

The addition reaction of  $R\cdot$  to  $O_2$

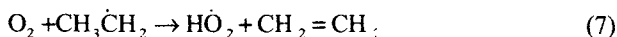


is exothermic: for primary, secondary, and tertiary alkyl radicals  $\Delta H_6 \approx 118 \pm 9$  kJ/mol, for allyl and benzyl radicals the enthalpy (by the absolute value) is much lower and depends on the strength of the C—H bond of the corresponding RH

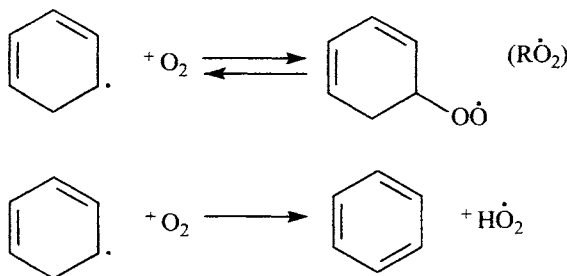
$$-\Delta H_6 = D_{R-O_2} = D_{R-H} - 274 \text{ kJ/mol} \quad (11.5)$$

This results in the situation that for hydrocarbons with the weak C—H bond this reaction occurs as a reversible reaction. For triphenylmethyl radicals the equilibrium constant is  $K_6 = 485$  l/mol (373 K), so that  $[R\cdot]/[RO_2\cdot] = 1$  at  $[O_2] = 2 \cdot 10^{-3}$  mol/l, that is, the concentration of  $O_2$  in the hydrocarbon contacting with air. Reaction (6) occurs very rapidly: in the gas phase with a constant of  $10^{10}$ – $10^9$  l/(mol s), and in the liquid phase with a diffusional rate constant of  $10^9$ – $10^8$  l/(mol s).

Along with the addition reaction, dioxygen enters the abstraction reaction with alkyl radicals similar to the disproportionation of radicals



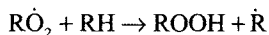
This reaction occurs much more slowly than the addition reaction. It plays a noticeable role in the high-temperature gas-phase oxidation of hydrocarbons with weak C—H bonds. This results in the parallel formation of  $ROOH$  and  $H_2O_2$  through  $\dot{R}O_2$  and  $\dot{H}O_2$



The rate constant  $k_7 = 10^4$  l/(mol s) (323 K),  $E_7 \approx 30$  kJ/mol, and the higher the temperature, the higher the  $k_7/k_6$  ratio.

### 11.1.3. Reaction of $\text{RO}_2^\cdot$ with C—H bond

This reaction occupies the central place in the chain oxidation of organic compounds



In most cases, this is precisely the reaction that limits chain propagation and determines the oxidation rate. Since the strength of the O—H bond in hydroperoxide is independent of the structure of the alkyl substituent R and even of the replacement of R by H, then reaction (2) is exothermic for hydrocarbons with  $D_{\text{R—H}} < D_{\text{ROO—H}} = 365 \text{ kJ/mol}$  (olefins, alkylaromatic hydrocarbons) and endothermic for hydrocarbons with  $D_{\text{R—H}} > 365 \text{ kJ/mol}$  (paraffinic and naphthenic hydrocarbons). The activation energy of this reaction is related by a linear correlation to  $D_{\text{R—H}}$

$$E_8 = 0.55(D_{\text{R—H}} - 144) \text{ kJ/mol.} \quad (11.6)$$

The ionization potential of RH ( $I_{\text{RH}}$ , eV) and the electron affinity  $E_A$  (eV) of  $\text{RO}_2^\cdot$  are significant for alkylaromatic hydrocarbons, as well as the steric factor ( $V_R$  is the substituent volume) for the attacked  $\alpha$ -C—H bond, so that  $k_8$  at 348 K depends on these factors as follows:

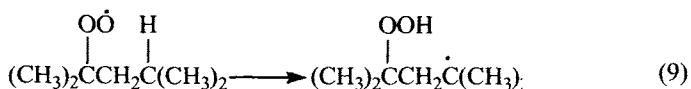
$$\log k_8 = 23.03 - 0.081D_{\text{R—H}} + 31.48/(I_{\text{RH}} - E_A) - 0.96V_R \quad (11.7)$$

The experimentally observed activation energies  $E$  change in the interval from 78 for the reaction of  $\text{R}'\text{CH}_3 + \text{RO}_2^\cdot$  to 20 kJ/mol for the reaction of  $\text{RO}_2^\cdot$  with 9,10-dihydroanthracene. The formation of the  $\text{RO}_2^\cdot \dots \text{H} \dots \text{R}$  transition state is associated with the entropy loss; therefore,  $A_8 < 10^7 \text{ l/(mol s)}$ , for the reaction of  $\text{RO}_2^\cdot$  with the C—H bond of paraffinic hydrocarbon  $\log A_8 = 9.0 \pm 0.2$ , and for the reaction of  $\text{RO}_2^\cdot$  with the  $\alpha$ -C—H bond of unsaturated or alkylaromatic hydrocarbon  $\log A_8 = 8.0 \pm 0.3$ .

Radicals  $\text{RO}_2^\cdot$ , primary and secondary alkylperoxyl radicals are close in activity, and tertiary radicals are by 4—8 times less active because of steric hindrances, which are created in the transition state by three alkyl groups; for tertiary  $\text{RO}_2^\cdot$  the above average  $A_8$  values should be decreased by 6 times. Peroxyl radicals of aldehydes  $\text{RCOOO}^\cdot$  possess very high activity, for which the  $k_8$  values being by 3—4 orders higher than those for  $(\text{CH}_3)_3\text{COO}^\cdot$  at 300 K. Since the  $\text{RO}_2^\cdot$  radical is polar, its attack to the C—H bond of a polar molecule (alcohol, ketone, etc.) results in the additional dipole-dipole interaction, which changes both  $E_8$  and  $A_8$ . In the reaction of  $\text{RO}_2^\cdot$  with polyfunctional compounds the multidipole interaction appears, which changes the  $k_8$  values to this or another side (see Chapter 6). The medium affects the reactivity of peroxyl radicals. In solvents with O—H groups, hydrogen bonds appear, which decreases the activity of  $\text{RO}_2^\cdot$ . In addition,  $\text{RO}_2^\cdot$  and the transition state are solvated by polar molecules. Donor-acceptor complexes appear in aromatic solvents.

#### 11.1.4. Isomerization of peroxy radicals

The free valence of the peroxy radical attacks both the C—H bond of another molecule and the C—H bonds of the radical if they are accessible for the attack. This isomerization results in the transformation of  $RO_2$  into the alkyl radical, for example,



Under the oxidation conditions, this reaction affords diatomic hydroperoxides, whereas reaction (8) gives monoatomic hydroperoxides. The analysis of geometry of the transition state for this isomerization showed that cyclic structures with one and two intermediate carbon atoms are formed without a substantial deformation of bond angles, that is, the attack should occur predominantly at the  $\beta$ - and  $\gamma$ -C—H bonds. The attack to the  $\alpha$ -position is very hindered due to the strong deformation of bond angles between the atoms forming the cyclic structure in the transition state. This agrees with the experimental data presented below ( $n$  is the number of  $\text{CH}_2$  groups in the  $(\text{CH}_3)_2\text{C}(\text{COO}\cdot)(\text{CH}_2)_n\text{CH}(\text{CH}_3)_2$  radical,  $k_9$  are presented at 373 K,  $k_9$  and  $A_9$  are in  $\text{s}^{-1}$ , and  $E_9$  are in kJ/mol).

$n$	$k_9$	$E_9$	$\log A_9$
0	0.2	94	12.5
1	18	73	11.5
2	8	71	11.0
3	1	79	11.0

Under oxidation conditions, this isomerization is a stage of intramolecular chain propagation. Competition between reactions (8) and (9) depends, naturally, on the structure of hydrocarbon and its concentration:  $v_8/v_9 = k_8[\text{RH}]/k_9$ . The ratio  $k_8/k_9 = 0.024$  l/mol for 2,4-dimethylpentane and 0.71 l/mol for n-pentane (373 K), i.e., in hydrocarbons with two (or more) tertiary C—H bonds in the  $\beta$ - and  $\gamma$ -positions the intramolecular attack of  $RO_2$  is more energetic.

#### 11.1.5. Addition of $RO_2$ at double bond

Peroxy radicals enter into the addition reaction with unsaturated compounds:



Reactions (6) and (10) alternate to give polymeric peroxide. The more stable the alkyl radical formed due to addition, the faster the addition reaction. Below we present the  $k_{10}$  values (l/(mol s)) for several monomers at 303 K.

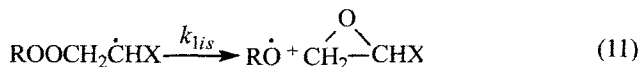
Monomer...	Vinyl acetate	Methyl acrylate	Methyl methacrylate	Styrene	$\alpha$ -Methylstyrene
$k_{10}$ .....	0.002	0.02	0.08	1.3	2.9

The  $k_{10}$  value also depends on the ionization potential of the double bond: the higher the ionization potential, the lower  $k_{10}$ . It is most likely that in the transition state a considerable transfer of the electron density occurs from the double bond to the oxygen atom of the attacking peroxy radical. For the same reason, acylperoxy radicals with a higher electron affinity add to the double bond by 2—3 orders of magnitude more rapidly than alkylperoxy radicals do. The steric factor also affects addition: the bulky substituent in the  $\alpha$ -position to the double bond impedes the addition of  $\text{RO}_2$ . In the reactions of  $\text{RO}_2$  with polyfunctional unsaturated esters, the effect of multipole interaction is manifested: polyesters (calculated per fragment) react more slowly than monoesters (see Chapter 6).

In oxidation of many unsaturated hydrocarbons, both reactions (abstraction and addition) occur in parallel to give a mixture of hydroperoxides and dialkyl or polyalkyl peroxides. The yields of the addition products of  $\text{RO}_2$  to the  $\pi\text{-C}=\text{C}$  bond of olefins are presented below for a series of olefins.

Olefin.....	Ethylene	Propylene	Hexene-1	Butene-1	Cyclohexene
$T, \text{K}$ .....	383	383	363	343	333
Yield, %....	100	50	33	26	4.4

The alkyl radicals formed due to the addition of  $\text{RO}_2$  to the double bond either react with  $\text{O}_2$  (reaction (6)) or decompose to form the oxide

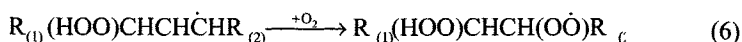
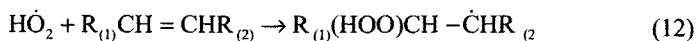


For many monomers such a decomposition occurs rather rapidly and successfully competes with reaction (1)

Monomer.....	Styrene	$\alpha$ -Methylstyrene	2-Butene	Trimethylethylene
$T, \text{K}$ .....	323	323	363	333
$k_{11}, \text{c}^{-1}$ .....	$7.6 \cdot 10^3$	$6.8 \cdot 10^4$	$9.1 \cdot 10^6$	$6.7 \cdot 10^6$

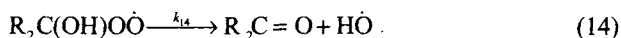
Oxides, whose yield depends on the oxygen pressure, are formed in parallel with alkyl and hydroperoxides due to this decomposition during olefin oxidation.

The oxidation of 1,2-substituted ethylene derivatives proceeds through the decomposition of the peroxy radical to olefin and  $\text{HO}_2$

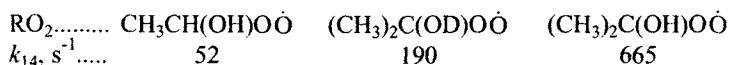




This results in the development of oxidation chain through the  $HO\cdot_2$  radicals, as in the case of cyclohexadienes. Alcohol oxidation occurs similarly where the decomposition reaction occurs in parallel with reaction (14)



The decomposition rate constants for these radicals at 295 K are presented below.

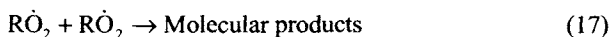
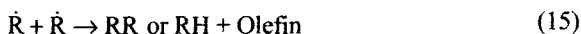


Decomposition occurs with sufficiently high activation energy,  $E_{14} = 56.4$  kJ/mol in the case of  $RO_2$  of isopropanol. The isotope effect ( $k_H/k_D = 3.5$ ) indicates the abstraction of H in the transition state.

#### 11.1.6. Disproportionation of peroxy radicals

ROOH formed in oxidation are intermediates and undergo decomposition.

These and other decomposition reactions will be considered in Section 11.3. Chain termination in oxidized hydrocarbons in the absence of inhibitors occur *via* bimolecular reactions

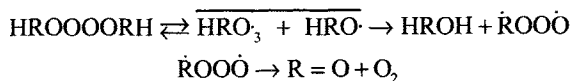


Reactions (15) and (16) occur in a solution with diffusional rate constants, and in the gas they occur with the frequency of bimolecular collisions (at rather high pressures). Under conditions of liquid-phase oxidation (laboratory and industrial), the condition  $[R\cdot] \ll [RO_2]$  is usually fulfilled, so that chain termination occurs mainly by reaction (17). The mechanism of this reaction is rather complicated and includes several stages

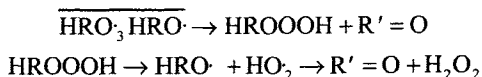




The contribution of stages to the overall process depends on the structure of R. For tertiary  $\text{RO}\cdot_2$ , stage (20) does not occur and the product of stage (21) is peroxide. Under conditions of equilibrium of stage (18), the total (measured in experiment) constant is  $k_{17} = K_{18}k_{19}k_{21}(k_{21} + k_{22})^{-1}$ , whereas at  $k_{18} \ll k_{19}$   $k_{17} = k_{18}k_{21}(k_{21} + k_{22})^{-1}$ . For tertiary  $\text{RO}\cdot_2$  disproportionation occurs rather slowly. For example, at 303 K for  $(\text{CH}_3)_3\text{COO}\cdot$   $2k_{17} = 1.5 \cdot 10^4$ , and for  $\text{Ph}(\text{CH}_3)_2\text{COO}\cdot$   $2k_{17} = 6 \cdot 10^3$  l/(mol s). Primary and secondary  $\text{RO}\cdot_2$  react much more rapidly: with rate constants of  $10^6$ – $10^8$  l/(mol s). For example, for the cyclohexylperoxyl radical  $2k_{17} = 7 \cdot 10^7 \exp(-6.7/RT) = 4.7 \cdot 10^6$  l/(mol s) (300 K). For secondary and primary  $\text{RO}\cdot_2$  the main stage of transformation of tetraoxide is reaction (20), so that  $k_{17} = K_{18}k_{20}(k_{18} + k_{20})^{-1}$ , and since  $k_{18} \gg k_{20}$ ,  $k_{17} = k_{20}k_{18}$ . Particular stages are characterized in more detail in Chapter 8. Note that there is another concept of the occurrence of stage (20) as a multistage reaction



This scheme explains, in particular, the formation of  $\text{H}_2\text{O}_2$  during the disproportionation of  $\text{RO}\cdot_2$



The presence of polar groups accelerates, as a rule, the disproportionation of peroxyl radicals.

### 11.2. Kinetics of initiated oxidation of organic compounds

In the presence of the initiator I or under the initiating action of light or radiation, chains are generated with the rate  $v_i$ , and the oxidation of RH proceeds as a chain process including reactions (1)–(6) (see Section 13.11). Usually  $v_i$  is so high that the decomposition of ROOH to radicals insignificantly contribute to initiation, so that during the experiment  $v_i = \text{const}$ , and oxidation develops as a chain non-branched reaction.

The reaction of  $\text{R}\cdot$  with  $\text{O}_2$  occurs, as we see, very rapidly, and in the presence of dissolved dioxygen ( $[\text{O}_2] > 10^{-4}$  M)  $[\text{R}\cdot] \ll [\text{RO}\cdot_2]$ . Therefore, reaction (8) limits chain propagation; chain termination occurs virtually only in reaction (17). In the presence of an initiator, as a rule, hydroperoxide decomposition does not play a noticeable role, so that  $v_i = k_i[\text{I}]$ . In the quasi-stationary regime,  $v_i = k_{17}[\text{RO}\cdot_2]^2$ , and

for long chains ( $k_{17}[\text{RH}][\text{RO}_2] \gg v_i$ ) the rate of chain oxidation is the following:

$$v = a[\text{RH}]v_i^{1/2}, \quad a = k_8 (2k_{17})^{-1/2} \quad (11.8)$$

This formula was repeatedly verified and confirmed by a large body of experimental material. The deviation from the linear dependence between  $v$  and  $[\text{RH}]$  is observed only when either RH or solvent have polar groups, which affects the solvation of the transition state and  $k_8$  and  $k_{17}$  values. In the case where chain propagation proceeds *via* reactions of intermolecular chain transfer (constant  $k_8$ ) and intramolecular isomerization of  $\text{RO}_2$  (constant  $k_9$ ), the equation for  $v$  takes the form

$$v = (k_8[\text{RH}] + k_9)(2k_{17})^{-1/2} v_i^{1/2} \quad (11.9)$$

In the case of short chains, initiation can noticeably contribute to the overall rate of the oxidation process, so that in the general case,

$$v = v_i + a[\text{RH}]v_i^{1/2} \quad (11.10)$$

The chain length is

$$v = k_8[\text{RH}][\text{RO}_2]/v_i = a[\text{RH}]v_i^{1/2}$$

so that with an increase in the initiation rate  $v$  decreases, and under the condition  $v_i \geq a^2[\text{RH}]^2$  oxidation proceeds as a non-chain radical process, among the products of which compounds formed in acts of chain termination predominate. The parameter decreases with the temperature decrease. Therefore, for each RH there is such a temperature  $T_{\text{min}}$  below which at the unchanged  $v_i$  oxidation already proceeds *via* the non-chain route. Below  $T_{\text{min}}$  are presented for a series of hydrocarbons calculated from the  $a$  values at  $v_i = 10^{-7}$  mol/(l s): cyclohexane (364 K), ethylbenzene (283 K), tetralin (247 K), and cumene (226 K).

The quasi-stationary regime of chain oxidation of RH is established within some time  $\tau$ . For the lifetime of the peroxy radical, *i.e.*, the time during which  $1 - ([\text{RO}_2]/[\text{RO}_2]_{\text{st}})$  changes by  $e$  times, we obtain  $\tau = 0.74(2v_i k_{17})^{-1/2}$ . For the interval of  $v_i$  changing from  $10^{-8}$  to  $10^{-6}$  mol/(l s) and variation of  $k_{17}$  from  $10^4$  to  $10^6$  l/(mol s)  $\tau$  changes from 0.1 to 100 s.

If the initiator concentration remains virtually unchanged during the time of experiment, then  $v_i = \text{const}$  and oxidation occurs with a constant rate. In fact, the initiator is consumed during oxidation, and the initiation rate decreases. If the initiator is the only source of radicals in the system, the oxidation kinetics is described by the equations ( $k_i = 2ek_d$ )

$$[\text{O}_2] = [\text{O}_2]_{\text{max}}[1 - \exp(-0.5k_d t)], \quad [\text{O}_2]_{\text{max}} = 2a[\text{RH}]k_d^{-1} \quad (11.11)$$

For a wide variation of the partial pressure of oxygen, such conditions are real-

ized under which reactions (15) and (16) noticeably contribute to chain termination. In this case, the oxidation rate depends on the partial oxygen pressure. At a very low concentration of dissolved dioxygen, reaction (6) limits chain propagation and chains terminate by reaction (15), so that the rate of the chain reaction

$$v = k_6 [O_2] [R] = k_6 (2k_{15})^{-1/2} [O_2] v_i^{1/2} \quad (11.12)$$

In a wide interval of changing  $[O_2]$ , the oxidation rate is related to  $[O_2]$  and  $[RH]$  by the correlation  $(v_\infty = k_8(2k_{17})^{-1/2}[RH]v_i^{1/2})$

$$\frac{[O_2]}{[RH]} \left( \frac{v_\infty^2}{v^2} - 1 \right) = \frac{k_8 k_{16}}{k_6 k_{17}} + \frac{k_8 k_{15} [RH]^2}{k_6 k_{17} [O_2]} \quad (11.13)$$

This rather complicated dependence can be approximated by a simpler formula

$$v = v_\infty (1 + \beta [O_2]^{-1})^{-1} \quad (11.14)$$

$\beta = [O_2]$  at which  $v = 0.5v_\infty$  and related to the rate constants of elementary steps by the correlation

$$\beta = 2(k_8 k_{17}^{1/2} k_6^{-1} k_{15}^{-1/2}) [RH] [(1 + 12 k_6 k_{16}^{-2} k_{17}^{-1/2})^{-1} - 1]^{-1}$$

The RH—O<sub>2</sub> system is two-phase; RH oxidation is preceded by the dissolution of dioxygen. If this dissolution occurs very rapidly, then  $[O_2] = \gamma p(O_2)$ , where  $\gamma$  is Henry's coefficient. However, with decreasing  $p(O_2)$  and increasing the oxidation rate, conditions are realized under which the process of O<sub>2</sub> dissolution begins to influence on the chain oxidation of RH. Oxygen rapidly saturates the thin surface layer of the liquid, and O<sub>2</sub> dissolution in the whole liquid bulk is usually limited by the rate of oxygen dissolution over the whole liquid mass by mixing. The rate of O<sub>2</sub> dissolution in RH thus depends on the interface surface, method and intensity of mixing, and oxygen concentration in the liquid; the dissolution process is described by the equation in which  $\kappa$  is the specific dissolution rate

$$d[O_2]/dt = \kappa(\gamma p_{O_2} - [O_2]) \quad (11.15)$$

In the quasi-equilibrium regime, the rates of oxygen dissolution and absorption by oxidized RH are equal

$$\kappa(\gamma p_{O_2} - [O_2]) = v = a[RH]v_i^{1/2} (1 + \beta [O_2]^{-1})^{-1} \quad (11.16)$$

which results after transformation in the following dependence of  $v$  on  $p_{O_2}$  and  $\kappa$ :

$$\frac{p_{O_2}}{v} = \frac{\beta}{(a[RH]v_i^{1/2} - v)} + \frac{1}{\gamma\kappa} \quad (11.17)$$

If  $\kappa$  is very high, so that  $[O_2] \approx \kappa \gamma p_{O_2}$ , then

$$v \approx a[RH]v_i^{1/2} (1 + \beta / \gamma p_{O_2})^{-1}$$

If, by contrast,  $\kappa$  is low, then  $v \approx \kappa \gamma p_{O_2}$ , that is, is limited by the rate of dioxygen dissolution. This consideration is approximate (it ignores the oxygen distribution over the RH volume) but allows one to estimate immediately from experimental data both the kinetic ( $\beta$ ) and physical ( $\kappa$ ) characteristics of the  $[O_2]$ -dependent oxidation process. Henry's coefficient for various hydrocarbons lies in the interval from 0.05 to 0.2 mol/(l MPa) at 300 K. The coupled oxidation of two hydrocarbons is described by the same kinetic equations as the copolymerization of two monomers (see Section 10.3).

### 11.3. Kinetics of autooxidation of hydrocarbons in liquid phase

Hydrocarbons are oxidized without the introduction of a radical source but this oxidation occurs with autoacceleration. This autoacceleration was explained in the framework of the theory of degenerate-branched chain reactions by the formation of an intermediate product, initiator. It was proved in 1930-50 that these products are hydroperoxides (see above). The Bach-Engler peroxide theory was thus merged with Semenov's theory of degenerate branching. Soviet scientists made the decisive contribution to the development of this area.

These reactions became widely studied in 1950-60 owing to N.M. Emanuel's initiation. The first studies of the decomposition of hydroperoxides formed during oxidation were performed as early as in the thirties: in 1931 H. Wieland and J. Mayer studied the decomposition of triphenylmethyl hydroperoxide, in 1935 S.S. Medvedev and A.Ya. Pod'yampol'skaya studied methyl hydroperoxide decomposition, and in 1939 K.I. Ivanov with co-workers studied the decomposition of  $\alpha$ -tetralyl hydroperoxide. In 1950 V. Langenbek and W. Pritzkow proposed the scheme of transformation of intermediate products of paraffin oxidation. A little later (1953) I.V. Berezin studied the composition of products and kinetics of cyclohexane oxidation.

In 1956 N.M. Emanuel, Z.K. Maizus, and L.G. Vartanyan, using the kinetic methods of investigation, studied the sequence of transformations of products in oxidized n-decane. The reactions of formation of radicals from hydroperoxides were studied in 1950-60. L. Beitman studied the kinetics of oxidation of several unsaturated compounds and showed in 1953 that ROOH decomposes to radicals by reactions of I and II orders. Several reactions of radical formation were discovered and studied in the sixties: the reaction of ROOH with the C—H bond of hydrocarbon (Z.K. Maizus, I.P. Skibida, N.M. Emanuel, 1960), the reaction of ROOH with the carbonyl group of

ketone (E.T. Denisov, 1962), the reaction of ROOH with carboxylic acid (L.G. Privalova, Z.K. Maizus, 1964), the reaction of ROOH with alcohol (E.T. Denisov, 1964), and the reaction of ROOH with the double bond of olefin (E.T. Denisov, L.N. Denisova, 1964). Theoretical aspects of the kinetics of oxidation as a chain degenerate-branched reaction were considered in 1959-62.

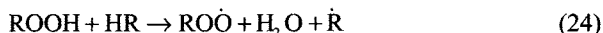
### 11.3.1. Decomposition of hydroperoxides to radicals

Hydroperoxides formed by oxidation have a weak O—O bond ( $D_{O-O} = 165$  kJ/mol) and in the gas phase they generate radicals in monomolecular decomposition



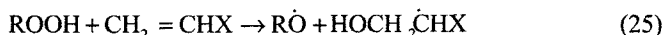
In the liquid phase their decomposition to radicals occurs more rapidly and with lower activation energy. For example, *tert*-butyl hydroperoxide in the gas phase decomposes with  $k_{23} = 5.0 \cdot 10^{13} \exp(-158/RT) = 5 \cdot 10^{-8} \text{ s}^{-1}$ , and in a chlorobenzene solution  $k_{23} = 4.0 \cdot 10^{12} \exp(-138/RT) = 1.8 \cdot 10^{-6} \text{ s}^{-1}$  (393 K). Mechanisms of hydroperoxide decomposition in organic compounds are diverse.

1. In saturated and alkylaromatic hydrocarbons hydroperoxides react with C—H bonds

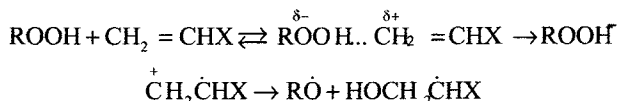


The weaker the C—H bond, the higher the rate constant. Cumyl peroxide reacts with cumene with the rate constant  $k_{24} = 5 \cdot 10^7 \exp(-109/RT) \text{ l/(mol s)}$ .

2. Hydroperoxide reacts with the  $\pi$ -bond of unsaturated compounds; the reaction is accompanied by the cleavage of the O—O bond



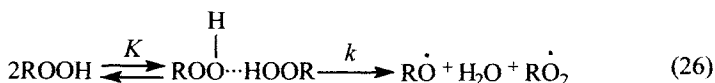
Probably, the reaction is preceded by the formation of a donor-acceptor complex, and the elementary act represents the electron transfer from the  $\pi$ -bond to the O—O group followed by its homolysis



*tert*-Butyl hydroperoxide reacts with styrene with  $k_{25} = 1.2 \cdot 10^4 \exp(-72/RT) \text{ l/(mol s)}$ . The polar structure of the transition state is indicated by the fact that reactions of polyatomic unsaturated esters with ROOH exhibit a pronounced effect of multidipole interaction: ROOH reacts more slowly with the double bond of polyatomic ester.

3. Hydroperoxides decompose to radicals through the preliminary formation of

an associate by the hydrogen bond



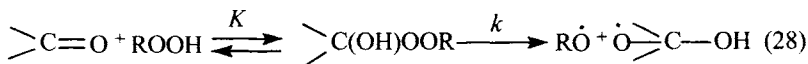
At low concentrations of ROOH when the fraction of associated molecules is low,  $v_i = 2ekK[\text{ROOH}]^2 = k_{26}[\text{ROOH}]^2$ , and in solutions of ROOH where almost all molecules are associated,  $v_i = 0.5ke[\text{ROOH}]$ . The transition of the initiation reaction from the second to first order with an increase in  $[\text{ROOH}]$  is really observed experimentally, for *tert*-butyl hydroperoxide  $0.5ek = 5.8 \cdot 10^7 \exp(-96/RT) \text{ s}^{-1}$ .

4. It is likely that hydroperoxides react similarly with alcohols



The rate of radical formation  $v_i = k_{23}[\text{ROOH}][\text{R}'\text{OH}]$  for  $[\text{R}'\text{OH}] \leq 1 \text{ mol/l}$ ; at higher concentrations  $v_i$  reaches a maximum and then decreases with an increase in  $[\text{R}'\text{OH}]$ . This is likely related to a change in the composition and reactivity of associates of hydroperoxide with alcohol.

5. Carbonyl compounds also accelerate the decomposition of hydroperoxides, which is due to the formation of labile peroxide compounds



The reaction of *tert*-butyl hydroperoxide with cyclohexane in a chlorobenzene medium is characterized by the constants:  $K = 7 \cdot 10^{-7} \exp(46/RT)$  and  $2ek = 3.6 \cdot 10^9 \exp(-109/RT) \text{ s}^{-1}$ .

6. Carboxylic acids also accelerate the decomposition of hydroperoxide to radicals; the rate of radical formation is  $v_i = k_{29}[\text{ROOH}][\text{R}'\text{COOH}]$ . It is assumed that the reaction is similar to that of ROOH with alcohol



Thus, in oxidized hydrocarbon where various oxidation products were formed and are present, the decomposition of hydroperoxides is parallel to several reactions. The question, which reaction prevails, was studied in such processes as the oxidation of cyclohexanol and isopentane.

### 11.3.2. Kinetic regularities of autoxidation

As already mentioned, the rate of chain initiation  $v_{i0}$  in oxidized organic compounds RH is low, so that the initiation rate increases with the accumulation of

ROOH, and at rather high [ROOH] the decomposition of hydroperoxide to radicals becomes the main radical source. If ROOH decomposes to radicals reacting with RH, whose concentration at the initial stages is constant, the generation of radicals from ROOH can be considered as a pseudo-molecular process with the rate  $v_i = k_i[\text{ROOH}]$ , where  $k_i = k_{23} + k_{24}[\text{RH}] + k_{25}[\text{CH}_2=\text{CHX}]$ . Since the rate of chain oxidation  $v = a[\text{RH}]v_i^{1/2}$  (see equation (13.10)) and  $v_i = v_{i0} + k_i[\text{ROOH}]$ , where  $k_i = k_{23} + (k_{24} + k_{25})[\text{RH}]$ , for autoxidation

$$v = a(v_{i0} + k_i[\text{ROOH}])^{1/2}[\text{RH}] \quad (11.18)$$

and in the case where all absorbed oxygen is transformed into hydroperoxide groups and the fraction of decomposed ROOH is small, the kinetics of oxygen absorption is described by the equation

$$\Delta[\text{O}_2]/t = a[\text{RH}]v_{i0}^{1/2} + b^2 t \quad (11.19)$$

where

$$a = k_8 k_{17}^{-1/2}, \quad b^2 = 1/4 a^2 k_{23}[\text{RH}]^2$$

At a very low  $a[\text{RH}]v_{i0}^{1/2}$  value ( $v_{i0}$  is very low) this equation gains a simpler form

$$\Delta[\text{O}_2]^{1/2} = bt \quad (11.20)$$

A diverse experimental material on the oxidation of individual organic compounds and mixtures of hydrocarbons agrees with this equation. At a comparatively high concentration, hydroperoxide decomposes with a noticeably rate *via* the bimolecular reaction, the rate being  $v_i = k_{26}[\text{ROOH}]^2$ . Therefore, the following dependence is observed between  $v$  and  $[\text{ROOH}]$ :

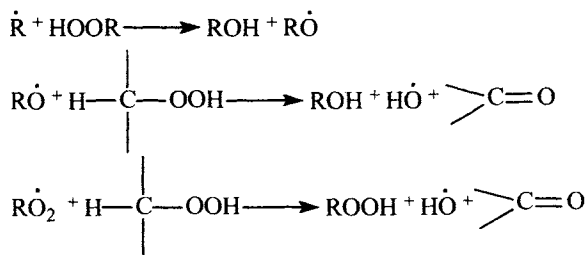
$$v^2/[\text{ROOH}] = a^2[\text{RH}]^2 k_{23} + a^2[\text{RH}]^2 k_{26}[\text{ROOH}] \quad (11.21)$$

All dependences considered above were obtained under the assumption that the quasi-stationary concentration of  $\text{RO}_2$  is established in the system very rapidly (during the time of heating of the reactor). This is valid only at such a sufficiently high  $v_{i0}$  at which the time of establishment of the quasi-stationary state  $\tau_{\text{st}} = 0.74(k_{17}v_{i0})^{-1/2}$  is shorter than the time of heating. Since the rates of chain initiation during the autoxidation of RH are often very low,  $\tau_{\text{st}}$  can be rather noticeable value. For example, at  $v_{i0} = 10^{-11} \text{ l}/(\text{mol s})$  and  $k_{17} = 10^5 \text{ l}/(\text{mol s})$   $\tau_{\text{st}} = 750 \text{ s}$  and the time of heating usually does not exceed 150 s. In these cases, formula (11.20) gains somewhat different form

$$\Delta[\text{O}_2]^{1/2} = b(t - \tau) \quad (11.22)$$

The same dependence is observed for inhibited autooxidation (in this case,  $\tau = f[\text{InH}]_0/v_{i0}$ ).

Hydroperoxides in oxidized RH decompose *via* the following three directions. First, they homolytically react with RH and products of its oxidation to form free radicals. Under the conditions of chain oxidation of RH, this decomposition does not result in a decrease in ROOH. Second, hydroperoxides are attacked by various radicals formed in the system, such as  $\text{RO}_2\cdot$ ,  $\text{RO}\cdot$ , and  $\text{R}\cdot$ , entering with them into reactions of the type



This results in the consumption of ROOH *via* the chain mechanism.

Finally, hydroperoxides are transformed into molecular products in heterolytic reactions with oxidation products (for example, under the action of acids) by the heterolytic decomposition on the reactor walls, under the action of the catalyst of heterolytic ROOH decomposition, which was specially introduced or randomly gotten into the system, and during the reaction in the cage of radicals formed from hydroperoxide. Let us consider the kinetics of RH oxidation at deep stages in this last case where ROOH decomposes in oxidized RH by the molecular reaction of a first order with the rate constant  $k_m$ . In this case (at  $k_m \gg k_{23}$ ), the maximum with respect to ROOH is achieved under the condition  $v = a[\text{RH}](k_{23}[\text{ROOH}])^{1/2} = k_m[\text{ROOH}]$ , from which  $[\text{ROOH}]_{\text{max}} = a^2 k_{23} k_m^{-1/2} [\text{RH}]^2$ , and the kinetics of ROOH formation and RH decomposition are described by the equations

$$[\text{ROOH}] = [\text{ROOH}]_{\text{max}} [1 - \exp(-k_m t/2)]^2 \quad (11.23)$$

$$[\text{RH}]^{-1} = [\text{RH}]_0^{-1} + k_{23} a^2 k_m^{-1} \{t + 2k_m^{-1} [\exp(-k_m t)/2 - 1]\} \quad (11.24)$$

and at rather high  $t$  ( $t \gg 2k_m^{-1}$ ) the kinetics of RH consumption is close to the bimolecular law

$$[\text{RH}]^{-1} \approx [\text{RH}]_0^{-1} + a^2 k_{23} k_m^{-1} (t - 2k_m^{-1}) \quad (11.25)$$

At deep stages of hydrocarbon oxidation, the self-retardation of the process is often observed, which is caused by the following facts.

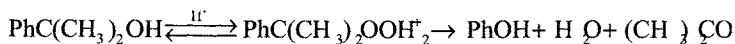
1. Such products as acids, hydroxy acids, and keto-alcohols, which result in the heterolytic decomposition of hydroperoxides, are formed and accumulated among

oxidation products. This is favored by an increase in the polarity of the medium due to the accumulation of water and polar oxygen-containing products. Therefore, in the above equations (11.23)-(11.25)  $k_m$  should be considered as a variable value  $k_m(t)$ .

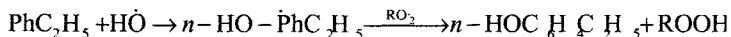
2. The accumulation of various intermediate products results in the situation that other radicals, in particular, hydroperoxyl, appear in the system in addition to  $RO_2$  and  $RH$ . They differ in reactivity; the appearance in the system of radicals less reactive than the initial  $RO_2$  results in the total decrease in the reactivity of the radical mixture, so that the effective value of the parameter  $a = k_8 k_{17}^{-1/2}$  decreases.

3. The decrease in the reactivity of all peroxy radicals is a result of the accumulation of hydroxyl-containing oxidation products: hydroperoxides, alcohols, acids, and water. They form with  $RO_2$  hydrogen bonds, which, naturally, decrease their reactivity.

4. The oxidation of aromatic compounds results in the accumulation of phenolic compounds, which are inhibitors of oxidation (see Section 11.4). Their formation is due to the accumulation of acids and heterolytic decomposition of  $ROOH$ , for example,



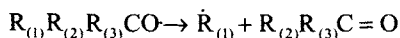
as well as by the homolytic decomposition of  $ROOH$  followed by the addition of the active hydroxyl radical to the aromatic ring of  $RH$  and its transformation into phenol, for example,



Very often all four factors act simultaneously, which results in the self-retardation of autoxidation at degrees of conversion of 40-50%.

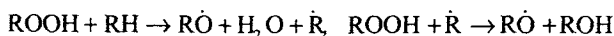
### 11.3.3. Autoxidation of polymers

The mechanism of autoxidation of solid polyolefins  $RH$  has many common features with hydrocarbon oxidation: polymers are oxidized by the chain route; the chain develops as alternation of acts of  $R\cdot$  with  $O_2$  and  $RO_2$  with  $RH$ ; in the absence of an inhibitor and at a sufficiently high  $[O_2]$  in polymer, chain oxidation occurs with autoacceleration because the hydroperoxide groups that formed are a source of initiation. However, there are several substantial distinctions. As already mentioned in Chapter 6, reactions resulting in polymer destruction play an important role. In initiated oxidation the main source of destruction is reactions of peroxide radicals, whereas in autoxidation the contribution of alkoxy radicals, which decompose in the reaction of the type



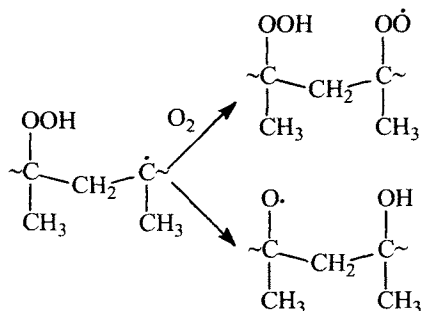
increases.

The source of macroradicals  $RO\cdot$  is macromolecules with hydroperoxide groups from which alkoxy radicals are formed in reactions of the type

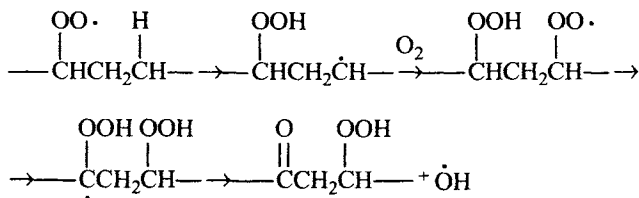


The more hydroperoxide groups were accumulated in the polymer, the higher is the rate of  $RO\cdot$  formation and their contribution to polymer destruction.

Another distinction of polymer autoxidation from the oxidation of hydrocarbons concerns reactions involving alkyl radicals. Under conditions of liquid-phase oxidation, usually all alkyl radicals are transformed into peroxy radicals (the reaction of  $R\cdot$  with  $O_2$  occurs very rapidly, see Chapter 4). In solid polymer the alkyl macroradical reacts with  $O_2$  much more slowly (see Chapter 6). This results for polypropylene (PP) oxidation, for example, in the fact that the following two reactions compete with commensurable rates:

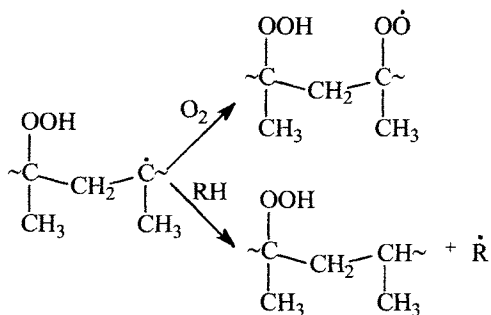


As a result, first, only a part of absorbed dioxygen is transformed into hydroperoxyl groups and a part is transformed into alcohol groups. Second, alkoxy radicals, which undergo destruction, appear. In the oxidation of PE, the reactions



lead to a similar result.

Since the competition of the reactions depends on  $[O_2]$ , the kinetics of ROOH accumulation depends on  $p(O_2)$ : the higher  $p(O_2)$ , the greater the fraction of absorbed dioxygen, which is transformed into hydroperoxyl groups. In addition, the competition appears between the reactions



Therefore, the composition of hydroperoxyl groups depends on the partial dioxygen pressure: the higher  $p(O_2)$ , the greater the fraction of block hydroperoxyl groups. Block hydroperoxyl groups decompose to radicals more rapidly than single groups. Therefore, the higher  $p(O_2)$ , the faster polymer autooxidation even under the conditions where initiated oxidation is independent of  $p(O_2)$ .

#### 11.4. Inhibition of oxidation reactions

##### 11.4.1. Kinetic classification of inhibitors

Alkyl and peroxy radicals alternating lead the chain process. Therefore, oxidation can be retarded by acceptors of both alkyl and peroxy radicals. Autooxidation develops as a self-initiated ROOH forming chain reaction. Hence, autooxidation can be retarded by the decomposition of hydroperoxide or decreasing the rate of its decomposition to radicals. According to the complicated oxidation mechanism, inhibitors in mechanism of their action can be divided into the following six groups.

##### *Inhibitors terminating chains by reaction with peroxide radicals*

Such inhibitors are aromatic compounds with comparatively weak O—H and N—H bonds (phenols, naphthols, aromatic amines, aminophenols, diamines). Compounds of this type possess reduction properties and rapidly react with peroxy radicals.

*Inhibitors terminating chains by reaction with alkyl radicals*

They are compounds that rapidly react with alkyl radicals: quinones, iminoquinones, methylenequinones, stable nitroxyl radicals, molecular iodine. Alkyl radicals rapidly react with oxygen. Therefore, inhibitors of this type are efficient under conditions where the concentration of dissolved dioxygen in the oxidized substance is low.

*Inhibitors decomposing hydroperoxides*

Compounds of this type are substances that rapidly react with hydroperoxides without formation of free radicals: sulfides, phosphites, arsenides, *etc.*, as well as metal thiophosphates and carbamates, various metal complexes. The reaction with hydroperoxide can occur stoichiometrically (sulfides, phosphites) and catalytically (metal complexes).

*Inhibitors as deactivators of metals*

Compounds of variable-valence metals decompose hydroperoxides to form free radicals, which accelerates oxidation. This catalyzed oxidation can be retarded by the introduction of a complex-forming agent, which forms a complex with the metal and is inactive toward hydroperoxide. Diamines, hydroxy acids, and other bifunctional compounds that form stable complexes with metals are used as inhibitors of this type.

*Inhibitors of cyclic chain termination*

The oxidation of some classes of substances (alcohols, aliphatic amines) gives peroxy radicals, which possess both oxidative and reductive actions. In these systems, a several inhibitors terminate chains and are regenerated again in acts of chain termination: catalytic chain termination takes place. The number of chain terminations depends on the ratio of the rates of inhibitor regeneration to its irreversible consumption. In several cases, multiple chain termination is observed in polymers. Inhibitors of multiple chain termination are aromatic amines, nitroxyl radicals, and compounds of variable-valence metals.

*Inhibitors of combined action*

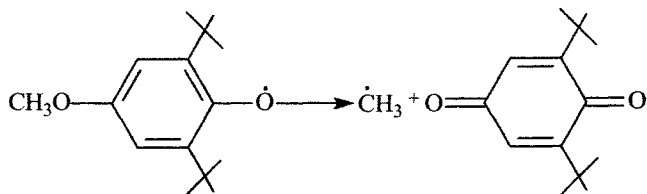
Some compounds retard oxidation entering simultaneously into several reactions. For example, they react with both alkyl and peroxy radicals (anthracene, methylenequinone), decompose hydroperoxides, and terminate chains in the reaction with  $\text{RO}_2$  (metal carbamates and thiophosphates). Such compounds are inhibitors of com-

bined action. The same group can enter into parallel reactions. For example, both  $R\cdot$  and  $RO_2\cdot$  react with the double bond of methylenequinone. A molecule often contains two or more functional groups, each of which enters into the corresponding reaction. For example, phenol sulfide reacts with hydroperoxide by its sulfide group and with  $RO_2\cdot$  by its phenol group. Finally, the initial inhibitor and products of its transformation can enter into reactions of different types.

Mixtures of inhibitors often possess a combined action. For example, when phenol and sulfide are introduced into the oxidized hydrocarbon, the first one retards by chain termination in the reaction with  $RO_2\cdot$ , and the second one decreases the rate of degenerate chain branching decomposing hydroperoxide. When two inhibitors enhance the retardation action of each other, we deal with synergism. When their retardation action is simply summated (for example, the induction period under the action of a mixture is equal to the sum of the induction periods under the action of each individual inhibitor), we have their additive retardation action. If the retardation action of a mixture is smaller than the sum of the retardation actions of each inhibitor, we have antagonism of inhibitors.

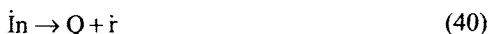
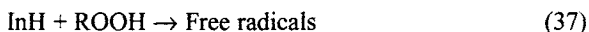
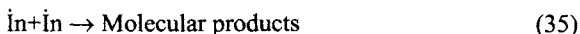
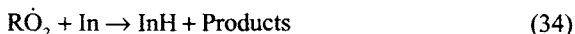
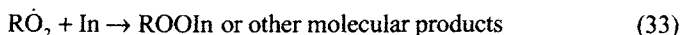
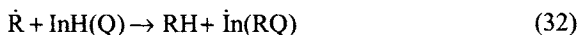
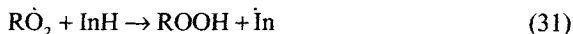
#### 11.4.2. Mechanism of inhibited oxidation of RH

The scheme of oxidation in the presence of the inhibitor InH, which reacts with peroxy radicals, and the inhibitor Q, which is an acceptor of alkyl radicals, includes several reactions involving radicals  $In\cdot$  formed from the inhibitor, namely, reactions of radical decay ( $In\cdot + In\cdot$ ,  $In\cdot + RO_2\cdot$ ) and reactions of chain propagation of the type  $In\cdot + RH$ ,  $In\cdot + ROOH$ , and decomposition of  $In\cdot$  to the molecule and radical capable of propagating the chain. This can be exemplified by the reaction



Being a reducing agent, the inhibitor is oxidized by not only the peroxy radical (this reaction results in chain termination) but also oxygen and hydroperoxide, which results in the consumption of the inhibitor without chain termination. Below we present the list of reactions involving an inhibitor; the reactions of  $R\cdot$  and  $RO_2\cdot$  in which an inhibitor does not participate are considered in Section 11.1 ( $R'OOR'$  is the initiator).





Quinolide peroxide  $InOOR$  is formed in the addition of  $RO_2$  to 2,4,6-tri-alkylphenoxyl radical. Phenoxyl with the alkoxy substituent in the para- or ortho-position react in the decomposition reaction (40) to form the alkyl radical and quinone.

Depending on the nature of the inhibitor and oxidation conditions, the mechanism of its action can be different. The mechanism can be identified by kinetic data, that is, reveal the key reactions, which determine the mechanism of inhibition action.

Depending on this or another set of key reactions, twelve basic mechanisms can be distinguished from the general scheme, each of which contains the minimum set of key reactions. Table 11.1 presents these mechanisms, key stages, and expressions for the rate and amount of absorbed oxygen at  $v_i = \text{const}$ .

The type of the mechanism of inhibition taking place in a particular system depends on the oxidizability of  $RH$ , structure and reactivity of the inhibitor, oxidation conditions ( $T$ ,  $[InH]$ ,  $[RH]$ ,  $[ROOH]$ ,  $[O_2]$ ,  $v_i$ ). For example, 2,6-di-*tert*-alkylphenoxyl radicals very slowly react with  $RH$  and  $ROOH$  and, hence, mechanisms IV and V are inappropriate for them. Mechanism IX is observed only for phenols with the alkoxy substituent in the para-position. Mechanisms X-XII are realized for acceptors of alkyl radicals, such as quinones and piperidineoxyls. Mechanism IV to occur needs a sufficiently weak C—H bond in the oxidized substance and a sufficiently reactive phenoxyl. In general, it is noteworthy that the strengths of the R—H and In—H bonds have the decisive significance for the inhibition mechanism. Table 11.2 contain the Polanyi-Semenov equations for reactions involving  $RH$ ,  $InH$ ,  $RO\cdot$ ,  $RO_2\cdot$ , and  $\dot{In}$ , where  $InH$  is phenol without *tert*-alkyl groups in the ortho-position

(group A) and with two *tert*-alkyl groups in positions 2 and 6 (group B).

Table 11.1. Equations of reaction rate  $v$  and oxygen absorption in time  $\Delta[\text{O}_2](t)$  at different mechanisms of inhibited oxidation

Mechanism	Key reactions	$v$	$\Delta[\text{O}_2](t)$
I	$\dot{r} + \text{RH}(k'_s)$ $\dot{r} + \text{InH}(k'_{31})$	$v_i(1 + k'_{31}[\text{InH}]/k'_s[\text{RH}])^{-1}$	$-(fk'_s[\text{RH}]/k'_{31})\ln(1 - at)$ $a = \frac{k''v_i}{fk'[\text{RH}]} \left( 1 + \frac{k'_{31}[\text{InH}]}{k'_s[\text{RH}]} \right)^{-1}$
II	(8), (31)	$v_i(1 + k'_{31}[\text{InH}]/k'_s[\text{RH}])$	$v_i t - k_8 k_{31}^{-1} [\text{RH}] \ln(1 - t/\tau)$
III	(8), (31)	$v_i k_8 [\text{RH}] / fk_{31} [\text{InH}]$	$\approx k_8 k_{31}^{-1} [\text{RH}] \ln(1 - t/\tau)$
IV	(8), (31), (33), (36)	$2k_8 [\text{RH}]^{3/2} (k_{36} v_i / fk_{31} k_8 [\text{InH}])^{1/2}$	$2v_o \tau (1 - \sqrt{1 - t/\tau})$
V	(8), (31), (-31), (33)	$k_8 [\text{RH}] (k_{31} [\text{ROOH}] v_i / fk_3 k_8 [\text{InH}]^{1/2})$	$\frac{v_o^2 \tau^2}{[\text{ROOH}]_0} (1 - \sqrt{1 - t/\tau})^2 + 2v_o \tau (1 - \sqrt{1 - t/\tau})$
VI	(8), (31), (37)	$k_8 [\text{RH}] (v_i + 2e_{37} k_{37} [\text{ROOH}] [\text{InH}] / fk_{31} [\text{InH}])$	$2v_o \tau (1 - \sqrt{1 - t/\tau})$

VII	(8), (31),	$\frac{k_8[\text{RH}](v_i + 2e_{38}k_{38}[\text{O}_2][\text{InH}]/fk_{31}[\text{InH}])}{2v_o(1-\sqrt{1-t/\tau})}$
VIII	(8), (31), (39)	$k_8[\text{RH}]v_i(1 + 2e_{39})/fk_{31}[\text{InH}] - k_8(k')_{31}^{-1}[\text{RH}]\ln(1-t/\tau)$
IX	(8), (31), (40)	$k_8[\text{RH}](k_{40}v_i/fk_{31}k_8[\text{InH}])^{1/2} 2v_o\tau(1-\sqrt{1-t/\tau})$
X	(6), (32)	$k_6[\text{O}_2]v_i/k'_{31}[\text{Q}] - k_6(k')_{31}^{-1}[\text{O}_2]\ln(1-t/\tau)$
XI	(6), (33), (36)	$k_6[\text{O}_2](k_8[\text{RH}]v_i/fk'_{31}k_8[\text{InH}])^{1/2} 2v_o\tau(1-\sqrt{1-t/\tau})$
XII	(6), (32)	$\frac{k_6[\text{O}_2](k_{31}[\text{ROOH}]v_i/fk'_{31}k_8[\text{Q}])^{1/2}}{[\text{ROOH}]_0} \left(1 - \sqrt{1-t/\tau}\right)^2 + 2v_o\tau(1-\sqrt{1-t/\tau})$

Notes.  $\tau = f[\text{InH}]_0 v_i^{-1}$  is the induction period of inhibited oxidation;  $v_o$  refers to  $t = 0$  when  $[\text{InH}] = [\text{InH}]_0$ .

Table 11.2. Equations for  $[\text{ROOH}] = f([\text{InH}])$  at hydrocarbon oxidation in the non-stationary regime ( $x = [\text{InH}]/[\text{InH}]_0$ )

Mechanism	Key reactions	$[\text{ROOH}]$	$a$
II	(8), (31)	$[\text{InH}]_0[1 - x + a\ln(1/x)]$	$k_8[\text{RH}]/k_{31}[\text{InH}]_0$
III	(8), (31)	$[\text{InH}]_0 a\ln(1/x)$	$k_8[\text{RH}]/k_{31}[\text{InH}]_0$
IV	(8), (31)	$a[\text{InH}]_0^{1/3} (1-\sqrt{x})^{2/3} (9fk_8^2 k_{36}/k_{23}k_{31}k_{33})^{1/3} [\text{RH}]$	
V	(8), (31) (-31), (33)	$a[\text{InH}]_0^{1/3} (1-\sqrt{x})$	$2k_8[\text{RH}](fk_{31}/k_{23}k_{31}k_{33})^{1/2}$
VI	(8), (31) (37)	$[\text{InH}]_0[a\ln(1/x) + b(1-x)]$	$k_8[\text{RH}]/k_{31}[\text{InH}]_0$ $b = 2k_8e_{37}[\text{RH}]/fk_{23}k_{31}$
VII	(8), (31), (38)	$[\text{InH}]_0 a\ln(1/x)$	$k_8[\text{RH}]/k_{31}[\text{InH}]_0$
VIII	(8), (31), (39)	$[\text{InH}]_0 a\ln(1/x)$	$k_8[\text{RH}](1 + 2e_{39})/k_{31}[\text{InH}]_0$
IX	(8), (31), (14)	$a[\text{InH}]_0^{1/3} (1-x)^{2/3} (9fk_8^2 [\text{RH}]^2 k_{40}/k_{23}k_{31}k_{33})^{1/3}$	
X	(6), (31)	$[\text{Q}]_0 a\ln(1/x)$	$k_6[\text{O}_2]/k_{31}[\text{Q}]_0$

$$\text{XI} \quad (6), (31), (8), \quad a[Q]_0^{1/3} (1-x)^{2/3} \left( 9fk_{31}^3 [Q]^2 [RH] / k_{23} k_{31} k_{33} \right)^{1/3} \\ (36)$$

$$\text{XII} \quad (6), (31), (-31), (33) \quad a[Q]_0^{1/2} (1-\sqrt{x}) \quad 2k_6[O_2] / (fk_{31} / k_{23} k_{31} k_{33})^{1/2}$$

#### 11.4.3. Inhibition of oxidation occurring in the regime of chain degenerate-branched reaction

If oxidation is carried out without an initiator, that is, in the autoxidation regime, it occurs with self-acceleration due to the initiation rate increasing during the reaction. It is very important that the temp of acceleration depends on the rate of chain oxidation, *i.e.*, there is a positive feedback between the processes of autoinitiation and chain oxidation of RH. This relationship is also manifested in the inhibition oxidation of organic compounds.

If in the chain initiated reaction when  $v_i = \text{const}$  the induction period is independent of the efficiency of retardation action of the inhibitor but is determined by its concentration, then during autoxidation the inhibitor is more slowly consumed when it more efficiently terminate chains because ROOH is more slowly accumulated and the retardation period increases. Then the initiated oxidation of hydrocarbons is retarded only by compounds terminating chains. Autoxidation is retarded by compounds decomposing hydroperoxides. This decomposition, if it is not accompanied by the formation of free radicals, decreases the concentration of the accumulated hydroperoxide and, hence, the autoxidation rate. Hydroperoxide decomposition is induced by compounds of sulfur, phosphorus and various metal complexes, for example, thiophosphate, thiocarbamates of zinc, nickel, and other metals.

Inhibited autoxidation is often characterized by critical phenomena reasoned by the autocatalytic character of the reaction and mentioned above feedback. Since hydroperoxide decomposes during oxidation, two different regime of inhibited oxidation appear: non-stationary and quasi-stationary with respect to hydroperoxide.

*Non-stationary regime.* For the non-stationary regime of oxidation, hydroperoxide is stable and does not virtually decompose within the induction period. This takes place when the rate constant of decomposition  $k_d < \tau^{-1}$ . Evidently, this regime is related to conditions of inhibited oxidation, as well as to the structure and reactivity of RH, ROOH, and inhibitor. Since the oxidation of RH and consumption of the inhibitor are interrelated, oxygen absorption can be quantitatively related to the consumption of the introduced inhibitor, using the following equations ( $v_{\text{InH}}$  is the rate of InH consumption):

$$v_i = v_{i0} + k_{23}[\text{ROOH}], \quad v_{\text{InH}} = v_i f \quad (11.26)$$

$$v = k_8[\text{RH}][\text{RO}_2\cdot] + k_{31}[\text{InH}][\text{RO}_2\cdot] \quad (11.27)$$

For each mechanism of inhibited oxidation,  $[\text{RO}_2]$  can be related to  $\text{InH}$  and  $\text{ROOH}$ , expressing this relationship mathematically and solving the system of two differential equations, which describe oxygen absorption and inhibitor consumption, and to express the amount of absorbed oxygen through the amount of the consumed inhibitor. For example, in the case of mechanism V when reactions (8), (31), (-31), and (33) are key (see Table 11.1), we obtain

$$\frac{d[\text{ROOH}]}{d[\text{InH}]} = \frac{f v}{v_i} = k_8 [\text{RH}] \left( \frac{fk_{-31}}{k_{23} k_{31} k_{33} [\text{ROOH}][\text{InH}]} \right)^{1/2}$$

$$[\text{ROOH}] = 2 k_8 [\text{RH}] (fk_{-31}/k_{23} k_{31} k_{33})^{1/2} ([\text{InH}]_0^{1/2} - [\text{InH}]^{1/2}) \quad (11.28)$$

For each mechanism this relationship has its intrinsic characteristic form.

Since  $v_{\text{InH}} = v_i/f$  and  $v_i$  increases during oxidation, the kinetics of inhibitor consumption is non-linear. In the initial oxidation period  $v_{\text{InH}} = v_{i0}/f$  and  $v_{\text{InH}}$  increases with the accumulation of hydroperoxide and becomes maximum to the end of the induction period.

*Quasi-stationary regime.* At rather high temperature or in the presence of a catalyst decomposing  $\text{ROOH}$ , hydroperoxide rapidly decomposes, and the quasi-stationary regime of oxidation with respect to hydroperoxide is established in the system when the rate of its decomposition becomes equal to the rate of formation. The concentration of hydroperoxide increases during oxidation because retardation weakens during the consumption of the inhibitor and the rate of  $\text{ROOH}$  formation increases. The necessary condition for the quasi-stationary regime of inhibited oxidation is the following inequality:  $k_{\Sigma\tau} \gg 1$ , where  $k_{\Sigma}$  is the total coefficient of  $\text{ROOH}$  consumption rate *via* all directions: decomposition to radicals, decomposition to molecular products, decomposition under the action of free radicals. The transition from the non-stationary to quasi-stationary regime is associated with the induction period  $\tau$ , which depends on the inhibitor and its concentration. This transition sometimes looks like the sharp exchange of autoxidation regimes and appears in critical phenomena.

*Critical phenomenon* in the inhibited autoxidation of hydrocarbons is expressed in the fact that at some inhibitor concentration, which is named critical  $[\text{InH}]_{\text{cr}}$  the dependence of the induction period on  $[\text{InH}]$  sharply changes, that is,  $d\tau/d[\text{InH}]$  at  $[\text{InH}] > [\text{InH}]_{\text{cr}}$  is much higher than at  $[\text{InH}] < [\text{InH}]_{\text{cr}}$ .

Let us consider mechanism III, key stages (2) and (7). When  $\text{In}\cdot$  does not participate in chain propagation, chains are linearly terminated and the chain length  $v$  is independent of  $v_i$  (see Table 11.1), then

$$v = v/v_i = k_8 [\text{RH}] / fk_{-31} [\text{InH}] \quad (11.29)$$

Consider the case of long chains ( $v \gg 1$ ). When the quasi-stationary regime with

respect to hydroperoxide is achieved, equilibrium is established between the rates of formation and decomposition of ROOH ( $[\text{ROOH}]_s$  is the stationary concentration)

$$v = k_{\Sigma}[\text{ROOH}]_s, v = v_i v, v_i = v_{i0} + k_i[\text{ROOH}]_s \quad (11.30)$$

After insertion and transformation, we obtain ( $\beta = k_i/k_{\Sigma}$ )

$$[\text{ROOH}]_s = \beta v v_{i0} / k_{23}(1 - \beta v) \quad (11.31)$$

It follows from this formula that the quasi-stationary regime is established only when  $\beta v < 1$  and, hence,  $[\text{InH}] > [\text{InH}]_{\text{cr}}$ , where

$$[\text{InH}]_{\text{cr}} = \beta k_8[\text{RH}] / k_{31} \quad (11.32)$$

At  $[\text{InH}] < [\text{InH}]_{\text{cr}}$  the process develops non-stationary in the presence of an inhibitor. The quasi-stationary regime is established in the already developed oxidation when chains terminate in reaction (6) and the equilibrium is achieved

$$\left. \begin{aligned} k_8 k_{17}^{-1/2} ([\text{RH}] v_{i0} + k_{23}[\text{ROOH}])^{1/2} &= k_{\Sigma} [\text{ROOH}]_s \\ [\text{ROOH}]_s &= k_8^2 [\text{RH}]^2 / k_{17} k_{\Sigma} \end{aligned} \right\} \quad (11.33)$$

The induction period of inhibited oxidation of RH at  $[\text{InH}] > [\text{InH}]_{\text{cr}}$  can be defined as the time during which the concentration of the inhibitor decreases from  $[\text{InH}]_0$  to  $[\text{InH}]_{\text{cr}}$

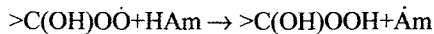
$$\tau = - \int_{[\text{InH}]_0}^{[\text{InH}]} \frac{d[\text{InH}]}{v_i} = \tau_0 [1 - x^{-1} (1 + \ln x)] \quad (11.34)$$

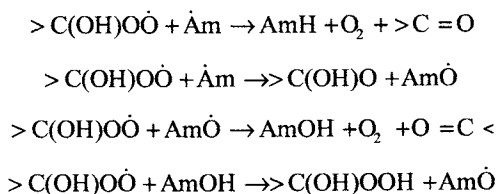
where  $\tau = f[\text{InH}]_0 / v_{i0}$  is the induction period in oxidized RH when  $v_i = v_{i0}$ , and  $x = f k_{31} [\text{InH}]_0 / (\beta k_8 [\text{RH}])$ .

#### 11.4.4. Multiple chain termination on inhibitors of oxidation

In some systems one inhibitor molecule can terminate many chains ( $f \gg 2$ ). This is observed when the starting inhibitor is formed again in the reaction of the active center ( $\text{R}\cdot$  or  $\text{RO}_2\cdot$ ) with the transformation product of the inhibitor ( $\text{In}\cdot$ ) or the inhibitor acts catalytically, transforming active  $\text{RO}_2\cdot$  into the low-active radical.

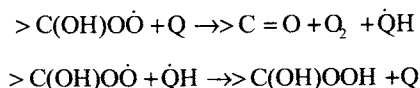
1. In oxidized alcohols (primary and secondary) hydroxyperoxyl radicals are formed, which possess a reductive effect. In the presence of inhibitors (aromatic amines AmH), cyclic reactions of chain termination involving aminyl and nitroxyl radicals appear





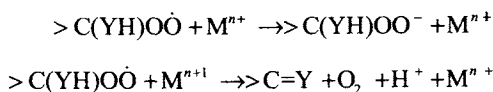
Similar reactions occur when aromatic amines are introduced into oxidized aliphatic amines, whose peroxy radicals also possess the reductive effect.

2. Quinones Q and iminoquinones retard alcohol oxidation entering into cyclic reactions with peroxy radicals

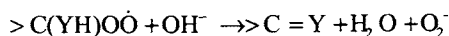


Cyclic termination on quinones is also observed in oxidized polypropylene where  $H_2O_2$  is formed by the decomposition of block hydroperoxyl groups. From  $H_2O_2$  radicals  $HO_2$  are formed by the exchange reaction and reduce quinones to the semi-quinone radical. Similar situation is observed for the oxidation of cyclohexadiene, which involves  $HO_2$  radicals.

3. Salts of variable-valence metals in the oxidation of alcohols and amines are typical negative catalysts ( $f \rightarrow \infty$ )

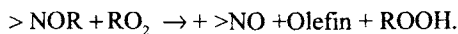


4. Bases are negative catalysts for alcohol oxidation, they transform active  $RO_2$  into inactive  $O_2^-$

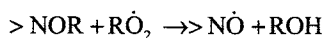


5. Stable nitroxyl radicals ( $>NO\cdot$ ) multiply terminate chains during polymer oxidation, which forms grounds for a high efficiency of sterically hindered amines as photostabilizers. Three mechanisms of cyclic chain termination involving nitroxyl radicals are known:

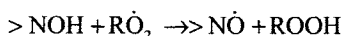
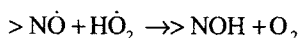
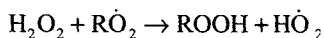
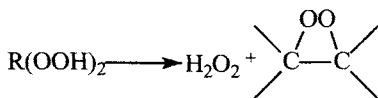
First:  $>NO + R \rightarrow NOR$



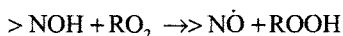
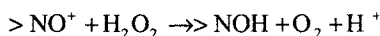
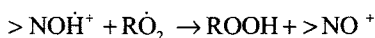
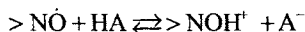
Second:  $>NOR \rightleftharpoons \overline{NO\cdot} + R\cdot \rightarrow NOH + Olefin,$



Third:



6. Intense abstraction of oxidation chains in which the stable nitroxyl radical multiply participates is provided by the three-component system: nitroxyl radical + hydrogen peroxide + acid (HA). Here the acid plays an important role. The mechanism of action is the following (RH-hydrocarbon):



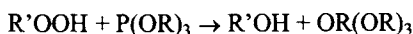
In this system the nitroxyl and acid act as catalysts and  $\text{H}_2\text{O}_2$  is consumed. A similar cyclic mechanism of chain termination takes place when the system alcohol + nitroxyl + acid or the system hydrogen peroxide + quinonimine + acid are introduced into oxidized hydrocarbon.

#### 11.4.5. Inhibitors of oxidation decomposing hydroperoxides

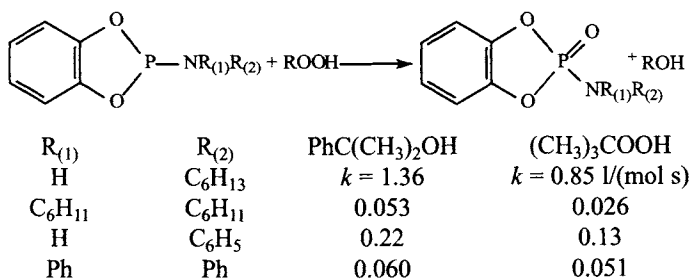
In the autooxidation of organic compounds the main source of free radicals is hydroperoxides formed in the reaction. It follows from this that the autooxidation rate can be retarded if the concentration of hydroperoxide is decreased by its decomposition. It should be kept in mind that two basically different directions of ROOH decomposition are possible: homolytic and heterolytic. The first direction results in the formation of free radicals and, hence, the intensification of homolytic decomposition only accelerates oxidation. By contrast, the heterolytic transformation of ROOH into molecular products (molecular decomposition) decreases the concentration of hydroperoxide and, correspondingly, the rate of its decomposition to radicals.

##### *Organophosphorus inhibitors*

Among various organophosphorus compounds, aryl phosphites found use as inhibitors of oxidation. Phosphites are rather rapidly oxidized by hydroperoxides to phosphates in the reaction



The reaction occurs with stoichiometry 1 : 1. Only sometimes stoichiometry somewhat differs from this ratio. For example, cumyl hydroperoxide oxidizes triphenyl phosphite in the stoichiometric ratio from 1.02 : 1 to 1.07 : 1, depending on the ratio of reactants. The reaction is bimolecular, trialkyl phosphites react with ROOH more rapidly than with aryl phosphites (see Table 11.1), and the activation energy depends on the phosphite structure and changes in an interval from 25 to 77 kJ/mol. The structure of hydroperoxide weakly reflects the rate of its reaction with phosphite, which is seen from the data for the reaction (303 K, C<sub>6</sub>H<sub>5</sub>CN)



The oxidation of phosphite with hydroperoxide is mainly heterolytic. This is indicated by the retention of optical activity in alcohol if hydroperoxide is optically active and in phosphate if phosphite is active. The more polar the solvent, the faster the reaction.

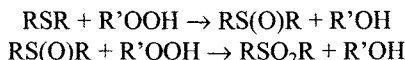
D.G. Pobedimskii showed that the homolytic reaction with the formation of free radicals occurs in parallel with heterolytic transformation. Manifestations of this phenomenon are diverse. The acceptor of free radicals, stable nitroxyl radical, is consumed in the reaction of hydroperoxide with phosphite. This reaction in ethylbenzene in the presence of oxygen is accompanied by chemiluminescence appeared by the disproportionation of peroxy radicals. Chemical polarization of <sup>31</sup>P nuclei was found in the oxidation product of phosphate by the NMR method. It was established that only a minor portion of the product had polarized nuclei. When phosphite is introduced into cumene containing hydroperoxide, the initiating (pro-oxidation) effect caused by radical formation is observed in the initial period. The yield of radicals is very low (0.01-0.02%) in the case of aliphatic phosphates and much higher (to 5%) for aromatic phosphites.

The homolytic reaction of phosphite with ROOH has higher activation energy than that of the heterolytic reaction; therefore, its fraction increases with temperature increasing. Phosphites react not only with hydroperoxides but also with peroxy radicals. Therefore, they are prone, on the one hand, to chain oxidation and, on the other hand, retard the chain oxidation of hydrocarbons and polymers by chain termination.

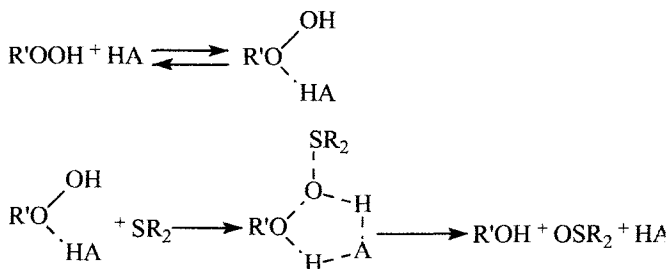
In a neutral solvent alkyl phosphites are oxidized with oxygen *via* the chain route in the presence of an initiator or under irradiation. Chains reach a size of  $10^4$ . The rate of oxygen absorption is proportional to  $v_i^{1/2}$ , which indicates the bimolecular mechanism of chain termination.

### *Sulfur-containing compounds*

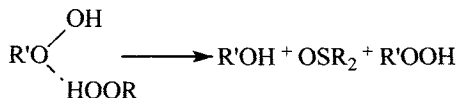
Sulfur-containing compounds are used as components of antioxidative polymer and lubricant additives. The mechanism of their retardation effect was intensively studied in the seventies and turned out to be rather complicated. In this mechanism, the reaction of these compounds with hydroperoxides occupies the central place. In 1945, G. Denison was first to show that dialkyl sulfides are oxidized by hydroperoxides to sulfoxides, the latter are oxidized to sulfones



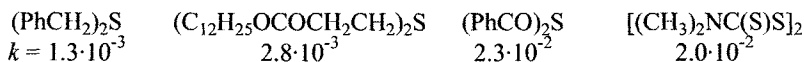
and hydroperoxide is reduced to alcohol. In the presence of alcohols and acids, the reaction is bimolecular, and the catalytic participation of the acid is assumed



In aprotic solvents the reaction rate is  $v = k[\text{R}_2\text{S}][\text{R}'\text{OOH}]^2$ , and the second order with respect to hydroperoxide is related to the fact that the second  $\text{R}'\text{OOH}$  molecule plays the role of acid



In some cases, the first order with respect to both sulfide and hydroperoxide is observed in aprotic solvents. Below we present the rate constants (l/mol s)) of the reaction of cumyl hydroperoxide with several sulfides in chlorobenzene at 353 K.



The detailed study of this reaction showed that it is accompanied by the forma-

tion of free radicals. The body of experimental facts and an analogy with other resembling system result in the following general scheme. Sulfide reacts with ROOH via two parallel reactions: heterolytic (*m*) and homolytic (*i*) generating radicals. In the case of the reaction of dilauryl dithiopropionate with cumyl hydroperoxide, the rate constants of these two reactions in chlorobenzene are the following:

$$k_m = 8 \cdot 10^4 \exp(-50/RT) \text{ l/(mol s)}$$

$$k_i = 2.5 \cdot 10^{14} \exp(-121/RT) \text{ l/(mol s)}$$

The ratio  $k_i/k_m$  is  $5 \cdot 10^{-4}$  at 300 K and increases with the temperature increase because  $E_i > E_m$ .

The reactions of sulfides with ROOH afford the products, which possess the catalytic effect and catalytically decompose hydroperoxides. Acid is the catalyst. This follows from the product composition: cumyl hydroperoxide decomposes to form phenol, and di-*tert*-butyl peroxide, the products of acidic catalytic decomposition, is mainly formed from *tert*-butyl hydroperoxide. Most researchers agree that this intermediate product-catalyst is  $\text{SO}_2$ , which reacts with ROOH as an acid.

As a whole, we can see a rather complicated pattern of the effect of sulfur-containing compounds on the oxidation of hydrocarbons and polymers. The starting compounds, first, reduce ROOH to alcohols and thus decrease the autoinitiation rate during autooxidation; second, free radicals are generated in the reaction with the same ROOH and oxidation is thus initiated; third, chains are slowly terminated in the reaction with  $\text{RO}_2$ . Intermediates of the transformation of sulfides and disulfides play an important role. Sulfenic acid  $\text{RSO}_2\text{H}$  formed by sulfoxide decomposition terminates chains in the reaction with  $\text{RO}_2$  but, along with this, initiates them in the reaction with ROOH. Acidic products ( $\text{SO}_2$ ,  $\text{H}_2\text{SO}_4$ ,  $\text{RSO}_2\text{H}$ ,  $\text{RSO}_3\text{H}$ ) decompose hydroperoxides predominantly to molecular products, *i.e.*, decrease autoinitiation. Along with this, they have an initiating effect decomposing ROOH to form radicals. In the oxidation of alkylaromatic compounds, the acidic decomposition of ROOH is accompanied by the formation of phenols, which terminate chains as inhibitors.

Metal complexes, first of all, dialkyl dithiophosphates and dialkyl dithiocarbamates of such metals as Zn, Ni, Ba, and Ca, are widely used for the stabilization of polymers and lubricants. Inhibitors of this type are inferior to phenols in efficiency at moderate temperatures (350–400 K) but exceed them at higher temperatures (430–480 K). The mechanism of action of inhibitors of this type is complicated. The reaction of these inhibitors with hydroperoxide plays a very important role in the complex mechanism of inhibition.

#### 11.4.6. Synergism of action of oxidation inhibitors

The mechanisms of action of inhibitors on the oxidation of organic compounds

are diverse. Inhibitors terminate chains in reactions with  $\text{RO}\cdot_2$  or  $\text{R}\cdot$ . The radicals formed from them are inactive or participate in chain termination by the reactions with  $\text{ROOH}$  or  $\text{RH}$ ; in several cases, cyclic reactions of chain termination appear. An inhibitor can reduce hydroperoxide or catalytically decompose it. Therefore, the introduction of two or more inhibitors into the oxidized hydrocarbon (or another compound) results in the appearance of different mechanisms of their mutual retardation effect.

All cases of retardation by mixtures of inhibitors can be reduced in their effect on the oxidation process to the following three ones: *additive effect* when the retardation effect of a mixture is equal to the sum of retardation effects of each component, *antagonism* when inhibitors impede each other, and *synergism* when the effect of a mixture is greater than the sum of retardation effects of the components.

The method for comparison of the retardation effect of various inhibitors and their mixtures from the duration of the retarding action, induction period, has been formed in laboratory practice long ago. The induction period is equal to the time period from the beginning of experiment to the moment of absorption of a certain amount of dioxygen or achievement of a certain well-measured oxidation rate. Therefore, three different cases of inhibitor effect on the autooxidation of  $\text{RH}$  can be expressed by the following inequalities ( $\tau$  is the induction period of the introduced mixture of inhibitors):

$$\begin{array}{l} \text{Synergism} \\ \tau_{\Sigma} > \sum_i \tau_i \end{array}$$

$$\begin{array}{l} \text{Additivity} \\ \tau_{\Sigma} = \sum_i \tau_i \end{array}$$

$$\begin{array}{l} \text{Antagonism} \\ \tau_{\Sigma} < \sum_i \tau_i \end{array}$$

Accepting the character of interaction of inhibitors and products formed from them, which results in synergism, as a basis, we can group the studied systems as follows.

1. One inhibitor terminates chains, and the second one decreases the autoinitiation rate decomposing  $\text{ROOH}$  or deactivating the catalyst, which destructs  $\text{ROOH}$  to radicals.
2. Two initial compounds (inhibitors or non-inhibitors) react to form an efficient inhibitor.
3. Intermediate products of inhibitor transformation interact and enhance the retardation effect of one on another.

The combined introduction of an inhibitor, which terminates chains, and a substance, which decomposes hydroperoxides, is widely used for the more efficient retardation of oxidation processes in polyolefins, resins, lubricants, and other materials. Various phenols, bisphenols, and aromatic amines are applied as an acceptor of  $\text{RO}\cdot_2$ , and aryl phosphites, esters of thiopropionic acid, dialkyl dithiopropionates and thiophosphates of zinc and nickel, and other similar compounds are introduced to

decompose ROOH. The induction period of the oxidized substrate is usually measured when mixtures of inhibitors with different ratios of components is introduced, and the ratio, which induces the longest retardation is determined.

The introduction of substance  $S$ , which decomposes ROOH, into the oxidized RH, naturally, decreases the current concentration of ROOH. This does not reflect the oxidation rate if the radical source is an initiator, which does not interact with  $S$ , light, or radiation, but results in the retardation of autoinitiated oxidation when the main radical source is hydroperoxide. The initial stage of autooxidation in the absence of the acceptor  $RO\cdot_2$  is described by the parabolic time law  $\Delta[O_2]^{1/2} = bt$ , where  $b = 0.5k_8 k_{23}^{1/2} k_{17}^{1/2} [RH]$ . The introduction of  $S$  changes the situation: a discrepancy between the absorbed dioxygen and  $[ROOH]$  appears from the very beginning due to the decomposition of ROOH. If  $S$  decomposes hydroperoxide only *via* the molecular route in the bimolecular reaction with the rate  $v_{ROOH} = k_S [ROOH][S]$ , and the decay of one  $S$  molecule results in the decay of  $f_S$  molecules of ROOH, then the rate of ROOH accumulation is the following:

$$d[ROOH]/dt = a[RH](v_{i0} + k_{23}[ROOH])^{1/2} - (k_{\Sigma} + k_S[S])[ROOH] \quad (11.35)$$

During the very intensive decomposition of hydroperoxide, the quasi-stationary oxidation regime with the quasi-stationary concentration  $[ROOH]_S$  is established within the time  $t \sim (k_S[S]_0)^{-1}$

$$[ROOH]_S = \frac{a^2 k_{23} [RH]^2}{2(k_{\Sigma} + k_S [S])} \left\{ 1 + \left[ 1 + \frac{4v_{i0}(k_{\Sigma} + k_S [S])^2}{a^2 k_{23}^2 [RH]^2} \right]^{1/2} \right\} \quad (11.36)$$

The rate of chain initiation  $v_{i0}$  is usually very low, so that

$$[ROOH]_S \approx \frac{a^2 k_{23} [RH]^2}{(k_{\Sigma} + k_S [S])^2} \approx k_{23} \left( \frac{a[RH]}{k_S [S]} \right)^2 \quad (11.37)$$

if the  $S$  inhibitor is introduced in such high concentration that  $k[S] \gg k_{\Sigma}$ . The induction period caused by the introduction of  $S$ , if it is determined as the time within which  $S$  decreases to the concentration  $[S]_r = k_{\Sigma}/k_S$ , is the following:

$$\tau_S = \int_0^{k_{\Sigma}/k_S} \frac{d[S]}{v_S} = \frac{f_S k_S}{2a^2 k_{23} k_S [RH]^2} \left\{ \left( \frac{k_S [S]_0}{k_{\Sigma}} \right)^2 + \frac{4k_S [S]_0}{k_{\Sigma}} + 2 \ln \frac{k_S [S]_0}{k_{\Sigma}} \right\} \quad (11.38)$$

When the inhibitor is introduced in the concentration  $[S]_0 \gg k_{\Sigma}/k_S$ , the expression is simplified

$$\tau_S \approx f_S k_S [S]_0^2 / 2 a^2 k_{23} k_\Sigma [RH]^2 \quad (11.39)$$

In this case, the higher  $k_S$  and  $f_S$  and  $\tau \sim [S]_0^2$ , the longer the retardation period. Evidently, the retardation of oxidation with the introduction of  $S$  appears when a sufficiently high concentration is introduced:  $[S]_0 > k_\Sigma/k_S$ . If the decomposition of ROOH by the inhibitor  $S$  occurs so rapidly that  $[ROOH]_S < v_{io}/k_{23}$ , then during the induction period the amount of formed (and decomposed) during the induction period ROOH is equal to  $v v_{io}$ , and the induction period is  $\tau_S = f_S [S]_0 / v_{io}$ . Thus, even in this most favorable regime  $S$  is consumed in  $v$  times more rapidly than free radicals are generated. Remind for comparison that the highly efficient acceptor  $RO_2$  is consumed, under similar conditions, with the rate  $v_{io}/f$  and  $\tau_o = f[InH]_0/v_{io}$ .

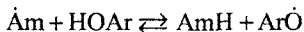
It follows from this that the inhibitor  $S$  retards oxidation if it proceeds through the chain route ( $v > 1$ ) and the main initiating agent is hydroperoxide that formed ( $k_{23}[ROOH] > v_{io}$ ). The noticeable retardation of oxidation is observed if such an amount of the inhibitor is introduced when  $k_S > k_\Sigma$ . There is one more substantial circumstance. Almost all substances reacting with ROOH decompose it both heterolytically (constant  $k_S$ ) and homolytically (constant  $k_{Si}$ ). The retarding rather than initiating effect of  $S$  is manifested when

$$\beta_S = k_{Si}/k_S \ll k_{23}/k_S = \beta$$

i.e., the fraction of homolysis of ROOH in the reaction with  $S$  is much smaller than that of its spontaneous homolysis under oxidation conditions.

#### *Synergism caused by interaction of intermediate products of inhibitors*

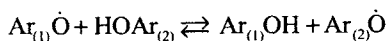
Synergism is observed when binary mixtures of some phenols and aromatic amines are introduced into hydrocarbon. It is related to the interaction of inhibitors and radicals formed from them. For the combined introduction of phenyl-N- $\beta$ -naphthylamine and 2,6-di-*tert*-butylphenol into oxidized ethylbenzene ( $v_i = \text{const}$ , 343 K), phenol is consumed first, and amine begins to consume only after its disappearance, although  $RO_2$  reacts with amine more rapidly ( $k_{31} = 1.3 \cdot 10^5$  l/(mol s), 333 K) than with phenol ( $k_{31} = 1.3 \cdot 10^4$  l/(mol s), 333 K). This phenomenon is caused by the equilibrium



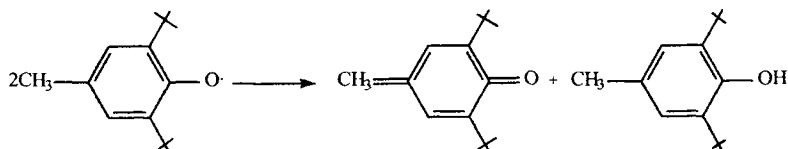
It is shifted to the right, if  $D_{N-H} > D_{O-H}$ . For example, the equilibrium constant of the reaction of the diphenylaminy radical with 2,4,6-tri-*tert*-butylphenol in  $CCl_4$  at 348 K is equal to  $(5 \pm 1) \cdot 10^3$ . In the general case,  $-RT \ln K = \Delta H = D_{O-H} - D_{N-H}$ . For the combined introduction of amine and phenol, this equilibrium decreases the concentration of aminyl radicals if  $D_{O-H} < D_{N-H}$ . It is assumed that the aminyl radicals propagate the chain in the reaction with RH, and sterically hindered phenoxyls formed from phenol do not participate in chain propagation and decay only in the

reaction with  $\text{RO}_2$ , which results in synergism during the autoxidation of hydrocarbon.

Synergism was observed for the combined introduction of two phenols, one of which is necessarily 2,6-di-*tert*-butylphenol. The initiated oxidation of 9,10-dihydroanthracene is not almost retarded by 2,4,6-tri-*tert*-butylphenol ( $10^{-4}$  mol/l at 333 K) but *p*-methoxyphenol in the same concentration retards oxidation. The induction period is doubled if both phenols are introduced in the same concentration, that is, both phenols participate in chain termination if they are introduced in combination. This is explained by the exchange reaction



One more mechanism of synergic interaction of phenols has recently been discovered by V.A. Roginskii when he studied the disproportionation of phenoxyl radicals. Phenoxyl radicals disproportionate if contain C—H groups in the *ortho*- or *para*-position, for example, 2,4,6-tri-*tert*-butylphenoxyl does not disproportionate and the ionol radicals enter into the reaction



The study of cross-disproportionation of phenol radicals of ionols and  $\alpha$ -tocopherol allowed one to establish that this reaction is much faster than homodisproportionation

	Ionol	$\alpha$ -Tocopherol	Ionol + $\alpha$ -tocopherol
$2k_{\text{disp}}, \text{ l}/(\text{mol s}) (323 \text{ K})$	$8.7 \cdot 10^3$	$2.2 \cdot 10^3$	$1.8 \cdot 10^5$

In this reaction tocopherol is regenerated due to phenoxyl of ionol.

As a result, fast cross-disproportionation decreases the total concentration of the phenoxyl radicals and participation of phenoxyls in chain propagation and reduces the most active phenol (tocopherol more rapidly reacts with  $\text{RO}_2$  than ionol); the methylenequinone that formed, in turn, terminates chains in the reaction with  $\text{RO}_2$ .

#### *Synergism caused by interaction of initial reactants*

The cases when the initial substances (inhibitors or non-inhibitors) interact to form labile or stable products, inhibitors, are rather abundant. Very often one of these substances is an inhibitor, so that this interaction results in the more efficient retardation, *i.e.*, synergetic effect.

As we convinced, phosphites retard oxidation by the reduction of ROOH to ROH. Compounds of variable-valence metals, on the contrary, catalyze oxidation decomposing ROOH to free radicals. Under some conditions, binary mixtures of phosphites (triethyl phosphite, triphenyl phosphite, various aryl phosphites) with metal complexes ( $\text{Cu}^+$ ,  $\text{Co}^{2+}$ ,  $\text{Ni}^{2+}$ ,  $\text{Fe}^{2+}$ , and others) efficiently catalyze the oxidation of hydrocarbons and polymers. This is due to the formation of complexes between the metal salt and phosphite, which react very actively with  $\text{RO}\cdot_2$  to terminate oxidation chains. For example, chain termination in oxidized styrene at 293 K is characterized for phosphites  $(\text{RO})_3\text{P}$  and their complexes with CuCl by the following parameters:

Phosphite	$k_{31}$ , l/(mol s)	$f$
$\text{P}(\text{OPh})_3$		Does not react
$\text{Cu}[\text{POPh}_3]\text{Cl}$	$6 \cdot 10^4$	3.0
$[2\text{-C}(\text{CH}_3)_3, 4\text{-CH}_3\text{C}_6\text{H}_3\text{O}]_3\text{P}\cdot\text{CuCl}$	$5 \cdot 10^4$	0.06
$[2\text{-C}(\text{CH}_3)_3, 4\text{-CH}_3\text{C}_6\text{H}_3\text{O}]_3\text{P}\cdot\text{CuCl}$	$3.4 \cdot 10^5$	1.4
$2[2\text{-C}(\text{CH}_3)_3, 4\text{-CH}_3\text{C}_6\text{H}_3\text{O}]_3\text{P}\cdot\text{CuCl}$	$4.8 \cdot 10^5$	0.9

It is seen that the complex reacts much more vigorously with  $\text{RO}\cdot_2$  than the ligand (phosphite) and with the higher coefficient  $f$ . Along with  $\text{RO}\cdot_2$ , these complexes react rapidly with ROOH to transform it predominantly into molecular products.

### Chain branched reactions

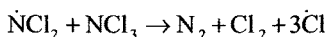
Chain branched reactions have several substantial distinctions from chain non-branched reactions. The mechanism of these reactions was discovered by N.N. Semenov with coworkers and by S. Hinshelwood with coworkers in 1925-1928. N. N. Semenov, Yu.B. Khariton, and Z.F. Volta. Studied the conditions of ignition of phosphor vapors and established that the transition from the absence of the reaction to the blowback of vapor occurs at a rigidly specified oxygen pressure, which depends on the diameter of the vessel. In 1928 Semenov proposed the chain branched mechanism of the process involving oxygen atoms.

In the twenties S. Hinshelwood studied the oxidation of hydrogen by oxygen. This reaction is also characterized by limits on pressure (lowest and upper) within which the mixture ignites. In 1928 Hinshelwood proposed the chain branched scheme of the process where excited water and oxygen molecules perform branching. The detailed study of the reaction of hydrogen with oxygen in Hinshelwood's and Semenov's laboratories allowed the authors to develop and substantiate the mechanism of this chain branched reaction involving hydrogen and oxygen atoms and hydroxyl radicals. Investigations of V.N. Kondrat'ev played an important role in the development of the theory of branched chain reactions. He found the hydroxyl radical in burning dihydrogen and studied its behavior and reactivity.

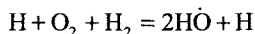
#### *12.1. Theory of chain branched reaction*

The chain radical reaction takes place if reactants are transformed through active intermediate species, viz., atoms and radicals, and reactions involving them form the closed cycle of transformations, and chain propagation occurs more rapidly than termination. The chain reaction is branched if it contains such a stage in which one radical or atom generates the formation of several atoms and radicals. As a result, under favorable conditions during the reaction the concentration of active centers increases and, correspondingly, the reaction rate increases. This often results in ignition or explosion. If branching occurs due to the interaction of an atom (radical) with a molecule, 3 particles with an unpaired electron (in the general case,  $2n + 1$ ) are formed from one particle owing to the conservation of the number of electrons in the system. An increase in the number of particles can occur in one stage; for example, in the

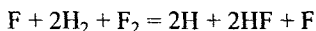
chain reaction of  $\text{NCl}_3$  decomposition it occurs according to the scheme



This act is exothermic ( $\Delta H = -146$  kJ/mol), although 3 chlorine atoms are formed in it instead of one  $\cdot\text{NCl}_2$  radical. For hydrogen burning, branching proceeds in two successive acts (see Section 14.3) according to the empirical equation



Such a stoichiometric branching reaction is endothermic, its  $\Delta H = +79$  kJ/mol. In the chain reaction of dihydrogen with fluorine branching proceeds through three successive stages (see below) according to the empirical equation



and is accompanied by the heat liberation ( $\Delta H = -102$  kJ/mol). All known chain branched reactions are exothermic.

Stoichiometric equation	$-\Delta H$ , kJ/mol
$2\text{H}_2 + \text{O}_2 = 2\text{H}_2\text{O}$ ,	484
$2\text{CO} + \text{O}_2 = 2\text{CO}_2$	566
$\text{P}_4 + 5\text{O}_2 = \text{P}_4\text{O}_{10}$	3067
$\text{H}_2 + \text{F}_2 = 2\text{HF}$	537

Critical, or limiting phenomena are an important kinetic peculiarity of branched chain reactions, which distinguishes them from other reactions, including chain. Systems, which are transformed by the mechanism of chain branched reactions, are characterized by conditions when the reaction occurs very slowly and conditions when the reactions occurs rapidly, often with explosion. The transition from one regime to another occurs with an insignificant change in the conditions in the region of their critical value. For example, phosphor vapors at the unchanged  $[\text{P}_4] : [\text{O}_2]$  ratio react with dioxygen in the region of  $p$  pressure, which is between two limiting pressures  $p_1$  and  $p_2$ :  $p_1 < p < p_2$ . At  $p < p_1$  and  $p > p_2$  phosphor vapors do not react with dioxygen. The ignition region also depends on the composition of the mixture, so that the critical condition of ignition is described by the equation ( $C_1$  and  $C_2$  are constants)

$$C_1 + C_2[\text{O}_2]^2 + [\text{O}_2][\text{P}_4] = 0 \quad (12.1)$$

The region of development of chain branched reaction is temperature-dependent. At an unchanged composition of the mixture and  $p = \text{const}$ , there is a temperature above which the fast reaction is observed and below which the reaction does not occur. In the  $p - T$  coordinates the ignition region for the chain branched reaction looks like a peninsula with a cape ( $T_{\min}$ ), so that at  $T < T_{\min}$  the reaction does not

occur at any pressure in the system. The limiting phenomena are explained by the general theory of chain branched reactions.

In the chain non-branched reaction the concentration of active centers  $n$  depends only on the initiation ( $v_i$ ) and termination rates ( $v_t = gn$ , where  $g$  is the specific rate of chain termination in the presence of an inhibitor  $\text{InH}$ ,  $g = k_{\text{InH}}[\text{InH}]$ ), in the quasi-stationary regime  $n = v_i/g$ .

The situation is basically different for the chain branched reaction. Branching acts provide a possibility for progressive increasing the concentration of active centers in time. For chain termination and branching in the reaction of a first order with the specific rates  $g$  and  $f$ , respectively, the rate of changing the concentration of active centers  $n$  is described by the equation

$$dn/dt = v_i - (g - f)n \quad (12.2)$$

Two basically different regimes of the reaction are possible. Quasi-stationary, when  $g > f$ , i.e., termination predominates over branching; then  $n = v_i/(g - f) = \text{const}$ , beginning from  $t \geq (g - f)^{-1}$ ; and non-stationary, when  $f > g$ , i.e., branching predominates. In this case, the concentration of active centers continuously increases in time, and if the consumption of reactants and changes in time of  $v_i$ ,  $g$ , and  $f$  are ignored, then

$$n = v_i(f - g)^{-1}(e^{(f - g)t} - 1)$$

The equality  $f = g$  is the critical condition for the transition of the system from one state to another. Thus, the chain reaction with branching occurs as a self-accelerating process only when active centers enter into branching acts more rapidly than into termination acts.

#### *Ignition limits with respect to pressure*

At a low pressure in the reactor, active centers rapidly reach the reactor wall, are adsorbed on it, and recombine: chains terminate on the wall. If the probability of recombination on the wall is low ( $\epsilon \ll 1$ ), then chain termination occurs after multiple collisions of the active center with the surface and is not limited by their diffusion to the surface. In this case, the concentration of active centers is the same in the bulk of the whole volume, and the rate of chain termination is the following:

$$v_t = gn = 250(S/V)\bar{u}\epsilon n \quad (12.3)$$

where  $S$  and  $V$  are the surface and volume of the reactor, respectively; and  $\bar{u}$  is the mean thermal velocity of particles movement.

Chain branching usually occurs in the reaction of the active center with the molecule with the rate

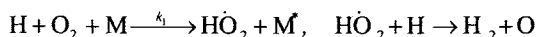
$$v_f = k_f [\text{reactant}] n = 10^{-3} k_f p (RT)^{-1} n$$

where  $\gamma p$  is the partial pressure of the reactant.

The critical transition is observed when the equality  $f = g$  or  $v_f = v_t$  is fulfilled, from which the expression for the lowest critical pressure follows

$$p_1 = 10^3 g RT / \gamma k_f \quad (12.4)$$

This pressure can be achieved by either changing the concentration of reactants or the introduction of an inert gas because this is the total pressure of the mixture. An increase in the pressure results in the situation when active centers decay more often by the triple collision of the active center with two particles, due to which the chain terminates. For example, for hydrogen oxidation the chain terminates in the reaction (M is the third particle)



In this case, the rate of chain termination is

$$v_t = 2 \cdot 10^3 k_t \gamma p^2 (RT)^{-2} n$$

The critical condition  $v_f = v_t$  results in the upper limit with respect to pressure

$$p_2 = 10^{-3} k_f RT / 2 k_t \quad (12.5)$$

#### *Temperature dependence of the ignition region*

Since  $k_f$  depends on temperature according to the exponential law  $\exp(-E_f/RT)$  and the frequency of triple collisions is  $z \sim u^2 \sim T$ , then

$$p_2 = p_2^0 \exp(-E_f / RT)$$

increases with temperature increasing. On the contrary,  $p_1$  decreases with the temperature increase because always  $E_g < E_f$  and

$$p_1 = p_1^0 \exp(E_f - E_g) / RT$$

Due to this opposite temperature run, both limits converge at the temperature  $T_M$  ("cape of the ignition peninsula," Fig. 12.1) when  $p_1 = p_2$ . This temperature is determined by the equality

$$T_M = (2 E_f - E_g) / [R \ln(p_2^0 / p_1^0)] \quad (12.6)$$

At  $T < T_M$  the chain branched reaction does not occur, that is,  $T_M$  is the critical temperature below which chain ignition is impossible. At  $T > T_M$  chains terminate on the surface and in the bulk more rapidly than branching and, therefore, the progres-

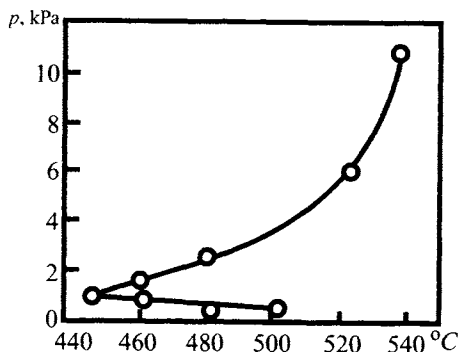


Fig. 12.1. Ignition peninsula of the stoichiometric mixture of dihydrogen and dioxygen.

sive development of the reaction is impossible.

#### *Critical sizes of the reactor*

If chain termination on the wall occurs rather efficiently ( $\epsilon \sim 1$ ), then near the lowest limit with respect to pressure chain termination is limited by the diffusion of active centers to the surface. In these cases, the critical condition depends on the competition of two processes: effective collision of the active center with the reactant followed by chain branching and collision of the active center with the wall with chain termination. This

process produces a gradient of the concentration of active centers over the reactor cross section: the closer to the surface, the lower the concentration of active centers. The rigid solution to this problem can be obtained in the framework of the diffusion equation. For the cylindrical reactor, the solution of this equation results in the expression  $p_1 = 23Dd^2$ , where  $d$  is the diameter of the vessel. Since in gas the diffusion coefficient is  $D = D_0 p^{-1}$ , the critical condition  $g = f$  takes the form

$$k_f f p_1 (RT)^{-1} = 23 D_0 RT d^{-2} p_1^{-1}$$

and for the lowest limit with respect to pressure we obtain the expression

$$p_1 = RT/d \left( 23 D_0 / \gamma k_f \right)^{2/3} \quad (12.7)$$

It follows from this formula that a critical size (diameter) of the reaction vessel also exists: chain ignition is observed in a large reactor, and it is not in a small reactor. As in the case of chain termination in the kinetic regime, critical conditions depend on the shape of the vessel (for a planar vessel  $g = 9.9DRTd^{-1}$ , for a spherical vessel  $g = 39.5DRTd^{-1}$ ).

#### *Kinetics of the branched chain reaction*

In the stationary regime where  $g > f$ , the kinetics of the branched chain reaction resembles the kinetics of the non-branched chain reaction and

$$v = k_p[RH]n = a_p n = [a_p v / (g - f)](1 - e^{-(g-f)t}) \approx a_p v_i / (g - f) \quad (12.8)$$

The chain branched reaction in the non-stationary regime occurs in a different manner. In this case,  $f > g$  and the concentration of active centers continuously

increases during the reaction, the rate of the process increases similarly

$$v = a_p n = (v_i a_p / \varphi)(e^{gt} - 1) \approx (v_i a_p / f) e^{*t} \quad (12.9)$$

where  $\varphi = f - g$ .

In the region of the lowest limit of pressure, the diffusion of a particle to the vessel surface occurs for  $10^{-1}$ - $10^{-3}$  s, that is,  $g$  is  $10^2$  to  $10^4$  s $^{-1}$ , respectively; in the non-stationary regime, we can accept the range of  $f$  values is  $10$ - $10^3$  s $^{-1}$ ; therefore, the process develops in time very rapidly.

Since the reaction proceeds with autoacceleration and its occurrence can be noticed experimentally only when some rate  $v = v_{\min}$  is achieved, the induction period  $\tau$  is observed, which can be determined as the time of achievement of  $v = v_{\min}$ , and since  $v$  is expressed by equation (12.9), then  $\tau = \varphi^{-1} \ln(v_{\min}/\text{const})$ , where  $\text{const} = a_p v_i \varphi^{-1}$ . It follows from this that  $\tau \varphi = \text{const}$ . On the other hand, the limits of chain ignition  $p_1$  and  $p_2$  are the roots of the equation  $\varphi = 0$  and, hence,  $\varphi$  can be expressed through  $p_1$  and  $p_2$  in the form  $\varphi = \text{const}(p - p_1)(p_2 - p)$ . From this we can obtain a relationship between the induction period and  $p_1$  and  $p_2$

$$\tau_u = \text{const}/[(p - p_1)(p_2 - p_1)] \quad (12.10)$$

As we will see, experimental data on hydrogen combustion agree well with these correlations.

At the first sight, it follows from formulas (12.2) and (12.9) that the concentration of active centers and reaction rate should continuously increase in the course of the reaction. In fact, this is not the case because of the consumption of the starting reactants. Since both the branching rate and the overall rate of the chain process depend on the concentration of reactants, the ratio between the branching and termination factors changes during the reaction. Since  $\gamma \sim [\text{reactant}] \sim (1 - \eta)$ , where  $\eta$  is the conversion, and  $g$  is independent of  $\eta$ , then such a moment takes place in the reaction course when  $\gamma = \gamma_0(1 - \eta)$  becomes equal to  $g$  and then the reaction transits to the quasi-stationary regime after all centers are consumed. The presence of the critical (limiting) depth of oxidation is characteristic of the chain branched reaction, as well as other critical phenomena. These questions will be considered in more detail for the reaction  $\text{H}_2 + \text{O}_2$ .

## 12.2. Combustion of hydrogen

Combustion of hydrogen is a model reaction, which allowed the detailed study of the mechanism of the chain branched process. The scheme-minimum and  $A$  and  $E$  values for the elementary reaction are presented in Table 12.1, from which it follows that chain branching occurs in reactions (2) and (3), and step (2) is limiting (for

numeration of steps, see Chapter 11). Chain termination occurs either on the wall (which predominates at low pressures) or in the bulk. Using the method of quasi-stationary concentrations to obtain the approximate solution, we assume  $d[\dot{\text{O}}\text{H}]/dt = d[\text{O}]/dt = 0$ . The kinetics of changing the concentration of hydrogen atoms in the reaction is described by the equation

$$d[\text{H}]/dt = v_i + \varphi[\text{H}] \quad (12.11)$$

where  $\varphi = 2k_2[\text{O}_2] - k_4 - k_5[\text{O}_2][\text{M}]$ .

The critical condition separating the stationary and non-stationary regimes has the form

$$2k_2[\text{O}_2] = k_4 + k_5[\text{O}_2][\text{M}] \quad (12.12)$$

Table 12.1. Rate constants of elementary steps of dihydrogen combustion

No.	Reaction	$A$ , $\text{l}/(\text{mol s})$ or $\text{l}^2/(\text{mol}^2 \text{s})$	$E$ , $\text{kJ/mol}$
0	$\text{H}_2 + \text{O}_2 \xrightarrow{k_0} 2\dot{\text{O}}\text{H}$	$2.5 \cdot 10^9$	163
1	$\text{H}_2 + \dot{\text{O}}\text{H} \xrightarrow{k_1} \text{H}_2\text{O} + \text{H}$	$2.2 \cdot 10^{10}$	22
2	$\dot{\text{H}} + \text{O}_2 \xrightarrow{k_2} \dot{\text{O}}\text{H} + \text{O}$	$1.5 \cdot 10^{11}$	70
3	$\text{H}_2 + \text{O} \xrightarrow{k_3} \text{H}\dot{\text{O}} + \dot{\text{H}}$	$2.5 \cdot 10^{10}$	41
4	$\dot{\text{H}} + \text{wall} \xrightarrow{k_4} 0.5\text{H}_2$	—	—
5	$\dot{\text{H}} + \text{O}_2 + \text{M} \xrightarrow{k_5} \text{H}\dot{\text{O}}_2 + \text{M}$	$3.6 \cdot 10^9$	0
6	$\dot{\text{H}} + \text{H}_2\text{O} \xrightarrow{k_6} \text{H}_2 + \dot{\text{O}}\text{H}$	$9.910^{10}$	85
7	$2\dot{\text{H}} + \text{M} \xrightarrow{k_7} \text{H}_2 + \text{M}$	$3.6 \cdot 10^9$	0
8	$2\text{H}\dot{\text{O}}_2 \xrightarrow{k_8} \text{H}_2\text{O}_2 + \text{O}_2$	$10^{10}$	0
9	$\text{H}_2\text{O}_2 + \text{M} \xrightarrow{k_9} 2\text{OH} + \text{M}$	$7.4 \cdot 10^{14}$	196
10	$2\dot{\text{O}}\text{H} + \text{M} \xrightarrow{k_{10}} \text{H}_2\text{O}_2 + \text{M}$	$1.1 \cdot 10^{10}$	-8
11	$\dot{\text{H}} + \text{H}_2\text{O}_2 \xrightarrow{k_{11}} \text{H}_2\text{O} + \dot{\text{O}}\text{H}$	$4.2 \cdot 10^{11}$	38

#### *Lowest ignition limit*

At a low pressure  $k_4 \gg k_5[\text{O}_2][\text{M}]$  and the critical condition takes the form  $2k_2[\text{O}_2] = k_4$  (chain termination in the kinetic region) and  $p_1 = k_4/(2k_2\gamma_{\text{O}_2})$ , where  $\gamma_{\text{O}_2} = [\text{O}_2]/p$ . For the diffusion regime of chain termination, the critical condition for the lowest limit is the following:

$$2k_2[\text{O}_2] = 23D_0/(d^2p) \quad (D = D_0 \text{ with } p = p_0 = 1)$$

and for the cylindrical vessel

$$p_1 = (23D_0)^{1/2}(2k_2\gamma_{\text{O}_2}d^2)^{-1/2}$$

#### *Upper ignition limit*

At a sufficiently high pressure  $k_5[\text{O}_2][\text{M}] \gg k_4$ , and the critical condition is  $2k_2[\text{O}_2] = k_5[\text{O}_2][\text{M}]$  or  $p_2 = 2k_2/k_5$ .

The non-stationary regime is possible if the inequality is fulfilled in the kinetic region:  $k_4 < 2k_2[\text{O}_2]$ ,  $k_5[\text{M}] < 2k_2$ , or  $k_4 < 2k_2\gamma_{\text{O}_2}^{-1}p$ ,  $k_5p < 2k_2$ ; in the diffusion region

$$23D_0d^{-2}p^{-1} < 2k_2[\text{O}_2] > k_5[\text{O}_2][\text{M}]$$

or

$$23D_0d^{-2}p^{-1} < 2k_2\alpha'p > k_5a'p^2$$

Since  $k_2$  is strongly temperature-dependent ( $E_2 = 71$  kJ/mol), the region in which the reaction occurs in the non-stationary regime represents in the  $p$ - $T$  coordinates the "ignition peninsula" (see Fig. 12.1).

In the developed chain branched reaction of dihydrogen oxidation, hydrogen and oxygen atoms,  $\text{HO}\cdot$  and  $\text{HO}_2\cdot$  radicals are formed in non-equilibrium concentrations. Therefore, the works on experimental detection of these species were of great significance. The formation of atomic hydrogen was proved by warming of a thermocouple immersed into a reactor where the reaction of dihydrogen oxidation took place. When the capillary of the thermocouple is covered with a composition, for example,  $\text{ZnO} \cdot \text{Cr}_2\text{O}_3$ , on the surface of which hydrogen atoms rapidly recombine, it is warmed much more strongly than the capillary, whose surface is rather inert toward atomic hydrogen. Hydroxyl was detected in the hydrogen flame using the method of linear absorption developed in the thirties by V.N. Kondratiev. With the development of ESR, this method allowed the proof of the formation of hydrogen atoms, hydroxyl radicals, and  $\text{HO}_2\cdot$  radicals during hydrogen combustion.

In the non-stationary regime, *i.e.*, inside the "ignition peninsula," the reaction proceeds with self-acceleration. Near the lowest ignition limit  $p_1$  in the kinetic regime of chain termination on the wall and a small depth, the reaction kinetics is described in the first approximation by the system of only two differential equations

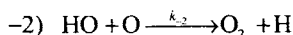
$$\begin{aligned} d[\text{H}]/dt &= v_i + 2k_2[\text{O}_2][\text{H}] - k_4[\text{H}] \\ -d[\text{O}_2]/dt &= v_i + k_2[\text{O}_2][\text{H}] \end{aligned}$$

This assumes the quasi-stationary regime respectively to the O and  $\text{HO}\cdot$  species. Beginning from the moment  $t'$ , chain initiation can be ignored ( $v_i \ll k_2[\text{O}_2][\text{H}]$ ). Then the combined solution of these equations gives a simple correlation between

the amount of reacted dioxygen  $\Delta[\text{O}_2] = [\text{O}_2]_0 - [\text{O}_2]$  and the concentration of the formed atomic hydrogen

$$[\text{H}] = 2\Delta[\text{O}_2] + (k_4/k_2)\ln(1 - \Delta[\text{O}_2]/[\text{O}_2]_0) \quad (12.13)$$

This expression is approximate and valid for small reaction depths near the lowest limit  $p_1$ . At higher pressures and burning-out depth, it is necessary to take into account several additional reactions. First, hydrogen evolution on the vessel wall due to reaction 4 (Table 12.1). Second, chain termination involving the O and HO-species often becomes noticeable with a decrease in  $[\text{H}_2]$  and, hence,  $[\text{H}\cdot]$  in the course of the process. Third, at sufficiently high concentrations of the O and HO-species, reaction (-2) begins to occur with a noticeable rate



in which the number of active centers decreases. This is the so-called *negative interaction of chains*. Taking into account this reaction, the kinetics of accumulation of hydrogen atoms takes the non-linear form

$$d[\text{H}]/dt = v_i + \varphi[\text{H}] - k[\text{H}]^2 \quad (12.14)$$

where  $\varphi = 2k_2 - k_4$ , and  $k = 2(k_2^2/k_{-2})([\text{O}_2]/[\text{H}_2])^2$ .

Equation (12.14) well describes the oxidation of hydrogen at any degrees of its burning-out.

Since the lowest ignition limit of the  $\text{H}_2 + \text{O}_2$  mixture is related to chain termination on the vessel wall, beginning from the thirties numerous publications were devoted to heterogeneous chain termination and the influence of the vessel walls on the kinetics of this reaction. In the kinetic region of chain termination when  $\varepsilon d/\lambda < 1$ , where  $\varepsilon$  is the probability of active center decay at its collision with the wall, the rate constant of chain termination in the reaction of hydrogen atoms with the surface is  $k_4 = \beta \varepsilon u/d$ , where the coefficient  $\beta = 1$  for a cylinder and  $\beta = 1.5$  for a sphere. The probability  $\varepsilon$  of the reaction of H with the surface depends on the material covering the wall and changes in wide limits. In the case of quartz covered with  $\text{K}_2\text{B}_4\text{O}_7$ ,  $\varepsilon = 10^{-5}$ ; for glass it varies from  $10^{-3}$  to  $10^{-2}$ ; for metals Al, Ti, and Ni it is from 0.1 to 0.5; and for platinum  $\varepsilon = 1$ . Hydrogen atoms react with the quartz surface with the activation energy  $\varepsilon = 0.5\exp(-23.4/RT)$ . Therefore, the lowest limit depends on the character of the surface. For example, for the  $2\text{H}_2 + \text{O}_2$  stoichiometric mixture at 713 K in a vessel with a diameter of 6.5 cm  $p_1 = 38$  Pa, and in the presence of an iron rod ( $d = 2$  mm)  $p_1 = 168$  Pa, i.e., by 4.3 times higher due to intense chain termination on the metal surface.

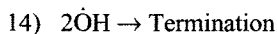
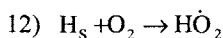
The decay of particles on the surface was considered until recently as the only heterogeneous reaction of chain carriers. Adsorption of atoms and radicals were equated to termination and it was believed that the efficiency of this termination is

unchanged in time. Heterogeneous termination was identified to the reaction of the first kinetic order with respect to the concentration of chain carriers.

However, it was established in early seventies that these starting positions, generally speaking, are not valid. They allow one to describe satisfactorily only ignition conditions rather than the kinetics of the process. Comparison with experiment finds a quantitative divergence in all main regularities. The totality of factors, which cause the observed divergences, was revealed. The main of them are the following factors.

1. Participation of some adsorbed atoms and radicals in chain propagation and branching. 2. Reversible chemical modification of the surface during combustion. 3. Bimolecular reactions between chain carriers even near the first limit determining non-linear branching and linear chain termination.

Each factor was found experimentally using modern methods of investigation. The indicated heterogeneous and homogeneous reactions result in the non-linear dependence of the chain process rate on the concentration of chain carriers. For example, the atoms and atomic groups on the surface, which appear during chain combustion and are responsible for important observed regularities of the process as a whole, were identified from IR spectra. The characteristic times of heterogeneous chain development were determined. They are comparable with the times of homogeneous stages. In particular, for dihydrogen combustion, the following reactions occurs ( $H_s$  is the adsorbed hydrogen atom):



As a result of the first two reactions, the adsorbed hydrogen atom returns to the gas phase as the active  $\cdot OH$  center. Thus, the adsorbed atom continues the reaction chain in the cases when the  $HO_2$  radical that formed reacts with H. Evidently, the greater the amount of atomic hydrogen in the bulk, the greater fraction of the  $HO_2$  radicals enters into the reaction with H, and this implies that the efficiency of heterogeneous chain termination depends on the concentration of atomic hydrogen. In fact, it follows from this reaction scheme that the total rate constant of H atoms decay on the surface is the following:

$$k_{ts} = k_{ts}^0 [1 - \beta k_{13} [H] / (k_{13} + k_{15} [H])] \quad (12.15)$$

where  $\beta$  is the fraction of the  $HO_2$  radicals adsorbed from the gas phase.

Outside the ignition region and in the induction period, the concentration of H is very low and  $k_{ts} = k_{ts}^0$ .

The ignition limit corresponds to this  $k_{ts}$  value. In the started combustion the concentration of H atoms is rather high, so that

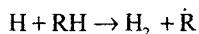
$$k_{13}[\text{H}] \gg k_{14} \quad \text{and} \quad k_{ts} = k_{ts}^0 (1 - \beta)$$

*i.e.*,  $k_{ts}$  becomes lower in the absence of combustion and at the limit. Therefore, the process occurs more rapidly than it follows from the theory, which treats  $k_{ts}$  as unchanged during the reaction. Indeed, this is observed in several chain processes in the presence of various surfaces.

In other cases, such a strong chemical modification of the surface takes place that the probability of adsorption changes, resulting, e.g., in an increase in  $k_{ts}$  during combustion. This retards combustion.

The following regularities of chain combustion are also caused by heterogeneous factors of the type: isothermal multiple self-ignition in a closed volume, new critical phenomena inside the ignition region in the isothermal regime, isothermal heterogeneous flame propagation, hysteresis of the kinetics of the chain process, induction of one chain reaction by another reaction due to the participation of adsorbed chain carriers, heterogeneous chain branching resulting in localization of isothermal flame at the surface even under conditions when chain termination occurs mainly on the surface, escape of atoms of the crystalline lattice into the gas phase under the action of chain carriers, *etc.* The observed regularities are inherent in the whole class of branched processes, *i.e.*, they have a general character. Evidently, these factors also act under non-isothermal conditions.

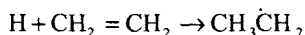
Works on the inhibition of dihydrogen combustion by additives of various substances play an important role in studies of this reaction. Among active species formed in this system atomic hydrogen is formed in the greatest amount and provides chain branching (see Table 12.1). Atomic hydrogen rapidly enters into such reactions as H abstraction



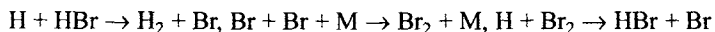
abstraction of the halogen atom (Cl, Br, I)



and adds rapidly at the double bond

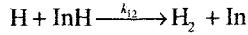


Alkyl radicals and halogen atoms formed in these reactions do not branch and do not propagate chains; therefore, reactions of this type result in chain termination. In some cases, cyclic mechanisms of chain termination appear, as in the case of HBr,



When a substance-inhibitor InH, which rapidly reacts with the hydrogen atom, is

introduced into the  $\text{H}_2 + \text{O}_2$  system, the  $\text{In}\cdot$  radical formed from it does not participate in chain propagation and branching



and changes the critical conditions of chain ignition. Near the lowest limit, the critical condition gains the form

$$2k_2[\text{O}_2] = k_4 + k_{12}[\text{InH}] \quad (12.16)$$

It follows from this that the shift of the lowest limit  $\Delta p_1 = p_{1,\text{InH}} - p_1$  is the following:

$$\Delta p_1/p_1 = k_{12}\gamma_{\text{InH}}/(2k_2\gamma_{\text{O}_2} - k_{12}\gamma_{\text{InH}}) \quad (12.17)$$

where  $p_{\text{O}_2} = \gamma_{\text{O}_2}p$ , and  $p_{\text{InH}} = \gamma_{\text{InH}}p$ .

A similar expression can be obtained when the upper limit with respect to pressure is shifted ( $\Delta p_2 = p_{2,\text{InH}} - p_2$ )

$$\Delta p_2/p_2 = k_{12}\gamma_{\text{InH}}/(2k_2\gamma_{\text{O}_2}) \quad (12.18)$$

If the inhibitor is very active and introduced on a sufficient concentration, ignition becomes impossible. This corresponds to the condition

$$\gamma_{\text{InH}} < (2k_2/k_{12})\gamma_{\text{O}_2} \quad (12.19)$$

Below we present the data illustrating the efficiency of some compounds as inhibitors of this process.

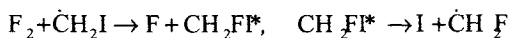
Inhibitor	$k_{12}$ , l/(mol s)	$2k_2/k_{12}$ (700 K)	$2k_2/k_{12}$ (800 K)
$\text{C}_2\text{H}_6$	$7.8 \cdot 10^{10} \exp(-38/RT)$	$1.6 \cdot 10^{-2}$	$3.1 \cdot 10^{-2}$
$\text{PhCH}_3$	$3.2 \cdot 10^{10} \exp(-25/RT)$	$4.2 \cdot 10^{-3}$	$1.1 \cdot 10^{-2}$
$\text{C}_2\text{H}_4$	$4.0 \cdot 10^{10} \exp(-27/RT)$	$4.5 \cdot 10^{-4}$	$5.6 \cdot 10^{-4}$
HCl	$2.3 \cdot 10^{10} \exp(-15/RT)$	$9.5 \cdot 10^{-4}$	$3.1 \cdot 10^{-3}$
HBr	$6.2 \cdot 10^{10} \exp(-9/RT)$	$1.4 \cdot 10^{-4}$	$5.2 \cdot 10^{-4}$

It is seen from the presented examples that ethylene and hydrogen bromide possess high activity, and the efficiency of inhibitors decreases with temperature increasing. The latter is associated with the fact that  $E_{12} < E_2$ .

### 12.3. Chain reactions with energy branching

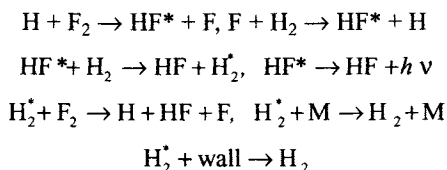
In oxidation reactions, such as  $\text{H}_2 + \text{O}_2$ ,  $\text{P}_4 + \text{O}_2$ ,  $\text{CS}_2 + \text{O}_2$ ,  $\text{CO} + \text{O}_2$ , chain branching occurs when atoms and radicals interact with molecules. A new class of

chain reactions was discovered using fluorination reactions as an example: reactions with energy chain branching. The characteristic feature of these reactions is the formation of noticeable amounts of vibration-excited molecules, which react to increase the number of atoms or radicals in the system. Excited molecules are formed in strongly exothermic reactions. In fluorination reactions, this is due to the fact that the F—F bond is comparatively weak (159 kJ/mol) and the C—F bonds (469 kJ/mol in CH<sub>3</sub>F) and the H—F bond (565 kJ/mol) are strong. Since the reaction of R· with F<sub>2</sub> is exothermic, it affords the RF\* molecule with a high probability. If this molecule has a bond close in strength to the excitation energy of the molecule, dissociation occurs and the number of radicals in the system increases, that is, branching takes place. For example, for the fluorination of methyl iodide, branching proceeds *via* the reactions

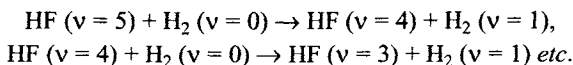


This mechanism became possible because the first stage occurs with energy release  $q = D_{\text{C—F}} - D_{\text{F—F}} = 308$  kJ/mol, which is close to the strength of the C—I bond in CH<sub>2</sub>FI ( $D_{\text{C—I}} = 234$  kJ/mol) and, evidently, the energy liberated in exothermic acts serves as the source of branching.

Hydrogen fluorination was studied in detail. This reaction occurs with self-ignition typical of branched chain reactions, which appears in a certain ( $p_1 < p < p_2$ ) range of pressures of the H<sub>2</sub> + F<sub>2</sub> mixture as in the case of hydrogen combustion. In the self-ignition regions, the reaction kinetics is described by the law  $e^{\phi t}$ . The reaction mechanism includes the following elementary steps:



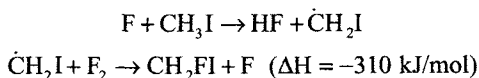
The first two reactions are exothermic:  $\Delta H = -406$  for the H + F<sub>2</sub> reactions and  $\Delta H = -130$  kJ/mol for the F + H<sub>2</sub> reaction. The dissociation energy of F<sub>2</sub> is 159 kJ/mol. Thus, the energy, which exceeds much the strength of the F—F bond is released in the first reaction, which is a basis for the development of energy chain branching under these conditions. The energy released in the reaction of F with H<sub>2</sub> is concentrated by 60% (240 kJ/mol) as the vibrational energy of HF. Due to the resonance between the vibrational levels of HF and H<sub>2</sub>, excitation is rapidly transmitted from HF\* to H<sub>2</sub> as a result of cascade processes ( $\nu$  is the vibrational energy level)



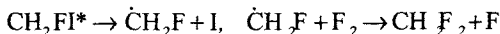
Polar HF molecules rapidly donate their energy as radiation, whereas the relaxation of vibration-excited hydrogen molecules occurs much (by 4 orders) more slowly. Therefore, these are precisely the molecules that act as energy carriers and react with  $F_2$  to result in branching. Comparison of the mechanisms of two chain reactions ( $H_2 + O_2$  and  $H_2 + F_2$ ) allows us to formulate the distinction between chain branched reactions and chain reactions with energy chain branching. Both chain reactions are branched due to their high exothermicity ( $\Delta H = -484$  kJ/mol for  $H_2 + O_2$  and  $-540$  kJ/mol for  $H_2 + F_2$ ). The source of branching is the elementary act of the atom with the molecule:  $H + O_2$  and  $H + F_2$ , respectively. However, in the chain branched reaction branching occurs as a sequence of chemical acts, which multiple the number of active centers ( $H + O_2 \rightarrow HO\cdot + O$ ;  $O + H_2 \rightarrow HO\cdot + H$ ), and in energy branching intermediate stages of energy transfer and reactions of excited molecules ( $HF^* + H_2 \rightarrow HF + H^*_2$ ;  $H^*_2 + F_2 \rightarrow H + HF + F$ ) play an important role. Undoubtedly, the appearance of excited molecules does not result, in many cases, in chain branching because this requires several conditions.

The reaction of fluorine with deuterium occurs *via* the mechanism similar to the reaction of  $F_2$  with  $H_2$ ; however, the lowest limit with respect to pressure in the  $F_2 + D_2$  mixture is much higher than that for  $F_2 + H_2$ . This indicates that in the  $F_2 + D_2$  system branching occurs more slowly because the energy (quantum) of vibrational excitation of  $D^*_2$  is by 13 kJ/mol lower than that for  $H^*_2$ .

In the above examples chain branching occurs as if in the bimolecular reaction of the vibration-excited molecule with  $F_2$ . Another type of branching occurs in the reaction of methyl iodide



The energy exceeding the energy of the C—I bond (234 kJ/mol) is concentrated in the formed excited molecule, and hence, the formation of the excited molecule is followed by its decomposition



Luminescence is observed during the reaction, and the concentration of atomic iodine reaches 10% of the initial concentration of fluorine. Branching is limited by the monomolecular decomposition of the vibration-excited molecule.

#### 12.4. Chemical lasers based on chain reactions

As it is known, a laser (optical quantum generator) generates coherent electromagnetic waves. Its operation is based on the forced emission of photons under the

action of an external electromagnetic field. With this purpose, such an inverse population of species in the excited state with the  $E_2$  energy is created in the working body (for example, gas) of the radiation source that the number of excited species exceeds the number of non-excited species with the energy  $E_1$ . Then when the electromagnetic wave with the frequency  $\omega = (E_2 - E_1)hL^{-1}/2\pi$  passes through the medium, its intensity increases due to acts of induced light emission by excited species. The amplification of the electromagnetic wave due to forced emission results in the exponential increase in its intensity  $I$  during passing the pathway  $z$

$$I = I_0 \exp[(\alpha - \beta)z] \quad (12.20)$$

where  $I = I_0$  at  $z = 0$ ,  $\alpha$  is the coefficient of quantum amplification, and  $\beta$  is the coefficient total losses.

The coefficient  $\alpha \sim (N^* - N)$ , and amplification is possible only when  $\alpha > \beta$ , *i.e.*, the condition  $\alpha = \beta$  is critical.

Light generation occurs in a cavity, which usually has the cylindrical shape with mirrors at the edges. The inverse population of molecules is created by this or another method in the working body. Photons emitted in the medium pass near excited molecules and result in the emission of new photons, *etc.* The photons, which were randomly emitted along the cavity axis, are multiply reflected from the mirrors and generate an avalanche of such photons in the medium. The cavity length is chosen in such a way that a whole number of waves fall in its length, so that the multiple reflections of photons result in the appearance in the cavity of standing waves, whose intensity is enhanced as an avalanche. Coherent radiation directed along the cavity axis is generated in the laser. One of the mirrors is made semi-transparent or with a hole for the radiation to exit from the cavity. The inverse population of the working medium in the laser is achieved by various methods, for example, by the irradiation of the working medium with special lamps; a gas discharge is used; an electron beam is passed; gas-dynamic method. In one of the methods, namely, chemical, a portion of the energy released in the reaction is used.

Several requirements are imposed on the chemical reaction used in a chemolaser.

1. Since excited species must appear in the system, only an exothermic reaction can serve as their source. The energy released in it ( $E = -\Delta H$ ) should exceed the excitation energy of the species, which serve as the radiation source. For example, in the reaction of H with  $F_2$  an energy of 408 kJ/mol is released (see 12.3), which is enough to excite HF to the vibration level with the quantum number  $v = 10$ .

2. The excited species relaxes; therefore, such species should be formed rapidly because only in this case we can create the situation with inversely populated species in the system. For example, the reaction of F with  $H_2$  occurs rapidly. At room temperature this reaction occurs in one of forty bimolecular collisions.

3. The laser to work needs that a considerable part of this energy would be trans-

formed in the energy formed used for the creation of laser radiation. Therefore, it is very important how the released energy is distributed between different types of energy of species (translational, rotational, vibrational, electronic).

Various deactivation processes have a strong influence of the power and other characteristics of the laser. All these forms are combined most favorably in fluorohydrogen lasers. Therefore, we consider this system in more detail.

The reaction of H with  $F_2$  occurs with a high rate constant

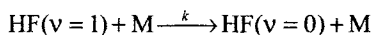
$$k_1 = 10^{11} \exp(-10/RT) = 1.8 \cdot 10^9 \text{ l/(mol s)} (298 \text{ K})$$

As a result of this exothermic reaction, the HF product is obtained in the vibration-excited state. The probability of  $HF^*$  formation at the vibration level is  $P(v) = 0.07$  ( $v = 3$ ),  $0.14$  ( $v = 4$ ),  $0.35$  ( $v = 5$ ), and  $0.44$  ( $v = 6$ ). The reaction of F with  $H_2$  occurs also rapidly

$$k_2 = 1.6 \cdot 10^{11} \exp(-7/RT) = 9.4 \cdot 10^9 \text{ l/(mol s)} (298 \text{ K})$$

The probability is  $P(v) = 0.7$  ( $v = 1$ ),  $0.55$  ( $v = 2$ ), and  $0.28$  ( $v = 3$ ).

As already mentioned, processes of energy transfer are very important. The energy transfer of the type  $V \rightarrow T, R$  (transition of the vibrational energy to translational or rotational) results in the deactivation of species, which serve as a source of laser radiation. The deactivation rate depends on the species M with which HF collides and on temperature. The rate constants of the process are presented below.



M	T, K	k, l/(mol s)
HF	295-1000	$3 \cdot 10^{11} T^{-1} + 7.1 \cdot 10^5 T$
Ar	800-2400	$1.7 \cdot 10^{-3} T^{3.05}$
He	1350-4000	$5.5 \cdot 10^{-8} T^{4.46}$
F	1400-4100	$127^{2.85}$
$H_2$	295-610	$167^{2.28}$
$F_2$	350	$2 \cdot 10^6$

On colliding of two molecules, the vibrational energy is transited from one molecule to another. In this transition the vibrational quantum number changes by unity. The probability of the transition depends on the energy of transition in both molecules. The transition occurs rapidly when these energies are close.

There are two types of HF lasers: one of them works on the basis of the non-chain reaction, and others use the chain reaction in the  $H_2 + F_2$  system. In the first case, fluorine atoms are generated from the fluorine-containing compound by this or another method (photolysis, electric charge, electron beam, *etc.*). The fluorine atoms react

with hydrogen molecules to form vibration-excited HF molecules, which are the source of laser radiation. Some such systems are presented below.

System	Pressure, kPa	Pulse duration, $\mu\text{s}$	Energy, K
NF <sub>3</sub> —CH <sub>4</sub> (H <sub>4</sub> )	1.3-5.0	1	0.025
SF <sub>6</sub> —C <sub>3</sub> H <sub>8</sub>	6	0.25	7.5
SF <sub>6</sub> —H <sub>2</sub>	20	0.20	11
F <sub>2</sub> —H <sub>2</sub>	133	0.025	2500

The efficiency of such laser, i.e., the ratio of the laser radiation energy to the energy of initiated electric discharge, is 4%, that is, low. For the creation of highly powerful lasers the chain reaction has an obvious advantage over the non-chain reaction because in these lasers the chemical energy ( $\Delta H$ ) of the chain process is the main energy source. The laser using the chain reaction  $\text{H}_2 + \text{F}_2$  operates in the pressure interval  $p_1 < p < p_2$ , where  $p_1$  and  $p_2$  are the lowest and upper limits of ignition. The inert gas is helium. Since the chain reaction appears spontaneously, the inhibitor (molecular oxygen) is added to the mixture to control the reaction, and a light flash is used for initiation. A portion of the energy of excited molecules is consumed to branching. Therefore, the spectrum of this laser contains lines corresponding to the transitions  $\text{HF}(v) \rightarrow \text{HF}(v-1)$  for  $v \leq 4$ . Below we present the wavelengths corresponding to different transitions in HF, depending on the rotational quantum number  $J$ .

Transition $v \rightarrow v-1$	Rotational quantum number $J$ of HF molecules						
$1 \rightarrow 0$	5	6	7	8	9	10	
$\lambda$ (mkm)	2.672	2.707	2.743	2.782	2.822	2.865	
$2 \rightarrow 1$	2	3	4	5	6	7	8
$\lambda$ (mkm)	2.696	2.727	2.760	2.795	2.831	2.870	2.910
$3 \rightarrow 2$	3	4	5	6	7	8	9
$\lambda$ (mkm)	2.853	2.888	2.925	2.963	2.004	2.047	2.093
$4 \rightarrow 3$	1	2	3	4	5	6	7
$\lambda$ (mkm)	2.922	2.954	2.989	3.026	3.064	3.105	3.148

The laser pulse duration depends on the composition of the mixture and varies in an interval of 2—12  $\mu\text{s}$ . The maximum emission intensity, for example, for the mixture  $\text{H}_2 : \text{F}_2 : \text{He} = 1 : 2 : 40$ , reaches  $500 \text{ W/cm}^2$ .

The electric efficiency of the transformation of the pulse energy into the laser energy achieves 160%, and the output energy of the laser is to 2500 J. The specific energy initiated by pulse photolysis reaches 80% J/l. These characteristics draw the HF laser to pulse CO<sub>2</sub> and CO lasers. For more detailed information about the branch chain reactions see Bibliography.

### Methods for studying chain reactions

Methods for studying chain reactions appeared and were improved in parallel with their discovery and study. Experimental evidence for the chain mechanism of the process and participation in it of free atoms and radicals gained significance at the first stage of development of the kinetics of chain reactions (1920-1940). It seems reasonable to consider briefly these proofs.

*High quantum yield.* According to Einstein's law of photochemical equivalence, one photon is absorbed by one molecule to induce a chemical transformation of only this molecule. If the quantum yield is  $\Phi > 1$ , this indicates the photoinitiated chain process. For the first time  $\Phi \gg 1$  (up to  $10^6$ ) was observed by M. Bodenstein for the reaction of  $\text{Cl}_2$  with  $\text{H}_2$  (1913).

*Initiator of chain reaction.* If the reaction proceeds via the chain mechanism, the introduction of a substance, which decomposes to radicals under experimental conditions, accelerates this reaction. Very often the chain process, for example, polymerization, does not occur without an initiator. The yield of the reaction products per decomposed initiator is always higher than unity.

*Influence of wall.* When the chain reaction occurs in the gas phase, chain termination very often occurs both in the bulk and on the wall. Therefore, the chain reaction is very sensitive; its rate depends on the material of the reactor wall, its preliminary treatment, and sizes and shape of the reaction vessel.

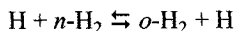
*Inhibitors of chain reactions.* A simple reaction cannot be retarded by minor additives of various substances. The chain reaction is retarded by an inhibitor, viz., the substance reacting with active centers and thus terminating chains. Inhibition of chain reactions was predicted by Christiansen and used for the first time by H. Backstrom as evidence for the chain mechanism of oxidation of sulfite and benzaldehyde (1926).

#### *13.1. Methods of identification of radicals and intermediate products of chain reaction*

*The method of metallic mirrors* was first to be used for the identification of radicals formed in the gas mixture (F. Paneth, 1929). Later the toluene method appeared (M. Szwarc, 1947): participation of radicals was concluded from the formation of

dibenzyl from toluene added to the reaction mixture. Then researchers began to use widely the ESR method for the identification of radicals and study of the kinetics of their transformation. However, we often meet the situation when the concentration of radicals is so low that the ESR method does not allow their detection. Then compounds, traps of free radicals, are used, such as  $(\text{CH}_3)_3\text{CN}(\text{O})$ . The latter reacts with a free radical to give the stable nitroxyl radicals detected by the ESR method.

Participation of atomic hydrogen in this or another reaction can be concluded from the *ortho-para*-conversion of hydrogen. In the equilibrium state hydrogen consists of 75% *ortho*-dihydrogen (nuclear spins are parallel) and 25% *para*-dihydrogen (nuclear spins are antiparallel). If only *para*-dihydrogen is introduced into the system, its transformation in the reaction mixture into *ortho*-dihydrogen indicates the generation of hydrogen atoms because *ortho-para*-conversion occurs in the reaction



Hydrogen atoms recombine especially intensely on the surface of some compounds, for example, on the  $\text{ZnO}\cdot\text{Cr}_2\text{O}_3$  mixed oxide. Recombination is accompanied by heat liberation (436 kJ/mol). The presence of hydrogen atoms in the system is indicated by warming of the thermocouple, the surface of the capillary of which is covered with this compound.

When radicals  $\text{R}\cdot$  collide with electrons, the probability of formation of the  $\text{R}^\cdot$  ions is much higher than on bombardment of molecules containing the R residue. This fact is used in mass spectrometry for the identification of free radicals in gas. G. Eltenton proposed this method in 1942.

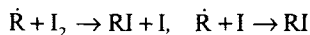
Along with the listed above phenomenological, physical, and analytical methods for revealing the chain mechanism of the reaction, a rich arsenal of various purely kinetic methods of investigation was created during 75 years of development of this area. We will briefly describe them below.

### 13.2. Method of free radical acceptors

Radical generation is the necessary stage of the chain process, which limits its rate. If a radical acceptor is introduced into the system, it reacts, first, with radicals and is consumed, and second, retards the chain process, *i.e.*, is its inhibitor.

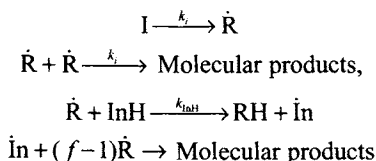
The generation rate of free radicals can be measured from the consumption of the radical acceptor  $\text{InH}$  (inhibitor of the chain reaction, counter of free radicals). Stable free radicals are most frequently used as alkyl radicals: nitroxyl, phenoxyl, and diphenylpicrylhydrazyl. Inhibitors of oxidation, *viz.*, phenol, naphthols, and aromatic amines, are applied for accepting peroxy and alkoxy radicals.

The consumption rate of the radical acceptor  $v_{\text{InH}}$  is related to the initiation rate  $v_i$  by the correlation  $v_i = f v_{\text{InH}}$ . If the acceptor is a stable radical, then most frequently  $f = 2$  because the radical formed from the acceptor reacts with another radical. For example, the consumption of  $\text{I}_2$  during alkyl radical generation in a solution is performed by the reaction



When the initiator decomposes to radicals, only some free radicals escape from the cage into the bulk and react with the acceptor. Therefore, the correlation  $v_i = 2e v_d$  or  $k_i = 2ek_d$ , where  $e$  is the probability of radical pair to escape to the solution, is valid for the decomposition rate of the initiator  $v_d$  and initiation rate  $v_i$  measured from the consumption of the acceptor. This simple correlation is valid when the initiator decomposes only homolytically and does not undergo induced decomposition.

An experiment is usually conducted in such a manner that the initiator concentration remains almost unchanged and the condition  $v_i = \text{const}$  is fulfilled. After measuring  $v_{\text{InH}}$ ,  $v_i$  is calculated, the dependence between  $v_i$  and  $c_A$ ,  $v_i$  and  $c_B$  (in the binary system) is found, and  $k$ :  $k_i = v_i/c_A$  (monomolecular decomposition),  $v_i = k_i/c_A^2$  (bimolecular decomposition of A), or  $v_i = k_i/c_A c_B$  (bimolecular reaction between A and B) is calculated. Several conditions must be fulfilled for the consumption rate of the inhibitor (radical acceptor) InH equals the initiation rate with an accuracy to the coefficient  $f$ . Let us consider the simplified scheme of reactions in a solution containing the initiator I and inhibitor InH



It is evident that

$$v_{\text{InH}} = f^1 k_i [\text{I}] \quad \text{if } f k_{\text{InH}} [\text{InH}] [\text{R}\cdot] \gg 2k_i [\text{R}\cdot]^2$$

or

$$f k_{\text{InH}} [\text{InH}] \gg (2k_i k_i [\text{I}])^{1/2}$$

that is, it is necessary that the inhibitor is introduced in a sufficiently high concentration

$$[\text{InH}] \gg (2k_i k_i [\text{I}])^{1/2} f^{-1} k_{\text{InH}}^{-1}$$

Assume that  $2k_i = 10^8 \text{ l}/(\text{mol s})$ ,  $f k_{\text{InH}} = 10^6$ , and  $k_i [\text{I}] = 10^{-6} \text{ mol}/(\text{l s})$ , then  $[\text{InH}]$

$\gg 10^{-5}$  mol/l. The optimum concentration of the acceptor is chosen from two concepts. On the one hand, as shown above, it is necessary that the acceptor "intercepts" almost all radicals, *i.e.*,  $[\text{InH}] > [\text{InH}]_{\min}$ . On the other hand, during the time of experiment  $t$  a considerable portion of the acceptor, *e.g.*,  $1/p$  part of its, should be consumed, *i.e.*,  $f[\text{InH}] < pk_i[\text{I}]t$ . Combining both inequalities, we obtain

$$(k_t k_i)^{1/2} / f k_{\text{InH}} [\text{I}]^{1/2} \ll [\text{InH}] / [\text{I}] < p f^{-1} k_i t \quad (13.1)$$

that is there is a certain interval of ratios of the concentrations of the acceptor to initiator in which this acceptor can be used for measuring  $k_i$ .

Sometimes the induction period of the chain reaction (for example, oxidation or polymerization) is measured rather than the consumption of the radical acceptor. In this case, known concentrations of the initiator and inhibitor (radical acceptor) are introduced into the system. If during the induction process the initiator remains the only source of free radicals and the inhibitor is consumed only in the reaction with free radicals and all chains terminate in the reaction of the radicals with inhibitor, then

$$v_i = f[\text{InH}] \text{ and } k_i = f[\text{InH}]_0 / t[\text{I}]_0$$

The measurement of the initial rate of consumption of the radical acceptor makes it possible to determine only  $k_i$ . If the experiment is carried out in such a way that the all substance-initiator decomposes within this time, then both  $k_d$  and  $k_i$  can be determined from the kinetic curve of consumption of the free radical acceptor. In these experiments the acceptor is added in excess for all radicals formed from the initiator would react with the acceptor. The rate of acceptor consumption under these conditions is the following:

$$-d[\text{InH}]/dt = (2ek_d/f)c_0 \exp(-k_d t) \quad (13.2)$$

and the kinetics of its consumption is described by the equation

$$\log\{([\text{InH}]_0 - [\text{InH}]_\infty) / ([\text{InH}] - [\text{InH}]_\infty)\} = 0.43 k_d t \quad (13.3)$$

Using the slope of the straight line in the coordinates  $\log(13.3)$ - $t$ , we find  $k_d$ , and the difference  $[\text{InH}]_0 - [\text{InH}]$  allows us to determine the probability of escape of radicals from the cage

$$e = 0.5 / f([\text{InH}]_0 - [\text{InH}]) / [\text{I}]_0 \quad (13.4)$$

In these experiments the same precautions as in the previous method have to be taken

$$[\text{InH}] > [\text{InH}]_{\min} = (2k_t k_i [\text{I}])^{1/2} / f k_{\text{InH}}$$

and  $k_i$  and  $k_d$  obtained from the experiment should be independent of  $[\text{InH}]_0$ .

### 13.3. Methods of chain reaction initiation

The study of the kinetics of the chain reaction makes it possible to establish the limiting stage of chain propagation and the character of chain termination and to obtain the quantitative kinetic characteristic of the chain process as a ratio of rate constants of limiting stages. The study of the rate of the chain process at different initiation rates is also significant.

#### Initiation rate

In the system where the chain reaction can develop, initiation with the known specified rate is created by either the introduction of an initiator, which decomposes to radicals with the known rate constant, or photochemically, or under the action of penetrating radiation ( $\gamma$  beams,  $\beta$  beams). The dependence of the chain reaction rate  $v$  on the initiation rate  $v_i$  allows one to judge about the character of chain termination. If  $v \sim v_i$ , chain termination has the first order with respect to the concentration of active centers; if  $v \sim v_i^{1/2}$ , it has the second order. In the liquid phase in the absence of an inhibitor, chains termination is monomolecular, and the rate of the chain reaction, e.g., polymerization of the monomer  $M$ , is

$$v = v_i + k_p (2k_t)^{-1/2} [M] v_i^{1/2} \quad (13.5)$$

The empirical dependence of  $v$  on  $v_i^{1/2}$  makes it possible to determine the parameter  $a = k_p(2k_t)^{-1/2}$ , which characterizes the rate of the chain process. Knowing this parameter, one can find the  $k_p$  value, if the rate constant  $k_t$  or the ratio  $k_p/2k_t$  are known or measured by the independent method (see Section 15.3.2). The parameter  $a$  allows one to measure the initiation rate for a non-studied radical source. If this source is the initiator  $I$ , then  $v_i = k_i[I]$ , and  $k_i$  is determined from a series of experiments with different initial concentrations of the initiator using the equation

$$k_i = v^2/a^2[M]^2[I]_0 \quad (13.6)$$

The parameter  $a$  allows one to estimate the upper limit with respect to  $v_i$  when the process proceeds *via* the chain pathway, that is, when  $v > 1$ . Since

$$v = v/v_i = k_p (2k_t)^{-1/2} [M] v_i^{-1/2}$$

then  $v > 1$  of the condition is fulfilled

$$v_i < k_p^2 [M]^2 / 2k_t \quad (13.7)$$

Since the reaction rate measured experimentally  $v > v_{\min}$  (where  $v_{\min}$  is the low-

est limit determined in experiment), the interval of reaction rate in the chain regime accessible for studying is determined by the inequality

$$v_{\min} < v < k_p^2 [M]^2 / 2k_i \quad (13.8)$$

Since the ratio  $k_p^2/2k_i$  decreases with temperature decreasing (always  $E_p > E_i$ ), then  $T_{\min}$  exists below which the reaction in the chain regime cannot be reproduced and studied.

When the initiator is used in such experiments, it is important that its decomposition to radicals occurs, on the one hand, with a sufficiently high rate and, on the other hand, not very rapidly for the condition  $v_i \approx \text{constant}$  is fulfilled during the time of the experiment, that is,  $k_d \ll t^{-1}$  (where  $t$  is the time of the experiment). This condition is expressed by the inequality

$$2k_i v_{\min}^2 / k_p^2 [M]^2 [I] \leq k_i \ll t^{-1} \quad (13.9)$$

For  $v_{\min} = 10^{-7}$  mol/(l s),  $[I] = 0.1M$ , and  $t = 10^3$  s, this inequality takes the form

$$10^{-16} [2k_i / (k_p^2 [M]^2)] \leq 10^{-3} k_i \ll 1 \quad (13.10)$$

#### *Method of mixed initiation*

The cases when the components of the system participate in both chain initiation and propagation are met rather often. For example, the introduction of alcohol and hydroperoxide into oxidized hydrocarbon, first, results, in the additional initiation (see Section 11.3) and, second, changes the ratio  $k_p(2k_i)^{-1/2}$  due to the participation of both components in chain propagation (peroxyl radicals of hydrocarbon react with ROH and ROOH, which changes the composition and concentration of the radicals). The method of studying is the following.

The initiator I for which  $k_i$  is known is introduced into the system where the chain reaction develops, for example, RH is oxidized and radicals are generated with the unknown rate  $v_{i,x}$ . A series of experiments with different concentrations of I is performed, and the rate of the chain reaction is measured in each experiment. If chain termination is bimolecular, the rate of the chain reaction ( $v \gg v_i$ ) is related to the initiator concentration by the ratio

$$v^2 = k_p^2 (2k_i) - 2[RH]^2 (v_i + k_i [I]) \quad (13.11)$$

Using the linear dependence of  $v^2$  on  $[I]$ , which has the form  $v^2 = A + B[I]$ , the coefficients  $A$  and  $B$  along with the following magnitudes are determined:

$$v_{ix} = k_i A / B, \quad k_p^2 (2k_i)^{-1} = B [I] / k_i [RH]^2$$

The conditions are selected in such a way that, first, the reaction proceeds *via* the chain route (inequality (13.8) is fulfilled); second, during the time of the experiment

$v_i \approx \text{const}$  (inequality (13.9)); and third,  $v_{ix}$  and  $k_i[I]$  should be commensurable, *i.e.*, the inequality  $0.5v_{ix} \leq k_i[I] \leq 5v_{ix}$  should be valid.

This method can also be applied when active centers decay in the reaction of the first order. In this case, the dependence of  $v$  on  $[I]$  is linear

$$v = k_p(k_t)^{-1}[RH](v_{ix} + k_i[I])$$

The method can also be used when chains terminate simultaneously in reactions of the first and second orders, then

$$k_i[I] + v_{ix} = Av^2 + Bv \quad (13.12)$$

$$A = 2k_t(k_p[RH])^{-2}, B = k_t'(k_p[RH])^{-1} \quad (13.13)$$

Three experiments with different concentrations of the initiator make it possible to calculate  $v_{ix}$ ,  $A$ , and  $B$ .

#### *Autoinitiated regime of chain reaction*

The opposite situation is observed in autoxidation reactions of organic compounds when the rate of radical generation increases during in the reaction course due to the formation of hydroperoxides. If ROOH decomposes to radicals in the reaction of the first order, then in the initial moment when the rate of ROOH formation is much higher than the rate of its decomposition

$$v = k_p(2k_t)^{-1/2}[RH]v_i^{1/2}, \quad v_i = v_{io} + k_i[ROOH]$$

and the kinetics of hydroperoxide accumulation is described by the formula

$$[ROOH]/t = 0.25a^2[RH]^2k_it + a[RH]v_{io} \quad (13.14)$$

where  $v_{io}$  is the rate of radical generation without participation of ROOH;  $a = k_p(2k_t)^{-1/2}$ .

Very often the rate of chain generation is so low that at rather long time the term  $a[RH]v_{io}$  in equation (13.14) can be neglected. Then the kinetics of ROOH accumulation is described by the simple expression

$$\Delta[O_2]^{1/2} = [ROOH]^{1/2} = 0.5a[RH]k_i^{1/2}t \quad (13.15)$$

Since the coefficient  $a$  can easily be determined in experiments on the initiated oxidation of RH, the rectification of the dependence by (13.15) allows one to determine the rate constant  $k_i$ . Rectifying the experimental results by (13.14), we can estimate the rate chain initiation  $v_{io}$ .

At a rather high concentration of ROOH, the radicals are generated by the bimolecular reaction with the rate  $k_i'[ROOH]^2$ , so that the total rate of radical generation

$$v_i = v_{io} + k_i[ROOH] + k_i'[ROOH]^2$$

The kinetics of accumulation of ROOH when its decomposition is insignificant and  $v_{i0}$  is very low and described at rather high  $t$  and  $[\text{ROOH}]$  by the expression

$$\Delta \ln[\text{ROOH}] = k_p[\text{RH}](k_i/2k_t)^{1/2}t + \ln(k_i/4k_i') \quad (13.16)$$

which makes it possible to estimate  $k_i$  at known  $k_p(2k_t)^{-1/2}$ .

### 13.4. Photochemical methods for studying elementary steps

The study of the kinetics of chain reactions in the stationary regime allows one to determine a combination of the rate constants  $k_p(2k_t)^{1/2}$  for bimolecular chain termination and  $k_p/k_i$  for chain termination in the first-order reaction. Non-stationary kinetic methods should be used for the estimation of the absolute values of rate constants. The sector method and the method of photochemical aftereffect found wide use in studying the mechanism of radical polymerization reactions.

#### 13.4.1. Sector method (method of intermittent irradiation)

The theory of this method was developed by D. Chapman, F. Briers, and E. Walters in 1926. However, only in 1937 this method was experimentally applied and used for studying the radical polymerization of vinylic compounds (H. Melville, 1937).

The method is applied for measuring the lifetime of active centers (atoms and radicals) in chain reactions with square chain termination. The method is based on the periodical initiation with light of formation of active centers and the change in the duration of light and dark periods from experiment to experiment.\* When the duration of the dark period is shorter than the lifetime of the active center (the sector is rapidly rotated), the reaction occurs rapidly, as under continuous initiation, with the rate  $(1+r)^{-1}$ , where  $r$  is the ratio of the dark to light periods, and the rate is  $v_f \sim v_i^{1/2}(1+r)^{-1/2}$ . At a long duration of the dark period (the sector rotates slowly), the reaction occurs only in irradiation periods, and the average rate is  $v_s \sim v_i^{-1}(1+r)^{-1/2}$ .

The transition from one regime to another occurs at such a dark period, whose duration is commensurable with the lifetime of the active center leading the chain reaction. The method is based on the dependence of the chain length on the initiation rate at square chain termination ( $v \sim v_i^{-1/2}$ ).

For the intermittent irradiation, the rate of chain transformation of RH is the following:

\* The light and dark periods are alternated using a rotating disk with slits (sectors).

$$v_o = k_p(v_i/2k_i)^{1/2}[\text{RH}]$$

At the fast rotation of the disk when the dark period is  $k_d \ll (2k_i v_i)^{-1}$ , the concentration of radicals corresponds to the average initiation rate  $v_i(1+r)^{-1}$ , where  $r = t_d/t_l$  and  $v_f = v_o(1+r)^{-1/2}$ . At the slow rotation of the disk, the reaction occurs only during the irradiation period, and the average rate during many periods is the following:

$$v_s = v_o(1+r)^{-1}$$

The ratio is

$$v_f/v_s = (1+r)^{1/2} = 2 \text{ at } r = 3$$

The transition from one regime to another occurs at

$$t_d \approx (2k_i v_i)^{-1/2}$$

The experiment is performed as follows (Fig. 13.1). The reaction mixture is placed in a thermostatted vessel 6 with transparent planar-parallel walls. The vessel is irradiated with the light with such a wavelength that generates radicals. Disk 4 is placed in the point where the beams are focused and is rotated. The reaction rate is measured by this or another method from experiment to experiment, and the empirical dependence of the  $v/v_o$  ratio on  $\log t_d$  is plotted,  $t_d$  is found from the rotation velocity of the disk and the ratio between the sizes of the dark and light sectors (usually  $r = 3$ ). This empirical dependence is compared with the theoretical one, and  $2k_i v_i$  is determined by comparison, and from this  $2k_i$  is calculated. The initiation rate is measured by the methods of inhibitors (see above) or through the chain reaction rate and the  $k_p/2k_i$  ratio.

The sector method provides reliable results when such conditions are fulfilled as uniform initiation over the whole reactor volume, rectangular (or close to it) shape of the light pulse (this is achieved by bringing the light beam to the point where the light beam is crossed by the disk), long chains, square character of the chain termination, and the absence (or a low rate) of the dark reaction.

The sector method can be used in the cases when chains terminate both quadratically

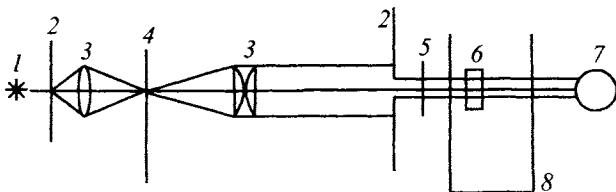


Fig. 13.1. Scheme of the sector installation: 1, light source; 2, diaphragms; 3, lenses; 4, rotating disk; 5, filter; 6, reaction cell; 7, photomultiplier; and 8, thermostat.

and linearly. However, in these cases, the ratio between  $k_t'$  and  $2k_t$  should be elucidated in special experiments (from the plot of  $v_0$  vs.  $v_i$ ) and  $v/v_0$  should be compared with  $\log m$  at the corresponding parameter

$$\gamma = k_t'[(k_t')^2 + 8k_tv_i]^{-1/2} \quad (13.17)$$

In the case of the dark initiation reaction, it should also be taken into account because the  $v/v_0$  ratio depends on the  $v_i/v_{id}$  ratio, where  $v_{id}$  is the rate of dark initiation. The sector method is used for measurements of reaction rate constants of radicals leading polymerization and oxidation. It allows one to measure  $2k_t$  from  $10^8$  l/(mol s) and lower, the error being usually  $\pm 25\%$ .

Using  $\Delta[R'H]$  and stationary rate  $v$  at the known  $v_i$  value,  $k_t$  can be determined. The method can be used only for chain photochemically initiated reactions. Rather reliable measurement of  $k_t$  and  $k_t'$  is possible when the time of chain development is longer than 1 s.

#### 13.4.2. Method of photochemical pre-effect and aftereffect

At the photochemical initiation of the chain effect, after the light was switched on, some time period passes until the stationary radical concentration and constant reaction rate are established. This is used for measuring the rate constant of chain termination. If chains terminate linearly, then after switching-on the light

$$d[\dot{R}]/dt = v_i + k_t'[\dot{R}], \quad [\dot{R}]_0 = 0, \quad d\Delta[R'H]/dt = k_p[R'H][\dot{R}] \quad (13.18)$$

$$[\dot{R}] = v_i(k_t')^{-1}(1 - e^{-k_t't})$$

At a low degree of conversion  $[R'H] = [R'H]_0$ , we have

$$\begin{aligned} \Delta[R'H] &= k_p(k_t')^{-1}v_i[R'H]_0[t + k_t'(e^{-k_t't} - 1)] \approx \\ &\approx k_p(k_t')^{-1}v_i[R'H]_0[t - (k_t')^{-1}] \end{aligned} \quad (13.19)$$

(at long  $t$ ), which allows one to find  $k_t'$  by the extrapolation of the asymptotic straight line of accumulation  $\Delta[R'H]$  to  $t = 0$ .

If chains terminate quadratically, then

$$d[\dot{R}]/dt = v_i - 2k_t[\dot{R}]^2$$

and

$$[\dot{R}] = (v_i / 2k_t)^{1/2}[(e^\tau - 1)/(e^\tau + 1)]$$

where  $\tau = 2(v_i k_t)^{1/2}t$ ;

$$\Delta[R'H] = \frac{k_p[R'H]}{2k_t} [\ln(e^\tau + 1) - \frac{1}{2} \tau - \ln 2] \approx \frac{k_p[R'H]}{2k_t} (at - \ln 2)$$

$$a = (2v_i k_t)^{1/2} \quad (13.20)$$

which makes it possible to find  $2k_t v_i$  and calculate  $k_t$  by the extrapolation of the asymptotic kinetic straight line of accumulation  $\Delta[R'H]$  to  $t = 0$  (the segment  $t = (2v_i k_t)^{-1/2} \ln 2$  is cut, Fig. 13.2).

Light switching-off results in not the instant stop of the chain reaction but in its gradual decay. If chain terminate linearly and the light was switched off in the moment  $t = 0$ , then

$$d[\dot{R}]/dt = -k'_t [\dot{R}] \text{ and } [\dot{R}] = v_i (k'_t)^{-1} \exp(-k'_t t)$$

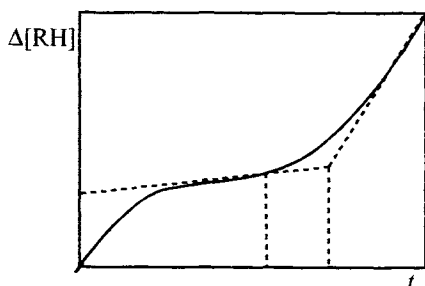
$$\Delta[R'H] = k_p (k'_t)^{-2} v_i [RH]_0 = v/k'_t \quad (13.21)$$

where  $v$  is the stationary rate of the chain reaction, and  $k'_t = v/\Delta[R'H]$ .

For square chain termination, some low initiation rate  $v'_i$  should be retained after light switching-off. Then after light switching-off the following amount the substance reacts due to the non-stationary concentration of radicals in the moment  $t = 0$ :

$$\Delta[R'H] = k_p(2k_t)[R'H]_0 \ln(1 + \xi)/2, \text{ where } \xi = v_i/v'_i \quad (13.22)$$

The use of the method is restricted by the systems where the amount of the substance  $\Delta[R'H] = v\tau$ , which exceeds the sensitivity of the analytical monitoring method, enters into the reaction during the lifetime of the active center.



### 13.5. Methods of studying liquid-phase oxidation of organic compounds

The described above methods are universal and used for studying various chain reactions. In addition, several kinetic methods based on the specificity of the liquid-phase oxidation of organic compounds were developed in the six-

Fig. 13.2. Kinetic curve of the chain reaction for switching-off ( $t = 0$ ) and switching-on the light (the moment is marked by arrow) in the photochemical aftereffect method.

ties. Below we briefly describe these methods.

### 13.5.1. Chemiluminescence methods

Liquid-phase oxidation of organic compounds is accompanied by weak chemiluminescence, which was found in 1959 by R.F. Vasil'ev, V.Ya. Shlyapintokh, and O.N. Karpukhin. Chemiluminescence is due to the fact that the disproportionation of secondary peroxide radicals affords triplet-excited ketone. The yield of excited molecules of ketone is  $10^{-3}$ - $10^{-2}$  per disproportionation act. The most part of excited molecules is quenched; the emission yield is  $10^{-5}$ - $10^{-3}$  quanta per excited molecule. The low quantum luminescence yield results in the low luminescence intensity.

To study chemiluminescence, a glass thermostatted reactor is placed in a light-proof chamber, hydrocarbon (most frequently it is well-studied ethylbenzene), an initiation source, and photosensitizer are introduced, and oxidation is performed along with continuous oxygen bubbling. 9,10-Dibromoanthracene or europium chelate (europium tris-thenoyl trifluoroacetate with phenanthroline) is used as the photosensitizer. The luminescence appeared during the reaction is collected by a mirror reflector and amplified by a photomultiplier, and the resulting signal is recorded using a self-recorder. The luminescence intensity appeared during oxidation is proportional to the rate of  $\text{RO}_2\cdot$  disproportionation, and in the quasi-stationary regime of the initiation rate

$$I = 2k_t\eta_{\text{ch}}[\text{RO}_2\cdot]^2 = \eta_{\text{ch}}v_i \quad (13.23)$$

where  $\eta_{\text{ch}}$  is the quantum yield of chemiluminescence.

To determine the unknown initiation rate, experiments with the known  $v'_i$  and unknown initiation rate  $v_i$  are carried out under identical conditions, measuring the chemiluminescence intensities  $I_{\text{ch}}$  and  $I'_{\text{ch}}$ , respectively. The initiation rate is found from the formula

$$v_i = v'_i(I_{\text{ch}}/I'_{\text{ch}}) \quad (13.24)$$

The chemiluminescence method was widely used for studying the decomposition of initiators. Since

$$I_{\text{ch}} = \eta_{\text{ch}}v_i, \quad v_i = 2ek_d[I]$$

$I_{\text{ch}}$  decreases in time with the decomposition of the initiator, so that  $k_d$  and  $e$  can be measured from the chemiluminescence kinetics

$$\ln(I_{\text{ch}}/I_{0,\text{ch}}) = k_d t \quad (13.25)$$

and

$$e = v_i/2k_d[I]_0$$

where  $v_i$  is determined from formula (13.22).

Chemiluminescence can be used for monitoring  $[\text{RO}_2\cdot]$  and in the non-stationary regime. If oxidation is carried out with the initiation of radicals by the light with the rate  $v_i$ , then  $[\text{RO}_2\cdot] = (v_i/2k_t)^{1/2}$  and the luminescence intensity  $I_{\text{o, ch}}$  correspond to this regime. After the light was switched off, the  $\text{RO}_2\cdot$  concentration decreases according to the equations (for numeration of the constants, see Chapter 11)

$$-d[\text{RO}_2\cdot]/dt = 2k_t[\text{RO}_2\cdot]^2, [\text{RO}_2\cdot]_0/[\text{RO}_2\cdot] - 1 = 2k_t[\text{RO}_2\cdot]_0 t$$

The decrease in the luminescence intensity is described by the formula

$$(I_{\text{o, ch}}/I)^{1/2} - 1 = (2k_t v_i)^{1/2} t \quad (13.26)$$

Using the slope of the straight line in the coordinates  $(I_{\text{o, ch}}/I_{\text{ch}})^{1/2} - t$ , the lifetime of  $\text{RO}_2\cdot$  can be determined:  $\tau = (2k_t v_i)^{-1/2}$ , and  $2k_t$  is found at the known  $v_i$ . The method of oxygen aftereffect was used rather often to find  $k_t$ . The method is based on the fast initiation of the  $\text{RO}_2\cdot + \text{initiator}$  system with oxygen. This is accompanied by a change in the luminescence intensity in time from  $I_{\text{o, ch}}$  at  $t = 0$  to  $I_{\infty, \text{ch}}$  at  $t \rightarrow \infty$ :  $I_{\text{o, ch}}$  corresponds to the concentration  $[\text{RO}_2\cdot]_0 = [\text{R}\cdot]_0$  in the moment  $t = 0$  when the concentration of  $\text{R}\cdot$  is determined by their recombination in the absence of  $\text{O}_2$

$$[\text{R}\cdot] = (v_i/2k'_t)^{1/2} \quad (13.27)$$

where  $k'_t$  is the rate constant of decay (recombination and disproportionation) of  $\text{R}\cdot$ .

The changing in  $I_{\text{ch}}$  in time is related to the establishment of the quasi-stationary concentration

$$[\text{RO}_2\cdot]_{\text{st}} = (v_i/2k_t)$$

Alkyl radicals decay with the diffusionally controlled rate and  $k_t \approx 10^8 \div 10^{10}$  l/(mol s), and  $\text{RO}_2\cdot$  decay much more slowly ( $k_t \approx 10^5 \div 10^7$  l/(mol s)) and, therefore,  $[\text{RO}_2\cdot]_{\infty} \gg [\text{RO}_2\cdot]_0$ , and luminescence enhances in time. The  $2k_t$  rate constant is found from the plot  $\ln(I_{\text{o, ch}}/I_{\text{ch}}) - t$

$$2k_t = \frac{v_i^{-1/2}}{2t} \ln \frac{I_{\infty, \text{ch}}^{1/2} + I_{\text{ch}}^{1/2}}{I_{\infty, \text{ch}}^{1/2} - I_{\text{ch}}^{1/2}} \quad (13.28)$$

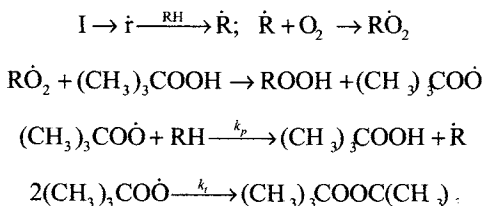
Several conditions must be fulfilled in the chemiluminescence method. Experiments should be carried out in hydrocarbon, whose oxidation affords secondary (or primary) peroxy radicals. The method was well approbated for ethylbenzene. It is important that all radicals of the initiator would react with hydrocarbon, finally exchanging to secondary peroxy radicals. The initiator must not quench chemiluminescence. Since oxygen possesses a quenching capability, experiments must be carried out at such partial pressures of  $\text{O}_2$ , which provide the fast transformation of  $\text{R}\cdot$  into  $\text{RO}_2\cdot$ , but the quenching effect of  $\text{O}_2$  is minimum. A photosensitizer is intro-

duced to enhance weak luminescence. In addition, it should be kept in mind that other processes, in particular, intracage radical recombination, could induce luminescence in oxidized systems.

### 13.5.2. Oxidation in the presence of hydroperoxide

The measure of oxidizability of the RH substance is the parameter  $2k_p(2k_t)^{-1/2}$ , which includes the characteristic of the reactivity of RH and  $\text{RO}_2\cdot$  with respect to RH and  $k_t$ . To characterize the reactivity of RH in the reaction with  $\text{RO}_2\cdot$ , it is necessary to measure the rate constants of a series of hydrocarbons  $\text{R}_i\text{H}$  with the peroxy radical of the same type. In 1962, J. Thomas and C. Tolman established that the introduction of tetralyl hydroperoxide in oxidized cumene retards its oxidation. They explained the retardation effect of  $\text{ROOH}$  by the fast exchange reaction of cumylperoxy by tetralylperoxy radicals, which rapidly into the disproportionation reaction. Later, the method using this effect was developed (J. Howard, K. Ingold, 1967).

The method is based on the oxidation of RH in the presence of an initiator and hydroperoxide, for example,  $(\text{CH}_3)_3\text{COOH}$ . Hydroperoxide reacts rapidly with peroxy radicals, for example, tetralyl hydroperoxide reacts with  $(\text{CH}_3)_3\text{COO}\cdot$  with the rate constant  $k = 10^6 \exp(-19/RT) = 530$  at 303 K and 2200 l/(mol s) at 373 K. Therefore, at rather high its concentration, the  $\text{RO}_2\cdot$  radicals are rapidly exchanged for the  $(\text{CH}_3)_3\text{COO}\cdot$  radicals, which participate in both chain propagation and termination. The scheme of chain oxidation of RH in the presence of  $(\text{CH}_3)_3\text{COOH}$  includes the following key reactions:



Hydroperoxide is introduced in such a concentration that  $\text{RO}_2\cdot$  are virtually completely exchanged for  $(\text{CH}_3)_3\text{COO}\cdot$ . To be sure in this, the dependence of the rate on the peroxide concentration is detected and such a concentration is chosen at which  $v = \text{const}$ . Usually  $v$  increases with an increase in  $(\text{CH}_3)_3\text{COOH}$  because for  $(\text{CH}_3)_3\text{COO}\cdot$   $k_t$  is much lower than those for many other  $\text{RO}_2\cdot$ . Under these conditions, the rate of chain oxidation of RH at  $v \gg 1$  is the following:

$$v = k_p [\text{RH}] (2k_t)^{-1/2} v_i^{1/2} \quad (13.29)$$

and the rate constant for the reaction of  $(\text{CH}_3)_3\text{COO}\cdot$  with RH is found from the formula

$$k_p^{\text{RH}} = v v_i^{1/2} (2k_t)^{1/2} [\text{RH}]^{-1} \quad (13.30)$$

For  $(\text{CH}_3)_3\text{COO}\cdot$ ,

$$2k_t = 8 \cdot 10^{10} \exp(-10/RT) \text{ l/(mol s)}.$$

Changing RH from experiment to experiment, one can obtain a series of  $k_p^{\text{RH}}$ , which characterizes the reactivity of various RH toward the same type of peroxy radicals, and the change of hydroperoxide from experiment to experiment allows one to obtain the reactivity of different  $\text{RO}_2\cdot$  toward the chosen RH. The concentration of hydroperoxide, which provides the entire exchange of  $\text{RO}_2\cdot$ , depends on the  $[(\text{CH}_3)_3\text{COOH}]/[\text{RH}]$  ratio and activity of RH: the higher the latter, the more hydroperoxide needs to be introduced. At sufficiently high temperatures, one can do without an initiator because hydroperoxide itself becomes the radical source. If it decomposes to radicals by the reaction of a first order with the constant  $k_i$ , then  $k_p^{\text{RH}}$  is found from the formula

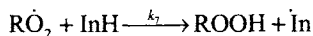
$$k_p^{\text{RH}} = v(2k_t)^{1/2} [\text{RH}]^{-1} (k_i[(\text{CH}_3)_3\text{COOH}])^{-1/2} \quad (13.31)$$

### 13.6. Methods for studying inhibitors of chain reactions

The mechanism of the inhibitor effect was studied in detail in chain reactions of oxidation of various compounds, first of all, hydrocarbons. It was studied in most detail for phenols. The developed procedures can find wider use, and we consider them using oxidation reactions as an example.

#### *Initial rate of inhibited oxidation (polymerization)*

In the cases when the In. radical formed from the InH inhibitor is not involved in chain propagation, chain termination proceeds *via* the reaction



and the rate of the inhibited chain reaction ( $k_2$  is referred to the stage of chain propagation, see Chapter 6) is

$$v = v_i + (k_2[\text{RH}]/f k_7[\text{InH}])v_i \quad (13.32)$$

Measuring the initial oxidation rate when  $[\text{InH}] \approx [\text{InH}]_0$  during the measurement time, we can determine the ratio of the constants

$$k_7/k_2 = \frac{v_i}{v - v_i} \frac{[\text{RH}]}{f[\text{InH}]_0} \quad (13.33)$$

Taking the series of inhibitors and knowing the  $k_2$  rate constant for the system  $\text{RH} \rightarrow \text{RO}_2^\cdot$ , we can determine  $k_7$ . The majority of rate constants of reactions of peroxy radicals with phenols were thus measured. Expressions (13.32) and (13.33) are valid in the case when all chains terminate on the inhibitor, *i.e.*, the following condition is fulfilled:

$$fk_7[\text{InH}] \gg (k_6v_i)^{1/2} \quad (13.34)$$

In the general case, when chains terminate in the reaction of both  $\text{RO}_2^\cdot$  with  $\text{InH}$  and  $\text{RO}_2^\cdot$  with  $\text{RO}_2^\cdot$ , the following correlation is valid:

$$\frac{v_o}{v_v} - \frac{v_v}{v_o} = \frac{fk_7[\text{InH}]}{(k_6v_i)^{1/2}} \quad (13.35)$$

where  $v = v - v_1$ ,  $v_o = v$  at  $[\text{InH}] = 0$ , and the chain length  $v_o \gg 1$ ,  $k_6$  is referred to the reaction of  $\text{RO}_2^\cdot$  with  $\text{RO}_2^\cdot$ . The following conditions need to be fulfilled for the efficient use of this method.

1. Inhibited oxidation should occur in the chain regime, otherwise the difference  $v - v_i$  will be very small and cannot be measured exactly. When accepting  $v_{\min} = 4$ , then

$$[\text{InH}]_o < k_2[\text{RH}]/4fk_7 \quad (13.36)$$

2. During the time of measuring the initial rate (the time of experiment  $t$ ), only a small portion of the inhibitor (for example, 15%) should be consumed. This implies that the inhibitor should be introduced in a sufficiently high concentration. Since the inhibitor is consumed with the rate  $v_i/f$ , we have the inequality

$$[\text{InH}]_o \gg v_i t / f \quad (13.37)$$

Evidently, the method makes it possible to measure such  $k_7$  for which the condition is fulfilled

$$k_7/k_2 < [\text{RH}]/28v_i t \quad (13.38)$$

Therefore, we have to select such  $\text{RH-InH}$  pairs and temperature that the  $k_7/k_2$  ratio falls in the region convenient for measurements. If the inhibitor reacts with  $\text{RO}_2^\cdot$  ( $k_7$ ) and with  $\text{R}^\cdot$  ( $k'_7$ ) (this case is realized in oxidized alcohols and polymers), the method allows one to determine both rate constants. With this purpose, a series of experiments is carried out at different partial oxygen pressures, changing the ratio of concentration  $[\text{R}^\cdot]/[\text{RO}_2^\cdot]$  from experiment to experiment. The ratio of the  $k_7/k_2$  and  $k'_7/k_1$  rate constants are found from the plot, which in the analytical form looks as follows:

$$\frac{v_0}{v} - \frac{v^2}{v_0^2} = \frac{fk_7[\text{InH}]}{k_2[\text{RH}]} + \frac{fk'_7[\text{InH}]}{k_1\gamma p_{\text{O}_2}}$$

where  $v_0 = v$  at  $[\text{InH}]_0 = 0$ ,  $k_1$  is referred to the reaction  $\text{R}\cdot + \text{O}_2$ ; and  $\gamma$  is Henry's coefficient for  $\text{O}_2$  in RH.

#### *Rate of inhibited oxidation as a time function*

The inhibitor is consumed in the course of the chain reaction. If all chains terminate on the inhibitor, it is consumed with a constant rate equal to  $v_i/f$ . Therefore, the inverse rate of inhibited oxidation linearly decreases in time

$$\frac{1}{v - v_i} = \frac{k_7}{k_2} \frac{f[\text{InH}]_0}{v_i[\text{RH}]} - \frac{k_7 t}{k_2[\text{RH}]} \quad (13.39)$$

The plot  $(v - v_i)^{-1} - t$  makes it possible to determine both  $k_7/k_2$  and  $v_i$ . The method imposes less rigid restrictions on the RH-InH system and allows one to extend the  $k_7/k_2$  range, which can be measured.

#### *Kinetics of inhibited oxidation*

The  $k_7/k_2$  ratio can also be estimated from the oxidation kinetics, measuring in time the amount of absorbed oxygen. The integration of equation (13.28) results in the expression ( $v \gg v_i$ )

$$\Delta[\text{O}_2] = \frac{k_2[\text{RH}]}{k_7} \ln \left( 1 - \frac{v_i t}{f[\text{InH}]_0} \right) \quad (13.40)$$

Another simpler method was also proposed: the kinetic curve is plotted in the inverse coordinates:  $\Delta[\text{O}_2]^{-1} - t^{-1}$ . The initial region of the kinetic curve is transformed into the straight line, whose slope allows the determination of the  $k_7/k_2$  ratio

$$\frac{\Delta[\text{O}_2]^{-1}}{\Delta(t^{-1})} = \frac{k_7}{k_2} \frac{f[\text{InH}]_0}{[\text{RH}]} \frac{1}{v_i} \quad (13.41)$$

This procedure makes it possible to still more extend the range of measured  $k_7/k_2$  and to study even such systems in which  $v \approx 1$  at  $t = 0$ .

#### *Method of competing reactions*

The same species, viz., peroxy radical participates in reactions of chain propagation and termination. Therefore, the  $\text{RH}-\text{InH}-\text{RO}_2\cdot$  system can be treated as the system of competing reactions, where RH and InH compete for the same species, peroxy radical. As a result of the reaction of  $\text{RO}_2\cdot$  with RH,  $\text{ROOH}$  is formed or the  $\text{O}_2$  molecule is absorbed, whereas in the reaction of  $\text{RO}_2\cdot$  with InH the latter is con-

sumed. When in the experiment on inhibited oxidation we follow the consumption of the inhibitor and formation of hydroperoxide, then it turns out that they are related by the simple correlation

$$[\text{ROOH}] - \Delta[\text{InH}] = \frac{k_2 [\text{RH}]}{k_7} \ln \frac{[\text{InH}]_0}{[\text{InH}]} \quad (13.42)$$

At rather long chains  $\Delta[\text{InH}]$  is low compared to  $[\text{ROOH}]$  and can be neglected. The advantage of the method is that it is applicable at both  $v_i = \text{const}$  and variable  $v_i$ , that is, under conditions of autoinitiated inhibited oxidation. If hydroperoxide rapidly decomposes during inhibited oxidation, it is more reliable to use the amount of absorbed oxygen  $\Delta[\text{O}_2]$  instead of  $[\text{ROOH}]$ . The method can be used at both  $v > 1$  and  $v \approx 1$  and under conditions when only some chains terminate on the inhibitor.

*Estimation of  $k_7$  from the kinetics of inhibitor consumption*

When the inhibitor is introduced in such a concentration that all chains terminate on it, and the rate of its consumption is independent of its concentration and equals  $v_i/f$ . This is used for the determination of the initiation rate. At rather low concentration of InH, the rate of its consumption depends on its concentration, which can be used for the determination of the rate constant  $k_7$ . If the concentration of InH is so low that in its presence peroxy radicals decay in the reaction with each other, then the rate of its consumption

$$-d[\text{InH}] / dt = k_7 [\text{InH}][\text{RO}_2\cdot] = (k_7 / \sqrt{k_6}) [\text{InH}] v_i^{1/2} \quad (13.43)$$

and the inhibitor is consumed by the reaction of a first order

$$[\text{InH}] = [\text{InH}]_0 e^{-kt}, \quad k = k_7 k_6^{-1/2} v_i^{1/2} \quad (13.44)$$

In a more general case, peroxy radicals decay in two reactions  $\text{RO}_2\cdot + \text{RO}_2\cdot$  and  $\text{RO}_2\cdot + \text{InH}$ , so that

$$k = \frac{k_7}{\sqrt{k_6}} v_i^{1/2} \left( 1 - \frac{k_7 [\text{InH}]}{\sqrt{k_6} v_i} \right) \quad (13.45)$$

To determine  $k_7$ , such a hydrocarbon is chosen for peroxy radicals of which  $k_6$  is known, the initiator is introduced, and the consumption of the inhibitor is monitored (for example, spectrophotometrically) during the experiment. From each experiment using (13.44),  $k$  is determined, and the extrapolation of  $k$  to  $[\text{InH}]_0 = 0$  gives  $k_7 k_6^{-1/2}$ , and  $k_7$  is calculated. The use of this method requires a highly sensitive method for analysis for the inhibitor and such a choice of conditions that allows one to monitor the inhibitor using standard methods. If the duration of the experiment  $t$  is minimum,  $k \leq t^{-1}$  can be measured and, hence,  $k_7 \leq k_6^{1/2} v_i^{-1/2} t^{-1}$ . The range of measuring  $k_7$  can

be extended if the experimental series is performed with different  $[\text{InH}]_0$  and such  $[\text{InH}]_0 = [\text{InH}]^{1/2}$  is determined (empirically) at which

$$v_{\text{InH}} = v_i/2f, \text{ that is, } f v_{\text{InH}} = 1/2 v_i$$

In this case, we have

$$k_7 = v_i^{1/2} k_6^{1/2} / 2 f [\text{InH}]^{1/2} \quad (13.46)$$

The range of measuring  $k_7$  can be extended by selecting  $\text{RH}(\text{RO}_2\cdot)$  with higher  $k_6$ .

#### *Chemiluminescence methods of measuring $k_7$*

Liquid-phase oxidation when secondary peroxy radicals lead chains is characterized by chemiluminescence when the disproportionation of two secondary peroxy radicals affords triplet-excited ketone, which is the emitter of luminescence



The chemiluminescence intensity is  $I \sim [\text{HR}'\text{OO}\cdot]^2 \sim v_i$  (in the quasi-stationary regime). When the inhibitor is introduced, the concentration of  $\text{RO}_2\cdot$  decreases and, hence, the chemiluminescence intensity decreases. The change in the intensity with the introduction of the inhibitor, for example, phenol, is related to  $[\text{InH}]$  by the correlation ( $I_0$  and  $I$  are the chemiluminescence intensities in oxidized RH in the absence and presence of the inhibitor, respectively)

$$(I_0/I)^{1/2} = 1 + (1.1 k_7 / \sqrt{v_i k_6}) \quad (13.47)$$

Using the plot of  $I$  vs.  $[\text{InH}]$ , one finds  $k_7$  at known  $v_i$  and  $k_6$ . The inhibitor is consumed during the experiment, and therefore, the chemiluminescence intensity increases. The kinetic curve of chemiluminescence is s-shaped. The maximum angular coefficient of the chemiluminescence curve is

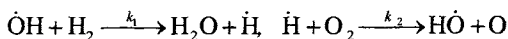
$$[d(I_0/I)/dt]_{\text{max}} = 0.22 k_7 v_i^{1/2} / k_6 \quad (13.48)$$

The expression is valid in the cases when the products of inhibitor transformation are inactive as inhibitors or initiators. In some special cases, the introduction of the inhibitor (amine) into the oxidized substance does not quench but, by contrast, enhances chemiluminescence (see Chapter 11).

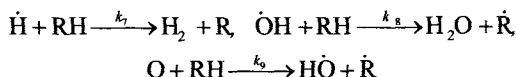
### *13.7. Method for shifting limits of chain ignition*

The chain branched reaction is characterized by the upper  $p_2$  and lower  $p_1$  limits of ignition with respect to pressure when the branching rate is equal to the rate of chain termination. Using the shift of the ignition limit because of the introduction of

the substance reacting with active centers, one can determine the rate constant of this reaction. For hydrogen combustion, chains propagate and terminate by the reactions (see Chapter 11)



When the substance RH is introduced, the following reactions occur



which can decrease the concentration of active centers (the  $\text{R}\cdot$  radical cannot branch the chain as H). Therefore, the introduction of RH decreases the upper limit  $p_2$  and increases the lower limit  $p_1$ . The shift of  $p_2$  and  $p_1$  can be used to calculate  $k_7$ .

$$\frac{[\text{O}_2]}{[\text{RH}]} \frac{\Delta p_2}{p_2} = \frac{k_7}{2k_2} + \left( \frac{k_8}{2k_2} + \frac{k_9}{k_1} \right) \frac{[\text{O}_2]}{[\text{H}_2]} \quad (13.49)$$

When the lower limit is shifted under the conditions when reactions (8) and (9) can be neglected,  $\Delta p_1/p_1 = (k_7/2k_2)(p_{\text{RH}}/p_1)$ . Since  $k_2$  is known ( $\log k_2 = 11.9 - 70/\Theta$ ),  $k_7$  is found from the  $k_7/(2k_2)$  ratio ( $\Theta = 2.3RT$ ).

## Part 5

### Homogeneous catalysis

#### *Chapter 14*

### **General Kinetic Regularities in Homogeneous Catalysis**

Homogeneous catalysts and enzymes accelerate processes with rather complicated kinetics. As a rule, several substrates are involved in reactions, multistage chemical transformations and electron transfer inside enzymes is often observed, and the cooperative interaction of active sites, positive and negative feedback, etc. are met.

In this chapter we consider some problems of the formal kinetics of homogeneous catalytic and enzymatic reactions. Since many public editions are devoted to the kinetics of chemical and enzymatic reactions, here we revise briefly only general problems. A great attention is given to sections directly associated with the specific problems of catalysis. The theory of elementary acts of chemical and enzymatic processes is presented in Chapters 4 and 6.

#### *14.1. General principles of homogeneous and enzyme catalysis*

A large group of scientists, including the present authors, believe that a chemical catalytic process, as well as an enzymatic reaction a certain sequence of elementary chemical steps. Each of these steps proceeds by “ordinary” laws of chemical kinetics. The accelerating action of a catalyst is accounted for by the fact that its active centers become involved in such chemical reactions with substrate molecules and with such rates, which lead to an increase in the velocity of the process as a whole. Within the framework of these concepts, enzymes are characterized by a set of certain specific properties, which have been “polished off” in the course of biological evolution.

According to modern concepts, the occurrence of a catalytic reaction proceeds at a sufficient rate provided by the following factors ("**selection**" rules) operating in concert.

**The Thermodynamic Feasibility of the Process as a Whole.** The change in the positive standard Gibbs energy ( $\Delta G^0$ ) must not be greater than about 20-25 kJ/mol.

**Smooth Thermodynamic Relief.** The catalyst involved in a chemical process alters the path of the reaction in a favorable direction providing smooth thermodynamic relief of the process. In other words, the catalyst should avoid deep energy "holes" and high "hills" along the reaction path.

**Proximity and Orientation Effects of the Substrate Molecules and Catalytic Site.** The preliminary approach of two reacting particles during complex catalyst-substrate formation, resulting from the interaction of the groups that do not participate directly in subsequent chemical reactions (**binding groups**), increases the rate constant of the reaction by about  $10^2$  times. The precise orientation of the substrate relative to **catalytic groups** may provide an acceleration of  $10^2$  to  $10^6$  times, depending on the type of the reactions. For the reaction involving three and more molecules, the additional acceleration due to these effects may be considerably greater. The proximity and precise orientation prevents a loss of entropy converting a multimolecular reaction to a unimolecular one.

**Low Energy Activation in Each Step.** In certain cases, the rules "the better the thermodynamics of the step, the lower energy activation" (Polanyi-Semenov, Bronsted equations, for example) are fulfilled. Among factors determining low energy activation of elementary chemical steps are concerted and multi-electron mechanisms, mechanical stress on substrate and catalytic groups, optimum polarity and electrostatic field in the active site cavity.

**Favorable Quantum-Mechanical Factors.** According to theory, the rate constant of an elementary step of a chemical process ( $k$ ) depends significantly on the value of resonance integral  $V$ , which is proportional to the overlap integral  $S$ . The latter characterizes the degree of positive overlap of the electron wavefunctions. If the overlap is very significant, frequencies of electronic motion exceed the frequencies of nuclear motion with characteristic times  $t = 10^{-12}$  to  $10^{-13}$  s. In this case, adiabatic approximation is valid and  $k$  does not depend on  $V$ . If the overlap is slight, i.e., the centers are separated by a large distance or electronic transition are symmetrically forbidden, then  $k$  is proportional to  $V^2$ . Another quantum-mechanical selection rule, the principle of the total spin conservation follows from the law of momentum conservation.

**Effective Synchronization of Nuclei in a Chemical Concerted Reaction.**

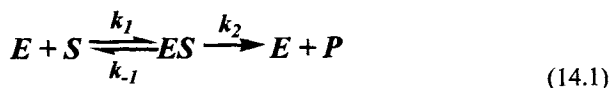
In a concerted adiabatic process the transition from the initial to transition states occurs upon motion of nuclei (taking about  $10^{-13}$  s) in a certain direction, which is only possible path that leads to reaction products. Obviously, the statistic thermal nature of chemical processes limits the number of nuclei, which can be involved in a signal elementary step. In such cases, the value of synchronization factor ( $\alpha_{\text{syn}}$ ), which quantitatively characterized possibility of the concerted process can be markedly lower than 1.

**Formation of Ensembles of Catalysts.** Capacity to be Regulated Formation of ordered catalytic ensembles can facilitate, to the great extent, accessibility of substrates in consecutive chemical and enzyme reactions. Capacity of catalysts to be or not to be active in proper space and proper time is of great importance especially in biological cells.

*14.2. Simple catalytic reactions*

The transformation of substrate S under the catalyst action, for example, enzyme E, occurs, as a rule, through the formation of the catalyst—substrate complex.

The simplest reaction scheme is the following:



Since in many cases the stationary regime with respect to the ES complex is established rather rapidly ( $10^{-3}$  to  $10^{-2}$  s), it is usually accepted that  $dE/dt \approx 0$ . Under the condition that the concentration of the substrate [S] is much greater than that of the catalyst  $[E]_0$  and the substrate is insignificantly consumed during the experiment, we obtain the following expression for the rate:

$$v = \frac{k_1 k_2 [E]_0 [S]_0}{k_1 [S] + k_{-1} + k_2} \quad (14.2)$$

where  $K_m = (k_{-1} + k_2)/k_1$  is named the Michaelis constant (after the author of the equation);  $v_{\text{max}} = k_2[E]_0$ . The Michaelis constant numerically equals the substrate concentration at which  $v = v_{\text{max}}/2$ .

Several methods for transformation of the Michaelis equation were proposed for finding  $K_m$  and  $v_{max}$ . They are shown in Fig. 14.1.

In the case where  $k_{-1} \gg k_2$ ,  $K_m = K_S = k_{-1}/k_1$ , i.e., equal to the dissociation constant of the ES complex named the substrate constant.

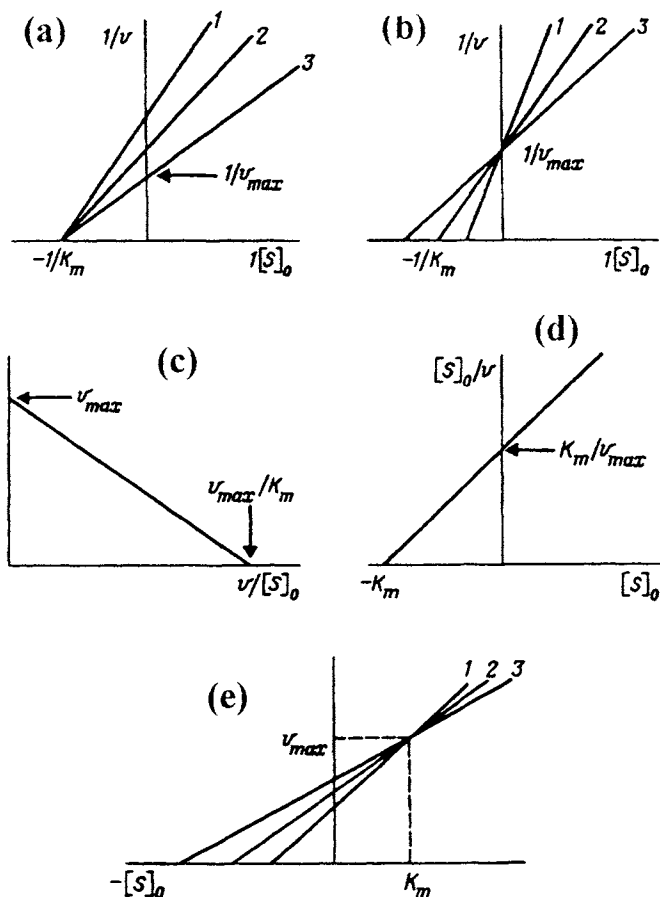


Fig. 14.1. Types of anamorphoses used for the determination of the parameters in the Michaelis equation ( $K_m$  is the Michaelis constant;  $v_{max}$  is the maximum rate; 1—3 correspond to the systems with different parameters  $v_{max}$  (a),  $K_m$  (b), or substrate concentration (e)).

The values of the constants in the Michaelis equation can be found by the analysis of the data on the pre-stationary kinetics, for example, from the kinetic curve of changing the concentration of the ES complex

$$[ES] = \frac{[E]_0[S]_0}{(K_m + [S]_0)} [1 - \exp\{-k_1[S]_0 + k_{-1} + k_2)t\}] \quad (14.3)$$

The stationary reversible reaction occurred according to (16.1) is described by the kinetic equation

$$v = \frac{v_S K_{mS}^{-1}[S] - v_P K_{mP}^{-1}[P]}{1 + K_{mS}^{-1}[S] + K_{mP}^{-1}[P]} \quad (14.4)$$

Indices S and P are referred to the maximum rates and Michaelis constants for the substrate and product, respectively:

$$v_S = k_2[E]_0, v_P = k_{-1}[E]_0, \\ K_{mP} = (k_{-1} + k_2), K_{mS} = (k_{-1} + k_2)/k_{-2} \quad (14.5)$$

For the reactions, whose rate depends on the degree of protonation of the catalyst, for example, when the  $\text{EH}^+$  form is active and  $\text{EH}_2^{2+}$  and E are inactive, the effective constant is the following:

$$K_m(H^+) = K_m(1 + K_a[H^+]^{-1} + K_b[H^+]^{-1})^{-1} \quad (14.6)$$

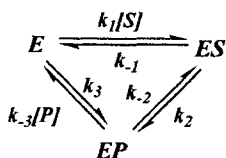
where  $K_a$  and  $K_b$  are the association constants for the  $\text{EH}^+$  and  $\text{EH}_2^{2+}$  complexes, respectively.

### 14.3. Methods of analysis of kinetic schemes

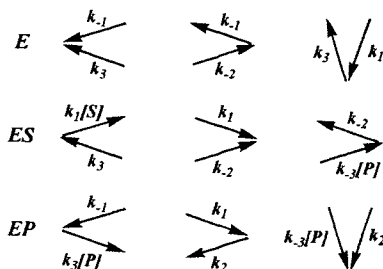
Equations, which substantially simplify calculations for stationary processes, were proposed to find a relationship between the experimentally measured rates of enzymatic reactions and the corresponding set of the rate constants for particular stages and concentration of the reactants.

The equations proposed by E. King and K. Altman can be illustrated by the enzymatic reaction with one substrate. The scheme of reactions is written as a

triangular cycle where the vertices correspond to the states of the enzyme and each arrow reflects the stage and indicates its direction



A set of consequently arranged arrows leading to a given point in the plot corresponds to each state: for each stage the arrow length is equal to the rate constant value (or the product of the rate constant by the concentration)



The fraction of each state of the enzyme (the  $[E_i]/[E]_0$  ratio value) is proportional to sum of products of arrow lengths; the sum contains three terms (in the case of  $n$  state,  $n$  terms), and each product contains two cofactors (in the general case,  $n - 1$ ). For the presented example,

$$\begin{aligned} [E]/[E]_0 &\propto k_{-1}k_3 + k_{-1}k_{-2} + k_3k_2, \\ [ES]/[E]_0 &\propto k_1k_3[S] + k_1k_{-2}[S] + k_{-3}k_{-2}[P], \\ [EP]/[E]_0 &\propto k_{-1}k_{-3}[P] + k_1k_2[S] + k_{-3}k_2[P] \end{aligned}$$

These values should be inserted into the kinetic equation

$$\frac{d[P]}{dt} = \frac{\{k_3[EP] - k_{-3}[E][P]\}[E]_0}{[E] + [ES] + [EP]}$$

As a result, we get

$$\frac{d[P]}{dt} = \frac{\{k_1 k_2 k_3 [S] - k_{-1} k_{-2} k_3 [P]\}}{\left\{ \frac{k_{-1} k_3 + k_{-1} k_{-2} + k_2 k_3 + (k_1 k_3 + k_1 k_{-2} + k_1 k_2)[S] + (k_{-1} k_{-3} + k_2 k_{-3} + k_{-2} k_{-3})[P]}{k_1} \right\}}$$

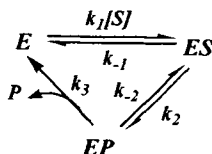
If the product is formed irreversibly ( $k_{-2} = k_{-3} = 0$  and  $k_3 \gg k_{-2}$ ), the equation takes the form of classical Michaelis equation

$$\frac{d[P]}{dt} = \frac{v_{\max} [S]}{[S] + K_m}$$

where

$$v_{\max} = k_2 [E]_0, K_m = (k_{-1} + k_2) / k_1$$

Another, more general method of analysis of complicated kinetic schemes (method of directed graphs) is illustrated by the irreversible reaction with one substrate and one product. The reaction scheme is written as a graph, viz., diagram plotted of nodal points (E, ES, EP) characterizing the state of the enzyme and connecting lines



Trees (array of branches (arrows) connecting all nodes of the graph without cycle formation) are drawn up to each node of the graph. The branch value is equal to the rate constant or the product of the rate constant by the concentration. The tree value is the product of the branch values along the given route. The determinant of the node  $D_i$  is the sum of the tree values converging at the given node.

For the case considered, the set of the branches coincides with the set of the arrows in the scheme by E. King and K. Altman. The rate of the irreversible enzymatic reaction at  $k_{-3} = 0$  is the following:

$$v = \frac{k_1 D_1 [E]_0}{D_1 + D_2 + D_3},$$

$$D_1 = k_{-1}k_{-2} + k_{-1}k_3 + k_2k_3, D_2 = k_3k_1[S] + k_2k_1[S], D_3 = k_1k_2$$

In the general case,

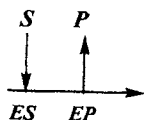
$$v = \frac{\sum k_j D_j [E]_0}{\sum D_j}$$

where  $D_j$  corresponds to the states of the enzyme from which products are isolated;  $k_j$  are the rate constants of product formation; summation in the denominator is performed over all states of the enzyme.

#### 14.4. Kinetic classification of catalytic reactions

According to Klelend's classification, three types of mechanisms are distinguished. The mechanism is named ordered if its set of kinetic constants and dissociation constants of products and substrates in the expression for the enzymatic reaction rate depends on the order of addition of substrates or the order of product isolation. This dependence is absent for the non-ordered mechanism. The "ping-pong" mechanism corresponds to the case where one or more molecules of the product are isolated before other substrate molecules add to the enzyme macromolecule. One should additionally take into account the numbers of kinetically substantial substrates or products in the reaction, which are designated as mono-, bi-, tri-, tetra-, etc. "Iso" is used for designation of mechanisms including the stage of isomerization between two stable enzyme forms.

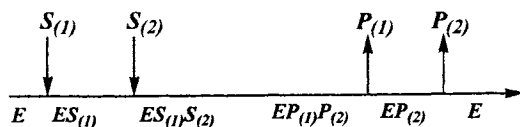
The simple reversible reaction with one substrate and one product is attributed to the mono,mono type and graphically presented as follows:



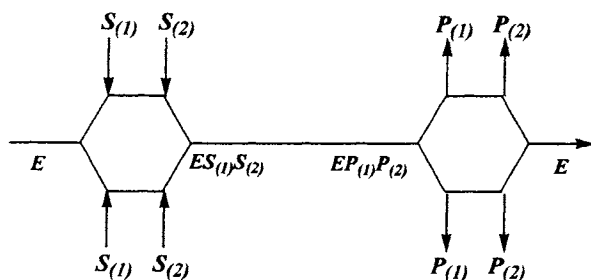
ES and EP are the enzyme—substrate and enzyme—product complexes.

The following diagrams performed in the simplified variants correspond to more complicated reaction mechanisms.

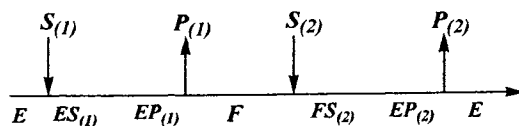
Ordered bi,bi mechanism (two substrates; two products)



Non-ordered bi,bi mechanism



“Ping-pong” bi,bi mechanism (fragment oscillates between two stable forms E and F)

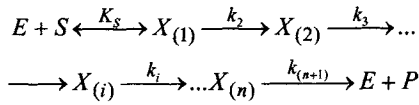


#### 14.5. Kinetic equations of multistage catalytic reactions

Three-stage reaction with one substrate

$$\begin{aligned}
 E + S &\xrightleftharpoons[k_{-1}]{k_1} ES \xrightleftharpoons[k_{-2}]{k_2} EP \xrightleftharpoons[k_{-3}]{k_3} EP_2 \xrightarrow{k_4} E + P_2 \\
 v &= \frac{k_2 k_3 k_4 [E]_0}{k_2 k_3 + k_2 k_{-3} + k_{-2} k_{-3} + k_2 k_4 + k_{-2} k_4 + k_3 k_4}, \\
 k_1 k_m &= \frac{k_{-1} k_{-2} k_3 + k_{-1} k_{-2} k_4 + k_{-1} k_3 k_4 + k_2 k_3 k_4}{k_2 k_3 + k_2 k_{-3} + k_{-1} k_{-3} + k_2 k_4 + k_{-2} k_4 + k_3 k_4}
 \end{aligned} \tag{14.7}$$

For the reaction with n irreversible stages,

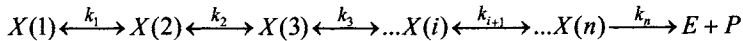


the kinetic analysis gives the expressions

$$v = [E]_0 \left/ \sum_{i=2}^{n+1} 1/k_i \right. \tag{14.8}$$

$$K_m = \frac{(K_S / k_2)}{\sum_{i=2}^{n+1} 1/k_i} \tag{14.9}$$

For the reaction with n reversible and the last irreversible stages, we have



The process rate  $v$  is related to the rate constants of elementary steps  $k_i$  and  $k_{-i}$  and the equilibrium constant  $K_i = k_i/k_{-i}$  by the following expression:

$$v = [E]_0 \left/ \sum_{i=1}^n A_i \right.,$$

where

$$A_n = 1/k_n, A_{n-1} = 1/k_{n-1} + K_{n+1}/k_n,$$

$$A_i = 1/k_i + K_i/k_{i+1} + \dots + K_i K_{i+1} \dots K_{j-1}/k_j + \dots + K_i \dots K_{n-1}/k_n,$$

$$i < j < n$$

For the ordered bi,bi mechanism (reaction with two substrates and one central complex), we have

$$v = (k_1 k_2 k_3 k_4 [S_{(1)}][S_{(2)}] - k_{-1} k_{-2} k_{-3} k_{-4} [P_{(1)}][P_{(2)}])[E]_0 / \Sigma,$$

$$\Sigma = k_{-1}(k_{-2} + k_{-3})k_4 + k_{-1}(k_{-2} + k_3)k_{-4}[P_{(2)}] +$$

$$+ k_1(k_{-2} + k_3)k_4[S_{(1)}] + k_{-1}k_{-2}k_{-3}[P_{(1)}] + k_2 k_3 k_4[S_{(2)}] +$$

$$+ (k_{-1} + k_{-2})k_{-3}k_{-4}[P_{(1)}][P_{(2)}] + k_1 k_2 (k_3 + k_4)[S_{(1)}][S_{(2)}] +$$

$$+ k_1 k_2 k_{-3}[S_{(1)}][P_{(1)}][S_{(2)}] + k_1 k_{-2} k_{-3}[S_{(1)}][P_{(1)}] +$$

$$+ k_2 k_{-3} k_{-4}[S_{(2)}][P_{(1)}][P_{(2)}] + k_2 k_3 k_{-4}[S_{(2)}][P_{(2)}]$$
(14.10)

For the non-ordered bi,bi mechanism, the expression for  $v$  corresponds to the previous case at  $k_1 = k_2$ ,  $k_{-1} = k_{-2}$ ,  $k_3 = k_4$ , and  $k_{-3} = k_{-4}$ .

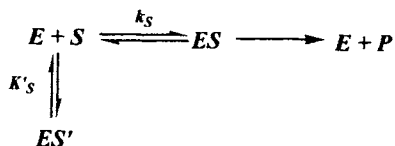
In the simplest variant, for the irreversible reaction ( $k_{-3} = k_{-4} = 0$ ) and under the condition where  $k_3 \ll k_{-1}$ , we have

$$v = \frac{k_3 [E]_0}{1 + K_{S_{(1)}}/[S_{(1)}] + K_{S_{(2)}}/[S_{(2)}] + K_{S_{(1)}} K_{S_{(2)}}/([S_{(1)}][S_{(2)})]}$$

where  $K_{S_{(1)}}$  and  $K_{S_{(2)}}$  are the substrate constants for the addition of the first and second substrate molecules, respectively.

If the reaction is carried out at the saturating concentration of one of the substrates, the equation presented can be reduced to the Michaelis equation.

The non-productive binding of the substrate resulting in the formation of the  $ES'$  inactive complex according to the scheme



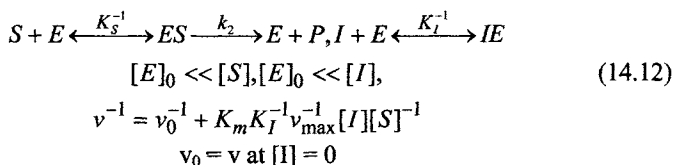
is described by the following expression for rate of substrate transformation:

$$v = \frac{k_2[E]_0[S]_0}{K_S + \left(1 + \frac{K_S}{K_I}\right)[S]_0} \quad (14.11)$$

#### 14.6. Inhibitors and activators in catalysis

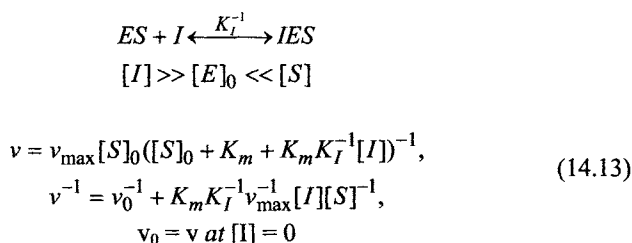
Effects of catalyst inhibition and activation are substantial for regulating their activity in complicated, in particular, physiological, systems. Inhibitor methods serve as a tool for studying the structure and mechanism of the catalytic effect of active sites. Below we describe the most often met types of inhibition and activation. The graphical methods for analysis of kinetic data are illustrated in Fig. 14.2.

**Reversible inhibition.** Competitive inhibition: inhibitor I competes with the substrate for the active site of enzyme



$K_I$  can be found from the slope of the straight line in the  $[v]^{-1}$ — $[S]_0^{-1}$  coordinates.

Competitive-less inhibition (Fig. 14.2, d): the inhibitor forms an inactive complex with the enzyme-substrate complex



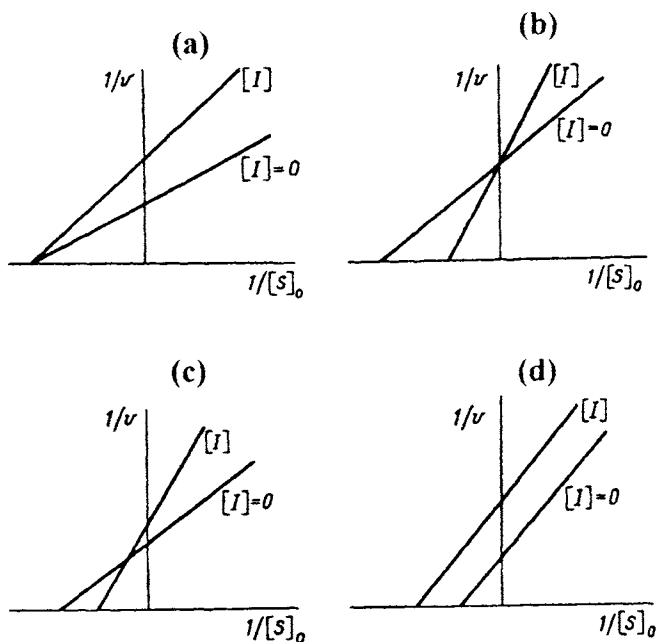
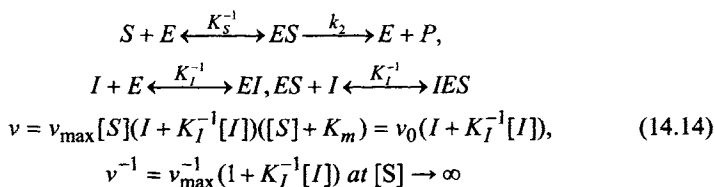
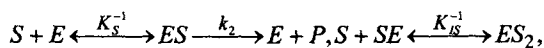


Fig. 14.2. Graphical representation of different inhibition mechanisms: a, non-competitive; b, competitive; c, mixed; and d, competitive-less inhibition.

Non-competitive inhibition (Fig. 14.2, a): addition of the inhibitor to the enzyme outside the active site to form the inactive form of the catalyst ( $[S] \gg [E]$ )



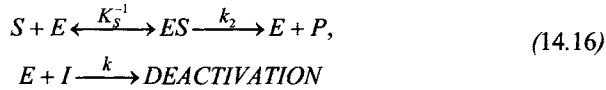
Non-competitive inhibition by substrate: the second substrate molecule affords the inactive complex with E



$$v = k_2[S][E]_0([S] + K_m + K_{IS}^{-1}[S]^2)^{-1},$$

$$\left\{ \frac{[S]}{v} - \frac{dv}{d[S]} \right\}^{-1} [S]^{-1} = (k_2[E]_0)^{-1} + K_{IS}^{-1} / (k_2[E]_0) \quad (14.15)$$

**Irreversible inhibition.** Inhibitors of this type react with the enzyme to irreversibly deactivate it. The enzyme activity decreases in time, unlike reversible inhibition when the degree of deactivation is time-independent under steady-state conditions



$$-\frac{dE}{dt} = K[I][E] = k[I][E](K_m + [S])^{-1} = k'[E] \quad (14.17)$$

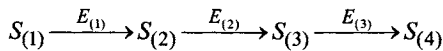
$$\text{At } [E]_0 \ll [S] \text{ and } [E]_0 \ll [I]$$

$$[E] = [E]_0 (K_m + [S])^{-1} e^{-kt},$$

$$v = k_2[E]_0[S](K_m + [S])^{-1} e^{-k't},$$

where  $t$  is the time from the moment of the enzyme mixing with the inhibitor to the moment of substrate addition.

**Allosteric inhibition** is the type of inhibition, which occurs in enzymatic systems catalyzing several successive reactions if the effect of one of the enzymes reacting in the beginning of the process is suppressed by one or several products of subsequent enzymatic reactions. For the system of three enzymes, we have



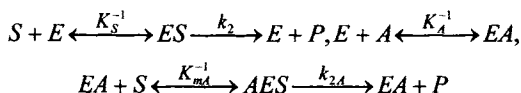
When the substrate of enzyme  $E_{(3)}$  simultaneously competitively inhibits enzyme  $E_{(1)}$ , the rates of substrate transformation are the following:

$$v_1 = \frac{v_{\max 1}[S_{(1)}]}{[S_{(1)}] + K_{m(1)}(1 + [S_{(3)}]K_I)}; v_2 = \frac{v_{\max 2}[S_{(2)}]}{[S_{(2)}] + K_{m(1)}}; \quad (14.18)$$

$$v_3 = \frac{v_{\max 3}[S_{(3)}]}{[S_{(3)}] + K_{m(1)}}$$

No inhibition occurs at  $v_{\max 3} \gg v_{\max}[S_{(3)}] \approx 0$ ; at  $v_{\max 3} \ll v_{\max 1}$ , the rate  $v_1 = v_{\max 3}$ .

**Reversible activation.** If activator A adds reversibly, in the simplest case we have



$$v = k_2 K_m^{-1} + k_{2A} K_{mA}^{-1} [A] [E]_0 [S] / (1 + K_m^{-1} [S] + K_A^{-1} [A] + K_{mA}^{-1} [A] [S]),$$

$$\frac{[E]_0}{v} = \frac{K_{mA}^{-1} + K_{mA}^{-1} K_A^{-1} [A]}{k_2 K_m^{-1} + k_{2A} K_{mA}^{-1} K_A^{-1} [A]} + \frac{1 + K_A^{-1}}{k_2 K_m^{-1} + k_{2A} K_{mA}^{-1} K_A^{-1} [A]} \frac{1}{[S]}$$

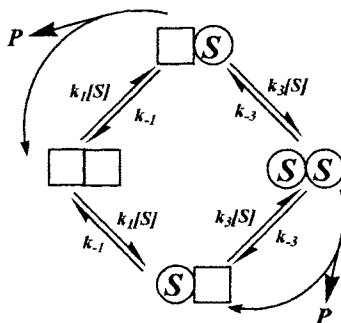
#### 14.7. Kinetics of cooperative processes

A cooperative system can be defined as a system of interacting elements. In this system, the thermodynamic state and rate of changing in this state for each element at any time moment depends, in the general case, on the state of all others. As applied to the enzymatic catalysis, mainly two senses are put into the concept of cooperativeness. First, enzymes including several catalytic or regulating centers are considered. It is assumed that the thermodynamic and kinetic parameters of chemical transformations on each center depend on the state (for example, degrees of coverage with reactants) of the others. Second, the enzyme is presented as a cooperative ensemble of component-elements, for example, amino acid moieties and water molecules. In both senses, the cooperativeness of the system is that the equilibrium constant  $K$  or rate  $k$  values of particular steps are considered dependent on the state of other elements of the system. Below we present examples illustrating the specific features of the kinetics of cooperative processes.

The term allosterism is widely used in enzymology. It characterizes the effect of mutual indirect influence of reactant-effectors (substrates, inhibitors, or activators) bound to different spatially separated centers of the enzyme. Let us consider two types of such systems.

*14.7.1. Homotropic allosteric systems with direct cooperativeness (Koshland, Nemeti, Volmer model or Volkenstein model)*

An enzyme macromolecule contains  $n$  identical sites (subunits). The thermodynamic and kinetic properties of each subunit depend on the fact whether the adjacent subunit is free or occupied with substrate molecules. The following scheme corresponds to the two-centered system in which the square designates the state of the subunit unoccupied with the substrate and the circle designates the state occupied with the substrate:



and

$$v = \frac{2k_2[E]_0[S](\beta K + \alpha[S])}{\beta K^2 + 2\beta K[S] + [S]^2} \quad (14.19)$$

where  $\alpha = k_4/k_2$ ,  $\beta = K'K$ ,  $K = (k_1 + k_2)$  and  $K' = (k_3 + k_4)/k_3$ .

Cooperativeness appears at  $\alpha \neq 1$  and  $\beta \neq 1$ .

Conditions for the inflection point in the  $v(S)$  curve:

$\alpha < 0.5$  and any  $\beta$ ; (2)  $1 > \alpha > 0.5$  and  $\alpha / (2\alpha + 1) > \beta > \alpha^2 / (2\alpha - 1)$ ; (3)  $\alpha > 1$  and  $\alpha^2 / (2\alpha^2 - 1) > \beta > \alpha(2\alpha - 1)$ .

The maximum is possible at  $\alpha < 0.5$  and any  $\beta$ .

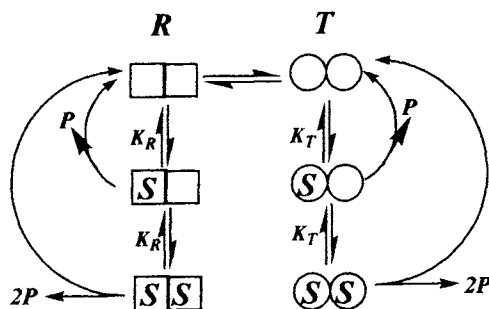
The so-called Hill coefficient characterizing the sharpness of changing the  $v(S)$  function is described by the expression

$$n = \frac{d \log[v_{\max} / (v_{\max} - v)]}{d \log[S]} \quad (14.20)$$

At small  $[S]$   $n = 2$ ; for the system of  $m$  identical centers  $n = m$ . The coefficient can be used to estimate the number of centers in the system.

#### 14.7.2. Homotropic system with indirect cooperativeness (Mono, Shanzhe and Wineberg model)

A dimer from a subunit, as a whole, can exist in two or several symmetrical conformational state,  $R$  and  $T$ ; the ligand affinity characterized by the equilibrium constants  $K_R$  and  $K_T$  changes with changing the state of oligomer



The mathematical expression for the process rate  $v$ , depending on  $[S]$ , resembles, in general, equation (16.20). The distinction is the absence of the linear term with respect to  $[S]$  in the denominator and its presence in the nominator. As shown for  $O_2$  binding with hemoglobin, it is difficult to choose between the models in the multi-centered systems from the kinetic data only.

### 14.7.3. Allosteric interactions in dissociating enzymatic systems

The dissociation process of catalyst (enzyme) molecules to subunits can change the reactivity of active sites (Kurganov B.I). Therefore, the catalyst activity can be controlled by changing its concentration and varying concentrations of substrates, inhibitors, and environmental conditions.

For the simplest system in which the catalyst dissociates to two subunits  $e$ :  $E \longleftrightarrow 2e$  and the rate of equilibrium establishment is higher than that of the catalytic reaction, the overall catalytic activity  $a$  depends on the specific activities of dimer  $a_1$  and monomer  $a_2$ , equilibrium rate constant  $K_0$ , and initial concentration of the enzyme  $[E]_0$

$$a = a_1 + (a_2 - a_1) \frac{\sqrt{1 + 8K_0[E]_0} - 1}{\sqrt{1 + 8K_0[E]_0} + 1} \quad (14.21)$$

The experimental plot of the reaction rate vs. initial enzyme concentration is a criterion for the dissociative mechanism. The shift of the equilibrium due to different bindings of the substrate by the dimer and monomer results in the deviation from the simple Michaelis equation because the effective binding constant  $K$  becomes a function of the local Michaelis constants for the dimer  $K_{mE}$  and monomer  $K_{me}$  and initial substrate concentration  $[S]_0$

$$K_{\text{exp}} = K_0 \frac{1 + [S]_0/K_{mE}}{1 + [S]_0/K_{me}} \quad (14.22)$$

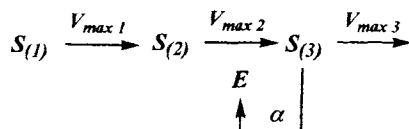
The  $K$  value depends analogously on the corresponding binding constants  $K_{FE}$  and  $K_{Fe}$  and concentration of the effector  $[F]_0$  (inhibitor or activator)

$$K_{\text{exp}} = K_0 \frac{1 + [S]_0/K_{mE}}{1 + [S]_0/K_{me}} \frac{1 + [F]_0/K_{FE}}{1 + [F]_0/K_{Fe}} \quad (14.23)$$

As follows from equation (14.22), if  $K_{FE}K_{Fe} < [F]_0$ , at certain ratios of the inhibition (activation) constants either positive or negative cooperative effects can be observed: depending on the fact which form of the catalyst, dimeric or monomeric, is more catalytically active and more strongly binds effector molecules.

#### 14.7.4. Oscillation allosteric catalytic processes

Oscillations of transformation rates and substrate concentrations in time appear in catalytic chains under certain conditions in the presence of a feedback between particular catalytic reactions. Let us consider the following reaction as an example:



where  $v_{\max 1}$ ,  $v_{\max 2}$ , and  $v_{\max 3}$  are the maximum rates of the corresponding stages described by the simple Michaelis equations and constants  $K_{m1}$ ,  $K_{m2}$ , and  $K_{m3}$ ;  $\alpha$  is the coefficient taking into account the degree of activation of the catalyst for the transformation  $S_{(2)} \rightarrow S_{(3)}$  by the product  $S_{(3)}$  with the constant  $K_{m\alpha} = [S_{(3)}]/(K_{m\alpha} + [S_{(3)}])$ .

In the simplified case when the transformation  $S_{(1)} \rightarrow S_{(2)}$  occurs with the constant rate  $v_1$  and  $[S_{(i)}] \ll K_{mi}$ , the following equations are valid:

$$\begin{aligned}
 \frac{d[S_{(2)}]}{dt} &= v_{\max 1} - v_{\max 2} \frac{[S_{(2)}]}{K_{m2}} \frac{[S_{(3)}]}{K_{m\alpha}[S_{(3)}]}, \\
 \frac{d[S_{(3)}]}{dt} &= v_{\max 2} \frac{[S_{(2)}][S_{(3)}]}{K_{m2}K_{m\alpha}} - v_{\max 3} \frac{[S_{(3)}]}{K_{m3}}
 \end{aligned}$$

Analysis of these equations indicates a possibility of different oscillation regimes, which are qualitatively illustrated in Fig. 14.3. The main reason for the appearance of oscillations is the presence of the feedback, which is the activation of the catalyst E with the substrate  $S_{(3)}$ .

An increase in the concentration of this substrate results in the autocatalytic acceleration of the substrate  $S_{(2)}$  consumption. The catalytic process almost ceases when the concentration of this substrate decreases substantially. Then the continuing feed of the substrate  $S_{(2)}$  and consumption of the substrate  $S_{(3)}$  again bring the system to the autocatalytic regime. Such cycles can multiply be repeated.

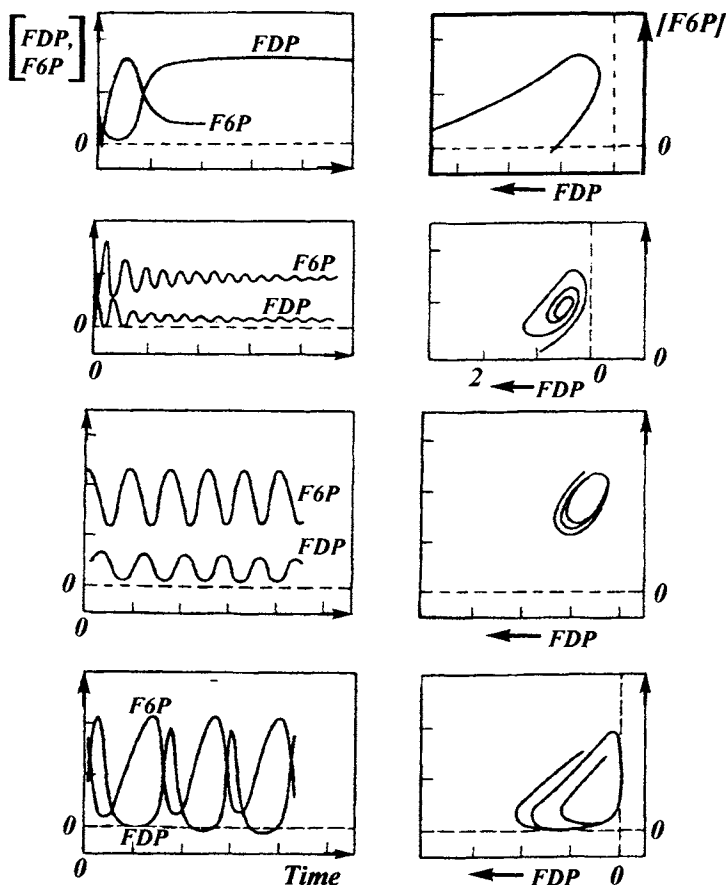


Fig. 14.3. Time plots of the substrate concentrations (a) and the corresponding bifurcation plots. Curves of oscillation regimes (b) in the system with the feedback (FDP is fructosodiphosphate, F6P is fructoso-6-phosphate).

#### 14.8. On the methods of studying the mechanism of catalytic reactions

The formal kinetics methods in combination with methods of detection of fast processes, as shown above, make it possible to establish the sequence and rate constants of individual steps of the catalytic process. The next stage of research is the establishment of occurrence of each step.

Among approaches to the establishment of reaction mechanisms, we can distinguish direct ones, associated with the direct detection of intermediate radical, ionic, or molecular species during the chemical reaction, and indirect methods.

In indirect methods researchers use experimental dependence of the rates of the process or individual steps on the steric and electronic properties of substrates and inhibitors, on the polarity, donor-acceptor ability of the solvent, ionic strength, various additives reacting with intermediate species (for example, radicals), etc. The methods for quantitative account of some of these effects are presented in chapters considering the factors influencing the rate of chemical reactions and correlations. Let us concentrate our attention on two approaches, which are significant for the establishment of the mechanism: isotope substitution method and measurement reaction rates in magnetic fields. The application of the first method is traditional in catalysis. The use of the second method has just been started.

The thermodynamic and kinetic isotope effects are mainly due to the differences in frequencies of isotope vibrations in the initial, transition, and final states (Chapter 8). The tunneling isotope effects become considerable, for example, when vibrational frequencies of bonds near the activation barrier exceed  $1000\text{ cm}^{-1}$  at the barrier value  $E > 20RT$ . Under these conditions, a proton tunnels approximately twofold more rapidly than deuterium. The tunneling isotope effect increases substantially with the temperature decrease.

According to estimations from the Marcus equations, the replacement of hydrogen by deuterium in water results in the isotope effect of increasing the electron transfer rate due to a change in the energy of medium reorganization. At room temperature the rate changes by 1.5—2 times. The dependence of the reaction rate on the concentration of  $D_2O$  in the sample is used to establish the number of protons involved in the limiting step. If the change in the rate is proportional to the concentration of  $D_2O$ , at this step one proton adds or eliminates. The second order indicates the participation of two protons.

In pH depending reactions, enzymatic reactions for instance, one has to take into account that when  $H_2O$  is replaced by  $D_2O$  the concentration of hydrogen ions changes, which is described by the equation  $pH = pD + 4$ , and  $pK_a$  of active groups increases by 0.2—0.5.

A new type of the isotope effect, viz., magnetic isotope effect, has recently been discovered. The theory of influence of the magnetic field on the rate of chemical reactions is based on the fundamental law of angular momentum conservation. Naturally, this law also concerns the intrinsic angular momentum of electrons and nuclei (spin). Therefore, any changes in the total spin are

forbidden in systems without interactions of electron spins with orbital momentum or with spins of nuclei. This prohibition is partially lifted when the interactions above are present because channels appear for angular momentum transmittance to other electrons and nuclei. The efficiency of electron-nuclear, spin-spin, and spin-orbital interactions depends on the magnetic field intensity. These interactions cause the influence of the magnetic field on chemical processes, whose rate depends on the population of certain spin states of the system.

Consider the problem about the mechanism of influence of the magnetic field for the recombination of the radical pair  $A\downarrow + B\uparrow \rightarrow A\uparrow\downarrow B$ . Figure 14.4 illustrates the influence of the external magnetic field intensity  $H_0$  on the process, whose rate is proportional to the population of the singlet level in the radical pair. This process can be exemplified by the back recombination of charge separation from the singlet state in photosynthesis, which is detected by the delayed fluorescence. In the absence of the magnetic field ( $H_0 = 0$ ), the triplet level  $T$  is degenerate.

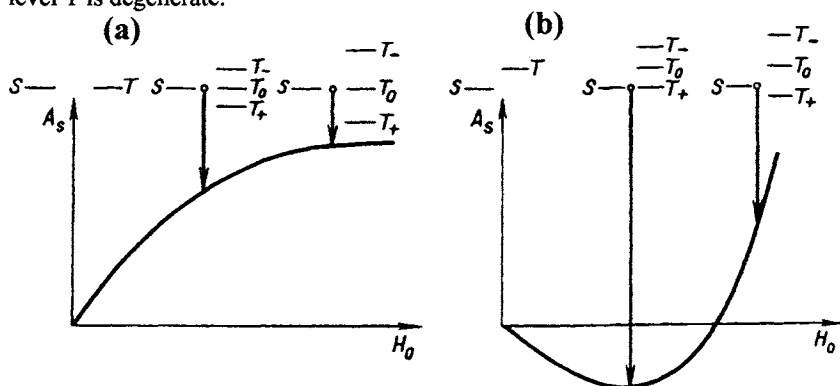


Fig. 14.4. Influence of the permanent magnetic field on the population of the singlet level  $A_S$  dependent of the rate of singlet-triplet transition  $S \rightarrow T$  in the radical pair: a, in the absence of exchange interaction ( $J = 0$ ); b, for exchange interaction ( $J > 0$ ).

When the magnetic field is applied, the  $T$  level is split into three levels:  $T_+$ ,  $T_0$ , and  $T_-$ . The efficiency of the transition  $S \rightarrow T$  decreases due to the differences in the  $k_{S \rightarrow T}$  values for transitions to different triplet levels. The  $S \rightarrow T_0$  transition is more efficient than those to other levels. With an increase in the field intensity  $H_0$  the  $T_+$  and  $T_-$  levels more and more remove from the initial state (the position of  $T_0$  remains unchanged) and thus make a smaller contribution to the  $S \rightarrow T$  transition. The relative population of the  $S$  level

increases, and the recombination rate enhances. With the further increase in  $H_0$  the  $T_+$  and  $T_-$  levels become so remote that the  $S \rightarrow T_{\pm}$  transition becomes insignificant, that is, the recombination rate becomes insensitive to the change in  $H_0$ .

The qualitatively different situation is observed for a sufficiently strong exchange interaction between the components of the radical pair. In this case, in the absence of magnetic field, the energy levels of the system are split into two levels: singlet  $S$  and triplet  $T$  with the energy difference equal to  $2J$ . The magnetic field application splits the triplet levels and approaches the  $T_+$  level to the  $S$  level. This favors an increase in the probability of the  $S \rightarrow T_+$  transition, a decrease in the relative population of  $S$ , and, hence, a decrease in the recombination rate  $v$  (minimum). With the further increase in  $H_0$  the  $S$  and  $T_+$  levels begin to remote, and the  $v(H_0)$  dependence is saturated in the limit. The minimum point satisfies the equality  $J = h^{-1}g\beta H_{min}$ , which can be used for the calculation of  $J$ .

Nuclear polarization effects on the rate of enzymatic reactions contributes significantly to the investigation of the kinetics and mechanism of electron transfer processes in catalytic systems.

Recently, new approaches and new twist of traditional methods of investigation intermediates in chemical homogeneous catalysts and enzymes have been developed. These methods include nano-, pico- second, and femto-second time resolved optical, fluorescence and Resonance Raman techniques, Fourier-transform Infrared Spectroscopy, nano-second T-jump, pulse and high resolution ESR, method of transition state analogues (transition state discrimination inhibitors), chemical trapping of enzyme-substrates intermediates, monitoring enzymes reactions with mass spectrometry, affinity and photoaffinity labelling methods. Ways of regulation of enzyme activity, specificity and stability by the site-directed mutagenesis, chemical modification and use of organic solvents have been developed.

One of the most promising approaches for elucidation of enzyme catalytic mechanisms and designing new catalysts is a "directed evolution", method of purposeful mutation of non-enzymatic proteins to evolve desired activity mimicking native enzymes. Another important trend in chemical and enzyme catalysis is the growing role of theoretical calculation of thermodynamic parameters of enzyme reactions, computer analysis of X-ray structural models, taking from Data Base, computer modeling of structure of chemical catalysts and enzymes and their interaction with substrates and inhibitors, and theoretical construction of transition and pretransition states of reactions of interest.

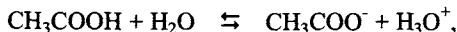
The modern kinetic methods make it possible to establish the sequence of steps of enzymatic processes, measure the rate constants of particular stages in an interval of  $10^{-4}$  to  $10^{+12} \text{ s}^{-1}$ , and study the mechanisms of elementary steps and estimate the thermodynamic possibility of their occurrence.

## Acid-base catalysis

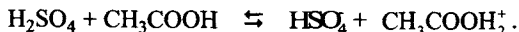
### 15.1. Acids and bases

Reactions involving acids and bases represent a very large and important section of modern chemistry. They are widely used in chemical synthesis and technology, and many biochemical reactions occur with participation of acids. Charge transfer reactions occupy the central place in this area.

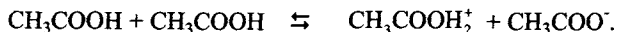
J.N. Brönsted gave (1923) the classical definition of acids. An acid is a compound capable of donating a proton, and a base is a compound capable of withdrawing a proton. Protic acids (Brönsted acids) include oxygen-containing inorganic acids ( $\text{H}_2\text{SO}_4$ ,  $\text{HNO}_3$ ,  $\text{HClO}_4$ , and others), hydrogen halides, organic oxygen-containing acids  $\text{RCOOH}$  ( $\text{HCOOH}$ ,  $\text{CH}_3\text{COOH}$ , etc.), phenols ( $\text{C}_6\text{H}_5\text{OH}$ ,  $\text{NO}_2\text{C}_6\text{H}_4\text{OH}$ , and others), alcohols, diketones in the enolic form, nitro compounds, for example,  $(\text{NO}_2)_3\text{CH}$ ,  $\text{HCN}$ , and other hydrogen-containing compounds including hydrocarbons. A molecule (for example,  $\text{HCl}$ ), anion (for example,  $\text{HSO}_4^-$  and  $\text{H}_2\text{PO}_4^-$ ), and cation (for example,  $\text{NH}_4^+$ ) can act as an acid. Molecules with a lone electron pair ( $\text{H}_2\text{O}$ ,  $\text{NH}_3$ ,  $\text{R}_3\text{N}$ ,  $\text{R}_2\text{O}$ ,  $\text{ROH}$ ,  $\text{C}_6\text{H}_6$ ,  $\text{R}_3\text{P}$ ) and anions, such as  $\text{SO}_4^{2-}$ ,  $\text{CH}_3\text{CO}_2^-$ ,  $\text{OH}^-$ , act as bases. Acid  $\text{HA}$  manifests itself as a proton donor only in the presence of base  $\text{B}$ , so that the proton transfer is a reaction of the type  $\text{B} + \text{HA} \rightleftharpoons \text{BH}^+ + \text{A}^-$  in which  $\text{HA}$  donating a proton is transformed into the acid  $\text{BH}^+$ . Depending on the partner, the same substance can behave as either an acid or a base: for example, in an aqueous solution acetic acid acts as an acid donating a proton to the solvent :



However, when sulfuric acid is dissolved in anhydrous acetic acid, the latter acts as a base:

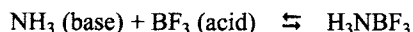


In autoprotolysis  $\text{CH}_3\text{COOH}$  also acts as both an acid and a base according to the dissociation equilibrium



The study of solid hydrates of strong acids, such as nitric, chloric, and sulfuric acid, showed that a proton, being added to water, forms the  $\text{H}_3\text{O}^+$  ion with the planar or oblate pyramidal structure. The bond between the proton and water molecule is very strong. According to the estimation from the thermodynamic cycle, it is 710 kJ/mol (in the gas phase). The heat of dissolution of  $\text{H}_3\text{O}^+$  in water is estimated as 380 kJ/mol. In an aqueous solution, as shown by spectral studies, the  $\text{H}_5\text{O}_2^+(\text{H}_2\text{OH}_2^+)$  ion is most stable. Superacids, for example,  $\text{HSbF}_6$  and  $\text{HSO}_3\text{SbF}_6$ , are very active proton donors in nonaqueous solutions.

Aprotic acids (Lewis acids) exist (and are used as catalysts) along with protic acids. Lewis acid is a substance capable of being an acceptor for an electron pair of a base. Lewis acids:  $\text{BF}_3$ ,  $\text{AlCl}_3$ ,  $\text{SO}_3$ ,  $\text{Ag}^+$ ,  $\text{H}^+$ . Lewis bases are substances that act as donors of an electron pair, for example,

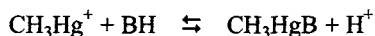


The definitions of a base according to Brönsted (proton acceptor) and Lewis (electron pair donor in the reaction with an acid) virtually coincide. However, the definitions of an acid diverge, as we can see. The Brönsted acid is a proton donor, and the Lewis acid is an acceptor of a base (a substance bearing an unshared electron pair).

Pearson introduced (1966) a concept of hard and soft acids and bases. Hard acids form more stable compounds with hard bases, and soft acids form more stable compounds with soft bases.

Bases	
Hard	Soft
$\text{H}_2\text{O}$ , $\text{OH}^-$ , $\text{CH}_3\text{COO}^-$ , $\text{ROH}$ , $\text{RO}^-$ , $\text{RO}_2^-$ , $\text{NH}_3$ , $\text{RNH}_2$ , $\text{F}^-$ , $\text{Cl}^-$ , $\text{PO}_4^{2-}$	$\text{R}_2\text{S}$ , $\text{RSH}$ , $\text{RS}^-$ , $\text{I}^-$ , $\text{SCN}^-$ , $\text{R}_3\text{P}$ , $\text{CN}^-$ , $\text{C}_2\text{H}_4$ , $\text{C}_6\text{H}_6$ , $\text{H}^-$ , $\text{R}^-$
Acids	
$\text{H}^+$ , $\text{Li}^+$ , $\text{Na}^+$ , $\text{K}^+$ , $\text{Mg}^{2+}$ , $\text{Ca}^{2+}$ , $\text{Al}^{3+}$ , $\text{BF}_3$ , $\text{AlCl}_3$ , $\text{RCO}^+$	$\text{Cu}^+$ , $\text{Ag}^+$ , $\text{Hg}^+$ , $\text{Pd}^{2+}$ , $\text{CH}_3\text{Hg}^+$ , $\text{I}_2$ , $\text{Br}_2$ , $\text{ICN}$

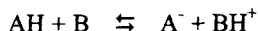
The degree of hardness or softness is determined in an aqueous solution by the state of equilibrium:



Here  $\text{CH}_3\text{Hg}^+$  is the soft acid, and  $\text{H}^+$  is the hard acid. If  $K > 1$ , base B is soft, and when  $K > 1$ , the base is hard.

### 15.2. Acid-base equilibrium

Equilibrium proton transfer in the general form is the reaction of the following type:



The water molecule acts as a base in an aqueous solution, dissociation constant  $K_a = [\text{A}^-][\text{H}_3\text{O}^+]/[\text{HA}]$ .

The dissociation of acids to anions in aqueous solutions is due to a high energy of ion hydration. In a vacuum water dissociation to  $\text{H}^+$  and  $\text{OH}^-$  requires an energy of 1630 kJ/mol, whereas in the liquid phase the dissociation of water occurs with an expense of 60 kJ/mol only. When the hydration of protons is presented as a stepwise process, the change in the enthalpy by steps is the following:



Total energy release due to  $\text{H}^+$  hydration is  $\sim 1090 \text{ kJ/mol}$ , and 540 kJ/mol is liberated due to the hydration of the hydroxyl ion. The stable state in an aqueous solution is the  $\text{H}_5\text{O}_2^+$  ion in which the proton is fluctuated between two oxygen atoms of two water molecules.

Strong acids and bases in strongly dilute aqueous solutions are completely dissociated. The situation is more complicated in concentrated solutions where the solution is characterized by *acidity*  $h_0$ . It is determined from the degree of protonation of the reference base B, which is introduced into the solution in a very low concentration

$$h = K \frac{[\text{BH}^+]}{[\text{B}]} = \frac{a_{\text{H}_3\text{O}^+}}{a_{\text{H}_2\text{O}}} \frac{\gamma_{\text{B}}}{\gamma_{\text{BH}^+}} \quad (15.1)$$

where  $a$  are activities, and  $\gamma$  are activity coefficients.

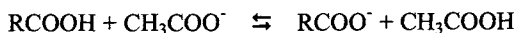
Nitroaniline and its derivatives are used as indicators. *Acidity function*  $H_0 = -\log h_0$  for mixtures of sulfuric acid with water has the following values:

% $\text{H}_2\text{SO}_4$ .....	10	30	50	75	85	95	100
$H_0$ .....	-0.31	-1.72	-3.38	-6.56	-8.14	-9.85	-12.2

Such a wide range of changing  $h_0$  (12 orders of magnitude) can be covered due to a high change in  $pK_a$  of nitroanilines used as indicators, depending on substituents in the molecule. For example, for *m*-nitroaniline  $pK_a = 2.50$ , for 2,4-dinitroaniline

$pK_a = -4.53$ , and for 2,4,6-trinitroaniline  $pK_a = -10.10$ . Acidity function  $H_0$  was introduced by Hammett and named after him. In later studies, other classes of base-indicators were also used for the determination of  $H_0$  and different acidity values of concentrated solutions of acids were obtained ( $H^{\text{III}}$  for indicators N,N-dialkylnitroanilines,  $H_I$  for alkylated indols,  $H_A$  for amides of acids, and  $H_R$  for triphenylcarbinols).

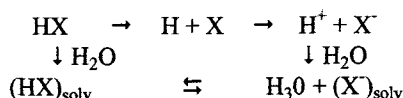
Dissociation of acids and bases is accompanied by a change in thermodynamic parameters. For example, the dissociation of acetic acid in  $H_2O$  at 298 K is characterized by  $\Delta H = -0.46$ ,  $T\Delta S = -27.6$ , and  $\Delta G = 27.14$  kJ/mol. For an uncharged base (for example,  $H_2O$ ) the thermodynamic parameters are determined by the acid structure. Below we present these values ( $T = 298$  K) for several acids at equilibrium of the type



R.....	$(CH_3)_3C$	H	$ClCH_2$	$C_6H_5$	$n-C_6H_4NO_2$
$\Delta G_0$ .....	1.55	-5.77	-10.78	-3.13	-7.52
$\Delta H^0$ .....	-2.55	0.29	-4.22	2.21	0.58
$T\Delta S$ .....	-4.10	6.06	6.56	5.35	8.11
$pK_a$ .....	5.03	3.75	2.87	4.21	3.44

It is seen that alkyl substituents impede the dissociation of carboxylic acid, and the Cl substituent in chloroacetic acid facilitates its dissociation ( $\Delta G = -11$  kJ/mol). Evidently, this is the result of charge delocalization on the  $ClCH_2COO^-$  anion decreasing the energy of anion formation.

Haloid acids strongly differ in degree of dissociation. Using them as an example, it is fruitful to analyze factors that influence the enthalpy of dissociation of these compounds in a vacuum and in an aqueous solution considering the following cycle:



Below we present  $D_{HX}$ ,  $E_X$  (electron affinity of X), enthalpies (in kJ/mol) of dissociation of HX to ions in the gas ( $\Delta H_g^0$ ) and water  $\Delta H_{H_2O}^0$ , enthalpies of hydration of HX,  $\Delta H_{HX}^0$  and  $pK_a$

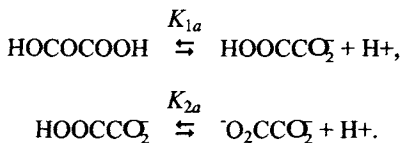
	HF	HCl	HBr	HI
$D_{HX}$ .....	568	430	368	297
$E_X$ .....	334	347	326	297
$\Delta H_g^0$ .....	1547	1392	1354	1312
$\Delta H_{H_2O}^0$ ...	0	-50	-50	-46
$\Delta H_{HX}^0$ .....	-50	-17	-21	-25
$pK_a$ .....	3	-7	-9	-10

As can be seen, HF differs substantially in degree of dissociation from other haloids. This is mainly due to the fact that  $D_{\text{HX}}$  for HF is much higher than those for other HX and, hence, its  $\Delta H_{\text{H}_2\text{O}}^0$  is much higher than those for other hydrogen halides.

The degree of dissociation of inorganic oxy acids  $\text{XO}_n(\text{OH})_m$  depends, naturally, on the nature of X. It depends very strongly on the number of oxygen atoms  $n$  and is virtually independent of the number of carboxyl groups  $m$ . It is seen from the following comparison (the  $\text{p}K_a$  values in  $\text{H}_2\text{O}$  at  $T = 298 \text{ K}$  are given in parentheses):  $\text{ClOH}$  (7.2),  $\text{ClO}(\text{OH})$  (2.0),  $\text{ClO}_2(\text{OH})$  (-1.0),  $\text{ClO}_3(\text{OH})$  (-10);  $\text{SO}(\text{OH})_2$  (1.99),  $\text{SO}_2(\text{OH})_2$  (< 0);  $\text{SeO}(\text{OH})_2$  (2.6),  $\text{SeO}_2(\text{OH})_2$  (< 0);  $\text{NO}(\text{OH})$  (3.3),  $\text{NO}_2(\text{OH})$  (-1.4);  $\text{PO}(\text{OH})_3$  (2.1),  $\text{HPO}(\text{OH})_2$  (1.8),  $\text{H}_2\text{PO}(\text{OH})$  (2.0);  $\text{IOH}$  (10.0),  $\text{IO}(\text{OH})_5$  (1.6).

Such a strong effect of the groups ( $\text{Y}=\text{O}$ , where Y is nonmetal) on  $\text{p}K_a$  of acids is explained according to the electrostatic model by the fact that the larger the volume of the ion, the lower the Gibbs energy of anion formation. The quantum theory explains the stabilization of oxygen-containing anions by a decrease in the energy of the molecular orbital due to the delocalization of electrons of the anion over several bonds.

Polyatomic acids are characterized by multistep dissociation, e.g.



The second dissociation constant is always lower than the first one:

Acid.....	Oxalic	Malonic	Succinic	Adipic
$\text{p}K_{1a}$ .....	1.23	2.83	4.19	4.42
$\text{p}K_{2a}$ .....	4.19	4.69	5.48	5.41

This distinction is related to the fact that the energy of formation of the bicharged anion is higher than that of the monocharged anion due to the energy of mutual repulsion of two negative charges.

Paraffinic hydrocarbons do not possess acidic properties. These properties are manifested by aromatic hydrocarbons. For example, indene reacts as an acid with strong bases, its  $\text{p}K_a$  is estimated as 18-23 units. The acidity increases when some electron-acceptor group, e.g., is included into the composition of the hydrocarbon molecule. For example, for acetone  $\text{p}K_a = 20$ . The inclusion of two carbonyl groups into the molecule enhances its acidic properties. For example, for acetylacetone  $\text{CH}_3\text{COCH}_2\text{COCH}_3$   $\text{p}K_a = 9$ , and for ketoester  $\text{CH}_3\text{COCH}_2\text{COOC}_2\text{H}_5$   $\text{p}K_a = 10$ . Acidic dissociation is characteristic of nitro compounds (for  $\text{CH}_3\text{NO}_2$   $\text{p}K_a = 10$ ) and

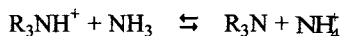
acid nitriles:  $\text{CH}_3\text{CN}$   $\text{p}K_a = 25$ ,  $\text{CH}_2(\text{CN})_2$   $\text{p}K_a = 11.2$ , and  $\text{CH}(\text{CN})_3$   $\text{p}K_a = -5$ .

Aromatic compounds in the electron-excited state possess a higher acidity than in the ground state. Acidity also depends on the fact whether the excited state is triplet or singlet. This is illustrated by the following examples ( $\text{p}K_a$  values are presented):

	$S_0$ state	$S_1$ state	$T$ state
$\beta$ -Naphthol.....	9.5	3.1	7.9
$\beta$ -Naphthoic acid.....	4.2	6.6	4.1
$\beta$ -Naphthylammonium....	4.1	-2	3.2

For bases, as for acids, the degree of dissociation and its thermodynamic parameters depend on the structure.

The dissociation of the ammonium ion ( $\text{NH}_4^+ \rightleftharpoons \text{NH}_3 + \text{H}^+$ ) in water is characterized by the parameters  $\Delta G = 52.71$ ,  $\Delta H = 51.83$ , and  $T\Delta S = -0.88$  kJ/mol at  $T = 298$  K. Below we present the thermodynamic parameters for several amines in an aqueous solution at equilibrium of the type ( $T = 298$  K)

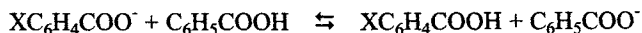


$\text{R}_3\text{N}....$	$\text{CH}_3\text{NH}_2$	$(\text{CH}_3)_2\text{NH}$	$(\text{CH}_3)_3\text{N}$	$\text{PhNH}_2$	$\text{o-ClC}_6\text{H}_4\text{NH}_2$	$\text{cis-C}_5\text{H}_{10}\text{NH}$
$\Delta G^\circ....$	7.82	8.82	3.22	-26.50	-37.70	10.57
$\Delta H^\circ....$	2.88	2.17	-14.92	-22.10	-22.10	1.67
$T\Delta S^\circ..$	-4.93	-10.99	-18.14	4.40	10.95	8.90
$\text{p}K_b....$	10.62	10.77	9.80	4.60	2.63	11.12

It can be seen that, depending on the amine structure,  $\Delta G$  changes in a wide interval from +10 to -38 kJ/mol.

Dissociation of acids and bases depends very strongly on the solvent. The solvent SH often acts itself as an acid, and the strength of the dissolved base or acid depends on its acid-base properties. Acetonitrile is a weaker acid and base than water, its ion product being  $3 \cdot 10^{-29}$ . Therefore, in acetonitrile HBr, HCl, and  $\text{H}_2\text{SO}_4$  dissociate incompletely, unlike their dissociation in water. In acetonitrile  $\text{p}K_a = 5.5$  for HBr, 7.3 for  $\text{H}_2\text{SO}_4$ , and 8.9 for HCl. Thus, acetonitrile is a differentiating solvent. Carboxylic acids also dissociate in it to a lower extent than in water: the difference between  $\text{p}K_a$  of  $\text{CH}_3\text{CN}$  and  $\text{H}_2\text{O}$  is 14.

The dielectric constant of the medium has a substantial effect on acid dissociation in solvents of the same type. This aspect was studied in detail for substituted benzoic acids at equilibrium of the type



Water and several alcohols served as solvents. In the framework of the electrostatic model for media with different  $\epsilon$ , the equilibrium constant is related to the radii

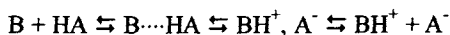
of the anions  $r_o$  and  $r$  by the correlation

$$\ln K = \ln K_{\infty} + \frac{E^2}{2kT\epsilon} \left( \frac{1}{r_o} - \frac{1}{r} \right) \quad (15.2)$$

According to this, we observed, in fact, a linear dependence between  $\ln K$  and  $1/\epsilon$  with a positive or negative slope. For *m*-nitrobenzoic acid, *e.g.*, this dependence has the form

$$\ln K = 0.48 + 30.2\epsilon^{-1} \quad (15.3)$$

In aprotic solvents with low  $\epsilon$  the acid and base form associates by the hydrogen bond and ion pairs

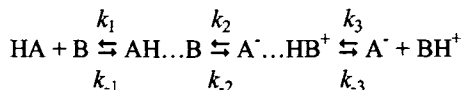


In these cases, the acid-base equilibrium is characterized by several equilibrium constants.

### 15.3. Proton transfer rate constants

Proton transfer reactions occur, as a rule, very promptly. Special methods were developed to measure rates of these reactions: methods of temperature jump, pressure drop, electric field pulse, and dielectric absorption; ultrasonic method; several electrochemical methods, and method of absorption line broadening of protons and  $^{17}\text{O}$  in NMR spectra (see Chapter 8). These methods allow the measurement of rate constants of bimolecular reactions in the  $10^6$ – $10^{11}$  l/(mol·s) interval. Results of measurements by different methods sometimes diverge dramatically. For example, for the reaction of  $\text{H}_3\text{O}^+$  and  $\text{CH}_3\text{COO}^-$  the rate constant values obtained by different electrochemical methods lie in an interval of  $(1.9) \cdot 10^{10}$  l/(mol·s) ( $\text{H}_2\text{O}$ , 298 K).

The transfer of a proton from an acid to base occurs in a solution by several steps and can be presented by the following scheme:

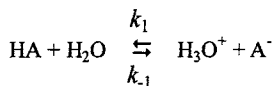


The experimentally measured rate constants of the forward ( $k_{AB}$ ) and backward ( $k_{BA}$ ) reactions have the form

$$k_{AB} = k_1 k_2 k_1 / \Sigma, \quad k_{BA} = k_3 k_2 k_{-1} / \Sigma, \quad \Sigma = k_3 k_{-1} + k_{-1} k_2 + k_3 k_2$$

At a very fast proton transfer in the  $\text{AH} \cdots \text{B}$  pair the equilibrium is established

between  $\text{AH}\cdots\text{B}$  and  $\text{A}^-\cdots\text{HB}^+$ , so that  $[\text{A}^-\cdots\text{HB}^+]/[\text{AH}\cdots\text{B}] = K_2 = k_2/k_{-2}$ . In addition, in many cases,  $k_1 \approx k_{-3}$ , *i.e.*, particles leave the cage with close diffusion rate constants. In these cases,  $k_{\text{AB}} = 0.5k_1K_2$  and  $k_{\text{BA}} = 0.5k_{-3}K_2^{-1}$ . The collision frequency of particles is substantially affected by their electric charges and dielectric constant of the solvent (see Chapter 8): unlike charges meet more often and like charges meet more rarely than neutral particles (rate constant  $k_{\text{D}}$ ). Proton transfer rate constants in water ( $T = 298 \text{ K}$ ) for several weak acids measured by electrochemical methods are presented below.



HA.....	HCOOH	CH <sub>3</sub> COOH	ClCH <sub>2</sub> COOH	Picolinic	Maleic	H <sub>3</sub> BO <sub>3</sub>
$k_1, \text{s}^{-1}$ .....	$6 \cdot 10^4$	$5 \cdot 10^5$	$2 \cdot 10^6$	$1 \cdot 10^6$	$3 \cdot 10^8$	$1 \cdot 10^3$
$k_2, \text{l}/(\text{mol} \cdot \text{s})$ .	$1 \cdot 10^9$	$2 \cdot 10^{10}$	$1 \cdot 10^{10}$	$7 \cdot 10^{10}$	$2 \cdot 10^{10}$	$2 \cdot 10^{12}$

It is seen that ion association occurs with the diffusion rate constant of an order of  $10^{10 \pm 1} \text{ l}/(\text{mol} \cdot \text{s})$ . The transfer of a proton from an acid to a water molecule requires an energy ( $\Delta G > 0$ ) and occurs, therefore, more rapidly or slowly. The following rule can be used for the approximate estimation of the proton transfer rate constant in the transition states  $\text{O}\cdots\text{H}-\text{O}$ ,  $\text{N}\cdots\text{H}-\text{O}$ , and  $\text{N}\cdots\text{H}-\text{N}$  in aqueous solutions:

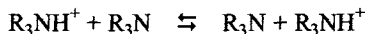
$$k \approx 10^{10} \text{ l}/(\text{mol} \cdot \text{s}) \text{ at } \text{p}K_{\text{a}} > 0,$$

$$k < 10^{10} \text{ l}/(\text{mol} \cdot \text{s}) \text{ at } \text{p}K_{\text{a}} < 0.$$

The proton transfer from the ammonium ion to hydroxyl ( $\text{H}_2\text{O}$ ,  $298 \text{ K}$ , NMR method) occurs very promptly

Ion.....	$\text{NH}_4^+$	$\text{CH}_3\text{NH}_3^+$	$(\text{CH}_3)_2\text{NH}_4^+$	$(\text{CH}_3)_3\text{NH}^+$
$k, \text{l}/(\text{mol} \cdot \text{s})$ ....	$3 \cdot 10^{10}$	$4 \cdot 10^{10}$	$3 \cdot 10^{10}$	$2 \cdot 10^{10}$

The proton exchange between the ammonium ion and amine occurs somewhat more slowly, *i.e.*, the reaction of the type:



$\text{R}_3\text{N}$ .....	$\text{NH}_3$	$\text{CH}_3\text{NH}_2$	$(\text{CH}_3)_2\text{NH}$	$(\text{CH}_3)_3\text{N}$
$k, \text{l}/(\text{mol} \cdot \text{s})$ ....	$1.2 \cdot 10^9$	$4 \cdot 10^8$	$4 \cdot 10^7$	$3 \cdot 10^7$

Exchange reactions in water occur very rapidly (NMR method):

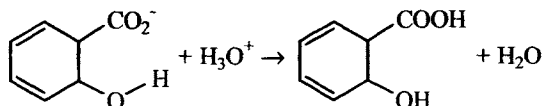
Reaction	$k$ , l/(mol·s) (298 K)	$E$	$A$
$\text{H}_3\text{O}^+ + \text{H}_2\text{O} \cdots \cdots$	$1 \cdot 10^{10}$	11	$9 \cdot 10^{11}$
$\text{OH}^- + \text{H}_2\text{O} \cdots \cdots$	$5 \cdot 10^9$	20	$2 \cdot 10^{12}$
$\text{H}_3\text{O} + \text{OH}^- \cdots \cdots$	$1.4 \cdot 10^{11}$	10	$9 \cdot 10^{12}$

The last reaction occurs so promptly that the diffusion-express mechanism is proposed for it where the proton transfer occurs due to the displacement of protons along hydrogen bonds



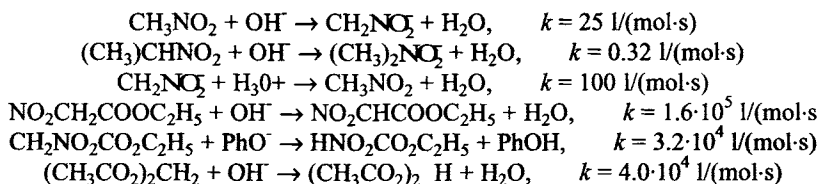
The distance at which a proton is transferred is, on the average, 0.8 nm, which is approximately threefold longer than the ion radius. The proton transfer to the negatively charged anion of the acid occurs, by contrast, much more slowly than the collision of neutral particles in water. For example,  $\text{OH}^-$  reacts with anions of phosphoric acids with a rate constant of  $2 \cdot 10^9$  for  $\text{HPO}_4^{2-}$ ,  $4.7 \cdot 10^8$  for  $\text{HP}_2\text{O}_7^{3-}$ , and  $2.1 \cdot 10^8$  l/(mol·s) for  $\text{HP}_3\text{O}_{10}^{4-}$ . The higher the anion charge, the slower the proton transfer because the repulsion potential between  $\text{OH}^-$  and the acid anion is higher.

When the intramolecular hydrogen bond is formed in the acid, this retards the proton exchange. For example, the salicylate ion reacts with the hydrogen ion



with a rate constant of  $6.4 \cdot 10^9$ , and similar carboxylate ions without a hydrogen bond react with  $k = 3.8 \cdot 10^{10}$  l/(mol·s).

The transfer of a proton from the C—H acid to the hydroxyl ion occurs slowly, although  $\Delta G < 0$ , i.e., the process is thermodynamically favorable. Several examples ( $\text{H}_2\text{O}$ , 298 K) are presented below.



Evidently, in the case of C—H acids, the proton transfer occurs with an activation energy even for the exothermic reaction.

### 15. 4. Quantum-chemical theory of proton transfer

The quantum-chemical proton transfer theory was developed by R.R. Dogonadze, A.M. Kuznetsov, and V.G. Levich in 1967. In the framework of this concept, the reaction  $AH + B \rightleftharpoons A^- + BH^+$  is considered as the transition of the system from the initial to final potential energy surfaces. Each of these surfaces is a function of the coordinate of a proton  $r$  (distance  $A...H$ ), distance  $R$  between  $A$  and  $B$ , and a set of coordinates  $q$  describing the nonequilibrium solvation of the  $AH...B$  pair. The transition between terms  $U_i$  and  $U_f$  occurs according to the Franck-Condon principle. The change in the electron state occurs much more promptly (within  $10^{-15} \div 10^{-16}$  s) than the change in the position of the proton ( $10^{-14}$  s) and solvent molecules surrounding the  $AH...B$  pair ( $10^{-12} \div 10^{-13}$  s). Therefore, the electron density redistribution on the reacting particles occurs at almost unchanged coordinates of the nuclei and is possible when  $\Delta U$  is close to zero. The transition of the system from the initial to final states is possible by two basically different routes.

1. **Adiabatically.** Due to the vibrational excitation the  $A-H$  bond is stretched to the critical value  $r^*$  at which terms  $U_i$  and  $U_f$  are overlapped. The process occurs as a smooth transition of the system with overcoming of the potential barrier.

2. **Tunneling transition.** The  $A-H$  bond elongates to the critical  $r^*$  value, and then the tunneling transfer of a proton occurs from level  $U_i$  to level  $U_f$ . This transition can take place if the vibrational levels of the proton in the initial and final states are equalized. This is achieved due to the thermal fluctuation of orientation of solvent dipoles. In the framework of the model, this looks like a change in the coordinates of the molecules from the  $q$  to  $q^*$  values. The tunneling proton transfer occurs in this state.

The total probability  $w$  of the proton transfer from  $A$  to  $B$  is described by the expression

$$w = \frac{1}{kT} \int_0^{\infty} \exp\left(-\frac{W}{kT}\right) P(W) dW \quad (15.4)$$

where the function  $P(W)$  is the probability of proton tunneling with the energy  $W$ , and the exponential term reflects the fraction of states of the system, which has the energy  $W$  at a specified temperature.

The  $P(W)$  function increases with  $W$  and is temperature independent. Each system and temperature are characterized by an optimum energy  $W^*$  at which the proton transfer occurs. The following three cases are possible. 1. The optimum energy  $W^*$  is close to the activation energy  $E$ , that is, coincides with the height of the activation barrier. The reaction occurs adiabatically. The  $A-H$  bond is stretched to the  $r^*$  value at which the  $U_i$  and  $U_f$  terms are overlapped. 2. The  $W^*$  value is close to zero, and proton tunneling between the ground vibrational levels of the initial and final states is most favorable. 3. The optimum energy  $W^*$  occupies an intermediate

position between zero and  $E$ . The proton is first excited, i.e., the system transits from the zero to excited levels with the  $W^*$  energy, and then the proton tunnels.

Proton tunneling from one potential well into another results in the splitting of the initial levels into  $\Delta E_H$ , so that the equality of the  $U_i$  and  $U_f$  levels is fulfilled only with an accuracy to  $\Delta E_H = U_f \pm \Delta E_H$ . It follows from this that the transition configuration of the whole system  $q^*$ , taking into account the solvation jacket, at which the energies of the proton levels are equalized, is retained for a short time interval  $t_s$ . This is precisely the time during which a proton is transferred, adiabatically or by tunneling. The adiabaticity of the process is determined by the parameter  $\gamma_p$ :

$$\gamma_p = (\Delta E_H/2)^2 / \hbar v_s \Delta F_s \quad (15.5)$$

where  $v_s$  is the thermal rate of motion of molecules, dipoles of the medium;  $\Delta F_s$  is the rate of changing the proton energy during the motion of dipoles of the medium near the transition configuration.

The proton has time to transit from the initial to final states under the condition  $\gamma_p > 1$ . Electron terms change similarly. The transition between the  $U_i$  and  $U_f$  terms occurs near  $r^*$  in the region of values of proton coordinates  $\Delta r^*$  where  $U_i = U_f \pm \Delta E_e$ ,  $\Delta E_e$  being the splitting of electron levels when the system exists in the state  $q^*$ . The criterion of adiabaticity of electron transfer is determined by the parameter

$$\gamma_e = \Delta E_e^2 / (4\hbar v_p \Delta F_p) \quad (15.6)$$

where  $v_p$  is the rate of proton motion, and  $\Delta F_p$  is the rate of changing the electron energy during proton motion near the transition configuration.

At  $\gamma_e > 1$  an electron has time to change its state during a time sufficient for the proton transfer. A. The reaction is adiabatic if  $\gamma_p > 1$  and  $\gamma_e > 1$ . In this case, transmission coefficient  $k = 1$ . The proton is transferred adiabatically if  $\gamma_e > 1$  and  $\gamma_p < 1$ . Transmission coefficient  $\kappa = \gamma_p < 1$ . Several factors affect the ratio between the adiabatic and tunneling proton transfer. First, temperature. The temperature increase increases the fraction of the AH...B pairs, which possess the  $E$  energy and, therefore, the rate of transformation increases with the potential barrier. At temperatures  $T > T_{ad}$  the reaction occurs only adiabatically. If the barrier is considered as the interception of two parabolic curves, then

$$T_{ad} = (E/R) (3L\hbar v_H/16E)^{2/3} \quad (15.7)$$

where  $v_H$  is the vibration frequency of a proton at the lowest vibrational level of A—H ( $v_H \approx 10^{14} \text{ s}^{-1}$ ).

Since the probability of proton tunneling is independent of the proton, at sufficiently low temperatures  $T < T_{tun}$  the transfer of the proton occurs by its tunneling

$$T_{tun} = (\Delta W_0)^2 / 8.6ER, \quad (15.8)$$

where  $\Delta W_0$  is the energy of the zero vibrational level of the proton in the transition state

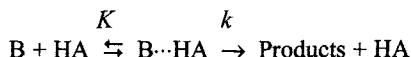
$(0.5h\nu_0L)$ .

The transition from the adiabatic to tunneling proton transfer affects the temperature dependence of the transfer rate constant in such a way that the activation energy decreases with decreasing  $T$  and at  $T < T_{\text{tun}}$   $d \ln k / d(1/T) = 0$ . The distance of proton tunneling has a very strong effect on the tunneling rate: the shorter the distance, the higher the  $\Delta E_{\text{H}}$  splitting and, correspondingly, the higher the tunneling probability. The relation between  $\Delta r^*$  and  $\Delta E_{\text{H}}$  is characterized by the following figures:

$\Delta r^*$ , nm.....	0.06	0.05	0.04	0.03
$\Delta E_{\text{H}}$ , kJ/mol.....	$8.4 \cdot 10^{-3}$	$7.1 \cdot 10^{-2}$	0.42	16.8

### 15.5. Theory of acid-base catalysis

The protonation of a molecule, its transformation into an ion often makes it labile and creates possibilities for transformation into these or other products. Therefore, acid catalysis is widely abundant, acids catalyze the very diverse reactions of addition, substitution, and elimination. The simplest scheme of the acid-catalytic reaction includes two steps



The complex of reactant B with acid HA can be an ionized form of the molecule ( $\text{BH}^+$ ), ion pair ( $\text{BH}^+$ ,  $\text{A}^-$ ) or complex with the hydrogen bond ( $\text{B} \cdots \text{HA}$ ). Polar molecules of the solvent participate in the formation of each form. At the first equilibrium step, product B acts as the base, which withdraws a proton from acid HA. The second irreversible step limits the process. The base-catalyzed reaction has a similar character. In this case, HA is the reactant and base B is the catalyst, which is regenerated in the subsequent stage of conversion. When the concentration of the catalyst (acid or base) is varied in wide limits, reactive complexes with different compositions are formed and the same products are formed *via* several routes of conversion of the initial reactant. Often the acid (base) forms nonreactive complexes with the reactant (equilibrium constant  $K$ ), which affects, of course, the reaction rate. The observed rate constant of the catalytic transformation of B into products is the following:

$$k = \frac{v}{[\text{B}]} = \frac{\sum_i k_i (a_{\text{AH}} K_i') \gamma_{\text{B}}}{1 + \sum (a_{\text{AH}} \gamma_{\text{B}} / K_i \gamma_{\text{HA}}) + \sum_j (a_{\text{AH}} \gamma_{\text{B}} / K_j' \gamma_{\text{HA}})} \quad (15.9)$$

where  $K_i$  is the constant of equilibrium formation of the  $i$ -th reactive complex B.HA, and  $K_j'$  is the constant of equilibrium formation of the  $j$ -th nonreactive complex.

Information on the composition of reactive complexes are obtained from experi-

mental data on measuring  $k_{\text{exp}} = v/[B]$  in the solvent with the unchanged composition with the variation of the catalyst concentration in wide limits. The simplest dependence is obtained when B and HA are bound to form one reactive complex. In this case,

$$k_{\text{exp}} = k a_{\text{HA}} \gamma_{\text{B}} \gamma_{\text{BHA}}^{-1} (K + a_{\text{HA}} \gamma_{\text{B}} / \gamma_{\text{BHA}})^{-1} \quad (15.10)$$

In aqueous solutions of strong acids, this dependence is usually well fulfilled. At  $K \ll a_{\text{HA}} \gamma_{\text{B}} \gamma_{\text{BHA}}^{-1}$  the constant  $k_{\text{exp}} = k$ , at  $K \gg a_{\text{HA}} \gamma_{\text{B}} \gamma_{\text{BHA}}^{-1}$  the constant  $k_{\text{exp}} = kK^{-1} \times a_{\text{HA}} \gamma_{\text{B}} \gamma_{\text{BHA}}$ . When the reactant is transformed through its protonated form  $\text{BH}^+$ , we experimentally observe the dependence of the type  $K/h_0 = \text{const}$ ,  $k_{\text{exp}}(h_0 a_{\text{H}_2\text{O}})^{-1} = \text{const}$  or  $k_{\text{exp}}(h_0 a_{\text{H}_2\text{O}}^2)^{-1} = \text{const}$ . If the first of these plots is observed, this implies that the protonated form of the reactant  $\text{BH}_3\text{O}^+$  is transformed. For example, the pinacolonic rearrangement in concentrated  $\text{H}_2\text{SO}_4$ . The second dependence is observed, e.g., for the dehydration of 2-phenyl-2-propanol in  $\text{H}_2\text{SO}_4$ . In this case, the water complex with the protonated form of the reactant is reactive. The dependence of the third type is observed for oxygen atom exchange in methanol, which occurs in sulfuric acid.

When the B.HA nondissociated complex is transformed, the plots  $k_{\text{exp}}[\text{HA}] = \text{const}$  take place. This is observed, e.g., for the dehydration of  $\beta$ -phenyl- $\beta$ -hydroxypropionic acid in  $\text{H}_2\text{SO}_4$ . If the reaction complex has the composition B.HA. $\text{H}_2\text{O}$ , the equality  $k_{\text{exp}}/a_{\text{HA}} a_{\text{H}_2\text{O}} = \text{const}$  takes place. This dependence is observed, e.g., for cis-cinnamic acid in  $\text{H}_2\text{SO}_4$ .

For catalysis by weak acids in aqueous solutions, both  $\text{H}_3\text{O}^+$  ions and nondissociated acids manifest activity. In this case, in dilute solutions

$$v = (k_{\text{H}} [\text{H}_3\text{O}^+] + k_{\text{HA}} [\text{HA}]) [\text{B}] \quad (15.11)$$

The introduction of a salt into the solution changes the catalytic activity of acids and bases. In the case of weak acids and bases, their degree of dissociation changes with changing the activity of the  $\text{H}_3\text{O}^+$  and  $\text{HO}^-$ .

For acid- and base-catalyzed reactions, in 1924 J.H. Brönsted and Ch.J. Pedersen empirically established correlations of the type

$$k_{\text{HA}} = aK_a^\alpha \text{ and } k_{\text{B}} = b(1/K_a)^\beta \quad (15.12)$$

where  $k_{\text{HA}}$  and  $k_{\text{B}}$  are the rate constants of reactions catalyzed by the acid and base, respectively;  $K_a$  is the acid dissociation constant of AH and  $\text{BH}^+$ , respectively; and  $a$ ,  $b$ ,  $\alpha$ , and  $\beta$  are empirical constants.

These correlations were the first example of linear correlations of free energies (see Chapter 8). They are well fulfilled under the following conditions: (1) a series of one-type acids and bases is considered; (2) in this series the reaction mechanism remains unchanged; and (3) each reaction is not accompanied by specific catalytic

effects. When  $K_a$  changes in a wide range (by  $15 \div 25$  orders of magnitude), the plot  $\log k - \log K_a$  now has the nonlinear character, that is, the parameters change: the higher the reactivity, *i.e.*,  $k_{AH}$ , the lower  $a$ .

The isotope effect, which appears when AH is replaced by AD and H in the reactant is replaced by D, plays an important role in studying acid-catalytic reactions. In particular, deuterated water dissociates to ions to a less extent than  $H_2O$ : the ratio of ion products  $K_w^{H_2O} : K_w^{D_2O} = 7.47$  and  $K_w^{H_2O} : K_w^{T_2O} = 16.4$  (298 K). For oxy acids in  $H_2O$  and  $D_2O$  the  $K_a^H : K_a^D$  ratio is  $2.5 \div 4.5$ . The replacement of H by D in acids and bases at the bonds, which are not involved in dissociation, results in the secondary isotope effect. This effect is usually low, although exclusions are known:  $K_a(HCO_2H)/K_a(DCO_2H) = 1.08$ ,  $K_a(CH_3COOH)/K_a(CD_3COOH) = 1.03$ ,  $K_a(CH_3NH_3^+)/K_a(CD_3NH_3^+) = 1.14$ , and  $K_a(CH_3)_3NH_4/K_a(CD_3)_3NH_4^+ = 1.61$ .

When a standard solvent is replaced by deuterated one, for example,  $H_2O$  by  $D_2O$ , we have the isotope effect by solvent with a complex character. The kinetic isotope effect is characteristic of proton transfer reactions. It depends on the following factors: type of the dissociated bond, change in enthalpy, and character of the elementary step of proton transfer (adiabatic or tunneling). For the adiabatic character of the reaction, the isotope effect is maximum for the thermally neutral reaction. The main contribution to the isotope effect is made by the difference in zero energies  $\Delta E_0$  of stretching vibrations of the A—H and A—D bonds. The  $k_H/k_D$  values are presented below, the effect is due to  $\Delta E_0$  only for different types of A—H bonds ( $T = 298$  K).

Bond.....	C—H	N—H	O—H	S—H
$\exp(E_0/RT)....$	6.9	8.5	10.6	6.0

Evidently, the isotope effect decreases with temperature increase. Another factor can also appear with temperature decrease: a noticeable contribution of the tunneling mechanism to proton transfer.

Tunneling electron transfer is characterized by high values of isotope effect  $k_H/k_D$ . The isotope effect is maximum at  $\Delta G = 0$ . It depends very strongly on the  $\Delta r^*$  distance at which H and D tunnelate

$$k_H/k_D = \exp(15.3\Delta r^{*2}) \quad (15.13)$$

and equals 4 at  $\Delta r^* = 0.03$  nm and 250 at  $\Delta r^* = 0.06$  nm.

## 15.6. Reactions catalyzed by acids and bases

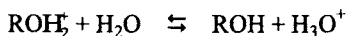
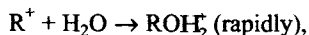
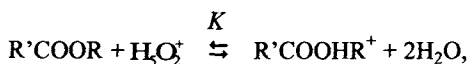
## 15.6.1. Hydrolysis of esters and esterification

The reaction of ester hydrolysis and backward reaction of esterification of carboxylic acids are studied in detail. Ester hydrolysis is catalyzed by both hydrogen ions and hydroxyl ions, that is, is an example of specific acid-base catalysis. Two different methods for the cleavage of ester bonds are possible and observed experimentally: acyl-oxygen and alkyl-oxygen

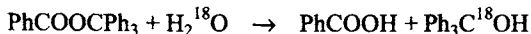


Ch. Ingold divided all known mechanisms of ester hydrolysis into 6 groups.

1. Monomolecular acid hydrolysis and esterification of the alkyl-oxygen bond cleavage (mechanism  $A_{AL}1$ ):



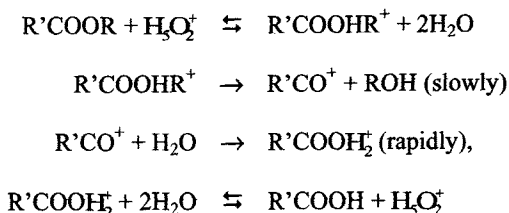
The second step limits the whole process in such a way that the hydrolysis rate  $v = kK[RCOOR][H_3O_2^+]$ . The second and third steps, rigidly speaking, are reversible; in the presence of alcohol and acid, the esterification process occurs in the backward direction. This mechanism is characterized by the following properties: the water oxygen goes into the alcohol, which is detected in experiments with water containing the  $^{18}O$  isotope; the optically active alcohol residue R under hydrolysis is racemized; the hydrolysis rate depends on the structure of the alcohol residue; and the steric effect is absent. The transfer of the  $^{18}O$  isotope was observed for the acid hydrolysis of triphenyl methylbenzoate in aqueous dioxane



Predominantly racemic alcohol is formed by the hydrolysis of optically active methylethylisohexyl carbonylacetate in an aqueous solution of dioxane. The optically active alcohol itself is very slowly racemized under these conditions (medium, acid). Esters of tertiary alcohols, for example, tert-butyl acetate in aqueous solutions, are hydrolyzed by the  $A_{AL}1$  mechanism. This is related to a relative stability of terti-

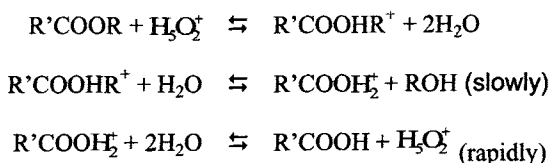
ary carbocations.

2. Monomolecular acid hydrolysis and esterification with the cleavage of the acyl-oxygen bond ( $A_{AC1}$ ). The mechanism includes the following steps:

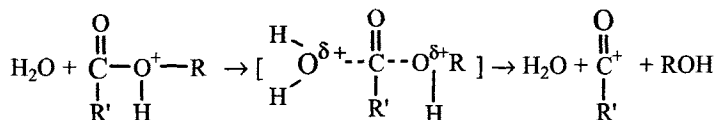


The second step is limiting. This mechanism has the following characteristic properties. When hydrolysis is performed in water in the presence of  $^{18}\text{OH}_2$ , oxygen transits from water to acid (see steps 3 and 4). Unlike the  $A_{AC2}$  mechanism (see below), ester is not enriched in the  $^{18}\text{O}$  isotope differently than through backward esterification. The optically active configuration  $\text{R}'$  is retained during hydrolysis. The steric effect is absent. In particular, methyl trimethylbenzoate is hydrolyzed in sulfuric acid by this mechanism. The  $A_{AC1}$  mechanism is also characterized by higher values of activation entropy ( $\Delta^\ddagger S > 0$ ) than those for  $A_{AC2}$  (see below). When the conditions of hydrolysis change, its mechanism can change.

3. Bimolecular acid hydrolysis and esterification with acyl-oxygen bond cleavage ( $A_{AC2}$ ). Unlike the  $A_{AC1}$  mechanism, in this case, the ester is cleaved by the attack of  $\text{H}_2\text{O}$  at the protonated form of ester



The second step is limiting. It can be presented as the nucleophilic attack of water at the protonated form of ester, namely:



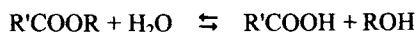
As for the  $A_{AC1}$  mechanism, in this case,  $^{18}\text{O}$  from  $^{18}\text{OH}_2$  is transited into the acid but hydrolysis is accompanied by the enrichment of nonhydrolyzed ester in  $^{18}\text{O}$  as well due to the reversibility of the second step. The hydrolysis rate better correlates with  $\text{H}_3\text{O}^+$  than with  $h_o$ . The  $A_{AC2}$  mechanism is characterized by lower values of activation entropy. The optically active configuration  $\text{R}'$  is retained. The steric effect

is observed. The steric influence of substituents on hydrolysis by the  $A_{AC}2$  mechanism is reflected by the parametric equation

$$\log k = \log k_o + \delta E_s \quad (15.14)$$

where  $E_s$  is the steric constant of the substituent in the acid residue.

Below we present several examples for the reaction of the type ( $T = 298\text{ K}$ )



R	Solvent	$\delta$	$\log k_o$
CH <sub>3</sub>	H <sub>2</sub> O	0.63±0.02	-3.16
	H <sub>2</sub> —CH <sub>3</sub> OH (50%)	0.94±0.04	-2.89
C <sub>2</sub> H <sub>5</sub>	H <sub>2</sub> O	1.12±0.02	-2.51
	H <sub>2</sub> —CH <sub>3</sub> OH (23%)	1.17±0.25	-3.25
CH <sub>2</sub> Cl	H <sub>2</sub> O	1.11±0.18	-2.83
	H <sub>2</sub> —CH <sub>3</sub> OH (36%)	0.99±0.25	-2.83

The  $A_{AC}2$  mechanism is widely abundant, it is characteristic of hydrolysis of primary and secondary alcohols of carboxylic acids in dilute solutions of strong acids.

Since the  $A_{AC}2$  and  $A_{AC}1$  mechanisms are rather close and it is difficult to distinguish one from another, they are often unified. The mechanisms of hydrolysis with the acyl—oxygen (rate constant  $k_{AC}$ ) and alkyl—oxygen ( $k_{AL}$ ) bond cleavage can be distinguished by exchange with <sup>18</sup>O in water enriched in this isotope. In addition, hydrolysis occurs slowly in water containing no acid (constant  $k_o$ ).

Hydrolysis often occurs in parallel *via* two mechanisms with the rate

$$v = (k_{AC} + k_{AL}) [R'COOR][H_3O^+] + k_o[R'COOR]$$

The catalytic hydrolysis of *tert*-butyl acetate in water is characterized by the following parameters:

$$k_o = 2 \cdot 10^{12} \exp(-112/RT) = 5.0 \cdot 10^{-8} \text{ s}^{-1}$$

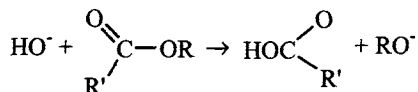
$$k_{AC} = 7.9 \cdot 10^7 \exp(-72/RT) = 2.0 \cdot 10^{-5} \text{ l/(mol}\cdot\text{s)}$$

$$k_{AL} = 1.3 \cdot 10^{16} \exp(-115/RT) = 9.6 \cdot 10^{-5} \text{ l/(mol}\cdot\text{s)}$$

It is seen that hydrolysis with the alkyl-oxygen bond cleavage predominates, which is especially characteristic of tertiary alcohols (see above). At the same time, hydrolysis with the acyl-oxygen bond cleavage occurs to a great extent, probably, by

the  $A_{AC2}$  mechanism.

4. Bimolecular base hydrolysis with acyl-oxygen bond cleavage ( $B_{AC2}$ ). The hydroxyl ion attacks the carboxyl group resulting in nucleophilic substitution

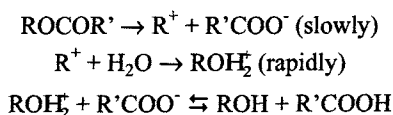


The first step limits the process. It is reversible, in principle, but due to the fast reaction of the acid with base the equilibrium is shifted to the right, so that hydrolysis proceeds irreversibly. The cleavage of the acyl—oxygen bond was proved by different methods. The alkaline hydrolysis of neopentyl acetate affords neopentyl alcohol, that is, the alcohol residue is not isomerized. Therefore,  $R^+$  is not eliminated because, in this case, neopentyl alcohol would isomerize to tert-amyl alcohol. Alcohol residues are not either isomerized during the alkaline hydrolysis of crotyl ( $R = -CH_2CH=CHCH_3$ ) and 1-methylallyl ( $R = CH_2-CH=CHCH_3$ ) acetates, which also indicates acyl—oxygen bond cleavage. This is also evidenced by experiments on the alkaline hydrolysis of esters in water enriched in the  $^{18}O$  isotope in which the  $^{18}O$  oxygen is transformed into acid rather than alcohol. Substituents in the acid residue have a strong inductive (reflected by the  $\rho^*$  coefficient) and steric ( $\delta^*$  coefficient) effects on the reaction. Below we present the parameters of the correlation biparametric Taft equation ( $T = 298\text{ K}$ )

$$\log k = \log k_0 + \rho^* \sigma^* + \delta E_s \quad (15.15)$$

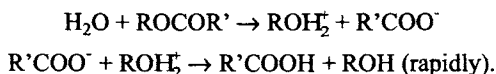
R	Solvent	$\rho^*$	$\delta$	$\log k_0$
CH <sub>3</sub>	H <sub>2</sub> O	2.45±0.05	0.80±0.05	1.58
C <sub>2</sub> H <sub>5</sub>	H <sub>2</sub> O	2.32±0.02	0.79±0.02	1.41
	H <sub>2</sub> O—C <sub>2</sub> H <sub>5</sub> OH (68%)	2.22±0.11	1.12±0.03	0.37
CH <sub>2</sub> CH <sub>2</sub> CH <sub>3</sub>	H <sub>2</sub> O	1.00±0.05	1.51±0.05	1.35
CH <sub>2</sub> CH=CH <sub>2</sub>	H <sub>2</sub> O	1.67±0.07	0.42±0.13	0.71
CH <sub>2</sub> Cl	H <sub>2</sub> O	2.5±0.23	1.01±0.18	3.61
(CH <sub>2</sub> ) <sub>3</sub> Cl	H <sub>2</sub> O	1.66±0.07	0.41±0.12	0.61
Ph	H <sub>2</sub> O—dioxane (33%)	2.64±0.24	0.79±0.11	1.14

5. Monomolecular base hydrolysis with alkyl—oxygen bond cleavage ( $B_{AL1}$ ). As in the case of acid hydrolysis, hydrolysis with the alkyl—oxygen bond cleavage is also possible. Selecting the corresponding structure of the medium ester, we can perform the following mechanism:



This mechanism is characterized by the following properties. Oxygen ( $^{18}\text{O}$  isotope) transits from water into alcohol. If the alcohol residue in ester is optically active (the carbon atom bound to oxygen is asymmetric), hydrolysis is accompanied by alcohol racemization. If the R radical is the substituted allyl group, hydrolysis is accompanied by alcohol isomerization. Hydrolysis is accelerated by electropositive (for example,  $\text{CH}_3\text{O}$ ) groups in the alcohol residue and electronegative groups (for example,  $\text{NO}_2$ ) in the acid residue. The steric effect is absent because the monomolecular process limits the reaction. An increase in the solvent polarity favors the reaction. The hydrolysis and alcoholysis of esters of triphenylmethyl alcohol, tert-butyl alcohol, and allyl alcohols proceed *via* the  $B_{\text{AL}}1$  mechanism.

6. Bimolecular base hydrolysis with alkyl-oxygen bond cleavage ( $B_{\text{AL}}2$ ). This mechanism is observed in rare cases and includes the attack of the water molecule at the carbon atom of the alcohol residue as the limiting step

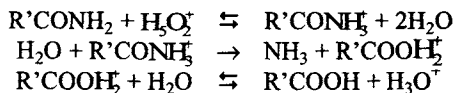


Specific features of the mechanism: the reaction occurs in the absence of acid; its rate is independent of pH in some interval of its change. Oxygen from water transits to alcohols (experiments in water enriched in  $^{18}\text{O}$ ). If the  $\alpha$ -C atom of the alcohol residue is asymmetric, the inversion of the optical activity occurs during hydrolysis. Steric effect also influences the reaction rate. This mechanism was established for lactone hydrolysis:  $\gamma$ -propiolactone,  $\beta$ -butyrolactone, and lactone of malic acid.

Comparison of the rate constants of acid  $k_{\text{A}}$  and base  $k_{\text{B}}$  hydrolyses shows that  $k_{\text{A}} \ll k_{\text{B}}$ . This is the result of the difference in activation energies: the activation energy of hydrolysis by the  $\text{OH}^-$  ion is much lower than that by the hydrogen ion. For the hydrolysis of acetates of aliphatic alcohols, this difference  $E_{\text{A}} - E_{\text{B}} = 24$  kJ/mol. Close values of the  $E_{\text{A}} - E_{\text{B}}$  difference are obtained for the hydrolysis of amides of aliphatic acids ( $E_{\text{A}} - E_{\text{B}} = 26$  kJ/mol) and acetone enolization ( $E_{\text{A}} - E_{\text{B}} = 30$  kJ/mol).

### 15.6.2. Hydrolysis of amides of acids

Hydrolysis occurs under the acid action according to the bimolecular law with the rate  $v = k_{\text{A}}[\text{A}_{\text{mide}}][\text{H}_3\text{O}^+]$ . The following mechanism ( $A_{\text{AC}}2$ ) is assumed:



Hydrolysis is limited by the second step, which can be considered as the nucleophilic attack of water at the acyl C atom. The acid hydrolysis rate depends on the inductive and steric effects of substituents in the acid residue. The following corre-

lation is fulfilled for the hydrolysis of  $\text{RCONH}_2$  in  $\text{H}_2\text{O}$  at 338 K:

$$\lg k [l/(\text{mol}\cdot\text{s})] = -4.22 - 3.40\sigma^* + 1.10 E_s$$

for the hydrolysis of compounds of the type  $\text{RCON} \begin{array}{c} \boxed{+} \\ \text{N} \end{array}$  ( $\text{H}_2\text{O}$ , 303 K):

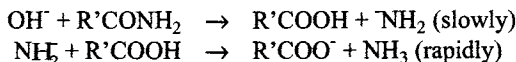
$$\lg k [l/(\text{mol}\cdot\text{s})] = -4.00 - 7.69\sigma^* + 1.25 E_s$$

and for  $\text{CH}_3\text{CONHR}$  ( $\text{H}_2\text{O}$ , 338 K):

$$\lg k [l/(\text{mol}\cdot\text{s})] = -3.37 - 2.36\sigma^* + 0.41 E_s$$

The hydrolysis of amides substituted by tert-alkyl occurs under the action of sulfuric acid with the abstraction of the tert-alkyl group and formation of nonsubstituted amide and tertiary alcohol. N-tert-butylamides of formic and acetic acids are hydrolyzed in such a way.

The hydrolysis of amides of acids under the action of an alkali occurs *via* the  $B_{AC2}$  mechanism. The following mechanism is proposed:



It cannot be ruled out that the first step proceeds through the  $\text{R}'\text{C}(\text{O}^-)(\text{OH})\text{NH}_2$  intermediate, which then is rapidly decomposed to acid and  $\text{NH}_2^-$ . The reversible formation of this intermediate is favored by the fact of the partial enrichment of amide in the  $^{18}\text{O}$  isotope when hydrolysis is carried out in water containing this isotope. The correlation equations for the alkaline hydrolysis of amides are presented below

$$\text{RCONH}_2 \text{ (338 K, H}_2\text{O)} \quad \lg k = -2.99 - 2.48\sigma^* + 1.30 E_s$$

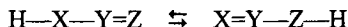
$$4\text{-X-C}_6\text{H}_4\text{CONH}_2 \text{ (353 K, H}_2\text{O - C}_2\text{H}_5\text{OH, 32 \%)} \quad \lg k = -4.16 + 1.16\sigma$$

$$4\text{-X-C}_6\text{H}_4\text{CO-cyclo-NC}_3\text{H}_3\text{N} \text{ (303 K, H}_2\text{O)} \quad \lg k = -2.25 - 1.30\sigma + 0.32 \sigma_R^*$$

As in the case of ester hydrolysis, the alkaline hydrolysis of amides occurs more rapidly than acid hydrolysis. For example, the ratio  $k_B/k_{HA} = 17$  for  $\text{CH}_3\text{CONH}_2$  in  $\text{H}_2\text{O}$  at 338 K. The  $\rho^*$  coefficient is higher in absolute value for acid hydrolysis than that for alkaline hydrolysis.

### 15.6.3. Keto-enol tautomerism

This tautomerism is a particular case of prototropic tautomerism of the type

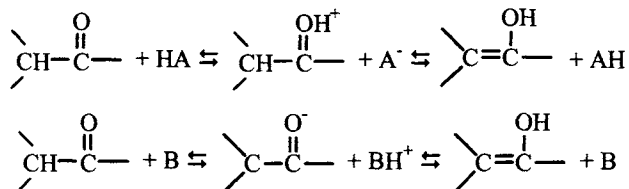


which is catalyzed by acids and bases. The enolic form is at equilibrium with the ketonic form if the equilibrium is rapidly established. The stability of the enolic form

depends on the structure of the molecule. Below we present (in %) the equilibrium concentrations of the enolic forms in the liquid phase at 298 K for several compounds.

$\text{CH}_3\text{COCH}_3$ $3.5 \times 10^{-4}$	<i>cyclo</i> - $\text{C}_6\text{H}_{10}\text{O}$ 0.20	$\text{CH}_3\text{COCH}(\text{CH}_3)\text{CO}_2\text{C}_2\text{H}_5$ 4	$\text{PhCOCH}_2\text{CO}_2\text{C}_2\text{H}_5$ 21
$\text{CH}_3\text{COCH}(\text{C}_2\text{H}_5)\text{COCH}_3$ 28	$\text{CH}_3\text{COCH}(\text{COOC}_2\text{H}_5)_2$ 69	$\text{CH}_3\text{COCH}_2\text{CH}_3$ 80	

Ketone enolization is catalyzed by both acids and bases



and is an example of general acid catalysis. Various kinetic variants are also possible, which can sufficiently be considered using acid catalysis as an example.

1. The first equilibrium is very promptly established ( $k_1 \ll k_{-1}$  and  $k_2 \ll k_{-1}$ ), and the process is limited by the second step. In this case,  $[\text{>CHCROH}^+] = K_1[\text{HA}][\text{>CHCRO}]$  and  $v = k_2 K_1 [\text{Ketone}][\text{HA}]$ . If the solution contains other bases along with ketone, acid dissociation and the participation of several proton-donor species in the reaction should be taken into account (see below). The reaction rate  $v = k_2 [\text{Ketone}] \sum_i K_i [\text{A}_i\text{H}]$ .

2. The formed protonated ketone form undergoes fast transformation ( $k_1 \ll k_{-1}$  and  $k_2 \gg k_{-1}$ ). Then the process is limited by the first step and  $v = k_1 [\text{Ketone}][\text{HA}]$ . Both cases are kinetically indiscernible.

3. Finally, the third case where the rates of steps  $k$  and  $k_{-1}$  are commensurable results in the expression

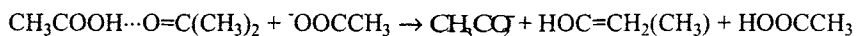
$$v = k_1 k_2 (k_{-1} + k_2)^{-1} [\text{Ketone}][\text{HA}][\text{A}^-]^{-1} \quad (15.16)$$

4. If step 2 occurs very slowly, and  $k_1$  and  $k_{-1}$  are commensurable, the protonated ketone form is present in the solution in noticeable amounts.

Since keto-enol tautomerism is accelerated by both acids and bases (the case of general acid-base catalysis), the reaction rate increases with both pH increase and decrease (V-shaped dependence). For example, the rate of acetone enolization in an acetate buffer is related to concentrations of the reactants by the following expression ( $\text{H}_2\text{O}$ , 298 K):

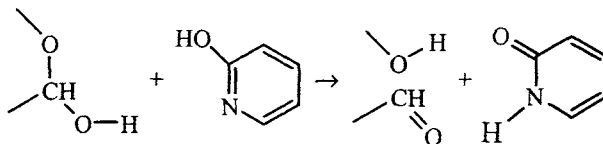
$$\begin{aligned}
 v = & 5 \cdot 10^{-10} [\text{H}_2\text{O}] + 1.6 \cdot 10^{-3} [\text{H}_3\text{O}^+] + 15 [\text{OH}^-] + \\
 & + 5.0 \cdot 10^{-6} [\text{CH}_3\text{COOH}] + 1.5 \cdot 10^{-5} [\text{CH}_3\text{COO}^-] + \\
 & + 2.0 \cdot 10^{-5} [\text{CH}_3\text{COOH}][\text{CH}_3\text{COO}^-]
 \end{aligned}
 \quad (15.17)$$

The last term reflects acetone enolization during the concerted attack of the acid and base at acetone, which can be presented as concerted proton abstraction and addition



In this reaction the acid donates a proton to the carbonyl group of acetone, and the acetate ion simultaneously abstracts a proton from the methyl group.

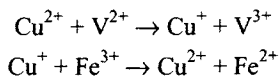
The high efficiency of this combined attack is related to the existence of bifunctional catalysts of prototropic enolization. A molecule of these catalysts contains both acidic and basic groups. For example, 2-hydroxypyridine is such a catalyst. It catalyzes glucose mutarotation 7000-fold more efficiently than a mixture of phenol and pyridine (298 K,  $\text{H}_2\text{O}$ , catalyst concentration 0.001 M). Keto acids,  $\beta$ -diketones, and pyrazole have a similar catalytic effect. The transformation scheme is the following:



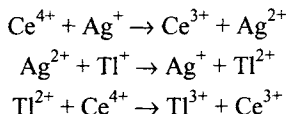
The efficiency of catalysts of this type is due to the cyclic transition state in which the concerted transfer of two protons occurs. Enzymes accelerating polypeptide hydrolysis function according to this principle.

### Redox catalysis

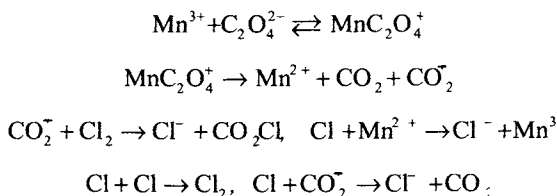
Transition metal ions react with other ions and radicals in electron transfer reactions. Such reactions often occur very rapidly. Redox catalysis is based on this capability of some metal ions of serving efficient mediators in electron transfer reactions. This type of catalysis has a wide propagation for ionic redox reactions. For example,  $\text{Fe}^{3+}$  ions very slowly oxidize  $\text{V}^{2+}$  ions. The introduction of copper ions accelerates this process because the faster sequence of reactions is observed in their presence:



Silver ions catalyze the reaction of  $\text{Ce}^{4+}$  ions with  $\text{Ti}^{+}$ :



Since a free radical is always formed in the reaction of an ion with a molecule during electron transfer, these redox systems are generators of free radicals. They are used for the initiation of reactions of radical polymerization, oxidation, and chlorination. For example, manganese ions initiate the chain oxidation of oxalate ions with chlorine in an aqueous solution. The process includes the following steps:

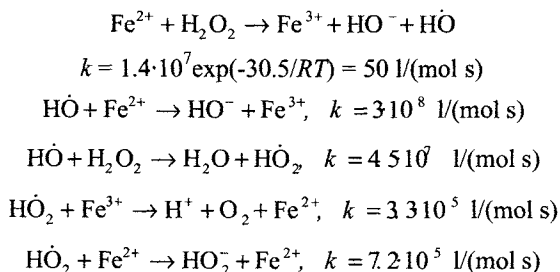


Active intermediate products often appear in the redox reaction, and autocatalysis is observed. The oscillating regime of the process is often observed in these systems. Redox reactions play a very important role in living organisms where they form a basis for enzymatic processes of respiration, nitrogen fixation, and removal of products harmful for the organism.

### 16.1. Catalysis of hydrogen peroxide decomposition by iron ions

Catalysis of  $\text{H}_2\text{O}_2$  decomposition by iron ions occupies a special place in redox catalysis. This was precisely the reaction for which the concept of redox cyclic reactions as a foundation of this type of catalysis was formulated. The detailed study of steps of this process gave several valuable data on the mechanism of redox catalysis. The catalytic decomposition of  $\text{H}_2\text{O}_2$  is an important reaction in the system of processes that occur in the organism.

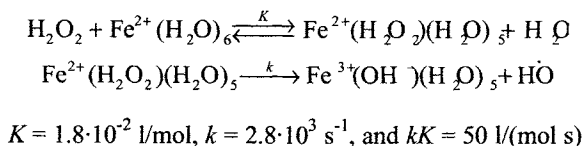
The catalytic decomposition of  $\text{H}_2\text{O}_2$  in the presence of the  $\text{Fe}^{2+}$  and  $\text{Fe}^{3+}$  ions includes the following steps ( $\text{H}_2\text{O}$ ,  $T = 298 \text{ K}$ , acidic medium):



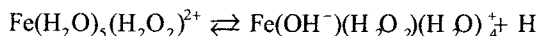
The first step, being the slowest, limits the process and, hence, the rate of  $\text{H}_2\text{O}_2$  decomposition is  $v = k[\text{H}_2\text{O}_2][\text{Fe}^{2+}]$ , and  $k$  depends on the pH of the medium. The stoichiometric ratio of the consumed  $\text{H}_2\text{O}_2$  and  $\text{Fe}^{2+}$  depends on the ratio of the reactants

$$\Delta[\text{H}_2\text{O}_2]/\Delta[\text{Fe}^{2+}] = 1/2 + (K'[\text{H}_2\text{O}_2]/[\text{Fe}^{2+}])$$

The transfer of an electron from  $\text{Fe}^{2+}$  to  $\text{H}_2\text{O}_2$  is intrasphere, being preceded by the incorporation of  $\text{H}_2\text{O}_2$  into the internal coordination sphere of the  $\text{Fe}_{aq}^{2+}$  ion

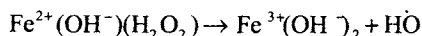


The reaction is accelerated with an increase in the pH of the solution. This is caused first by the hydrolysis of the  $\text{Fe}(\text{H}_2\text{O}_2)^{2+}$

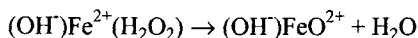


and the faster electron transfer in this complex. Two variants are accepted in the lit-

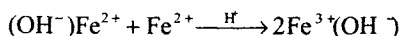
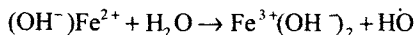
erature, namely, one-electron transfer



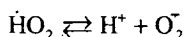
and two-electron transfer to form the ferryl ion



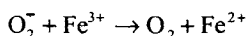
Then the ferryl ion either reacts with water to form the hydroxyl radical, or oxidizes another  $\text{Fe}^{2+}$  ion



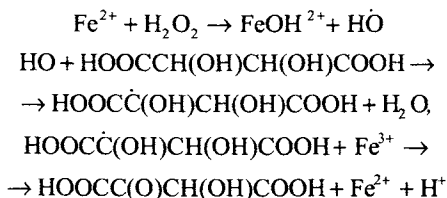
Thus, two routes of transformation are possible for the  $\text{Fe}^{2+}\cdot\text{H}_2\text{O}_2$  complex: one-electron to form the hydroxyl radical and two-electron to form the ferryl ion. It is difficult to prove experimentally the formation of the ferryl ions because they are very active, so that this route of interaction of  $\text{H}_2\text{O}_2$  with  $\text{Fe}^{2+}$  remains hypothetical to a great extent. Another change in the mechanism of  $\text{H}_2\text{O}_2$  decomposition with pH increasing is related to the acidic dissociation of  $\text{HO}_2\cdot$  ( $\text{p}K_a = 4.4$ )



The  $\text{O}_2^{\cdot-}$  ion possesses a low electron affinity (42 kJ/mol in a vacuum) and is a reducing agent. Therefore, it rapidly reacts, in particular, with  $\text{Fe}^{3+}$



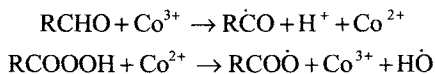
The oxidation of organic compounds by the Fenton reagent is associated, as it is clear now, with the generation of hydroxyl radicals. For example, the oxidation of tartaric acid includes the following reactions as key steps:



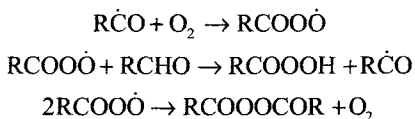
which in combination form a cycle. Other organic compounds are oxidized similarly.

### 16.2. Catalysis of hydrocarbon oxidation with dioxygen by transition metals

Salts of variable-valence metals are widely used in technological processes for the preparation of various oxygen-containing compounds from hydrocarbon raw materials. The principal mechanism of acceleration of RH oxidation by dioxygen in the presence of salts of heavy metals was discovered by C. E. H. Bawn for benzaldehyde oxidation (1951). Benzaldehyde was oxidized with dioxygen in a solution of acetic acid, cobalt acetate being the catalyst. The oxidation rate was  $v \sim [\text{PhCHO}]^{3/2}[\text{Co}^{3+}]^{1/2}[\text{O}_2]^0$ . The rate of radical generation was measured by the inhibitor method and turned out to be  $v_i = k_i[\text{PhCHO}][\text{Co}^{3+}]$ ,  $k_i = 3 \cdot 10^9 \exp(-61.9/RT)$  l/(mol s). The reaction rate of  $\text{Co}^{3+}$  with benzaldehyde was measured in independent experiments (from the consumption of  $\text{Co}^{3+}$  in the absence of oxygen): the rate constant of this bimolecular reaction coincided with  $k_i$ . Thus, in this process the limiting step of initiation is the reduction of  $\text{Co}^{3+}$  with aldehydes, and the complete cycle of initiation reactions includes the reactions

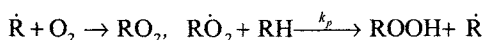


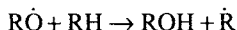
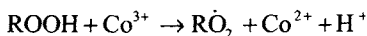
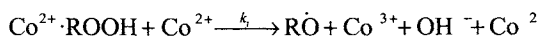
and the formation of perbenzoic acid occurs due to the chain reaction including the steps



Catalysis is caused by the fact that the radicals are generated by the oxidized form of the catalyst in the reaction with aldehydes, and the reduced form of the catalyst is rapidly oxidized by perbenzoic acid formed in the chain reaction.

Alkylaromatic hydrocarbons, such as tetralin, ethylbenzene, and cumene, are oxidized in a solution of acetic acid in the presence of cobalt acetate via somewhat different mechanism. In these systems, after some rather short acceleration period, a constant oxidation rate  $v \sim [\text{RH}]^2$  is established: it is independent of either the catalytic concentration, or the partial oxygen pressure. The stationary concentration of hydroperoxide  $[\text{ROOH}]_{\text{st}} \sim ([\text{RH}]/[\text{Co}^{2+}])^2$  corresponds to the constant oxidation rate. In a nitrogen atmosphere the hydroperoxide decomposes with the rate  $v = k[\text{ROOH}][\text{Co}(\text{Ac})_2]^2$ . These results agree with the following scheme of chain oxidation:





The reaction of  $\text{Co}^{2+}$  with ROOH limits initiation. In the quasi-stationary regime, the rate constants of formation and decomposition of hydroperoxide are equal

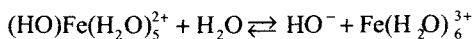
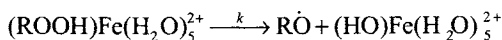
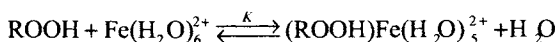
$$k_p[\text{RH}][\text{RO}_2\cdot] = k_i K [\text{ROOH}][\text{Co}^{2+}]^2$$

$$[\text{RO}_2\cdot]^2 = k_i K [\text{ROOH}][\text{Co}^{2+}]^2 / 2k_t$$

so that  $[\text{ROOH}]_{\text{st}} = k_p^2 [\text{RH}]^2 / 2k_t k_i K [\text{Co}^{2+}]^2$ , and the oxidation rate is  $v_{\text{st}} = (k_p[\text{RH}])^2 / 2k_t$ .

The dependence of the oxidation rate  $v$  on catalyst concentration looks somewhat paradoxical: the reaction is catalyzed by the cobalt ions but  $v$  is independent of their concentration. This is due to the fact that initiation occurs by the reaction of hydroperoxide with the catalyst but the process is limited in the quasi-stationary regime by the rate of chain oxidation of the hydrocarbon. In essence, the catalyst transforms the chain process into non-chain due to the high initiation rate.

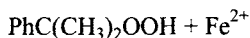
As in the case with hydrogen peroxide, radical generation by the reaction of metal ions with hydroperoxide consists of several steps. In an aqueous solution, as in the case of  $\text{H}_2\text{O}_2$ , first ROOH is substituted in the internal coordination sphere of the ion followed by the transfer of an electron from the ion to ROOH accompanied by the subsequent cleavage to  $\text{RO}\cdot$  and  $\cdot\text{OH}$ , for example,



The total constant  $k_{\text{exp}} = kK$  weakly depends on the hydrocarbon residue, which is seen from the following data ( $T = 298 \text{ K}$ ):



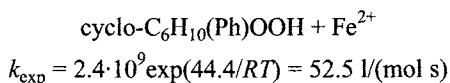
$$k_{\text{exp}} = 2.04 \cdot 10^8 \exp(-41/RT) = 12.9 \text{ l}/(\text{mol s}),$$



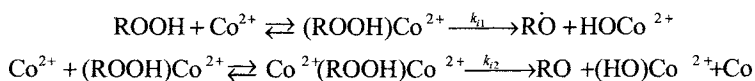
$$k_{\text{exp}} = 3.55 \cdot 10^8 \exp(-38/RT) = 16.6 \text{ l}/(\text{mol s}),$$



$$k_{\text{exp}} = 3.80 \cdot 10^8 \exp(-35.5/RT) = 59 \text{ l}/(\text{mol s}),$$



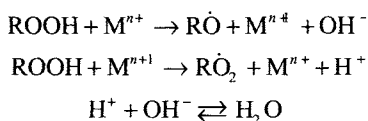
However, the ligand environment substantially reflects the  $k$  value (cf. the data for  $\text{Fe}(\text{P}_2\text{O}_7)^{2-}$  and  $\text{Fe}^{2+}$ ). In the acetic acid the reaction of cobalt ions with ROOH proceeds via two channels: through the mono- and binuclear cobalt complexes



Due to this,  $v_i = (k_{i1}[\text{Co}^{\text{II}}] + k_{i2}[\text{Co}^{\text{II}}]^2)[\text{ROOH}]$ , at 333 K in  $\text{CH}_3\text{COOH}$  for  $(\text{CH}_3)_3\text{COOH}$   $k_{i1} = 2.2 \cdot 10^{-2} \text{ l}/(\text{mol s})$  and  $k_{i2} = 0.62 \text{ l}^2/(\text{mol}^2 \text{ s})$ . Similarly, in the case of the  $\text{Co}^{\text{II}}$  complex with ethylenediamine tetraacetate in the mixture  $\text{CH}_3\text{COOH} : \text{H}_2\text{O} = 1 : 1$  at 308 K  $k_{i1} = 7.2 \cdot 10^{-5} \text{ l}/(\text{mol s})$  and  $k_{i2} = 6.1 \cdot 10^{-3} \text{ l}^2/(\text{mol}^2 \text{ s})$ .

In the case of cobalt ions, the inverse reaction of  $\text{Co}^{\text{III}}$  reduction with hydroperoxide occurs also rather rapidly. In aqueous acidic solutions  $k_i = 1.35 \cdot 10^{-2} \text{ l}/(\text{mol s})$  (293 K). The efficiency of redox catalysis is especially pronounced if we compare the rates of thermal homolysis of hydroperoxide with the rates of its decomposition in the presence of ions, for example, cobalt. *tert*-Butyl hydroperoxide decomposes in a chlorobenzene solution with the rate constant  $k_d = 3.6 \cdot 10^{12} \exp(-138/RT) = 10^{-9} \text{ s}^{-1}$  (293 K): at the concentration  $[\text{Co}^{2+}] = 10^{-4} \text{ M}$   $k_{i1}[\text{Co}^{2+}] = 2.2 \cdot 10^{-2} \cdot 10^{-4} = 2.2 \cdot 10^{-6} \text{ s}^{-1}$ ; thus, the specific decomposition rates differ by three orders of magnitude, and this difference can be increased by increasing the catalyst concentration. The kinetic difference between the homolysis of the O—O bond and redox decomposition of ROOH is reasoned by the difference in the thermodynamic routes of decomposition in these cases. The homolysis of ROOH at the O—O bond requires the energy expenditure equal to the strength of this bond (130–150 kJ/mol).

The redox cycle

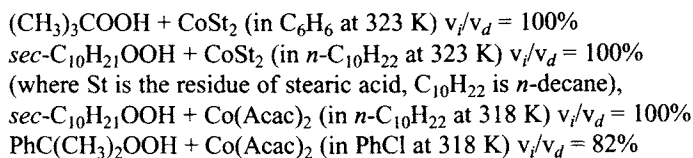


requires an energy expenditure (per ROOH molecule) of only  $\Delta H = 1/2(D_{\text{O—O}} + D_{\text{O—H}} - D_{\text{HO—H}}) = 10 \text{ kJ/mol}$ . This results in the great difference in rates of the catalytic and non-catalytic decompositions of ROOH.

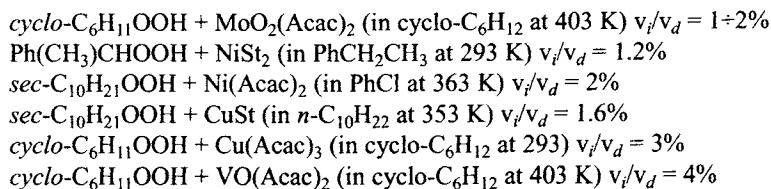
In real systems (hydrocarbon- $\text{O}_2$ -catalyst), various oxidation products, such as alcohols, aldehydes, ketones, bifunctional compounds, are formed in the course of oxidation. Many of them readily react with ion-oxidants in oxidative reactions. Therefore, radicals are generated via several routes in the developed oxidative process, and the ratio of rates of these processes changes with the development of the

process. Reactions of this type are considered in Chapter 10.

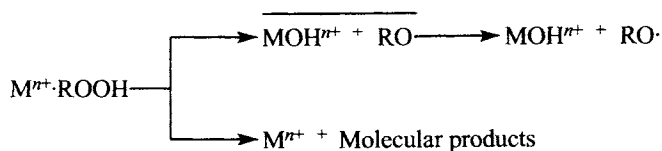
According to the Haber—Weiss scheme, in the framework of which we considered the catalytic decomposition of ROOH, all ROOH molecules decompose under the action of ions only to free radicals, i.e., one-electron redox decomposition occurs. Both rates of catalytic decomposition of ROOH (from the consumption of ROOH) and the rate of generation of free radicals (from the consumption of the acceptor of free radicals or initiation rate of the chain process of RH oxidation or  $\text{CH}_2=\text{CHX}$  polymerization) were measured for a series of systems (ROOH-catalyst-solvent). The comparison of these two processes showed that there are many systems, indeed, where the rate of ROOH decomposition and radical generation virtually coincide ( $v_i \approx v_d$ ). This is observed, for example, in the systems



However, there are many systems in which  $v_i \ll v_d$ , for example,



The decrease in  $v_i$  compared to  $v_d$  can be explained by the cage effect. However, the cage effect of a pair of radicals in low-viscosity liquids are characterized by the ratios  $v_i/v_d \approx 0.4 \div 0.8$ , so that the  $v_i/v_d$  ratios lower than 20% do not agree with the cage effect (see Chapter 7). In addition, at the cage effect  $E_i + E_d = \Delta E_i \gg E_D$ , and the activation energy of diffusion of a particle is  $5 \div 10$  kJ/mol. In experiment these systems (ROOH + metal complex) often exhibit very high  $\Delta E_i$  of 40–70 kJ/mol. This indicates the parallel occurrence of two different reactions: homolytic to form radicals and heterolytic to form molecular products. Thus, the general scheme of transformations of hydroperoxide in the coordination sphere of the metal has the form

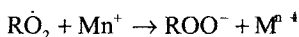


The cage effect is a component of this scheme. It takes place of the  $\text{RO} \cdot$  radical rapidly (within the time of the cage existence) reacts with the metal ion in the oxi-

dized state.

The question about the competition of the homolytic and heterolytic catalytic decomposition of ROOH is tightly associated with the question about the products of this decomposition. This can be exemplified by cyclohexyl hydroperoxide, whose decomposition affords cyclohexanol and cyclohexanone. When decomposition is catalyzed by cobalt salts, cyclohexanol prevails among the products ([alcohol] : [ketone] > 1) because only homolysis of ROOH occurs under the action of the cobalt ions to form RO· and RO<sub>2</sub>·: the first of them are mainly transformed into alcohol (in the reactions with RH and Co<sup>2+</sup>), and the second radicals are transformed into alcohol and ketone (ratio 1 : 1) due to the disproportionation (see Chapter 11). Heterolytic decomposition predominates for catalysis by chromium stearate (see above), and ketone prevails among the decomposition products (ratio [ketone] : [alcohol] = 6 in cyclohexane at 393 K). These precisely such ions that can exist in more than two different oxidation states (chromium, vanadium, molybdenum) are prone to the heterolytic decomposition of ROOH, and this seems to be mutually related.

Peroxyl radicals with a strong oxidative effect along with ROOH are continuously generated in oxidized organic compounds. They rapidly react with ion-reducing agents

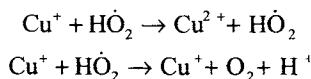


Below we present the rate constants for several systems

Ion	Radical	Medium	T, K	k, l/(mol s)
Cu <sup>+</sup>	HO <sub>2</sub> ·	H <sub>2</sub> O	296	4.3·10 <sup>9</sup>
Fe <sup>2+</sup>	HO <sub>2</sub> ·	H <sub>2</sub> O, 0.5M H <sub>2</sub> SO <sub>4</sub>	296	7.2·10 <sup>6</sup>
MnO <sub>4</sub> <sup>-</sup>	HO <sub>2</sub> ·	H <sub>2</sub> O, pH 3	296	7.9·10 <sup>6</sup>
Mn(EDTA) <sup>2+</sup>	PhC(CH <sub>3</sub> ) <sub>2</sub> OO·	CH <sub>3</sub> COOH	333	1.0·10 <sup>6</sup>
Co(EDTA) <sup>2+</sup>	PhC(CH <sub>3</sub> ) <sub>2</sub> OO·	CH <sub>3</sub> COOH	333	3.8·10 <sup>5</sup>
Co(Acac) <sub>2</sub>	~CH <sub>2</sub> CH(OO·)Ph	PhCl	353	5.0·10 <sup>4</sup>

Under the conditions where the chain oxidation process occurs, this reaction results in chain termination. In the presence of ROOH with which the ions react to form radicals, this reaction is disguised. However, in the systems where hydroperoxide is absent and the initiating function of the catalyst is not manifested, the latter has the retarding effect on the process. It was often observed that the introduction of cobalt, manganese, or copper salts into the initial hydrocarbon did not accelerate the process but vice versa results in the induction period and elongates it. The induction period is caused by chain termination in the reaction of RO<sub>2</sub>· with Mn<sup>II</sup>, and cessation of retardation is due to the formation of ROOH, which interacts with the catalyst and thus transforms it from the inhibitor into the component of the initiating system. Some peroxyl radicals (HO<sub>2</sub>·, >C(OH)OO·, >C(NHR)OO·) can either oxidize or

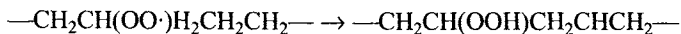
reduce, for example,



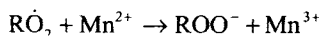
In systems where such radicals appear (alcohols, amines, some unsaturated compounds), variable-valence metal ions manifests themselves as catalysts for chain termination (see Chapter 11). The reaction of the ions with peroxy radicals appears also in the composition of the oxidation products, especially at the early stages of oxidation. For example, the only primary oxidation product of cyclohexane autooxidation is hydroperoxide: the other products, in particular, alcohol and ketone, appear later as the decomposition products of hydroperoxide. In the presence of stearates of such metals as cobalt, iron, and manganese, all three products (ROOH, ROH, and ketone) appear immediately with the beginning of oxidation and in the initial period (when ROOH decomposition is insignificant), they are formed in parallel with a constant rate. The ratio of rates of their formation is determined by the catalyst. The reason for this behavior is evidently related to the fast reaction of  $\text{RO}_2\cdot$  with the catalyst. Thus, the reaction of peroxy radicals with variable-valence ions manifests itself in the kinetics as well (the induction period appears under certain conditions), and alcohol and ketone are formed in parallel with ROOH from  $\text{RO}_2\cdot$  among the oxidation products.

The variety of functions of the catalyst is pronounced, in particular, in the technological catalytic oxidation of *n*-paraffins to aliphatic acids. This technology consists of several stages among which the central place is occupied by oxidation. It is conducted at 380–420 K in a series of reactors, the catalyst being a mixture of salts of aliphatic acids of  $\text{K}^+$  and  $\text{Mn}^{2+}$  or  $\text{Na}^+$  and  $\text{Mn}^{2+}$ . The alkaline metal salt stabilizes (makes it more soluble and stable) the manganese salt.

Many-year studies revealed the many-sided role of the catalyst (manganese ions). First, they ( $\text{Mn}^{2+}$  and  $\text{Mn}^{3+}$ ) react with hydroperoxide that formed and decompose it to generate radicals and thus initiate the chain oxidation process. Second, isomerization of  $\text{RO}_2\cdot$  of the following type vigorously occurs in oxidized paraffin (without a catalyst):

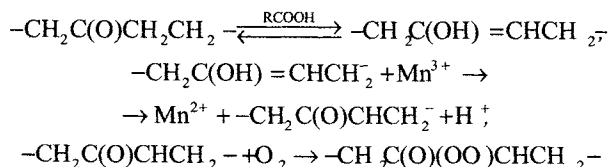


due to which polyfunctional compounds are formed and, finally, acids containing functional groups (oxy acids, keto acids, etc.), and this is very unfavorable for obtaining the target product (aliphatic acids). In the presence of the catalysts the reaction of  $\text{Mn}^{2+}$  with the peroxy radical successfully competes with the former reaction



due to which the fraction of bifunctional compounds decreases and the yield of

aliphatic acids increases. Third, the  $\text{Mn}^{3+}$  ions formed in the reactions of  $\text{Mn}^{2+}$  with  $\text{ROOH}$  and  $\text{RO}_2\cdot$  successfully react rather rapidly and oxidize carbonyl compounds



Two carboxylic acids are the final product of this ketone oxidation. As a result, the content of ketones in the system decreases, and the yield of aliphatic acids increases. Fourth, the accumulation of alcohols in the systems sharply retards the developed process, that is, results in the so-called limiting depth of oxidation. The hydroxyperoxyl radical is formed by the attack of  $\text{RO}_2\cdot$  at the alcohol group



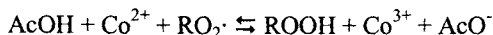
The  $\text{Mn}^{2+}$  and  $\text{Mn}^{3+}$  ions react with these radicals to result in catalytic chain termination. As alcohol is accumulated, the fraction of hydroperoxyl radicals increases among all peroxy radicals, and in parallel the rate of chain termination in the reaction of the ions with these radicals increases. The chain process ceases when the termination rate becomes higher than the rate of radical generation involving manganese ions. Thus, there are some limits of effecting on the oxidation process (depth, rate) for variable-valence metals used as catalysts.

### 16.3. Cobalt-bromide catalysis

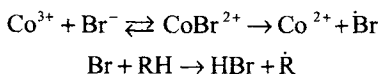
A cobalt-bromide catalyst is a mixture of cobalt and bromide salts in the presence of which hydrocarbons are oxidized with oxygen. Acetic acid or a mixture of carboxylic acids serves as solvents. The catalyst is used in the technology of production of arylcarboxylic acids by the oxidation of methylaromatic hydrocarbons (toluene, p-xylene, polymethylbenzenes). The catalyst was discovered as early in the 1950s, and the mechanism of catalysis was studied by many researchers. The experimentally developed scheme of the catalyst effect was proposed by I. V. Zakharov.

We showed in the previous section that hydrocarbon oxidation catalyzed by cobalt salts occurs under the quasi-stationary conditions with the rate  $v_{\text{max}} = 2(k_p[\text{RH}])^2/k_t$ , which is independent of the catalyst. This limit with respect to the rate is caused by the fact that at the fast catalytic decomposition of the ROH that formed the process is limited by the reaction of  $\text{RO}_2\cdot$  with RH. The introduction of the bromide ions into the system makes it possible to surmount this limit because creates a new route of hydrocarbon oxidation. In the reactions with  $\text{ROOH}$  and  $\text{RO}_2\cdot$  the  $\text{Co}^{2+}$

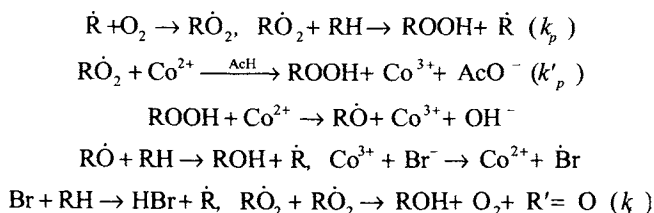
ions are oxidized into  $\text{Co}^{3+}$ , which in the reaction with ROOH are reduced to  $\text{Co}^{2+}$  and do not participate in initiation



However, in the presence of the  $\text{Br}^-$  ions, the  $\text{Co}^{3+}$  ions are reduced to  $\text{Co}^{2+}$ , and the Br atoms that formed participate, which is very important in chain propagation



These reactions result in an additional route of chain propagation, which allows one to exceed the rate limit, which is due to the mechanism of action of only variable-valence ions. In fact, the initial rate of RH transformation in the presence of the cobalt-bromide catalyst is determined by the rate of two reactions, namely, of  $\text{RO}_2\cdot$  with RH ( $k_p$ ) and of  $\text{RO}_2\cdot$  with  $\text{Co}^{2+}$  ( $k_p$ ), followed by the reactions of  $\text{Co}^{3+}$  with  $\text{Br}^-$  and of Br with RH. The general scheme includes the following steps (written in the simplified form):



Two reactions indicated above limit this process under the conditions of fast ROOH decomposition, so that the oxidation rate of RH is

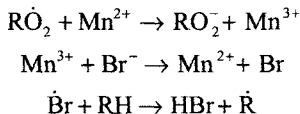
$$v = 2(k_p[\text{RH}] + k'_p[\text{Co}^{2+}])^2/k_t$$

The expression is valid for oxidation with excess of bromide ions over cobalt ions (the conditions of fast oxidation of  $\text{Co}^{3+}$ ). The experimental data agree with this dependence. Below we present the  $k_p$ ,  $k'_p$ , and  $E'_p$  values for three hydrocarbons (343 K, acetic acid)

RH	$k_p$ , l/(mol s)	$k'_p$ , l/(mol s)	$E'_p$ , kJ/mol
Toluene	1.6	$6.1 \cdot 10^2$	42
p-Xylene	4.5	$7.2 \cdot 10^2$	41
Ethylbenzene	5.4	$1.9 \cdot 10^2$	31

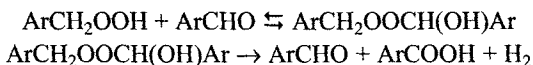
It is seen that  $k'_p \gg k_p$ , and the dependence of the reaction rate on the catalyst concentration makes it possible to increase it by increasing the catalyst concentration. Still higher oxidation rates are achieved when hydrocarbons are oxidized in the

presence of the catalytic system including the Co, Mn, and Br-ions. The Mn-Br binary system is less efficient than the cobalt-bromide catalyst. Synergism of the mutual catalytic effect of the Co and Mn ions is due to the fact that the  $\text{Co}^{2+}$  ions rapidly decompose hydroperoxide, and bivalent manganese ions very rapidly react with  $\text{RO}_2^\cdot$ , so that in the presence of  $\text{Mn}^{2+}$  the chain is more efficiently propagated in the reactions



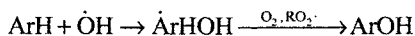
The peroxy radical of ethylbenzene reacts with  $\text{Mn}^{2+}$  in acetic acid with the rate constant  $k = 9.7 \cdot 10^4 \text{ l}/(\text{mol s})$  (347 K), which is by approximately two orders of magnitude higher than that with the  $\text{Co}^{2+}$  ions.

As alkylaromatic hydrocarbon (toluene, p-xylene, etc.) is oxidized, aldehydes appear; radicals and peracids formed from them play an important role. First, aldehydes react rather rapidly with the  $\text{Co}^{3+}$  and  $\text{Mn}^{3+}$  ions, which intensifies oxidation. Second, acylperoxy radicals appeared from aldehydes are very active and rapidly react with the initial hydrocarbon. Third, aldehydes forms with primary hydroperoxide an adduct, which decomposes to form aldehyde and acid



This creates a possibility of transforming ROOH into aldehydes omitting the stage of alcohol.

Generalizing the known data and established experimental peculiarities of action of the cobalt-bromide catalyst, we have to emphasize its following advantages. This catalyst makes it possible to increase the oxidation rate of alkylaromatic hydrocarbons due to the intense participation of the catalyst itself ( $\text{Co}^{2+}$ ,  $\text{Co}^{3+}$ ,  $\text{Br}^-$ , and  $\text{Br}^\cdot$ ) in chain propagation. It provides the fast transformation of intermediate products (hydroperoxide, aldehydes) into the final product, viz., acid. Finally, it makes it possible to oxidize hydrocarbon to a significant depth, and when the RH molecule contains several methyl groups, the catalyst allows all these groups to be transformed into carboxyls. This last specific feature is insufficiently studied so far. Perhaps, it is associated with the following specific features of oxidation of alkylaromatic hydrocarbons. The thermal decomposition of ROOH affords hydroxyl radicals, which give phenols after their addition at the aromatic ring

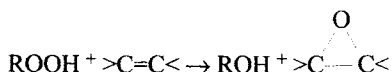


In addition, alkylaromatic hydroperoxide  $\text{ArCH}_2\text{OOH}$  under the acid action is heterolytically transformed into phenol and formaldehyde. Phenols are accumulated

and retard the oxidation process at early stages when the amount of methylcarboxylic acids (intermediate products) is yet low and they have no time to be oxidized further. In the presence of the catalyst during the intense generation of  $\text{RO}_2\cdot$  and  $\text{Co}^{3+}$ , phenols are rapidly oxidized and do not retard the process, which makes it possible to achieve the complete oxidation of all methyl groups in the hydrocarbon molecule to carboxyl groups.

#### 16.4. Catalytic epoxidation of olefins by hydroperoxides

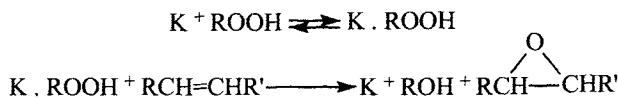
Olefin epoxidation by alkyl hydroperoxides occupies an important place among catalytic oxidation reactions. This process occurs according to the following stoichiometric equation:



The catalysts of this process are vanadium, molybdenum, tungsten, niobium, chromium, and titanium compounds. The yield of oxide calculated per olefin is close to 100%, and that per hydroperoxide reaches 85—95% and depends on the catalyst, temperature, and depth of conversion.

The first observation concerning catalytic olefin epoxidation was made in 1950 by E. Hawkins. He discovered oxide formation from cyclohexene and octane-1 during the decomposition of cumyl hydroperoxide in the medium of these hydrocarbons in the presence of vanadium pentaoxide. In 1963-1965 the Halcon Co. developed and patented the process of preparation of propyleneoxide and styrene from propylene and ethylbenzene in which the key stage is the catalytic epoxidation of propylene by ethylbenzene hydroperoxide. In 1965 N. Indictor and W. Brill published the work in which they studied the epoxidation of several olefins by tert-butyl hydroperoxide catalyzed by acetylacetonates of several metals. They observed the high yield of oxide (close to 100% with respect to hydroperoxide) for catalysis by molybdenum, vanadium, and chromium acetylacetonates. The low yield of oxide (15—28%) was observed in the case of catalysis by manganese, cobalt, iron, and copper acetylacetonates. The further studies showed that, indeed, the molybdenum, vanadium, and tungsten compounds are most efficient as catalyst for epoxidation. Atoms and ions of these metals possess vacant orbitals and easily form complexes due to the interaction with electron pairs of other molecules, in particular, with olefins and hydroperoxides. The epoxidation of the double bond by hydroperoxide with these catalysts is heterolytic. It is not accompanied by the formation of free radicals (the initiating effect of this reaction on oxidation is absent, inhibitors do not influence on catalytic epoxidation). The catalyst forms a complex with hydroperoxide, and this

complex epoxidizes olefin. Therefore, the initial epoxidation period is described by the seemingly simple kinetic scheme (K is catalyst)

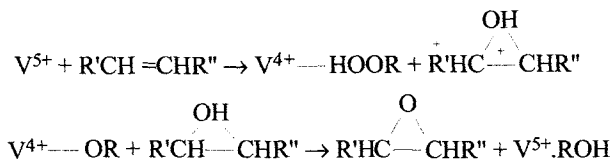


The dependence of the epoxidation rate on the concentrations of olefin and hydroperoxide is described by the Michaelis—Menten equation

$$v = kK_p[\text{Olefin}][ROOH][K](1 + K_p[ROOH])^{-1}$$

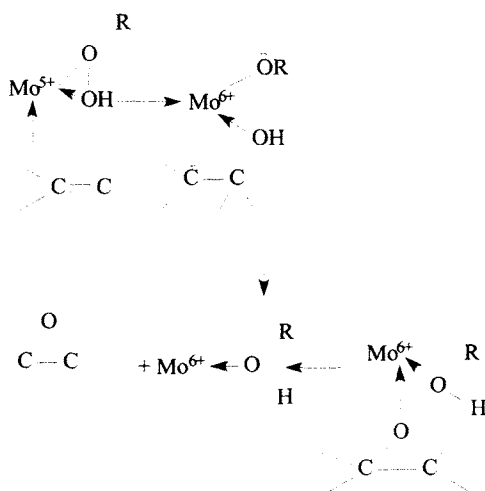
The catalyst is preliminarily oxidized to the state of the highest valence (vanadium to  $V^{5+}$ ; molybdenum to  $Mo^{6+}$ ). Only the complex of hydroperoxide with the metal in the highest-valence state is catalytically active. Alcohol that formed upon epoxidation is complexes with the catalyst. As a result, competitive inhibition appears, and the effective reaction rate constant, i.e.,  $v/[\text{Olefin}][ROOH]$ , decreases in the course of the process. Water, which acts by the same mechanism, is still more efficient inhibitor. Several hypothetical variants were proposed for the detailed mechanism of epoxidation.

1. The simplest mechanism includes stages of catalyst oxidation to the highest-valence state, the formation of a complex with ROOH, and the reaction (bimolecular) of this complex with olefin (E. Gould, R. Hiatt, K. Irwin, 1968).



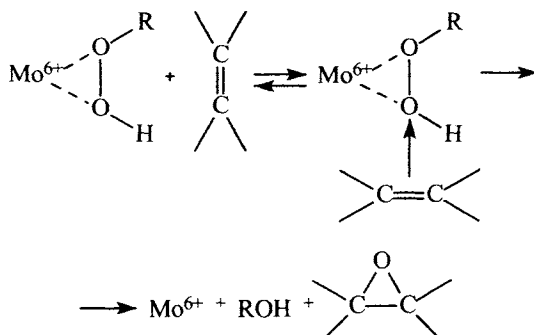
The first two stages (oxidation of  $V^{IV}$  to  $V^V$  and complex formation) were proved but the third stage predicting the heterolysis of the O—O bond with the addition of  $OH^+$  at the double bond is speculative. Heterolysis of this type is doubtful because of the very high energy of the heterolytic cleavage of  $RO—OH$  to  $RO^+$  and  $OH^-$ .

2. From the energetic point of view, the epoxidation act should occur more easily (with a lower activation energy) in the coordination sphere of the metal when the cleavage of one bond is simultaneously compensated by the formation of another bond. For example, E. Gould proposed (in 1974) for olefin epoxidation on molybdenum complexes the following (schematic) mechanism:

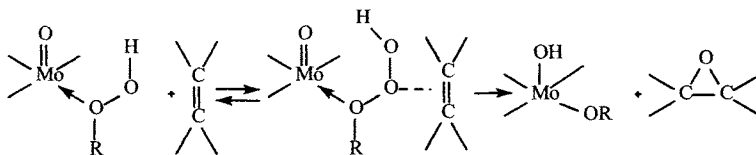


This scheme differs from the previous one by the fact that the heterolysis of the  $\text{O}-\text{O}$  bond occurs in the internal coordination sphere of the complex and is compensated by the formation of the  $\text{C}-\text{O}$  bond.

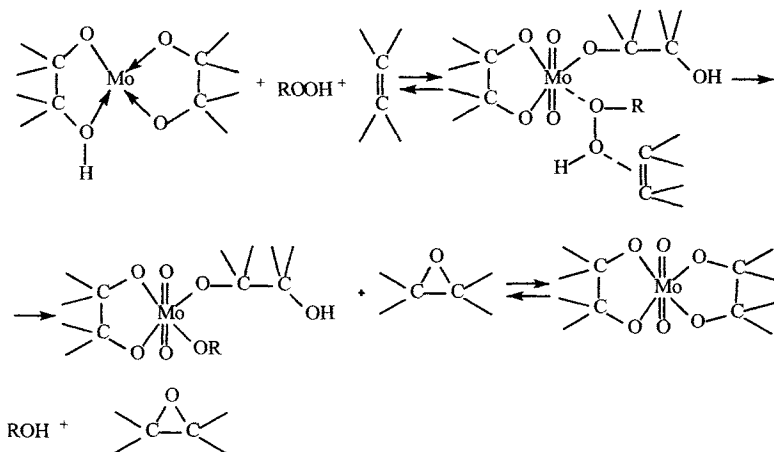
3. The complex in which olefin is bound by the donor-acceptor bond to the oxygen atom of hydroperoxide and exists in the secondary coordination sphere is also considered in the literature (V.N. Sapunov, 1974)



4. The proofs were obtained that the  $\text{Mo}=\text{O}$  group as a proton acceptor participates in epoxidation. In this connection, the following scheme taking into account this circumstance was proposed (R. Sheldon, 1973):



The formation of molybdenum complexes with diols (formed by olefin oxidation) was proved for the use of the molybdenum catalysts. Therefore, the participation of these complexes in the developed epoxidation reaction is assumed (R. Sheldon, 1973)



All schemes presented are similar and conventional to a great extent. It is characteristic that the epoxidation catalysts also result in the heterolytic decomposition of hydroperoxides (see Section 16.2) at which heterolysis of the O—O bond also occurs. Thus, there are no serious doubts that it occurs in the internal coordination sphere of the metal-catalyst. However, its specific mechanism and the structure of unstable catalyst complexes that formed are unclear. The activation energy of epoxidation is lower than that of the catalytic decomposition of hydroperoxides; therefore, the yield of oxide per consumed hydroperoxide decreases with the temperature increase.

### 16.5. Oscillating oxidation reactions

The rate of the chemical process usually changes with time smoothly: decreases with the consumption of reactants or increases and passes through a maximum in

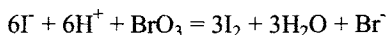
autocatalytic processes. According to this, the concentration of reaction products smoothly changes in time, and the kinetic curves have only one maximum or minimum if any. However, the systems were discovered in which the concentration of intermediate products oscillates, i.e., periodically passes through a maximum and a minimum. The amplitude of oscillations of the product concentration can decrease, increase, or remain unchanged for a long time. This regime was observed first for the decomposition of hydrogen peroxide catalyzed by iodine (V. Bray, 1921). Hydrocarbon oxidation in the gas phase is accompanied by the appearance of cold flame, which often flashes periodically (D. Townend, 1938, propane oxidation). B.P. Belousov was first to observe (1958) in redox systems the oscillation of concentrations of ion-oxidants ( $\text{Ce}^{4+}$  and  $\text{Ce}^{3+}$ ) for the oxidation of malonic acid catalyzed by cerium ions. Later A.M. Zhabotinsky showed (1964) that the oscillation regime is retained if malonic acid is replaced by another substrate with the activated  $\text{CH}_2$  group and cerium ions are replaced by manganese ions. He proposed the mechanism explaining this phenomenon. The more detailed and quantitative substantiated mechanism of this reaction was proposed by R. Noyes, R. Field, and E. Keresch (1972).

The main processes occurring in this system are the following: bromate oxidizes trivalent cerium to tetravalent;  $\text{Ce}^{4+}$  oxidizes bromomalonic acid, being reduced to  $\text{Ce}^{3+}$ . The bromide ion, which inhibits the reaction, is isolated from the oxidation products of bromomalonic acid. During the reaction the concentration of the  $\text{Ce}^{4+}$  ions (and  $\text{Ce}^{3+}$ ) oscillates multiply passing through a maximum and a minimum. The shape of peaks of concentrations and the frequency depend on the reaction conditions. The autooscillation character of the kinetics of the cerium ions disappears if  $\text{Ce}^{4+}$  or  $\text{Br}^-$  are continuously introduced with a low rate into the reaction mixture. The autooscillation regime of the reaction takes place only in a certain interval of concentrations of reactants:  $[\text{Malonic acid}] = 0.013 \div 0.5 \text{ M}$ ;  $[\text{KBrO}_3] = 0.013 \div 0.063$ ;  $[\text{Ce}^{3+}] + [\text{Ce}^{4+}] = 10^{-4} \div 10^{-2}$ ;  $[\text{H}_2\text{SO}_4] = 0.5 \div 2.4$ ;  $[\text{KBr}]$  - traces ( $2 \cdot 10^{-5}$ ). The oscillation regime begins after some time period after mixing of reactants; however, if a mixture of  $\text{Ce}^{3+}$  and  $\text{Ce}^{4+}$  corresponding to the established regime is introduced, autooscillations begin immediately. The period of vibrations ranges from 5 to 500 s depending on the conditions. The following data are known concerning the mechanism of particular stages.

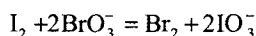
Hydroxybromomalonic acid (ROH) is brominated by  $\text{BrOH}$  and  $\text{Br}_2$ , and dibromomalonic acid that formed decomposes to form bromide ion, which inhibit the oxidation of  $\text{Ce}^{3+}$  with bromate. The autooscillation regime is observed in the  $\text{BrO}_3^-$ -cerium ions-reducing agent systems where the reducing agent is oxaloacetic, acetonedicarboxylic, citric, or malic acids; acetoacetic ester, and acetylacetone (all compounds contain the  $\beta$ -diketone group and are readily brominated in the enolic form).

The oscillation regime is observed in the oxidation of iodide ions by  $\text{BrO}_3^-$  ions. The kinetics of this reaction and its mechanism were studied in detail by O. Sitrey and I. Epstein (1986). The process was studied in a jet reactor. The oscillating regime

is observed when the concentration of iodide ions changes in an interval of  $5 \cdot 10^{-7}$ – $4 \cdot 10^{-2}$  M (bromate was introduced in excess with respect to iodide ions). The process occurs in two stages. The first stage is completed by the oxidation of  $I^-$  to  $I_2$  and proceeds according to the stoichiometric equation



with the rate  $v = 45[I^-][BrO_3^-][H^+]$  ( $T = 298$  K). The second stage is described by the stoichiometric equation



It proceeds autocatalytically: first  $I_2$  is transformed into  $BrI$ , which then is slowly transformed into  $Br_2$  and  $IO_3^-$ . In the oscillation regime, the concentration of  $Br^-$  changes from minimum to its maximum by almost 10 times, and the oscillation period is about 90 s ( $T = 298$  K,  $[BrO_3^-] = 5 \cdot 10^{-3}$ ,  $[I^-] = 2.5 \cdot 10^{-3}$ ,  $[H_3O^+] = 1.5$  M). The process includes the following stages (the rate constant is referred to  $T = 298$  K, water is solvent):

Reaction	k
$BrO_3^- + I^- + 2H_3O^+ \rightarrow HBrO_2 + HOI + 2H_2O$	$45 \text{ l}^3/(\text{mol}^2 \text{ s})$
$HBrO_2 + HOI \rightarrow HIO_2 + HOBr$	$10^9 \text{ l}/(\text{mol s})$
$I^- + HOI + H_3O^+ \rightarrow I_2 + 2H_2O$	$3.1 \cdot 10^{12} \text{ l}^2/(\text{mol}^2 \text{ s})$
$I_2 + 2H_2O \rightarrow I^- + HOI + H_3O^+$	$2.2 \cdot 10^2 \text{ l}^2/(\text{mol}^2 \text{ s}^{-1})$
$BrO_3^- + HOI + H_3O^+ \rightarrow HBrO_2 + HIO_2 + H_2O$	$8 \cdot 10^2 \text{ l}^2/(\text{mol}^2 \text{ s})$
$BrO_3^- + HIO_2 \rightarrow IO_3^- + HBrO_2$	$1.6 \cdot 10^4 \text{ l}/(\text{mol s})$
$HOBr + I_2 \rightarrow HOI + IBr$	$8 \cdot 10^7 \text{ l}/(\text{mol s})$
$IBr + HOI \rightarrow I_2 + HOBr$	$1 \cdot 10^2 \text{ l}/(\text{mol s})$
$IBr + 2H_2O \rightarrow HOI + Br^- + H_3O^+$	$30 \text{ s}^{-1}$
$HOI + Br^- + H_3O^+ \rightarrow IBr + 2H_2O$	$1 \cdot 10^8 \text{ l}^2/(\text{mol}^2 \text{ s})$
$Br^- + HBrO_2 \rightarrow HOBr + BrO^-$	$2 \cdot 10^6 \text{ l}/(\text{mol s})$
$HOBr + Br^- + H_3O^+ \rightarrow Br_2 + 2H_2O$	$8 \cdot 10^9 \text{ l}^2/(\text{mol}^2 \text{ s})$
$Br_2 + 2H_2O \rightarrow HOBr + Br^- + H_3O^+$	$1.1 \cdot 10^2 \text{ s}^{-1}$
$2H_3O^+ + Br^- + BrO_3^- \rightarrow HBrO_2 + HOBr + 2H_2O$	$2.1 \text{ l}^3/(\text{mol}^3 \text{ s})$
$HBrO_2 + HOBr + 2H_2O \rightarrow BrO_3^- + Br^- + 2H_3O^+$	$1 \cdot 10^4 \text{ l}/(\text{mol s})$
$Br^- + HIO_2 + H_3O^+ \rightarrow HOI + HOBr + H_2O$	$6 \cdot 10^5 \text{ l}^2/(\text{mol}^2 \text{ s})$
$HOI + HOBr + H_2O \rightarrow Br^- + HIO_2 + H_2O^+$	$2 \cdot 10^8 \text{ l}/(\text{mol s})$
$HIO_2 + HOBr \rightarrow IO_3^- + Br^- + 2H_3O^+$	$2.2 \cdot 10^8 \text{ l}/(\text{mol s})$
$BrO_3^- + IBr + 2H_2O \rightarrow IO_3^- + Br^- + HOBr + H_2O$	$0.8 \text{ l}/(\text{mol s})$

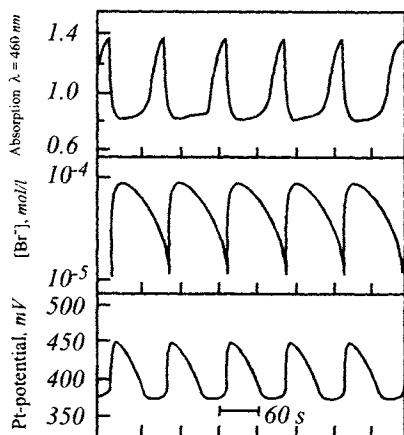
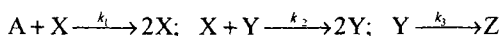


Fig. 16.1. Kinetics of changing the light absorption by  $I_2$  ( $\lambda = 460$  nm), concentration of  $Br^-$ , and potential of the Pt electrode in the system where the reaction of  $BrO_3^-$  with  $I^-$  occurs ( $[BrO_3^-]_0 = 5 \cdot 10^{-3}$  M,  $[I^-]_0 = 2.5 \cdot 10^{-3}$  mol/l,  $[H^+] = 1.5$  M,  $T = 298$  K).

The system of differential equations, which describes the process on the basis of all stages presented above, agree well with experiment and reproduces the oscillation regime of the process (Fig. 16.1).

One of the simplest schemes, which make it possible to describe the autooscillation regime, was considered by Lotka



The quasi-stationary state, if the system has achieved it, would have the form

$$c_{Xs} = k_3/k_2 \text{ and } c_{Ys} = k_1 c_{A0}/k_2$$

where  $c_A = c_{A0}$  in the course of the whole process.

To describe the behavior of the system near the quasi-stationary state, the variables are introduced

$$\xi = c_{Xs} - c_X \text{ and } \eta = c_{Ys} - c_Y$$

changes in  $\xi$  and  $\eta$  are described by the equations

$$d\xi/dt = -k_2\eta(\xi - c_{Xs}) \approx -k_2\eta c_{Xs}$$

$$d\eta/dt = k_2\xi(\eta + c_{Ys}) \approx k_2\xi c_{Ys}$$

whose solution has the form

$$c_1 \exp(-\lambda_1 t) + c_2 \exp(-\lambda_2 t)$$

where  $\lambda_1$  and  $\lambda_2$  are the roots of the equation

$$\lambda_2 = k_2^2 c_{Xs} c_{Ys}, \quad \text{i.e.} \quad \lambda = \pm i k_2 (c_{Xs} c_{Ys})^{1/2} = i (k_2 c_{Xs} c_{Ys})^{1/2}$$

The imaginary roots imply that  $c_X$  and  $c_Y$  undergo oscillation changes but never become equal to  $c_{Xs}$  and  $c_{Ys}$ , and at  $c_A = c_{A0}$  they remain unattainable. It can be shown that the system in the coordinates  $c_X - c_Y$  executes the cyclic motion around zero (zero has the coordinates  $c_X = c_{Xs}$ ,  $c_Y = c_{Ys}$ ).

As a rule, the transition from one equilibrium state to another with changing the conditions (temperature, concentration) occurs smoothly and via the same route for the motion both "from bottom" and "from top." However, in some systems the kinetic hysteresis is observed, viz., the transition from one state to another via different routes. The example is the photochemical dissociation of  $N_2O_4$

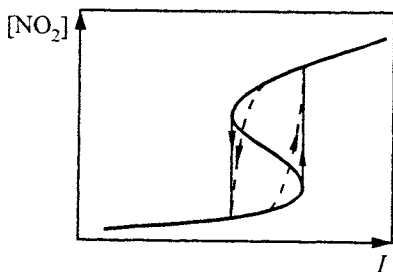
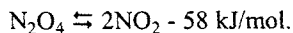


Fig. 16.2. Hysteresis phenomenon at the photochemical dissociation of  $N_2O_4$  ( $I$  is the light intensity).



Under irradiation with visible light, which is absorbed by only  $NO_2$ , the mixture is warmed, and the equilibrium shifts toward  $NO_2$ . If irradiation is started at the temperature above 240 K, the transition from bottom up and back occurs via the same curve in the coordinates  $[NO_2] - I$ .

At a lower initial temperature, the transitions "from bottom up" and "from top down" occurs via different routes (Fig.

16.2), that is, hysteresis is observed. This phenomenon is caused by the feedback between the degree of dissociation of  $N_2O_4$  and temperature of the gas under its continuous irradiation. The higher the concentration of  $NO_2$ , the more intense its absorption of the light and the higher the temperature of the gas. At a certain ratio between the temperature, rate constants of the direct and inverse reactions, heat capacity, and heat removal, the ambiguous transition of the system from one state to another appears, i.e., kinetic hysteresis.

## Catalysis by metal complexes

Catalysis by metal complexes in the liquid phase is presently a very important area in chemistry. Intense development of this field is due to several evident advantages of such catalysts. They are characterized by high catalytic activity, capability of reacting only with specific substrates (specificity) and in a specific position (selectivity).

Presently the number of industrial processes using metal complex catalysts is continuously increasing. They include such "classical" large-tonnage processes as polymerization on the Ziegler catalysts, olefin oxidation by molecular oxygen to aldehydes, hydroformylation of saturated compounds, preparation of acetic acid from methanol and carbon monoxide, synthesis of adiponitrile from butadiene, and others.

Metal complex catalysts allowed under mild conditions several reactions, which were previously unknown in chemistry, *viz.*, reduction of molecular nitrogen to hydrazine and ammonia, alkane activation and oxidation, water photodecomposition, *etc.*

Finally, due to relative simplicity of kinetic and physicochemical studies in the liquid phase and potentialities for wide varying of the structure and properties of the catalyst and medium, metal complex systems are convenient objects for the solution of basically novel problems of catalysis as a whole.

In this chapter, we consider the mechanisms of metal complex catalysis.

### *17.1. Electronic structure and catalytic properties of metal complexes*

The main features of metal complex catalyst are caused by a set of orbitals (*s*-, *p*-, *d*-, and *f*-orbitals) in a transition metal ion (Fig. 17.1-3). They interact with orbitals of ligands and substrates. The catalytic properties of complexes depend strongly on the properties of partially occupied *d*-orbitals of the metal tending to binding with neutral molecules, namely, substrates, which can donate electrons (CO, olefins, dienes, *etc.*). The substrate is activated during its coordination.

The formation of the  $\sigma$ - and  $\pi$ -bonds with the  $d$ -orbitals of the metal ion is illustrated in Fig. 17.1 using ethylene molecule coordination as an example. The formation of the  $\sigma$ -bond results in the shift of the electron density from the bonding orbital of the substrate to the metal ion. The inverse process occurs simultaneously in the  $\pi$ -system, that is, density on ethylene increases. These effects lead to the activation of the molecule and elongate the C—C bond. In the general case, due to the opposite direction of electron motion depending on the nature of the metal and other ligands, different effects are possible associated with an increase (or decrease) in the electrostatic charge on the substrate, change in its acid-base and nucleophilic (or electrophilic) properties, and change in the polarizability.

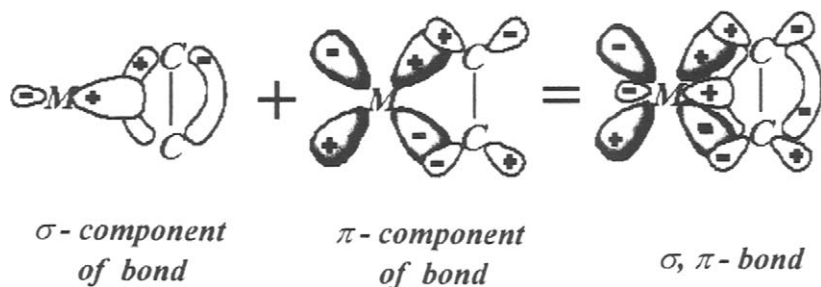


Fig. 17.1. Scheme of overlapping of molecular orbitals of ethylene and  $d$ -orbitals of the transition metal.

The main results of catalysis are approximately equal energies of all intermediate stages (smooth thermodynamic relief) of the process and low activation energies at each stage.

For this purpose, the catalyst has to possess optimum thermodynamic parameters, for example, the redox potential  $E^0$  corresponding to this process. As shown in practice, metal complexes with different structures are characterized by a very broad range of  $E^0$  values. For example, for dicyclopentadienyl complexes of transition metals, depending on the nature of the central atom, the  $E^0$  value ranges from  $-3$  to  $+2$  eV. The change in the donor-acceptor properties of substituents in the cyclopentadiene ring of ferrocene changes  $E^0$  by several electron volts.

Donor-acceptor effects in  $\sigma$ - and  $\pi$ -coordination systems can favor a decrease in the activation energies of particular stages of the catalytic processes

(by changing the nature of the central atom, ligands, and properties of the medium).

The ability to be in coordinationally unsaturated states is substantial for the catalytic properties of metal complexes. In this case, substrate molecules can be arranged sterically close to each other, which substantially increases the probability of their direct interaction.

The capability of changing the coordination number during chemical transformation increases the number of possible reaction routes in the coordination sphere of the metal complex.

We would like to mention two parameters among other parameters of metal complexes substantial for the catalytic properties. The first parameter is related to the steric effects of bulky ligands, which are characterized, in particular, by the canonical angle (angle of the cylindrical cone with the vertex remote at a certain distance from the coordinated atom of the ligand). The volume and shape of the ligand affect the stability of the complex and its ability to perform selective reactions. The second property was generalized by K. Tolman as the "rule of 18 valent electrons." Electrons donated by the central metal atom and two electrons from each ligand are included into the number of valent electrons. The relative stability of such diamagnetic complexes provides a higher probability of their participation as intermediates in complex catalytic processes.

### *17.2. Specific features of electronic structure of transition metal clusters*

Complexes containing several interacting metal atoms are named clusters. Metal atoms in clusters bound by chemical forces are localized at rather short distances for efficient overlap of their valent orbitals. This overlap results in the system of molecular delocalized states (Fig. 17.2).

The energies of these states are close to the energies of the initial atomic states. Their difference does not exceed values of an order of the energy of interaction of atoms. Molecular orbitals with different symmetries are formed from atomic orbitals of atoms composing the cluster. The levels of each type of symmetry are approximately uniformly dispersed over the  $E$  energy interval, that is, the group of tight levels of the nearest excited states consists of levels with different symmetries.

Small local changes in the electron density result in slight changes in the forces acting on the nuclei in the cluster. Therefore, it can be accepted that the displacement of equilibrium positions of the nuclei during the redox process is small. The small rearrangement of the nuclear system during electron transitions favors multielectron transfers involving clusters because synchronization of the

motion during transfer is facilitated due to small nuclear displacements in the system.

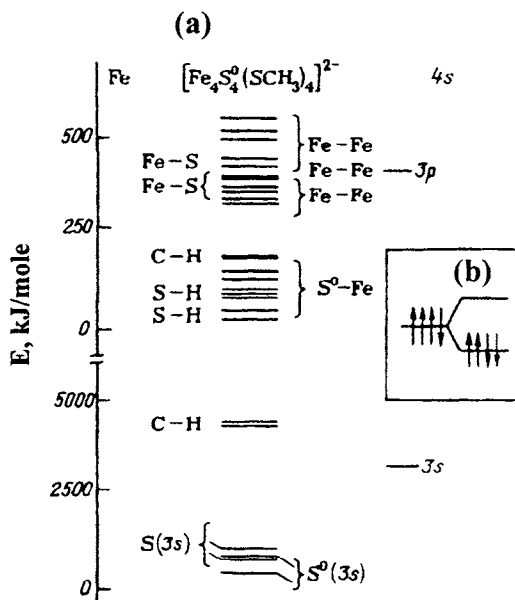


Fig. 17.2. Scheme of energy levels (a) in the iron-sulfur tetranuclear cluster and scheme of electron population of the highest orbitals (b). When the charge of the cluster changes by the addition or elimination of an electron, the cluster system can add or donate one to two electrons without a substantial change in energy and configuration. Therefore, it is characterized as a system with the great electron capacity (I.B. Bersuker).

Clusters possess a pronounced capability of multiorbital binding of ligands when, *e.g.*, electrons are transferred from the occupied *d*-orbitals of the metal to the antibonding orbitals of the ligand with the simultaneous back transfer from the bonding orbitals of the ligand to the unoccupied *d*-orbitals of the metal. Multiorbital binding is illustrated in Fig. 17.3. by the formation of the binuclear  $N_2$  complex.

Multiorbital binding can be characterized in chemical terms as parallel donor-acceptor and dative interactions of the metal complex with the substrate. An advantage of multiorbital binding over one-orbital binding is the possibility of a much stronger change in the electronic structure of the substrate during coordination. The matter is that during one-orbital binding the noticeable transfer

of the electron density is prevented by the charge resulting in the appearance of the electric field directed opposite the transfer. For multiorbital binding, the coordination of bonds of the substrate can change more considerably due to the effect of charge compensation because of the unlikely directed transfers.

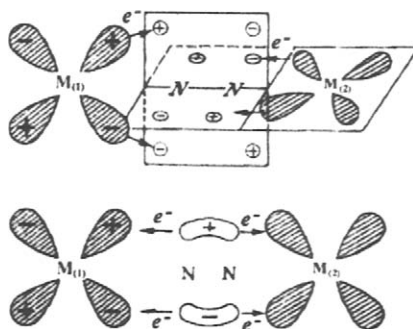


Fig. 17.3. Scheme of multiorbital overlap of the  $d$ -orbitals of metal atoms with the orbitals of  $N_2$  in the binuclear complex.

In addition, the charging effect in clusters is less significant because of the transferred charge distribution over the atoms of the cluster due to the delocalization of the  $d$ -states of the cluster. The atomic  $d$ -orbitals are rather strongly localized due to which two electrons on one  $d$ -orbital undergo strong Coulomb repulsion. The formation of the molecular orbital delocalized over many centers from the atomic  $d$ -orbitals in the cluster decreases the Coulomb repulsion due to an increase in the average distance between electrons.

As mentioned above, clusters have many closely lying levels of different types of symmetry. Therefore, the interaction with other molecules or a change in the electronic state of complexes provides a high probability that orbitals with the corresponding symmetry would be included in this process. This results in the possibility of "avoiding" reaction pathways, which are forbidden in symmetry and multiplicity.

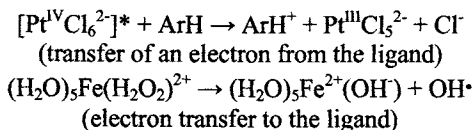
Due to the listed properties, clusters are promising catalysts of redox processes. This type of catalysis is very abundant in the nature.

### 17.3. Mechanisms of reactions in the coordination sphere of metal complexes

#### 17.3.1. Electron transfer

Electron transfer, which can be complete or partial, occurs at the appropriate combination of redox potentials of the central atom and ligands.

The complete electron transfer is usually postulated in reactions of photoexcited complexes and complexes in the ground state, which have high positive and negative  $E_0$  values. The following reactions are presented as an example:



Inner-sphere incomplete charge transfer occurs, in particular, in complexes of molecular oxygen with the copper dipyriddy complex  $[\text{dipy}_2\text{CuO}_2^+]$  in which the oxidation state of copper is intermediate between I and II.

The interaction of the catalytic center with the substrate can proceed *via* the peripheral mechanism when the stage-to-stage transfer is impeded for thermodynamic reasons due to a high barrier at one of the stages, and the one-stage two-electron process is more thermodynamically favorable. This process is likely exemplified by the oxidation of  $\text{Fe}^{\text{II}}$  to  $\text{Fe}^{\text{IV}}$  with hypochlorous acid (Yu.N. Kozlov, A.P. Purnal').

#### 17.3.2. Complex formation

Complex formation with the substrate is the key stage of many catalytic processes. The formation of the following types of organometallic complexes is most typical in catalysis: alkyl  $\pi$ -complexes, carbene complexes,  $\pi$ -complexes of substrates with the saturated bond (olefin, acetylene and allyl, complexes with carbon oxides), hydrazine complexes, and complexes with molecular oxygen and nitrogen. The structure of a ruthenium complex with  $\text{CO}_2$  obtained on the basis of an *ab initio* study is presented in Fig. 17.4.

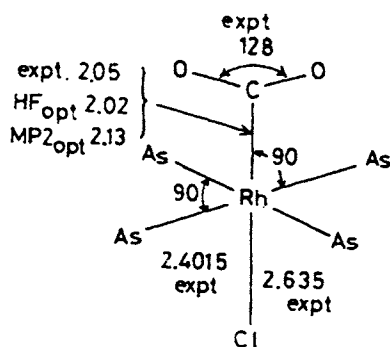


Fig. 17.4. Structure of  $\text{Rh}(\text{AsH}_3)_4(\text{CO}_2)$  complex (Sakaki et al., *Inorg. Chem.* **28**,103-109,1989). Reproduces with permission.

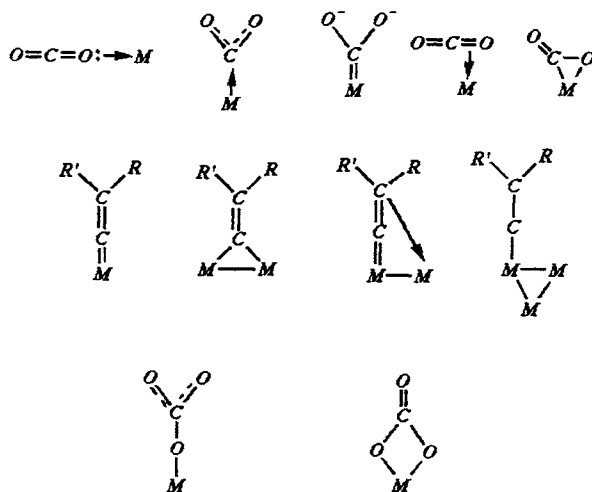


Figure 17.1 illustrates possible variants of the interaction of the orbitals of the central atom with the substrate in olefin complexes to form  $\sigma$ - and  $\pi$ -bonds. Above we present possible methods for complex formation of carbon dioxide, carbene, and carbonate.

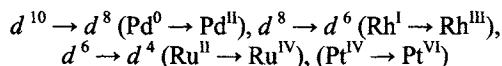
The catalytic role of various complexes was considered in sections devoted to the corresponding catalytic reactions.

### 17.3.3. Oxidative addition and reductive elimination

Complexes of several low-valence metals ( $\text{Fe}^0$ ,  $\text{Ru}^0$ ,  $\text{Co}^I$ ,  $\text{Pt}^{II}$ , and others) can add  $\text{X—Y}$  molecules to form two covalent bonds:  $\text{M} + \text{XY} \leftrightarrow \text{X—M—Y}$ . Molecular hydrogen, oxygen, halogen derivatives, arenes, alkanes, *etc.* act as such molecules. Since the formal oxidation state increases by two units, the process was named the oxidative addition, and the inverse process was named the reductive elimination.

The possibility of oxidative addition is determined by several factors, such as the presence of two free coordination sites, the difference between the bond energies  $E_{\text{X—Y}}$  and the sum  $E_{\text{M—X}} + E_{\text{M—Y}}$ , the positive overlap and energy correspondence of orbitals of the metal and substrate, and the absence of steric hindrances. For example, the oxidative addition of  $\text{H}_2$  to  $\text{Pt}(\text{PH}_3)_2$  is exothermic,  $\Delta H = 67 \text{ kJ/mol}$ .

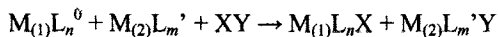
Since in such molecules as  $\text{H}_2$ ,  $\text{RH}$ , and  $\text{RCl}$  the lowest unoccupied orbitals have a rather high energy, the tendency to oxidative addition of small molecule is most pronounced for low-valence metals with the highest occupied  $d$ -orbitals. The typical redox transitions are



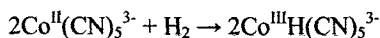
Oxidative addition to the central metal atom is favored by ligands increasing the electron density on the metal. The formation of alkane  $\text{RH}$  from the alkylhydride complex ( $\text{R—M—H}$ ) is an example of reductive elimination.

### 17.3.4. Homolytic and heterolytic addition

In homolytic addition fragments of the substrate molecule  $\text{X—Y}$  add to two metal-containing molecules with the change in the oxidation state of each metal by unity

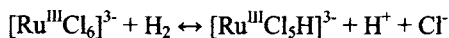


The example of this reaction is



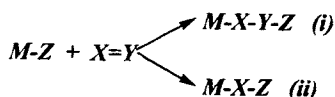
The factors that influence on this process are analogous to those favoring oxidative addition.

In heterolytic addition the oxidation state of the metal remains unchanged, and one of the fragments of the  $X-Y$  substrate transforms into the ionized state as it takes place in the addition of molecular hydrogen to ruthenium(III) hexachloride

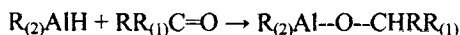


### 17.3.5. Insertion and migration of internal ligands

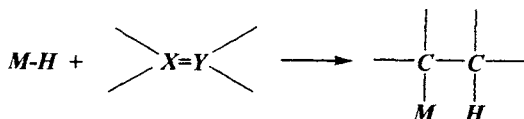
In the general case, the insertion of the ligand is described by the scheme



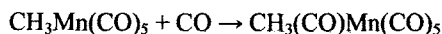
The Al, B, Rh, Mo, Ti, Mn, Fe, and Pd atoms act as M in these reactions. The  $X=Y$  bonds are presented by such bonds as  $C=C$ ,  $C=N$ ,  $N=N$  and  $C=O$ , and  $C=N-R$ . An example of reaction I is the insertion of the polar ketone group at the polar  $AlH$  bond



The low-polarity bonds of olefins are inserted into the low-polarity  $M-H$  and  $M-C$  bonds in complexes of the  $d^1$ -,  $d^2$ -, and  $d^9$ -metals (for example,  $\text{MH}_2$ ,  $\text{Cp}_2$ )



The second type of insertion can be illustrated by the insertion of carbon monoxide into manganese methylpentacarbonyl



The migration of one ligand from the metal atom to another ligand is possible inside the coordination sphere



$\sigma$ - $\pi$ -Rearrangements of the type



can also be attributed to processes of internal ligand migration.

Similar transformations are stimulated by a change in the coordination number of the central atom due to the addition or elimination of the external ligand, *e.g.*, amine (L) in the reaction

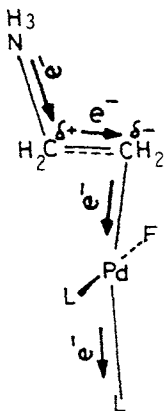
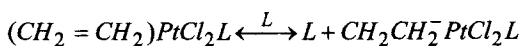
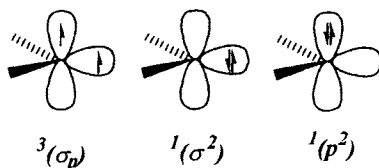


Fig. 17.5. Scheme of nucleophilic attack of  $NH_3$  on a coordinated olefin assisted by palladium complex (Sakaki et al., *Inorg. Chem.* **26**, 2499-2505, 1987). Reproduced with permission.

The special role in reactions (hydrogenation, dehydrogenation, carbonylation, alkene isomerization, chain growth, *etc.*) involving coordination compounds

belongs to carbenes (as ligands), whose simplest representative is methylene ( $\text{:CH}_2$ ). This molecule exists in three states



The triplet  $^3(\sigma_p)$  state with the HCH angle about  $135^\circ$  is the most stable configuration. Energy of 38 kJ/mol is required for the transformation to the excited singlet state  $^1(\sigma^2)$ . The latter state is most reactive in one-stage addition to multiple C=C bonds and insertion at the C—H, H—H, and other ordinary bonds. In the majority of reactions the methylene derivatives exhibit the electrophilic properties. However, strong  $\pi$ -donor substituents, for example, MeO, favor nucleophilic reactions.

The palladium -assisted nucleophilic attack on a coordinated olefin studied by *ab-initio* semiquantitative method is presented in Fig. 17.5.

The combination of the mechanisms listed in the coordination sphere of the metal results, in most cases, in the equality of the energies of intermediate states and low energy barriers to catalytic processes.

#### 17.4. Hydrogenation and activation of C—H bonds

The addition of molecular hydrogen to unsaturated compounds does not occur due to the high energy barrier caused by the quantum-chemical prohibition and high bond energy in  $\text{H}_2$ .

However, we know numerous homogeneous catalytic reactions occurred with a high rate under the action of low-valence complexes of such metals as Ru, Rh, Co, Pt, Pd, Mn, *etc.* The typical ligands of such complexes are phosphines, CO,  $\text{Cl}^-$ ,  $\text{CN}^-$ , and others. Clusters of the Pd, Pt, Ni, and Os metals are used in recent years. The structure of one of these complexes obtained by the Hartree-Fock-Slate transition state method is presented in Fig. 17.6

The key stage of the catalytic reaction is the formation of the hydride M—H complex with the simultaneous coordination of the unsaturated X=Y bond of the substrate to the metal atom. Then the unsaturated bond (for example, CO) reacts with the M—H bond followed by the addition of the second hydrogen atom.

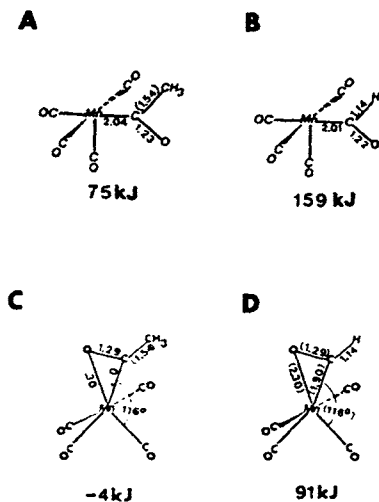
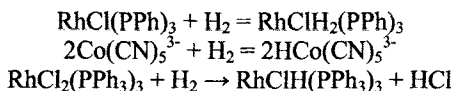


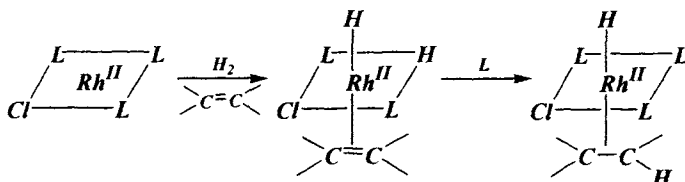
Fig. 17.6. Structures and energies of  $\text{CH}_3\text{C(O)Mn(CO)}_4$  and  $\text{HC(O)Mn(CO)}_4$ . The energies (kJ mol<sup>-1</sup>) are relative to the parent  $\text{CH}_3\text{Mn(CO)}_5$  and  $\text{HMn(CO)}_5$  molecules, respectively. Bond distances are given in Å (Ziegler et al., *J. Am. Chem. Soc.* **108**, 612-617, 1982). Reproduced with permission.

The hydride complex can be formed *via* three mechanisms: oxidative addition (1), homogeneous (2) or heterolytic (3) addition. These three processes are presented below.

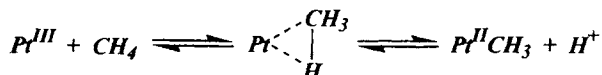


The limiting stage of the process is, as a rule, the intracomplex migration of hydride to the unsaturated bond, as it is assumed, *e.g.*, for the so-called Wilkinson complex

The subsequent isomerization stages with hydride migration and reductive elimination of alkane complete the catalytic cycle.



In the above reaction the second hydrogen atom adds to ethylene by the migration of the hydride atom already present in the complex. This mechanism is designated by the symbol  $\eta^4$ . In another,  $\eta^3$ -mechanism, which involves  $\text{Co}(\text{CN})_5^{3-}$ , the insertion of the unsaturated bond into the hydride complex is followed by the oxidative addition of the  $\text{H}_2$  molecule accompanied by the elimination of the hydrogenated product and regeneration of the catalyst. The following reactions occur between methane molecules and protons of the medium and in halogenation and hydroxylation of hydrocarbons in the presence of  $\text{Pt}^{\text{II}}$  tetrachloride:



At room temperature  $k_1 = 3 \cdot 10^{-3} \text{ l}/(\text{mol} \cdot \text{s})$ ,  $k_{-1}[\text{H}^+]/k_2 = 1.75 \cdot 10^{-2} \text{ M}$  and  $k_3 = 0.14 \text{ s}^{-1}$ ; the reaction proceeds through the formation of the metal-alkyl complex, whose formation was detected by NMR.

The coordinationally unsaturated intermediate rhodium complex was proved experimentally at low temperatures ( $-55^\circ\text{C}$ ). The formation of the C—C bond is catalyzed by bivalent palladium complex. It is assumed that the activation of aromatic compounds is facilitated due to the preliminary  $\pi$ -coordination of the substrate to the metal atom. The examples of other reactions involving low-valence metal complexes are presented in the next section.

The interaction of  $\text{CO}_2$  with the H ligand in  $\text{CuH}(\text{PH}_3)$  complex through the charge-transfer from the H ligand to  $\text{CO}_2$  and the electrostatic interaction between the  $\text{Cu}^+$  and (O) atoms is schematically shown in Fig. 17.7. These interactions correspond to a four-center-like transition state.

In strongly acidic media, for example, in  $\text{CF}_3\text{COOH}$ , hydrogenation begins from the protonation of the substrate followed by the addition of hydride to the radical cation that formed.

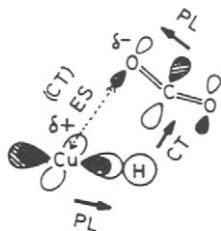


Fig. 17.7. Interactions in complex  $\text{CuH}(\text{PH}_3)$  with  $\text{CO}_2$  proposed on the basis of *ab initio* study (Sakaki et al., *Inorg. Chem* **28**, 2583-2590, 1986). Reproduced with permission.

In the present time many catalytic systems have been proposed in which various unsaturated compounds, viz., alkenes, alkanes, dienes, aromatic and heterocyclic compounds, aldehydes, ketones, and nitro compounds, are hydrogenated by molecular hydrogen. Selecting the corresponding catalysts and reaction conditions, one can achieve a high selectivity and perform reactions that afford asymmetrical compounds.

Under specific conditions, hydrogenation can proceed through a series of one-electron stages. A similar mechanism likely takes place when nitrobenzene is reduced in aprotic solvents in the presence of  $\text{PtCl}_2$ ,  $\text{NaBH}_4$ , and hydroquinone. It is assumed that the catalyst donates electrons to the substrate molecule, and hydroquinone protonates the reduced intermediate. Phenylhydroxylamine is the final reaction product.

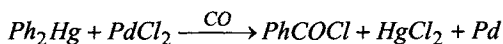
Several other hydrogenating agents are used in addition to dihydrogen. For example, in the presence of the  $\text{CoCl}_2$ ,  $\text{FeCl}_2$ , and  $\text{RhCl}(\text{CO})(\text{PPh}_3)_2$  catalysts,  $\text{NaBH}_4$  hydrogenates alkenes and amines. Organic compounds, such as silanes, alcohols, acids, dioxane, piperidine, and several inorganic complexes, e.g.,  $\text{Mo}(\text{CO})_6$ , can serve as sources of hydrogen and electrons in the corresponding reactions.

An interesting type of reactions including the activation of chemically inert C—H bonds is based on oxidative addition. This process appears, in particular, in isotope exchange of alkanes with molecular hydrogen.

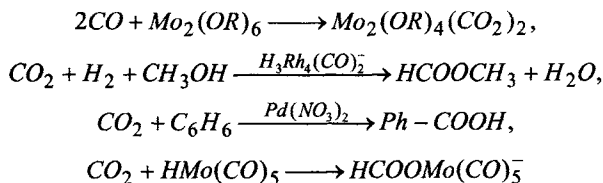
### 17.5. Carbonylation, carboxylation, hydroformylation and hydrochlorination

Homogeneous catalysts based on complexes of low-valence transition metals favor the reactions of carbon monoxide and formate with molecular hydrogen,





Catalytic systems involving such an inert molecule as carbon dioxide in the reaction have been proposed in recent years, for example,



These reactions, most likely, also involve the stages described above of oxidative addition and intracomplex insertion.

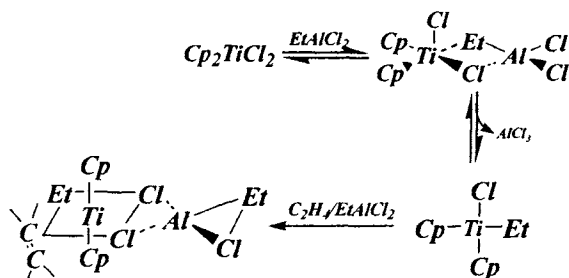
The examples presented convincingly demonstrate possibilities of using low-valence transition metal complexes in various catalytic reactions.

### 17.6. Polymerization, oligomerization, and metathesis

Organic compounds with multiple bonds in the presence of complexes containing transition metals (Ti, Rh, W, Mo, Re, Ni, and others) can undergo various transformations to afford polymeric, oligomeric, and isomeric products. Despite a variety of catalytic mechanisms, these processes are characterized by several general properties including the stages of formation of low-valence coordinationally unsaturated intermediates, coordination of unsaturated bonds, and intracomplex insertion. In many cases, the activation of the intermediate complex occurs due to the alkylation of the central metal atom.

The Ziegler—Natta catalysts are most efficient in heterogeneous and homogeneous polymerization of olefins. They consist of two main components: complexes of metals of Groups IV—VII and halide groups.

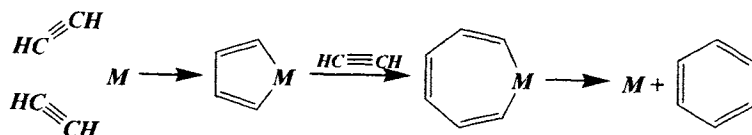
One of the most active homogeneous catalytic systems includes bivalent titanium complexes and alkylaluminum chloride. The reaction is assumed to proceed *via* the following scheme:



These stages result in the formation of the active form of the catalyst. The next is the key stage of ethylene insertion at the methane-alkyl bond, whose multiple repetition results in the polymeric chain growth. The reaction ceases when the metal in the catalytic complex is reduced to the trivalent state.

Non-stereoregular atactic polymer is obtained in homogeneous catalytic systems during propylene polymerization. The stereoregular polymer is obtained when heterogeneous catalysts are used. Oligomerization is the formation of products with a higher molecular weight than the initial substrates but insufficient to consider them polymers. Catalysts of alkene oligomerization are the Ziegler—Natta contacts, metal (Ni, Co, Rh, Fe, Cr) carbonyl complexes, and dimeric complexes of the  $\text{Rh}_2(\text{CF}_3\text{COO})_4$  type. Two types of oligomerization are distinguished: cyclic and linear.

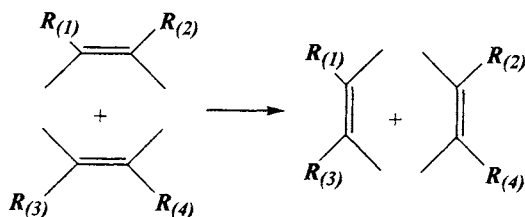
The cyclic process can be illustrated by acetylene cyclotrimerization to benzene by a transition metal in a low oxidation state. At the first stage, two acetylene molecules give the five-membered cycle involving the central M atom, and the insertion of the third acetylene molecule increases the number of atoms in the cycle to seven followed by the rearrangement to benzene



Ethylene is dimerized similarly involving nitrile and acetylene derivatives to butene on the Ziegler catalysts.

The  $\text{Ni}^{2+}$  and  $\text{Co}^{2+}$  complexes with phosphine ligands are most active in the presence of alkylaluminum chlorides in the linear oligomerization of alkenes. These reactions also involve, most likely, the stages of substrate coordination,  $\sigma$ - $\pi$ -rearrangement, insertion, and reductive elimination.

Metathesis is the redistribution of unsaturated bonds between alkene or alkyne molecules



These reactions are catalyzed by systems similar to the Ziegler—Natta contacts, in particular, those containing tungsten hexachlorides, molybdenum and rhenium pentachlorides in the presence of alkylaluminum chlorides.

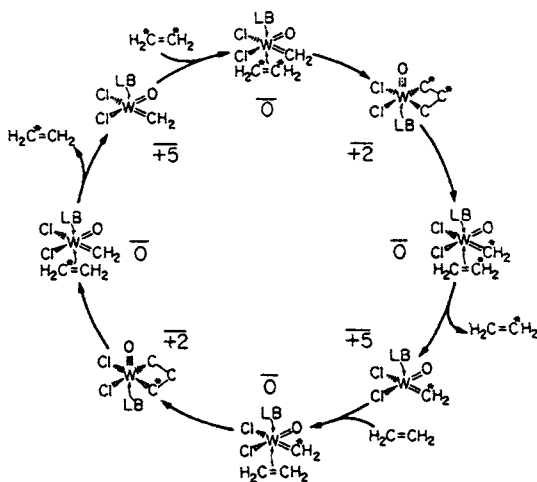
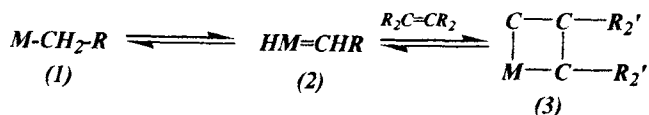


Fig. 17.8. The full catalytic cycle for metathesis by W oxo-alkylidene with Lewis base. Energies are DG3000 in kcal/mol (Rappe A.K and Goddard III, W.A., *J. Am. Chem. Soc.* **104**, 448-456, 1982). Reproduced with permission.

The most probable mechanism of metathesis is that involving a metal-alkyl complex, which transforms into a metal-carbene complex, e.g., according to the scheme



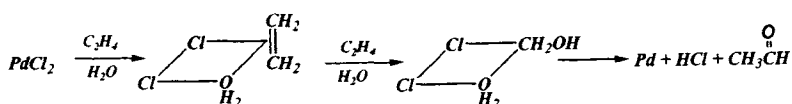
Complex (2) coordinates the second olefin molecule. Then stages of  $\sigma$ - $\pi$ -isomerization, metallocycle formation,  $\sigma$ - $\pi$ -isomerization, and escape of the newly formed  $RCH=CR'_{(2)}$  molecule from the coordination medium are assumed.

Fig. 17.8 shows the full catalytic cycle for metathesis by a tungsten complex.

### 17.7. Oxidation

Transition metal complexes can be included into the catalytic processes by the coordination and activation of the substrate or oxidant.

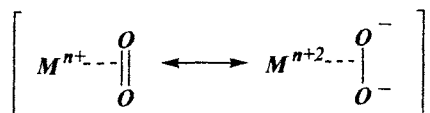
The Waker process exemplifies the first type of process. It is the reaction of oxidation of ethylene and other olefins to acetaldehyde in the presence of  $Pd^{II}$  and  $CuCl_2$  salts in an aqueous hydrochloride solution. The reaction is assumed to occur through the scheme



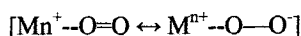
The key stage of the process is  $\pi$ - $\sigma$ -rearrangement with the insertion at the Pd—OH bond and elimination of a proton. At the subsequent stages, metallic palladium is reoxidized by  $CuCl_2$  and  $O_2$  to the initial state.

Aromatic compounds, including toluene and xylene, enter into analogous catalytic processes. The stages of coordination and formation of the  $\equiv C-Pd$  covalent bond are also postulated for oxidative dimerization and oxidative coupling of olefins and aromatic compounds. Olefin oxidation is also catalyzed by the  $Hg^{II}$  and  $Tl^{III}$  complexes.

Many complexes of molecular oxygen with transition metal ions are known. In all cases, the electron density shifts from the metal to O<sub>2</sub>. According to this fact, the complexes of the "peroxide" complexes are distinguished

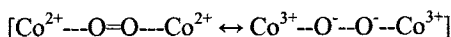


They are typical of metals with the  $d^8$ - ( $Ir^+$ ,  $Co^+$ ) and  $d^{10}$ - ( $Pt^0$ ,  $Pd^0$ ,  $Ni^0$ ) configurations with electron-donor, *e.g.*, phosphorus, ligands and ligands of the "superoxide" type



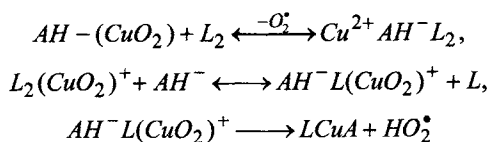
The latter type is presented by the  $Co^{2+}$ ,  $Co^{3+}$ ,  $Mn^{3+}$ , and  $Fe^{2+}$  complexes with porphyrin and other macrocyclic ligands and the  $Ti^{4+}$ ,  $Mo^{6+}$ , and  $V^{5+}$  complexes.

The complexes described above and binuclear systems of the type



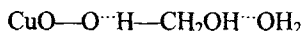
are highly stable in redox reactions and are "keepers" and carriers of O<sub>2</sub>.

The  $Cu^{2+}$  and  $Fe^{2+}$  complexes are used for the activation of the inert oxidant, *viz.*, molecular oxygen. The inclusion of O<sub>2</sub> into the coordination sphere of these metals results in the reaction of inner-sphere transfer of one or two electrons and a series of subsequent redox processes. Let us consider some reactions involving 2,2'-dipyridyl complex  $L_2Cu^{2+}$ , which catalyzes the oxidation of different substrates of the  $AH_2$  type (malonic and ascorbic acids)



In this reaction the key stage is the inner-sphere transfer and an electron and proton followed by the escape of the active radical species  $HO_2^*$  into the solution.

It is most likely that the different, more thermodynamically favorable mechanism takes place in the oxidation of alcohols, in particular, methanol. It is the inner-sphere two-electron transfer of the hydride ion from the alcohol molecule to oxygen



Simultaneously a proton is transferred from the carbon atom of alcohol to the solvent. Other mechanisms of oxidative processes in the presence of metal complexes are also presented in the literature. For example, the  $\text{Co}^{\text{III}}$ ,  $\text{Mn}^{\text{III}}$ , and  $\text{Pt}^{\text{IV}}$  complexes oxidize olefins presumably by the one-electron mechanism. The reaction of  $\text{O}_2$  with cobalt dicyclopentadienyl derivatives is accompanied by the oxidation of  $\alpha$ -diketones and *o*-quinones.

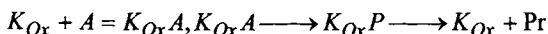
### 17.8. Metal complex electrocatalysis

A promising direction based on the combination of stages of metal complex catalysis with electrode processes has recently been developed.

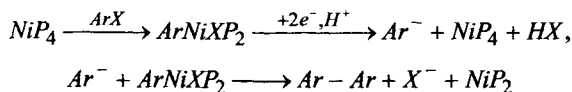
Two types of electrocatalytic processes are distinguished. The first type includes the outer-sphere transfer of an electron to the catalyst molecule in the oxidized form ( $K_{\text{ox}}$ ), which performs the further catalytic process of transformation of the substrate *S* into the product *Pr* in a solution



Another type of electrocatalysis includes the formation of an intermediate complex between the catalyst and substrate and further reaction according to the scheme



Efficient electrocatalysis can be exemplified by dehalogenation of aryl and alkyl halides ( $\text{ArX}$ ). The direct electrochemical reduction of these compounds requires very low redox potentials ( $-1.6$  V). However, in the presence of the zero-valence nickel tetraphosphine complex, efficient dehalogenation *via* the scheme



occurs.

Another example is the catalytic reduction of compounds bearing the triple bond ( $\text{N}_2$ ,  $\text{C}_2\text{H}_2$ ,  $\text{CO}$ ). The system containing  $\text{Mo}^{\text{III}}$ ,

dipalmitoylphosphatidylcholine, and phosphines reduces molecular nitrogen to ammonia on the mercury cathode in a protic medium.

Non-catalytic reactions are very non-efficient under the conditions of an electrode process because the direct one-electron reduction of this molecule to  $\text{CO}_2$  needs the potential about  $-2$  V. The catalysts, viz.,  $\text{Re}(\text{bipy})(\text{CO})_3\text{Cl}$  and  $[\text{Re}(\text{bipy})_2(\text{CO})_2]^{2+}$  complexes and  $\text{Ni}^{2+}$  and  $\text{Co}^{2+}$  derivatives, allow the reduction of carbon dioxide to  $\text{CO}$  and  $\text{H}_2$  under much milder conditions.

Ni-complexes has been proved to be efficient in the electrocatalysis (Fig. 17.9) Electrocatalysis turned out to be efficient in a series of other reactions, such as water oxidation to molecular oxygen on iron(III) and cobalt(III) hydroxides, oxidation of hydrocarbons by hydrogen peroxide and molecular oxygen in the presence of iron ions and hemin derivatives.

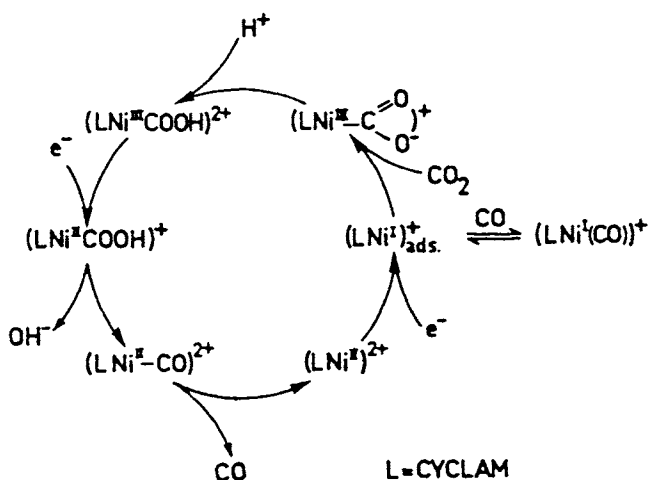


Fig. 17.9. Postulated mechanistic cycle for the electrocatalytic reduction of  $\text{CO}_2$  into  $\text{CO}$  by Ni cyclam $^{2+}$  in water (Beley et al., J. Chem. Soc. 108, 7461-7467). Reproduced with permission.

### 17.9. Water oxidation

The life giving process of water decomposition in containing manganese photosynthetic systems still remains one of the most challenging problems to

biochemists and chemists. The evolution dioxygen from water in a cluster of transition metals in the biological systems at the absorption of light quanta of low energy can occurs by a sequence of elementary steps: four one-electron steps of oxidation of the manganese complex and, most probably and by one four-electron step of O<sub>2</sub> evolution . In approaching this problem, a number of artificial manganese clusters and other transition metal clusters were synthesized and investigated (Shilov, 1997; Rüttinger and Dismukes, 1997)

The crystallographic structures of the  $[\text{Mn}_2(\text{2OHsalpn})_2]^{2-}$  complex of different oxidative states (-,0,+) have been determined (Gelasko et al., 1997). These molecules form dimers with both of the ligands spanning both Mn ions with the alkoxide on the backbone of the ligand bridging the metals. The following metal-metal distances were obtained: Mn(II)-Mn(II) = 3.33 Å, Mn(II)-Mn(III) = 3.25 Å, Mn(III)-Mn(III) = 3.36 Å, Mn(III)-Mn(IV) = 3.25 Å. Significant structural changes in the polyhedra of X-ray structures of a series of dimanganese complexes and terpyridine dimanganese oxo complexes across the range of metal oxidation states, have been observed. The authors suggested that these changes are reminiscent of the carboxylate shift in metal carboxylate in the natural complex. It also illustrates how alkoxide ligands can participate in an analogous alkoxide shift to generate a binding site for an incoming ligand, such as MeOH, or a substrate, such as H<sub>2</sub>O<sub>2</sub>.

A series of dimanganese complexes,  $[\text{Mn}_2\text{III,IV}(\mu\text{-O})_2(\text{terpy})_2(\text{H}_2\text{O})_2]^{3+(1)}$ ,  $[\text{Mn}_2\text{III,IV}(\mu\text{-O})_2(\text{terpy})_2(\text{CF}_3\text{CO}_2)_2]^+$ , (2), and  $[\text{Mn}_2\text{III,III}(\mu\text{-O})(\text{terpy})_2(\text{CF}_3\text{CO}_2)_4]$  (terpy = 2,2':6,2''-terpyridine) have been crystallographically characterized (Baffert et al., 2002). The electrochemical behavior of complex (2) in CH<sub>3</sub>CN shows that while this complex could be oxidized into its stable manganese(IV,IV) species its reduced form manganese(III,III) is very unstable. A model water oxidation complex  $[\text{H}_2\text{O}(\text{terpy})\text{Mn}(\text{O})_2\text{Mn}(\text{terpy})\text{OH}_2](\text{NO}_3)_3$  (terpy is 2,2':6',2''-terpyridine), containing a di-μ-oxo manganese dimer, was synthesized and structurally characterized (Limburg et al., 2001). This complex catalyzes the dioxygen evolution. Oxygen-18 isotope labeling showed that water is the source of the oxygen atoms in the evolved dioxygen. Another functional model for photosynthetic water oxidation, the complex,  $[(\text{terpy})(\text{H}_2\text{O})\text{MnIII}(\text{O})_2\text{MnIV}(\text{OH}_2)(\text{terpy})](\text{NO}_3)_3$  (terpy = 2,2':6,2''-Terpyridine,) has been synthesized and characterized This complex catalyzes O<sub>2</sub> evolution from either KHSO<sub>5</sub> (potassium oxone) or NaOCl via an intermediate complex  $[(\text{terpy})(\text{SO}_4)\text{MnIV}(\text{O})_2\text{MnIV}(\text{SO}_4)(\text{terpy})]$ . Dioxygen evolution in systems containing cubane-type tetramers,  $[\text{Ru}_4(\text{CO})_{12}(\mu_3\text{-Se})_4]$  and  $[(\text{dpp})_6\text{Mn}_4\text{O}_4]$  (dpp- =diphenyl phosphinate anion), have been indicated (Rüttinger and Dismukes., 2000).

### 17.10. Long-range electron transfer (LRET)

LRET between donor (D) and acceptor (A) centers can occur by three mechanisms: 1) direct transfer which involves direct overlap between electron orbitals of the donor and acceptor, 2) consecutive electron jumps via chemical intermediates with a fixed structure, and (3) superexchange via intermediate orbitals.

In direct LRET the direct electronic coupling between D and A is negligible and this mechanism is not practically realized in condensed media being non-competitive with the consecutive and superexchange processes. In theoretical consideration of the consecutive LRET a relevant theory of ET in two-term systems can be applied.

Of considerable interest is the superexchange process. According to the Fermi Golden Rule, the non-adiabatic ET rate constant is strongly dependent on electronic coupling between the donor state D and acceptor state A connected by a bridge ( $V_{AB}$ ) which is given by an expression derived from the weak perturbation theory

$$V_{AB} = \frac{\sum V_{A\alpha} V_{\alpha B}}{\Delta E_{\alpha}} \quad (17.1)$$

where  $V_{A\alpha}$  and  $V_{\alpha B}$  are the couplings between bridge orbitals and acceptor and donor orbitals, respectively, and  $\Delta E_{\alpha}$  is the energy of the bridge orbitals relative to the energy of the donor orbital. The summation over  $\alpha$  includes both occupied and unoccupied orbitals of the bridge. This approach was extended to a more general case, where D is connected to A by a number of atomic orbitals. A special, so-called “artificial intelligence”, search procedure was devised to select the most important amino acid residues, which mediate long-range transfer (Siddarth and Marcus, 1993).

A semi-empirical approach for the quantitative estimation of the effect bridging the group on LRET was developed by Likhtenshtein (1993, 1995). The basic idea underlying this approach is an analogy between superexchange in electron transfer and such electron exchange processes as triplet-triplet energy transfer (TTET) and spin-exchange (SE). The ET rate constant is proportional to the square of the resonance integral  $V_{ET}$ .

All three integrals  $V_{ET}^2$ ,  $J_{SE}$  and  $J_{TT}$  are related to the overlap integral ( $S_i$ ), which quantitatively characterizes the degree of overlap of orbitals involved in these processes. Thus

$$V_{ET}^2, J_{SE}, J_{TT} \propto S_i^n \propto \exp(-\beta_i R_i) \quad (17.2)$$

where  $R_i$  is the distance between the interacting centers and  $\beta_i$  is a coefficient which characterizes the degree of the integral decay. The spin exchange and TT phenomena may be considered an idealized model of ET without or with only a slight) replacement of the nuclear frame. Thus, the experimental dependence of exchange parameters  $k_{TT}$  and  $J_{SE}$  on the distance between the exchangeable centers and the chemical nature of the bridge connecting the centers may be used for evaluating such dependences for the resonance integral in the ET equations (Eq. 17.2).

Remarkable progress has been made in the elucidation processes of electron transfer in biological and model systems. This progress has been achieved through massive and concentrated applications of the entire arsenal of modern chemical, biochemical and physical methods. Biochemistry and biophysics provide isolated and functionally well-characterized samples of electron transfer in biological objects. Synthetic chemistry and genetic engineering allowed purposeful modification of biological and model molecules. Structural methods including X-ray analysis and all kinds of spectroscopy from Gamma-resonance to nuclear magnetic resonance reveal the detailed chemical structure of proteins with natural and artificial donor and acceptor sites. The most advanced theories of electron transfer have been used to analyze the experimental data.

For example, s was shown in large series works, (H.Gray and his colleagues) by varying the position of the ruthenium complexes relative to metalloproteins redox-active sites, it has been possible to estimate experimentally the coupling factor and its dependence on the distance between the redox centers and the chemical nature of the intermediate medium. It was shown that electron transfer in the modified proteins occurs for distance up to 16 Å significantly faster than it would in a vacuum or aqueous medium.

The experimental data on dependence of rate constants of electron transfer  $k_{ET}$  on the distance between the centers ( $\Delta R$ ) is approximated by the following equation (Dutton, P.L.; Likhteshtein. G.I.)

$$k_{ET} \sim \exp(-\beta_i \Delta R) \quad (17.3)$$

Figure 17.10 shows that the logarithm of maximum rates of electron transfer in reaction centers (RCs) of purple bacteria and green plants photosystem I (PSI) spanning 12 order of magnitude for intraprotein ET reaction as a function of the edge- to edge distance generates an approximate linear relationship with  $\beta = 1.3 \text{ \AA}^{-1}$ .

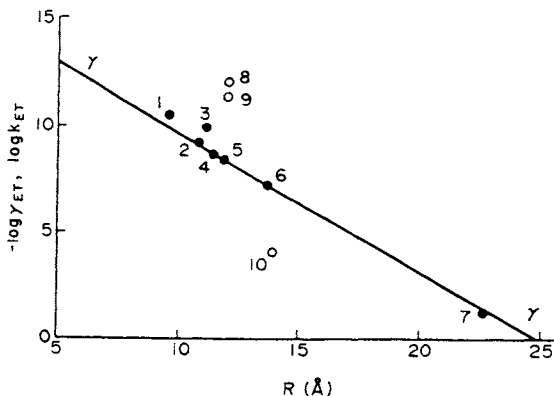


Fig. 17.10. Dependence of maximum rate constant of ET on the edge-to-edge distance in photosynthetic reaction centers of bacteria and plant photosystem. The straight line is related to the dependence of the attenuation parameter for spin exchange ( $\gamma_{SE}$ ) in homogeneous "non-conducting" media. Filled circles (Likhstenshtein, G.I., *J. Photochem. Photobiol. A: Chem.* **96**, 79-92, 1996). Reproduced with permission.

### 17.11. Concerted reactions. Synchronization factor

In order to explain the high efficiency of many chemical and enzymatic processes, wide use is made of the concepts of energetically favorable, concerted mechanisms. In a concerted reaction a substrate is simultaneously attacked by different active reagents with acid and basic groups, nucleophile and electrophile, or reducing and oxidizing agents. It may however be presumed, that certain kinetic limitations exist on the realization of reactions which are accompanied by a change in the configuration of a large number of nuclei. (Bordwell, F.G., 1970, Likhstenshtein, G.I., 1974).

According to a simplified theory (Alexandrov, 1976), a concerted reaction occurs as a result of the simultaneous transition (taking approximately  $10^{-13}$  s) of a system of independent oscillators, with the mean displacement of nuclei  $\phi_0$ , from the ground state, to the activated state in which this displacement exceeds for each nuclei a certain critical value ( $\phi_{cr}$ ). If  $\phi_{cr} > \phi_0$  and the activation energy of the concerted process  $E_{syn} > nRT$ , the theory gives the following expression for the synchronization factor which is the ratio of the pre-exponential factors of the synchronous and simple processes:

for each nuclei a certain critical value ( $\varphi_{cr}$ ). If  $\varphi_{cr} > \varphi_0$  and the activation energy of the concerted process  $E_{syn} > nRT$ , the theory gives the following expression for the synchronization factor which is the ratio of the pre-exponential factors of the synchronous and simple processes:

$$\alpha_{syn} = \frac{n}{2^{n-1}} \left( \frac{nRT}{\pi E_{syn}} \right)^{\frac{n-1}{2}} \quad (17.4)$$

where  $n$  is the number of vibrational degrees of freedom of the nuclei participating in the concerted transition.

At  $\varphi_{cr} < \varphi_0$  and  $E_{syn} < nRT$ ,

$$\alpha_{syn} = \frac{n}{2^{n-1}} \quad (17.5)$$

In fact, in the frame of the Alexandrov model, when the average thermal energy of the system ( $E_{av} = nRT$ ) exceeds the energy of the activation barrier, the process can be considered as activationless. Analysis of Eqs. 17.4 and 17.5 provides a clear idea of the scale of the synchronization factor, and the dependence of this factor on the number of  $n$  and therefore on the number of broken bonds and the energy activation (Fig. 17.11).

For example, at moderate energy activation 20-40 kJ/mole, typical for enzymatic reactions, the incorporation of each new nucleus into the transition state can lead to a ten-fold decrease in the rate of the process.

Therefore, in the case of an effective concerted mechanism, the decrease of the synchronization probability ( $\alpha_{syn}$ ) with increasing  $n$  must be compensated for by an appreciable decrease in the activation energy.

The models of concerted processes discussed above are only a crude approximation of the motion of a complex system of nuclei along the reaction coordinate. However, such an approximation apparently permits one to choose between the possible reaction mechanisms. The reliability of such a choice increases through a comparative examination of alternative reaction coordinates.

17.12. The principle of "optimum motion" in elementary acts of chemical and enzymatic processes

From the point of view of general concepts of chemical reactions, the less nuclei change their position in the course of an elementary step, the lower reorganization the energy and, therefore, the energy of the activation of the step (principle of "minimum motion"). On the hand, involving several acid-base, donor-acceptor and redox groups in concerted reaction can markedly decrease the reaction activation energy. Nevertheless, have led to the formulation of the

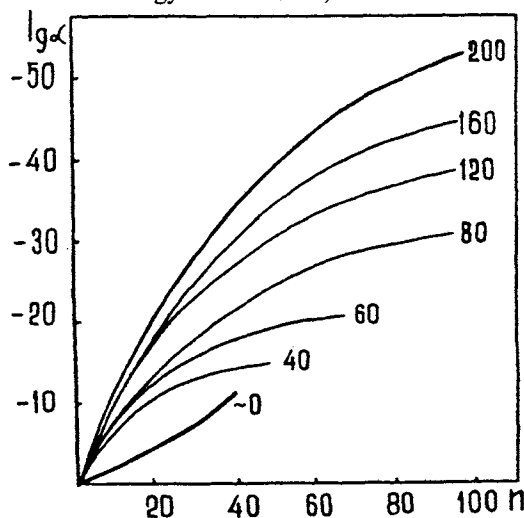


Fig. 17.11. Theoretical dependences of the synchronization factor ( $\alpha_{\text{syn}}$ ) on the number of degrees of freedom ( $n$ ) of the nuclei involved in a concerted reaction. The curves have been constructed in accordance with Eqs 2.44 and 2.45. (Likhtenshtein, G.I., *Chemical Physics of Redox Metalloenzyme Catalysis*, Springer-Verlag, Berlin.. 1988). Reproduced with permission

principle of "optimum motion" (Likhtenshtein, 1974). According to this principle, the number of nuclei whose configuration is changed in the elementary act of a chemical reaction must be sufficiently large to provide favourable energetics for the step and, at the same time, sufficiently small for the maintenance of a high value of the synchronization probability during motion along the reaction pathway to the reaction products.

The condition preferring the concerted reaction as opposite to the direct with a rate constant  $k_{\text{dir}}$  and energy of activation  $E_{\text{dir}}$  is the inequality

$$\frac{k_{syn}}{k_{dir}} > \alpha_{syn} \exp\left(\frac{E_{dir} - E_{syn}}{RT}\right) \quad (17.6)$$

Though the estimates that illustrate the principle of "optimal motion" are based on simplified models and approximation formulas (2.44 – 2.46), they have, nevertheless, made it possible to draw some conclusions which are apparently useful in taking into account the treatment of complex elementary acts of chemical and biochemical processes

In transition state theory, the rate of an adiabatic chemical reaction depends only on the difference between free energy in initial and transition states. From point of view of thermodynamics, formation of an intermediate complex can not give any preference to the process as compared with a collision complex.

Nevertheless, the formation of a preliminary (pretransition) structure on the reaction coordinate can constrain the system of nuclear motions that do not lead to reaction products and, therefore, accelerate the process. It is necessary to stress that this acceleration is not caused by entropy reason, but by the optimization of the synchronization factor.

### *17.13. Multi-electron mechanisms of redox reactions. Switching molecular devices*

There are a considerable number of reactions in which the products contain two electrons, more than the starting compounds, and the consecutive two-step one-electron electron transfer process proves to be energetically unfavorable. In such cases, it is presumed that the two-electron process occurs in one elementary two-electron step. An example of a two-electron process is the hydride transfer, when two electrons are transported together with a proton.  $\text{BH}_4^-$ , hydroquinones and reduced nicotinamides are typical hydride donors. A specific feature of quinones is the capacity to accept and then to reversibly release electrons one by one or two electrons as a hydride. Therefore, quinones can serve as a molecular device, which can switch consecutive one-electron process to single two-electron process.

Another possible two-electron mechanism involves the direct transport of two electrons from a mononuclear transition metal complex to a substrate (S). Such a transport alters sharply the electrostatic states of the systems and obviously requires a substantial rearrangement of the nuclear configuration of ligands and polar solvent molecules. For instance, the estimation of the synchronization factor ( $\alpha_{syn}$ ) for an octahedral complex, with Eq. 2.44 shows a very low value of  $\alpha_{syn} = 10^{-7}$  to  $10^{-8}$  and, therefore, a very low rate of reaction.

The probability of two-electron processes, however, increases sharply if they take place in the coordination sphere of a transition metal, where the reverse compensating electronic shift from the substrate to metal occurs. Involvement of bi- and, especially, polynuclear transition metal complexes and clusters and synchronous proton transfer in the redox processes may essentially decrease the environment reorganization, and, therefore, provide a high rate for the two-electron reactions.

The reduction of molecular nitrogen to ammonium and water oxidation to molecular oxygen causes six- and four-electron transfer to occur eventually in these reactions, respectively. Such processes obviously cannot occur in a single step. Analysis of the thermodynamics of plausible intermediates rules out one- and two-electron transfers for both reactions and only four-electron mechanisms are energetically allowed. Evidently, the direct transport of four electrons from (or to) a mononuclear or even binuclear transition metal complex appears to be ruled out. Practically the only possible variant of the four-electron mechanism is the conversion in the coordination sphere of a transition metal polynuclear complex.

The multi-electron nature of the energetically favorable process does not evidently impose any new, additional restriction on its velocity. Within a coordination sphere the orbital overlap is effective and, therefore the resonance integral  $V$  is high. The strong delocalization of electrons in clusters, polynuclear complexes in clusters and polynuclear complexes reduces to a minimum the reconstitution of the nuclear system during electronic transitions and, therefore, provides a high value for the synchronization factor.

An important feature of polynuclear transition metal complexes in redox enzymes and its chemical models is their ability to evolve inert molecules, such as  $N_2$ ,  $O_2$ , and  $H_2O$  into inner-sphere chemical conversion under ambient condition to  $N_2O_4$ ,  $H_2O_2$  and  $O_2$ , correspondingly. According to thermodynamic estimations, the formation of  $N_2H_2$ ,  $HO_2$  and  $HO$  as intermediates in the above mentioned processes is energetically strongly unfavorable. Therefore, these reactions include multi-electron elementary steps. It is necessary to stress that realization of elementary four-electron redox reaction is provided by a simultaneous transport of additional number electrons from the nearest electron donating or electron-accepting centers, that is to say, metal clusters or polynuclear complexes and subsequent proton transfer. Examples of the multielectron processes in biological reaction are presented in Chapter 18.

## Enzymes as catalysts

### 18.1. Basic concepts and definitions

*Enzymes* are biological catalysts of the protein nature, which accelerate chemical reactions and are necessary for the living activity of organisms. Enzymatic catalysis is characterized by high substrate specificity (in some cases, stereospecificity), selectivity with respect to specific bonds of the substrate, and capability of fine regulating the activity under the action of effectors (activators and inhibitors).

The majority of enzymes are active in a comparatively narrow interval of pH 4—9 and temperatures (273—293 K). Experimental activation energies of enzymatic reactions are low (20—60 kJ/mol).

Many enzymes consist of the protein macromolecule (*apoenzyme*) and *cofactor* (prosthetic group), viz., non-protein molecule (ion, complex), which together with the protein forms an active catalyst. In other cases, protein functional groups of polypeptide chains play the role of the cofactor.

*Active site of enzyme* is a combination of functional groups, peptide bonds, and hydrophobic regions in the enzymatic protein molecule, where chemical transformations occur.

*Coenzyme* is a complicated organic or metalloorganic compound (cofactor), which successively binds to two different enzymes during the catalytic reaction and participates in the chemical transformation.

Isosteric effects are caused by the direct interaction between two substrate or inhibitor molecules or enzyme regions; allosteric effects are related to the mutual influence of spatially separated enzymatic sites localized on different subunits.

Homotropic allosteric effect appears in the system with identical ligands, and heterotropic allosteric effect is manifested for interaction between different ligands.

Multi-site systems in which the kinetic and thermodynamic parameters of the same site depend on filling of other sites by substrate or effector molecules are named cooperative.

Oligomer is a system consisting of a certain number of identical subunits, viz., protomers.

*Productive binding* of the substrate by the enzyme appears in the cases where the improvement of complex formation in the substrate series (decrease in the substrate constant) either increases the maximum transformation rate or has no effect on this rate. Opposite effects are observed for *non-productive binding*.

The International Biochemical Union recommends characterizing the *catalytic activity of enzyme* by the "catal" unit (symbol cat) corresponding to the transformation of one mole of the substrate per second. The molar catalytic activity is expressed in cat/mole of enzyme.

### 18.2. Main statements of enzymatic catalysis theory

Unique catalytic properties of enzymes are caused by two main specific features of their structure: polyfunctional character of the active site and capability of conformational transitions, which, in turn, is associated with the intramolecular mobility of protein globules of enzymes.

Specificity of enzymes is related to the complementary structure of their active site to the structure of substrates. The active site is arranged, as a rule, in the macromolecular cavity of the enzyme and is formed from different chain regions of the protein globule. According to the Koshland theory, the complimentary structure is induced, namely, at the moment of interaction with the active site, the substrate induces such change in the enzyme geometry which corresponds to the optimum (for the specific reaction) orientation of groups directly involved in the chemical transformation of the substrate (catalytic groups). In the case of bulky substrates, multi-site sorption occurs in the active site due to the dispersion, hydrophobic, and electrostatic interactions and hydrogen bonds. Small molecules, such as  $O_2$ ,  $N_2$ , and  $H_2O$ , directly react with transition metal atoms. However, in this case, binding is also multi-site, for example, in binuclear complexes and clusters or involving metal-less groups. For instance, in the case of the complex formation of the  $O_2$  molecule in hemoglobin with the  $Fe^{2+}$  ion, a hydrogen bond is formed with the protonated histidine residue in the vicinity of the active site.

The main reasons for the considerable acceleration of chemical processes by enzymes compared to a non-enzymatic process can be formulated as follows.

1. Due to the binding contact functional groups and hydrophobic regions, enzyme sharply increases the concentration of the substrate in the active site and performs its precision orientation relative to the catalytic groups. This provides the acceleration of the process by  $10^4$ — $10^7$  times.

2. The presence of nucleophilic and electrophilic groups or a whole set of redox sites in the active site increases the probability of synchronous acid-base and multi-electron redox stages, which are characterized by a lowered activation energy.

3. Multi-point binding of substrates and the appearance of the unique structure inside the active site cavity favors the stabilization of electronic configurations lying along the reaction coordinate, the formation of pretransition state, which energy is close to the transition state energy, and equalization of levels of the intermediate states.

4. The protein globule of an enzyme provides unique opportunities for the creation of the local dielectric medium optimum for a specified process. The dielectric properties of the active site created due to both the closest and remote electric charges can be controlled during the reaction by conformational transitions.

5. The presence of redox and acid-base sites in the steric vicinity in the active sites makes it possible to perform elementary acts of conjugated processes. For example, the protonation of the redox site enhances its withdrawing ability, and the oxidation of the site can favor its deprotonation. The formation of hydrogen and other donor-acceptor bonds also influences on the redox properties of reactants. Another function of such bonds is the precision orientation of catalytic groups at all stages of the process in the active site.

6. According to the R. Lumry concept, a change in the conformation of protein macromolecules during the formation and transformation of enzyme-substrate complexes disturbs these contacts and form others, results in the conformational pressure on the substrate and catalytic groups, which favors a decrease in the energy barriers of the reaction. The rule of mutual compensation of the free energy of the chemical reaction and conformational energy of the macromolecule is fulfilled, resulting in smoothening of the energy relief of the overall process.

7. The dynamic structure of protein macromolecules of enzymes postulated by R. Lumry, K. Lindershtrom-Lang, and D. E. Koshland appears as the local thermal mobility of particular regions and the capability of induced conformational transitions. The hindered intramolecular mobility of proteins plays the main role in realization of such functionally important properties of enzymes as dynamic adaptation of the enzyme shape to the structure of catalytic and substrate groups, which changes during the chemical reaction, allosteric interaction between spatially separated sites, and realization of the principle of complementarity of free energies and induced correspondence.

8. Changes in the conformation of macromolecules of the enzyme and substrate can occur in such a way that the conformational result of one stage favors the beginning of the next stage. These mechanisms are favored by the domain (unit) structure of protein globules of enzymes.

9. When organized in protein and membrane ensembles, enzymes gain additional possibilities for the functional and structural interaction by processes of electron and substrate transfer and through allosteric effects.

The above catalytic features of enzymes, which can naturally be explained in terms of the concepts of the chemical kinetics, are inherent, to some extent, in standard chemical catalysts. However, in the case of enzymes, they are especially pronounced and, mainly, act in combination.

### *18.3 Chemical Mechanisms of Enzyme Reactions*

#### *18.3.1 Overview*

Creating enzymes in the processes of biological evolution, the Nature used whole arsenal of mechanisms of chemical reactions including covalent catalysis, general acid/base catalysis, electrostatic catalysis, desolvation, strain or distortion of a substrate, concerted reactions, short- and long-range electron transfer, multielectron transfer, “switching” mechanism and donor-acceptor catalysis (See Chapter 17).

Specific forces maintaining enzymes native structure and providing its interactions with substrates and inhibitors are similar to those we meet in chemistry. They are covalent bonds, ionic (electrostatic) interactions, ion-dipoles and dipole-dipole interactions, hydrogen bonds, charge transfer complexes, hydrophobic interactions, and van der Waals Forces.

Enzyme commission of the International Union of Biochemistry and Molecular Biology (IUBMB) established two enzyme nomenclatures systematic and trivial. According the systematic nomenclature all enzymes are divided upon 6 classes: 1. Oxidoreductases; 2. Transferases; 3. Hydrolases; 4. Lyases cleaving C-C; C-O, C-N bonds; 5. Isomerases, and 6. indication of bond formed.

Table 18.1 illustrates tremendous acceleration of the reaction rate of a chemical reaction in enzymatic process as compared with noncatalytic one.

Table 18.1. Rate enhancement of enzymes ( $k_{\text{cat}}$  and  $k_{\text{uncat}}$  are the rate constants of catalytic and uncatalytic reactions, respectively)

Enzymes	$k_{\text{cat}}/k_{\text{uncat}}$
Nitrogenase	$>10^{50}$
Methan monooxygenase	$>10^{20}$
Fumarase	$7.2 \times 10^{17}$
Carboxypeptidase	$1.3 \times 10^{13}$
Adenosine deaminase	$2.1 \times 10^{12}$
Phosphotriesterase	$2.8 \times 10^{11}$
Carbonic anhydrase	$7.7 \times 10^6$
Catalytic antibodies	$102-10^5$

An information about types of chemical enzymatic reactions of the main catalytic groups is presented in Table 18.2.

Table 18.2. Chemical reactions accelerated by enzymes.

Chemical Reaction	Group or molecule attacked	Enzyme	Catalytic groups
Hydrolysis by peptidases	peptide bond	$\alpha$ -chymotrypsin	Ser-OH, His-Im
Hydrolysis by esterases	ester bond	acetylcholinesterase	Ser-OH
	ester bond	$\beta$ -glucosidase	Gly-COOH
Phosphorilations	phosphate	glucose-6-phosphatase	Ser-OH
Oxidation	aldehyde	glyoxalase	glutathion
	C-H	alcohol dehydrogenase	pyridine
	C-H	D-amino acid oxidase	flavin
	C-H	methanol dehydrogenase	pyrroloquinoline
	H <sub>2</sub> O <sub>2</sub>	catalase	hemin

	DH <sub>2</sub>	peroxidase	hemin
Reduction	NO <sup>3-</sup>	nitrate reductase	
	N <sub>2</sub>	nitrogenase	(Fe <sub>7</sub> Mo) cofactor
Hydroxylation	C-H	phenol hydroxylase	flavin
	C-H	cytochrome P-450	heme
	C-H	methane monooxygenase	[Fe (III)] <sub>2</sub>
	C-H	ascorbate oxidase	Cu <sup>2+</sup>
Deoxygenation	Catechol	catechol dioxygenase	Fe(III)
	C-H	prostaglandin-H synthetase	hemin
Substitution	O-C	disaccharide phosphorilase	COOH
Carboxylations	H <sub>2</sub> C=C<	PEP-carboxykinase	Mn <sup>2+</sup>
Decarboxylation	CH <sub>2</sub> COO <sup>-</sup>	acetoacetate decarboxylase	Lys-NH <sub>2</sub>
Isomerization	C-OH	aldose-ketose isomerase	B:, HB <sup>+</sup>
	OPO <sub>3</sub> <sup>2-</sup>	phosphomutase	Ser-OH
Elimination and addition	COH	enolase	Mg <sup>2+</sup>
	COH	Aconitase	Fe <sub>4</sub> S <sub>4</sub>
Aldol reaction	COH	fructose 1,6-diphosphate Aldolase	His-Im, Zn <sup>2+</sup>
Metylation	N(CH <sub>3</sub> ) <sub>2</sub>	Methionine synthetase	cobalamin
Rearrangements	C-0	Chorismate mutase	

#### 18. 4. Mechanisms of chosen enzyme reactions.

*α-Chymotrypsin.* The enzyme accelerates hydrolysis of protein and peptides by more than 10<sup>7</sup> times as compared with nonenzymatic reaction. *α*-chymotrypsin used so called charge relay system, a catalytic triad Asp-102, His-57 and Ser-195, for performing the covalent and electrostatic catalysis. The most

important property of the triad is a substantial increase the nucleophilic capacity of the Sr-95 OH group as a result of the charge relay shifting H to imidazole, which is in turn activated by the carboxylic group of Asp-102. This group possesses high nucleophilic power, being ducked in local media of polarity, which is markedly lower than polarity of bulk water.

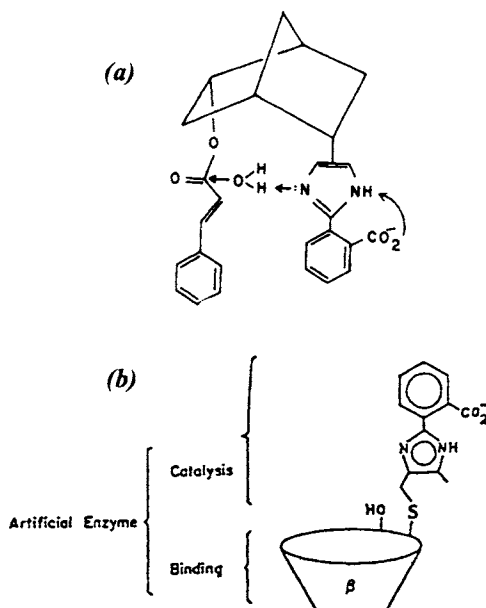


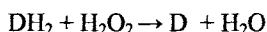
Fig. 18.1. The mechanism of action of "artificial chymotrypsin" (a); Complete model of acylchymotrypsin (a) and miniature organic model of chymotrypsin (b) (D'Souza and Bender, 1987). Reproduced with permission.

The most promising direction of the enzyme modeling is the synthetically mimicking the nature of the binding site and the active site in terms in close similarity of catalytic groups, stereochemistry, interatomic distances and the mechanism of action of the enzyme. Mimicking of the "proton-transfer relay" proposed for the mechanism of action of chymotrypsin is the brilliant example of such a work (D'Souza and Bender, 1987). The miniature organic model of chymotrypsin build up on the basis of a cyclodextrin and the mechanism of

hydrolysis *m*-tert-butylphenyl acetate has been constructed (Fig. 18.1). The catalytic activity of the "artificial chymotrypsin" in the hydrolysis of *m*-tert-butylphenyl acetate ( $k_{\text{cat}} = 2.8 \times 10^2 \text{ s}^{-1}$ ,  $K_M = 13 \times 10^5 \text{ M}$ ) was found to be close to activity of chymotrypsin in the hydrolysis of *p*-nitrophenyl acetate ( $k_{\text{cat}} = 1.1 \times 10^2 \text{ s}^{-1}$ ,  $K_M = 4 \times 10^5 \text{ M}$ ).

***β-Glucosidases.*** These enzymes catalyzing the hydrolysis of oligosacchrides use covalent catalysis. Activated carboxylic group, for example Glu387, in the active site of *Sulfolobus solfataricus*, forms the covalent C-O bond with a substrate, followed by the bond hydrolysis.

***Peroxidases, Catalase, Cytochrome P-450.*** The hemin-containing enzymes peroxidases and catalase catalyze the oxidation of electron-donor molecules ( $\text{DH}_2$ ) by hydrogen peroxide according to the following scheme



Various electron donors may serve as substrates: phenoles, amines, alcohols, and  $\text{H}_2\text{O}_2$  (for catalase).

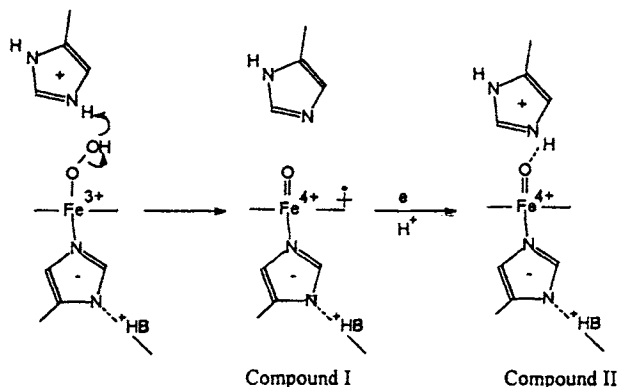
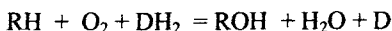


Fig. 18.2. Compounds I and II as active intermediates in peroxidase and catalase reactions (Shilov A.E.)

Fig. 18.2 illustrates the first decisive steps of the reaction with formation of compounds I and II possessing high oxidizing capacity (the values of redox potentials are  $E_I = 970 \text{ mV}$  and  $E_{II} = 950 \text{ mV}$ , respectively. Two-electron oxidation of hemin- $\text{Fe}^{+3}$  group to compound I proceeds with the synchronous

assistance of protonated imidazole of histidine. Compounds I and II oxidize a substrate by two electron hybrid reaction (substrate ethanol, for instance) or two consecutive one-electron processes (*p*-aminophenol, for example).

The protoheme IX containing enzyme Cytochrome P-450 catalyzes hydroxylation of organic substrates, i.e. hydrocarbons, organic acids, amines, etc. according the following scheme:



where  $\text{DH}_2$  is the reducing agent (NADH or NADPH). The protoheme IX fives ligand is a sulfur. Proposed reaction cycle for cytochrome P450 is presented in Fig. 18.3.

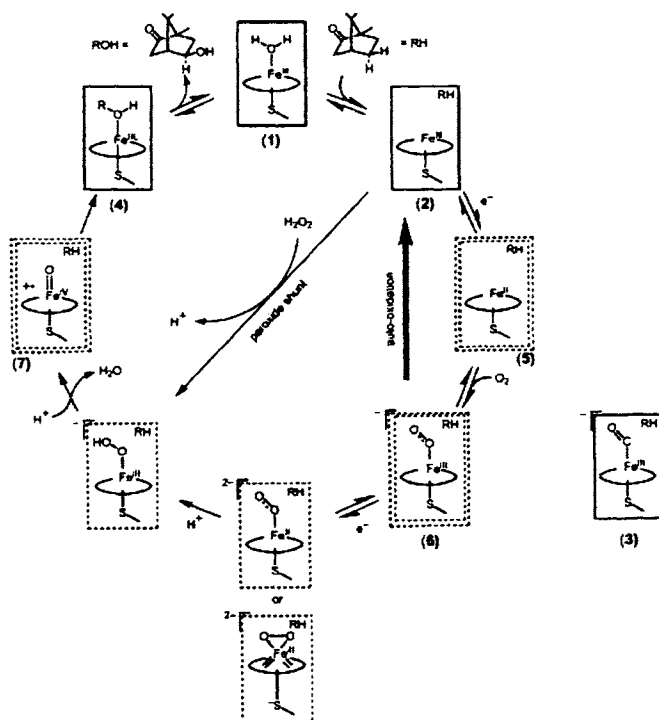


Fig. 18.3. The catalytic pathway of cytochrome P450cam (Schlichting I. et al. Science **287**, 1615-1622, 2000). Reproduced with permission.

Reaction pathway of a camphor hydroxylation catalyzed  $\beta$  - cytochrome P450 consists of the following principle stages: substrate binding by the heme active site with sulfur as a fifth ligand (1); addition of first electron (5); binding of dioxygen (6); addition a second electron and two protons with formation of the activated oxygen intermediate (most probably an Compound I analog) (7); its reacts with camphor to produce 5-exo-hydroxycamphor

The first principle breakthrough in mimicking the enzymatic hydroxylation reaction was pionireeng work of Groves and his colleagues. The first synthetic analog which closely mimicked the chemistry of cytochrome P450 was chloro- $\alpha,\beta,\gamma,\delta$ -tetraphenylporphinatoiron (III) [Fe(III)TPP(Cl)]with iodozylbenzene as the oxidant to effect the stereospecific epoxidation of oleins and hydroxylation of cyclohexane. This compound may be considered as an analog of oxoiron (IV) cation radical of protoporphyrin IX.

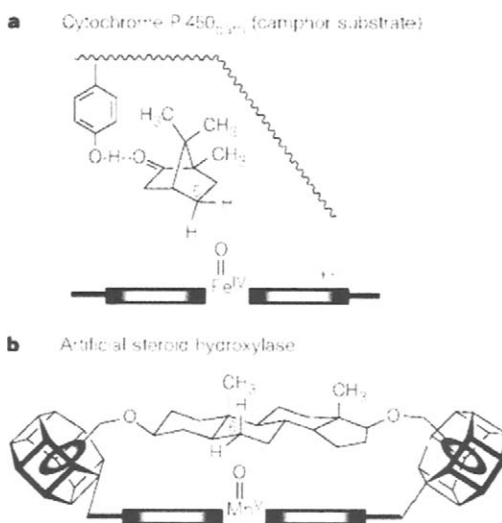


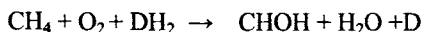
Fig. 18.4. Schematic presentation of the Cytochrome P-450<sub>cam</sub> active site (a) and the Breslow model of steroid hydroxylase (Groves J.T., *Nature* **389**, 329-330, 1997). Reproduced with permission.

In model system developed by Breslow and his coworkers (Breslow et al., 1997), four cyclodextrin groups were attached to a synthetic manganese porphyrin (Fig. 18.4). A substrate steroid was captured by hydrophobic central

cavities of the doughnet shaped heptamylose sugars and the five-turnover hydroxylation occurred only at carbon 6 of the substrate.

*Ascorbate Oxidase.* The enzyme catalyzes the oxidation of ascorbate to dihydroascorbate and water by  $O_2$  and contains three types of copper complexes mononuclear  $Cu^{+2}$  (I) and  $Cu^{+2}$ (II) and binuclear  $[Cu^{+2}]_2$  (III). The redox potential of the primary electron acceptor of  $Cu^{+2}$ (I)  $E_0 = 500$  mV, which is quite sufficient for the one electron oxidation of ascorbate ( $E_0 = 310$  mV) but is not enough for the one-electron reduction of  $O_2$  ( $E_0 = -330$  mV). The most probable mechanism of reaction involves two consecutive one-electron reduction of the copper complexes followed by the two-electron reduction of  $O_2$  in the binuclear  $[Cu^{+2}(III)]_2$  complex accompanied by synchronuos proton transfer.

*Methane Monooxygenase.* In microorganisms utilizing methane an enzyme, methane monooxidase, has been detected, which catalyzes the reaction



The electron donor ( $DH_2$  is NADH). The binuclear structure of the enzyme active center and proposed catalytic cycle are presented in Fig. 18.5.

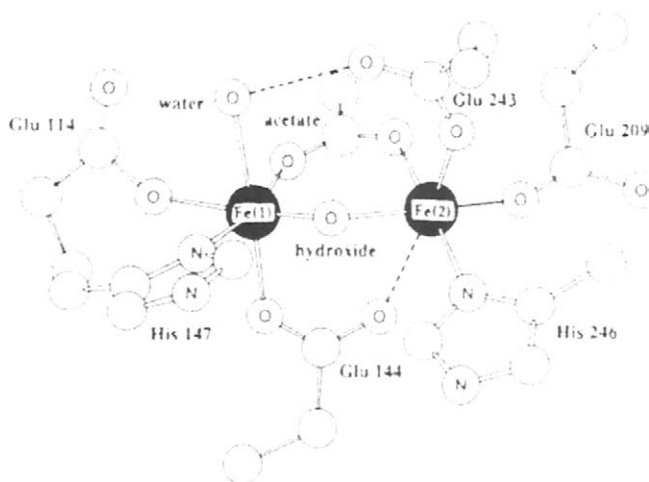


Fig. 18.5 Structure of active center of MMO (Rosenzweig A.C. et al. *Nature* **366**, 537-543, 1993). Reproduced with permission.

The most probable mechanism of the reaction is an oxygen activation with formation of the ferryl structure followed by the formation a free methyl radical reacting with oxygen atom.

The model  $[\text{Fe}_2\text{OL}(\text{OBz})](\text{ClO}_4)_2$  complex was prepared by the interaction of a polydentate ligand 2,6-bis[3-[N,N-di(2-pyridylmethyl)amino]propoxy]benzoic acid (LH) with  $\text{Fe}(\text{ClO}_4)_3$  in the presence of  $\text{NaOBz}$ . (Trukhan et al. 1998). In this structure, one bridging carboxylate (in L) is fixed, and the other (in OBz) remains mobile, retaining the capability for substitution reactions and occupying two labile coordination sites. This complex catalyzes selective oxidation of methane to  $\text{MeOH}$  by  $\text{H}_2\text{O}_2$ .

**Nitrogenase.** The central enzyme of biological nitrogen fixation catalyzes the reduction of molecular nitrogen to ammonia by biological (ferredoxin) and non-biological ( $\text{S}_2\text{O}_4^{2-}$ ) reducing agents with assistance of hydrolysis of ATP:

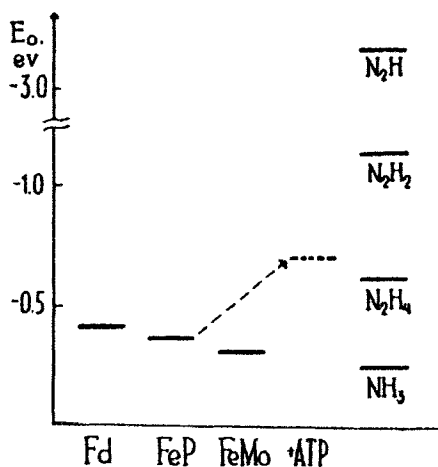
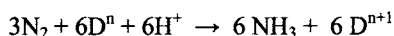


Fig. 18.6. The energy profile of a nitrogenase reaction.  $E_0$  is the standard redox potential of the reactants, intermediates and products of the reaction; Fd = ferredoxin; FeP = Fe protein; FeMo = FeMo protein. The arrow indicates the increase of the reduction potential upon ATP hydrolysis (Likhtenshtein G.I. *Chemical Physics of Redox Metalloenzyme Catalysis*, Springer-Verlag, Berlin, 1988). Reproduced with permission.

The active form of nitrogenase is formed upon the combined action of two components: a protein containing  $[\text{Fe}_4\text{S}_4]$  cluster (FeP) and iron-molybdenum protein (FeMoP) with two  $[\text{Fe}_8\text{S}_8]$  centers, so-called P-clusters, and two iron-molybdenum cofactors (FeMoCo).

Since the time of Daniel Rutherford, who discovered molecular nitrogen about 200 years ago, this gas has served as an example of an inert substance. From the works of Pauling (1962) it follows that the energy of the first bond being broken is very high (560 kJ/mol). In 1970 Likhtenshtein and Shilov advanced the supposition that the enzyme nitrogenase by-passed the above mentioned energy difficulties by way of realizing a reaction mechanism that provides the rupture of two bonds in  $\text{N}_2$  with simultaneous compensation due to the formation of four new bonds with two transition atoms. This mechanism was provisionally termed the four-electron mechanism in which the reduction potential per bond involving the formation of hydrazine derivative is much lower than in the case of one- or two-electron mechanisms (18.6).

The better way for realizing such a mechanism is involving polynuclear complexes of transition metals. This conclusion was confirmed by studies of isolated nitrogenase and model systems (Fig. 18.7). This reaction is proceeded by consecutive four long-distance electron transfer along the path  $\text{FeP} \rightarrow \text{P-cluster} \rightarrow \text{FeMoCo}$ . The decisive step of reduction of  $\text{N}_2$  occurs in polynuclear FeMoCo most probably by four-electron mechanism.

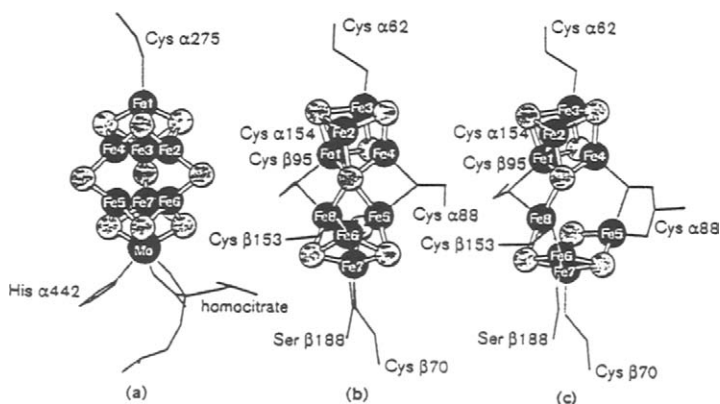
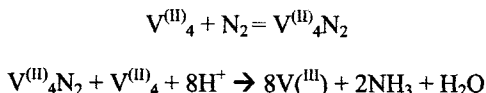
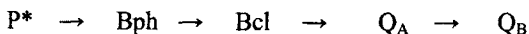


Fig. 18.7. Structural models of FeMo cofactor (a), the dithionate reduced P-cluster (b), and oxidized P-cluster (c) (Rees and Howard, 2000). Reproduced with permission

The first break through the problem of involving  $N_2$  in a chemical reaction in relative mild conditions was made in pioneering work of Volpin and Shur (1964). These authors demonstrated first reactions of dinitrogen reduction by such reducing agents as  $Al-AlBr_3$ ,  $LiAlH_4-AlBr_3$  in aprotic media in the presence transition metals ( $FeCl_3$ ,  $MoCl_5$ ,  $CrCl_3$ ). In the 1970's, on the basis of the concept of the multi-electron mechanism of dinitrogen reduction in polynuclear transition metal complexes (Likhtenshtein and Shilov, 1970), dinirogen reduction of hydrazine and ammonia in protic media (methanol, water) involving relative weak reducing agents was discovered (Shilov A.E. with colleagues). The first systems discovered were heterogeneous and included metal hydroxides  $Mo(OH)_3-Ti(OH)_3$  or  $V(OH)_2-Mg(OH)_2$ , which can be considered as giant clusters of transition metals. As a model of biological dinitrogen fixation,  $N_2$  was reduced by  $Ti^{3+}$ ,  $Cr^{2+}$ , or  $V^{2+}$  in the presence of Mo compounds in aqua and alcohol solutions, while CO strongly inhibited redaction. The principal product was hydrazine, although  $N_2$  was reduced to  $NH_3$  at higher temperatures. The more recent advantages in modeling the nitrogenase reaction was the discovering complexes of V(II) and catechol in the protic media (Nikonova L.A. and Shilov A.E.) in presence of which the following reactions take place:

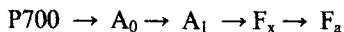


*Photosynthetic Reaction Centres (RC's).* The conversion of solar energy to chemical energy with a quantum yield close to unity proceeds by the mechanism of photoseparation of charges in the RC's of photosynthetic bacteria. The following scheme of electron transfer in the Rc of photosynthetic bacteria has been shown to take place:



where  $P^*$ , the bacteriochlorophyll dimer  $(Bcl)_2$  in the excited singlet state, is the primary donor, Bcl is bacteriochlorophyll, Bph is the bacteriopheophytin, and  $Q_A$  and  $Q_B$  are the primary and secondary quinone acceptors respectively. This process leads to the formation of the cation radical  $P^+$ , which is a strong oxidizing agent with  $E_0 = 0.8$  eV, and reduced quinone, which is a sufficiently strong reducing agent with  $E_0 = 0$  eV.

In the RC of PSI, the primary photochemical steps occurs along the cascade of the redox centers,



where P700 is the chlorophyll dimer,  $A_0$  is chlorophyll,  $A_1$  is phyloquinone and  $F_x$  and  $F_a$  are the  $Fe_4-S_4$  clusters.

One of the authors of this monograph (Likhtenshtein, 1974) suggested that rapid electron transfer in the reaction centers in the forward direction and the slow transfer in reverse direction may be accounted for the mechanism of long-distance electron transfer. It was assumed that in such systems donor and acceptor centres are at an optimum distance from each other and are separated by non-conductive medium. As it is seen in Fig. 18.8., this prediction was confirmed by X-ray analysis

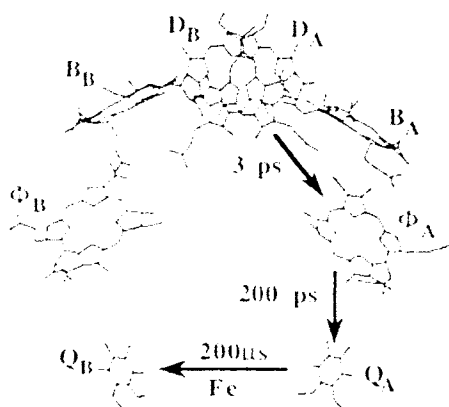


Fig. 18.8. Structure of the cofactors of the RC from Rb. Sphaeroides. Phytyl and isoprenoid tails have been omitted for clarity. Electron transfer proceeds preferentially along the A branch as shown by the arrows with characteristic times as indicated (Rees et al., *Annu. Rev. Biochem.* **38**, 607-633. 1989). Reproduced with permission.

For the purpose of modeling photosynthetic systems a congruent and systematic set of well-designed models have been synthesized and their photochemical and photophysical properties were characterized (Gust D., Wasielewski, M.R., and their colleagues). Effect of the chemical structure of donor and acceptor centers, energy of the donor center in excited state and donor, distance between the centers and their mutual orientation, nature and length of spacer tethered the donor and acceptor, solvent and temperature were investigated. For example, a series of Zn porphyrin-quinone dyads and two porphyrins-quinone tryads have been synthesized (Sessler J.L.). In the first group of complexes the photoinduced charge separation (PCS) occurred on time scale of  $< 1$  ps, while in the triad the excitation formed a transition species for about 60 ps. In these systems the thermal recombination was found to be very fast.

*18.5. Protein Intramolecular Dynamics and Catalytic Activity of Enzymes.*

The present concept of the intramolecular dynamics of proteins is based on a hypothesis put forward in 1950-1960s. First, Lumry and Eyring assumed that the interaction of a substrate with enzyme was accompanied by a certain distortion of the structure of both the substrate and the enzyme. Later, this concept was developed into the theory of "complementarity" of free energy of the chemical reaction in the enzyme active center and enzyme conformational free energy. In so doing, energy redistribution occurs in such a way that the energy profile of the process, as a whole, is eventually flattened. Another basis of the modern concept of protein molecular dynamics is the Linderstrom-Lang hypothesis regarding the structural fluctuation of the protein macromolecule, which is visible in the ability of inner peptide groups to exchange hydrogen atoms for water protons. According to the Koshland "induced-fit" theory, the conformational structure of the enzyme can be induced to fit the structure of the substrate during their interaction.

At a later stage, the concepts of protein dynamics were supplemented by the principle of dynamic adaptation of the enzyme conformational structure to the substrate configuration in a consecutive reaction to the enzyme. Such an adaptation promotes both the first step of precise orientation and the subsequent chemical steps, without allowing cleavage of the contacts needed for the chemical mechanism.

In the 1960s and 1970s, much indirect evidence was obtained in favor of protein intramolecular mobility, i.e. the entropy and energy specificity of enzyme catalysis, compensation phenomena. The first observations made concerned the transglobular conformational transition during substrate-protein interaction, the reactivity of functional groups inside the protein globule, and proteolysis.

From the late 1960s to the early 1970s, more direct approaches to the investigation of protein dynamics were intensively developed. Its distinctive feature was the application of physical methods, such as NMR, optical spectroscopy, fluorescence, differential scanning calorimetry, X-ray and neutron scattering, as well as physical labelling. The purposeful application of the approaches made it possible to obtain detailed information on the mobility of different parts of protein globules and to compare it with both the functional characteristics and stability of proteins and with results of the theoretical calculation of protein dynamics (M. Karplus).

The essential contribution when tackling the problem, especially at the early stages of a study of protein dynamics, was the development and use of biophysical labelling methods.

The basic idea underlying the physical labelling approach is the modification of the chosen sites of the object in question by specific compounds, which are bound covalently (labels) and/or non-covalently (probes), whose properties make it possible to trace the state of the surrounding biological matrix by appropriate physical methods. The following main types of compounds are used as labels and probes to monitor the dynamic parameters of proteins: (1) centers with unpaired electrons (stable nitroxide radicals, radical pairs and paramagnetic complexes) exhibit electron spin resonance (ESR), (2) luminescent fluorescence and phosphorescence chromophores, and (3) Mossbauer atoms (e.g.  $^{57}\text{Fe}$ ) which gives the nuclear  $\gamma$ -resonance (NGR) spectra.

Data on the intramolecular dynamics of proteins obtained by the physical labelling approach combined with other dynamical and complementary methods may be briefly summarised as follows.

At low temperatures and in dry samples, protein macromolecules exhibit only high frequency low-amplitude harmonic nuclear vibrations with  $t_c = 10^{12} - 10^{14} \text{ s}^{-1}$  and amplitude  $A = 0.01 - 0.05 \text{ \AA}$ . This type of motion takes place in all proteins, at all temperatures and degrees of humidity, and apparently is not directly related to their functions and stability

Non-harmonic low frequency ( $t_c = 10^7 - 10^9 \text{ s}^{-1}$ ) and relatively high amplitude motions ( $0.2 \text{ \AA}$  and more) appear at certain critical temperatures,  $180 - 210 \text{ K}$ , and degree of hydration ( $10 - 30\%$ ) depending on protein structure. Protein conformational flexibility in the nanosecond and subnanosecond time scale was revealed in theoretical calculations in experiments on fluorescence quenching of the buried tryptophane residues, spin labelling and on protein NMR.

The comparative analysis of the experimental data obtained by a whole arsenal of independent methods revealed a new type of intramolecular mobility of protein globules (Likhtenshtein 1976). This type of intermolecular mobility consists of the movement of the relatively large and rigid parts of the protein macromolecules. Such hinge-like oscillation of the tightly packed polypeptide blocks does not give a measurable contribution to the overall heat capacity and the helicity degree of polypeptide chains, but it strongly affects the mobility of the Mössbauer labels firmly bound to the protein blocks, the mobility of spin and fluorescence labels and native chromophores located in cavities between the blocks, etc. At a later stage, the mechanism proposed was confirmed by independent experimental and theoretical investigations. The considerable body of experimental and theoretical evidences indicate that the capacity of a protein globule to change conformation as a result of intramolecular dynamics is an inherent property of these macromolecules and necessary prerequisite for their functional activity, recognition and capacity to be regulated.

At physiological ambient conditions, all above mentioned physical methods indicate intramolecular hinge-bending (blocks, domain) mobility of protein globules and surrounding media in the nanosecond temporal region. As shown, these modes of mobility are essential for biochemical processes, such as long-distance electron transfer in photosynthesis, substrate hydrolysis by  $\alpha$ -chymotrypsin, heme protein liganding, model photoredox reactions, etc.

As an example, photosensitive systems are convenient objects for analysing a possible correlation between the dynamic and functional properties of proteins. After a short light pulse, it is possible to observe a chemical reaction and to trace the dynamical state of the matrix with the aid of internal and external physical labels.

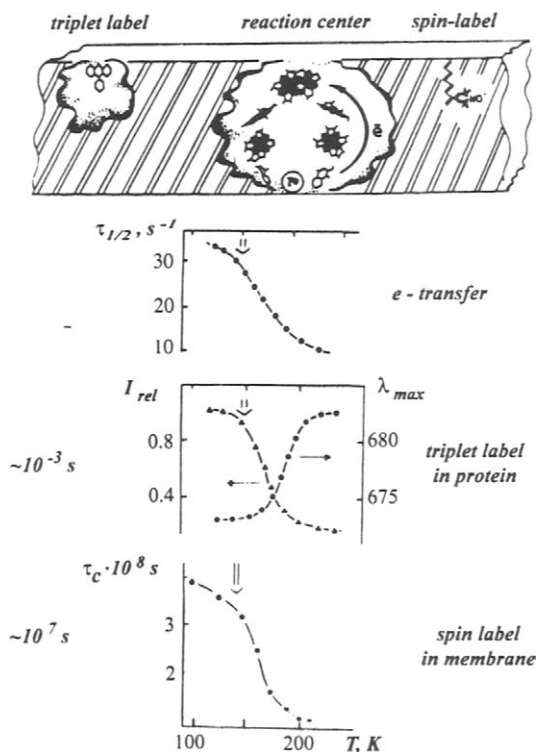


Fig. 18.9. Temperature dependences of the parameters of physical labels on chromatophores from *R. rubrum*: (a) Schematic diagram of the locations of spin and triplet labels. (b) Experimental data:  $\tau_{1/2}$  is the characteristic time of electron transfer from the reduced primary acceptor to the oxidized primary donor (Likhtenshtein G.I., *J. Photochem. Photobiol. A: Chem.* **96**, 79-92, 1996). Reproduced with permission.

As it is seen from Fig. 18.9 that the emergence of an electron from the primary photosynthetic cell, e.g., transport from the primary acceptor  $A_1$  to the secondary acceptor  $A_2$ , takes place only under conditions where the labels record the mobility of the protein moiety in the membrane with  $t_c > 10^7 \text{ s}^{-1}$ . The rate of another important process, recombination of the primary product of charge separation, i.e., reduced primary acceptor ( $A_1^-$ ) and oxidized primary donor ( $D_1^+$ ), falls from  $10^3$  to  $10^2 \text{ s}^{-1}$  when dynamic processes with  $t_c = 10^3 \text{ s}^{-1}$  occur.

Spin and fluorescent labelling experiments on intramolecular dynamics of hyperthermostable -glycosidase indicate a higher rigidity of the enzyme protein globule as compared with the relevant non-thermostable enzymes, as well as clear-cut correlation between conformational mobility and the catalytic activity of the enzyme active site at high temperature ( $90\text{--}100^\circ \text{C}$ )

As was mentioned in Section 18.2, the most important specific feature of enzymes is their multi-center nature. It is this feature, which is responsible for the main advantages of enzymes, such as the binding and orientation of substrates, synchronous elementary acts and the possibility that a multi-step process occurs with an optimal rate for each step. However, an analysis of concrete reactions shows that these advantages cannot occur in rigid structures. Chemical enzymatic processes are accompanied by multi-contact substrate-enzyme interactions and by a significant change in size of the reaction complex. Some bonds are broken, new ones are formed, and the covalent binding is changed to van der Waals contacts and vice versa. It is obvious that the structure of the protein matrix must fit the varying shape of the reaction complex in all the process steps. Even such a simple process as electron transfer must be completed with a structural reorganisation in which electronic-conformational interaction takes place.

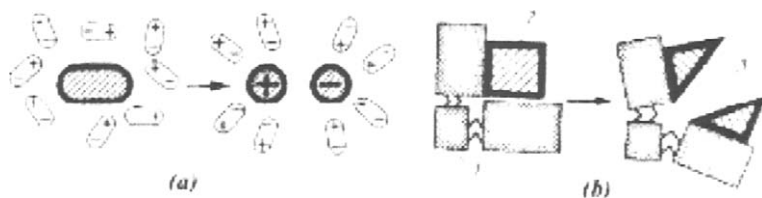


Fig. 18.10. Illustration of the principle of dynamic adaptability: (a) – orientational adaptation of the surrounding molecules toward the system of appearing charges; (b) – block mechanism of adjustment of the form of active center of changing configuration of reaction chemical complex (1 – active center, 2 – substrate, 3 – product).

This general property of the protein may be defined as dynamic adaptability (Fig. 18.10).

### 18.6. Energy and entropy parameters of enzymatic processes

The plots of the rate and equilibrium constants vs. temperature are used in experiment (see Chapter 1) to determine the energy ( $E_a$ ) and entropy ( $\Delta S^\ddagger$ ) activation parameters. (The thermodynamic parameters can also be determined by direct calorimetric measurements.) However, applying equations of the chemical kinetics to enzymatic reactions, as to any real processes in the condensed phase, one should keep in mind that due to the complex (non-elementariness) of these processes, the parameters determined from the temperature plots of the rate constants of stages of substrate transformation  $k$ , substrate affinity constants  $K_S$ , inhibition constants  $K_I$ , and others are effective integral parameters, which reflect the whole complicatedness of the process: the presence of intermediate microstages (which are not outwardly manifested), participation of the protein matrix of the enzyme, rearrangement of solvent species, and others).

The majority of enzyme-catalyzed reactions, unlike similar non-enzymatic reactions, have lower effective activation energies. The entropy parameters of enzymatic reactions take any various values from  $-100$  to  $+100$  eu, which corresponds to an interval of pre-exponential factors of  $10^{10}$ . The entropy factor is often sensitive to the structure of the substrate and enzyme, to the temperature and pH. Many cases of anomalously high and anomalously low  $E_a$  and  $\Delta S^\ddagger$  values were observed compared to those for simple model reactions. A sharp break of experimental linear plots of  $\log K_S$  and  $\log K_I$  vs.  $1/T$  are often met, which indicates the jumped change in the effective energies and entropies of the reactions in a narrow temperature range.

We know many cases when the change in the activation energy or enthalpy of the process with the same enzyme at the variation of the chemical structure of the substrate, inhibitor, or activator is accompanied by the parallel change in the activation energy and entropy. In this case, the following relationship are approximately fulfilled:

$$E_a = \alpha_c + \beta_c \Delta S^\ddagger \quad (18.1)$$

where  $\alpha_c$  and  $\beta_c$  are the empiric coefficients, which are constant for the given series.

The differences in energies reach  $60$  kJ/mol, which, according to equations (18.1) should result in changes in the rate or equilibrium constants by almost 10 orders of magnitudes. However, these changes are compensated in the Arrhenius equation by great (to  $200$  eu) changes in entropy, and the difference between the real constants is much lower. Relationships similar to (18.1) were named *compensation*. Analysis of experimental data showed that the coefficient  $\beta$  in the

equation describing the data on the Michaelis and inhibition constants are close to the average temperatures of experiments  $T_{av}$ . The same correlation obeys for the data obtained for the same enzyme in different temperature regions. For the kinetic parameters corresponding to different substrates, activators, or inhibitors, as a rule,  $\beta_c > T_{av}$ . The examples for compensation effects for rotational diffusion of the nitroxide spin labels attached to  $\beta$ -glucosidase and catalytic rate constant are presented in Fig. 18.11. The similar correlation was also observed for electron transfer reactions involving metal mediators.

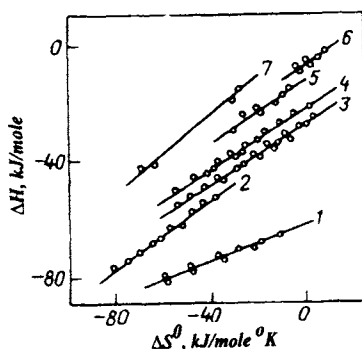


Fig. 18.11. Compensation relationships for the reactions of liganding of hemoglobin and myoglobin (1-7 different ligands and various pH).

The anomalies in the thermodynamic and kinetic parameters of enzymatic processes, including compensation effects, can be explained in general features from the assumption that chemical elementary steps on enzymes are accompanied by the rearrangement of the structure of protein globules and surrounding water. Thus, the experimentally measured  $E_{exp}$  and reflect not only properties of chemical reactions but also the cooperative properties of the water-protein matrix (G.I. Likhtenshtein, R. Lumri).

### 18.7. Enzyme catalysis today and chemistry of the 21st century

One of the top creations of Nature, biological catalysis, appears as challenging problem to chemists of the 21st century. The unique catalytic properties of enzyme are its precise specificity, selectivity, high rate, and capacity to be regulated. Classical and modern physical chemistry, chemical

kinetics, organic, inorganic and quantum chemistry provide an arsenal of physical methods and establish a basis for investigation of structure and action mechanism of enzyme. The general properties of enzymes, the “ideal” chemical catalysts, are formation of intermediates, smooth thermodynamic relief along the reaction coordinate, fulfillment of all chemical selection rules, the ability to proceed and to stop in proper time and proper space, and compatibility with the ambient media. These properties are made possible by multifunctional active centers, by the unique structure of protein globules, possessing both rigidity and flexibility, and the formation of catalytic ensembles.

Outstanding catalytic and regulator properties of enzymes which catalyze various chemical reactions with high rates, specificity and selectivity in mild conditions (ambient temperature, normal pressure, neutral aqua media) have long been a matter of interest to chemists. A greater knowledge of principles of structure and mechanism of enzymes and realization of these principles in chemistry would signify a new decisive step in the development of a theory of kinetics and catalysis and its application in industry (Shilov, 1997; Groves, 1997; Holm et al., 1996; Diekmann et.al. 2002). On the another hand, chemical model studies can be used to elucidate enzyme mechanism, along with designs of haptens, catalytic antibodies, inhibitors and medicines (R.B. Silverman).

The terms “mimicking enzymatic processes” or “chemical models of enzymes” have no monosemantic and exact definition. In some cases mimicking involves proceeding a fast and specific chemical reaction catalyzed by an enzyme in mild conditions. In other cases, attempts to construct chemical structures similar to a enzyme active site and to imitate different steps of an enzymatic process are made. Depending on knowledge about the detail structure and action mechanism of a target enzyme, starting positions of chemist are also divers.

At present, the following general steps of mimicking enzymatic processes may be formulated.

1. Previous detail analysis of existing data on structure and action mechanism of an enzyme, which together with experience and chemical intuition of the investigator would allow to compose a realistic working program providing optimal conditions for each stage of the enzymatic processes.

2. Choice of basic (primary) catalytic groups directly involved in the catalytic process. These groups may be nucleophilic and electrophilic reagents, general acids and bases, complexes of transition metals of given valence, etc. It is necessary to emphasize that the chemical reactivity of these reagents, as well as the activity of correspondent catalytical groups in the active sites of enzymes, have to be optimum to provide smooth thermodynamic relief in all steps of the process.

3. Selection of secondary groups which can regulate the reactivity of the attacking groups. For instance, adjacent basic imidazol or carboxylate can strengthen nucleophilic properties of a hydroxyl or acid groups can assist to reactions of electrophilic reagents. For helping along redox processes with participation of transition metals, adjacent acid and basic charged groups can be useful. At multi-electron processes, presence of transition metal clusters in the vicinity of primary metal atoms plays a key role.

4. Optimum disposition of primary and secondary catalytic groups within a single super molecule or on a polymer or membrane template for its sterical adjusting to attack to a substrate.

5. Including in the catalytic system additional residues which can form portions capable to bound and to precisely orient substrate molecule.

6. A matrix, carrying the model catalysis active site, should provide unimpeded entrance reagents and exit of products, and free room for conversion of each intermediates (the dynamic adaptation). In other words, the matrix should exhibit optimum molecular dynamics similar to intramolecular dynamics of proteins.

7. Each stage of the catalytic process should obey to "principle of optimum motion" (Section 14.11). Eventually, constrained pretransition state complex that activates cleavage or formation of chemical bonds, have to be formed. Realization of this last requirement is the most challenging and difficult problem of mimicking enzymes processes.

Mimicking an enzymatic processes it is not need to copy structure of protein and coenzyme groups and all stages of this process. In the course of evolution, the Nature created enzymes in specific conditions in certain media and utilized certain "building materials". Besides chemical functions, enzymes bear many other obligations serving as units of complicated enzymatic and membrane ensembles. These conditions not always were the most favorable for catalytic properties and stability the enzymes.

Biochemistry returns to chemistry a plenty of knowledge about nearly "ideal" catalysts, the enzymes as catalysts close to the enzymes and opens the way for chemical modeling of enzyme reactions. Mimicking of enzyme processes is one of the perspective trends in chemistry of 21<sup>st</sup> century. This area does only first steps, nevertheless demonstrate advantages as in elucidation of mechanism of specific enzymes enzyme but in realization of effective catalytic processes as,  $N_2$  reduction in mild conditions, oxidation carbohydrates, conversion light energy to chemical energy,

## **Bibliography**

### ***CHAPTER 1***

- Alberty, R. A. 1987, Physical Chemistry, Wiley, New York, .
- Bamford C. H. and Tipper C. F. H., 1969, Comprehensive Chemical Kinetics, vol. 1, Elsevier, Amsterdam.
- Benson S. W., 1960, The Foundations of Chemical Kinetics, McGraw – Hill, New York.
- Connors K. A., 1990,. Chemical Kinetics, Wiley, New York.
- Denisov, E. T. 1988, Kinetics of Homogeneous Chemical Reactions, Vysshaya Shkola, Moscow (in Russian).
- Kondratiev V. N. and E. E. Nikitin, 1981, Gas – Phase Reactions, Springer – Verlag, Berlin.
- Laidler, K. J 1987, Chemical Kinetics, Harper and Row, New York.
- I. Mills, 1988, Quantities, Units, and Symbols in Physical Chemistry, Blackwell Sci. Publications, New York.
- Pilling M. J. and Seakins P. W., 1995, Reaction Kinetics, Oxford University Press, Oxford.
- Van't Hoft, J. H. 1884, Etudes de dynamique chimique, Muller und Co., Amsterdam.

### ***CHAPTER 2***

- Gilbert R.G. and Smith S.C., 1990, Theory of Unimolecular and Recombination Reactions. Blackwell, Oxford.
- Green W.H. Jr., Moore, C.B. and Polik, W.F., 1992, Transition States and Rate Constants for Unimolecular Reactions. Ann. Rev. Chem., 43, 591–626.
- Kondratiev, V.N. and Nikitin, E.E., 1981, Gas Phase Reactions. Kinetics and Mechanisms. Springer, Berlin.
- Nikitin, E.E., 1974, Theory of Elementary Atomic and Molecular Processes in Gases. Clarendon, Oxford.
- Steinfeld, I.J., Francisco, J.S. and Hase, W.L., 1989, Chemical Kinetics and Dynamics. Prentice Hall, Englewood Cliffs, New Jersey.

Truhlar, D.G., Garrent, B.C. and Klippenstein, S.J., 1996, Current Status of Transition-State Theory. *J. Phys. Chem.*, 100, 12771 – 12800.

### **CHAPTER 3**

Baev, V.M. and Latz, T., 1999, Toscek Laser Intracavity Absorption Spectroscopy. *Appl. Phys. B* 69, 171 – 202.

Bagratashvili, V.N., Letchov, V.S., Makarov, A.A. and Ryabov, E.A., 1985, Multiple Photon Infrared Laser Photophysics and Photochemistry. Harwood Academic Publishers, Chur, London, Paris, New York.

Demtröder, W., 1983, Laser Spectroscopy. Springer Verlag, Berlin, Heidelberg, New York.

Kluger, D.S., Ed., 1983, Ultrasensitive Laser Spectroscopy. Academic Press, New York, London.

Rabek, J.F., 1982, Experimental Methods in Photochemistry and Photophysics. Parts 1 and 2. John Wiley and Sons, Chichester, New York, Brisbane, Toronto, Singapore.

Sherer, J.J., Paul, J.B., O'Keefe, A. and Saykally, R.J., 1997, Cavity Ringdown Laser Absorption Spectroscopy: History, Development, and Application to Pulsed Molecular Beams. *Chem. Rev.*, 97(1), 25 – 51.

### **CHAPTER 4**

Ashfold, M.N. and Baggot, J.E., 1987, Molecular Photodissociation Dynamics. Royal Society of Chemistry, London.

Butler, L. J. and Neumark, D.M., 1996, Photodissociation Dynamics. *J. Phys. Chem.*, 100, 12801-12816.

Crim, F.F., 1996, Bond-selected Chemistry: Vibrational State Control of Photodissociation and Bimolecular Reaction. *J. Phys. Chem.*, 100, 12725-12734.

Lewine, R.D. and Bernstein, R.B., 1987, Molecular Reaction Dynamics and Chemical Reactivity. University Press, New York, Oxford.

Moore, C. B. and Smith, W., Ian, 1996, State-Resolved Studies of Reactions in Gas Phase. *J. Phys. Chem.*, 100, 12848-12865.

Sarkisov, O.M. and Umanskii, S.Ya., 2001, Femtochemistry. *Russian Chem. Rev.*, 70(6), 449 – 469.

Whitehead, J.C., Ed., 1988, *Selectivity in Chemical Reactions*. Kluwer Academic Publisher.

Zewail, A.H., 2000, Femtochemistry: Atomic-Scale Dynamics of the Chemical Bond., *J. Phys. Chem. A*, 104, 5660-5694.

### **CHAPTER 5**

Alfassi, Z.B., Ed., 1999, *General Aspects of the Chemistry of Radicals*, Wiley, New York.

Caldin, E.F., 1964, *Fast Reactions in Solution*, Blackwell, Oxford.

Calef, D.F. and Derutch, J.M., 1983, Diffusion – Controlled Reactions, *Ann. Rev. Phys. Chem.*, 34, 493.

Denisov, E.T., 1981, Mechanisms of homolitic decomposition of molecules in the liquid phase, *Itogi Nauki i Tekhniki, Seriya Kinetika i Kataliz*, (in Russian), VINITI, Moscow.

Griller, D., 1984, *Landolt – Bornstein Handbook, New Series, Vol. 13, Subvolume a*, Ed. H. Fisher, Springer – Verlag, Berlin.

### **CHAPTER 6**

Basolo, F. and Pearson, R.G., 1967, *Mechanisms of Inorganic Reactions*, Wiley, New York.

Entelis, S.G. and Tiger, R.P., 1973, *Kinetics of Reactions in Liquid Phase* (in Russian), Khimiya, Moscow.

Glasstone, S., Laidler, K.J. and Eyring, H., 1941, *The Theory of Rate Processes*, McGraw-Hill, New York.

Hammett, L P., 1970, *Physical Organic Chemistry*, McGraw-Hill, New York.

Hynes, J.T., 1985, Chemical Reaction Dynamics in Solution, *Ann. Rev. Phys. Chem.*, 36, 573.

Ingold, C.K., 1969, *Structure and Mechanism in Organic Chemistry*, Cornell University Press, London.

Laidler, K J., 1987, *Chemical Kinetics*, Harper and Row, New York.

Maskill, H., 1985, *The Physical Basis of Organic Chemistry*, Clarendon, Oxford.

Moelwyn – Hughes, E.A., 1971, *The Chemical Statics and Kinetics of Solutions*, Academic Press, London.

Shorter, J., 1982, *Correlation Analysis of Organic Reactivity*, Research Studies Press, Chichester.

### **CHAPTER 7**

Alfassi, Z.B., Ed., 1999, *General Aspects of the Chemistry of Radicals*, Wiley, New York.

Bamford, C.H. and Tipper, C.F.H., Eds., 1976, *Comprehensive Chemical Kinetics*, Vol. 18, Elsevier, Amsterdam.

Benson, S.W., 1968, *Thermochemical Kinetics*, Wiley, New York.

Denisov, E.T., 1974, *Liquid – Phase Reactions Rate Constants*, IFI/Plenum, New York.

Fisher, H., Ed., 1984 and supplements, 1997, *Landolt – Bornstein, New Series*, Vol. 13, Subvolumes a-e, *Radical Reaction Rate Constants*, Springer-Verlag, Berlin.

Kerr, J.A. and Moss, S.J., 1981, *CRC Handbook of Bimolecular and Termolecular Gas Reactions*, Vol. 1,2, CRC Press, Boca Raton.

Kochi, J.K., Ed., 1973, *Free Radical*, Vol. 1, 2, Wiley, New York.

Kondratiev, V.N. and Nikitin, E.E., 1981, *Gas – Phase Reactions*, Springer-Verlag, Berlin.

Semenow, N.N., 1958 *Some Problems of Chemical Kinetics and Reactivity*, Vol.1, 2, Pergamon Press, London.

Walling, C., 1962, *Free Radicals in Solution*, Wiley, New York.

### **CHAPTER 8**

Allcock, H.R. and Lampe, F.W., 1981, *Contemporary Polymer Chemistry*, Prentice Hall, Englewood Cliffs, New Jersey.

Bamford, C.H. and Tipper, C.F.H., Eds., 1985, *Comprehensive Chemical Kinetics*, Vol. 24, Elsevier, Amsterdam.

Caldin, E.F., 1964, *Fast Reactions in Solution*, Blackwell, Oxford.

- Cram, D.J., 1965, *Fundamentals of Carbanion Chemistry*, Academic Press, London.
- Hammes, G.G., Ed., 1973, *Investigation of Rates and Mechanisms of Reactions*, Wiley, New York.
- Hammett, L.P., 1970, *Physical Organic Chemistry*, New York, McGraw-Hill, New York.
- Hynes, J.T., 1985, *Chemical Reaction Dynamics in Solution*, *Ann. Rev. Phys. Chem.*, 36, 573.
- Kochi, J.K., Ed., 1977, *Free Radicals*, Vol. 1, 2, Wiley, New York.
- Laidler, K.J., 1987, *Chemical Kinetics*, Harper and Row, New York.
- Moelvin – Hughes, E.A., 1971, *The Chemical Statics and Kinetics of Solutions*, Academic Press, London.

### **CHAPTER 9**

- Bamford, C.H. and Tipper, C.F.H., Eds., 1972, *Comprehensive Chemical Kinetics*, Vol. 5, Elsevier, Amsterdam.
- Denisov, E.T., Denisova, T.G. and Pokidova, T.S., 2002, *Handbook of Free Radical Initiators*, Wiley, New York.
- Ingold, C.K., 1969, *Structure and Mechanism in Organic Chemistry*, Cornell University Press, London.
- Koenig, T., 1973, Chapter 3 in *Free Radicals*, Vol. 1, 113, Ed. J.K. Kochi, Wiley, New York.
- Sergeev, G.B. and Smirnov, V.V., 1985, *Molecular Halogenation of Olefins*, (in Russian), Izdatelstvo Moscow University, Moscow.

### **CHAPTER 10**

- Billingham, N.C. and Jenkins, A.D., 1976, *Comprehensive Chemical Kinetics*, Eds. C.H. Bamford and C. H. F. Tipper, Elsevier, Amsterdam, Vol. 14A, 419.
- Denisov, E.T. and Azatyan, V.V., 2000, *Inhibition of Chain Reactions*, Gordon and Breach, London.
- Ito, O., 1999, *General Aspects of the Chemistry of Radicals*, 209, Ed. Z.B. Alfassi, Wiley, New York.

Kondratiev, V.N. and Nikitin, E.E., 1981, Gas – Phase Reactions, Springer – Verlag, Berlin.

Laidler, K.J., 1987, Chemical Kinetics, Harper and Row, New York.

Laidler, K.J. and Loucks, L.F., 1972, Comprehensive Chemical Kinetics, Vol. 5, 1, Eds. C.H. Bamford and C.F.H. Tipper, Elsevier, Amsterdam.

Moad, G. and Solomon, D.H., 1995, The Chemistry of Free Radical Polymerization, Pergamon, New York.

Pilling, M.J. and Seakins, P.W., 1995, Reaction Kinetics, Oxford University Press, Oxford.

Semenov, N.N., 1958-1959, Some Problems of Chemical Kinetics and Reactivity, Vol. 1, 2, Pergamon Press. London.

Walling, C., 1957, Free Radicals in Solution, Chapman and Hall, New York.

## **CHAPTER 11**

Bamford, C.H. and Tipper, C.F.H., Eds., 1980, Comprehensive Chemical Kinetics, Vol.16, Elsevier, Amsterdam.

Denisov, E.T. and Azatyan, V.V., 2000, Inhibition of Chain Reactions, Gordon and Breach, London.

Denisov, E.T. and Denisova, T.G., 2000, Handbook of Antioxidants CRC Press, Boca Raton.

Denisov, E.T., Mitskevich, N.I. and Agabekov, V.F., 1977, Liquid – Phase Oxidation of Oxygen – Containing Compounds, Consultants Bureau, New York.

Emanuel, N.M., Denisov, E.T. and Maizus, Z.K., 1967, Liquid-Phase Oxidation of Hydrocarbons, Plenum Press, New York.

Emanuel, N.M. and Gal, D., 1984, Oxidation of Ethylbenzene, (in Russian) Nauka, Moscow.

Hamid, S.H., Ed., 2000, Handbook of Polymer Degradation, Dekker, New York.

Howard, J.A., 1972, Adv. Free Radical Chem., 4, 49.

Lundberg, W.O., Ed., 1961, Autoxidation and Antioxidants, Interscience Publishers, Wiley, New York.

Semenov, N.N., 1958-1959, Some Problems of Chemical Kinetics and Reactivity, Vol. 1, 2, Pergamon Press. London.

**CHAPTER 12**

Billingham, N.C. and Jenkins, A.D., 1980, *Comprehensive Chemical Kinetics*, Vol. 17, Eds. C.H. Bamford and C. H. F. Tipper, Elsevier, Amsterdam.

Benson, S.W., 1960, *The Foundations of Chemical Kinetics*, McGraw – Hill, New York.

Denisov, E.T. and Denisova, T.G., 2000, *Handbook of Antioxidants*, CRC Press, Boca Raton.

Hinshelwood, C. and Williamson, A., 1934, *The Reaction between Hydrogen and Oxygen*, Clarendon Press, Oxford.

Jordan, P.C., 1979, *Chemical Kinetics and Transport*, Plenum Press, New York.

Kondratiev, V.N. and Nikitin, E.E., 1981, *Gas – Phase Reactions*, Springer – Verlag, Berlin.

Senenov, N.N., 1935, *Chemical Kinetics and Chain Reactions*, Oxford University Press, London.

Semenov, N.N., 1958-1959, *Some Problems of Chemical Kinetics and Reactivity*, Vol. 1, 2, Pergamon Press, London.

**CHAPTER 13**

Benson, S.W., 1960, *The Foundations of Chemical Kinetics*, McGraw – Hill, New York.

Caldin, E.F., 1964, *Fast Reactions in Solution*, Blackwell, Oxford.

Denisov, E.T. and Azatyan, V.V., 2000, *Inhibition of Chain Reactions*, Gordon and Breach, London.

Emanuel, N.M., Denisov, E.T. and Maizus, Z.K., 1967, *Liquid-Phase Oxidation of Hydrocarbons*, Plenum Press, New York.

Hammes, G.G., Ed., 1973, *Investigation of Rates and Mechanisms of Reactions*, Wiley, New York.

Howard, J.A., 1972, *Adv. Free Radical Chem.*, 4, 49.

Laidler, K.J., 1987, *Chemical Kinetics*, Harper and Row, New York.

Moelwyn – Hughes, E.A., 1971, *The Chemical Statics and Kinetics of Solutions*, Academic Press, London.

Shlyapintoth, V.Ya., Karpukhin, O.N., Postnikov, L.M., Tsepalov, V.F., Vichutinskii, A.A. and Zakharov, I.V., 1968, *Chemiluminescence Techniques in Chemical Reactions*, Consultance Bureau, New York.

#### **CHAPTER 14**

Bugg, T., 1997, *An Introduction of Enzyme and Coenzyme Chemistry*, Blackwell Science, Cambridge, MA.

Cornish-Bowden, A., 2001, *Fundamentals of Enzyme Kinetics*, Portland Press, London.

Cornish-Bowden, A., 1995, *Analysis of Enzyme Kinetic Data*, Oxford University Press, Oxford.

Fersht, A., 1999, *Structure and Mechanism of Protein Science: A Guide to Enzyme Catalysis and Protein Folding*. W.H. Freeman and Co., UK.

Gutfreund, H., Ed., 1995, *Kinetics for the Life Sciences: Receptors, Transmitters and Catalysis*. Cambridge University Press, Cambridge, UK.

Hammes, G.G., 2000, *Thermodynamics and Kinetics for Biological Science*, John Wiley and Sons, NY.

Kurganov, B.I., 1979, *Allosteric Enzymes*, Nauka, Moscow.

Leninger, A.L., Nelson, D.L. and Cox, M.M., 1993, *Principles of Biochemistry*, Worth Publishers, NY.

Likhtenshtein, G.I., 1988, *Chemical Physics of Redox Metalloenzymes*, Springer Verlag, Heidelberg.

Shramm, V.L. and Purich, D.L., Eds., *Methods in Enzymology* 308, Enzyme Kinetics and Mechanism, Part E, Academic Press, San Diego.

Varfolomeev, C.D. and Gurevich, K.G., 1999, *Bikinetika. A Practical Course*. Grand. Moscow.

#### **CHAPTER 15**

Bell, R.P., 1941, *Acid – Base Catalysis*, Clarendon Press, Oxford.

Bell, R.P., 1973, *The Proton in Chemistry*, Chapman and Hall, London.

Benson, S.W., 1960, *The Foundations of Chemical Kinetics*, McGraw – Hill, New York.

- Caldin, E.F., 1964, *Fast Reactions in Solution*, Blackwell, Oxford.
- Hammett, L.P., 1970, *Physical Organic Chemistry*, McGraw – Hill, New York.
- Laidler, K.J., 1987, *Chemical Kinetics*, Harper and Row, New York.
- Lewis, G.N., 1923, *Valency and the Structure of Atoms and Molecules*, Reinhold, New York.

### **CHAPTER 16**

- Amis, E.S., 1966, *Solvent Effects on Reaction Rates and Mechanisms*, Academic Press, New York.
- Basolo, F. and Pearson, R.G., 1967, *Mechanisms of Inorganic Reactions*, Wiley, New York.
- Denisov, E.T., 1974, *Liquid – Phase Reactions Rate Constants*, IFI/Plenum, New York.
- Denisov, E.T., Denisova, T.G. and Pokidova, T.S., 2002, *Handbook of Free Radical Initiators*, Wiley, New York.
- Waters, W.A., 1963, *Mechanisms of Oxidation of Organic Compounds*, Methuen, London.

### **CHAPTER 17**

- Adams, R.D., Ed., 1998, *Catalysis by Di- and Polynuclear Metal Clusters Complexing. Chemistry of Metal Clusters*, Ed., F. Allert Cotton.
- Bhaduri, S. and Mukesh, D., 2000, *Homogeneous Catalysis. Mechanisms and Industrial Applications*, Wiley-Interscience, N.Y.
- Cornils, B. and Herrmann, W.A., 2002, *Applied Homogeneous Catalysis with Organometallic Compounds*, Second Editions. John Wiley and Sons, New York.
- Gates, B.C., 1991, *Catalytic Chemistry*, John Wiley and Sons, New York.
- Hill C.L., 1989, *Activation and Functionalization of Alkanes*, John Wiley and Sons, New York.
- Likhtenshtein G.I., 2002, *New Trends in Enzyme Catalysis and Mimicking Chemical Reactions*, Kluwer Academic, New York.

Malleran, J.L., Legros, J.Y., and Fiaud, J.C., 1997, *Handbook of Palladium Catalyzed Organic Reactions: Synthetic Aspect and Catalytic Cycles*, Academic Press, New York.

Mathey, F. and Sevin, A., 1996, *Molecular Chemistry of Transition Elements*, John Wiley and Sons, New York.

Masel R.I., 2001, *Chemical Kinetics and Catalysis*. Wiley-Interscience, New York.

Meunier, B., Ed., 2000, *Biomimetic Oxidations Catalyzed by Transition Metal Complexes*, Imperial College Press, London.

Murahashi, S.I., 1999, *Transition Metal Catalyzed Reactions*, Chemistry for the 21<sup>st</sup> Century Monograph, YUPAC.

Parshell, G.W. and Ittel, S.D., 1992, *Homogeneous Catalysis: the Application and Chemistry of Catalysis by Soluble Transition Metal Complexes*. John Wiley and Sons, New York.

Pross, A., 1995, *Theoretical and Physical Principles of Organic Reactivity*, John Wiley and Sons, New York.

Sheldon, R.A., 1994, *Metalloporphyrins in Catalytic Oxidation*, Marcel Dekker, New York.

Shilov A.E., 1997, *Metal Complexes in Biomimetical Reactions. N<sub>2</sub> Fixation, Activation and Oxidation of Alkanes, Chemical Models of Photosyntheses*, CRC.

Shilov, A.E., Ed., 1986, *Fundamental Research in Homogeneous Catalysis*. Gordon and Breach Science Publishers. New York.

Spessard, G.O. and Meissler, G.L., 1996, *Organometallic Chemistry*, Prentice Hall, New Jersey.

Wilkins, R.G., 1991, *Kinetics and Mechanism of Reactions of Transition Metal Complexes*, VCH, Weinheim.

Yoshida, S., Sakaki, S., and Kobayashi, H., 1994, *Electronic Processes in Catalysis*., KODASHA (Tokio), VCH, Weinheim.

## **CHAPTER 18**

Bertini I., Gray, H., Lippard, S.J., and Valentine, J.S. (Eds.) ,1994, *Bioinorganic Chemistry*. University Science Books, Mill Valley, California.

Bixon, M. and Jortner, J., 1999, Electron transfer - from isolated molecules to biomolecules, in Jortner, J. and Bixon. (eds.), *Advances in Chemical Physics* 107, Part 1, John Wiley & Sons. NY, 35-202.

Bruice, T. and Benkovic, S.J. ,2000, Chemical basis for enzyme catalysis, *Biochemistry* 39, 6267-6274.

Fersht A. ,1999, *Structure and Mechanism of Protein Science : A Guide to Enzyme Catalysis and Protein Folding*. W.H. Freeman and C.

Gray, G.H. and Winkler, J.R. ,1996. Electron transfer in proteins. *Annu. Rev. Biochem.* 65, 537-561.

Fersht A. ,1999, *Structure and Mechanism of Protein Science: A Guide to Enzyme Catalysis and Protein Folding*. W.H. Freeman and Co. UK.

Gutfreund, H. (ed.) ,1995, *Kinetics for the Life Sciences: Receptors, Transmitters and Catalysis*. Cambridge University Press, Cambridge, UK

Likhtenshtein, G.I. ,1993, *Biophysical Labeling Methods in Molecular Biology*, Cambridge University Press, N.Y.

Leninger, A.L., Nelson,D.L.,Cox, M.M. (1993) *Principles of Biochemistry* Worth Publishers. N.Y.

Likhtenshtein G.I. (1979 )*Multinuclear Redox Metalloenzymes*, Moscow, Nauka.

Likhtenshtein G.I. (1988)(*Chemical Physics of Redox Metalloenzymes*. Heidelberg, Springer-Verlag.

Lippard, S.J. and Berg, J.M. (1994) *Principles of Bioorganic Chemistry*. University Science Books, Mill Valley, CA.

Lumry, R. (1995) On the Interpretation of Data From Isothermal processes, in

Johnson, M. and Ackers (eds.) *Methods in Enzymology* 259, *Energetics of Biological Macromolecules*. Acad. Press, San-Diego, pp. 628-720.

Lumry, R. (1995) *The New Paradigm for Protein Research*, in Roger G.B.. *Protein-Solvent Interactions*. Dekker, N. Y.1-141

Lumry, R. and Gregory, R.B. (1986) Free energy management in protein reactions. Concepts, complications and compensation, in G.R. Welch (ed), *The Fluctuating Enzymes*, Wiley, New York, pp. 3-185.

Marcus, R.A. (1999) Electron transfer past and future, in Jortner, J., Bixon, M. (eds.)

*Advances in Chemical Physics* 107, Part 1, John Wiley & Sons. N.Y., pp. 1-6.

Marcus, R. A. and Sutin, N. (1985) *Electron Transfer in Chemistry and Biology*, Biochim. Biophys. Acta 811, 265-322.

Orme-Johnson, W. H. (1992) Nitrogenase Structure: Where To Now? Science 257,1639-1640.

Perutz, M.F. (1992) Introductory Lecture: What are enzyme structures telling us? Faraday Discussion 93, 1-12.

Reedijk, J. and Bouwman, E. (eds) (1994) *Bioinorganic Catalysis* (2nd Edition, Revised and Expanded) Marcel Dekker, Inc., New York, N. Y.

Rees, D.C. and Howard, J.B. ,2000, Nitrogenase: standing at crossroads, Curr. Opin. Chem. Biol. 4, 559-566.

R.B. Silverman, 2000, *The Organic Chemistry of Enzyme-catalyzed Reactions*. Academic Press, San Diego., pp. 717

Shilov A.E. ,1997, *Metal Complexes in Biomimetical Reactions. N<sub>2</sub> Fixation, Activation and Oxidation of Alkanes,, Chemical Models of Photosyntheses*, CRC Press, Boca Raton, New-Yorkpp.

SyrtsovaL. A. and Timofeeva, E. A. ,2001, Electron Transfer Coupled with ATP Hydrolysis in Nitrogenase, Bull. Russian Acad, Sci. (Chemistry) 50, 1789-1794.

Semenov, N.N., Shilov, A.E., and Likhenshtein, G.I. ,1975, Polynuclear processes in chemistry and biology, Dokl. Acad. Nauk. SSSR, 221, 1374-1377.

Tikhanovitch, I.A., Provorov, N.A., Romanov, V.I., and Newton, W.E. (eds.) ,1995, *Nitrogen Fixation: Fundamentals and Applications*, Kluwer Academic Publishers, Dodrecht.

Adams R.D. (Ed.),1998, *Catalysis by Di-and Polynuclear Metal Cluster Complexing (Chemistry of Metal Clusters)*. F.Allert Cotton,

Gates B.C. *Catalytic Chemistry* (1991) John Wiley and Sons, New-York,.

Hammes G.G. (2000) *Thermodynamics and Kinetics for the Biological Sciences*. John Wiley and Sons, New-York,.

Yosshida S., Sakaki S., Koboyashi H. *Electronic Processes in Catalysis: A quantum Chemical Approach in Catalysis* (1994) John Wiley and Sons, New-York,

Murahashi S.I. *Transition Metal Catalyzed Reactions (Chemistry for the 21<sup>st</sup> Century)* YUPAC, 1999, pp 512

## INDEX

### Absorption coefficient 158

Abstraction 166, 210-211, 214, 216-222,  
224-229, 231-232, 234, 244-245, 322,  
324, 337

Acceptors 349

Acid 254, 358, 362

- base equilibrium 432
- catalysis 254, 441
- catalyzed reactions 442

Acidity 435

- function 432

Acids 311, 430

- aprotic 431
- dissociation of
- hard 431
- polyatomic 434
- protic 430
- soft 431
- strong 432, 442
- super 431
- weak 442

Action

- energy 179
- inhibitors 362

Activated complex 164

Activation

- by collisions 98
- chemical 99, 101
- energy 5, 13-15, 58, 141-142, 154, 157,  
161, 163-164, 171-172, 178, 186, 190,  
196-197, 202-203, 206, 208-212, 215,  
217-223, 225, 228-229, 231-232, 234-  
235, 240, 246, 257-259, 260, 305-306,  
308, 310-312, 316, 318, 323-325, 332-  
333, 335, 343, 502

entropy 164, 168, 170, 187, 521

- of molecules 14
- thermal 100
- volume 311

Active site of enzyme 502

Addition 201, 208, 210-217, 238, 245, 255-  
256, 309,  
336, 441

Addition reaction 207, 210, 214-215, 323,  
334, 337

Adiabatic

- channels 65

- reaction 164

- terms 36

Affinity and photoaffinity labeling methods  
428

Agents 256

Alcoxyl radicals 232

Alfrey and Price scheme 202

Alignment of reactivity 243

Alkoxy radicals 141, 236, 348

Alkyl

- macroradicals 348
- peroxy radicals 335
- radicals 141, 197, 217, 334, 349

Allosteric

- inhibition 419
- dissociation of enzymatic systems 423

Allosterism 421

$\alpha$ -Chymotrypsin 507

Aminyl radicals 198

Amplitude 162

- of vibrations 206

Analysis of kinetic schemes 410

Anisotropic reactivity 142

Apoenzyme 502

Arrhenius 5

- equation 206
- law 13, 14
- parameters 306, 310

Arrhenius, S. 4

Ascorbate oxidase 512

Aspartatamino transferase

Auto-

- catalysis 452
- catalytic reactions 5
- initiated regime of chain reaction 392

Autoxidation 344, 347-349, 355, 359

- of hydrocarbons 342
- of polymers 347-348

### Bach, A. N. 5

Bach-Engler peroxide theory 342

Bamford and Jenkins scheme 203

Base(s) 430

- -catalyzed reactions 442
- hard 431
- soft 431

- strong 432
- Beitman, L. 342
- Belousov, B. P. 468
- Berezin, I. V. 342
- Berthelot, M. 3, 4
- Bessel function 155, 241
- $\beta$ -Glucosidases 509
- Bimolecular reactions 15, 43, 143, 154-155, 158, 160, 164-166, 180, 215, 242, 256-257, 310, 318, 331, 333, 338
- rate constants of 22, 155, 157, 161, 164, 167-168, 183, 241
- Biradicals 237
- Bjerrum, N. 175, 251
- Boag, J. 157
- Bodenstein, M. 317
- Boltzmann distribution 32
- Bond
  - energy 252, 314-315
  - dissociation energies 219
- Braun constant 181
- Bray, V. 468
- Briers, F. 393
- Brill, W. 464
- Brønsted, J. N. 178, 430, 442
- Brønsted and Lewis acids 316
- Brownian motion 146, 149, 241
  
- Cage** 142, 145, 150, 152-155, 160-161, 170, 173, 185, 241, 243
- Cage effect 143-144, 146-147, 149, 151-152, 154, 189-190, 247
- Calculation methods 48
  - empirical 48
  - of rate constants of elementary reactions 46
- Carbanions 256
- Carbenes 237-238
- Carbonylation 485
- Carboxylation 485
- Catalase 509
- Catalysis 442
  - by metal complexes 472
  - cobalt-bromide 461
  - of hydrocarbon oxidation 455, 509
  - of hydrogen peroxide decomposition 453, 509
  - redox 452
- Catalyst-substrate complex 408,
- Catalytic
  - decomposition of ROOH 458
  - epoxidation of olefins 464
  - reaction 311
- Cation 251
- Chain
  - degenerate-branched reaction 343, 355
  - generation 331, 333
  - initiation 317
  - length 321, 326, 340
  - non-branched reactions 317, 339
  - oxidation 340, 347
  - propagation 317-319, 326-328, 335, 339-341, 366
  - radical mechanisms 315
  - reactions 184, 317, 319-322, 325, 327-328, 379-381
  - termination 317, 320-321, 326-327, 338, 340-341
- Chandrasekar, S. 139
- Chapman, D. 393
- Charge of the ion 251
- Charge transfer complexes (CTC) 159, 312-314
- Chemical
  - concerted reaction
  - kinetics 1, 3, 4, 5
  - lasers 381
  - models of enzymes 523
- Chemiluminescence 8, 200
- Chemiluminescence methods 397, 404
- Christiansen 317
- Cis-trans*-Isomerization 195, 305
- Claisen rearrangement 195
- Classical trajectory 21, 48
- Clusters 474, 476
- Coenzyme 502
- Cofactor 502
- Coherent anti-Stokes Raman spectroscopy 88
- Coherent elementary reactions 16
- Colliding particles 38
- Collins, F. 139
- Collision 17
  - cross section 18
  - elastic 18
- Compensation
  - effect 183,, 517, 521
  - phenomena 183, 517, 521

- Competitive-less inhibition 417
- Complementarity of free energy 517
- Complexes
  - activated 57
  - long-lived intermediate 44
  - of halogens with olefins 315
  - of molecular oxygen
  - Van-der-Waals 133
- Concentration of reactants 1, 9
- Concerted
  - decomposition 184, 186-188, 200
  - reactions 408,
- Configuration
  - collinear 39
  - noncollinear 39
  - space 49
- Conformation of macromolecules 505, 517
- Conjugated reactions 5
- Conjugation effect 179-180
- Conservation of orbital symmetry 322-323
- Constant 5
  - of equilibrium 5, 441
- Contact 251
- Conversion 10, 13
- Cooperative
  - interaction 502
  - processes, 420
- Copolymerization 203
- Correlation equations 178
- Coulomb interaction 313
- Critical
  - phenomena 355-356
  - pressure
  - size (diameter) of reaction vessel
  - size of reactor
  - temperature 137
- Cross
  - disproportionation 366
- Crossed molecular beams 19, 68
- Cyclic
  - chain termination 350, 357
  - mechanisms of chain termination
  - termination 358
- Cyclization 194, 306
- Cytochrome P-450 510
- D**antus, M. 134
- Debye, P. 142
- Decarboxylation 153
- Decomposing hydroperoxide inhibitors
- Decomposition 144-145, 148-154, 186, 196, 306-309, 318-320, 322, 337-338, 342-343, 356
  - of molecules 146, 184, 190, 305, 307
  - with chimerical interaction 184, 188
- Decyclization 306
- Degrees of freedom 64
  - adiabatic 64
- Denison, G. 361
- Density function 138
- Dielectric constant 15, 169, 173, 177, 203, 251, 253, 258, 312, 435
- Diels-Alder reactions 309
- Diene synthesis 309
- Diffusion 139-142, 151-154, 161, 166, 239
  - coefficient D 139, 149
  - -controlled reactions 136, 139, 243
  - rate constant 141, 199, 253, 334, 338, 437.
- Dihydrogen combustion
- Dimerization 309, 311
- Dioxygen 331, 334
- Dioxygen dissolution 341-342
- Dipole 171-173
  - dipole-dipole interaction 170, 172-173, 312
  - moment 169, 177, 179-180, 258, 311
- Directed evolution method 428
- Dispersion forces 251, 312
- Disproportionation 141, 154, 197-199, 320, 334, 338-339
- Dissociation 131, 253-254, 435
  - constant 178
  - constants of acids 178
  - energy 212, 231
  - of acids 432, 433, 435
- Distribution 175
  - .bimodal 122
  - function 120
  - Maxwell-Boltzmann 125
  - prior 121
- Distributions
  - energy 109
  - rotational 107
  - vibrational 107
- Dogonadze, R. R. 439
- Domain structure of protein globules 505, 518

- Donor-acceptor
  - complexes 332, 335, 343
  - interaction 173
- Dorfman, L. 157
- Drago and Wieland 314
- Dynamic approach 46
  
- E**instein, A 317.
- Einstein's law 386
- Electron
  - affinity 226, 313, 335, 433
  - capacity 505, 518
  - transfer 406, 477, 494
- Electronegativity 178
- Electronic subsystem 37
- Electronically adiabatic process 37
  - coupling
- Electronically excited molecules 103, 131
- Electrophilic 256
- Elementary
  - chemical act 133
  - reactions 2, 16, 42
  - coherent
  - gas phase 16
  - steps 2, 16, 319, 331
  - totality of 16
  - volume of phase space 54
- Elimination 255-256, 308, 441
- Emanuel, N. M. 342
- Empirical methods 48
- Encounter theory 5, 161, 164, 167, 242
- Endothermic
  - process 40
  - reactions 223
- Energy
  - branching 379-381
  - diagram 115
  - of stabilization of the radical 202
  - transfer 383
- Engler, G. 5
- Ensembles of catalysts
- Enthalpy 137, 164, 170, 176-177, 201, 208, 218, 222-223, 229, 231, 251, 309, 314, 331, 334, 433
- Entropy 164, 176, 198, 201, 251, 259, 309, 314
- Enzyme nomenclatures 505
- Epstein, I. 468
  
- Equilibrium 314, 328, 432, 436
  - concentration 161
  - constant 34, 125, 164, 175-176, 202, 242, 253, 310, 314, 334
  - rate constant 27
- ESR method 387
- Esson, W. 4
- Esterification 444
- Evans 202
- Excited
  - molecules 380
  - state 311, 382, 435
  - state, triplet or singlet 435
- Exothermic reactions 223, 322, 382-383
  
- F**ast reactions 139
- Femtochemistry 93, 128
- Femtosecond
  - light pulse 128, 134
  - spectroscopy 92
- Fermi Golden Rule 494
- Fick's law 139
- Field, R. 468
- Field effect 179
- Flow reactor 71
- Force constant 206-210, 219-220, 224-225
- Forces 240
- Fourier components 129
- Franck, J. 144
- Free
  - radicals 157, 191, 196, 202, 316, 320-321
  - valence 319-322
  - volume 138, 162, 167, 170
- Frenkel, Y. I. 137, 144
- Frequency factor 332
- Function of density 137
  
- G**eneration of radicals 345
- Geometry of the transition state 205
- Gershenzon, Yu. M. 113
- Gibbs
  - activation energy 172, 243-244
  - energy 203
  - solvation energies 251
- Gould, E. 465
- Grunwald, E. 174

Guggenheim, E. 161

Guldberg, C. M. 4

**H**aber-Weiss scheme 458

Halogenation 315

Hamilton function 48, 55

Hamiltonian

- isolated atomic fragments 47
- isolated diatomic fragments 47
- of the *N*-atomic system 47

Hammett

- constant, 181, 203
- equation 178, 180

Hammett, L. 178, 433

Harcourt, V. 4

Hard cage 154

Hawkins, E. 464

Heat of reaction 202

Henry's coefficient 341-342

Heterolytic

- dissociation 252
- reactions 255, 346

Heterotropic allosteric effect 502

HF lasers 383

Hiatt, R. 465

High activation energy 308, 323, 338

Hinge-like oscillation 504, 518

Hinshelwood, S.

Hoff, J. Van't 3

Hole theory of diffusion 141

Holes 138

Homolytic

- addition 479
- decomposition 307, 479

Homotropic allosteric effect 502

Howard, J. 399

Hydration 251

Hydrogen

- bonds 173, 180, 253, 312, 335
- fluorination 380

Hydrogenation and activation of C-H bonds 482

Hydrolysis 4, 254, 256

- bimolecular acid 445
- bimolecular base 447-448
- monomolecular acid 444-445
- monomolecular base 447
- of esters 444

Hydroperoxide decomposition 342-345, 355-356, 359

Hydroperoxides 342-343, 346, 363

Hydroxyl radical 234

Hyper-Raman light scattering 87

Hysteresis phenomenon 471

**I**ndicator, N. 464

Induced conformational transitions 504, 517

Induction period 355-357, 363-364

Inductive effect 178-180

Ingold, C.K. 256, 399, 444

Inhibited oxidation 400

Inhibition 348, 355

Inhibition constants 521, 521

Inhibitor 321, 325-326, 349-351, 355-356, 359, 362-364, 386

Initiation 145, 327-329, 340

Initiation rate 321, 328, 390

Initiator 144, 148, 184, 318, 328, 339-340, 355, 386

Innersphere transfer 491

Insertion and migration of internal ligands 480

Intermediate 2, 5, 6, 157, 305, 362-363, 365

Intracavity laser spectroscopy 79

Intramolecular

- chain transfer 340
- dynamics 133, 134, 504
- dynamics of protein 504s
- mobility of proteins 504

Ion 177, 250, 257-258

- dipole interaction
- pairs 176, 251-252
- recombination 253-254
- strength 175

Ionic

- mechanisms 315
- -strength 176

Ionization 250, 252-254, 308

- of molecules 159, 252
- potential 313, 335, 337

Ionizing strength *Y* 174

Ion-dipole interaction

Ions 15, 141, 175, 178, 250-251, 254, 260

- transition metal

Irreversible inhibition 419

Irwin, K. 465  
 Isomerization 145, 191-194, 254, 305-306  
   - of molecules 254, 305, 336  
 Isosteric effects  
 Isoteric effects  
 Isotope effect 338, 443, 426  
 Ito and Matsuda scheme 203  
 Ivanov, K. I. 342  
 Ivans, M. 178

### Karpukhin, O. N. 397

Keene, J. 157  
 Keresh, E. 468  
 Keto-enol tautomerism 449-450  
 Kimbell, G. 139  
 Kinetic  
   - curve 7, 9, 15  
   - equations 12  
   - isotope effects  
   - theory of liquids 137, 138  
   - methods 2  
 Kinetics 158, 329, 339-340  
 Kinetics of inhibited oxidation 402  
 King-Altman method 412  
 Kirkwood 169  
 Kistiakovski, V. A. 5  
 K  nig, T. 148, 151  
 Kondrat'ev, V. N.  
 Konovalov, D. P. 5  
 Koshland theory 503, 517  
 Krim, F. 108  
 Kuznetsov, A. M. 439

### Landau-Zener probability 131

Laser 382  
   - absorption spectroscopy 76  
   - induced heating of gas mixture 74  
   - induced fluorescence spectroscopy 83  
   - magnetic resonance 77  
   - spectroscopy 109  
 Lasers 158  
 Law of mass action 3, 8, 13  
 Lenard-Jones potential 162  
 Levich, V. G. 439  
 Lewis acids 431  
 Lifetimes 149, 340  
 Light generation 382

Limiting step 327-328  
 Limits on pressure  
 Linear  
   - accelerator 159  
   - correlations 180, 182  
 London forces 312  
 Long-distance electron transfer (LDET) 494  
 Long-lived complex 111, 115, 127  
 Lotka 470  
 Luminescence 381  
 Lumry concept 504

### MacLachlan, A. 157

Macrokinetics 2  
 Macromolecules 239, 244-245  
 Macroradicals 244-245  
 Magnetic isotope effect 426  
 Main catalytic groups  
 Maizus, Z. K. 342  
 Mass spectrometry 88, 109, 428  
 Matheson, M. 157  
 Matrix elements 51  
 Mayer, J. 342  
 McCarthy, R. 157  
 Mechanical strain 246  
 Mechanism(s) 1  
   - of inhibited oxidation 353  
   - of inhibition 352  
   - of inhibitor action 352  
   - of the chemical process 2  
 Medvedev, S. S. 342  
 Melville, H. 393  
 Menshutkin, N. A. 4, 178  
 Messi parameter 38  
 Metal complex electrocatalysis 492  
 Metal complexes 362, 362, 473  
 Metathesis 487  
 Methane monooxygenase  
 Method  
   - for shifting limits of chain ignition 404  
   - of activated complex 53  
   - of competitive reactions 193, 402  
   - of directed graphs 410  
   - of free radical acceptors 387  
   - of metallic mirrors 386  
   - of mixed initiation 391  
   - of molecular orbitals 47  
   - of semiclassical approximation 49

- of temperature jump 254
- Methyl radical 213
- Michaelis
  - constant 408
  - equation 408
- Microscopic rate constants 25
  - of unimolecular reaction
- Migration 194
- Migration of group 193
- Mimicking enzymatic processes
- Molecular
  - beams 127
  - collisions 4
  - complexes 160, 166, 174, 311-312, 315
  - delocalized states
  - mechanism 316
  - mobility 153-156, 240
  - reactions 322
- Molecule-dipoles 250
- Monomolecular
  - acid hydrolysis 444-445
  - base hydrolysis 447
  - reactions 256, 320
- Mulliken, R.S. 313
- Multi-
  - center nature
  - dipole effect 172
  - dipole interaction 215, 233, 332
  - electron elementary steps 499, 514
  - electron mechanisms of redox reactions
  - orbital binding 475, 476
  - orbital binding of ligands 475, 476
  - photon absorption 87, 102, 134
  - point binding of substrates 504
  - stage catalytic reactions 414
- Multiphon absorption
- Multiple chain termination 350, 357
  
- N**anosecond T-jump 428
- Negative catalysts 358
- Nitrogenase 513
- Non-
  - adiabatic ET
  - adiabatic process 52, 129
  - bonding orbital 211, 224
  - competitive inhibition 418
  - concerted decomposition 184, 187, 200
  - equilibrium kinetics 2
  - ordered mechanism 418
  - productive binding 502
  - stationary regime 354-355
- Normal liquids 136
- Noyes, R. 139, 147, 150, 151, 468
- Nuclear synchronization
- Nucleophilic
  - agent 256-257
  - attack 258
  - reactant 256-257, 259
  - substitution 256-257, 259
  
- O**lefin oxidation 472
- Oligomer-503
- Oligomerization 503
- Optically active molecule 151
- Optimum motion principle
- Orbital
  - overlap 311
  - symmetry 311
- Order
  - constant 10, 11
  - of chain reaction 326
  - of the reaction 8
- Ordered mechanism 413
- Organophosphorus inhibitors 359
- Oriental frequency 240
- Oriental interaction 312
- Ortho-para*-conversion of hydrogen 387
- Oscillation allosteric catalytic processes 424
- Ostwald, W. 5
- Overlap integral S 473, 474
- Overlapping of molecular orbitals
- Oxidation 319, 331, 335, 337, 339-340, 344, 347-348, 351, 355-357, 362, 367, 490
- Oxidation of hydrogen
- Oxidative addition 479
- Ozone 248
  
- P**aneth, F. 386
- Parabola model 231
- Parabolic
  - model 205, 207, 217-219, 223, 232
  - model addition 205
- Pauling L. 226

- Pean de Saint Gilles, L. 3, 4  
 Pearson 431  
 Pedersen, K. 178, 442  
 Period of conversion 15  
 Peripheral mechanism 502  
 Peroxidases  
 Peroxyl radicals 199, 216, 232, 335-338, 349, 351  
 Phase space 49  
 Photoactivation 28  
 Photochemical  
 - generation 318  
 - methods 393  
 - pre-effect and after-effect 395  
 Photodecomposition 150, 152  
 Photodissociation 102, 104, 129, 134, 147  
 Photolysis 144-145, 158  
 Photons 382  
 Photosynthetic reaction centers (RS's) 515  
 Physical labeling approach 518  
 $\pi$ -bonds 211, 229-230  
 Ping-pong mechanism 413  
 Pod'yampol'skaya, A. Ya. 342  
 Polanyi-Semenov equations 178, 223  
 Polar  
 - effect 179, 215, 231  
 - interaction 232  
 - molecules 15, 178, 231, 257  
 Polarizability 312  
 Polarization 173-174  
 Polychronous kinetics 245-246  
 Polymer matrix 154, 156  
 Polymeric matrix 154, 239  
 Polymerization 400, 487  
 Polymers 152-153, 155, 238, 242, 244-246, 347  
 Polynuclear transition metal complexes  
 Popov, A. A. 247  
 Porter, J. 157  
 Potential  
 - curve 37  
 - energy curves 129  
 - energy surface 37, 39, 46  
 Pre-exponential factor 14, 155, 157, 163-164, 177, 206, 240, 305, 308, 310, 332-333  
 Pre-stationary kinetics 408  
 Pretransition state 504  
 Principle  
 - of cyclicity 320  
 - of detailed balancing 33  
 - of dynamic adaptation 504, 520  
 - of non-annihilation of free valence 319  
 of optimal motion 504  
 - of reversibility 32  
 Probability of radical escape 144, 147  
 Productive binding  
 Propagation 321, 327, 329  
 Protein  
 - and membrane ensembles 505  
 - dynamics 504  
 - intramolecular dynamics 504, 517, 518  
 Proton 430  
 transfer 436, 438-439, 504  
 Protonation  
 of a molecule 441, 504  
 of the redox site 504  
 Proximity and orientation effects 407, 503  
 Pulse  
 - and high resolution ESR  
 - laser photolysis 157  
 - photolysis 157  
 - radiolysis 157, 159
- Quantum**  
 - -chemical methods 204  
 - -chemical theory 439  
 - -mechanical factors  
 - theory 434  
 - yield 144, 148, 150, 317, 386  
 Quasi-  
 - equilibrium regime 341  
 - stationary concentration 345  
 - stationary regime 325-327, 329, 340, 356-357, 364  
 Quinolide peroxide 352
- RRKM theory** 101  
 Rabinovich, B. S. 306  
 Rabinovich, E. 144  
 Racemization 145  
 Radical 231, 320  
 - acceptor 146-147, 158  
 - anion 159  
 - generation 332  
 - ions 141  
 - pairs 152, 190

- reactions 184, 231, 238, 244
- Radicals 158-159, 184, 229, 245, 318-319, 322-324
- Radius 251
- Radius (radii) of the atom 214, 227
- Raman light scattering 86
- Rate 259, 305
  - constant 8-11, 13, 15, 46, 140-143, 145-146, 148, 150, 152, 154, 156-158, 160-161, 163-166, 168, 178, 185, 187, 190, 193-194, 196, 199, 203, 216, 240, 247, 253, 257, 259-260, 320, 323, 334, 362, 436-437
  - of the chemical reaction 3, 5, 6
- Reactant
  - concentration 1, 9, 10, 13, 14
  - consumption 11
- Reactants 2
- Reaction
  - elementary 46
  - mechanism 306
  - order 8, 9, 10
  - path 40
  - products 109
  - rate 1, 6, 7, 8, 9, 10, 14, 258, 353
- Reactions
  - direct 111
  - elementary 26
  - endoergic 40
  - isomerization 45
  - microscopic 119, 124
  - non-adiabatic 117
  - of the first order 4, 326-327
  - of the second order 4, 326, 328
  - oscillating oxidation 467
  - pseudo-diffusion 142
  - rebounding 44
  - recombination 44, 198
  - simple bond cleavage 44
  - slow 166
  - stripping 44
  - superfast chemical 131
  - thermal 27
    - electronically adiabatic 110
    - thermally neutral
  - unimolecular 27, 44, 98, 102
  - with concerted rearrangements of bonds 308
- Reactivity 245, 322-323
- Reactivity of reactants 2, 4, 242
- Recombination 139, 141-142, 144-145, 150-154, 157-158, 166, 196-198, 254, 320, 327
- Redox
  - catalysis 452
  - potential  $E_0$  473,
  - systems 318
- Reductive elimination 479
- Relaxation of molecules 381
- Repulsion
  - forces 311
  - in the transition state 214
- Resonance
  - integral
- Reversible inhibition 417
- Rigid cage 239-240
- Ring-Down spectroscopy 82
- Rotational
  - angular momenta 103
  - diffusion 142-143, 154, 241
  - excitation 126
  - frequency 240
  - motion 152
  - relaxation 173
- Rule of 18 valent electrons 474
- Russel 200
  
- S<sub>N</sub>2 reaction 258**
- Sapunov, V. N. 466
- Sato formula 224
- Scheme of the mechanism 2
- Sector method 393
- Segmental mobility 245
- Self-retardation 346
- Selectivity 323
- Semenov, N. N. 178, 202
- Semenov's theory of degenerate branching 342
- Semiclassical approximation 52
- Semiempirical calculations 47
- Sheldon, R. 466
- Shilov, N. A. 5
- Shlyapintokh, V. Y. 397
- Shock tubes 73
- Sitrey, O. 468
- Six-membered cycle 192-193
- Smoluchowski, M. 139
- Solution volume 251

Solvate  
 Solvate-separated 251  
 Solvate shell 175, 177, 250-251, 258  
 Solvation 173, 234-235, 250  
 - Gibbs energy 169  
 - Number 250  
 - number SN 250  
 -  
 Specificity of enzymes 503  
 State  
 - excited  
 - singlet excited  
 - triplet excited  
 Static reactor 69  
 Stationary regime  
 Steps  
 - microscopic 16  
 Stepwise substitution 236  
 Steric  
 - effect 229-230  
 - factor 142, 153, 314, 337  
 - hindrance 217  
 Stoichiometric coefficients 6  
 Stokes radius 250  
 Stretching  
 - strain 247  
 - vibration 219  
 Structural fluctuation  
 Structure 2  
 Substitution 236, 255-256, 441  
 Substrate 256  
 Substrate affinity constants 521  
 Sulfur-containing compounds 361  
 Super-exchange process 495  
 Supersonic jet 67  
 Switching molecular devices  
 Symmetry of interacting orbitals 316  
 Synchronization 472  
 - factor 496  
 - of nuclei 496  
 Synchronous  
 - mechanism 309  
 - substitution 236  
 Synergism 362-363, 365-366  
 Szwarc, M. 386

**T**aft, R. 178  
 Taft

- constant 181  
 - equations 178, 181  
 Taylor, Ch. 178  
 Temperature coefficient 15  
 Termination 325-326, 329  
 Theory  
 - of absolute reaction rates 5  
 - statistical  
 - of bimolecular reactions 58  
 - of unimolecular reactions 62  
 Thermal electronically adiabatic reactions  
 Thermally neutral reaction 222  
 Thermodynamic  
 - feasibility of the process 407  
 Thermolysis 318  
 Thiyl radical 203  
 Thomas, J. 399  
 Time  
 - of conversion 10  
 - resolved techniques  
 Tolman, C. 399  
 Trajectory calculations 123  
 Transglobular conformational transition  
 Trans-hybridization delay 244-245  
 Transition  
 - metal clusters 474, 476  
 - metal ions 452  
 - state 128-130, 154, 169, 171, 173, 179, 187, 191-192, 197-198, 210-211, 217, 219, 224-227, 232, 240, 260, 306, 308, 310-311, 316, 324, 331, 336-338, 343  
 - state theory 168, 173, 182, 188  
 - state volume 157  
 Translational motion 152  
 Transmission factor 56  
 Trialkylboron 236  
 Trimolecular reaction 332-333  
 Triplet repulsion 210-212, 224-228  
 Tunneling transition 439  
 Turning point of reaction path 126

**U**pper limit of pressure  
 Urri and Kharash 191

**V**an der Graaf accelerator 159  
 Vartanyan, L. G. 342  
 Vasil'ev, R. F. 397

Vibration  
- excited 128  
- frequency 162  
- of atoms 206  
Vibrational overtones 108  
Vibrationally excited molecules 105, 123,  
132, 381  
Viscosity 142-143, 145, 147, 149-151, 154,  
163, 185, 197, 239-240  
Volume of the activated complex 185

**W**aage, P. 4  
Waite, T. 139  
Waker process 490  
Walters, E. 393  
Wave package 129  
Wieland, H. 342  
Wilhelmy, L. F. 3  
Winstein, S. 174  
Woodward-Hofmann rule 310, 322

**Z**habotinsky, A. M. 468  
Ziegler catalysts 472  
Ziegler-Natta catalysts 487